UNIVERSITEIT VAN PRETORIA
UNIVERSITY OF PRETORIA
YUNIBESITHI YA PRETORIA

Under the trapdoor - Resolving the taxonomy and phylogeography of the trapdoor spider genus *Stasimopus* (Mygalomorphae: Stasimopidae) of the Karoo

By

Shannon Brandt

[14009669]

Catherine L. Sole

Robin Lyle

Submitted in fulfilment of the requirements for the degree

Doctor of Philosophy

(Zoology)

Department of Zoology and Entomology

In the Faculty of Natural and Agricultural Sciences

University of Pretoria

February 2023

© University of Pretoria

“Nothing in life is to be feared, it is only to be understood. Now is the time to understand more so that we may fear less”

- Marie Curie

© University of Pretoria

Summary

Under the trapdoor - Resolving the taxonomy and phylogeography of the trapdoor spider genus *Stasimopus* (Mygalomorphae: Stasimopidae) of the Karoo

Student: Shannon Brandt[1]

Supervisors: Prof. Catherine L. Sole[1] and Robin Lyle[2]

Departments: [1]Department of Zoology and Entomology, University of Pretoria, Hatfield, Pretoria, 0002, South Africa.

[2]Agricultural Research Council – Plant Health and Protection, Biosystematics, Roodeplaat, Pretoria, 0035, South Africa.

Degree: Doctor of Philosophy (Zoology)

Keywords: *Stasimopus*, Mygalomorphae, Phylogenetics, Species delimitation, Geometric morphometrics, Integrative Taxonomy, Phylogeography, Karoo, Morphology, Identification

Abstract

Stasimopus is a genus of cork-lid trapdoor spider under the infraorder Mygalomorphae. The genus is endemic to southern Africa, but is largely understudied. This study was undertaken to understand the true species diversity and history of this genus in the Karoo region of South Africa. The Karoo is a semi-arid, unique and sensitive ecosystem which is facing pressure for development due to economic incentives. This area has long been neglected, with few studies investigating the fauna and their phylogeographic history.

The first two data chapters are dedicated to finding new methods to aid in species identification. The identification of *Stasimopus* as well as mygalomorph species generally has been a long-standing challenge. This is due to their conservative morphologies and the lack of quantifiable characters. For this reason, species delimitation methods as well as geometric morphometrics were explored to find ways to aid species identification. Multiple coalescent based species delimitation methods were used in chapter 2 to attempt to determine the number of different species present for *Stasimopus* in the region. These methods were tested against the morphological identifications and monophyletic groupings. The species delimitation proved unfruitful, as they appear to delimit population structure rather than species. This is likely due to extensive population structuring, which is common in mygalomorph spiders. The second methodology was to test whether the historically

© University of Pretoria

used eye patterns are a valid character for species identification and if so, to implement geometric morphometric techniques to attempt to separate species. The results showed significant phylogenetic signal for ocular patterns in both sexes, validating its use for species identification. Species and morphospecies show distinct clustering in morphospace, but there is overlap due to the continuous shape of the character. The methodology of applying geometric morphometrics to quantify ocular patterns shows great promise for distinguishing species, but a larger sample size is required to test this more conclusively.

The third data chapter is the first integrative taxonomy for *Stasimopus* of the Karoo region of South Africa. The study found that the diversity of the genus is significantly higher than previously believed including the description of nine new species. This chapter also highlights the pitfall of using only morphological data as the male of *S. maraisi* was incorrectly assigned to the female based on morphology. A description of the genetically matched *S. maraisi* male was completed as well as the original male being assigned to a new species.

The final data chapter unravelled the phylogeographic patterns of the genus in the Karoo. It was found that 15 species occur in the region and that the genus radiated in the Karoo in the early Paleocene. Most species radiated between the late Eocene and the Miocene, which is mirrored by some mygalomorph spiders in the arid region of Western Australia. The Tankwa Karoo has been tentatively identified as a Pleistocene glacial cycle refugia for the species *S. leipoldti*. The species *S. maraisi* was found to have undergone extensive population expansion in the mid-Miocene leading to its extensive modern range. This chapter also highlights the large number of short-range endemics present in the Karoo, which are of great conservation concern.

© University of Pretoria

Research outputs

Peer-reviewed journal articles:

Mitchell, S. (Brandt, S.), Lyle, R. and Sole, C. L. (2020). Teratological cases of the ocular patterns in the South African endemic trapdoor spider genus *Stasimopus* Simon (1892) (Araneae, Mygalomorphae, Stasimopidae). African Zoology, 55 (4): 363-367.

Conference presentations:

Oral presentations:

Mitchell, S. (Brandt, S.), Lyle, R. and Sole, C. L. The species delimitation of the endemic trapdoor spider genus *Stasimopus* Simon, 1892 (Araneae: Mygalomorphae: Stasimopidae) in the Karoo. Oral presentation delivered at Zoological Society of Southern Africa Conference, Skukuza, MP, South Africa, 2019.

Mitchell, S. (Brandt, S.), Lyle, R. and Sole, C. L. The species delimitation of the endemic trapdoor spider genus *Stasimopus* Simon, 1892 (Araneae: Mygalomorphae: Stasimopidae) in the Karoo. Oral presentation delivered at the University of Pretoria, Zoology and Entomology department Annual General Meeting (AGM), Pretoria, GP, South Africa, 2019.

Mitchell, S. (Brandt, S.), Lyle, R. and Sole, C. L. The phylogeography and radiation of an endemic trapdoor spider genus, *Stasimopus* Simon (1892) (Araneae, Mygalomorphae, Stasimopidae) in the Karoo, South Africa. Oral presentation delivered at the University of Pretoria, Zoology and Entomology department Annual General Meeting (AGM), Pretoria, GP, South Africa, 2020.

Mitchell, S. (Brandt, S.), Lyle, R. and Sole, C. L. Geometric morphometric analysis of ocular patterns in the endemic trapdoor spider genus *Stasimopus* Simon, 1892. Oral presentation delivered at the International Congress of Zoology, Cape Town, WC, South Africa [ONLINE], 2021.

Mitchell, S. (Brandt, S.), Lyle, R. and Sole, C. L. Geometric morphometric analysis of ocular patterns in the endemic trapdoor spider genus *Stasimopus* Simon, 1892. Oral presentation delivered at the University of Pretoria, Zoology and Entomology department Annual General Meeting (AGM), Pretoria, GP, South Africa, 2021.

© University of Pretoria

List of abbreviations

°C	degree Celsius
16S	16S ribosomal ribonucleic acid
A	Atlas region
AB	Agulhas Bank
ABDG	Automatic Barcode Gap Discovery
AFFZ	Agulhas-Falkland Fracture Zone
ALE	Anterior lateral eye
AME	Anterior median eye
AMGS	Albany Museum, Grahamstown, South Africa
AMNH	American Museum of Natural History, New York, USA.
AP	Agulhas Plateau
AP1	Antarctic Peninsula
Ar	Armenian microplate
B	Burma
BCE	Before the Common Era
BMNH	Natural History Museum, London, United Kingdom
bPTP	Bayesian Poisson Tree Processes
C	Caribbean
CA	Central Atlantic
CAS	California Academy of Sciences, San Francisco, USA.
cm	centimetre
CO1	Cytochrome c oxidase subunit 1
CO_2	Carbon dioxide
DFZ	Davie Fracture Zone
DML	Drönning Maud Land
DNA	Deoxyribonucleic acid
do	dorsal
DSI	Department of Science and Innovation
E	Etendeka basalts
EBIS	Ecological and Biodiversity Importance and Sensitivity
EF-1ɣ	Elongation Factor 1 gamma
EWM	Ellsworth Island
FBIP	Foundational Biodiversity Information Program
FI	Falkland Islands
FP	Falklands Plateau
FPB	Falkland Plateau Basin
GFS	Gastre Fault System
GM	Gulf of Mexico
GMYC	General Mixed Yule Coalescent
I	Iberia
Ir	Iranian microplate

© University of Pretoria

K – Pg	Cretaceous – Paleogene
Km^2	square kilometre
KT	Cretaceous – Tertiary
L	Lebombo
LA	Luderitz Arch
LGM	Last Glacial Maximum
M	Malaya
MCP	Mozambique Coastal Plain
MEB	Maurice Ewing Bank
mm	millimetre
MOQ	Median ocular quadrangle
MPT	Mid-Pleistocene Transition
MR	Mozambique Ridge
MRCA	Most Recent Common Ancestor
MY	Million years
MYA	Million years ago
NCA	National Collection of Arachnida
Ne	Effective population size
NM	National Museum, Bloemfontein, South Africa.
NRF	National Research Foundation
OB	Orange river Basin
pl	Prolateral
P	Parana basalts
PLE	Posterior lateral eye
PME	Posterior median eye
PPRI	Plant Protection Research Institute
rl	Retrolateral
RV	Rocas Vardes
S	Sumatra
SB	Somali Basin
SAMC	Iziko Museum of Cape Town, Cape Town, South Africa
SANBI	South African National Biodiversity Institute
SEA	Strategic Environmental Assessment
SKA	Square Kilometre Array
ST	Southern Tibet microplate
T	time
TP	Tristan plume
TMSA	Ditsong Museum of Natural History
v	Ventral
WB	Walvis Basin
WS	Weddell Sea
YA	years ago
ZMBH	Museum für Naturkunde, Heidelberg, Germany

© University of Pretoria

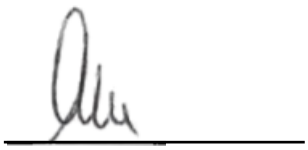
Declaration

I declare that the thesis, which I hereby submit for the degree Doctor of Philosophy in Zoology at the University of Pretoria, is my own work and has not previously been submitted by me for a degree at this or any other tertiary institution.

Ethics statement

The author, whose name appears on the title page of this thesis, has obtained, for the research described in this work, the applicable research ethics approval.

The author declares that she has observed the ethical standards required in terms of the University of Pretoria's Code of Ethics for Researchers and the Policy guidelines for responsible research.



Shannon Brandt

31 August 2022

Disclaimer

Each chapter within this study, except chapters 1 and 6, have been written in paper format for publication at various journals, hence the formats are all different.

The paper (published by S. Brandt, R. Lyle and C. Sole) included in the end of this thesis has already been published in African Zoology and will thus appear plagiarised. This may be the reason for a higher-than-expected plagiarism score.

© University of Pretoria

Acknowledgements

I would like to thank my parents, Charmain, Brett and Lindsay for your never wavering support and interest in a topic far removed from your own. Thank you for believing in me for my entire academic career not only the last four years. Thank you to the Brandt family, Natacha and Jonathan, thank you for providing me with a steady home environment and support which made this endeavour easier. Keagan and Kelsey, thank you for providing me with frequent comedic relief. My husband, Dylan, thank you for supporting and believing in me more than I could possibly expect. You picked me up when I ran into obstacles with your wisdom, that if it were easy, everyone would have a Ph.D. I appreciate you all immensely.

I would like to thank my supervisors, Catherine Sole and Robin Lyle. You are both incredibly inspirational role models of strong women in science. I cannot articulate how much your knowledge, support and guidance has benefitted me in the last six years. You have been pivotal in shaping me into the woman I am not only in my career but in my everyday life. Thank you for the opportunity to work with you both.

Thank you to Carmen Jacobs for assisting with sequence generation which contributed to this thesis. Elme Brand, thank you for assisting with field work to collect the specimens. Thank you to you both for being great lab partners in the beginning of this project. I would like to thank Prof. Christian Pirk for his assistance with the statistics underlying the geometric morphometric chapter of this thesis.

Thank you to the many friends whose support and interest was always appreciated. Tshepiso, thank you for assistance on fieldwork and being the person who I could always turn to as we went through all of this together. Laughing with you about the peculiarities of a Ph.D. always made everything seem easier.

Lastly, I would like to acknowledge the NRF for funding most of my academic career and in particular this project (grant numbers: 120190 and 139125). The Karoo BioGaps project was also instrumental in funding, as well as arranging all the sampling localities (grant number: 98864).

© University of Pretoria

Table of contents

Chapter 1 General Introduction 1

1.1. The geological history of the Karoo basin 1

1.2. The modern-day Karoo region 8

1.3. Karoo BioGaps Project 10

1.4. Background on the infraorder Mygalomorphae 11

1.5. Mygalomorphae fossil record and divergence dating 13

1.6. Taxonomic history of *Stasimopus* 16

1.7. Genetics 17

1.8. Phylogenetics 18

1.9. Species delimitation 19

1.10. Geometric morphometrics 21

1.11. Integrative taxonomy 24

1.12. Phylogeography 25

1.13. Rationale 26

1.14. Aims and objectives 27

References 28

Chapter 2 The phylogenetic structure and coalescent species delimitation of an endemic trapdoor spider genus, *Stasimopus* (Araneae, Mygalomorphae, Stasimopidae) in the Karoo region of South Africa. 40

1. Introduction 42

2. Methods and Materials 44

2.1. Taxon sampling 44

2.2. Morphological identification 45

2.3. DNA extraction, sequencing and alignment 46

2.4. Phylogenetic analysis 47

2.5. Species delimitation 48

© University of Pretoria

3. Results 51
3.1. Field survey 51
3.2. Phylogenetic analysis 51
3.3. *Stasimopus* phylogenies and identities 51
3.5. Species delimitation 55
4. Discussion 61
4.1. *Stasimopus* phylogenies 61
4.2. Uncertainty in the phylogenies 62
4.3. Coalescent species delimitation 62
5. Conclusion 65
References 66
Supplemetary material 72

Chapter 3 Geometric morphometric analysis of ocular patterns as a species identifier in the South African endemic trapdoor spider genus *Stasimopus* Simon 1892 (Araneae, Mygalomorphae, Stasimopidae)……..89
1. Introduction 92
2. Methods and Materials 93
2.1. Specimen selection 93
2.2. Geometric morphometric data capture 95
2.3. Phylogenetic analyses 96
2.4. Statistical analyses 96
2.5. Pilot study for error testing 99
3. Results 100
3.1. Phylogenetic signal and relationships 100
3.1. Separtation of species or morphospecies 103
4. Discussion 107
4.1. Phylogenetic relationship to eye pattern 107
4.2. Eye patterns as an identifier 108
References 110
Supplemetary material 117

© University of Pretoria

Chapter 4 An integrative taxonomy of the *Stasimopus* of the Karoo with the description of nine new *Stasimopus* Simon 1892 species a *Stasimopus maraisi* male Hewitt 1914……134

1. Introduction……136
2. Methods and Materials……137
   - 2.1. Specimen collection……137
   - 2.2. Taxonomic methods……138
   - 2.3. Phylogenetic analyses……139
   - 2.4. Geometric morphometric analysis of ocular patterns……140
   - 2.5. List of abbreviations……140
3. Results……141
   - 3.1. Morphological character matrices……141
   - 3.2. Phylogenetic results……142
   - 3.3. Geometric morphometric ocular patterns……145
   - 3.2. Integrative taxonomy……146
   - 3.3. Taxonomic results……149
4. Discussion……200
   - 4.1. Karoo species diversity……200
   - 4.2. Integrative taxonomy……200
5. Conclusion……201

References……203

Supplemetary material……209

Chapter 5 Phylogeography and diversification of an endemic trapdoor spider genus, *Stasimopus* Simon 1892 in the Karoo……213

1. Introduction……215
2. Methods……217
   - 2.1. Taxon sampling……217
   - 2.2. Sequence data generation……217
   - 2.3. Divergence dating……218
   - 2.4. Demography analyses……219
   - 2.5. Haplotype networks……220
   - 2.5. Mantel test and isolation by distance……220

© University of Pretoria

3. Results 221
3.1. Divergence dating 221
3.2. Demographic history 224
3.3. Mantel test 225
4. Discussion 227
4.1. Divergence dating 227
4.2. Demography 228
4.3. Mantel test and geographic influence 229
5. Conclusion 230
References 231
Supplemetary material 241

Chapter 6 General discussion 250
1. General discussion 250
2. Future directions 256
3. Conclusion 257
References 258

Appendix A Expanded methodologies ....
1. Methods for divergence dating (Chapter 5) 263
2. Geometric morphometric pilot study background (Chapter 3) 267

Appendix B Additional publication ....
1. Teratological cases of the ocular patterns in the South African endemic trapdoor spider genus *Stasimpus* Simon (1892) (Araneae, Mygalomorphae, Stasimopidae) 272

© University of Pretoria

Chapter 1

General introduction

1.1. The geological history of the Karoo basin

The Karoo basin of South Africa in combination with four other basins globally form the Gondwanan foreland basins which were formed by collisions and terrain accretion tectonics along Gondwana's southern edge (Götz and Ruckwied, 2014; King, 1978). The Karoo basin sedimentation dates from the late Carboniferous to the middle Jurassic (323 – 174 MYA) (Johnson et al., 2006). During this time the sedimentation recorded the gradual change from a glacial environment to an arid desert, as South Africa changed in latitude from the polar region towards the tropics (Johnson et al., 2006; Meadows and Watkeys, 1999; Tankard et al., 1982a). The Karoo basin is the only basin globally to record this 200 MY change in its sedimentation (Johnson et al., 2006). It spans 700,000 km^2, covering 60% of South Africa's land surface (Johnson et al., 2006). Only the south-western portion of this is the modern-day Karoo region. Due to the geological history of the basin, it is now of large economic value due to expansive coal deposits (Holness et al., 2016; Johnson et al., 2006).

The main basin was formed by the gradual subsidence of cratonic crust in the late Carboniferous period (323 – 298 MYA) (Johnson et al., 2006). At this point in time, South Africa was located above the polar ice caps and there were global temperature reductions, leading to a drop in sea level and widespread ice cover (Johnson et al., 2006; Meadows and Watkeys, 1999; Scheffler et al., 2003; Tankard et al., 1982a). A marine incursion extended in from the west, which led to a heterogenous marine ice sheet over the basin (Johnson et al., 2006; Tankard et al., 1982a).

The Dwyka rock group was then deposited into this glaciated Precambrian bedrock during the late Carboniferous – early Permian period (Johnson et al., 2006). The deposition was due to increasing temperatures leading to the erosion of debris from the highlands (Johnson et al., 2006). The debris and melted ice then filled the valley forming the Dwyka group (Johnson et al., 2006). At this time, the first terrestrial ecosystems resembling those today were formed leading to a radiation of terrestrial life (Meadows and Watkeys, 1999). It is reported that the Ecca basin would have held large forests with temperatures of 30 °C and 3000 mm of annual rain (Meadows and Watkeys, 1999). These were the conditions that led to the rich fossil fuel seams present today (Götz and Ruckwied, 2014).

During the Permian period (298 – 251 MYA) there was a rise in sea level (due to melted ice sheets), this led to the Ecca group deposit (Johnson et al., 2006; Tankard et al., 1982a). The deposit consists of various formations, each with their own environmental conditions (Johnson et al., 2006). The Prince Albert and Whitehill formations were both carried into the basin due to melting ice sheets (Johnson et al., 2006). Volcanic activity in the subduction zone led to ash layers being deposited,

Department of Zoology and Entomology
University of Pretoria

© University of Pretoria

creating the basin plain tributaries and submarine fans of the Fort Brown, Laingsburg, Ripon, Stoorsteensberg and Vischkuil formations (Johnson et al., 2006). The Kookfontien formation was a continuation of the pro-delta sedimentation after the gravity flow of the Stoorsteensberg formation (Johnson et al., 2006). The Tierberg formation was deposited as mud in the shallow water of the North of the Karoo trench (Johnson et al., 2006). The Collingham, Pietermaritzburg, Vryheid, Volksrust and Waterford formations were also formed at this time (Johnson et al., 2006). These events led to the progradation of the delta-front and the movement of plain sediments into the Ecca sea (Johnson et al., 2006; Tankard et al., 1982a). At this time the Karoo basin was landlocked and still experiencing a marine incursion (Tankard et al., 1982a). The environment resembled the modern-day Black Sea, only shallower and larger (Tankard et al., 1982a). Through time the Ecca sea experienced cycles of shallowing and deepening (Tankard et al., 1982a).

In the late Permian (259 – 251 MYA), the Beaufort group began to form with the Adelaide lower subgroup. This subgroup was deposited subaerially as the upper delta plain and fluvial mud (Johnson et al., 2006). The flood plain was waterlogged for this period (Johnson et al., 2006). By the early Triassic (251 – 247 MYA), the environment was becoming more arid, leading to active subsidence (Götz and Ruckwied, 2014; Johnson et al., 2006; Tankard et al., 1982a). The environment was predominated by meandering rivers or floodplains and was inhabited by small carnivores and large herbivores (Johnson et al., 2006; Meadows and Watkeys, 1999). This is captured in the Tarkastad upper subgroup of the Beaufort group (Johnson et al., 2006).

Globally an important event took place at the Permian–Triassic boundary (248 MYA) which is marked by a mass extinction event, after which abundant diversification occurred (Meadows and Watkeys, 1999). In the beginning of the late Triassic period (237 MYA), the environment was a peat swamp with a cool, wet climate (Johnson et al., 2006). The Molteno formation deposition was due to bedload dominated rivers flowing from a tectonically active source across braided plains (Johnson et al., 2006). As the late Triassic progressed the climate was warming and becoming more arid, this led to rivers becoming broader, shallower and more ephemeral as captured in the Elliot formation (Johnson et al., 2006). At the end of the late Triassic and early Jurassic (201 MYA), there was progressive warming and desiccation (Johnson et al., 2006). This is seen in the Clarens formation, which was the deposition of shallow playa lakes (Johnson et al., 2006). In the same period, the Cape orogeny occurred and this formed the Cape Fold Belt mountain range which forms part of the Gondwanide fold belt (extending to the Falkland Islands, Argentina and Antarctica) (Newton et al., 2006). This orogeny event involved the southern-most part of the Karoo foreland basin (Newton et al., 2006).

The sedimentation of the Main Karoo basin ended with the beginning of magmatic activity and minor basaltic lava flows (Johnson et al., 2006; Tankard et al., 1982a). This was due to the breakup of Gondwana, but initiated 20 MY earlier during the Jurassic (Tankard et al., 1982a). The main volcanism occurred between 200 – 190 MYA, but acid volcanism continued until 140 MYA

© University of Pretoria

(Tankard et al., 1982a). This caused a mass local extinction event in the early Jurassic (180 MYA), which had a global effect (Duncan and Marsh, 2006; Meadows and Watkeys, 1999). The whole of southern Africa was covered in basaltic lava due to the intrusive dolerite suite being a feeder system to the flood basalt eruptions (Duncan and Marsh, 2006). This occurrence is responsible for the network of sills and dykes present in the modern-day Karoo (Duncan and Marsh, 2006).

The break-up of Gondwana began in the Jurassic period and is still continuing today (Meadows and Watkeys, 1999; Watkeys, 2006). Watkeys (2006), broke the break-up of Gondwana from a southern African context into five stages as seen in Figures 1 - 5 (Watkeys, 2006). The first stage occurs from 180 – 175 MYA and documents the rifting, but no separation of the super continent (Figure 1a) (Watkeys, 2006). At this time, Tethys I (ocean) which shared a passive margin with Gondwana was subducting beneath Laurasia causing the formation of a new oceanic ridge resulting in the development of Tethys II (Figure 1) (King, 1978; Watkeys, 2006). Karoo volcanism occurred 183 MYA, the cause of this is unknown but is thought to be either due to a plume, subduction event or lithospheric stretching (Duncan and Marsh, 2006; Watkeys, 2006). The volcanism caused softening, leading to weak zones allowing for continental drift to occur at a later stage (Watkeys, 2006). The second stage occurred 175 – 155 MYA and features a major fracture forming across Gondwana, followed by microplate rotation (Figure 2) (Watkeys, 2006). Stage three is defined between 155 – 135 MYA, at this time Gondwana was broken up into two plates due to a strike-slip movement (Figure 3) (Watkeys, 2006). The one plate consisted of Africa and South America (West Gondwana) and the other of Madagascar, India, Antarctica and Australia (Figure 3a) (East Gondwana) (Watkeys, 2006). These plates slid past each other and initiated movement along the Proto-pacific linked system, rifting the landscape of the Agulhas bank (Figure 3) (Watkeys, 2006). During stage four (135 – 115 MYA), West Gondwana split in two (extraction of the Falkland plateau, 133,5 MYA) resulting in the Agulhas-Falkland fracture zone (Figure 4) (King, 1978; Watkeys, 2006). A strike-slip movement caused the first oceanic crust development around South Africa (Watkeys, 2006). Approximately 132 MYA the Etendeka volcanics of Namibia erupted, these flood volcanics form part of the Parana continental flood basalt province in Africa (Figure 4) (Watkeys, 2006). At this time Africa and South America were moving westwards on one plate (Watkeys, 2006). Another important event occurred 137 MYA with the formation of the Tristan da Cunha plume beneath the Parana basin of South America (Figure 4) (Watkeys, 2006). The plate containing Africa and South America continued to move until the Fault-Falkland-Agulhas fracture was above the plume (132 MYA) (Watkeys, 2006). The plume then initiated sea-floor spreading leading to the split of Africa and South America (Watkeys, 2006). Africa started to travel eastwards (Watkeys, 2006). The final stage (115 – 90 MYA) saw the split of Antarctica and Australia and the final break between Africa and South America (Figure 5) (Watkeys, 2006). By the Tertiary there was an 800 km shallow ocean between Liberia and Brazil (Axelrod and Raven, 1978). This ocean however, was populated with many islands which were stepping stones for taxa (Axelrod and Raven, 1978).

© University of Pretoria

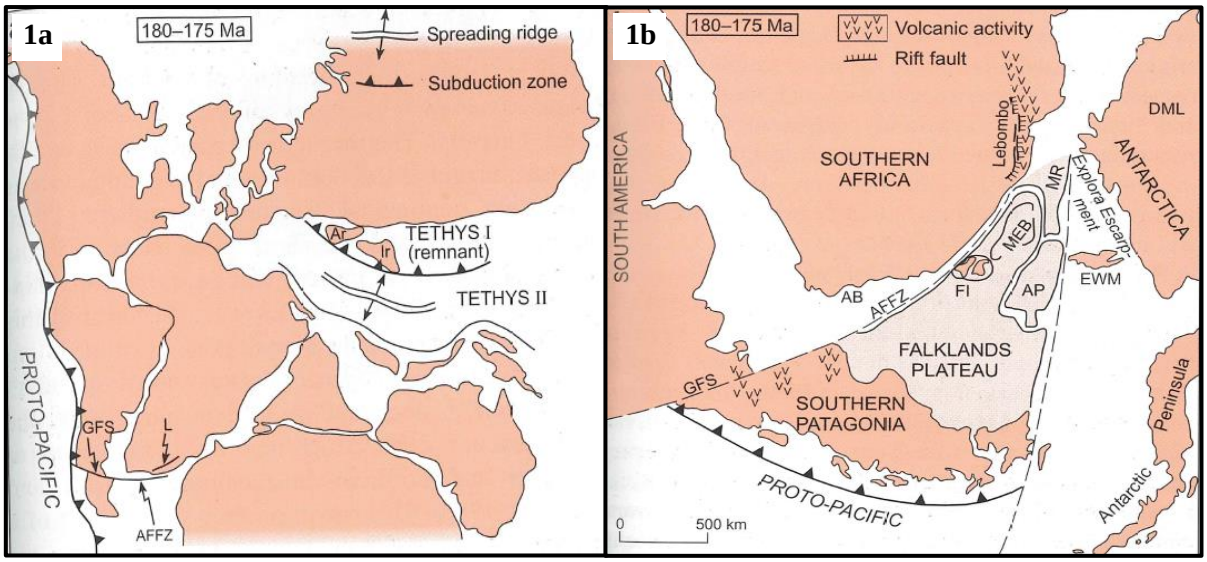


Figure 1. Taken from Watkeys (2006). Stage 1 of Gondwana break-up (180 - 175 MA). (a) Illustration of the break-up Pangaea. (b) Illustration of the southern African environment during the break-up of Pangaea. Abbreviations: AB: Agulhas Bank; AFFZ: Agulhas-Falkland Fracture Zone; AP: Agulhas Plateau; Ar: Armenian microplate; DML: Drönning Maud Land; EWM: Ellsworth Island; FI: Falkland Islands; GFS: Gastre Fault System; Ir: Iranian microplate; L: Lebombo; MEB: Maurice Ewing Bank; MR: Mozambique Ridge.

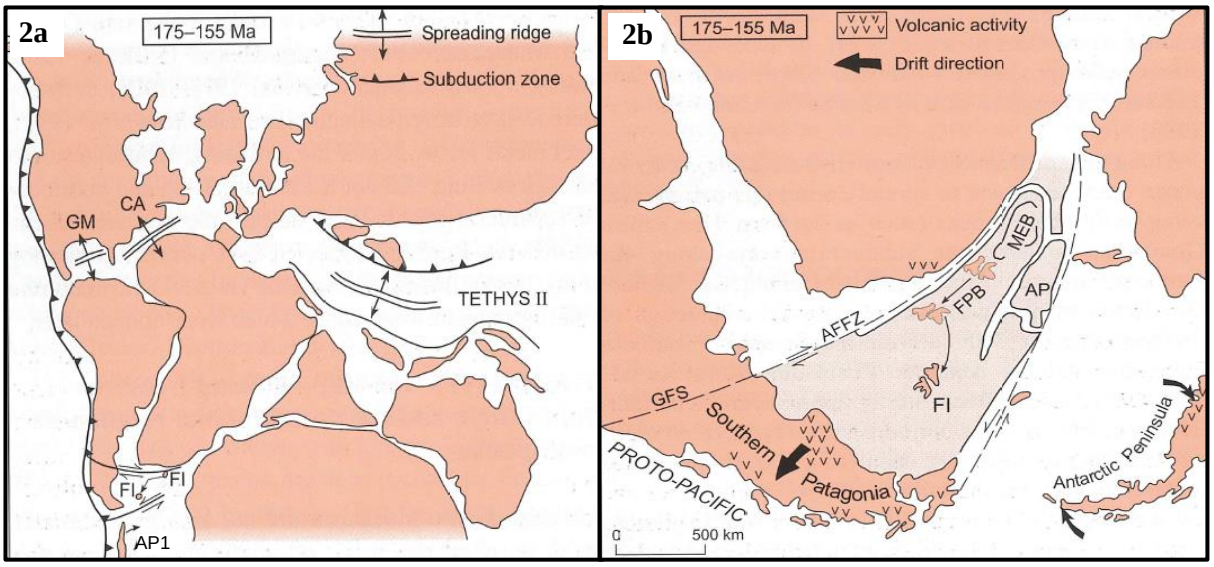


Figure 2. Taken from Watkeys (2006). Stage 2 of Gondwana break-up (175 - 155 MA). (a) Illustration of the break-up Pangaea. (b) Illustration of the southern African environment during the break-up of Pangaea. Abbreviations: AFFZ: Agulhas-Falkland Fracture Zone; AP: Agulhas Plateau; AP1: Antarctic Peninsula; CA: Central Atlantic; FI: Falkland Islands; FPB: Falkland Plateau Basin; GFS: Gastre Fault System; GM: Gulf of Mexico; MEB: Maurice Ewing Bank.

© University of Pretoria

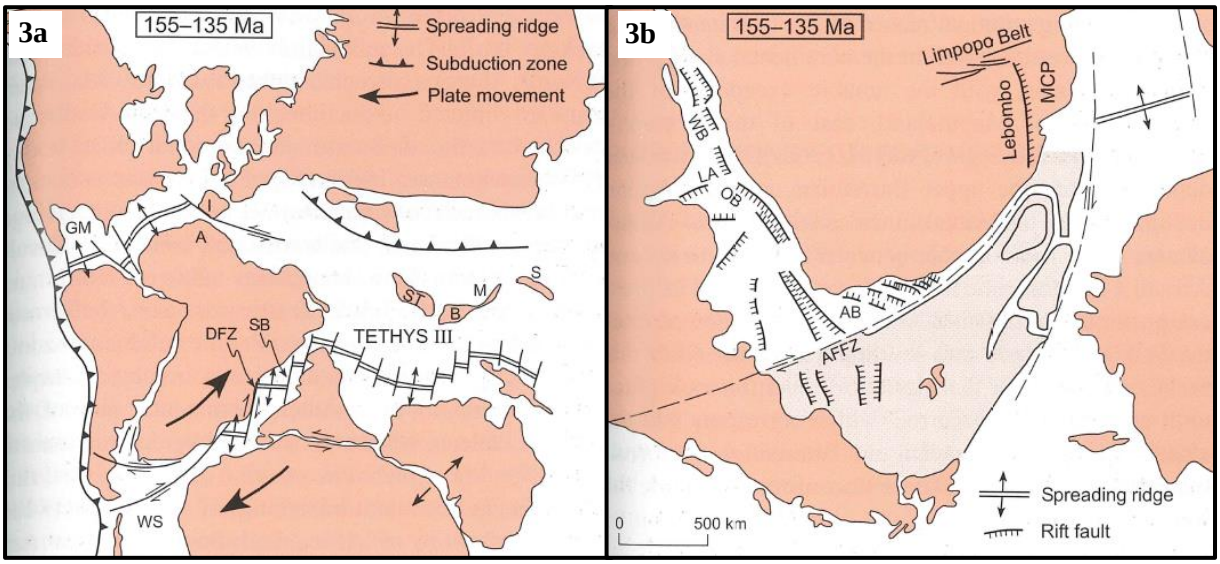


Figure 3. Taken from Watkeys (2006). Stage 3 of Gondwana break-up (155 - 135 MA). (a) Illustration of the break-up Pangaea. (b) Illustration of the southern African environment during the break-up of Pangaea. Abbreviations: A: Atlas region; AB: Agulhas Bank; AFFZ: Agulhas-Falkland Fracture Zone; B: Burma; DFZ: Davie Fracture Zone; GM: Gulf of Mexico; I: Iberia; LA: Luderitz Arch; M: Malaya; MCP: Mozambique Coastal Plain; OB: Orange River Basin; S: Sumatra; SB: Somali Basin; ST: Southern Tibet microplate; WB: Walvis Basin; WS: Weddell Sea.

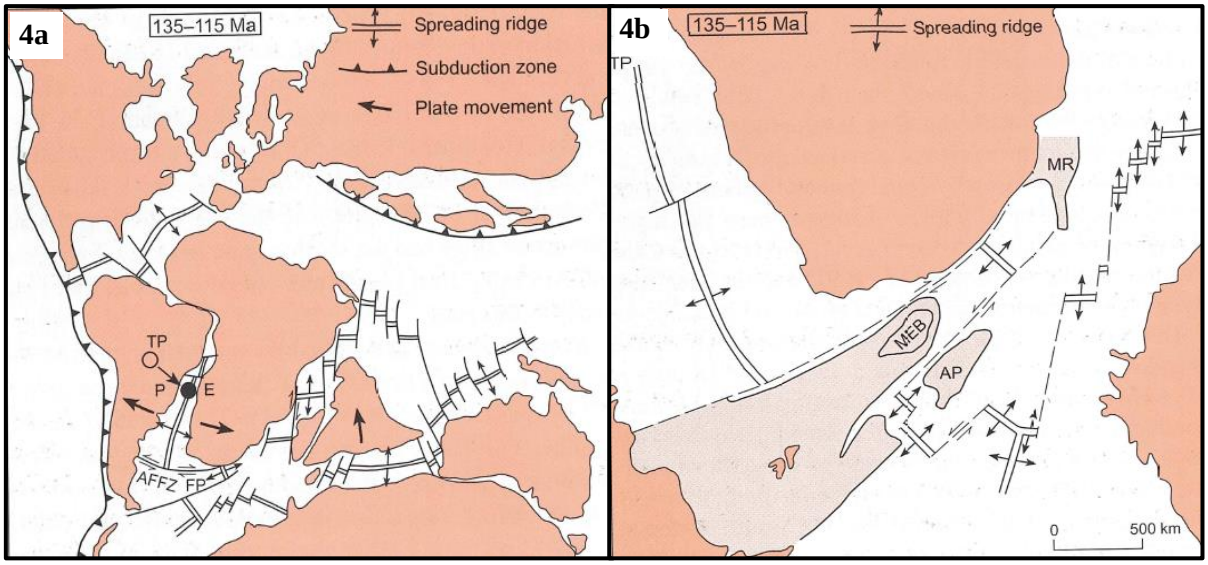


Figure 4. Taken from Watkeys (2006). Stage 4 of Gondwana break-up (135 - 115 MA). (a) Illustration of the break-up Pangaea. (b) Illustration of the southern African environment during the break-up of Pangaea. Abbreviations: AFFZ: Agulhas-Falkland Fracture Zone; AP: Agulhas Plateau; E: Etendeka basalts; FP: Falklands Plateau; MEB: Maurice Ewing Bank; MR: Mozambique Ridge; P: Parana basalts; TP: Tristan plume.

© University of Pretoria

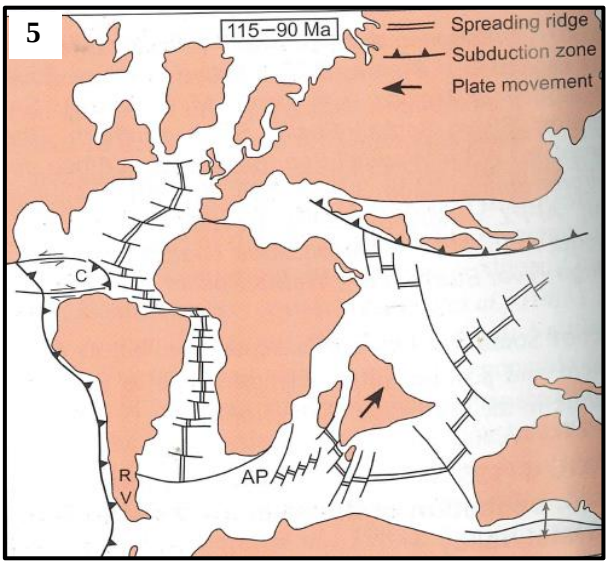


Figure 5. Taken from Watkeys (2006). Stage 5 of Gondwana break-up (115 - 90 MA). Illustration of the break-up Pangaea. Abbreviations: AP: Agulhas Plateau; C: Caribbean; RV: Rocas Vardes.

The present costal geography was in place by the end of the Cretaceous and global temperatures were temperate (66 MYA) (Meadows and Watkeys, 1999; Tankard et al., 1982b). The Cretaceous – Tertiary (KT) (Cretaceous – Paleogene (K–PG)) boundary saw another mass extinction event, which led to the extinction of the dinosaurs and thus, the radiation of mammals and grasses (Meadows and Watkeys, 1999). The Palaeocene (66 – 56 MYA) saw global temperatures higher than modern times, which contributed to the radiation events (Meadows and Watkeys, 1999). It is believed that the environment would have been a subtropical forest in the Karoo, changing to temperate forest in the Cape (Axelrod and Raven, 1978). The sea-level maximum was reached in the middle Eocene and lasted until 30 MYA, at this time the global temperatures had risen past that of the Palaeocene (Meadows and Watkeys, 1999; Tankard et al., 1982b). The Eocene – Oligocene boundary (38 MYA) saw changing climates and thus large changes in fauna and is known as the ‘great divide’ (Meadows and Watkeys, 1999). In the late Oligocene (25 MYA) the Circum-Antarctic current formed which resulted in the separation of low- and high- altitude oceanic temperatures (Tankard et al., 1982b). This was due to the separation of Antarctica from the South Tasmanian rise (Axelrod and Raven, 1978). At a similar time, an upwelling of cold water and the beginning of the cold Southern Ocean occurred leading to widespread aridity and declines in temperatures in the western parts of southern Africa (Meadows and Watkeys, 1999; Tankard et al., 1982b). These two factors had a large effect on life at the time (Axelrod and Raven, 1978).

During the late Oligocene to early Miocene, the western portion of the Karoo is estimated to have been populated by Cape sclerophyll vegetation, the east by subtropical natal laurel forest and the central interior by savanna-woodland (Axelrod and Raven, 1978). During the Miocene, the Antarctic

© University of Pretoria

circumpolar current become more intense, leading the global climate to become cooler (Byrne et al., 2008). In the mid-Miocene (17 MYA) Antarctica was completely frozen, which influenced the formation of the Benguela current, the Karoo at the time had moist tropical climates (Meadows and Watkeys, 1999). In the late Miocene (10 MYA) there was an acceleration of sea-floor spreading and ridge expansion leading to oceanic transgression and the onset of aridity (Meadows and Watkeys, 1999; Tankard et al., 1982b). Episodic sea-floor spreading and the inflation and contraction of the mid-oceanic ridge occurred, leading to fluctuations in sea levels (Tankard et al., 1982b). At the end of the Miocene, Africa experienced epeirogenic uplift, leading to isolation (Axelrod and Raven, 1978). In the Pliocene, global environments are estimated to have been wetter and warmer than today (Byrne et al., 2008; Rix et al., 2015). This is believed to be caused by the contraction or collapse of Antarctic ice which led to sea level rises (Byrne et al., 2008).

During the Pleistocene (2.58 MYA) there were high sea levels due to alternating glaciation cycles of the northern hemisphere causing the African climate to become increasingly cool and arid (Barlow et al., 2013; Tankard et al., 1982b). The alternating glacial and interglacial cycles is known to have had global impacts on species ranges (Potts et al., 2013). There is, however, evidence that the Fynbos and Succulent Karoo biomes of South Africa were decoupled from these effects and rather experienced localised climate stability, this is thought to have led to the extensive biodiversity and endemism of these areas present today (Potts et al., 2013). It is believed that at this time, aridity was heightened due to less evaporation of the colder seas and lower sea levels causing more exposed land (Byrne et al., 2008). An important event during this epoch was the Mid-Pleistocene Transition (MPT) which occurred 1.2 MYA and 800,000 YA (Chalk et al., 2017). Before the MPT in the early Pleistocene glacial-interglacial climates occurred in cycles of approximately 40,000 years, whereas after the MPT the cycles gradually intensified to between 80,000- and 120,000-year cycles (Chalk et al., 2017). This led to the late Pleistocene having longer, dustier and cooler ice ages which was largely influenced by lower CO_2 levels and the stabilisation of continental ice sheets (Chalk et al., 2017). The global ice sheets were at their maximum, 21,000 –16,000 YA (known as the Last Glacial Maximum – LGM), causing South Africa to have temperatures 5 – 6 °C cooler than present (Meadows and Watkeys, 1999; Potts et al., 2013; Stone, 2014). At the time of the LGM there is evidence for drier conditions in the east of southern Africa (including most of the Karoo) whereas the west and southwest were wetter (Stone, 2014). There is however no true consensus for the time period or duration of the LGM (Hughes et al., 2013; Potts et al., 2013; Stone, 2014). Paleoenvironmental records suggest that temperatures in South Africa were increased by 5°C from 15,000 – 7000 YA (Scott et al., 1995). The Nama Karoo vegetation at this time had changed from treeless grassland with dwarf shrubs to a more woodland environment whereas, the Succulent Karoo shifted from grasslands, dwarf shrublands and fynbos to a more succulent dominated environment (Scott et al., 1995). The period of 11,000 – 10,000 YA was particularly important during this biome shift, as the cool late Pleistocene conditions transitioned to the warm Holocene conditions (Scott et al., 1995).

© University of Pretoria

Temperatures then increased to 2 °C warmer than present day during the Holocene hypsithermal (7000 – 6500 YA) (Meadows and Watkeys, 1999). The continual changes in oceanic circulation and the epeirogenic uplift of the subcontinent led to the gaining of a more continental climate (larger differences between summer and winter temperatures) and thus, the aridification of southern Africa in the late Cenozoic (King, 1978; Tankard et al., 1982b; van Zinderen Bakker, 1987).

Further desertification of the Karoo region has been traced back to historical land use (Hoffmann et al., 1999). The Karoo has historically and in modern times largely had land use dedicated to the farming of sheep, cattle, ostrich and game (Hoffmann et al., 1999). The farmers in the 1760 – 1780s settled around water sources and implemented the Kraaling system for keeping livestock (Archer, 2000; Hoffmann et al., 1999). This led to over grazing, lower plant cover, erosion and eventually land degradation (Archer, 2000; Hoffmann et al., 1999). These conditions were exacerbated due to the continual prolonged drought periods the Karoo experiences (Hoffmann et al., 1999). In the 1990s a rotational grazing system was implemented leading to higher plant cover and thus lower erosion which is still in use today (Archer, 2000; Hoffmann et al., 1999).

1.2. The modern-day Karoo region

The Karoo region of South Africa does not encompass the entire Karoo basin, but is rather an arid/semi-arid area that spans one third of the land surface of South Africa over four provinces (Northern Cape, Western Cape, Eastern Cape and Free State) (Henschel et al., 2018). The current day climate and aridity of the Karoo is caused by the circumpolar westerly airstream, the southern subtropical high pressure (anticyclone) belt and the north flowing Benguela current (bringing cool air from the ocean) (Desmet and Cowling, 1999). The more local conditions are affected by the raised interior plateau and shielding to the south due to the Cape Fold Mountain belt (Desmet and Cowling, 1999).

The characteristic weather conditions of the Karoo encompasses high temperatures, little to no cloud cover and low relative humidity (Desmet and Cowling, 1999). As expected from the continentality and altitude of the area, the lowest mean minimum temperatures are towards the center of the region (Desmet and Cowling, 1999). There is no general trend with wind patterns in the Karoo region, but rather the winds are local and caused by topographical factors (Desmet and Cowling, 1999).

Rainfall in the greater Karoo area follows a east-west and a south-north gradient (East and South have higher precipitation) and the same trend is observed with rainfall variability (Desmet and Cowling, 1999). Rainfall is not the only source of precipitation in the Karoo. Dew plays an important role in certain times of the year in each region (Desmet and Cowling, 1999). The probability of experiencing frost in winter is 50 % for the entire Karoo region (Desmet and Cowling, 1999). The

© University of Pretoria

Karoo comprises of two separate biomes, namely Nama Karoo and Succulent Karoo, which are distinguished by climate and vegetation (Figure 6) (Henschel et al., 2018).

The Nama Karoo is on the central plateau in the Western portion of the country (Mucina et al., 2006b). The biome experiences summer rainfall, which is unreliable due to phenomenon such as the Southern Oscillation (El Nino effect) and prolonged periods of drought are common (Desmet and Cowling, 1999; Henschel et al., 2018). Dew is most abundant in the autumn months (April – May) in the summer rainfall region (Desmet and Cowling, 1999). The vegetation is dominated by dwarf shrub vegetation which are xeromorphic (Desmet and Cowling, 1999; Werger, 1978). Succulents do occur towards the west (boardering the Succulent Karoo) and grasses are more common towards the east (Werger, 1978). This is the second largest biome in South Africa covering 260,295 km^2 (Henschel et al., 2018; Mucina et al., 2006b). This region has been divided into three bioregions (Griqualand West and Bushmanland, the Great Karoo and central Lower Karoo, and lastly the Upper Karoo and Eastern Cape Midlands) (Henschel et al., 2018; Mucina et al., 2006b). This is also further divided into 14 different vegetation types (Henschel et al., 2018; Mucina et al., 2006b). Due to past land use practices approximately 60 % of the biome has moderate to severe degradation of soils and vegetation (Mucina et al., 2006b). Only 2 % of the entire Nama Karoo biome is under conservation (Henschel et al., 2018).

The Succulent Karoo covers a belt from Lüderitz (Namibia) through Namaqualand and includes smaller encloves of Hantam, Tanqua, Roggeveld and the little Karoo (Mucina et al., 2006a). The general biome experiences winter rainfall (100 – 200 mm anually) which is more reliable and aids in the sustainability of vegetation (Desmet and Cowling, 1999; Henschel et al., 2018). Dew is most abundant in midwinter (July and August) (Desmet and Cowling, 1999). In the Succulent Karoo fog is an important source of soil moisture, but is not measured in rainfall data (Desmet and Cowling, 1999; Henschel et al., 2018). The vegetation is dominated by succulent plants and following good rains, by annuals (Asteraceae and Brassicaceae) (Desmet and Cowling, 1999; Werger, 1978). This biome is the fourth largest in South Africa and covers 87,001 km^2 (Henschel et al., 2018; Mucina et al., 2006a). This area is divided into six different bioregions (Richtersveld, Namaqualand Hardeveld, Namaqualand Sandveld, Knersvlakte, Trans-Escarpment Succulent Karoo and the Rainshadow valley Karoo) and 63 separate vegetation units (Henschel et al., 2018; Mucina et al., 2006a). The succulent Karoo is bordered by the Cape Fold mountains, which caused isolation leading to high levels of endemisim and species richness of hopliniid beetles, aculeate Hymenoptera, reptiles and arachnids (Milton and Dean, 1999). There is a portion of the succulent Karoo which occurs more inland, known as the Tanqua (or Tankwa) Karoo (Werger, 1978). This area is a valley surrounded by mountains and receives <150 mm of rainfall anually (Werger, 1978). The Succulent Karoo environment has similar counterparts globally such as the Atacama desest in Chile and the Baja California desert (Axelrod and Raven, 1978; Mucina et al., 2006a). It is however, the world's only entirely arid region diversity

© University of Pretoria

hotspot (Henschel et al., 2018; Mucina et al., 2006a). Despite high levels of endemisim and being a biodiversity hotspot, only 8 % of the biome is conserved (Henschel et al., 2018).

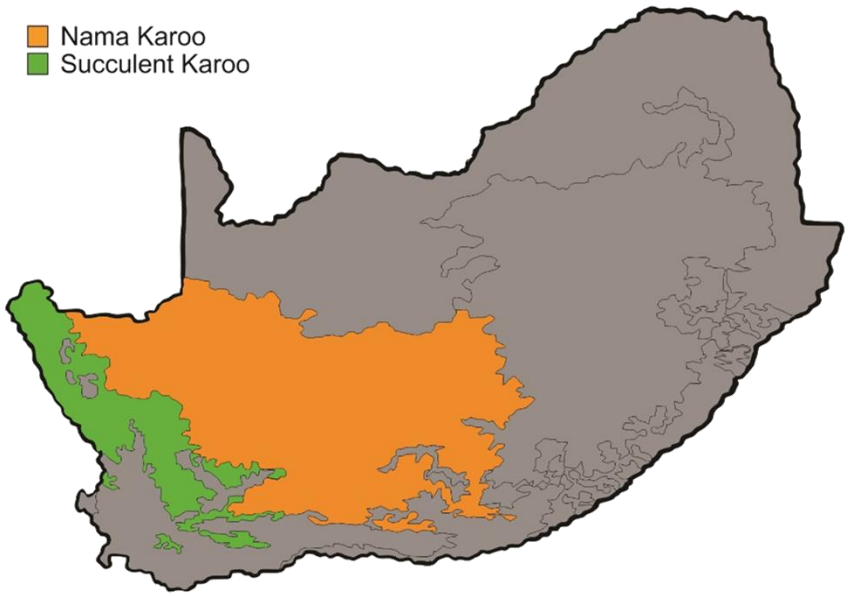


Figure 6. Map of South Africa indicating the two biomes investigated in this study. The Nama Karoo (orange) accounts for 260,295 km^2 of South Africa's land surface. The Succulent Karoo (green) covers 87,001 km^2.

1.3. Karoo BioGaps Project

The Karoo contains unique and sensitive ecosystems which respond poorly to disturbance and have slow recovery rates (Holness et al., 2016). This region has long been neglected in studies due to the assumption of low biodiversity in semi-arid regions (Roth-Monzón et al., 2018). This began to change in 2015 when the Karoo region was considered for shale gas exploration to lessen the country's dependence on coal and increase economic activity in the area (Holness et al., 2016). The South African Department of Environmental Affairs called for the beginning of a Strategic Environmental Assessment (SEA) to determine all the possible risk factors involved in Shale gas exploration in the region (Holness et al., 2016). In order to explore the biodiversity aspect of this, a collaborative project was undertaken by the South African National Biodiversity Institute (SANBI), the National Research Foundation (NRF), Foundational Biodiversity Information Program (FBIP) and the Department of Science and Innovation called the Karoo BioGaps project (Holness et al., 2016). The intention of the project was to produce a report on the state of biodiversity in the region to assist governmental policy-makers in making informed decisions about land-use change in the area (Holness et al., 2016). This became imperative as in previous years pressure for land use change increased due to economic incentives such as mining, farming, renewable energy, intensive shale gas exploration and the Square Kilometre Array (SKA) (Sethusa, 2016). This project sampled across 12 focal taxa representing most

© University of Pretoria

types of life present (Eardley, 2016). One of the taxa under study was Arachnida, which our study organism falls under, the genus *Stasimopus* Simon, 1892 (Stasimopidae).

In 2016 the use of the land for shale gas exploration was denied based on various risk factors such as insufficient water capacity, water pollution, loss of tourism and the discovery of high levels of biodiversity and important ecological processes (Holness et al., 2016). It was found in the SEA results that 55 % of the area outlined were not suitable for Shale gas development (Holness et al., 2016). This is due to being classified as Protected or level 1 or 2 of Ecological and Biodiversity Importance and Sensitivity (EBIS-1 or EBIS-2) as seen in Figure 7.

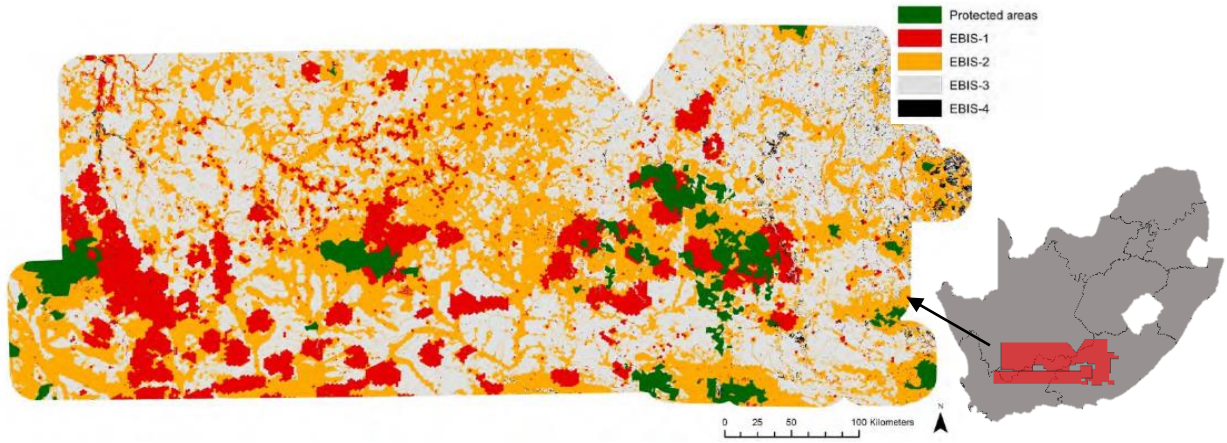


Figure 7. Taken from (Holness et al., 2016). Map of Ecological and Biodiversity Importance and Sensitivity in the study area with an inset map showing the location within South Africa. Protected areas (5 % of study area) are legally protected. EBIS-1 areas (13 % of study area) contain extremely sensitive features and are irreplaceable. EBIS-2 areas (37 % of study area) contain highly sensitive features and/or features that are important for achieving targets for representing biodiversity and/or maintaining ecological processes. Protected areas, EBIS-1 areas and EBIS-2 areas collectively meet targets for representation of biodiversity and maintenance of ecological processes in the study area. EBIS-3 areas (44 % of the study area) are natural areas that do not contain currently known sensitive or important features. In EBIS-4 areas (1 % of study area) there is no remaining natural habitat.

1.4. Background on the infraorder Mygalomorphae

The focal taxon for this study is within the spider infraorder Mygalomorphae, which includes trapdoor spiders, tarantulas and their relatives. The Mygalomorphae consists of 31 families, 368 genera and 3327 species (World Spider Catalog, 2022). The Mygalomorphae are an ancient group of spiders which are found in the fossil record since the late Triassic, but are believed to date back to the Carboniferous period (300 MYA) (Magalhaes et al., 2020; Opatova et al., 2020; Selden and Gall, 1992; Starrett et al., 2013). Despite all the elapsed time and diversification, this group of spiders has

© University of Pretoria

mostly retained plesiomorphic characters such as paraxially directed fangs, unspecialised spinnerets and two pairs of book lungs (Beavis et al., 2011; Dippenaar-Schoeman, 2002; Magalhaes et al., 2020; Opatova et al., 2020). The retention of ancestral traits has led to a group of spiders with highly conservative morphologies, which makes species level identifications incredibly challenging and has led to many inconsistencies within mygalomorph taxonomy (Wilson et al., 2018).

The life history traits of these spiders make them ideal candidates for biodiversity monitoring as well as for phylogenetic and phylogeographic studies (Ferretti et al., 2014; Hedin et al., 2013, 2015; Kremen et al., 1993; Leavitt et al., 2015; Newton et al., 2020; Rix et al., 2019; Satler at al., 2013; Wilson et al., 2018), but also make them difficult to define at species level. Mygalomorphs are exceptionally long lived for spiders, with an idiopid reportedly living to 43 years old (Mason et al., 2018). These spiders live in retreats comprising vertical burrows or chambers under rocks or on trees which are lined with silk (except for some arboreal species) (Dippenaar-Schoeman, 2002; Harrison et al., 2017; Mason et al., 2018; Wilson et al., 2023). The females lead sedentary lifestyles, only exiting the burrow to capture prey within reach of the burrow entrance (Engelbrecht and Prendini, 2011; Satler et al., 2013). The males however, are nomadic in nature, wandering to locate females and thus being the drivers of nuclear genome dispersal. This sexually dimorphic behaviour has affected the morphology of the spiders as seen in Figure 8. The offspring once mature enough will leave the mothers burrow but only move a few meters before making a new burrow to live in (Harrison et al., 2017). Due to these life history traits, mygalomorph spiders often experience geographic isolation through various processes which can lead to allopatric speciation and endemic species (Harrison et al., 2017; Opatova et al., 2020; Wilson et al., 2018). This behaviour also leads to extensive population structuring and the formation of “micro-clades” within phylogenies (Bond et al., 2001; Newton et al., 2020; Satler et al., 2013).

The importance of trapdoor spiders and other mygalomorphs is undervalued. Spiders are top invertebrate predators in terrestrial ecosystems and are thus important top-down ecosystem regulators (Capinera, 2008). Mygalomorphs feed on a wide variety of insects, arachnids, snails, amphibians and small reptiles (Dippenaar-Schoeman, 2002). Mygalomorph spiders are also an important food source for many animals, such as birds, centipedes, lizards, chameleons, baboons, mice, bats, honey badgers, scorpions, solifugs and other spiders (Dippenaar-Schoeman, 2002; Pérez-Miles and Perafán, 2017). Mygalomorph spiders are an important part of the life cycle of various parasites, including the orders of Hymenoptera, Diptera, some mites and nematodes (Dippenaar-Schoeman, 2002; Pérez-Miles and Perafán, 2017). Spiders are also important indicators of environmental quality when considering issues such as land-use change (Ferretti et al., 2012). Mygalomorph spiders are known to have painful bites which can lead to secondary infections, but most are not venomous to humans (Dippenaar-Schoeman, 2002; White, 2010). With the exception of the families Atracidae (genera: *Atrax* and *Hadronyche*) and Actinopodidae (genus: *Missulena*), he male of *Atrax robustus* (Sydney

© University of Pretoria

funnel-web) is considered the world's most venomous spider (Hedin et al., 2018; Opatova et al., 2020; White, 2010).

The focal taxon for this study is the genus *Stasimopus* Simon 1892 (African cork-lid trapdoor spider). *Stasimopus* falls under the family of Stasimopidae Bond, Opatova and Hedin 2020 and is endemic to Southern Africa. An endemic species in this context is a taxon whose distribution is geographically limited (Vernon, 1999). *Stasimopus* and the mygalomorphs of South Africa are poorly represented in our taxonomic and biodiversity records leading to large gaps in our knowledge. This is in part due to the difficulties in identification and the lack of surveying (Engelbrecht and Prendini, 2011).



Figure 8. Photographs of *Stasimopus hewitti* (Engelbrecht and Prendini, 2012), the black line indicates a 1cm scale bar. (A) Female of *S. hewitti*, which is robust and stocky due to a sedentary lifestyle. (B) Male of *S. hewitti*, which is slender and gracile due to a nomadic lifestyle.

1.5. Mygalomorphae fossil record and divergence dating

The oldest spider-like fossil was thought to be *Attercopus fimbriuguis* (order: Uraraneida) (Shear et al., 1987) found in Devonian (Givetian) sediments (Ayoub et al., 2007). This has however been reviewed and it is now considered a more basal lineage of arachnid which produced silk, but lacked spinnerets (Dunlop et al., 2020). The oldest Araneae fossil is now thought to be *Arthrolycosa* sp. (family: Arthrolycosidae) from the Carboniferous (Bashkirian stage) dated to 323 MYA and is assigned to the Mesothelae stem-group (Opatova et al., 2020). The Mygalomorphae fossils are separated by family in Table 1. There are 12 mygalomorph fossils whose identities are still undetermined which are not represented in Table 1 (Dunlop et al., 2020). Many extant mygalomorph families are not yet represented in the fossil record, including Stasimopidae (Dunlop et al., 2020).

© University of Pretoria

Table 1. Mygalomorph families currently represented in the fossil record. Extinct families are indicated by an asterisk. Information largely gathered from Dunlop et al., 2020.

Family	**Fossil**	**Period**	**Location**	**Reference**
Atypoidea	*Friularachne rigoi*	Triassic	Italy	Dalla Vecchia and Selden, 2013
Atypidae	*Ambiortiphagus ponomarenkoi*	Cretaceous	Mongolia	Eskov and Zonstein, 1990
	Atypus beigeli; A. juvenis; A. spinosus	Palaeogene	Baltic region	Wunderlich, 2011
	Atypus sp.	Palaeogene	Ukraine / Belarus	Perkovsky et al., 2018
Antrodiaetidae	*Cretacattyma raveni*	Cretaceous	Central Mongolia	Eskov and Zonstein, 2000
Mecicobothriidae	*Cretohexura coylei*	Cretaceous	Transbaikalia	Eskov and Zonstein, 1990
	Cretomegahexura platnicki	Cretaceous	Central Mongolia	Eskov and Zonstein, 1990
Dipluridae	*Cethegoides patricki*	Palaeogene	Baltic region	Wunderlich, 2017
	Clostes priscus	Palaeogene	Baltic region	Menge, 1869
	Cretadiplura ceara; Dinodiplura ambulacra	Cretaceous	Northeastern Brazil	Selden et al., 2006
	Edwa maryae	Triassic	Queensland	Raven et al., 2015
	Phyxioschemoides collembola	Cretaceous	Northern Myanmar	Wunderlich, 2015
	Seldischnoplura seldeni	Cretaceous	Northeastern Brazil	Raven et al., 2015
	Dipluridae sp.	Palaeogene	Baltic region	Wunderlich, 2004
	Dipluridae sp.	Neogene	Dominican Republic	Wunderlich, 2004
Calcaridae*	*Fossilcalcar praeteritus*	Cretaceous	Northern Myanmar	Wunderlich, 2015
Hexathelidae	*Rosamygale grauvogely*	Triassic	France	Selden and Gall, 1992

© University of Pretoria

	Alioatrax incertus	Cretaceous	Northern Myanmar	Wunderlich, 2017
Ctenizidae / Halonoproctidae	*Baltocteniza kulickae; Electrocteniza sadilenkoi*	Palaeogene	Baltic region	Eskov and Zonstein, 2000
	Ummidia damzeni; U. malonowskii	Palaeogene	Baltic region	Wunderlich, 2000
	Ummidia sp.	Palaeogene	Baltic region	Wunderlich, 2004
Cyrtaucheniidae	*Bolostromus destructus*	Neogene	Dominican Republic	Wunderlich, 1998
Barychelidae	*Psalistops hispaniolensis*	Neogene	Dominican Republic	Wunderlich, 1998
Theraphosidae	*Hemirraghus* sp.	Neogene	Mexico	García-Villafuerte, 2008
	Ischnocolinopsis acutus	Neogene	Dominican Republic	Wunderlich, 1998
Nemesiidae	*Cretamygale chasei*	Cretaceous	Isle of Wight	Selden, 2002
	Eodiplurina cockerelli	Palaeogene	Florissant, USA	Petrunkevitch, 1922
Microstigmatidae	*Parvomygale distincta*	Neogene	Dominican Republic	Wunderlich, 2004

Based on these fossils, many studies have performed divergence dating in order to date import divergences and radiation events in the evolutionary history of the Mygalomorphae. The first split in the Araneae tree of life splits into the Mesothelae and Opisthothelae (Araneomorphae and Mygalomorphae) is dated to 287 – 398 MYA (Fernández et al., 2018; Garrison et al., 2016). The Mesothelae are sister to all extant spiders, they differ due to the plesiomorphic traits of mid-ventral spinnerets and a segmented abdomen (Garrison et al., 2016). The Mygalomorphae infraorder is then split between Atypoidea (Atypidae and Antrodiaetidae) and Avicularioidea (the rest of Mygalomorphae) and is dated to 242 – 323 MYA based on the fossils *Rosamygale grauvogely* and *Arthrolycosa spp*. (Fernández et al., 2018; Garrison et al., 2016; Opatova et al., 2020). The split between Atypidae and Antrodiaetidae is dated to 242 – 100 MYA based on *Ambiortiphagus ponomarenkoi* and *R. grauvogely* (Ayoub et al., 2007; Magalhaes et al., 2020; Opatova et al., 2020). The spilt between the Bemmeridae / Theraphosidae and 'Nemesioidina' clade is considered between 242 – 125 MYA based on the fossils *R. grauvogely* and *Cretamygale chasei* (Opatova et al., 2020).

© University of Pretoria

This information can be used to draw useful conclusions about the evolution of Mygalomorphae spiders. An example of this is the conclusion that most spider families which existed 65 MYA survived the Cretaceous-Paleogene (K-Pg) extinction event, speaking to the resilience of the order (Penney et al., 2003). This was based on the fact that most Cretaceous fossils have extant relatives and is useful to inform researches on how the order may respond to future global events (Magalhaes et al., 2020; Penney et al., 2003).

1.6. Taxonomic history of Stasimopus

The placement of *Stasimopus* has been a conundrum for Mygalomorphae taxonomists for decades (Hedin and Bond, 2006; Opatova et al., 2020). Mygalomorph spiders have historically been described and taxonomically placed on the basis of male morphological characters. Features such as the shape of the palpal bulb, length of the pedipalp in relation to the first leg, spination patterns on the legs and eye patterns have been used (Engelbrecht and Prendini, 2012; Hendrixson and Bond, 2004). There is a high degree of sexual dimorphism present in these spiders which makes it extremely difficult to morphologically match the sexes to the correct species. The retention of ancestral traits has led to a group of spiders with highly conservative morphologies, which makes species level identifications incredibly challenging and is largely only possible for experts in the field.

The genus *Stasimopus* Simon 1892 (African cork-lid trapdoor spider) was originally classified in the family Ctenizidae. This was based on a range of plesiomorphic characteristics: three claws on the tarsi; in females claws are paired with few teeth; on the first and second legs are patches of dense short spines on the lateral surfaces on the distal segments in females; posterior spinnerets have domed distal segments; males have a simple, pyriform pedipalpal bulb; the chelicerae have two rows of teeth; fang's outer surface is smooth and a strongly procurved fovea on the carapace (Engelbrecht and Prendini, 2012). *Stasimopus* strays from the classic ctenizid genera as follows: The tibia of the third leg is not dorsally excavated; the anterior lobe of the maxillae is anteriorly produced; ocelli group is twice as wide as long (Engelbrecht and Prendini, 2012). This has invoked debate around the monophyly of Ctenizidae in regards to *Stasimopus*. The majority of studies find that Ctenizidae is not monophyletic but is rendered paraphyletic due the inclusion of the genus *Stasimopus* (Ayoub et al., 2007; Hedin and Bond, 2006; Opatova et al., 2013). Only Bond et al. (2012) found Ctenizidae (including *Stasimopus*) to be monophyletic using a total evidence phylogeny (molecular and morphology based).

In a study by Godwin et al. (2018), the family Ctenizidae underwent a major revision, in which it was split into two families, Halonoproctridae and Ctenizidae. The Halonoproctridae consists of the genera, *Bothriocyrtum*, *Conothele*, *Cyclocosmia*, *Hebestatis*, *Latouchia* and *Ummidia* (Godwin et al., 2018). However, older studies have considered splitting this family further in different ways

© University of Pretoria

(Ayoub et al., 2007; Bond et al., 2012). The most recent Mygalomorphae revision has placed *Stasimopus* into its own famly, Stasimopidae Bond, Opatova and Hedin 2020 (Opatova et al., 2020). Stasimopidae consists of 47 described species (World Spider Catalog, 2022), 25 of the 47 species are described from only one sex (19 female; 6 male). This increases the difficulty of specimen identification. An additional problem is the vagueness of these descriptions and the very slight differences in morphology between many of the species. The monophyly within the genus *Stasimopus* has not been tested to date (Engelbrecht and Prendini, 2012)

Due to the highly conservative nature of the morphology of the Mygalomorphae, it is not reliable to base taxonomy solely on morphology. Genetic methods are extremely useful to create phylogenies which can indicate divergent groups or separate evolutionary lineages. These phylogenies often can not objectively delimit what consitutes a species. To be able to define a species one should thus use multiple lines of evidence (morphological, genetic, ecological, etc.) (Bond et al., 2021; De Queiroz, 2007).

1.7. Genetics

Genetics is frequently used as a line of evidence when describing and distinguishing species. Genetics is considered the science of heredity and variation (Gayon, 2016). The field has an extensive history and has evolved into many other disciplines, such as classical genetics, molecular genetics, population genetics, epigenetics and many more (Gayon, 2016). The reason for the mass diversification of the field is that every time something new is discovered it leads to many new avenues for exploration. In this thesis the focus is on field of population/evolutionary genetics and thus the definition of heredity and variation is used.

Curiosity about the inheritance of characteristics is recorded back to the times of Hippocrates (c. 460 – 375 BCE) and Aristotle (384 – 322 BCE) (Cobb, 2006). These ideas were used to attempt to classify organisms for millennia but, it was not until Willi Hennig that a testable hypothesis framework was developed. Hennig in 1949 conceptualised the idea of using synapomorphies to create sister groups, and autapomorphies to distinguish between groups (Hennig, 1949; Renner, 2014). This led to his notion that only monophyletic groups should be taxonomically studied (Hennig, 1949; Renner, 2014). This was the key concept to be followed to understand the evolution of taxonomic groupings and allowed for the exploration of the field. The idea of evolution by natural selection, thus the concept of traits being favoured and perpetuated was put forward by Charles Darwin and Alfred Russell Wallace in 1858, but the underlying mechanism was not yet known (Durmaz et al., 2015; McClean, 2011). This mechanism was then described by Gregor Mendel in 1865 and he is considered the father of genetics (Cobb, 2006; Durmaz et al., 2015; Gayon, 2016; McClean, 2011). He described the process of gene inheritance including the ideas of segregation and independent assortment of genes (McClean, 2011). Over the subsequent years, major progress was made in the field of genetics,

© University of Pretoria

such as the discovery of the nuclin (F. Miescher 1871), chromosome behavior (A. Weismann 1887), mutations (H. de Vries 1900), the theory of chromosomal inheritance (W. Sutton and T. Boveri 1902) and the allele (W. Bateson 1902) (Durmaz et al., 2015; Gayon, 2016; McClean, 2011).

The next major breakthrough for evolutionary genetics was the formulation of the Hardy-Weinberg principle of genetic equilibrium by G. H. Hardy and W. Weinberg in 1908 (McClean, 2011). This principle is vital as it examines allele frequencies and the ways in which the equilibrium could be disturbed. The parsimony procedure was developed for phylogenetic tress in 1979 by Goodman and colleagues, followed by the maximum likelihood procedure (Felsenstien in 1981) (McClean, 2011). Along with progress in the theoretical aspect there were also breakthroughs in genetic techniques. These included the method of Sanger sequencing to determine the genetic code of a gene (by F. Sanger and W. Gilbert in 1977) and the Polymerase Chain Reaction (K. Mullis in 1985) to accumulate large amounts of DNA (Durmaz et al., 2015; McClean, 2011). Since then, technology has been improving rapidly leading to the next generation sequencing of today.

DNA sequences are of vital importance to unravel the evolutionary history of organisms and with the advancements made it has become a readily accessible tool. In 1977 sequence data was first used to examine the phylogenetic relationships between different organisms by Woese and Fox (Pace et al., 2012). Since then, population genetics and phylogenetics have become increasingly popular when trying to elucidate taxonomic problems and assess evolutionary history.

1.8. Phylogenetics

Phylogenetics is the study of evolutionary development and diversification of a taxonomic group based upon their relatedness (Brochu and Sumrall, 2001). The process entails the sequencing of one or more gene regions of the organisms' genome, in order to find synapomorphies (base pair similarities which share a common ancestor between taxa), which are used to determine relatedness of the taxa. This information is then used to build phylogenetic trees representing evolutionary history (Stamatakis, 2005). Phylogenetics is thus a tool with which to approach the fields of systematics and taxonomy in order to form formal biological classifications (Wiley and Lieberman, 2011).

Life history traits of *Stasimopus* as well as mygalomorphs in general as mentioned earlier, may lead to complex population structuring which may impact the speciation process (Harrison et al., 2017; Opatova et al., 2020; Wilson et al., 2018). A phylogenetic approach will provide an indication of the genetic diversity of the genus in the region. This will indicate the potential species present as well as their relation to one another. This information can then feed into species delimitation tools, phylogeographic analysis and integrative taxonomy to allow us to understand the species diversity and the underlying factors driving the diversification (Brochu and Sumrall, 2001).

© University of Pretoria

1.9. Species delimitation

The difficulty of identifying *Stasimopus* species morphologically has made their conservation status impossible to gauge as the actual species ranges are yet to be defined. The concept of a species is of vital importance in biology and related fields as a stable taxonomy is required in order to make accurate deductions in biodiversity, conservation, ecology and evolutionary studies (Bond et al., 2021; Fujita et al., 2012; Newton et al., 2020). Species have always been defined using species concepts, these various species concepts are often contradicting in the criterion used to define the species boundary (De Queiroz, 2007; Newton et al., 2020).

To ensure the viability of calling a group of organisms a species we need an iterative methodology of determining distinct evolutionary lineages – species delimitation methods fulfil this niche (Fujita et al., 2012). The action of species delimitation is the use of empirical data to determine species boundaries and the number of species and then using secondary lines of evidence to confirm the putative species. (De Queiroz, 2007; Fujita et al., 2012). Species and species delimitation are treated as hypotheses, in this way they can be proven or falsified given additional data. A method of species delimitation which is gaining favour by the scientific community is a coalescent approach.

This methodology has its foundations in population genetics and is thus an investigation of gene divergence within a genealogy (Kingman, 1982). According to Kingman (2000), the main concept driving coalescence is to follow the ancestral history of a gene further into the past while constructing the genes genealogy back to a singular common ancestor. Coalescent theory is thus a stochastic process of producing genealogies of sampled genetic sequences, the process samples from the tree tips (t = 0) and proceeds backwards in time (t increases) (Kingman, 1982; Minin et al., 2008). Individuals are coalesced in a pairwise manner until the most recent common ancestor (MRCA) is reached (Figure 9) (Kingman, 1982; Minin et al., 2008). This allows coalescent species delimitation to operate at the interface of two fields: phylogenetics and population genetics. Phylogenetics estimates the relationships among species while population genetics focuses on changes in allele frequencies which may lead to adaptation (Carstens et al., 2013).

The population genetics used for coalescence is grounded in the Fisher-Wright model, which describes evolution as genealogical relationships with transmission of genes forward through generations (Hein et al., 2005). This model has a few basic assumptions, such as no gene selection, mating which is random as well as a constant population size (Hein et al., 2005; Satler et al., 2013). Deviations from the assumptions are acceptable as the coalescent framework has several different models to account for the deviations. For example, the assumption of random mating can be circumvented by implementing stepping-stone models or continuous space models (Hein et al., 2005). In these models, populations can be split into separate demes where mating occurs randomly within a deme but seldom between demes – thereby accounting for an overall lack of random mating (Hein et al., 2005). Differing models exist for most types of deviation. which could violate any of the basic

© University of Pretoria

assumptions. The Wright-Fisher model thus defines a model of demography and reproduction within a genealogy (Fujita et al., 2012; Hein et al., 2005). The use of Fisher-Wright population genetics means that coalescent theory relies on demographic parameters such as divergence rates, times of lineage divergence, effective population size and a thoroughly produced phylogeny (Fujita et al., 2012).

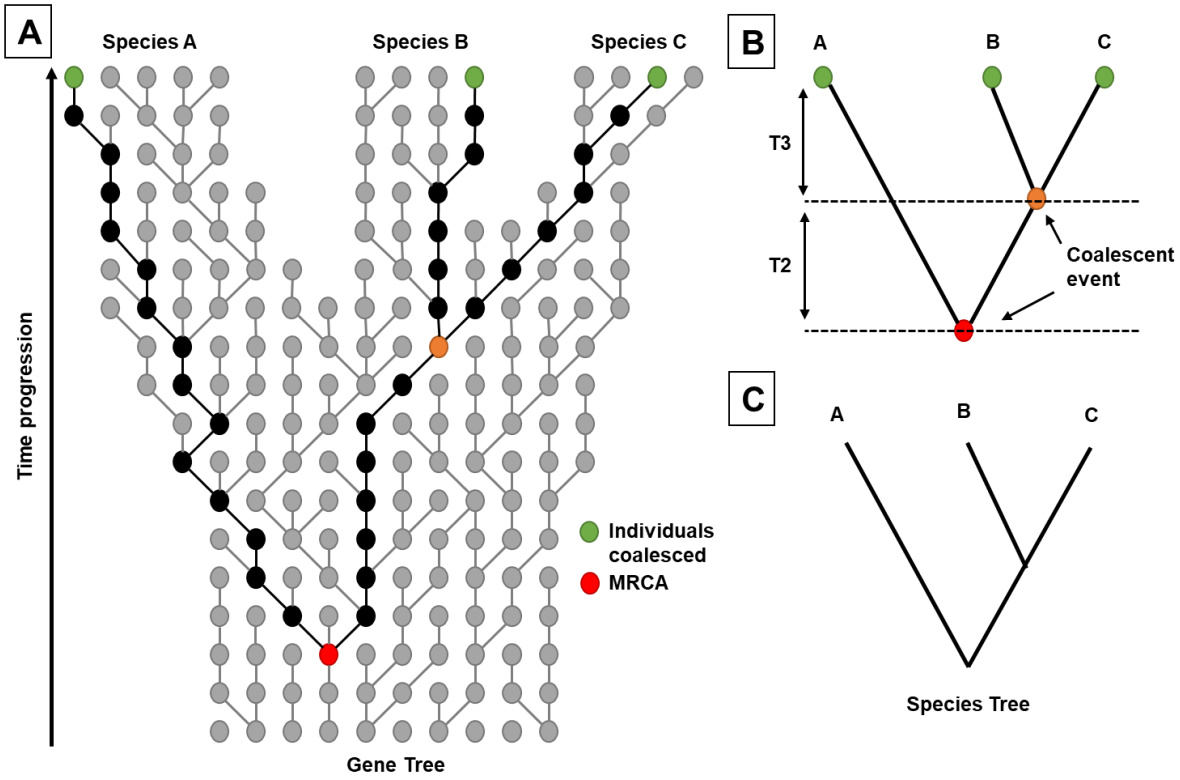


Figure 9. Representation of Kingman's Coalescent theory. A. The genealogy of three separate species (A-C) traced back through time to the Most Recent Common Ancestor (MCRA). The diagram shows non-overlapping generations where each grey dot is an individual gene copy which linked to its ancestor in the previous generation by a grey line. The green dots represent three sampled individuals which are traced back to their MRCA (red dot). B. This is a simpler version of A which indicates the coalescent events occurring at different times. T2 and T3 show the intercoalescent interval, i.e., the time between coalescent events. C. Represents the species tree of the gene tree shown in A.

Once the basis of the Fisher-Wright model is understood, and the assumptions are accounted for, one must select which coalescent approaches will be used. Discovery approaches are used in instances where prior knowledge is limited and populations or taxonomy is not adequately defined and putative groups must be created (Carstens et al., 2013). This is the case for *Stasimopus*, as it is very difficult to morphologically identify specimens into species and the taxonomy of the genus has

© University of Pretoria

never been explored. Defining putative groups can be done by a variety of methods, such as defining groups by basic morphological differences, geographic separation or the use of the coalescent genetic clustering approaches (Carstens et al., 2013; Fujita et al., 2012; Satler et al., 2013). Some of the more popular discovery approaches used are the General Mixed Yule Coalescent (GMYC) model (Pons et al., 2006), Bayesian Poisson Tree Processes (bPTP) (Zhang et al., 2013), O'Meara's Heuristic method (O'Meara, 2010) and the Automatic Barcode Gap Discovery (ABGD) (Puillandre et al., 2012). The ABDG methodology is not a coalescent methodology but rather makes use of a prior distance to determine genetic distance and define clusters. Numerous papers suggest that multiple approaches should be applied to a data set and that results which are congruent across the methodologies are to be considered to be reliable (Carstens et al., 2013; Fujita et al., 2012).

The coalescent model is thus capable of detecting separate lineages at shallow time depths, dating common ancestors and instilling additional confidence in the phylogeny (Fujita et al., 2012). Coalescent theory also allows for the estimation of current and historic population sizes directly from genetic data (Heled and Drummond, 2008). Demographic information such as effective population size (N_e) can provide insights into factors such as inbreeding, genetic drift and genetic diversity (Gill et al., 2013; Heled and Drummond, 2008). A major advantage of the coalescent approach is better objectivity, as specific probabilities of speciation events are produced which is sustained by evolutionary and population genetic history of the taxa (Carstens et al., 2013; Fujita et al., 2012; Fujita and Leaché, 2011).

Species delimitation techniques will be tested to determine if they can define putative species for the *Stasimopus* of the Karoo using the genetic diversity present. The results will be compared against the actual morphological identities of the species as well as monophyletic clusters to determine the accuracy of the species delimitation methodology on this group. If this proves successful then this could possibly be used to validate species identification.

1.10. Geometric morphometrics

The difficulty in resolving the taxonomic relationships of the Mygalomorphae has been discussed and as mentioned has historically relied on the morphology of species. The relationship between the morphological character and evolutionary history is usually unknown. This is an important aspect to determine as if the character is not informed by the evolutionary history of the taxa, it should not be used to identify nor describe species (Hendrixson and Bond, 2009). This is determined by testing for phylogenetic signal. Phylogenetic signal is based on the observation that closely related species tend to have similar morphological traits (Adams, 2014). Strong phylogenetic signal is present if specimens that are phenotypically more similar are more closely related than specimens that are phenotypically more distinct (Adams, 2014; Klingenberg and Gidaszewski, 2010). This is expected when organisms have experienced divergent evolution, but can be diluted by homoplasy due to

© University of Pretoria

convergence, parallel evolution and reversals (Klingenberg and Gidaszewski, 2010). If a character does have phylogenetic signal, then it can be used to differentiate species.

The next step would be to determine to what extent the characters shape can be quantified. Morphological characters used to identify taxonomic entities often use the comparison of anatomical shape (Adams et al., 2004). However, this can lead to vague descriptions such as the curvature of a line of eyes as “pro-curved’’ or ‘’retrocurved’’ (Engelbrecht and Prendini, 2012). This loses a lot of the possible variation of the shape, as it is not fully described.

To better describe the qualities of biological shape, the field of morphometrics was established. Morphometrics concerns the quantitative analysis of shape and falls into the field of statistics (Rodriguez-Mendoza, 2013). In this context the term shape refers to the geometric properties of an object which remain once the effects of size, position and orientation are removed (Mitteroecker and Gunz, 2009; Rodriguez-Mendoza, 2013; Seetah, 2014). As shape is a continuous morphological variable it is more difficult to place in quantitative terms to be used in order to compare individuals – morphometric analyses make it possible to identify discrete patterns in continuous data (Hendrixson and Bond, 2009; Zelditch et al., 2004a). There are two broad approaches to morphometrics, namely traditional / multivariate morphometrics and geometric morphometrics (Mitteroecker and Gunz, 2009; Rohlf and Marcus, 1993).

Multivariate morphometrics gained popularity in the 1960-1970s and is the use of standard measurements, such as lengths, widths and distances between objects (Jungers et al., 1995; Rohlf and Marcus, 1993). These distances are then standardised for size and compared between individuals to draw comparisons (Jungers et al., 1995). Statistical tests are used such as principal component analysis, generalised distances, discriminant functions and canonical variate analyses. Ratios and angles can also be used in this methodology (Rohlf and Marcus, 1993; Zelditch et al., 2004b). A downfall to this is that the original shape is lost as very little data is actually extracted from the object (Rohlf and Marcus, 1993). This method is still applicable if the data generated is adequate to draw strong comparisons.

Geometric morphometrics has the advantage of retaining all the data, but is more complex than traditional methods. The field was conceptualised in 1993 by Rohlf and Marcus and marked a revolution in morphometric techniques (Rohlf and Marcus, 1993). In geometric morphometrics, the entire structure being analysed is captured in either two-dimensional or three-dimensional coordinates of landmark points (Mitteroecker and Gunz, 2009; Rohlf and Marcus, 1993; Seetah, 2014; Zelditch et al., 2004c). Landmark points are positions on the structure being analysed which are biologically informative and homologous between specimens (Adams et al., 2004; Zelditch et al., 2004c). These coordinates then allow for the construction of transformation grids or thin-plate spines (Rohlf and Marcus, 1993). The transformation allows one to discriminate which differences are due to rotation or size of the organism and thus focus only on the morphologically informative aspects of the individuals (Mitteroecker and Gunz, 2009; Rohlf and Marcus, 1993). These aspects are then converted to

© University of Pretoria

principal warps which can be translated into taxonomic characters (Rohlf and Marcus, 1993). Morphometrics is thus a methodology of quantitatively describing continuous differences in the morphology of individuals.

Most spiders have eight eyes that are divided into different groups. The two front eyes which are most central are the anterior median eyes (AME), on either side of these are the anterior lateral eyes (ALE). In the row behind these is another pair of central eyes which are the posterior median eyes (PME), which are in the middle of the two posterior lateral eyes (PLE) (Figure 10) (Crews, 2011). The size and arrangement of these eyes are used to characterise different spiders at a range of taxonomic levels from family to species. For this the standard measurements tend to be eye diameter across the lens, inter-eye distances and the arrangement of the different eye pairs (Crews, 2011). Eye patterns have proven particularly useful at the family level within the araneomorphs which are significantly more advanced than the mygalomorphs and show a higher degree of morphological variation (Crews, 2011; Polotow and Brescovit, 2014). However, in the mygalomorphs, the differences in eye patterns are more subtle and are observable in the relative eye sizes and positions. Ocular patterns are often included in species descriptions of *Stasimopus* where they are considered diagnostic (Engelbrecht and Prendini, 2012; Hendrixson and Bond, 2004; Hewitt, 1910; Pocock, 1902). One such occasion in which it was used was in Engelbrecht and Prendini, (2012) where the distance of the anterior ocelli from the carapace margin, the curvature of the anterior and posterior ocular rows as well as the eye sizes relative to each other are all described. This is a step forward in using ocular patterns as an identifiable character for *Stasimopus*, but is not specific enough for the fine scale variation which exists between the species. In order to achieve this a more quantitative methodology is required.

The use of geometric morphometrics in this study will determine if firstly, eye patterns carry phylogenetic signal and secondly, if there is enough variation in the relative eye size and arrangement between different species of *Stasimopus* to be used as an identifier.



Figure 10. Structure of ocular pattern of an 8-eyed spider from the top view. The dashed line is the median line and the notations indicate the standard terminology used to explain each eye. The relative sizes and arrangement of the eyes is highly variable between families, genera and species.

© University of Pretoria

1.11. Integrative taxonomy

Taxonomy is the backbone of all the various fields of biology, and is the classification of organisms into a hierarchical structure based on shared characteristics. If the taxonomy of a species is incorrect, no true inference can be made about the organism's relation to another (Fujita et al., 2012). The key factor of taxonomy is the species concept used to classify organisms (Bond et al., 2021). A species concept is the theoretical definition of what constitutes a species. Species concepts are problematic as there are many alternative species definitions in use today (Newton et al., 2020). Due to the abundance of species concepts available today, there is often taxonomic inflation (attributing more species to a genus than is necessary based on conflicting lines of evidence) which muddies the waters of taxonomy (De Queiroz, 2007). The competing species concepts all have the same primary property: species as separately evolving metapopulations or lineages (De Queiroz, 2007). Yet they differ in their secondary properties, the biological species concept for example has the secondary property of reproductive isolation, whereas the phylogenetic species concept requires monophyly (De Queiroz, 2007). To simplify this concept, we define a species using the generalised species concept to separate and diagnose species. We thus identify species as separately evolving metapopulation lineages using multiple lines of evidence (De Queiroz 2007; Rix et al. 2018). Thus, the first criterion for identifying a species is that it must be a lineage, which is evolving separately from other such lineages (monophyletic) (Bond et al. 2021). The species delimitation is then proven or falsified by secondary properties, viewed as lines of evidence for the species delimitation (Yeates et al. 2011). Secondary properties are of vital importance as they may be what is used to actually identify the species (such as morphological characters), and because of this, numerous sources state the importance of using more than one line of evidence when looking at a species' taxonomy (Dayrat, 2005; De Queiroz, 2007; Fujita et al., 2012; Yeates et al., 2011). This is critically important when considering mygalomorph spiders and *Stasimopus* as they have historically been described using morphology which has led to the incorrect placement of the genus (Bond et al., 2012; Newton et al., 2020). Mygalomorph spiders have incredibly conservative morphologies and similar life history traits across the infraorder, this has led to a high degree of homoplasy in regards to morphology (Hamilton et al., 2011; Opatova et al., 2020; Wilson et al. 2023). This stresses the use of multiple lines of evidence when trying to describe species for the Mygalomorphae and when untangling their taxonomy (Newton et al., 2020). This issue thus calls for the use of integrated taxonomy and the use of diverse data types which in combination make a strong case for a species to be delineated and classified (Bond et al., 2021; Dayrat, 2005; De Queiroz, 2007; Fujita et al., 2012).

A main goal of this thesis is to create an integrated taxonomy for the *Stasimopus* of the Karoo, which will include genetic data (from three gene regions), morphology and geometric morphometric characters if applicable.

© University of Pretoria

1.12. Phylogeography

Phylogeography is the union of the fields of biogeography and phylogenetics. Biogeography is a science which strives to unravel the patterns of biological diversity throughout history and the effect of evolutionary events (Lomolino et al., 2010; Vernon, 1999). This would imply that as the factors affecting an organisms' distribution changes (vegetation, soil, climate), either the organisms' distribution would change in response, the organism will adapt or it will perish (Lomolino et al., 2010). The field of phylogenetics attempts to recover phylogenetic relationships between taxa and trace back through time a line of evolutionary decent.

Phylogeography applies the present geographic patterns of genotypes to make deductions about an organism's historical distribution and demography (Matshiner et al., 2010; Ochando et al., 2010). It must take into consideration the geography of the region, as well as the organisms' history in the region, when assessing a phylogeny as it may inform what drove the genetic history and current outcome (Avise, 2000). These fields thus allow for the identification of new species, insights into the process of speciation and a deeper understanding of the evolutionary history of a taxon (Gutiérrez-garcía and Vázquez-domínguez, 2011; Hedin, 1997; Wang and Yan, 2014).

Mygalomorph spiders are perfect model species for phylogeographic studies (Ferretti et al., 2014). The combination of behaviours displayed by the infraorder previously discussed, leads to extensive population structuring and isolated geographic locations for the populations, which is useful to analyse in phylogeographic studies (Ferretti et al., 2014; Hedin et al., 2013, 2015; Kremen et al., 1993; Leavitt et al., 2015; Newton et al., 2020; Rix et al., 2019; Satler et al., 2013; Wilson et al., 2018). To date, several phylogeographic studies have been performed on Mygalomorphae species (Beavis et al., 2011; Beavis & Rowell, 2006; Cooper et al., 2011; Ferretti et al., 2014; Graham et al., 2015, 2020; Hamilton et al., 2011; Harrison et al., 2017; Hedin et al., 2013, 2015; Hendrixson & Bond, 2007; Kornilios et al., 2016; Opatova et al., 2013, 2016, 2020; Rix et al., 2019; Starrett et al., 2018; Starrett & Hedin, 2007; Wilson et al., 2018).

Beavis et al. (2011) conducted a study on the phylogeographic differences between two species of Australian funnel web spiders. They found that a shared distribution of species does not necessarily imply a shared ancestral history, but rather that environmental change or events such as volcanic eruptions may affect ecological niches differently. Sympatric taxa could achieve the same distribution in a multitude of different ways due to differences in life history or in the case of this study, microhabitats (Beavis et al., 2011). There are many different drivers that may shape the phylogeography of a species which can lead to a multitude of global implications. Phylogeography is an invaluable tool for outlining areas for conservation efforts and predicting how species distributions may change in the face of environmental changes, such as global warming (Ferretti et al., 2014; Rolland et al., 2011). This is vital in light of the sensitivity of the Karoo ecosystem, the life history of *Stasimopus* and the drastic land-use and climate change predicted for the area. To date no

© University of Pretoria

phylogenetic studies on Mygalomorphae have been conducted in South Africa, nor have they been performed on the genus *Stasimopus.*

1.13. Rationale

This project was initially started as part of the Karoo BioGaps project discussed above. I was offered a part in the project for my Honours year in 2017 where a deep interest in this topic developed. This initial Honours project showed the range of genetic diversity present in *Stasimopus* in the Karoo region of South Africa, but also raised many more questions which have fueled this PhD thesis.

Firstly, how does this genetic diversity translate into species diversity? This seemed a simple question to answer, until the difficulty of morphological identification was discovered. Which then raised additional questions. What other methods can be used to delineate specimens into species? Species delimitation came up as a possible solution. Coalescent species delimitation has not been tested on this genus, and was a novel opportunity to apply set methodologies to a novel target. Another method of species' identification was in the description of the species themselves. Ocular patterns were historically used to identify *Stasimopus* species, but appeared vague and unrepeatable. I turned to geometric morphometrics with the aim of testing whether eye patterns could reliably be used to separate species of the genus. Geometric morphometrics has never been applied to the Stasimopidae and has never been used to test the validity of ocular patterns as a character in mygalomorph species descriptions. I now had two different methods to aid in the identification of our specimens other than morphology.

The next question became why is there so much genetic diversity in the Karoo, and what has shaped it? For this I decided to conduct the first phylogeographic study of Stasimopidae, focusing on the Karoo region. With all this information I aim to create the first integrative taxonomy for *Stasimopus*. The rationale for this study started with a simple question and led to questions of diversity, species delimitation techniques, the validity of identification characters and an understanding of the evolutionary history of the genus in the Karoo.

© University of Pretoria

1.14. Aims and objectives

The over-arching aim of this project was to: Determine which species of *Stasimopus* occur in this region of the Karoo and understand the relationships of the species within the genus. The second part of the project was to define methodologies which may aid in the identification of *Stasimopus* species (species delimitation and morphometrics). This information was then combined to create an integrative taxonomy using all the data generated. Lastly, I aimed to use phylogeography to understand the biogeographic history of *Stasimopus* and thereby gain an understanding of how change in this landscape may affect the genus. These aims are broken down and explored as follows:

Chapter 2: i) Determining the phylogenetic relationship between the various *Stasimopus* species within the Karoo region of South Africa and ii) determining whether coalescent species delimitation techniques can be used to determine species boundaries for the genus.

Chapter 3: iii) Determining if ocular patterns carry phylogenetic signal in the genus and iv) testing the viability of applying geometric morphometrics to the ocular pattern of *Stasimopus* species to determine if they can be used as quantitative characters to distinguish between species or morphospecies.

Chapter 4: v) Morphologically identifying all *Stasimopus* specimens found during the sampling of the Karoo region in 2017 and 2018, vi) describing all new *Stasimopus* species found, and vii) creating an integrative taxonomy for the *Stasimopus* of the Karoo based on morphology, molecular data and geometric morphometrics if applicable.

Chapter 5: (viii) Creating a dated phylogeny using the CO1, 16S and EF-1ɣ genes, (ix) creating haplotype networks for the *Stasimopus* populations observed and determine the gene flow between them, and (x) evaluating the phylogeographic pattern underlying the phylogeny and assess potential drivers thereof.

© University of Pretoria

References

Adams, D.C., 2014. A Generalized K Statistic for Estimating Phylogenetic Signal from Shape and Other High-Dimensional Multivariate Data. Systematic Biology 63, 685–697. https://doi.org/10.1093/sysbio/syu030

Adams, D.C., Rohlf, F.J., Slice, D.E., 2004. Geometric morphometrics: Ten years of progress following the 'revolution.' Italian Journal of Zoology 71, 5–16. https://doi.org/10.1080/11250000409356545

Archer, S., 2000. Technology and Ecology in the Karoo: A Century of Windmills, Wire and Changing Farming Practice. Journal of Southern African Studies 26, 675–696. https://doi.org/10.1080/03057070020008224

Avise, J.C., 2000. Phylogeography: the history and formation of species. Harvard University Press, Cambridge.

Axelrod, D.I., Raven, P.H., 1978. Late Cretaceous and Tertiary vegetation history of southern Africa, in: Werger, M.J.A. (Ed.), Biogeography and Ecology of Southern Africa. Springer, Dordrecht, pp. 77–130.

Ayoub, N.A., Garb, J.E., Hedin, M., Hayashi, C.Y., 2007. Utility of the nuclear protein-coding gene, elongation factor-1 gamma (EF-1γ), for spider systematics, emphasizing family level relationships of tarantulas and their kin (Araneae: Mygalomorphae). Molecular Phylogenetics and Evolution 42, 394–409. https://doi.org/10.1016/j.ympev.2006.07.018

Barlow, A., Baker, K., Hendry, C.R., Peppin, L., Phelps, T., Tolley, K.A., Wüster, C.E., Wüster, W., 2013. Phylogeography of the widespread African puff adder (*Bitis arietans*) reveals multiple Pleistocene refugia in southern Africa. Molecular Ecology 22, 1134–1157. https://doi.org/10.1111/mec.12157

Beavis, A.S., Rowell, D.M., 2006. Phylogeography of two Australian species of funnel web spider (Araneae: Mygalomorphae: Hexathelidae) in Tallaganda State Forest, New South Wales, in: Insect Biodiversity and Dead Wood: Proceedings of a Symposium for the 22nd International Congress of Entomology. pp. 23–29.

Beavis, A.S., Sunnucks, P., Rowell, D.M., 2011. Microhabitat preferences drive phylogeographic disparities in two Australian funnel web spiders. Biological Journal of the Linnean Society 104, 805–819. https://doi.org/10.1111/j.1095-8312.2011.01753.x

Bond, J.E., Godwin, R.L., Colby, J.D., Newton, L.G., Zahnle, X.J., Agnarsson, I., Hamilton, C.A., Kuntner, M., 2021. Improving Taxonomic Practices and Enhancing Its Extensibility - An Example from Araneology. Diversity 14(1), 5. https://doi.org/10.3390/d14010005

Bond, J.E., Hedin, M.C., Ramirez, M.G., Opell, B.D., 2001. Deep molecular divergence in the absence of morphological and ecological change in the Californian coastal dune endemic trapdoor spider *Aptostichus simus*. Molecular Ecology 10, 899–910. https://doi.org/10.1046/j.1365-294X.2001.01233.x

Bond, J.E., Hendrixson, B.E., Hamilton, C.A., Hedin, M., 2012. A reconsideration of the classification of the spider infraorder Mygalomorphae (Arachnida: Araneae) based on three nuclear genes and morphology. PLoS ONE 7, e38753. https://doi.org/https://doi.org/10.1371/journal.pone.0038753

© University of Pretoria

Brochu, C.A., Sumrall, C.D., 2001. Phylogenetic nomenclature and palaeontology. Journal of Paleontology 75, 754–757. https://doi.org/10.1666/0022-3360(2001)075<0754:PNAP>2.0.CO;2

Byrne, M., Yeates, D.K., Joseph, L., Kearney, M., Bowler, J., Williams, M.A.J., Cooper, S., Donnellan, S.C., Keogh, J.S., Leys, R., Melville, J., Murphy, D.J., Porch, N., Wyrwoll, K.H., 2008. Birth of a biome: insights into the assembly and maintenance of the Australian arid zone biota. Molecular Ecology 17, 4398–4417. https://doi.org/10.1111/j.1365-294X.2008.03899.x

Capinera, J.L., 2008. Spiders (Arachnida: Araneae), in: Capinera, J.L. (Ed.), Encyclopaedia of Entomology. Springer Science and Business Media, p. 3507.

Carstens, B.C., Pelletier, T.A., Reid, N.M., Satler, J.D., 2013. How to fail at species delimitation. Molecular Ecology 22, 4369–4383. https://doi.org/10.1111/mec.12413

Chalk, T.B., Hain, M.P., Foster, G.L., Rohling, E.J., Sexton, P.F., Badger, M.P.S., Cherry, S.G., Hasenfratz, A.P., Haug, G.H., Jaccard, S.L., Martínez-García, A., Pälike, H., Pancost, R.D., Wilson, P.A., 2017. Causes of ice age intensification across the mid-Pleistocene transition. Proceedings of the National Academy of Sciences of the United States of America 114, 13114–13119. https://doi.org/10.1073/pnas.1702143114

Cobb, M., 2006. Heredity before genetics: A history. Nature Reviews Genetics 7, 953–958. https://doi.org/10.1038/nrg1948

Cooper, S.J., Harvey, M.S., Saint, K.M., Main, B.Y., 2011. Deep phylogeographic structuring of populations of trapdoor spider *Moggridgea tingle* (Migidae) from southwestern Australia: evidence for long-term refugia within refugia. Molecular Ecology 20, 3219–3236. https://doi.org/10.1111/j.1365-294X.2011.05160.x

Crews, S.C., 2011. A revision of the spider genus *Selenops* Latreille, 1819 (Arachnida, Araneae, Selenopidae) in North America, Central America and the Caribbean. Zookeys 1–182. https://doi.org/10.3897/zookeys.105.724

Dalla Vecchia, F.M., Selden, P.A., 2013. A Triassic spider from Italy. Palaeontologica Polonica 58, 325–330. https://doi.org/10.4202/app.2011.0132

Dayrat, B., 2005. Towards integrative taxonomy. Biological Journal of the Linnean Society 85, 407–415. https://doi.org/10.1111/j.1095-8312.2005.00503.x

De Queiroz, K., 2007. Species Concepts and Species Delimitation. Systematic Biology 56, 879–886. https://doi.org/10.1080/10635150701701083

Desmet, P.G., Cowling, R.M., 1999. The climate of the Karoo - a functional approach, in: Dean, W.R.J., Milton, S.J. (Eds.), The Karoo: Ecological Patterns and Processes. Cambridge University Press, Cambridge, pp. 3–16.

Dippenaar-Schoeman, A.S., 2002. Baboon and Trapdoor Spiders of Southern Africa: An Identification Manual, Handbook. ed. Plant production research institute. Agricultural Research Council, Pretoria., Pretoria.

Duncan, A.R., Marsh, J.S., 2006. The Karoo Igneous Province, in: Johnson, M.R., Anhaeusser, C.R., Thomas, R.J. (Eds.), The Geology of South Africa. Council for Geoscience, Pretoria.

© University of Pretoria

Dunlop, J.A., Penney, D., Jekel, D., 2020. A summary list of fossil spiders and their relatives [WWW Document]. World Spider Catalog. URL http://wsc.nmbe.ch (accessed 5.25.20).

Durmaz, A.A., Karaca, E., Demkow, U., Toruner, G., Schoumans, J., Cogulu, O., 2015. Evolution of genetic techniques: Past, present, and beyond. BioMed Research International 2015. https://doi.org/10.1155/2015/461524

Eardley, C., 2016. BioGaps: a collaborative survey of Karoo biodiversity. Newsletter of Plan Production Research 5.

Engelbrecht, I., Prendini, L., 2011. Assessing the taxonomic resolution of southern African trapdoor spiders (Araneae: Ctenizidae; Cyrtaucheniidae; Idiopidae) and implications for their conservation. Biodiversity and Conservation 20, 3101–3116. https://doi.org/10.1007/s10531-011-0115-z

Engelbrecht, I., Prendini, L., 2012. Cryptic diversity of South African trapdoor spiders: Three new species of *Stasimopus* Simon, 1892 (Mygalomorphae, Ctenizidae), and redescription of *Stasimopus robertsi* Hewitt, 1910. American Museum Novitates 1–42. https://doi.org/https://doi.org/10.1206/3732.2

Eskov, K.Y., Zonstein, S.L., 1990. First Mesozoic mygalomorph spiders from the Lower Cretaceous of Siberia and Mongolia, with notes on the system and evolution of the infraorder Mygalomorphae (Chelicerata: Araneae). Neues Jahrbuch für Geologie und Paläontologie 178, 325–368.

Eskov, K.Y., Zonstein, S.L., 2000. The first ctenizoid mygalomorph spiders from Eocene Baltic amber (Araneida: Mygalomorphae: Ctenizidae). Paleontological Journal 34, S268–S274.

Fernández, R., Kallal, R.J., Dimitrov, D., Ballesteros, J.A., Arnedo, M.A., Giribet, G., Hormiga, G., 2018. Phylogenomics, Diversification Dynamics, and Comparative Transcriptomics across the Spider Tree of Life. Current Biology 28, 1489-1497.e5. https://doi.org/10.1016/j.cub.2018.03.064

Ferretti, N., González, A., Pérez–Miles, F., 2014. Identification of priority areas for conservation in Argentina: quantitative biogeography insights from mygalomorph spiders (Araneae: Mygalomorphae). Journal of Insect Conservation 18, 1087–1096. https://doi.org/10.1007/s10841-014-9718-5

Ferretti, N., Pompozzi, G., Copperi, S., Pérez-Miles, F., González, A., 2012. Mygalomorph Spider Community of a Natural Reserve in a Hilly System in Central Argentina. Journal of Insect Science 12, 1–16. https://doi.org/10.1673/031.012.3101

Fujita, M.K., Leaché, A.D., 2011. A coalescent perspective on delimiting and naming species: a reply to Bauer et al. Proceedings of the Royal Society B: Biological Sciences 278, 493–495. https://doi.org/10.1098/rspb.2010.1864

Fujita, M.K., Leaché, A.D., Burbrink, F.T., McGuire, J.A., Moritz, C., 2012. Coalescent-based species delimitation in an integrative taxonomy. Trends in Ecology & Evolution 27, 480–488. https://doi.org/10.1016/j.tree.2012.04.012

García-Villafuerte, M.Á., 2008. Primer registro fósil del género Hemirraghus (Araneae, Theraphosidae) en ámbar del Terciario, Chiapas, México. Revista Ibérica de Aracnología 16, 43–47.

© University of Pretoria

Garrison, N.L., Rodriguez, J., Agnarsson, I., Coddington, J.A., Griswold, C.E., Hamilton, C.A., Hedin, M., Kocot, K.M., Ledford, J.M., Bond, J.E., 2016. Spider phylogenomics: untangling the Spider Tree of Life. PeerJ 4, e1719. https://doi.org/10.7717/peerj.1719

Gayon, J., 2016. De Mendel à l'épigénétique : histoire de la génétique. Comptes Rendus Biologies Biologies 339, 225–230. https://doi.org/10.1016/j.crvi.2016.05.009

Gill, M.S., Lemey, P., Faria, N.R., Rambaut, A., Shapiro, B., Suchard, M.A., 2013. Improving Bayesian population dynamics inference: A coalescent-based model for multiple loci. Molecular Biology and Evolution 30, 713–724. https://doi.org/10.1093/molbev/mss265

Godwin, R.L., Opatova, V., Garrison, N.L., Hamilton, C.A., Bond, J.E., 2018. Phylogeny of a cosmopolitan family of morphologically conserved trapdoor spiders (Mygalomorphae, Ctenizidae) using Anchored Hybrid Enrichment, with a description of the family, Halonoproctidae Pocock 1901. Molecular Phylogenetics and Evolution 126, 303–313. https://doi.org/10.1016/j.ympev.2018.04.008

Götz, A.E., Ruckwied, K., 2014. Palynological records of the Early Permian postglacial climate amelioration (Karoo Basin, South Africa). Palaeobiodiversity and Palaeoenvironments 94, 229–235. https://doi.org/10.1007/s12549-013-0134-8

Graham, M.R., Santibáñez-López, C.E., Derkarabetian, S., Hendrixson, B.E., 2020. Pleistocene persistence and expansion in tarantulas on the Colorado Plateau and the effects of missing data on phylogeographical inferences from RADseq. Molecular Ecology 29, 3684–3701. https://doi.org/10.1111/mec.15588

Gruber, K., Harvey, M., Didham, R., Huey, J., 2017. Phylogeography of trapdoor spiders of the genus *Aname*: using genes and genomes to reveal biogeographic and evolutionary history (Master in Science). University of Western Australia.

Gutiérrez-garcía, T.A., Vázquez-domínguez, E., 2011. Comparative Phylogeography: Designing Studies while Surviving the Process. BioScience 61, 857–868. https://doi.org/10.1525/bio.2011.61.11.5

Hamilton, C.A., Formanowicz, D.R., Bond, J.E., 2011. Species delimitation and phylogeography of *Aphonopelma hentzi* (Araneae, Mygalomorphae, Theraphosidae): Cryptic diversity in North American tarantulas. PLoS ONE 6, e26207. https://doi.org/10.1371/journal.pone.0026207

Harrison, S.E., Harvey, M.S., Cooper, S.J.B., Austin, A.D., Rix, M.G., 2017. Across the Indian Ocean: A remarkable example of trans-oceanic dispersal in an austral mygalomorph spider. PLoS ONE 12, E0180139.

Hedin, M., 1997. Molecular Phylogenetics at the Population / Species Interface in Cave Spiders of the Southern Appalachians (Araneae: Nesticidae: *Nesticus*). Molecular Biology and Evolution 14, 309–324.

Hedin, M., Bond, J.E., 2006. Molecular phylogenetics of the spider infraorder Mygalomorphae using nuclear rRNA genes (18S and 28S): Conflict and agreement with the current system of classification. Molecular Phylogenetics and Evolution 41, 454–471. https://doi.org/10.1016/j.ympev.2006.05.017

© University of Pretoria

Hedin, M., Carlson, D., Coyle, F., 2015. Sky island diversification meets the multispecies coalescent – divergence in the spruce-fir moss spider (*Microhexura montivaga*, Araneae, Mygalomorphae) on the highest peaks of southern Appalachia. Molecular Ecology 24, 3467–3484. https://doi.org/10.1111/mec.13248

Hedin, M., Derkarabetian, S., Ramírez, M.J., Vink, C., Bond, J.E., 2018. Phylogenomic reclassification of the world's most venomous spiders (Mygalomorphae, Atracinae), with implications for venom evolution. Scientific Reports 8, 1636. https://doi.org/10.1038/s41598-018-19946-2

Hedin, M., Starrett, J., Hayashi, C., 2013. Crossing the uncrossable: Novel trans-valley biogeographic patterns revealed in the genetic history of low-dispersal mygalomorph spiders (Antrodiaetidae, *Antrodiaetus*) from California. Molecular Ecology 22(2), 508–526. https://doi.org/10.1111/mec.12130

Hein, J., Schierup, M.H., Wiuf, C., 2005. Gene genealogies, variation and evolution: A primer in coalescent theory. Systematic Biology 54, 986–987. https://doi.org/10.1080/10635150500354860

Heled, J., Drummond, A.J., 2008. Bayesian inference of population size history from multiple loci. BMC Evolutionary Biology 8, 1–15. https://doi.org/10.1186/1471-2148-8-289

Hendrixson, B.E., Bond, J.E., 2004. A new species of *Stasimopu*s from the Eastern Cape Province of South Africa (Araneae, Mygalomorphae, Ctenizidae), with notes on its natural history. Zootaxa 619, 1–14. https://doi.org/10.11646/zootaxa.619.1.1

Hendrixson, B.E., Bond, J.E., 2009. Evaluating the efficacy of continuous quantitative characters for reconstructing the phylogeny of a morphologically homogeneous spider taxon (Araneae, Mygalomorphae, Antrodiaetidae, *Antrodiaetus*). Molecular Phylogenetics and Evolution 53, 300–313. https://doi.org/10.1016/j.ympev.2009.06.001

Hennig, W., 1949. Zur Klärung einiger Begriffe der phylogeneischen Systematik, in: Forschungen und Fortschritte. Vol. 25, pp. 137–139.

Henschel, J.R., Hoffman, M.T., Walker, C., 2018. Introduction to the Karoo Special Issue: Trajectories of Change in the Anthropocene. African Journal of Range & Forage Science 35, 151–156. https://doi.org/10.2989/10220119.2018.1535214

Hewitt, J., 1910. Description of two trapdoor spiders from Pretoria (female of *Acanthodon pretoriae Poc.* and *Stasimopus robertsi*, n. sp.). Annals of the Transvaal Museum 2, 74–76.

Hoffmann, M.T., Cousins, B., Meyer, T., Petersen, A., Hendricks, H., 1999. Historical and contemporary land use and the desertification of the Karoo, in: Dean, W.R.J., Milton, S.J. (Eds.), The Karoo: Ecological Patterns and Processes. Cambridge University Press, Cambridge, pp. 257–273.

© University of Pretoria

Holness, S., Driver, A., Todd, S., Snaddon, K., Hamer, M., Raimondo, D., Daniels, F., Alexander, G., Bazelet, C., Bills, R., Bragg, C., Branch, B., Bruyns, P., Chakona, A., Child, M., Clarke, R.V., Coetzer, A., Coetzer, W., Colville, J., Conradie, W., Dean, R., Eardley, C., Ebrahim, I., Edge, D., Gaynor, D., Gear, S., Herbert, D., Kgatla, M., Lamula, K., Leballo, G., Lyle, R., Malatji, N., Mansell, M., Mecenero, S., Midgley, J., Mlambo, M., Mtshali, H., Simaika, J., Skowno, A., Staude, H., Tolley, K.A., Underhill, L., van der Colff, D., van Noort, S., von Staden, L., 2016. Biodiversity and Ecological Impacts: Landscape Processes, Ecosystems and Species, in: Scholes, R., Lochner, P., Schreiner, G., Snyman-Van der Walt, L., de Jager, M. (Eds.), Shale Gas Development in the Central Karoo: A Scientific Assessment of the Opportunities and Risks. CSIR, Pretor, pp. 7–1 to 7–72.

Hughes, P.D., Gibbard, P.L., Ehlers, J., 2013. Timing of glaciation during the last glacial cycle: evaluating the concept of a global ‘Last Glacial Maximum’ (LGM). Earth-Science Reviews 125, 171–198. https://doi.org/10.1016/j.earscirev.2013.07.003

Johnson, M.R., van Vuuren, C.J., Visser, J.N.J., Cole, D.I., Wickens, H., Robers, D.L., Brandl, G., 2006. Sedimentary rocks of the Karoo supergroup, in: Johnson, M.R., Anhaeusser, C.R., Thomas, R.J. (Eds.), The Geology of South Africa. Council for Geoscience, Pretoria.

Jungers, W.L., Falsetti, A.B., Wall, C.E., 1995. Shape, relative size, and size-adjustments in morphometrics. American Journal of Physical Anthropology 38, 137–161. https://doi.org/10.1002/ajpa.1330380608

King, L., 1978. The geomorphology of central and southern Africa, in: Werger, M.J.A. (Ed.), Biogeography and Ecology of Southern Africa. Springer, Dordrecht, pp. 1–17.

Kingman, J.F.C., 1982. The coalescent. Stochastic Processes and their Applications 13, 235–248. https://doi.org/10.1016/0304-4149(82)90011-4

Kingman, J.F.C., 2000. Origins of the Coalescent: 1974-1982. Genetics 150, 1461–1463. https://doi.org/10.1093/genetics/156.4.1461

Klingenberg, C.P., Gidaszewski, N.A., 2010. Testing and Quantifying Phylogenetic Signals and Homoplasy in Morphometric Data. Systematic Biology 59, 245–261. https://doi.org/10.1093/sysbio/syp106

Kremen, C., Cowell, R.K., Erwin, T.L., Murphy, D.D., Noss, R.F., Sanjayan, M.A., 1993. Terrestrial arthropod assemblages their use in conservation planning. Conservation Biology 7, 796–808.

Leavitt, D.H., Starrett, J., Westphal, M.F., Hedin, M., 2015. Multilocus sequence data reveal dozens of putative cryptic species in a radiation of endemic Californian mygalomorph spiders (Araneae, Mygalomorphae, Nemesiidae). Molecular Phylogenetics and Evolution 91, 56–67. https://doi.org/10.1016/j.ympev.2015.05.016

Lomolino, M. V, Riddle, B.R., Whittaker, R.J., Brown, J.H., 2010. Biogeography, forth. ed. Sinauer Associates, Inc., Sunderland, Massachusetts.

Magalhaes, I.L.F., Azevedo, G.H.F., Michalik, P., Ramírez, M.J., 2020. The fossil record of spiders revisited: implications for calibrating trees and evidence for a major faunal turnover since the Mesozoic. Biological Reviews 95, 184–217. https://doi.org/10.1111/brv.12559

Mason, L.D., Wardell-Johnson, G., Main, B.Y., 2018. The longest-lived spider: mygalomorphs dig deep, and persevere. Pacific Conservation Biology 24, 203. https://doi.org/10.1071/PC18015

© University of Pretoria

Matshiner, M., Hanel, R., Salzburger, W., 2010. Phylogeography and the speciation process in marine fishes and fishes from large freshwater lakes, in: Rutgers, D.S. (Ed.), Phylogeography. Nova Science Publishers, Inc, New York, pp. 1–29.

McClean, P., 2011. A History of Genetics and Genomics. North Dakota State University.

Meadows, M.E., Watkeys, M.K., 1999. Paleoenvironments, in: Dean, W.R.J., Milton, S.J. (Eds.), The Karoo: Ecological Patterns and Processes. Cambridge University Press, Cambridge, pp. 27–41.

Menge, A., 1869. Ueber einen Scorpion und zwei Spinnen im Bernstein. Schriften der Naturforschenden Gesellschaft in Danzig (Neue Folge) 2, 1–9.

Milton, S.J., Dean, W.R.J., 1999. The Karoo: past and future, in: Dean, W.R.J., Milton, S.J. (Eds.), The Karoo: Ecological Patterns and Processes. Cambridge University Press, Cambridge, pp. 314–318.

Minin, V.N., Bloomquist, E.W., Suchard, M.A., 2008. Smooth skyride through a rough skyline: Bayesian coalescent-based inference of population dynamics. Molecular Biology and Evolution 25, 1459–1471. https://doi.org/10.1093/molbev/msn090

Mitteroecker, P., Gunz, P., 2009. Advances in Geometric Morphometrics. Evolutionary Biology 235–247. https://doi.org/10.1007/s11692-009-9055-x

Mucina, L., Jürrgens, N., le Roux, A., Rutherford, M.C., Schmiedel, U., Elser, K.J., Powrie, L.W., Desmet, P.G., Milton, S.J., Boucher, C., Ellis, F., Lambrechts, J.J.N., Ward, R.A., Manning, J.C., Midgley, G.F., 2006a. Succulent Karoo Biome, in: Mucina, L., Rutherford, M.C. (Eds.), The Vegetation of South Africa, Lesotho and Swaziland. South African National Biodiversity Institute, Pretoria, pp. 220–299.

Mucina, L., Rutherford, M.C., Plamer, A.R., Milton, S.J., Scott, L., Lloyd, J.W., van der Merwe, B., Horae, D.B., Bezuidenhout, H., Vlok, J.H.J., Euston-Brown, D.I.W., Powrie, L.W., Dold, A.P., 2006b. Nama-Karoo Biome, in: Mucina, L., Rutherford, M.C. (Eds.), The Vegetation of South Africa, Lesotho and Swaziland. South African National Biodiversity Institute, Pretoria, pp. 324–347.

Newton, A.R., Shone, R.W., Booth, P.W.K., 2006. The Cape Fold Belt, in: Johnson, M.R., Anhaeusser, C.R., Thomas, R.J. (Eds.), The Geology of South Africa. Council for Geoscience, Pretoria.

Newton, L.G., Starrett, J., Hendrixson, B.E., Derkarabetian, S., Bond, J.E., 2020. Integrative species delimitation reveals cryptic diversity in the southern Appalachian *Antrodiaetus unicolor* (Araneae: Antrodiaetidae) species complex. Molecular Ecology 29, 2269–2287. https://doi.org/10.1111/mec.15483

Ochando, M.D., Reyes, A., Segura, D., Callejas, C., 2010. Phylogeography: its importance in insect pest control, in: Rutgers, D.S. (Ed.), Phylogeography. Nova Science Publishers, Inc, New York, pp. 31–56.

O'Meara, B.C., 2010. New Heuristic Methods for Joint Species Delimitation and Species Tree Inference. Systematic Biology 59, 59–73. https://doi.org/10.1093/sysbio/syp077

© University of Pretoria

Opatova, V., Arnedo, M.A., 2014a. From Gondwana to Europe: inferring the origins of Mediterranean *Macrothele* spiders (Araneae, Hexathelidae) and the limits of the family Hexathelidae. Invertebrate Systematics 24, 361–374.

Opatova, V., Arnedo, M.A., 2014b. Spiders on a hot volcanic roof: Colonisation pathways and phylogeography of the Canary Islands endemic trap-door spider *Titanidiops canariensis* (Araneae, Idiopidae). PLoS ONE 9, e115078. https://doi.org/10.1371/journal.pone.0115078

Opatova, V., Bond, J.E., Arnedo, M.A., 2013. Ancient origins of the Mediterranean trap-door spiders of the family Ctenizidae (Araneae, Mygalomorphae). Molecular Phylogenetics and Evolution 69, 1135–1145. https://doi.org/10.1016/j.ympev.2013.08.002

Opatova, V., Bond, J.E., Arnedo, M.A., 2016. Uncovering the role of the Western Mediterranean tectonics in shaping the diversity and distribution of the trap-door spider genus *Ummidia* (Araneae, Ctenizidae). Journal of Biogeography 43, 1955–1966. https://doi.org/10.1111/jbi.12838

Opatova, V., Hamilton, C.A., Hedin, M., de Oca, L.M., Král, J., Bond, J.E., 2020. Phylogenetic Systematics and Evolution of the Spider Infraorder Mygalomorphae Using Genomic Scale Data. Systematic Biology syz064. https://doi.org/10.1093/sysbio/syz064

Pace, N.R., Sapp, J., Goldenfeld, N., 2012. Phylogeny and beyond: Scientific, historical, and conceptual significance of the first tree of life. Proceedings of the National Academy of Sciences of the United States of America 109, 1011–1018. https://doi.org/10.1073/pnas.1109716109

Penney, D., Wheater, C.P., Selden, P.A., 2003. Resistance of spiders to Cretaceous-tertiary extinction events. Evolution 57, 2599. https://doi.org/10.1554/03-024

Pérez-Miles, F., Perafán, C., 2017. Behaviour and Biology of Mygalomorphae, in: Viera, C., Gonzaga, M.O. (Eds.), Behaviour and Ecology of Spiders. Springer International Publishing, Cham, pp. 29–54. https://doi.org/10.1007/978-3-319-65717-2_2

Perkovsky, E.E., Eskov, K.Y., Marusik, Y.M., 2018. First record of Atypidae (Araneae) in Rovno amber. Acta Arachnologica 67, 13–17.

Petrunkevitch, A.I., 1922. Tertiary spiders and opilionids of North America. Transactions of the Connecticut Academy of Arts and Sciences 25, 211–279.

Pocock, R.I., 1902. Descriptions of some new species of African Solifugae and Araneae. Annals and Magazine of Natural History 7, 6–27.

Polotow, D., Brescovit, A.D., 2014. Phylogenetic analysis of the tropical wolf spider subfamily Cteninae (Arachnida, Araneae, Ctenidae). Zoological Journal of the Linnean Society 170, 333–361. https://doi.org/10.1111/zoj.12101

Pons, J., Barraclough, T.G., Gomez-Zurita, J., Cardoso, A., Duran, D.P., Hazell, S., Kamoun, S., Sumlin, W.D., Vogler, A.P., 2006. Sequence-Based Species Delimitation for the DNA Taxonomy of Undescribed Insects. Systematic Biology 55, 595–609. https://doi.org/10.1080/10635150600852011

© University of Pretoria

Potts, A.J., Hedderson, T.A., Vlok, J.H.J., Cowling, R.M., 2013. Pleistocene range dynamics in the eastern Greater Cape Floristic Region: A case study of the Little Karoo endemic *Berkheya cuneata* (Asteraceae). South African Journal of Botany 88, 401–413. https://doi.org/10.1016/j.sajb.2013.08.009

Puillandre, N., Lambert, A., Brouillet, S., Achaz, G., 2012. ABGD, Automatic Barcode Gap Discovery for primary species delimitation. Molecular Ecology 21, 1864–1877. https://doi.org/10.1111/j.1365-294X.2011.05239.x

Raven, R.J., Jell, P.A., Knezour, R.A., 2015. *Edwa maryae gen. et sp. nov*. in the Norian Blackstone Formation of the Ipswich Basin – the first Triassic spider (Mygalomorphae) from Australia. Alcheringa 39, 259–263.

Renner, S.S., 2014. From Taxonomy to Phylogenetics: Life and Work of Willi Hennig. - By Michael Schmitt. Systematic Biology 63(3), 452–453. https://doi.org/10.1093/sysbio/syu012

Rix, M.G., Bain, K., Main, B.Y., Raven, R.J., Austin, A.D., Cooper, S.J.B., Harvey, M.S., 2019. Systematics of the spiny trapdoor spiders of the genus *Cataxia* (Mygalomorphae: Idiopidae) from south-western Australia: documenting a threatened fauna in a sky-island landscape. Journal of Arachnology 45(3), 395–423. https://doi.org/10.1636/0161-8202-45.1.451

Rix, M.G., Edwards, D.L., Byrne, M., Harvey, M.S., Joseph, L., Roberts, J.D., 2015. Biogeography and speciation of terrestrial fauna in the south-western Australian biodiversity hotspot. Biological Reviews 90, 762–793. https://doi.org/10.1111/brv.12132

Rix, M.G., Huey, J.A., Cooper, S.J.B., Austin, A.D., Harvey, M.S., 2018. Conservation systematics of the shield-backed trapdoor spiders of the nigrum-group (Mygalomorphae, Idiopidae, *Idiosoma*): integrative taxonomy reveals a diverse and threatened fauna from south-western Australia. ZooKeys 756, 1–121. https://doi.org/10.3897/zookeys.756.24397

Rodriguez-Mendoza, R., 2013. Population structure of the bluemouth, *Helicolenus dactylopterus* (Teleostei: Sebastidae), in the Northeast Atlantic and Mediterranean using geometric morphometric techniques. University of Vigo.

Rohlf, F.J., Marcus, L.F., 1993. A Revolution in Morphometrics. TREE 8, 129–132.

Rolland, J., Cadotte, M.W., Davies, J., Devictor, V., Lavergne, S., Mouquet, N., Pavoine, S., Rodrigues, A., Thuiller, W., Turcati, L., Winter, M., Zupan, L., Jabot, F., Morlon, H., 2011. Using phylogenies in conservation: new perspectives. Biology Letters 10–12. https://doi.org/10.1098/rsbl.2011.1024

Roth-Monzón, A.J., Mendoza-Hernández, A.A., Flores-Villela, O., 2018. Amphibian and reptile biodiversity in the semi-arid region of the municipality of Nopala de Villagrán, Hidalgo, Mexico. PeerJ 6, e4202. https://doi.org/10.7717/peerj.4202

Satler, J.D., Carstens, B.C., Hedin, M., 2013. Multilocus Species Delimitation in a Complex of Morphologically Conserved Trapdoor Spiders (Mygalomorphae, Antrodiaetidae, *Aliatypus*). Systematic Biology 62, 805–823. https://doi.org/10.1093/sysbio/syt041

Scheffler, K., Hoernes, S., Schwark, L., 2003. Global changes during Carboniferous–Permian glaciation of Gondwana: Linking polar and equatorial climate evolution by geochemical proxies. Geology 31, 605. https://doi.org/10.1130/0091-7613(2003)031<0605:GCDCGO>2.0.CO;2

© University of Pretoria

Scott, L., Steenkamp, M., Beaumont, P.B., 1995. Paleoenvironmental conditions in South Africa at the Pleistocene-Holocene transition. Quaternary Science Reviews 14, 937–947. https://doi.org/10.1016/0277-3791(95)00072-0

Seetah, T.K., 2014. Geometric Morphometrics and Environmental Archaeology, in: Smith, C. (Ed.), Encyclopaedia of Global Archaeology. Springer, New York, pp. 3029–3036. https://doi.org/10.1007/978-1-4419-0465-2_2123

Selden, P.A., 2002. First British Mesozoic spider, from Cretaceous amber of the Isle of Wight, southern England. Palaeontology 45, 973–983.

Selden, P.A., Casado, F.C., Mesquita, M. V, 2006. Mygalomorph spiders (Araneae: Dipluridae) from the Lower Cretaceous Crato Lagerstätte, Araripe Basin, north-east Brazil. Palaeontology 49, 817–826.

Selden, P.A., Gall, J.C., 1992. A Triassic mygalomorph spider from the northern Vosges, France. Palaeontology 35, 211–235.

Sethusa, T., 2016. Karoo BioGaps Project [WWW Document]. SANBI [ONLINE]. URL https://www.sanbi.org/karoo-biogaps-project/ (accessed 2.7.18).

Shear, W.A., Selden, P.A., Rolfe, W.D.I., Bonamo, P.M., Grierson, J.D., 1987. New terrestrial arachnids from the Devonian of Gilboa, New York. American Museum Novitates 2901, 1–74.

Stamatakis, A., 2005. Phylogenetics: Applications, Software and Challenges. Cancer Genomics and Proteomics 2, 301–306.

Starrett, J., Hedin, M., Ayoub, N., Hayashi, C.Y., 2013. Hemocyanin gene family evolution in spiders (Araneae), with implications for phylogenetic relationships and divergence times in the infraorder Mygalomorphae. Gene 524, 175–186. https://doi.org/10.1016/j.gene.2013.04.037

Stone, A.E.C., 2014. Last Glacial Maximum conditions in southern Africa: Are we any closer to understanding the climate of this time period? Progress in Physical Geography 38, 519–542. https://doi.org/10.1177/0309133314528943

Tankard, A.J., Jackson, M.P.A., Eriksson, K.A., Hobday, D.K., Hunter, D.R., Minter, W.E.L., 1982a. The intercratonic Karoo basin, in: Tankard, A.J., Jackson, M.P.A., Eriksson, K.A., Hobday, D.K., Hunter, D.R., Minter, W.E.L. (Eds.), Crustal Evolution of Southern Africa: 3.8 billion Years of Earth History. Springer-Verlag, New York, pp. 346–402.

Tankard, A.J., Jackson, M.P.A., Eriksson, K.A., Hobday, D.K., Hunter, D.R., Minter, W.E.L., 1982b. Changing climates and sea levels: The Cenozoic record, in: Tankard, A.J., Jackson, M.P.A., Eriksson, K.A., Hobday, D.K., Hunter, D.R., Minter, W.E.L. (Eds.), Crustal Evolution of Southern Africa: 3.8 billion Years of Earth History. Springer-Verlag, New York, pp. 433–454.

van Zinderen Bakker, E.M., 1987. Late Cenozoic Palaeoecology, in: Cowling, R.M., Roux, P.W. (Eds.), The Karoo Biome: A Preliminary Synthesis Part 2 - Vegetation and History. CSIR, Pretoria, pp. 96–99.

Vernon, C.J., 1999. Biogeography, endemism and diversity of animals in the Karoo, in: Dean, W.R.J., Milton, S.J. (Eds.), The Karoo: Ecological Patterns and Processes. Cambridge University Press, Cambridge, pp. 57–86.

© University of Pretoria

Wang, Y., Yan, G., 2014. Molecular Phylogeography and Population Genetic Structure of *O. longilobus* and *O. taihangensis* (Opisthopappus) on the Taihang Mountains. PLoS ONE 9. https://doi.org/10.1371/journal.pone.0104773

Watkeys, M.K., 2006. Gondwana break-up: a South African perspective, in: Johnson, M.R., Anhaeusser, C.R., Thomas, R.J. (Eds.), The Geology of South Africa. Council for Geoscience, Pretoria.

Werger, M.J.A., 1978. The Karoo-Namib region, in: Werger, M.J.A. (Ed.), Biogeography and Ecology of Southern Africa. Springer, Dordrecht, pp. 231–300.

White, J., 2010. Venomous animals: clinical toxicology, in: Luch, A. (Ed.), Molecular, Clinical and Environmental Toxicology: Volume 2: Clinical Toxicology. Springer Science and Business Media, pp. 233–274.

Wiley, E.O., Lieberman, B.S., 2011. Phylogenetics: Theory and Practice of phylogenetic systematics, Second. ed. John Wiley and Sons, Inc, New Jersey.

Wilson, J.D., Bond, J.E., Harvey, M.S., Ramírez, M.J., Rix, M.G., 2023. Correlation with a limited set of behavioural niches explains the convergence of somatic morphology in mygalomorph spiders. Ecology and Evolution 13(1). https://doi.org/10.1002/ece3.9706

Wilson, J. D., Hughes, J. M., Raven, R. J., Rix, M. G., & Schmidt, D. J., 2018. Spiny trapdoor spiders (*Euoplos*) of eastern Australia: Broadly sympatric clades are differentiated by burrow architecture and male morphology. Molecular Phylogenetics and Evolution 122, 157–165. https://doi.org/10.1016/j.ympev.2018.01.022

World Spider Catalog, 2022. World Spider Catalog Version 23.5 [WWW Document]. Natural History Museum Bern. https://doi.org/10.24436/2 (accessed 8.8.22).

Wunderlich, J., 1998. Beschreibung der ersten fossilen Spinnen der Unterfamilien Mysmeninae (Anapidae) und Erigoninae (Linyphiidae) im Dominikanischen Bernstein (Arachnida: Araneae). Entomologische Zeitschrift 108, 363–367.

Wunderlich, J., 2000. Zwei neue Arten der Familie Falltürspinnen (Araneae: Ctenizidae) aus dem Baltischen Bernstein. Entomologische Zeitschrift 110, 345–348.

Wunderlich, J., 2004. Introduction, general findings and conclusions, 3rd ed. Beiträge zur Araneologie.

Wunderlich, J., 2011. Some fossil spiders (Araneae) in Eocene European ambers. Beiträge zur Araneologie 6, 472–538.

Wunderlich, J., 2015. On the evolution and the classification of spiders, the Mesozoic spider faunas, and descriptions of new Cretaceous taxa mainly in amber from Myanmar (Burma) (Arachnida: Araneae), 9th ed. Beiträge zur Araneologie.

Wunderlich, J., 2017. New and rare fossil spiders (Araneae) in mid Cretaceous amber from Myanmar (Burma), including the description of new extinct families of the suborders Mesothelae and Opisthothelae as well as notes on the taxonomy, the evolution and the biogeography of the, 10th ed. Beiträge zur Araneologie.

© University of Pretoria

Yeates, D.K., Seago, A., Nelson, L., Cameron, S.L., Joseph, L., Trueman, J.W.H., 2011. Integrative taxonomy, or iterative taxonomy? Systematic Entomology 36, 209–217. https://doi.org/10.1111/j.1365-3113.2010.00558.x

Zelditch, M.L., Swiderski, D.L., Sheets, H.D., Fink, W.L., 2004a. Theory of Shape, in: Zelditch, M.L., Swiderski, D.L., Sheets, H.D. (Eds.), Geometric Morphometrics for Biologists: A Primer. Elsevier Academic Press, San Diego, pp. 73–104.

Zelditch, M.L., Swiderski, D.L., Sheets, H.D., Fink, W.L., 2004b. Ordination methods, in: Zelditch, M.L., Swiderski, D.L., Sheets, H.D. (Eds.), Geometric Morphometrics for Biologists: A Primer. Elsevier Academic Press, San Diego, pp. 153–187.

Zelditch, M.L., Swiderski, D.L., Sheets, H.D., Fink, W.L., 2004c. Landmarks, in: Zelditch, M.L., Swiderski, D.L., Sheets, H.D. (Eds.), Geometric Morphometrics for Biologists: A Primer. Elsevier Academic Press, San Diego, pp. 23–50.

Zhang, J., Kapli, P., Pavlidis, P., Stamatakis, A., 2013. A general species delimitation method with applications to phylogenetic placements. Bioinformatics 29, 2869–2876. https://doi.org/10.1093/bioinformatics/btt499

© University of Pretoria

Chapter 2

The phylogenetic structure and coalescent species delimitation of an endemic trapdoor spider genus, *Stasimopus* (Araneae, Mygalomorphae, Stasimopidae) in the Karoo region of South Africa

Shannon Brandt[1], Robin Lyle[2] and Catherine L. Sole[1]

[1] *Department of Zoology and Entomology, University of Pretoria, Hatfield, Pretoria, South Africa*

[2] *Agricultural Research Council – Plant Health and Protection, Biosystematics, Roodeplaat, Pretoria, South Africa*

This data chapter has been submitted as:

Brandt, S., Lyle, R. L., and Sole, C. L. 2023. The phylogenetic structure and coalescent species delimitation of an endemic trapdoor spider genus, *Stasimopus* (Araneae, Mygalomorphae, Stasimopidae) in the Karoo region of South Africa, to Molecular Phylogenetics and Evolution.

© University of Pretoria

Abstract

The Karoo region of South Africa is a unique and sensitive ecosystem which is facing pressure for development due to economic incentives such as mining, farming and shale gas exploration. The species diversity of many taxa in the area is largely unknown. A phylogenetic analysis of the cork-lid trapdoor spider genus, *Stasimopus* (Stasimopidae) was undertaken in order to gain insight into the relationships between the species that may be present in the area. The species within *Stasimopus* are challenging to identify and define using traditional morphological methods due to a high degree of morphological conservatism within the genus. For this reason, multiple coalescent based species delimitation methods were used to attempt to determine the species present for *Stasimopus* in the region which was tested against the morphological identifications and genetic clades (based on CO1, 16S and EF-1ɣ). We tested single-locus methods Automatic Barcode Gap Discovery (ABGD), Bayesian implementation of Poisson Tree Processes (bPTP) and General Mixed Yule- Coalescent (GMYC), as well as multi-locus Brownie. The phylogenetic analysis of *Stasimopus* in the Karoo showed that there is a high degree of genetic diversity within the genus. The species delimitation results proved unfruitful for the genus, as they appear to delimit population structure rather than species for most methods. Alternative methods should be investigated to aid in the identification of the species in order truly understand the species diversity of the genus.

Keywords

Trapdoor-spider, *Stasimopus*, Species delimitation, phylogenetics, Karoo

© University of Pretoria

1. Introduction

Mygalomorph spiders are notoriously difficult to study for a number of reasons such as outdated literature, the challenge of sampling these cryptic organisms, sexual dimorphism (making linking the sexes morphologically difficult) and their highly conservative morphologies (Wilson et al. 2018). This combination makes species level identifications and descriptions incredibly challenging, which leads to poorly defined conservation statuses across numerous mygalomorph taxa. Resolving this has become increasingly important with the reported population declines in these spiders especially as they tend to be short range endemics exposed to an ever-changing environment.

The spider infraorder Mygalomorphae is a primitive group of spiders which have largely retained their ancestral traits. These plesiomorphic characters include longitudinal fangs, no specialisation of the spinning structures and the retention of two pairs of book lungs (Beavis et al., 2011; Godwin et al., 2018). Mygalomorph spiders live in retreats comprising vertical silk-lined burrows or chambers under rocks or on trees (Dippenaar-Schoeman, 2002; Mason et al., 2018). The females lead sedentary lifestyles, only exiting the burrow to capture prey within reach of the burrow entrance (Engelbrecht and Prendini, 2011; Satler et al., 2013). The males however, are nomadic in nature, wandering to locate females and thus being the drivers of nuclear genome dispersal. Once mature enough the offspring will leave the mothers burrow but only move a few meters before making a new burrow to live in. This behaviour leads to extensive population structuring (Bond et al., 2001; Newton et al., 2020; Satler et al., 2013). Mygalomorph spiders have life history traits of long-life spans and sedentary habits, making them ideal candidates for both phylogenetic and phylogeographic studies as well as biodiversity monitoring (Ferretti et al., 2014; Kremen et al., 1993; Leavitt et al., 2015; Mason et al., 2018; Newton et al., 2020).

The focal taxon for this study is the genus *Stasimopus* Simon 1892 (African cork-lid trapdoor spider) of the family Stasimopidae (Opatova et al., 2020). *Stasimopus* is endemic to Southern Africa, consisting of 47 described species (World Spider Catalog, 2020), but the true diversity in the genus could be significantly higher (Engelbrecht and Prendini, 2011). Based on the taxonomic literature, five species of *Stasimopus* are known from within the part of the Karoo accessed in this study and two species from nearby the area (Dippenaar-Schoeman et al., 2010).

Stasimopus and other mygalomorphs were historically described and taxonomically placed on the basis of morphological characters. In *Stasimopus*, features such as the shape of the palpal bulb, length of the pedipalp in relation to the first leg, spination patterns on the legs and eye patterns are used for identification (Engelbrecht and Prendini, 2012; Hendrixson and Bond, 2004). The retention of ancestral traits has led to a group of spiders with highly conservative morphologies, which makes species level identifications challenging (Hamilton et al., 2014; Newton et al., 2020; Opatova et al., 2020; Rix et al., 2018). Genetic methods have been used to aid in the identification of mygalomorphs

© University of Pretoria

at species level by creating phylogenies, which indicate divergent groups or separate evolutionary lineages. To define a species one should start by using species delimitation methods and then confirm the putative species by using multiple lines of evidence, such as morphological, genetic and ecological data (De Queiroz, 2007; Derkarabetian and Hedin, 2014). Coalescent-based species delimitation makes use of molecular data to determine species boundaries (De Queiroz, 2007; Fujita et al., 2012). The coalescent approach provides objectivity, as specific probabilities of speciation events are produced which is sustained by the evolutionary and population genetic history of the taxa (Carstens et al., 2013; Fujita et al., 2012; Fujita and Leaché, 2011).

There are two broad types of delimitation approaches based on information availability: discovery approaches and validation approaches. Discovery approaches are used in instances where prior knowledge is limited and populations or taxonomy is not adequately defined and putative groups must be created (Carstens et al., 2013). This is done by the use of molecular methods or morphology (Carstens et al., 2013; Fujita et al., 2012; Satler et al., 2013). Species validation approaches require prior information such as predetermined species tree topologies and individuals already allocated to different putative species. It has been demonstrated that multiple delimitation approaches should be applied to a data set and that results which are congruent across the methodologies are considered reliable (Carstens et al., 2013; Fujita et al., 2012).

Species delimitation techniques have been employed to several mygalomorph groups with varying degrees of success (Hamilton et al., 2014; Hedin, 2015; Leavitt et al., 2015; Opatova and Arnedo, 2014; Satler et al., 2013, 2011). These largely empirical studies found that mygalomorph spiders tend to exhibit strong genetic structuring, leading to contentious species limits, thus species delimitation methods tend to oversplit the data (Hamilton et al., 2014; Leavitt et al., 2015; Opatova and Arnedo, 2014). These studies tend to rely on only a single gene region (usually mitochondrial) or only single locus methods, the delimitations can thus likely be improved by the addition of more gene regions (especially nuclear genes) or other delimiting characters such as morphology (Hedin, 2015; Satler et al., 2013). These studies did however find coalescent species delimitation useful for uncovering species complexes in cases of crypsis, such as Satler et al. (2013) for the *Aliatypus* genus in California. By uncovering cases of crypsis, or simply understanding the species diversity of a taxon, conservation efforts can be more directed and effective.

Concise and effective conservation is vital when dealing with sensitive ecosystems which have slow recovery to disturbance. An area for concern in South Africa is the Karoo region. This is a unique semi-arid area, in the interior of the country characterised by several mountain ranges. The Karoo is seeing large scale land use changes for mining, farming, renewable energy, intensive shale gas exploration and the Square Kilometre Array (SKA) (Sethusa, 2016). In 2016 the Karoo Biogaps project was undertaken to gain insight into the biodiversity standing of the region, which until then had never been fully assessed (Holness et al., 2016; Sethusa, 2016). This provided the opportunity to

© University of Pretoria

try to unravel the species diversity of *Stasimopus* in this unique ecosystem. This study is a stepping stone to increasing our understanding of the greater diversity of the entire genus, which given greater funding opportunities, should be addressed in the future.

This paper therefore aims to investigate i) the phylogenetic relationship between the various *Stasimopus* specimens within the Karoo region of South Africa and ii) to determine the species boundaries and estimate the number of species present in the region using coalescent species delimitation and confirm their accuracy against both the presence of monophyletic genetic clusters and morphological identification.

2. Methods and Materials

2.1. Taxon Sampling

Stasimopus specimens were collected from part of the Great Karoo, South Africa. The area is within the demarcated area for potential shale gas fracking. The boundary of the area is set approximately by the following coordinates: -30.88688, 26.29295 and -33.03079, 20.01661 (Figure 1). The sites were selected by the Karoo BioGaps team to cover the range of environmental conditions present in the region. A total of 79 sites were sampled, on average 50 km apart (Figure 1). *Stasimopus* specimens were collected at 55 of these sites. Females and juveniles were collected by actively excavating their burrows, while males were found active while crossing isolated roads on rainy evenings. All specimens were euthanised in a solution of cold alcohol and kept in an ice box. Specimens were later preserved in 80% ethanol in glass polytop vials for long term storage.

Additional recently collected museum specimens (*Stasimopus hewitti*) as well as individuals collected on other sampling trips from the Karoo area and Hluhluwe (Kwazulu-Natal) were included in the *Stasimopus* dataset. All locality information (except for GPS coordinates) is available in Table S1. GPS coordinates were omitted as the Karoo region is of conservation concern and the IUCN conservation statuses for *Stasimopus* species are completely unknown due to the lack of data. All newly collected material was deposited in the National Collection of Arachnida (NCA) of the Agricultural Research Council (ARC), Roodeplaat, South Africa.

© University of Pretoria

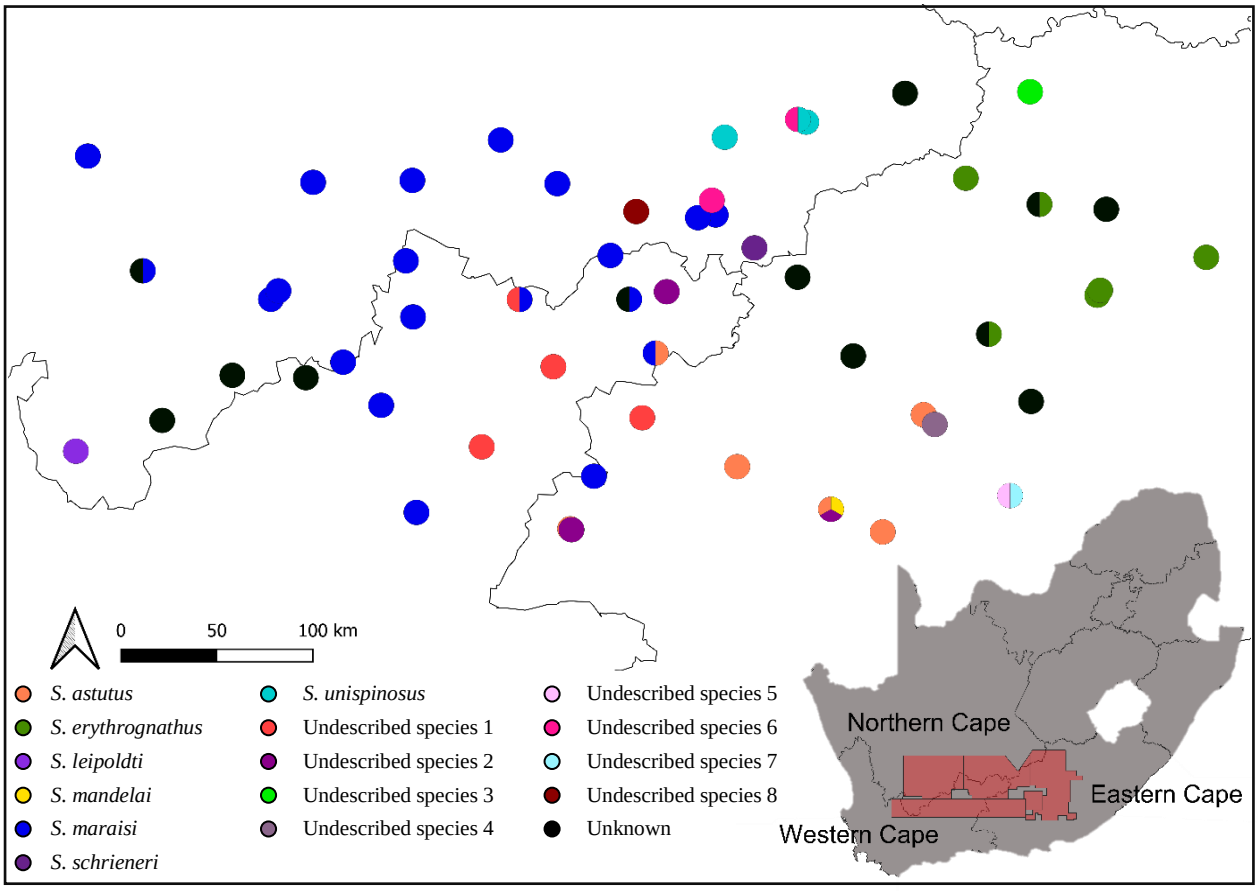


Figure 1. Map of the study area in the greater Karoo, in the south-western part of South Africa. Markers indicate the 55 sites where *Stasimopus* specimens were found. Specimens are divided into proposed morphospecies. Red polygons indicate areas identified for shale gas exploration. Map created in QGIS version 3.4.8-Madeira (2019), available at: http://qgis.osgeo.org.

2.2. Morphological identification

All adult specimens were examined against existing species descriptions and all type specimens of the genus. All adults were then assigned to morphospecies, based solely on the morphological species concept. Following this, species were assigned to existing species based on current species descriptions and types. All morphospecies which could not be classified into an existing species were classified as 'undescribed'. The examined morphological characters are in a character matrix available in Chapter 4.

© University of Pretoria

2.3. DNA extraction, sequencing and alignment

Genomic DNA was extracted from the removed third right leg of each specimen. DNA extraction was performed using the Macherey-Nagel NucleoSpin® Tissue kit (Düren, Germany) following the manufacturer's instructions.

Three genes were selected for sequencing to account for the differing mutational rate changes over time as well as different patterns of inheritance. These were ribosomal 16S, mitochondrial cytochrome c oxidase subunit 1 (CO1) and nuclear elongation factor 1 gamma (EF-1ɣ). The rationale for selecting these three gene regions was that they allow for the maximisation of phylogenetically informative data at a very fine genetic scale (species level variation). Histone H3 (H3) was also sequenced but was found to not be phylogenetically informative at this level. The phylogenetic topologies of the three genes will show if the gene trees reflect the species tree by congruence (Doyle, 1992; Maddison, 1997).

Genomic DNA was amplified by polymerase chain reaction (PCR) for the target genes using previously published primer sequences indicated in Table S2. Amplification mixtures were prepared to reach a final volume of 50 µL containing: 2.5 mM $MgCl_2$, 20 pmol of each primer, 10 mM dNTPs, 1 X PCR buffer, one unit of TaqDNApolymerase (Supertherm® DNA polymerase, Separation Scientific SA (Pty) Ltd, South Africa) or Emerald Amp®MAX HS PCR Mastermix (TAKARA BIO INC., Otsu, Shiga, Japan), for problematic samples as well as the EF-1ɣ gene region, in combination with 10-50 ng of extracted genomic DNA template. The PCR cycling parameters performed for the CO1 and 16S gene regions can be viewed in Table S3, and the parameters for EF-1ɣ were as stated in Table S4. Purification of the successful amplifications was done using the Macherey-Nagel NucleoSpin® Gel and PCR Clean-up kit (Düren, Germany) according to manufacturer's specifications. Samples which presented double bands were gel purified following the manufacturer's specifications. The BigDye® Terminator v3.1 Cycle Sequencing kit (Applied Biosystems, Foster City, USA) was used for the cycle sequence reactions in both sequence directions. The cycle sequencing products were precipitated using the standard protocol of sodium acetate and ethanol. All sequences generated were assembled in CLC Bio Main Workbench Version 6.9 (http://www.clcbio.com). All four gene regions were submitted to GenBank and the accession numbers are recorded in Table S1 (as well as sequence information for the selected outgroups). All the sequences generated from the barcoding CO1 region will be submitted to the Barcode of life database (BOLD).

The CO1, 16S and EF-1ɣ datasets were concatenated using FASconCAT v1.11 (Kück and Meusemann, 2010). The edited sequences for each gene were aligned using MAFFT online (Katoh, 2005; Katoh and Toh, 2008). The 'Auto' strategy for alignment was used in MAFFT followed by visual inspection.

© University of Pretoria

2.4. Phylogenetic Analysis

All analyses were applied to the individual gene regions and concatenated-molecular datasets for the *Stasimopus* data. The Akaike information criterion (AIC) and the Bayesian information criterion (BIC) were both implemented within jModelTest v2.1.7 (Posada, 2008).

Maximum likelihood (RAxML v8.1.20; Stamatakis, 2014) analyses were performed in RAxML implementing a General Time Reversible (GTR) model, with coding genes further partitioned for codon position. A maximum likelihood search was done to find the best tree, followed by bootstrapping for support of 1000 pseudoreplicates (Felsenstein, 1985).

For the Bayesian inference (MrBayes v3.2.5; Ronquist and Huelsenbeck, 2003) analyses, the parameters for each partition were unlinked in order to obtain separate estimates for each gene, the rate-prior was set to variable and flat Dirichlet-priors used. The analysis was run by two simultaneous Monte-Carlo-Markov-Chains, each with three hot and one cold chain (Drummond and Rambaut, 2007). This ran for 10,000,000 iterations, sampling every 500th iteration. This produced 20,000 trees of which the first 25% (5000) were discarded as burn-in.

Tracer v1.7.1 was used to confirm convergence (Rambaut et al., 2018). The individual runs per dataset were then compiled to ensure a normal distribution.

Outgroups were selected based on the most recent Mygalomorphae revision by Opatova et al. (2020). The sister clade to Stasimopidae in this study is the 'Venom clade', composed of Atracidae and Actinopodidae, represented by *Hadronyche* and *Actinopus* genera respectively. Additional outgroup representation was included with the nemesioids (genera: *Calisoga* (Nemesiidae), *Kiama* (Microstigmatidae), *Pionothele* (Pycnothelidae)) and an paratropidid (*Paratropis*) as this added additional support.

2.4.1. Ultrametric tree preparation

Two of the species delimitation methods tested require an ultrametric tree as a prior. To comply with this, ultrametric trees were constructed for each gene (some of the species delimitation approaches test only single locus data) using BEAST v1.10.4 (Suchard et al., 2018). For CO1 and 16S, a combined tree was produced as there is mitochondrial linkage (Rubinoff and Holland, 2005). The priors were set in BEAUTi (Suchard et al., 2018) as follows: The nucleotide substitution was set according to the results of jModelTest for each gene and codon partitioning was implemented for CO1 and EF-1ɣ; rate of molecular evolution to a relaxed clock with a lognormal distribution (this allows mutational rates to vary over the tree) (Michonneau, 2017); the MCMC chains were set to a chain length of 100,000,000 with echo states and log parameters to 1000. The last prior altered, was the model describing the branching pattern of the tree. For this prior we aimed to test two models for the GMYC method: the Yule model (all branching is covered by a constant speciation rate) and the Coalescent model with a

© University of Pretoria

constant population size (usually used for datasets which have individuals from the same species) (Michonneau, 2017). We decided to test both of these priors as it would allow for numerous (Yule model) or a few species (Coalescent model) (Michonneau, 2017). All other priors were left on the default settings in BEAUTi. Both files (Yule and Coalescent model priors) were then executed in BEAST. This was repeated four times per dataset and model to ensure convergence.

Tracer v1.7.1 was again used to confirm convergence (Rambaut et al., 2018). Log Combiner v1.10.4 (Suchard et al., 2018) was used to combine the tree files into one file per model and per gene and was set with a burn-in of 25,000,000.

2.5. Species delimitation

A variety of different species delimitation approaches were tested to determine i) if there is congruence among methods and ii) to test if these approaches can accurately delimit *Stasimopus* species given the strong population structuring of mygalomorph spiders. All the species delimitation results were tested against the morphological identifications of the specimens and monophyletic clusters, for this reason only identified adult specimens or juveniles whose identity could be inferred genetically were included.

2.5.1. Automated Barcode Gap Discovery (ABDG)

DNA barcoding has gained popularity in recent years. DNA barcoding is the use of short genetic markers to identify an organism to species level (Rubinoff and Holland, 2005). The CO1 gene is used for barcoding because it is one of the most conservative protein-coding genes in the mitochondrial genome; this makes it preferable for evolutionary time depths between species (Folmer et al., 1994). Mitochondrial genes such as CO1 are useful for species level or genus level analyses due to a higher number of variable/informative sites than nuclear loci (Rubinoff and Holland, 2005).

Automated Barcode Gap Discovery (Puillandre et al., 2012) uses the aligned gene sequences to determine species delimitations based upon the degree difference between individuals. The programme identifies the different thresholds for determining species boundaries specific to a particular taxon. This is done instead of the traditional method of having a set cut off divergence value *a priori* to determine species delimitations (Puillandre et al., 2012). The method uses the first barcode gap estimated at a distance limit deemed large enough to delimit intraspecific variation (using the population mutation rate estimated from the dataset) (Puillandre et al., 2012). This is given as the incursive value for the various P – distances partitions. The recursive value adds an additional step to this and takes into account the variability in mutation rate across the taxa in the dataset as well as the

© University of Pretoria

overlap of the intraspecific and interspecific variations (Puillandre et al., 2012). The recursive partition is thus considered more reliable (Puillandre et al., 2012).

The online tool was used (available at: http://wwwabi.snv.jussieu.fr/public/abgd/abgdweb.html) and the analysis parameters set to: pmin = 0.03; pmax = 0.6; x = 0.5; number of steps = 30, number of bins (Nb) = 50 and Kimura distance (TS/TV) left at the default setting (TS/TV = 2.0). The minimum and maximum p-value was determined iteratively by testing different combinations until more than one putative species was given as an output. For this reason, the range of intraspecific divergence values selected was between 0.0300 and 0.0618 as the species threshold. The species delimitations were then assessed for congruency against the morphological identifications, genetic clustering and other delimitation methods.

2.5.2. General Mixed Yule Coalescent (GMYC)

The GMYC model of species delimitation uses an algorithm which attempts to determine where a swap in branching pattern of a tree is due to a speciation event (which would place one lineage in a species) or due to coalescent events within a species (places multiple lineages in a species) (Michonneau, 2017; Pons et al., 2006).

The GMYC is applied to single locus data, for this reason EF-1ɣ and the combined CO1 / 16S were analysed separately. The ultrametric trees were then imported into R v3.4.3 (R Core Team, 2017) and analysed using the packages ape, paran and splits with the GMYC method (Dinno, 2014; Ezard et al., 2014; Paradis and Schliep, 2019). Both the Yule speciation and Coalescent speciation models were tested.

2.5.3. Bayesian Poisson Tree Processes (bPTP)

The Bayesian implementation of the Poisson Tree Processes (bPTP) model makes use of jumps in the branching patterns to determine differences between and within species. The model then links the number of nucleotide substitutions in a gene tree (the branch length) to model speciation events – assuming that there is a higher number of substitutions per site between species than within a species (Zhang et al., 2013).

To implement the PTP model with Bayesian support we used the bPTP server (Zhang et al., 2013). We performed the analyses EF-1ɣ and the combined CO1 / 16S separately. The RAxML tree with outgroup was uploaded and the rooted option was selected. All datasets were run for 500,000 MCMC generations. The burn-in was set to 0.25 and all other parameters were left on default.

© University of Pretoria

2.5.4. Brownie species delimitation

The heuristic method for species delimitation, produced by O'Meara (2009), makes use of the concept of gene tree congruence in a clade reflecting a cohesive species and incongruence of the gene trees for the clade reflecting variation within a species (O'Meara, 2010). Brownie takes gene trees as input files, performs a heuristic search comparing the topologies of the gene trees and locates areas where there is congruence in the gene trees (within a species) and areas of extensive incongruence (between species). This then sets species limits and estimates the species tree (O'Meara, 2010). The programme represents a species by a polytomy of the related samples. The programme does not inherently produce an estimation of uncertainty, but this can be estimated by bootstrapping (O'Meara, 2010).

Brownie v2.1.2 was run on a Mac OS (O'Meara, 2010). The ultrametric gene trees were imported to R v3.4.3 (R Core Team, 2017) and edited using the 'ape' package (Paradis and Schliep, 2019). This was done to remove tips for taxa which were not present across all three gene regions (14 taxa removed from CO1, 21 from 16S and 4 from EF-1ɣ). This was done as Brownie requires complete coverage of each gene. The edited individual ultrametric gene trees were used as the input data in NEXUS format in a combined file. The heuristic settings were all left on default. These analyses were repeated ten times to ensure consistent results.

The best trees selected by the program from each run were then used to create a consensus tree, from which another overall consensus tree was constructed using PAUP v4.0a (Swofford, 2002).

© University of Pretoria

3. Results

3.1. Taxon sampling

A total of 125 *Stasimopus* individuals were collected. An additional 4 *Stasimopus* individuals were genetically analysed from outside the study area. These additional samples were included to aid in the identification of the various lineages produced. At the majority of collecting sites only a few individuals were found during sampling. However, at a few sites, *Stasimopus* were especially abundant and easily found (due to high density or clear burrow entrances). The majority of specimens found were juveniles (61), followed by mature females (44) with few adult males collected (12). Seventeen morphospecies were morphologically assigned, nine of which could be assigned to existing *Stasimopus* species (*S. astutus*, *S. erythrognathus*, *S. hewitti*, *S. leipoldti*, *S. mandelai*, *S. maraisi*, *S. schrieneri*, *S. rufidens*, and *S. unispinosus*). While the other eight species did not match any existing species descriptions or type specimens and were denoted as 'undescribed'.

3.2. Phylogenetic analysis

The number of individuals and base pairs per gene region are summarised in Table S5. The table also indicates the nucleotide substitution model selected by jModelTest for the Akaike Information Criterion (AIC) and the Bayesian Information Criterion (BIC).

3.3. *Stasimopus* phylogenies and identities

Stasimopus is a well-supported monophyletic clade from the data (BS: 93; PP:0.97). The individual sample of *Stasimopus* cf. *rufidens* from Kwazulu-Natal (denoted as SUH) is sister to the rest of the *Stasimopus* samples (Figure 2). The remainder of the phylogram is then divided into 11 distinct genetic clades (Figure 2, A-K).

Clade K is composed of one individual, this is however with weak support. This individual being in its own evolutionary lineage is supported by the results of the species delimitation analyses and morphology. This individual could not be matched to any described species ('Undescribed species 7'). Clade J could not be identified as it is comprised of only juveniles and is likely a separate species. Clade I is a large clade, morphologically identified to be *Stasimopus maraisi*. Individuals from site 47 occur in both clades I and J, indicating synoptic species occurring at this locality. Clade H (BS: 96; PP: >0.95) consists of individuals from only locality 31. This lineage is supported by the species delimitation and does not match any previously described species morphologically and was donated as 'Undescribed species 3'. Clade G (BS: 92; PP: 0.99) has been morphologically identified as *S. unispinosus*, but the 02 samples could not be confirmed due to only being juveniles. Clade F (BS: 78; PP: 0.95) did not match any described species ('Undescribed species 1'). The terminal nodes

© University of Pretoria

of the clade have much higher support values than the internal nodes. Individuals from site 7 are placed in clade F and I, indicating another case of syntopic species. Clade E (BS: 93; PP: 0.97) did not match any described species ('Undescribed species 2'). Clade D has many samples which could not be identified (NCRA (2), 35 (2) and 53 (3)) as they are juveniles, whereas the rest were identified as *S. astutus*. Individuals from Site 38B and 35 occur in both clades D and I. Clade C is comprised solely of individuals from site 13, these samples have been identified as *S. leipoldti*. The most derived clades are A, and B. Clade B contains multiple morphologically distinct species, each represented by only a few individuals. These species are *S. mandelai*, *S. schrieneri*, 'Undescribed species 6'. and 'Undescribed species 8'. Individuals from site 05B are placed in clades C, F and H, individuals from site 59B are in both clades B and G, and individuals from SOUJ are in clades B, D and E. Clade A also comprises of multiple species. The two SH individuals are *Stasimopus hewitti*. One individual from locality 36 could also not be matched to any described species ('Undescribed species 5'). The most derived portion is an apparent species complex of *S. erythrognathus* and another species which did not match any existing species descriptions ('Undescribed species 4'). Individuals from site NCRA occur in clades A and E.

© University of Pretoria

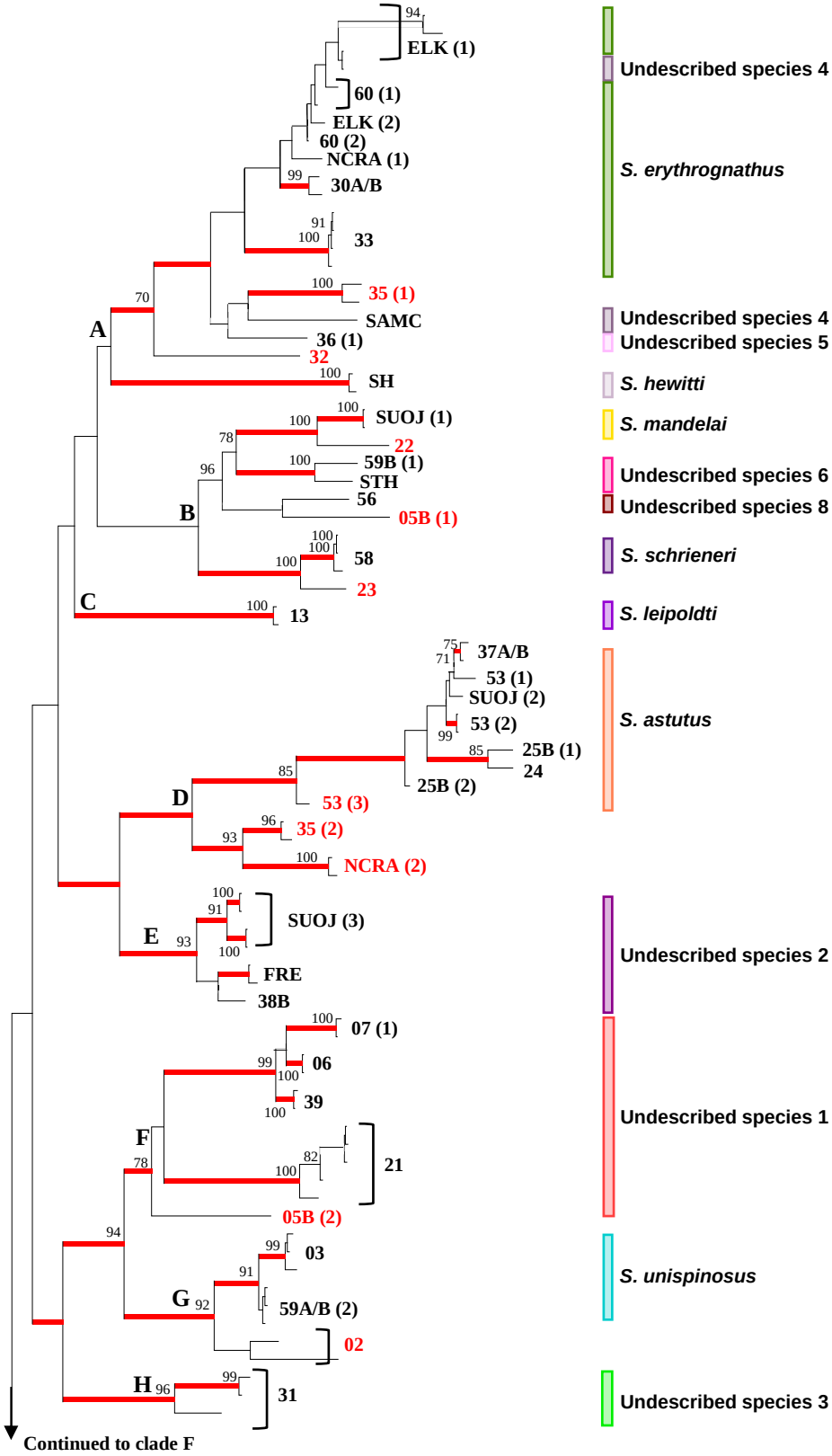


Figure 2 (Part A). Majority-rule (MrBayes) consensus tree for the concatenated dataset of CO1, 16S and EF-1ɣ for the *Stasimopus* dataset from the Karoo. Posterior probabilities above 0.95 are shown by the red bars. Bootstrap support values above 70 are given on the corresponding node. The morphologically identified species are indicated along the right. Specimens in red indicate juveniles that could not be morphologically identified or attributed to species clades. Broader clades are indicated on the tree.

© University of Pretoria

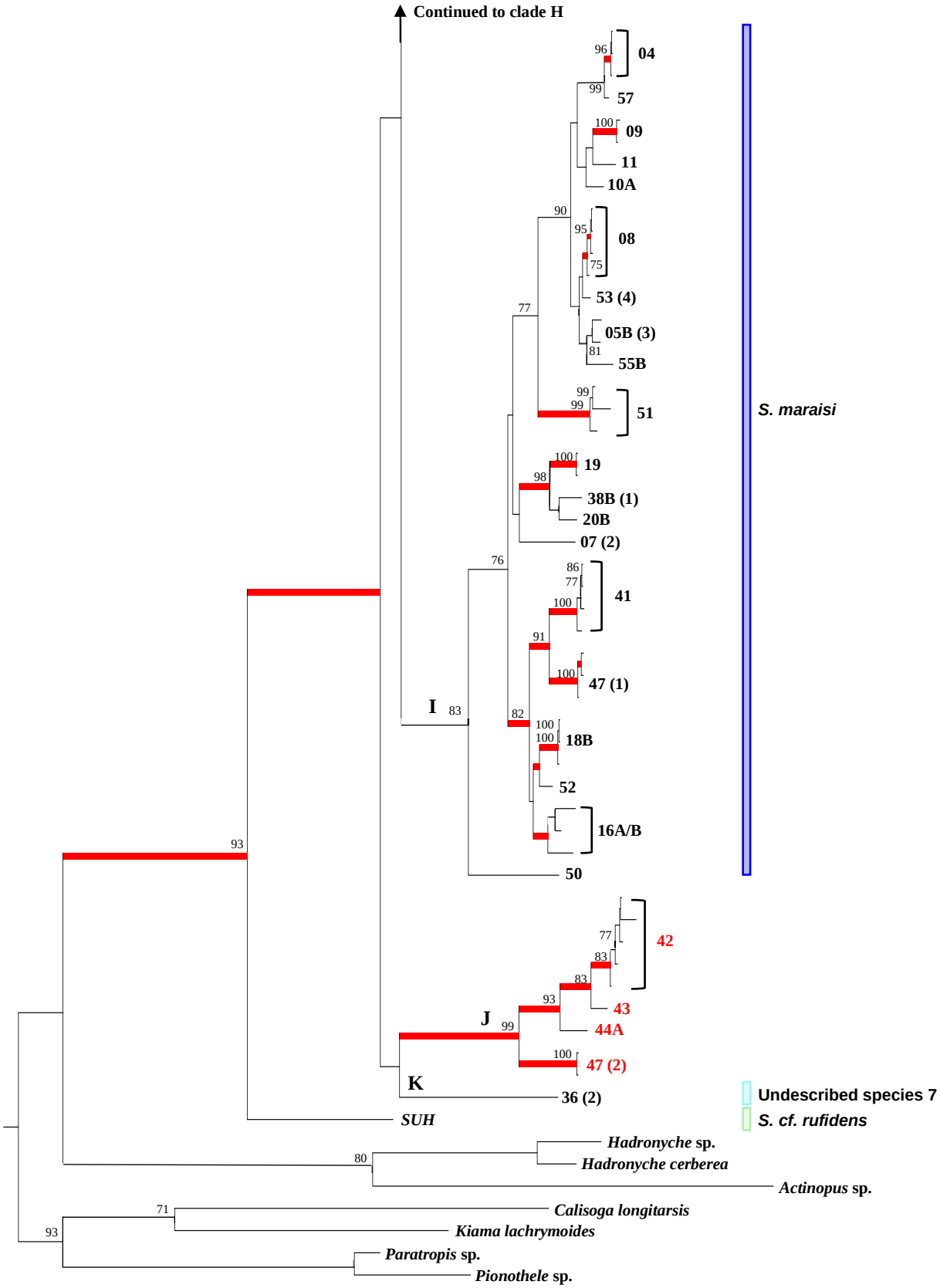


Figure 2 (Part B). Majority-rule (MrBayes) consensus tree for the concatenated dataset of CO1, 16S and EF-1ɣ for the *Stasimopus* dataset from the Karoo. Posterior probabilities above 0.95 are shown by the red bars. Bootstrap support values above 70 are given on the corresponding node. The morphologically identified species are indicated along the right. Specimens in red indicate juveniles that could not be morphologically identified or attributed to species clades. Broader clades are indicated on the tree.

© University of Pretoria

3.4. Species delimitation

3.4.1. Automated Barcode Gap Discovery species delimitation

ABDG produced various species delimitations based on the different prior maximal distance (P) values used in the input. The larger the P value given, the more split the data became (more species were delimited). When the P value was smaller than 0.0300, more than 60 species were delimited. When the P value was larger than 0.0623 only one species was delimited (Figure 3).

The initial distance value is more conservative in the number of species delimited than the recursive. The smallest distance value (P = 0.0623) classifies all the samples as one species (Grey, Figure 3). The incursive results for P 0.033 and 0.037 were identical, thus only 0.033 (I) is shown. The results of the 0.411 and 0.455 distance values were also identical and only 0.0455 is shown in Figure 3. The incursive results for P 0.0455 and 0.0561 were identical, thus only 0.0561 (I) is shown. This was again true for the distance values of 0.505 and 0.561, and only 0.0561 is shown.

Certain samples are consistently recovered as separate species. *Stasimopus hewitti* (SH02; thistle), *S. leipoldti* (13STAS02; blue violet), *S. unispinosus* (03STAS01, 03STAS02; cyan) and 'Undescribed species 7' (36STAS01; cadet blue), are all separate species on their own in all distance values except for P = 0.0623 (Figure 3). A few species are recovered most of the time (except for the distance values of 0.0561 (I) and 0.0623). These include 'Undescribed species 4'. (SAMC7293), 'Undescribed species 5', 'Undescribed species 8' and *S. schrieneri* (Figure 3). *Stasimopus astutus,* 'Undescribed species 1' and *S. maraisi* were only recovered at the lower distance values, whereas for 'Undescribed species 6' this is true of the middle-distance values (Figure 3). *Stasimopus erythrognathus,* 'Undescribed species 1' and 'Undescribed species 3' were never fully recovered as they were always overspilt and in the case of *S. erythrognathus* also had additional species included according to genetic clustering and morphology.

The species complex described in the phylogeny (Figure 2) is apparent here again between *S. erythrognathus* and 'Undescribed species 4', whereas ELKSTAS06 (ELK (1) – Figure 2) is never recovered as a separate species (Figure 3).

© University of Pretoria

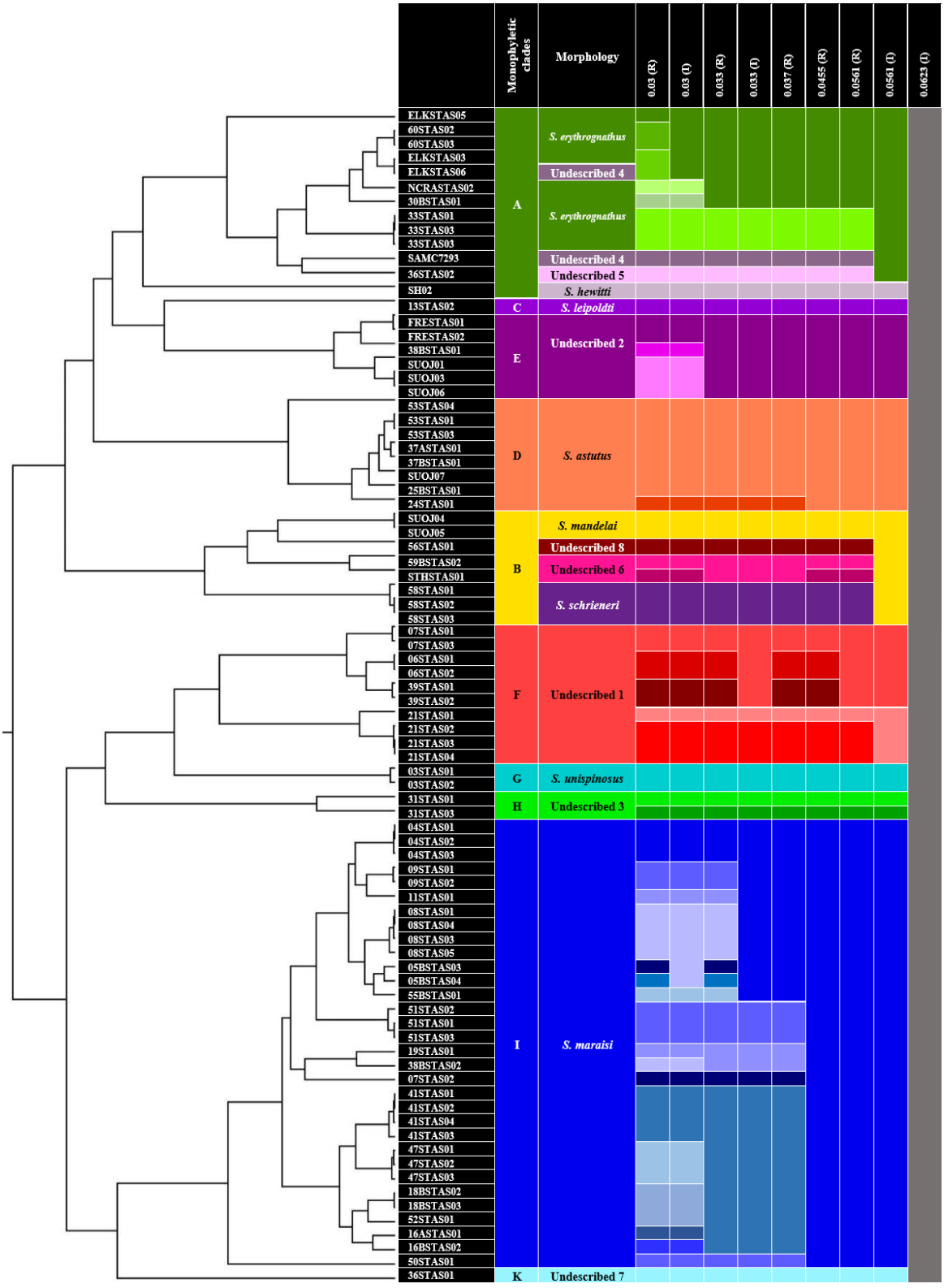


Figure 3. The species delimitations of the Automated Barcode Gap Discovery tool distance values on the cladogram of the CO1 data. The various partitions for different values of the prior maximal distance (P) are given in the first row. The recursive and incursive partitions are denoted by (R) and (I) respectively. The samples are split into their proposed species and monophyletic clades by the different coloured blocks in a pantone corresponding the *Stasimopus* phylogram (Figure 2).

© University of Pretoria

3.4.2. General Mixed Yule Coalescent (GMYC)

The General Mixed Yule Coalescent (GMYC) gave fairly similar results between the Yule and coalescent model of speciation for each gene region. The CO1_16S gene region presented with 2 putative species (coalescent Confidence interval (CI): 1-10–; yule CI: 1-4) and 2 distinct genetic clusters (coalescent CI: 1-7, yule CI: 1-4) which were identical for the Yule and Coalescent trees. The LR test was not significant for both. The results for the EF-1ɣ region were also not significant under the LR test and presented with more putative species. The coalescent model predicted 8 putative species (CI: 1-17) whereas the yule model predicted 18 putative species (CI: 1 - 24). The confidence ranges are exceptionally wide for this gene region. The putative species are given for each gene region in figures 4 and 5.

3.4.3. Bayesian Poisson Tree Process (bPTP)

The Bayesian Poisson Tree Process (bPTP) method of species delimitation results vary between the different gene regions. The two mitochondrial genes (CO1_16S) have a lower number of putative species (36 or 53) than the nuclear gene (29 or 75) (Table 1). There is a wide margin of error as the estimated number of species is a large range, approximately 30 species between the minimum and maximum for each gene region. The acceptance rate is much higher for EF-1ɣ (0.889) than CO1_16S (0.417). The putative species are given for each gene region in Figures 4 and 5. The number of species for each confidence interval is given in Table S6 as well as putative species acceptance rates in tables S7 – S8.

Table 1. The number of species delimited for each gene region (CO1_16S and EF-1ɣ) with the Bayesian Poisson Tree Process (bPTP) species delimitation methodology.

	CO1_16S	**EF-1ɣ**
Acceptance rate	0.417	0.889
Estimated number of species	26-68	29 - 76
Mean number of species	49.34	55.86
Bayesian Inference species estimation	53	75
Maximum likelihood species estimation	36	29

© University of Pretoria

3.4.4. Summary of single locus coalescent methods

The species delimitation results for linked CO1 and 16S are not congruent between the GMYC and bPTP methodologies (Figure 4). The bPTP method severely oversplit the dataset, whereas GMYC lumps the data when compared to the morphological identities of the specimens as well as the monophyletic clades. There are only a few individuals constituting a 'species' for the bPTP method while matching the morphology and genetic clusters: 'Undescribed species 4' (SAMC7293), 'Undescribed species 5', *S. hewitti*, *S. schrieneri*, *S. leipoldti*, *S. unispinosus* 'Undescribed species 8' and 'Undescribed species 7' (Figure 4).

EF-1ɣ species delimitation has a different result to the CO1_16S. The GMYC method is more conservative than the bPTP method with 8 or 18 putative species as opposed to 29 or 75 putative species (Figure 5). No species is congruent across methodologies. The phylogeny produced for the EF-1ɣ is however not in agreement with the morphological identifications.

Across the two separate gene regions' species delimitation results, no species are congruent and neither method could resolve the *S. erythrognathus* and 'Undescribed species 4' complex.

3.4.5. Brownie species delimitation

The results of the heuristic search run in brownie are inconclusive. The analyses produced 633 tree topologies from the ten runs. However, there is no true congruence between these trees. Individuals constantly swap between the different putative species – having no true placement. A 50% majority-rule consensus tree is shown as Figure S1. The tree has a hard polytomy, meaning that no real putative species could be delimited. When testing for accuracy within Brownie, either 51 or 53 species were constantly delimited (individuals in the species are not given).

© University of Pretoria

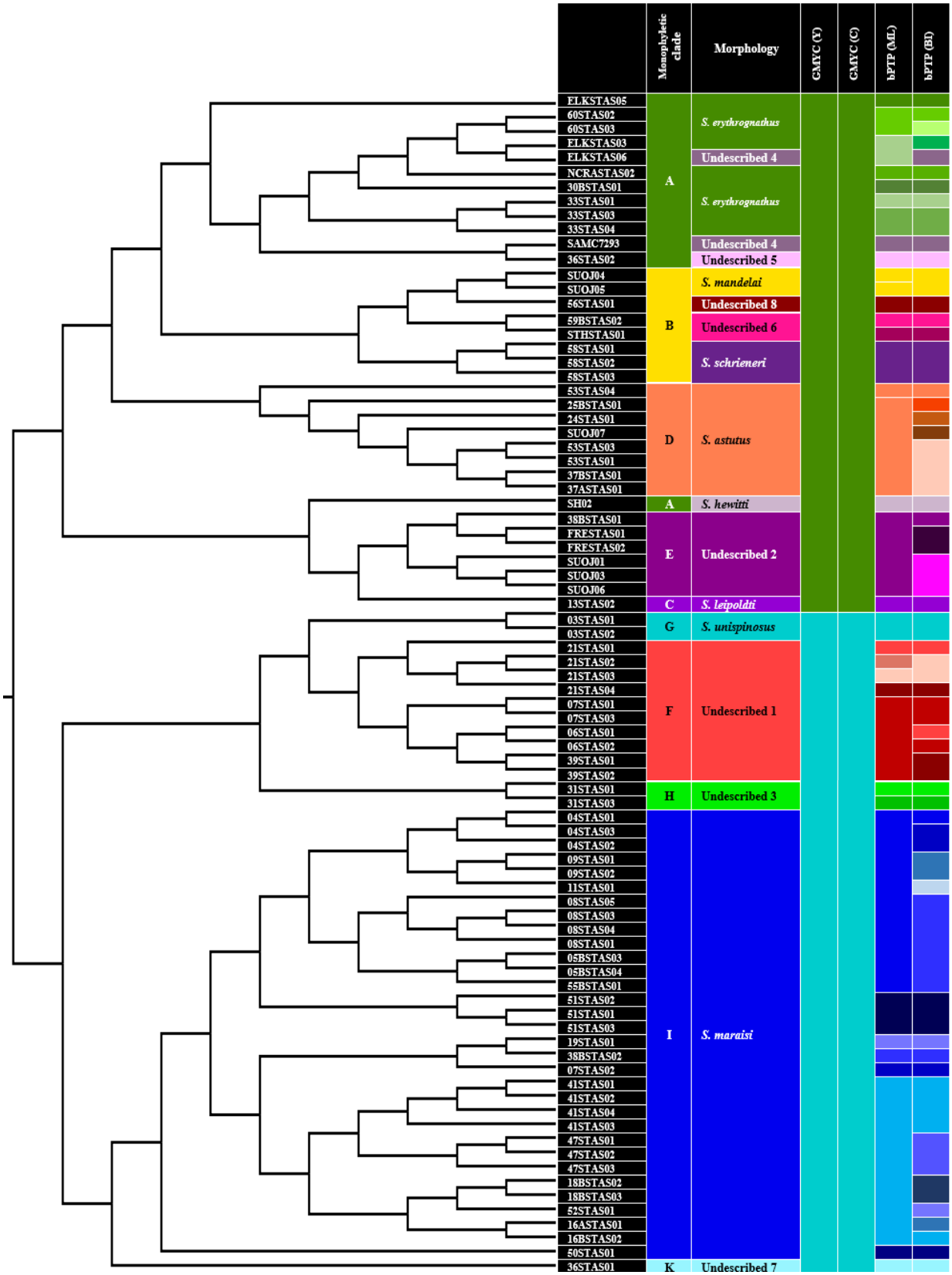


Figure 4. Combined results for cytochrome oxidase 1 (CO1) and ribosomal 16S bPTP and GMYC species delimitation. The results are overlaid on the CO1 and 16S cladogram. The samples are split into their proposed species and monophyletic clades by the different coloured blocks in a pantone corresponding the *Stasimopus* phylogram (Figure 2). The Yule and coalescent speciation models are indicated by (Y) and (C) respectively.

© University of Pretoria

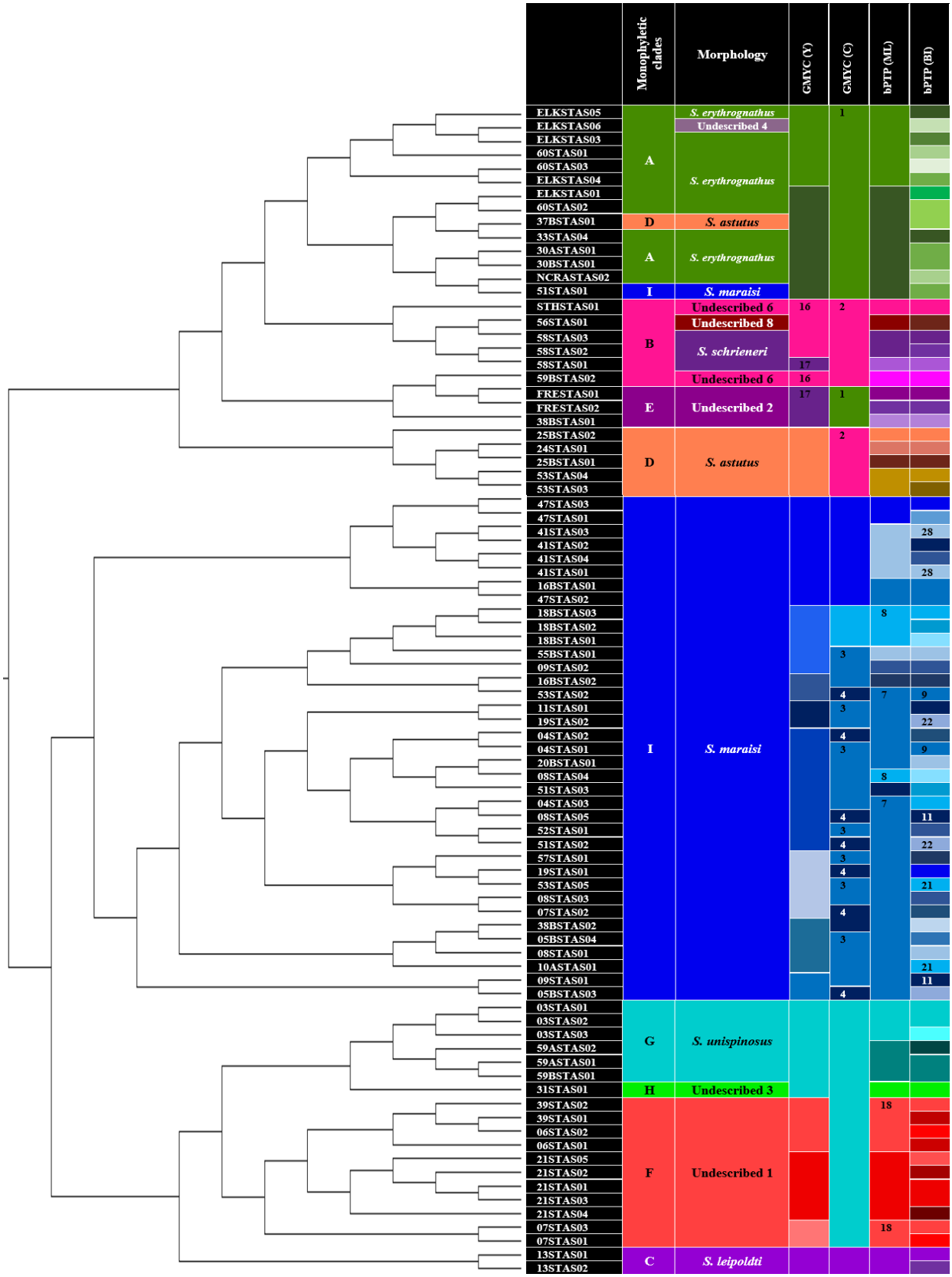


Figure 5. The elongation factor 1 gamma (EF-1ɣ) species delimitation results for the bPTP and GMYC. The results are overlaid on the EF-1ɣ cladogram. The samples are split into their proposed species and monophyletic clades by the different coloured blocks in a pantone corresponding the *Stasimopus* phylogram (Figure 2). The Yule and coalescent speciation models are indicated by (Y) and (C) respectively.

© University of Pretoria

4. Discussion

4.1. *Stasimopus* diversity

This study is the first detailed phylogenetic study on the group including the use of species delimitation methods. The study generated extensive sequence data for a severely understudied organism in a potentially threatened and sensitive ecosystem. These resources can be used in future studies to better understand the genus. The *Stasimopus* samples assessed in this study form a well-supported monophyletic clade. The phylogeny consists of 17 morphospecies and juvenile specimens which could not be identified, based on morphology. Fifteen species were only recovered from a single or few localities which were all in close proximity, indicating that these species are 'short-range endemics'. Short-range endemics are species which have a naturally narrow distribution (<10,000 km^2) (Harvey, 2002; Harvey et al., 2011; Mason et al., 2018). Short-range endemics often have life history traits such as poor dispersal ability, reliance on rare or fragmented habitats and low fecundity (Harvey et al., 2011). *Stasimopus*, like most of the Mygalomorphae, are known to exhibit sedentarily habits and have short dispersal distances (Leavitt et al., 2015). These factors would make a species which is a short-range endemic especially sensitive to climate change, degradation of the habitat or habitat loss (Harvey et al., 2011). This is vital information in light of the slew of land use change proposed for the Karoo region. The morphologically identified species *S. maraisi* and *S. erythrognathus* have wide distributions across the Karoo, and are not short-range endemics. Several species sampled appear to experience sympatry at multiple locations. This indicates that the species may have an unknown ecological niche separation or are syntopic in nature (Wilson et al. 2018).

The species *S. erythrognathus* distribution is not completely known but appears very wide (sampled in the eastern portion of the Karoo and the type locality being Worcester, which are 600 km apart) and likely extends to other unsampled parts of South Africa. There were no specimens found between these two localities during our sampling. This indicates that further sampling needs to be performed in order to determine if this whole range is still occupied or if these may be relict populations / remnants or perhaps a species complex.

Stasimopus erythrognathus and 'Undescribed species 4'. appear to form a genetic species complex as one specimen is 'Undescribed species 4' and falls within the *S. erythrognathus* clade . One specimen which is placed sister to the *S. erythrognathus* clade as is also 'Undescribed species 4'. All of these specimens were collected in the eastern Karoo and within fairly close geographic proximity. These two species are morphologically distinct and more gene regions are required to resolve the genetic complex found here.

The placement of *Stasimopus* cf. *rufidens*, from Hluhluwe (Kwazulu Natal) indicates that there is a great amount of genetic distance between the *Stasimopus* of the coastal area and that of the interior Karoo.

© University of Pretoria

4.2. Uncertainty in the phylogenies

Low support values on internal branches could be due to factors such as homoplasy, low genetic signal or incomplete lineage sorting (Buckley et al., 2006).

The incongruence of the ML and BI trees, as well as low support values may be the impact of missing data or an insufficient number of loci to resolve these relationships. Methods such as concatenation assume that the different genes used have moderately similar evolutionary histories, thus not considering that different genes evolve at different rates (mitochondrial genes evolve more rapidly than nuclear genes due to the pattern of inheritance) (Xi et al., 2016). Thus, when comparing a species for which only mitochondrial information is available to one with only nuclear information in the same phylogeny, would put the individual with the mitochondrial information on a longer branch. This may be the case with clade D of the *Stasimopus* phylogeny. This would make it appear as though there are different rates of evolution between the species which is untrue. Concatenation methods do however fair well with missing data if the data is evenly distributed among the taxa and gene regions (Xi et al., 2016). Our data sets had fairly evenly distributed missing data.

It is also noted that the phylogenetic inference and species delimitation may be impacted by the scattered phylogenetic sampling. The Karoo region was throughly sampled, but this region has no natural boundaries limiting the distribution of taxa, and thus their full ranges were not captured by these data. This may affect the accuracy of the species delimition models (Papadopoulou et al. 2009). These methods can also be affected by using 'singleton' representatives of species, this is however largely unavoidable when working with unforthcoming taxa (Ahrens et al. 2016). Future studies should expand on this sampling effort to better encapsulate the distribution of the genus as well as attempt to include multiple representatives of each species.

4.3. Coalescent species delimitation

Stasimopus as a genus is challenging to identify using morphology alone at species level. For this reason, use of coalescent based species delimitation was investigated as a tool to determine how many species can be identified from a genetic dataset and validated using both morphology and genetic clustering. It is also important to note that the study used not only mitochondrial data, but a nuclear region too.

The Automated Barcode Gap Discovery (ABDG) online tool delimited the most species in the largest partition (>0.03) which severely oversplit the CO1 dataset, placing each locality into its own species. This delimitation of 46 species is highly unlikely. This most likely reflects the genetic structure between sites, as a result of limited dispersal. A species delimitation study on the Nemesiidae returned a similar result where each locality was returned as a putative species, the over estimation is most likely due to genetic substructuring which occurs in mygalomorph spiders at small

© University of Pretoria

geographic scales (Leavitt et al., 2015). Another example of this was seen in Idiopidae studied in the Canary islands (Opatova and Arnedo, 2014). This appears to be the case with the 0.03 and 0.033 distance values. The largest distance value (0.0623) lumped all individuals into one species. The result of one species is inaccurate as from the males and females collected, 17 separate morphospecies were morphologically identified. This lumping is most likely because the barcode gap is overshot: (P) prior maximum divergence of the intraspecific diversity is too large and overshadows the interspecific diversity (Puillandre et al., 2012). The distance value with the closest results is 0.0561, where the initial distance value which suggests 13 species and recursive suggests 21. The recursive 0.0561 partition delimits most species correctly except the *S. erythrognathus* / 'Undescribed species 4' complex, and oversplits 'Undescribed species 1' and 'Undescribed species 6'. This partition being the most reliable is also supported by the fact that the recursive partition is usually considered more reliable than the incursive due to taking more factors in the dataset into account (Puillandre et al., 2012). This methodology appears to have delivered the most plausible results.

The Bayesian Poisson Tree Process (bPTP) results were the least conservative for the EF-1ɣ gene region, estimating 29 or 75 putative species. The number of putative species predicted for the CO1_16S region also appears to be unrealistically high too. The number of species predicted by this analysis would be lower (and possibly more accurate) if nodes with low support values (<0.80) are collapsed (Zhang et al., 2013). There is also incongruence between the gene tree produced for the EF-1ɣ dataset and the morphology. This is clear from the one *S. atutus* and *S. marasi* samples that are embedded in clade A. This pattern is however not seen in the mitochondrial gene tree, nor the combined tree. More nuclear genes need to be added to investigate this fully. This may in part be responsible for the poor performance of the species delimitation methods.

The General Mixed Yule Coalescent (GMYC) gave similar results between the coalescent and yule model of speciation for the CO1_16S dataset. The Yule model assumes a constant speciation rate across branches and is often used in cases where the individuals are from numerous species, whereas the Coalescent model (constant growth rate) is often used in cases with a few species (Michonneau, 2017). It appears that the speciation model of the ultrametric tree only had a significant effect on the EF-1ɣ data set where the number of delimited species changed from 18 (Yule) to 8 (Coalescent), but this result was not significant under the LR test. The species were however incorrectly delimited according to morphology and monophyletic clusters. The discrepancy between the mitochondrial genes (CO1 and 16S) and the nuclear gene in the number of putative species produced may be attributed to the fact that these two parts of the genome have very different rates of evolution. For the class Arachnida, the rate of mitochondrial evolution is on average 3.1 times faster than nuclear evolution (Allio et al., 2017). The GMYC appears to have lumped the CO1_16S dataset into only two species, which is in reality not feasible based on the monophyletic clades and morphology. GMYC is commonly cited as oversplitting data for the mygalomorph group due to the

© University of Pretoria

strong population structuring observed in spiders with sedentary lifestyles, whereas the opposite was observed (Hamilton et al., 2014; Hedin, 2015; Opatova and Arnedo, 2014; Satler et al., 2013).

As a whole, the single-locus methods of species delimitation performed poorly at delimiting species for the *Stasimopus* genus when validated against the morphological identifications as well as genetic clustering. There was no full congruence across methods for any of the gene regions. The Automated Barcode Gap Discovery (ABDG) shows the most promising results for the CO1 region, where both bPTP and GMYC incorrectly split the data. Overall, CO1 and DNA barcoding may need to be interpreted with caution when used in isolation, as it may not capture all the variation present and may be lacking some resolving power (Galtier et al., 2009). Galtier et al. (2009) found that many of the underlying principles of mitochondrial DNA which supports barcoding may be false. Some of these characteristics include mitochondrial DNA undergoes recombination, positive selection as well as an evolutionary rate which changes over time (Galtier et al., 2009). This emphasises that species delimitation cannot be performed using only a single gene region, as no single gene region is impervious to these factors. This means that multiple gene regions should be considered when delimiting species or that the species delimitation tools must be developed so that the variation between different gene regions is taken into account (Hedin et al., 2015).

Brownie (multilocus species delimitation) provided inconclusive results as no congruence was found between the trees produced by the analysis. A study conducted on frogs in South America by Correa et al. (2017) had the same result from analyses run by Brownie. They recovered a consensus tree with a hard polytomy – resulting in no reliable species being delimited (Correa et al., 2017).

From the results of the species delimitation analyses one of three scenarios are likely taking place. Firstly, there is the possibility that there are approximately 40 species of *Stasimopus* in this region of the Karoo. This result was recovered in part by all the methods, but is highly unlikely. Secondly, the *Stasimopus* of the Karoo are undergoing speciation. This may be a possibility as the life history traits of the genus makes them prime candidates to undergo allopatric speciation (Wilson et al., 2018). The largely sedentary lifestyles of females and limited dispersal of spiderlings tends to lead to extensive population structuring which are referred to as ‘microallopatric populations’ within a species (Bond et al., 2001; Satler et al., 2013). These populations may then remain isolated for extensive periods of time leading to speciation events. This scenario is supported by the short terminal branches of the phylogeny, which is a common indicator of speciation events. The last scenario is simply that due to the extensive population structure (microallopatric populations), the species delimitation methods used are not suitable for resolving the relationships and are prone to oversplitting the dataset (except for GMYC) (Satler et al., 2013). This scenario is supported as coalescent species delimitation techniques appear to delimit genetic structure, not species (Sukumaran and Knowles, 2017).

© University of Pretoria

5. Conclusion

The phylogenetic diversity of *Stasimopus* within the Karoo region of South Africa is higher than previously believed with eight undescribed species identified. *Stasimopus* and other trapdoor spiders have not been extensively researched, but are a significant part of the Karoo fauna. For this reason, they should be considered for inclusion in environmental impact assessments, evaluated for placement on the IUCN Red List and other conservation initiatives. It is suggested that species delimitation is not purely based on barcoding genes but a multi-locus approach should always be implemented. From the results of the species delimitation, we find that these methods are not suitable to delimit species for the genus as the population has extensive substructure at fine geographical scales, leading to 'microallopatric populations'. More research is needed to find gene regions which have greater resolution for this group of spiders. The way forward is to determine the evolutionary history and environmental pressures which may be causing the divergence in the populations by implementing a phylogeographic analysis of the data.

Acknowledgements

We would like to acknowledge Carmen Jacobs and Ishtiag Abdalla Mohammed for assistance with molecular work and phylogenetic analyses. Tshepiso Majelantle and Elmé Brand for their assistance on fieldwork. Equipment for field work was supplied by the Agricultural Research Council. We would like to thank the following institutions for loaning the specimens required for specimen identification: Albany Museum, Grahamstown, South Africa; The National Museum, Bloemfontein, South Africa; Ditsong Museum of Natural History, Pretoria, South Africa; Iziko Museum of Cape Town, South Africa; Museum für Naturkunde, Berlin, Germany; National Collection of Arachnida, Pretoria, South Africa.

Funding

The National Research Foundation (NRF) are acknowledged for funding to the second author. The first author would also like to acknowledge the National Research Foundation for funding (Grant no: 120190 and 139125). This work is based on the research supported in part by the Karoo BioGaps Project (NRF Grant Number 98864), which was awarded through the Foundational Biodiversity Information Programme (FBIP), a joint initiative of the Department of Science and Innovation (DSI), the National Research Foundation (NRF) and the South African National Biodiversity Institute (SANBI).

© University of Pretoria

References

Allio, R., Donega, S., Galtier, N., Nabholz, B., 2017. Large variation in the ratio of mitochondrial to nuclear mutation rate across animals: Implications for genetic diversity and the use of mitochondrial DNA as a molecular marker. Mol. Biol. Evol. 34, 2762–2772.

Ahrens, D., Fujisawa, T., Krammer, H.-J., Eberle, J., Fabrizi, S., Vogler, A. P., 2016. Rarity and Incomplete Sampling in DNA-Based Species Delimitation. Syst. Biol. 65, 478–494.

Ayoub, N.A., Garb, J.E., Tinghitella, R.M., Collin, M.A., Hayashi, C.Y., 2007. Blueprint for a High-Performance Biomaterial: Full-Length Spider Dragline Silk Genes. PLoS ONE 2, e514

Barley, A.J., Brown, J.M., Thomson, R.C., 2018. Impact of Model Violations on the Inference of Species Boundaries under the Multispecies Coalescent. Syst. Biol. 67, 269–284.

Beavis, A.S., Sunnucks, P., Rowell, D.M., 2011. Microhabitat preferences drive phylogeographic disparities in two Australian funnel web spiders. Biol. J. Linn. Soc. 104, 805–819.

Bond, J.E., Hedin, M.C., Ramirez, M.G., Opell, B.D., 2001. Deep molecular divergence in the absence of morphological and ecological change in the Californian coastal dune endemic trapdoor spider *Aptostichus simus*. Mol. Ecol. 10, 899–910.

Bond, J.E., Hendrixson, B.E., Hamilton, C.A., Hedin, M., 2012. A reconsideration of the classification of the spider infraorder Mygalomorphae (Arachnida: Araneae) based on three nuclear genes and morphology. PLoS ONE 7, e38753.

Buckley, T. R., Cordeiro, M., Marshall, D. C., Simon, C., 2006. Differentiating between Hypotheses of Lineage Sorting and Introgression in New Zealand Alpine Cicadas (*Maoricicada* Dugdale). Syst. Biol. 55, 411–425.

Cognato, A.I., Vogler, A.P., 2001. Exploring data interaction and nucleotide alignment in a multiple gene analysis of Ips (Coleoptera: Scolytinae). Syst. Biol. 50, 758–780.

Carstens, B.C., Pelletier, T.A., Reid, N.M., Satler, J.D., 2013. How to fail at species delimitation. Mol. Ecol. 22, 4369–4383.

Correa, C., Vasquez, D., Castro-Carrasco, C., Zuniga-Reinoso, A., Ortiz, J.C., Palma, R.E., 2017. Species delimitation in frogs from South American temperate forests: the case of *Eupsophus*, a taxonomically complex genus with high phenotypic variation. PLoS ONE 12, e0181026.

De Queiroz, K., 2007. Species Concepts and Species Delimitation. Syst. Biol. 56, 879–886.

Derkarabetian, S., Hedin, M., 2014. Integrative taxonomy and species delimitation in harvestmen: A revision of the western North American genus *Sclerobunus* (Opiliones: Laniatores: Travunioidea). PLoS ONE 9.

Diniz-Filho, J.A.F., Soares, T.N., Lima, J.S., Dobrovolski, R., Landerio, V.L., de Campos Telles, M.P., Rangel, T.F., Bini, L.M., 2013. Mantel test in population genetics. Genet. Mol. Biol. 36, 475–485.

Dinno, A., 2014. paran: Horn's test of Principle Components/ factors.

© University of Pretoria

Dippenaar-Schoeman, A.S., 2002. Baboon and Trapdoor Spiders of Southern Africa: An Identification Manual, Handbook. ed. Plant production research institute. Agricultural Research Council, Pretoria., Pretoria.

Dippenaar-Schoeman, A.S., Haddad, C.R., Foord, S.H., Lyle, R., Lotz, L., Helberg, L., Mathebula, S., van der Berg, A., van Niekerk, E., Jocque, R., 2010. First atlas of the spiders of South Africa (Arachnida: Araneae), in: SANSA Technical Report. p. 1160.

Doyle, J.J., 1992. Gene trees and species trees: Molecular systematic one-character taxonomy. Syst. Bot. 17, 144–163.

Dray, S., Dufour, A.-B., Thioulouse, J., 2018. Analysis of ecological data: Exploratory and Euclidean methods in environmental sciences. R package.

Drummond, A.J., Ho, S.Y.W., Phillips, M.J., Rambaut, A., 2006. Relaxed phylogenetics and dating with confidence. PLoS Biol. 4, 0699–0710.

Drummond, A.J., Rambaut, A., 2007. BEAST: Bayesian evolutionary analysis by sampling trees. BMC Evol. Biol. 7, 1–8.

Eardley, C., 2016. BioGaps: a collaborative survey of Karoo biodiversity. Newsletter of Plan Production Research 5.

Engelbrecht, I., Prendini, L., 2011. Assessing the taxonomic resolution of southern African trapdoor spiders (Araneae: Ctenizidae; Cyrtaucheniidae; Idiopidae) and implications for their conservation. Biodivers. Conserv. 20, 3101–3116.

Engelbrecht, I., Prendini, L., 2012. Cryptic diversity of South African trapdoor spiders: Three new species of *Stasimopus* Simon, 1892 (Mygalomorphae, Ctenizidae), and redescription of *Stasimopus robertsi* Hewitt, 1910. Am. Mus. Novit. 1–42.

Ezard, T., Fujisawa, T., Barraclough, T., 2014. splits: SPecies' LImits by Threshold Statistics.

Felsenstein, J., 1985. Confidence limits on phylogenetics: an approach using the bootstrap. Evol. 783–791.

Ferretti, N., González, A., Pérez–Miles, F., 2014. Identification of priority areas for conservation in Argentina: quantitative biogeography insights from mygalomorph spiders (Araneae: Mygalomorphae). J. Insect Conserv. 18, 1087–1096.

Folmer, O., Black, M., Hoeh, W., Lutz, R., Vrijenhoek, R., 1994. DNA primers for amplification of mitochondrial cytochrome c oxidase subunit I from diverse metazoan invertebrates. Mol. Mar. Biol. Biotechnol. 3, 294–299.

Fujisawa, T., Barraclough, T.G., 2013. Delimiting Species using Single-locus Data and the Generalized Mixed Yule Coalescent (GMYC) Approach. Syst. Biol. 44, 1–60.

Fujita, M.K., Leaché, A.D., 2011. A coalescent perspective on delimiting and naming species: a reply to Bauer *et al*. Proc. Royal Soc. B. 278, 493–495.

Fujita, M.K., Leaché, A.D., Burbrink, F.T., McGuire, J.A., Moritz, C., 2012. Coalescent-based species delimitation in an integrative taxonomy. Trends Ecol. Evol. 27, 480–488.

© University of Pretoria

Galtier, N., Nabholz, B., Glemin, S., Hurst, G.D.D., 2009. Mitochondrial DNA as a marker of molecular diversity: a reappraisal. Mol. Ecol. 18, 4541–4550.

Godwin, R.L., Opatova, V., Garrison, N.L., Hamilton, C.A., Bond, J.E., 2018. Phylogeny of a cosmopolitan family of morphologically conserved trapdoor spiders (Mygalomorphae, Ctenizidae) using Anchored Hybrid Enrichment, with a description of the family, Halonoproctidae Pocock 1901. Mol. Phylogenet. Evol. 126, 303–313.

Hamilton, C.A., Hendrixson, B.E., Brewer, M.S., Bond, J.E., 2014. An evaluation of sampling effects on multiple DNA barcoding methods leads to an integrative approach for delimiting species: A case study of the North American tarantula genus *Aphonopelma* (Araneae, Mygalomorphae, Theraphosidae). Mol. Phylogenet. Evol. 71, 79–93.

Harvey, M.S., 2002. Short-range endemism among the Australian fauna: some examples from non-marine environments. Invertebr. Syst. 16, 555–570.

Harvey, M.S., Johnson, M.S., Humphreys, W.F., 2011. Protecting the innocent: Studying short-range endemic taxa enhances conservation outcomes. Invertebr. Syst. 25, 1–10.

Hedin, M., 2015. High-stakes species delimitation in eyeless cave spiders (*Cicurina*, Dictynidae, Araneae) from central Texas. Mol. Ecol. 24, 346–361.

Hedin, M., Carlson, D., Coyle, F., 2015. Sky island diversification meets the multispecies coalescent – divergence in the spruce-fir moss spider (*Microhexura montivaga*, Araneae, Mygalomorphae) on the highest peaks of southern Appalachia. Mol. Ecol. 3467–3484.

Hein, J., Schierup, M.H., Wiuf, C., 2005. Gene genealogies, variation and evolution: A primer in coalescent theory. Syst. Biol. 54, 986–987.

Hendrixson, B.E., Bond, J.E., 2004. A new species of *Stasimopus* from the Eastern Cape Province of South Africa (Araneae, Mygalomorphae, Ctenizidae), with notes on its natural history. Zootaxa 619, 1–14.

Holness, S., Driver, A., Todd, S., Snaddon, K., Hamer, M., Raimondo, D., Daniels, F., Alexander, G., Bazelet, C., Bills, R., Bragg, C., Branch, B., Bruyns, P., Chakona, A., Child, M., Clarke, R.V., Coetzer, A., Coetzer, W., Colville, J., Conradie, W., Dean, R., Eardley, C., Ebrahim, I., Edge, D., Gaynor, D., Gear, S., Herbert, D., Kgatla, M., Lamula, K., Leballo, G., Lyle, R., Malatji, N., Mansell, M., Mecenero, S., Midgley, J., Mlambo, M., Mtshali, H., Simaika, J., Skowno, A., Staude, H., Tolley, K.A., Underhill, L., van der Colff, D., van Noort, S., von Staden, L., 2016. Biodiversity and Ecological Impacts: Landscape Processes, Ecosystems and Species, in: Scholes, R., Lochner, P., Schreiner, G., Snyman-Van der Walt, L., de Jager, M. (Eds.), Shale Gas Development in the Central Karoo: A Scientific Assessment of the Opportunities and Risks. CSIR, Pretoria, pp. 7–1 to 7–72.

Katoh, K., 2005. MAFFT version 5: improvement in accuracy of multiple sequence alignment. Nucleic Acids Res. 33, 511–518.

Katoh, K., Toh, H., 2008. Recent developments in the MAFFT multiple sequence alignment program. Brief. Bioinformatics. 9, 286–298.

Kingman, J.F.C., 1982. The coalescent. Stoch. Process their Appl. 13, 235–248.

Kingman, J.F.C., 2000. Origins of the Coalescent: 1974-1982. Genetics 150, 1461–1463.

© University of Pretoria

Kornilios, P., Thanou, E., Kapli, P., Parmakelis, A., Chatzaki, M., 2016. Peeking through the trapdoor: historical biogeography of the Aegean endemic spider *Cyrtocarenum* Ausserer, 1871 with an estimation of mtDNA substitution rates for Mygalomorphae. Mol. Phylogenet. Evol. 98, 300–313.

Kremen, C., Cowell, R.K., Erwin, T.L., Murphy, D.D., Noss, R.F., Sanjayan, M.A., 1993. Terrestrial Arthropod Assemblages: Their Use in Conservation Planning. Conserv. Biol.

Kück, P., Meusemann, K., 2010. FASconCAT: Convenient handling of data matrices. Mol. Phylogenet. Evol. 56, 1115–1118.

Kumar, S., Stecher, G., Tamura, K., 2016. MEGA7: Molecular Evolutionary Genetics Analysis Version 7.0 for bigger datasets. Mol. Biol. Evol. 33, 1870–1874.

Leavitt, D.H., Starrett, J., Westphal, M.F., Hedin, M., 2015. Multilocus sequence data reveal dozens of putative cryptic species in a radiation of endemic Californian mygalomorph spiders (Araneae, Mygalomorphae, Nemesiidae). Mol. Phylogenet. Evol. 91, 56–67.

Lemoine, F., Domelevo Entfellner, J.-B., Wilkinson, E., Correia, D., Dávila Felipe, M., De Oliveira, T., Gascuel, O., 2018. Renewing Felsenstein's phylogenetic bootstrap in the era of big data. Nature 556, 452–456.

Maddison, W.P., 1997. Gene trees in species trees. Syst. Biol. 46, 523–536.

Mantel, N., 1967. The detection of disease clustering and a generalized regression approach. Cancer Res. 27, 209–220.

Mason, L.D., Wardell-Johnson, G., Main, B.Y., 2018. The longest-lived spider: mygalomorphs dig deep, and persevere. Pac. Conserv. Biol. 24, 203.

Michonneau, F., 2017. Using GMYC for species delimitation. Zenodo.

Newton, L.G., Starrett, J., Hendrixson, B.E., Derkarabetian, S., Bond, J.E., 2020. Integrative species delimitation reveals cryptic diversity in the southern Appalachian *Antrodiaetus unicolor* (Araneae: Antrodiaetidae) species complex. Mol. Ecol. 29, 2269–2287.

Oksanen, J., Blanchet, F.G., Friendly, M., Kindt, R., Legendre, P., McGlinn, D., Minchin, P.R., O'Hara, R.B., Simpson, L, G., Solymos, P., Stevens, M.H.H., Szoecs, E., Wagner, H., 2019. vegan: Community Ecology Package.

O'Meara, B.C., 2010. New Heuristic Methods for Joint Species Delimitation and Species Tree Inference. Syst. Biol. 59, 59–73.

Opatova, V., Arnedo, M.A., 2014. Spiders on a hot volcanic roof: Colonisation pathways and phylogeography of the Canary Islands endemic trap-door spider *Titanidiops canariensis* (Araneae, Idiopidae). PLoS ONE 9, e115078.

Opatova, V., Hamilton, C.A., Hedin, M., De Oca, L.M., Král, J., Bond, J.E., 2020. Phylogenetic Systematics and Evolution of the Spider Infraorder Mygalomorphae Using Genomic Scale Data. Syst. Biol. syz064.

Papadopoulou, A., Monaghan, M. T., Barraclough, T. G., Vogler, A. P., 2009. Sampling Error Does Not Invalidate the Yule-Coalescent Model for Species Delimitation. A Response to Lohse (2009). Syst. Biol. 58, 442–444.

© University of Pretoria

Paradis, E., Schliep, K., 2019. Ape 5.0: An environment for modern phylogenetics and evolutionary analyses in R. Bioinformatics 35, 526–528.

Pons, J., Barraclough, T.G., Gomez-Zurita, J., Cardoso, A., Duran, D.P., Hazell, S., Kamoun, S., Sumlin, W.D., Vogler, A.P., 2006. Sequence-Based Species Delimitation for the DNA Taxonomy of Undescribed Insects. Syst. Biol. 55, 595–609.

Posada, D., 2008. jModelTest: Phylogenetic model averaging. Mol. Biol. Evol. 25, 1253–1256.

Puillandre, N., Lambert, A., Brouillet, S., Achaz, G., 2012. ABGD, Automatic Barcode Gap Discovery for primary species delimitation. Mol. Ecol. 21, 1864–1877.

R Core Team, 2017. R: A language and environment for statistical computing.

Rambaut, A., Drummond, A.J., Xie, D., Baele, G., Suchard, M.A., 2018. Posterior Summarization in Bayesian Phylogenetics Using Tracer 1.7. Syst. Biol. 67, 901–904.

Rix, M.G., Raven, R.J., Harvey, M.S., 2018. Systematics of the giant spiny trapdoor spiders of the genus *Gaius* Rainbow (Mygalomorphae: Idiopidae: Aganippini): documenting an iconic lineage of the Western Australian inland arid zone. J. Arachnol. 46, 438–472.

Ronquist, F., Huelsenbeck, J., 2003. MrBayes 3: Bayesian phylogenetic inference under mixed models. Bioinformatics 19, 1572–1574.

Ronquist, F., Huelsenbeck, J., Teslenko, M., 2011. MrBayes version 3.2 Manual: Tutorials and Model Summaries.

Rubinoff, D., Holland, B.S., 2005. Between two extremes: mitochondrial DNA is neither the panacea nor the nemesis of phylogenetic and taxonomic inference. Syst. Biol. 54, 952–961.

Satler, J.D., Carstens, B.C., Hedin, M., 2013. Multilocus Species Delimitation in a Complex of Morphologically Conserved Trapdoor Spiders (Mygalomorphae, Antrodiaetidae, *Aliatypus*). Syst. Biol. 62, 805–823.

Satler, J.D., Starrett, J., Hayashi, C.Y., Hedin, M., 2011. Inferring species trees from gene trees in a radiation of Californian trapdoor spiders (Araneae, Antrodiaetidae, *Aliatypus*). PLoS ONE 9, E25355.

Sethusa, T., 2016. Karoo BioGaps Project [WWW Document]. SANBI [ONLINE]. URL https://www.sanbi.org/karoo-biogaps-project/ (accessed 2.7.18).

Simon, C., Frati, F., Beckenbach, A., Crespi, B., Liu, H., Flook, P., 1994. Evolution, weighting and phylogenetic utility of mitochondrial gene sequences and a compilation of conserved polymerase chain reaction primers. Ann. Entomol. Soc. Am. 87, 651–702.

Stamatakis, A., 2014. RAxML version 8: a tool for phylogenetic analysis and post-analysis of large phylogenies. Bioinformatics 30, 1312–1313.

Stamatakis, A., Hoover, P., Rougennant, J., Renner, S., 2008. A rapid bootstrap algorithm for the RAxML web servers. Syst. Biol. 57, 758–771.

Suchard, M.A., Lemey, P., Baele, G., Ayres, D.L., Drummond, A.J., Rambaut, A., 2018. Bayesian phylogenetic and phylodynamic data integration using BEAST 1.10. Virus Evol. 4.

© University of Pretoria

Sukumaran, J., Knowles, L.L., 2017. Multispecies coalescent delimits structure, not species. PNAS. 114, 1607–1612.

Swofford, D.L., 2002. PAUP* Phylogenetic Analysis Using Parsimony (*and other methods), Version 4. ed. Sinauer Associates, Sutherland, Massachusetts.

Thanou, E., Kornilios, P., Poursanidis, D., Parmakelis, A., Arnedo, M.A., Chatzaki, M., 2017. Exploring the role of within-island ecogeographical factors: insights from the genetic diversity of Cretan trap-door spiders (*Cyrtocarenum cunicularium*, Ctenizidae: Araneae). Invertebr. Syst. 31, 506.

Veness, C., 2019. Movable Type Scripts: Calculate distance, bearing and more between Latitude/Longitude points.

Wilson, J. D., Hughes, J. M., Raven, R. J., Rix, M. G., Schmidt, D. J., 2018. Spiny trapdoor spiders (*Euoplos*) of eastern Australia: Broadly sympatric clades are differentiated by burrow architecture and male morphology. Mol. Phylogenet. Evol. 122, 157–165.

Wheeler, W.C., Coddington, J.A., Crowley, L.M., Dimitrov, D., Goloboff, P.A., Griswold, C.E., Hormiga, G., Prendini, L., Ramírez, M.J., Sierwald, P., Almeida-Silva, L., Alvarez-Padilla, F., Arnedo, M.A., Benavides Silva, L.R., Benjamin, S.P., Bond, J.E., Grismado, C.J., Hasan, E., Hedin, M., Izquierdo, M.A., Labarque, F.M., Ledford, J., Lopardo, L., Maddison, W.P., Miller, J.A., Piacentini, L.N., Platnick, N.I., Polotow, D., Silva-Dávila, D., Scharff, N., Szűts, T., Ubick, D., Vink, C.J., Wood, H.M., Zhang, J., 2017. The spider tree of life: phylogeny of Araneae based on target-gene analyses from an extensive taxon sampling. Cladistics 33, 574–616.

World Spider Catalog, 2020. World Spider Catalog Version 21.5 [WWW Document]. Natural History Museum Bern. https://doi.org/10.24436/2. (Accessed 17.7.20).

Xi, Z., Liu, L., Davis, C.C., 2016. The impact of missing data on species tree estimation. Mol. Biol. Evol. 33, 838–860.

Zhang, J., Kapli, P., Pavlidis, P., Stamatakis, A., 2013. A general species delimitation method with applications to phylogenetic placements. Bioinformatics 29, 2869–2876.

© University of Pretoria

Supplementary material

Table S1. Specimen information for all *Stasimopus* samples collected and outgroups selected for the genetic analyses. GenBank accession numbers are provided for all sequenced gene regions. Collection information for each specimen is provided.

No.	Species	CO1	Efɣ-1	16S	H3	Voucher codes	Museum Voucher
1	*Stasimopus* sp.	MK923763	MK923874	MK935573	OQ184933	02STAS01	NCA 2017/1834
2	*Stasimopus unispinosus*	MK923764	MK923875	MK935574	OQ184934	03STAS01	NCA 2017/1835
3	*Stasimopus unispinosus*	MK923765	MK923876	MK935575	---	03STAS02	NCA 2017/1836
4	*Stasimopus unispinosus*	MK923766	MK923877	---	---	03STAS03	NCA 2017/1837
5	*Stasimopus maraisi*	MK923767	MK923878	MK935576	---	04STAS01	NCA 2017/1839
6	*Stasimopus maraisi*	MK923768	MK923879	MK935577	---	04STAS02	NCA 2017/1840
7	*Stasimopus maraisi*	MK923769	MK923880	MK935578	---	04STAS03	NCA 2017/1841
8	*Stasimopus* sp.	MK923770	MK923881	MK935579	---	05BSTAS01	NCA 2017/1843
9	*Stasimopus* sp.	MK923771	MK923882	MK935580	---	05BSTAS02	NCA 2017/1844
10	*Stasimopus maraisi*	MK923772	MK923883	MK935581	---	05BSTAS03	NCA 2017/1845
11	*Stasimopus maraisi*	MK923773	MK923884	MK935582	---	05BSTAS04	NCA 2017/1846
12	Undescribed 1 / *S. hamartia* n. sp.	MK923774	MK923885	MK935583	---	06STAS01	NCA 2017/1849
13	Undescribed 1 / *S. hamartia* n. sp.	MK923775	MK923886	MK935584	---	06STAS02	NCA 2017/1850
14	Undescribed 1 / *S. hamartia* n. sp.	MK923776	MK923887	MK935585	OQ184935	07STAS01	NCA 2017/1852
15	*Stasimopus maraisi*	MK923777	MK923888	MK935586	---	07STAS02	NCA 2017/1853
16	Undescribed 1 / *S. hamartia* n. sp.	MK923778	MK923889	MK935587	---	07STAS03	NCA 2017/1854
17	*Stasimopus maraisi*	MK923779	MK923890	MK935588	---	08STAS01	NCA 2017/1855
18	*Stasimopus maraisi*	MK923780	MK923891	MK935589	---	08STAS03	NCA 2017/1857
19	*Stasimopus maraisi*	MK923781	MK923892	MK935590	OQ184941	08STAS04	NCA 2017/1858
20	*Stasimopus maraisi*	MK923782	MK923893	MK935591	---	08STAS05	NCA 2017/1859
21	*Stasimopus maraisi*	MK923783	MK923894	MK935592	---	09STAS01	NCA 2017/1861
22	*Stasimopus maraisi*	MK923784	MK923895	MK935593	---	09STAS02	NCA 2017/1862
23	*Stasimopus maraisi*	---	MK923896	MK935594	---	10ASTAS01	NCA 2017/1865
24	*Stasimopus maraisi*	MK923785	MK923897	MK935595	---	11STAS01	NCA 2017/1866
25	*Stasimopus leipoldti*	MK923786	MK923898	---	OQ184936	13STAS01	NCA 2017/1870
26	*Stasimopus leipoldti*	MK923787	MK923899	MK935596	---	13STAS02	NCA 2017/1871
27	*Stasimopus maraisi*	MK923788	---	MK935597	OQ184937	16ASTAS01	NCA 2017/1874
28	*Stasimopus maraisi*	MK923789	MK923900	---	---	16BSTAS01	NCA 2017/1875

© University of Pretoria

Table S1 (cont.). Specimen information for all *Stasimopus* samples collected and outgroups selected for the genetic analyses. GenBank accession numbers are provided for all sequenced gene regions. Collection information for each specimen is provided.

No.	Locality	Collection date	Collectors
1	SOUTH AFRICA, Northern Cape, Colesberg; BioGaps site 3050_2500	09/04/2017	S. Brandt, C. Sole, I. Engelbrecht, T. Majelantle
2	SOUTH AFRICA, Northern Cape, Richmond; BioGaps site 3105_2400	21/04/2017	S. Brandt, C. Sole, I. Engelbrecht, T. Majelantle
3	SOUTH AFRICA, Northern Cape, Richmond; BioGaps site 3105_2400	21/04/2017	S. Brandt, C. Sole, I. Engelbrecht, T. Majelantle
4	SOUTH AFRICA, Northern Cape, Richmond; BioGaps site 3105_2400	21/04/2017	S. Brandt, C. Sole, I. Engelbrecht, T. Majelantle
5	SOUTH AFRICA, Northern Cape, Richmond; near BioGaps site3130_2355	21/04/2017	S. Brandt, C. Sole, I. Engelbrecht, T. Majelantle
6	SOUTH AFRICA, Northern Cape, Richmond; near BioGaps site3130_2355	21/04/2017	S. Brandt, C. Sole, I. Engelbrecht, T. Majelantle
7	SOUTH AFRICA, Northern Cape, Richmond; near BioGaps site3130_2355	21/04/2017	S. Brandt, C. Sole, I. Engelbrecht, T. Majelantle
8	SOUTH AFRICA, Western Cape, Victoria West; BioGaps site 3155_2330	20/04/2017	S. Brandt, C. Sole, I. Engelbrecht, T. Majelantle
9	SOUTH AFRICA, Western Cape, Victoria West; BioGaps site 3155_2330	20/04/2017	S. Brandt, C. Sole, I. Engelbrecht, T. Majelantle
10	SOUTH AFRICA, Western Cape, Victoria West; BioGaps site 3155_2330	20/04/2017	S. Brandt, C. Sole, I. Engelbrecht, T. Majelantle
11	SOUTH AFRICA, Western Cape, Victoria West; BioGaps site 3155_2330	20/04/2017	S. Brandt, C. Sole, I. Engelbrecht, T. Majelantle
12	SOUTH AFRICA, Western Cape, Beaufort West; BioGaps site 3215_2305	20/04/2017	S. Brandt, C. Sole, I. Engelbrecht, T. Majelantle
13	SOUTH AFRICA, Western Cape, Beaufort West; BioGaps site 3215_2305	20/04/2017	S. Brandt, C. Sole, I. Engelbrecht, T. Majelantle
14	SOUTH AFRICA, Western Cape, Beaufort West; BioGaps site 3155_2250	20/04/2017	S. Brandt, C. Sole, I. Engelbrecht, T. Majelantle
15	SOUTH AFRICA, Western Cape, Beaufort West; BioGaps site 3155_2250	20/04/2017	S. Brandt, C. Sole, I. Engelbrecht, T. Majelantle
16	SOUTH AFRICA, Western Cape, Beaufort West; BioGaps site 3155_2250	20/04/2017	S. Brandt, C. Sole, I. Engelbrecht, T. Majelantle
17	SOUTH AFRICA, Northern Cape, Victoria West; BioGaps site 3120_2305	19/04/2017	S. Brandt, C. Sole, I. Engelbrecht, T. Majelantle
18	SOUTH AFRICA, Northern Cape, Victoria West; BioGaps site 3120_2305	19/04/2017	S. Brandt, C. Sole, I. Engelbrecht, T. Majelantle
19	SOUTH AFRICA, Northern Cape, Victoria West, BioGaps site 3120_2305	19/04/2017	S. Brandt, C. Sole, I. Engelbrecht, T. Majelantle
20	SOUTH AFRICA, Northern Cape, Victoria West; BioGaps site 3120_2305	19/04/2017	S. Brandt, C. Sole, I. Engelbrecht, T. Majelantle
21	SOUTH AFRICA, Northern Cape, Victoria West; BioGaps site 3105_2245	19/04/2017	S. Brandt, C. Sole, I. Engelbrecht, T. Majelantle
22	SOUTH AFRICA, Northern Cape, Victoria West; BioGaps site 3105_2245	19/04/2017	S. Brandt, C. Sole, I. Engelbrecht, T. Majelantle
23	SOUTH AFRICA, Northern Cape, Carnarvon; BioGaps site 3120_2215	19/04/2017	S. Brandt, C. Sole, I. Engelbrecht, T. Majelantle
24	SOUTH AFRICA, Northern Cape, Williston; BioGaps site 3110_2030	18/04/2017	S. Brandt, C. Sole, I. Engelbrecht, T. Majelantle
25	SOUTH AFRICA, Northern Cape, Laingsburg; BioGaps site 3240_2020	17/04/2017	S. Brandt, C. Sole, I. Engelbrecht, T. Majelantle
26	SOUTH AFRICA, Northern Cape, Laingsburg; BioGaps site 3240_2020	17/04/2017	S. Brandt, C. Sole, I. Engelbrecht, T. Majelantle
27	SOUTH AFRICA, Northern Cape, Fraserburg; near BioGaps site 3155_2125	17/04/2017	S. Brandt, C. Sole, I. Engelbrecht, T. Majelantle
28	SOUTH AFRICA, Northern Cape, Fraserburg; near BioGaps site 3155_2125	18/04/2017	S. Brandt, C. Sole, I. Engelbrecht, T. Majelantle

© University of Pretoria

Table S1 (cont.). Specimen information for all *Stasimopus* samples collected and outgroups selected for the genetic analyses. GenBank accession numbers are provided for all sequenced gene regions. Collection information for each specimen is provided.

No.	Species	CO1	Efŷ-1	16S	H3	Voucher codes	Museum Voucher
29	*Stasimopus maraisi*	MK923790	MK923901	MK935598	---	16BSTAS02	NCA 2017/1876
30	*Stasimopus maraisi*	MK923791	MK923902	---	---	18BSTAS01	NCA 2017/1882
31	*Stasimopus maraisi*	MK923792	MK923903	MK935599	---	18BSTAS02	NCA 2017/1883
32	*Stasimopus maraisi*	MK923793	MK923904	MK935600	---	18BSTAS03	NCA 2017/1884
33	*Stasimopus maraisi*	MK923794	MK923905	MK935601	OQ184942	19STAS01	NCA 2017/1885
34	*Stasimopus maraisi*	MK923795	MK923906	---	---	19STAS02	NCA 2017/1886
35	*Stasimopus maraisi*	MK923796	MK923907	---	---	20BSTAS01	NCA 2017/1887
36	Undescribed 1 / *S. hamartia* n. sp.	MK923797	MK923908	MK935602	OQ184943	21STAS01	NCA 2017/1888
37	Undescribed 1 / *S. hamartia* n. sp.	MK923798	MK923909	MK935603	---	21STAS02	NCA 2017/1889
38	Undescribed 1 / *S. hamartia* n. sp.	MK923799	MK923910	MK935604	---	21STAS03	NCA 2017/1890
39	Undescribed 1 / *S. hamartia* n. sp.	MK923800	MK923911	MK935605	---	21STAS04	NCA 2017/1891
40	Undescribed 1 / *S. hamartia* n. sp.	---	MK923912	MK935606	---	21STAS05	NCA 2017/1892
41	*Stasimopus* sp.	MK923801	MK923913	MK935607	---	22STAS01	NCA 2017/1897
42	*Stasimopus* sp.	MK923802	MK923914	---	---	23STAS01	NCA 2017/1899
43	*Stasimopus astutus*	MK923803	MK923915	MK935608	OQ184938	24STAS01	NCA 2017/1903
44	*Stasimopus astutus*	MK923804	MK923916	MK935609	OQ184939	25BSTAS01	NCA 2017/1906
45	*Stasimopus astutus*	MK923805	MK923917	MK935610	---	25BSTAS02	NCA 2017/1907
46	*Stasimopus erythrognathus*	MK923806	MK923918	---	---	30ASTAS01	NCA 2017/1913
47	*Stasimopus erythrognathus*	MK923807	MK923919	MK935611	OQ184940	30BSTAS01	NCA 2017/1914
48	*Stasimopus* sp.	MK923861	---	---	---	NCRASTAS01	NCA 2017/1915
49	*Stasimopus erythrognathus*	MK923862	MK923975	MK935675	---	NCRASTAS02	NCA 2017/1916
50	*Stasimopus* sp.	MK923863	---	MK935676	---	NCRASTAS03	NCA 2017/1917
51	Undescribed 3 / *S. venterstadensis* n. sp.	MK923808	MK923920	MK935612	---	31STAS01	NCA 2019/608
52	New species 3 / *S. venterstadensis* n. sp.	---	---	MK935613	---	31STAS02	NCA 2019/609
53	New species 3 / *S. venterstadensis* n. sp.	MK923809	---	MK935614	---	31STAS03	NCA 2019/610
54	*Stasimopus* sp.	MK923810	MK923921	MK935615	---	32STAS01	NCA 2019/603
55	*Stasimopus erythrognathus*	MK923811	---	MK935616	---	33STAS01	NCA 2019/625

© University of Pretoria

Table S1 (cont.). Specimen information for all *Stasimopus* samples collected and outgroups selected for the genetic analyses. GenBank accession numbers are provided for all sequenced gene regions. Collection information for each specimen is provided.

No.	Locality	Collection date	Collectors
29	SOUTH AFRICA, Northern Cape, Fraserburg; near BioGaps site 3155_2125	18/04/2017	S. Brandt, C. Sole, I. Engelbrecht, T. Majelantle
30	SOUTH AFRICA, Western Cape, Beaufort West; BioGaps site 3225_2205	16/04/2017	S. Brandt, C. Sole, I. Engelbrecht, T. Majelantle
31	SOUTH AFRICA, Western Cape, Beaufort West; BioGaps site 3225_2205	16/04/2017	S. Brandt, C. Sole, I. Engelbrecht, T. Majelantle
32	SOUTH AFRICA, Western Cape, Beaufort West; BioGaps site 3225_2205	16/04/2017	S. Brandt, C. Sole, I. Engelbrecht, T. Majelantle
33	SOUTH AFRICA, Western Cape, Prince Albert; BioGaps site 3255_2220	15/04/2017	S. Brandt, C. Sole, I. Engelbrecht, T. Majelantle
34	SOUTH AFRICA, Western Cape, Prince Albert; BioGaps site 3255_2220	15/04/2017	S. Brandt, C. Sole, I. Engelbrecht, T. Majelantle
35	SOUTH AFRICA, Eastern Cape, Willowmore; BioGaps site 3245_2315	14/04/2017	S. Brandt, C. Sole, I. Engelbrecht, T. Majelantle
36	SOUTH AFRICA, Eastern Cape, Willowmore; BioGaps site 3225_2335	14/04/2017	S. Brandt, C. Sole, I. Engelbrecht, T. Majelantle
37	SOUTH AFRICA, Eastern Cape, Willowmore; BioGaps site 3225_2335	14/04/2017	S. Brandt, C. Sole, I. Engelbrecht, T. Majelantle
38	SOUTH AFRICA, Eastern Cape, Willowmore; BioGaps site 3225_2335	14/04/2017	S. Brandt, C. Sole, I. Engelbrecht, T. Majelantle
39	SOUTH AFRICA, Eastern Cape, Willowmore; BioGaps site 3225_2335	14/04/2017	S. Brandt, C. Sole, I. Engelbrecht, T. Majelantle
40	SOUTH AFRICA, Eastern Cape, Willowmore; BioGaps site 3225_2335	14/04/2017	S. Brandt, C. Sole, I. Engelbrecht, T. Majelantle
41	SOUTH AFRICA, Eastern Cape, Graaff Reinet; BioGaps site 3145_2430	13/04/2017	S. Brandt, C. Sole, I. Engelbrecht, T. Majelantle
42	SOUTH AFRICA, Eastern Cape, Graaff Reinet; BioGaps site 3210_2445	13/04/2017	S. Brandt, C. Sole, I. Engelbrecht, T. Majelantle
43	SOUTH AFRICA, Eastern Cape, Jansenville; BioGaps site 3300_2455	12/04/2017	S. Brandt, C. Sole, I. Engelbrecht, T. Majelantle
44	SOUTH AFRICA, Eastern Cape, Somerset East; BioGaps site 3230_2510	12/04/2017	S. Brandt, C. Sole, I. Engelbrecht, T. Majelantle
45	SOUTH AFRICA, Eastern Cape, Somerset East; BioGaps site 3230_2510	12/04/2017	S. Brandt, C. Sole, I. Engelbrecht, T. Majelantle
46	SOUTH AFRICA, Eastern Cape, Tarkastad; BioGaps site 3150_2605	10/04/2017	S. Brandt, C. Sole, I. Engelbrecht, T. Majelantle
47	SOUTH AFRICA, Eastern Cape, Tarkastad; BioGaps site 3150_2605	10/04/2017	S. Brandt, C. Sole, I. Engelbrecht, T. Majelantle
48	SOUTH AFRICA, Eastern Cape, Cradock	10/04/2017	S. Brandt, C. Sole, I. Engelbrecht, T. Majelantle
49	SOUTH AFRICA, Eastern Cape, Cradock	10/04/2017	S. Brandt, C. Sole, I. Engelbrecht, T. Majelantle
50	SOUTH AFRICA, Eastern Cape, Cradock	10/04/2017	S. Brandt, C. Sole, I. Engelbrecht, T. Majelantle
51	SOUTH AFRICA, Eastern Cape, Kleinvie; near Biogaps site 3055_2540	12/05/2018	S. Brandt, C. Sole, I. Engelbrecht, E. Brand
52	SOUTH AFRICA, Eastern Cape, Kleinvie; near Biogaps site 3055_2540	12/05/2018	S. Brandt, C. Sole, I. Engelbrecht, E. Brand
53	SOUTH AFRICA, Eastern Cape, Kleinvie; near Biogaps site 3055_2540	12/05/2018	S. Brandt, C. Sole, I. Engelbrecht, E. Brand
54	SOUTH AFRICA, Eastern Cape, Grootdam; Biogaps site 3125_2610	13/05/2018	S. Brandt, C. Sole, I. Engelbrecht, E. Brand
55	SOUTH AFRICA, Eastern Cape, Farm Weltevreden; Biogaps site 3140_2640	13/05/2018	S. Brandt, C. Sole, I. Engelbrecht, E. Brand

© University of Pretoria

Table S1 (cont.). Specimen information for all *Stasimopus* samples collected and outgroups selected for the genetic analyses. GenBank accession numbers are provided for all sequenced gene regions. Collection information for each specimen is provided.

No.	Species	CO1	Efŋ-1	16S	H3	Voucher codes	Museum Voucher
56	*Stasimopus erythrognathus*	---	---	MK935617	---	33STAS02	NCA 2019/626
57	*Stasimopus erythrognathus*	MK923812	---	MK935618	---	33STAS03	NCA 2019/627
58	*Stasimopus erythrognathus*	MK923813	MK923922	MK935619	---	33STAS04	NCA 2019/628
59	*Stasimopus* sp.	MK923814	MK923923	MK935620	---	35STAS01	NCA 2019/620
60	*Stasimopus* sp.	MK923815	MK923924	MK935621	---	35STAS02	NCA 2019/621
61	*Stasimopus* sp.	MK923816	MK923925	---	---	35STAS03	NCA 2019/622
62	*Stasimopus* sp.	---	MK923926	MK935622	---	35STAS04	NCA 2019/623
63	Undescribed 7 / *S. finni* n. sp.	MK923817	---	MK935623	---	36STAS01	NCA 2019/605
64	Undescribed 5 / *S. theaei* n. sp.	MK923818	---	MK935624	---	36STAS02	NCA 2019/606
65	*Stasimopus astutus*	MK923819	---	MK935625	---	37ASTAS01	NCA 2019/638
66	*Stasimopus astutus*	MK923820	MK923927	MK935626	---	37BSTAS01	NCA 2019/635
67	Undescribed 2 / *S. dylani* n. sp.	MK923821	MK923928	MK935627	---	38BSTAS01	NCA 2019/676
68	*Stasimopus maraisi*	MK923822	MK923929	MK935628	---	38BSTAS02	NCA 2019/677
69	Undescribed 1 / *S. hamartia* n. sp.	MK923823	MK923930	MK935629	---	39STAS01	NCA 2019/660
70	Undescribed 1 / *S. hamartia* n. sp.	MK923824	MK923931	MK935630	---	39STAS02	NCA 2019/661
71	*Stasimopus maraisi*	MK923825	MK923932	MK935631	---	41STAS01	NCA 2019/636
72	*Stasimopus maraisi*	MK923826	MK923933	MK935632	---	41STAS02	NCA 2019/637
73	*Stasimopus maraisi*	MK923827	MK923934	MK935633	---	41STAS03	NCA 2019/683
74	*Stasimopus maraisi*	MK923828	MK923935	MK935634	---	41STAS04	NCA 2019/684
75	*Stasimopus* sp.	MK923829	MK923936	MK935635	---	42STAS01	NCA 2019/690
76	*Stasimopus* sp.	MK923830	MK923937	MK935636	---	42STAS02	NCA 2019/691
77	*Stasimopus* sp.	MK923831	MK923938	MK935637	---	42STAS03	NCA 2019/692
78	*Stasimopus* sp.	MK923832	MK923939	MK935638	---	42STAS04	NCA 2019/693
79	*Stasimopus* sp.	---	MK923940	MK935639	---	43STAS01	NCA 2019/678
80	*Stasimopus* sp.	MK923833	MK923941	MK935640	---	44ASTAS01	NCA 2019/662
81	*Stasimopus maraisi*	MK923834	MK923942	MK935641	---	47STAS01	NCA 2019/630
82	*Stasimopus maraisi*	MK923835	MK923943	MK935642	---	47STAS02	NCA 2019/631

© University of Pretoria

Table S1 (cont.). Specimen information for all *Stasimopus* samples collected and outgroups selected for the genetic analyses. GenBank accession numbers are provided for all sequenced gene regions. Collection information for each specimen is provided.

No.	Locality	Collection date	Collectors
56	SOUTH AFRICA, Eastern Cape, Farm Weltevreden; Biogaps site 3140_2640	13/05/2018	S. Brandt, C. Sole, I. Engelbrecht, E. Brand
57	SOUTH AFRICA, Eastern Cape, Farm Weltevreden; Biogaps site 3140_2640	13/05/2018	S. Brandt, C. Sole, I. Engelbrecht, E. Brand
58	SOUTH AFRICA, Eastern Cape, Farm Weltevreden; Biogaps site 3140_2640	13/05/2018	S. Brandt, C. Sole, I. Engelbrecht, E. Brand
59	SOUTH AFRICA, Eastern Cape, Rietrivier; near Biogaps site 3225_2540	14/05/2018	S. Brandt, C. Sole, I. Engelbrecht, E. Brand
60	SOUTH AFRICA, Eastern Cape, Rietrivier; near Biogaps site 3225_2540	14/05/2018	S. Brandt, C. Sole, I. Engelbrecht, E. Brand
61	SOUTH AFRICA, Eastern Cape, Rietrivier; near Biogaps site 3225_2540	14/05/2018	S. Brandt, C. Sole, I. Engelbrecht, E. Brand
62	SOUTH AFRICA, Eastern Cape, Rietrivier; near Biogaps site 3225_2540	14/05/2018	S. Brandt, C. Sole, I. Engelbrecht, E. Brand
63	SOUTH AFRICA, Eastern Cape; Biogaps site 3255_2535	14/05/2018	S. Brandt, C. Sole, I. Engelbrecht, E. Brand
64	SOUTH AFRICA, Eastern Cape; Biogaps site 3255_2535	14/05/2018	S. Brandt, C. Sole, I. Engelbrecht, E. Brand
65	SOUTH AFRICA, Eastern Cape, Aberdeen; near Biogaps site 3245_2405	14/05/2018	S. Brandt, C. Sole, I. Engelbrecht, E. Brand
66	SOUTH AFRICA, Eastern Cape, Aberdeen; near Biogaps site 3245_2405	14/05/2018	S. Brandt, C. Sole, I. Engelbrecht, E. Brand
67	SOUTH AFRICA, Eastern Cape, Willowmore.	15/05/2018	S. Brandt, C. Sole, I. Engelbrecht, E. Brand
68	SOUTH AFRICA, Eastern Cape, Willowmore.	15/05/2018	S. Brandt, C. Sole, I. Engelbrecht, E. Brand
69	SOUTH AFRICA, Western Cape, Beaufort West; Biogaps site 3235_2240	15/05/2018	S. Brandt, C. Sole, I. Engelbrecht, E. Brand
70	SOUTH AFRICA, Western Cape, Beaufort West; Biogaps site 3235_2240	15/05/2018	S. Brandt, C. Sole, I. Engelbrecht, E. Brand
71	SOUTH AFRICA, Northern Cape, Beaufort West; Biogaps site 3210_2150	16/05/2018	S. Brandt, C. Sole, I. Engelbrecht, E. Brand
72	SOUTH AFRICA, Northern Cape, Beaufort West; Biogaps site 3210_2150	16/05/2018	S. Brandt, C. Sole, I. Engelbrecht, E. Brand
73	SOUTH AFRICA, Northern Cape, Beaufort West; Biogaps site 3210_2150	16/05/2018	S. Brandt, C. Sole, I. Engelbrecht, E. Brand
74	SOUTH AFRICA, Northern Cape, Beaufort West; Biogaps site 3210_2150	16/05/2018	S. Brandt, C. Sole, I. Engelbrecht, E. Brand
75	SOUTH AFRICA, Western Cape, Beaufort West; Biogaps site 3215_2140	16/05/2018	S. Brandt, C. Sole, I. Engelbrecht, E. Brand
76	SOUTH AFRICA, Western Cape, Beaufort West; Biogaps site 3215_2140	16/05/2018	S. Brandt, C. Sole, I. Engelbrecht, E. Brand
77	SOUTH AFRICA, Western Cape, Beaufort West; Biogaps site 3215_2140	16/05/2018	S. Brandt, C. Sole, I. Engelbrecht, E. Brand
78	SOUTH AFRICA, Western Cape, Beaufort West; Biogaps site 3215_2140	16/05/2018	S. Brandt, C. Sole, I. Engelbrecht, E. Brand
79	SOUTH AFRICA, Northern Cape, Fraserburg; Biogaps site 3215_2115	16/05/2018	S. Brandt, C. Sole, I. Engelbrecht, E. Brand
80	SOUTH AFRICA, Northern Cape, Sutherland; Biogaps site 3230_2050	17/05/2018	S. Brandt, C. Sole, I. Engelbrecht, E. Brand
81	SOUTH AFRICA, Northern Cape, Williston; near Biogaps site 3150_2045	19/05/2018	S. Brandt, C. Sole, I. Engelbrecht, E. Brand
82	SOUTH AFRICA, Northern Cape, Williston; near Biogaps site 3150_2045	19/05/2018	S. Brandt, C. Sole, I. Engelbrecht, E. Brand

© University of Pretoria

Table S1 (cont.). Specimen information for all *Stasimopus* samples collected and outgroups selected for the genetic analyses. GenBank accession numbers are provided for all sequenced gene regions. Collection information for each specimen is provided.

No.	Species	CO1	Efγ-1	16S	H3	Voucher codes	Museum Voucher
83	*Stasimopus maraisi*	MK923836	MK923944	MK935643	---	47STAS03	NCA 2019/632
84	*Stasimopus* sp.	MK923837	MK923945	MK935644	---	47STAS04	NCA 2019/633
85	*Stasimopus* sp.	MK923838	MK923946	MK935645	---	47STAS05	NCA 2019/634
86	*Stasimopus maraisi*	MK923839	---	MK935646	---	50STAS01	NCA 2019/689
87	*Stasimopus maraisi*	MK923840	MK923947	MK935647	---	51STAS01	NCA 2019/640
88	*Stasimopus maraisi*	MK923841	MK923948	MK935648	---	51STAS02	NCA 2019/685
89	*Stasimopus maraisi*	MK923842	MK923949	MK935649	---	51STAS03	NCA 2019/686
90	*Stasimopus maraisi*	MK923843	MK923950	MK935650	---	52STAS01	NCA 2019/688
91	*Stasimopus astutus*	MK923844	---	MK935651	---	53STAS01	NCA 2019/647
92	*Stasimopus maraisi*	---	MK923951	MK935652	---	53STAS02	NCA 2019/648
93	*Stasimopus astutus*	MK923845	MK923952	MK935653	---	53STAS03	NCA 2019/649
94	*Stasimopus astutus*	MK923846	MK923953	MK935654	---	53STAS04	NCA 2019/650
95	*Stasimopus astutus*	---	MK923954	MK935655	---	53STAS05	NCA 2019/651
96	*Stasimopus maraisi*	MK923847	MK923955	MK935656	---	55BSTAS01	NCA 2019/680
97	Undescribed 8 / *S. teras* n. sp.	MK923848	MK923956	MK935657	---	56STAS01	NCA 2019/643
98	*Stasimopus maraisi*	---	MK923957	MK935658	---	57STAS01	NCA 2019/681
99	*Stasimopus schrieneri*	MK923849	MK923958	MK935659	---	58STAS01	NCA 2019/671
100	*Stasimopus schrieneri*	MK923850	MK923959	MK935660	---	58STAS02	NCA 2019/672
101	*Stasimopus schrieneri*	MK923851	MK923960	MK935661	---	58STAS03	NCA 2019/673
102	*Stasimopus unispinosus*	---	MK923961	MK935662	---	59ASTAS01	NCA 2019/654
103	*Stasimopus unispinosus*	---	MK923962	MK935663	---	59ASTAS02	NCA 2019/655
104	*Stasimopus unispinosus*	---	MK923963	MK935664	---	59BSTAS01	NCA 2019/617
105	Undescribed 6 / *S. ignis* n. sp.	MK923852	MK923964	MK935665	---	59BSTAS02	NCA 2019/653
106	*Stasimopus erythrognathus*	---	MK923965	MK935666	---	60STAS01	NCA 2019/645

© University of Pretoria

Table S1 (cont.). Specimen information for all *Stasimopus* samples collected and outgroups selected for the genetic analyses. GenBank accession numbers are provided for all sequenced gene regions. Collection information for each specimen is provided.

No.	Locality	Collection date	Collectors
83	SOUTH AFRICA, Northern Cape, Williston; near Biogaps site 3150_2045	19/05/2018	S. Brandt, C. Sole, I. Engelbrecht, E. Brand
84	SOUTH AFRICA, Northern Cape, Williston; near Biogaps site 3150_2045	19/05/2018	S. Brandt, C. Sole, I. Engelbrecht, E. Brand
85	SOUTH AFRICA, Northern Cape, Williston; near Biogaps site 3150_2045	19/05/2018	S. Brandt, C. Sole, I. Engelbrecht, E. Brand
86	SOUTH AFRICA, Northern Cape, Bakenskop; Biogaps site 3120_2140	20/05/2018	S. Brandt, C. Sole, I. Engelbrecht, E. Brand
87	SOUTH AFRICA, Western Cape, Basterspoortseleegte; near Biogaps site 3140_2210	21/05/2018	S. Brandt, C. Sole, I. Engelbrecht, E. Brand
88	SOUTH AFRICA, Western Cape, Basterspoortseleegte; near Biogaps site 3140_2210	21/05/2018	S. Brandt, C. Sole, I. Engelbrecht, E. Brand
89	SOUTH AFRICA, Western Cape, Basterspoortseleegte; near Biogaps site 3140_2210	21/05/2018	S. Brandt, C. Sole, I. Engelbrecht, E. Brand
90	SOUTH AFRICA, Western Cape, Matjiesfontein	21/05/2018	S. Brandt, C. Sole, I. Engelbrecht, E. Brand
92	SOUTH AFRICA, Western Cape, Waterkloof; near Biogaps site 3210_2345	22/05/2018	S. Brandt, C. Sole, I. Engelbrecht, E. Brand
93	SOUTH AFRICA, Western Cape, Waterkloof; near Biogaps site 3210_2345	22/05/2018	S. Brandt, C. Sole, I. Engelbrecht, E. Brand
94	SOUTH AFRICA, Western Cape, Waterkloof; near Biogaps site 3210_2345	22/05/2018	S. Brandt, C. Sole, I. Engelbrecht, E. Brand
95	SOUTH AFRICA, Western Cape, Waterkloof; near Biogaps site 3210_2345	22/05/2018	S. Brandt, C. Sole, I. Engelbrecht, E. Brand
96	SOUTH AFRICA, Western Cape, Gabrielspruit; Biogaps site 3140_2320	22/05/2018	S. Brandt, C. Sole, I. Engelbrecht, E. Brand
97	SOUTH AFRICA, Northern Cape, Sandkop; Biogaps site 3125_2330	22/05/2018	S. Brandt, C. Sole, I. Engelbrecht, E. Brand
98	SOUTH AFRICA, Northern Cape, Richmond; near Biogaps site 4143	23/05/2018	S. Brandt, C. Sole, I. Engelbrecht, E. Brand
99	SOUTH AFRICA, Northern Cape, Richmond; near Biogaps site 3135_2410	23/05/2018	S. Brandt, C. Sole, I. Engelbrecht, E. Brand
100	SOUTH AFRICA, Northern Cape, Richmond; near Biogaps site 3135_2410	23/05/2018	S. Brandt, C. Sole, I. Engelbrecht, E. Brand
101	SOUTH AFRICA, Northern Cape, Richmond; near Biogaps site 3135_2410	23/05/2018	S. Brandt, C. Sole, I. Engelbrecht, E. Brand
102	SOUTH AFRICA, Northern Cape, Hanover	24/05/2018	S. Brandt, C. Sole, I. Engelbrecht, E. Brand
103	SOUTH AFRICA, Northern Cape, ca. 6.6km ENE Hanover, 3km along R389 Noupoort, N side of road	24/05/2018	S. Brandt, C. Sole, I. Engelbrecht, E. Brand
104	SOUTH AFRICA, Northern Cape, Hanover	24/05/2018	S. Brandt, C. Sole, I. Engelbrecht, E. Brand
105	SOUTH AFRICA, Northern Cape, Hanover	24/05/2018	S. Brandt, C. Sole, I. Engelbrecht, E. Brand
106	SOUTH AFRICA, Eastern Cape, Kambrokop	25/05/2018	S. Brandt, C. Sole, I. Engelbrecht, E. Brand

© University of Pretoria

Table S1 (cont.). Specimen information for all *Stasimopus* samples collected and outgroups selected for the genetic analyses. GenBank accession numbers are provided for all sequenced gene regions. Collection information for each specimen is provided.

No.	Species	CO1	Efγ-1	16S	H3	Voucher codes	Museum Voucher
107	*Stasimopus erythrognathus*	MK923853	MK923966	MK935667	---	60STAS02	NCA 2019/665
108	*Stasimopus erythrognathus*	MK923854	MK923967	MK935668	---	60STAS03	NCA 2019/666
109	*Stasimopus erythrognathus*	---	MK923968	MK935669	---	ELKSTAS01	NCA 2019/611
110	*Stasimopus erythrognathus*	MK923855	MK923969	MK935670	---	ELKSTAS03	NCA 2019/613
111	*Stasimopus erythrognathus*	MK923856	MK923970	---	---	ELKSTAS04	NCA 2019/614
112	*Stasimopus erythrognathus*	MK923857	MK923971	MK935671	---	ELKSTAS05	NCA 2019/615
113	Undescribed 4 / *S. karooensis* n. sp.	MK923858	MK923972	MK935672	---	ELKSTAS06	NCA 2019/616
114	Undescribed 2 / *S. dylani* n. sp.	MK923859	MK923973	MK935673	---	FRESTAS01	NCA 2019/663
115	Undescribed 2 / *S. dylani* n. sp.	MK923860	MK923974	MK935674	---	FRESTAS02	NCA 2019/664
117	Undescribed 4 / *S. karooensis* n. sp.	MK923864	---	MK935677	---	SAMC7293	SAM-ENW-C007293
118	*Stasimopus hewitti*	---	---	MK935678	---	SH01	NCA 2019/695
119	*Stasimopus hewitti*	MK923865	---	MK935679	---	SH02	NCA 2019/696
120	Undescribed 2 / *S. dylani* n. sp.	MK923867	---	MK935682	---	SUOJ01	NCA 2019/697
121	Undescribed 2 / *S. dylani* n. sp.	MK923868	---	---	---	SUOJ02	NCA 2019/698
122	Undescribed 2 / *S. dylani* n. sp.	MK923869	---	MK935683	---	SUOJ03	NCA 2019/699
123	*Stasimopus mandelai*	MK923870	---	MK935684	---	SUOJ04	NCA 2019/700
124	*Stasimopus mandelai*	MK923871	---	MK935685	---	SUOJ05	NCA 2019/701
125	Undescribed 2 / *S. dylani* n. sp.	MK923872	---	MK935686	---	SUOJ06	NCA 2019/702
126	*Stasimopus astutus*	MK923873	---	MK935687	---	SUOJ07	NCA 2019/703
127	*Stasimopus cf. rufidens*	---	---	MK935681	---	SUH01	NCA 2019/704
128	*Hadronyche cerberea*	JN130348	---	---	---	OZ46_1.1_H	-
129	*Actinopus* sp.	KY017543	JQ358722	KY015695	---	ARAMY002873	MY2873
130	*Calisoga longitarsis*	---	DQ680314	KY015979	---	16S:ARAMY00028 1; EF-1γ: MY77	16S: AUM MY281
131	*Kiama lachrymoides*	---	---	KY015982	---	ARAMY002094	AUM MY2094
132	*Pionothele* sp.	---	KR182477	---	---	AUMS6718	DHL-2015
133	*Paratropis* sp.	KY017841	---	KY016026	---	ARAJB000013	-

© University of Pretoria

Table S1 (cont.). Specimen information for all *Stasimopus* samples collected and outgroups selected for the genetic analyses. GenBank accession numbers are provided for all sequenced gene regions. Collection information for each specimen is provided.

No.	Locality	Collection date	Collectors
107	SOUTH AFRICA, Eastern Cape, Kambrokop	25/05/2018	S. Brandt, C. Sole, I. Engelbrecht, E. Brand
108	SOUTH AFRICA, Eastern Cape, Kambrokop	25/05/2018	S. Brandt, C. Sole, I. Engelbrecht, E. Brand
109	SOUTH AFRICA, Eastern Cape, Farm Elandskuil	12/05/2018	S. Brandt, C. Sole, I. Engelbrecht, E. Brand
110	SOUTH AFRICA, Eastern Cape, Farm Elandskuil	12/05/2018	S. Brandt, C. Sole, I. Engelbrecht, E. Brand
111	SOUTH AFRICA, Eastern Cape, Farm Elandskuil	12/05/2018	S. Brandt, C. Sole, I. Engelbrecht, E. Brand
112	SOUTH AFRICA, Eastern Cape, Farm Elandskuil	12/05/2018	S. Brandt, C. Sole, I. Engelbrecht, E. Brand
113	SOUTH AFRICA, Eastern Cape, Farm Elandskuil	12/05/2018	S. Brandt, C. Sole, I. Engelbrecht, E. Brand
114	SOUTH AFRICA, Western Cape, Murraysburg.	21/05/2018	S. Brandt, C. Sole, I. Engelbrecht, E. Brand
115	SOUTH AFRICA, Western Cape, Murraysburg	21/05/2018	S. Brandt, C. Sole, I. Engelbrecht, E. Brand
117	SOUTH AFRICA, Pearston, Plains of Camdeboo Game Reserve	09/05/2010 / 26/06/2010	S. van Noort
118	SOUTH AFRICA, Gauteng, Wonderboom Distr.	-	-
119	SOUTH AFRICA, Gauteng, Wonderboom Distr.	-	-
120	SOUTH AFRICA, Eastern cape, Jansenville.	17/07/2015	I. Engelbrecht; D. Kambas
121	SOUTH AFRICA, Eastern cape, Jansenville.	17/07/2015	I. Engelbrecht; D. Kambas
122	SOUTH AFRICA, Eastern cape, Jansenville.	17/07/2015	I. Engelbrecht; D. Kambas
123	SOUTH AFRICA, Eastern cape, Jansenville.	17/07/2015	I. Engelbrecht; D. Kambas
124	SOUTH AFRICA, Eastern cape, Jansenville.	17/07/2015	I. Engelbrecht; D. Kambas
125	SOUTH AFRICA, Eastern cape, Jansenville.	17/07/2015	I. Engelbrecht; D. Kambas
126	SOUTH AFRICA, Eastern cape, Jansenville.	17/07/2015	I. Engelbrecht; D. Kambas
127	SOUTH AFRICA, KwaZulu-Natal, Ukuwela, Hhluhluwe	-	-
128	AUSTRALIA, New South Wales	Reference: (Beavis et al., 2011)	
129	ARGENTINA, Buenos Aires, Parque Leloir	Reference: CO1; 16S: (Wheeler et al., 2016); EF-1ɣ: (Bond et al., 2012)	
130	USA, California, vic Mariposa	Reference: (Wheeler et al., 2016); EF-1ɣ: (Ayoub et al., 2007)	
131	AUSTRALIA, New South Wales.	Reference: (Wheeler et al., 2016)	
132	-	Reference: (Leavitt et al., 2015)	
133	EF-1ɣ: ECUDOR, Jatun Sacha	Reference: (Bond et al., 2012)	

© University of Pretoria

Table S2. Summary of primers used in this study and their corresponding gene regions.

Gene Region	Primer name	Sequence	Primer references
CO1	HCO2198	5' - TAA ACT TCA GGG TGA CCA AAA - 3'	(Folmer et al., 1994)
	LCO1490	5' - GGT CAA CAA ATC ATA AAG ATA - 3'	
	C1-J-1751	5' - GGA TCA CCT GAT ATA GCA TTC CC - 3'	
16S	LRN-13398	5' - CGC CTG TTT AAC AAA AAC AT - 3'	(Simon et al., 1994)
	LR-J-12961	5' - TTT AAT CCA ACA TCG AGG - 3'	(Cognato and Vogler, 2001)
EF-1ɣ	EF1gF78	5’ - ATT GCB GCN CAG TAY AGY GG - 3’	(Ayoub et al., 2007)
	EF1gR1258	5’ - CCT TGR TTG AAY TTC TTT CC - 3’	
	CyrtEF1L	5’ - CAG TTA CGC GGT ACC ACT CT - 3’	(Kornilios et al., 2016)
	CyrtEF1R	5’ - CGC ATC TTG TCT AGC CTC TG - 3’	

Table S3. The PCR protocol used for CO1 and 16S gene regions. The annealing temperature was adjusted if a sample did not amplify.

Phase	Temperature (°C)	Time (s)	
Denaturation	94	300	
	94	15	**40 cycles**
Annealing	48-52	5	
Amplification	72	15	
	72	420	

Table S4. The PCR protocol used for EF-1ɣ gene region for both the initial and nested PCR. The initial PCR used the primers EF1g78 and EF1g1258 whereas the nested PCR used CyrtEF1L and CyrtEF1R. The annealing temperature was adjusted if a sample did not amplify.

Phase	Temperature (°C)	Time (s)	
Denaturation	94	180	
	94	60	**35 cycles**
Annealing	50 / 52	60	
Amplification	72	60	
	72	60	

© University of Pretoria

Table S5. Model of nucleotide substitution selected for each gene region. The contribution of base pairs and samples by each gene region to the combined phylogeny is given. The Akaike Information Criterion (AIC) and the Bayesian Information Criterion (BIC) were both produced by jModelTest.

Dataset	Gene region	Base pairs	Number of samples	Percentage individuals included in phylogeny (%)	AIC model	BIC model	Model selected
Stasimopus	CO1	401	111	86	TIM1+ I+ G (I=0.379; G=0.638)	TIM1+ I+ G (I=0.379; G=0.638)	**GTR+ I+ G (I=0.379; G=0.638)**
Stasimopus	16S	317	115	89.15	TIM3+ G (G=0.348)	TIM3+ G (G=0.348)	**GTR+ G (G=0.348)**
Stasimopus	CO1_16S	720	101	-	TPM1uf+ I+ G (I= 0.001; G=0.299)	TPM1uf+ I+ G (I= 0.001; G=0.296)	**GTR+ G (G=0.299)**
Stasimopus	EFɣ-1	539	103	79.84	TPM2uf+ I+ G (I=0.519; G=0.872)	HKY+ G (G=0.231)	**HKY+ G (G=0.231)**
Stasimopus	Combined	1257	129	-	TIM1+ I+ G (I=0.531; G=0.640)	TIM1+ I+ G (I=0.531, G=0.640)	**GTR+ I+ G (I=0.531, G=0.640)**

Table S6. Number of putative species delimited based on varying posterior probability cut off values for the species delimitation method of Bayesian Poisson Tree Process (bPTP). ML represents the Maximum Likelihood method and BI the Bayesian Inference method. The actual species delimited can be viewed in tables S7 – S8.

Gene Region	Methodology	PP>0.00	PP>0.50	PP>0.90	PP>0.95
CO1_16S	**ML**	11	7	4	14
	BI	14	21	5	13
EF	**ML**	17	6	2	4
	BI	44	19	3	9

© University of Pretoria

Table S7. The putative species predicted by the Bayesian Poisson Tree Process (bPTP) species delimitation methodology for the 16S and CO1 combined gene regions. The Bayesian inference and maximum likelihood results are presented and the support shown as a score out of 1.00.

Putative Species	CO1_16S (Bayesian Inference)		CO1_16S (Maximum Likelihood)	
	Individuals	Support	Individuals	Support
1	SH02	1.000	SH02	1.000
2	13STAS02	1.000	13STAS02	1.000
3	36STAS01	1.000	36STAS01	1.000
4	03STAS01, 03STAS02	0.780	39STAS02, 39STAS01, 07STAS03, 07STAS01, 06STAS02, 06STAS01	0.177
5	58STAS03, 58STAS02, 58STAS01	0.931	03STAS01, 03STAS02	0.780
6	SAMC7293	1.000	58STAS03, 58STAS02, 58STAS01	0.931
7	NCRASTAS02	1.000	SAMC7293	1.000
8	30BSTAS01	1.000	NCRASTAS02	1.000
9	ELKSTAS05	1.000	30BSTAS01	1.000
10	56STAS01	1.000	60STAS03, 60STAS02	0.485
11	50STAS01	1.000	ELKSTAS03, ELKSTAS06	0.501
12	SUOJ04, SUOJ05	0.506	ELKSTAS05	1.000
13	36STAS02	1.000	SUOJ03, SUOJ06, SUOJ01, FRESTAS01, FRESTAS02, 38BSTAS01	0.133
14	31STAS01	0.999	56STAS01	1.000
15	31STAS03	0.999	50STAS01	1.000
16	53STAS04	0.999	41STAS03, 41STAS02, 41STAS01, 41STAS04, 47STAS03, 47STAS01, 47STAS02, 18BSTAS03, 18BSTAS02, 52STAS01, 16BSTAS02, 16ASTAS01	0.249
17	07STAS02	0.992	25BSTAS01, 53STAS03, 53STAS01, 37BSTAS01, 37ASTAS01, 24STAS01, SUOJ07	0.233
18	51STAS01, 51STAS03, 51STAS02	0.886	53STAS04	0.999
19	55BSTAS01, 05BSTAS03, 05BSTAS04, 08STAS05, 08STAS03, 08STAS04, 08STAS01	0.346	07STAS02	0.992
20	25BSTAS01	0.766	36STAS02	1.000
21	53STAS03, 53STAS01, 37BSTAS01, 37ASTAS01	0.622	31STAS01	0.999
22	38BSTAS02	0.842	31STAS03	0.999
23	19STAS01	0.842	51STAS01, 51STAS03, 51STAS02	0.886

© University of Pretoria

Table S7 (cont.). The putative species predicted by the Bayesian Poisson Tree Process (bPTP) species delimitation methodology for the 16S and CO1 combined gene regions. The Bayesian inference and maximum likelihood results are presented and the support shown as a score out of 1.00.

Putative Species	**CO1_16S (Bayesian Inference)**		**CO1_16S (Maximum Likelihood)**	
	Individuals	**Support**	**Individuals**	**Support**
24	59BSTAS02	0.934	11STAS01, 09STAS02, 09STAS01, 04STAS03, 04STAS02, 04STAS01, 55BSTAS01, 05BSTAS03, 05BSTAS04, 08STAS05, 08STAS03, 08STAS04, 08STAS01	0.289
25	STHSTAS01	0.934	21STAS01	0.912
26	39STAS02, 39STAS01	0.693	33STAS04, 33STAS03	0.331
27	07STAS03, 07STAS01	0.674	33STAS01	0.660
28	24STAS01	0.673	21STAS04	0.617
29	SUOJ07	0.673	SUOJ04	0.494
30	SUOJ03, SUOJ06, SUOJ01	0.373	SUOJ05	0.494
31	38BSTAS01	0.746	38BSTAS02	0.842
32	FRESTAS01, FRESTAS02	0.649	19STAS01	0.842
33	04STAS03, 04STAS01	0.224	21STAS02	0.292
34	04STAS02	0.457	21STAS03	0.292
35	06STAS02	0.400	59BSTAS02	0.934
36	06STAS01	0.400	STHSTAS01	0.934
37	16ASTAS01	0.438		
38	16BSTAS02	0.448		
39	09STAS02, 09STAS01	0.539		
40	11STAS01	0.611		
41	ELKSTAS03	0.499		
42	ELKSTAS06	0.499		
43	41STAS03, 41STAS02, 41STAS01, 41STAS04	0.660		
44	47STAS03, 47STAS01, 47STAS02	0.613		
45	21STAS01	0.912		
46	52STAS01	0.452		
47	18BSTAS03, 18BSTAS02	0.234		
48	33STAS03, 33STAS04	0.331		
49	33STAS01	0.660		
50	60STAS02	0.515		
51	60STAS03	0.515		
52	21STAS04	0.617		
53	21STAS02, 21STAS03	0.325		

© University of Pretoria

Table S8. The putative species predicted by the Bayesian Poisson Tree Process (bPTP) species delimitation methodology for the EF-1ɣ gene region. The Bayesian inference and maximum likelihood results are presented and the support shown as a score out of 1.00.

Putative Species	EF-1ɣ (Bayesian Inference)		EF-1ɣ (Maximum Likelihood)	
	Individuals	Support	Individuals	Support
1	09STAS02	1.000	13STAS01, 13STAS02	0.513
2	16BSTAS02	1.000	24STAS01	0.664
3	58STAS01	1.000	25BSTAS02	0.829
4	20BSTAS01	0.994	31STAS01	0.911
5	57STAS01	0.987	55BSTAS01	0.912
6	38BSTAS02	0.981	51STAS03	0.954
7	05BSTAS04	0.971	08STAS05, 09STAS01, 52STAS01, 53STAS05, 10ASTAS01, 11STAS01, 07STAS02, 04STAS03, 19STAS01, 04STAS02, 08STAS03, 04STAS01, 53STAS02, 51STAS02, 19STAS02, 05BSTAS03, 08STAS01, 05BSTAS04, 38BSTAS02, 57STAS01,2 0BSTAS01	0.006
8	08STAS01	0.963	18BSTAS01, 18BSTAS03, 18BSTAS02, 08STAS04	0.270
9	04STAS01, 53STAS02	0.747	09STAS02	1.000
10	08STAS03	0.903	16BSTAS02	1.000
11	08STAS05, 09STAS01	0.427	FRESTAS01	0.407
12	51STAS03	0.954	FRESTAS02	0.407
13	55BSTAS01	0.912	38BSTAS01	0.705
14	31STAS01	0.911	58STAS01	1.000
15	ELKSTAS01	0.875	03STAS03, 03STAS02, 03STAS01	0.284
16	52STAS01	0.807	59ASTAS02, 59ASTAS01, 59BSTAS01	0.267
17	NCRASTAS02	0.593	21STAS04, 21STAS02, 21STAS05, 21STAS03, 21STAS01	0.228
18	60STAS03	0.809	39STAS01, 06STAS01, 39STAS02, 06STAS02, 07STAS01, 07STAS03	0.098
19	ELKSTAS06	0.652	25BSTAS01	0.446
20	04STAS02	0.739	53STAS03, 53STAS04	0.243
21	53STAS05, 10ASTAS01	0.337	56STAS01	0.293
22	51STAS02, 19STAS02	0.319	STHSTAS01	0.293
23	05BSTAS03	0.630	59BSTAS02	0.567
24	41STAS04	0.635	58STAS02, 58STAS03	0.416
25	38BSTAS01	0.705	47STAS03, 47STAS01	0.353
26	FRESTAS01	0.407	16BSTAS01, 47STAS02	0.338
27	FRESTAS02	0.407	41STAS03, 41STAS01, 41STAS02, 41STAS04	0.227
28	41STAS03, 41STAS01	0.221	60STAS03, ELKSTAS05, 60STAS01, ELKSTAS03, ELKSTAS04, ELKSTAS06	0.618
29	41STAS02	0.417	60STAS02, 33STAS04, 37BSTAS01, NCRASTAS02, 30ASTAS01, 30BSTAS01, 51STAS01, ELKSTAS01	0.102

© University of Pretoria

Table S8 (cont.). The putative species predicted by the Bayesian Poisson Tree Process (bPTP) species delimitation methodology for the EF-1ɣ gene region. The Bayesian inference and maximum likelihood results are presented and the support shown as a score out of 1.00.

Putative Species	EF-1ɣ (Bayesian Inference)		EF-1ɣ (Maximum Likelihood)	
	Individuals	Support	Individuals	Support
30	16BSTAS01, 47STAS02	0.338		
31	21STAS04	0.757		
32	08STAS04	0.730		
33	ELKSTAS04	0.499		
34	18BSTAS01	0.485		
35	60STAS02	0.508		
36	30ASTAS01, 30BSTAS01	0.203		
37	51STAS01	0.413		
38	ELKSTAS03	0.327		
39	21STAS02	0.564		
40	25BSTAS02	0.829		
41	33STAS04	0.234		
42	37BSTAS01	0.234		
43	24STAS01	0.664		
44	18BSTAS03	0.242		
45	18BSTAS02	0.242		
46	ELKSTAS05	0.163		
47	60STAS01	0.163		
48	39STAS01	0.361		
49	06STAS01	0.361		
50	59BSTAS02	0.567		
51	56STAS01	0.293		
52	STHSTAS01	0.293		
53	39STAS02	0.350		
54	06STAS02	0.350		
55	58STAS02	0.441		
56	58STAS03	0.441		
57	59ASTAS02	0.569		
58	59ASTAS01, 59BSTAS01	0.281		
59	25BSTAS01	0.446		
60	21STAS05	0.374		
61	21STAS03, 21STAS01	0.191		
62	11STAS01	0.272		
63	07STAS02	0.272		
64	47STAS03	0.343		
65	47STAS01	0.343		
66	53STAS03	0.203		
67	53STAS04	0.203		
68	07STAS01	0.427		
69	07STAS03	0.427		
70	13STAS02	0.487		
71	13STAS01	0.487		
72	03STAS03	0.552		
73	03STAS02, 03STAS01	0.279		
74	04STAS03	0.282		
75	19STAS01	0.282		

© University of Pretoria

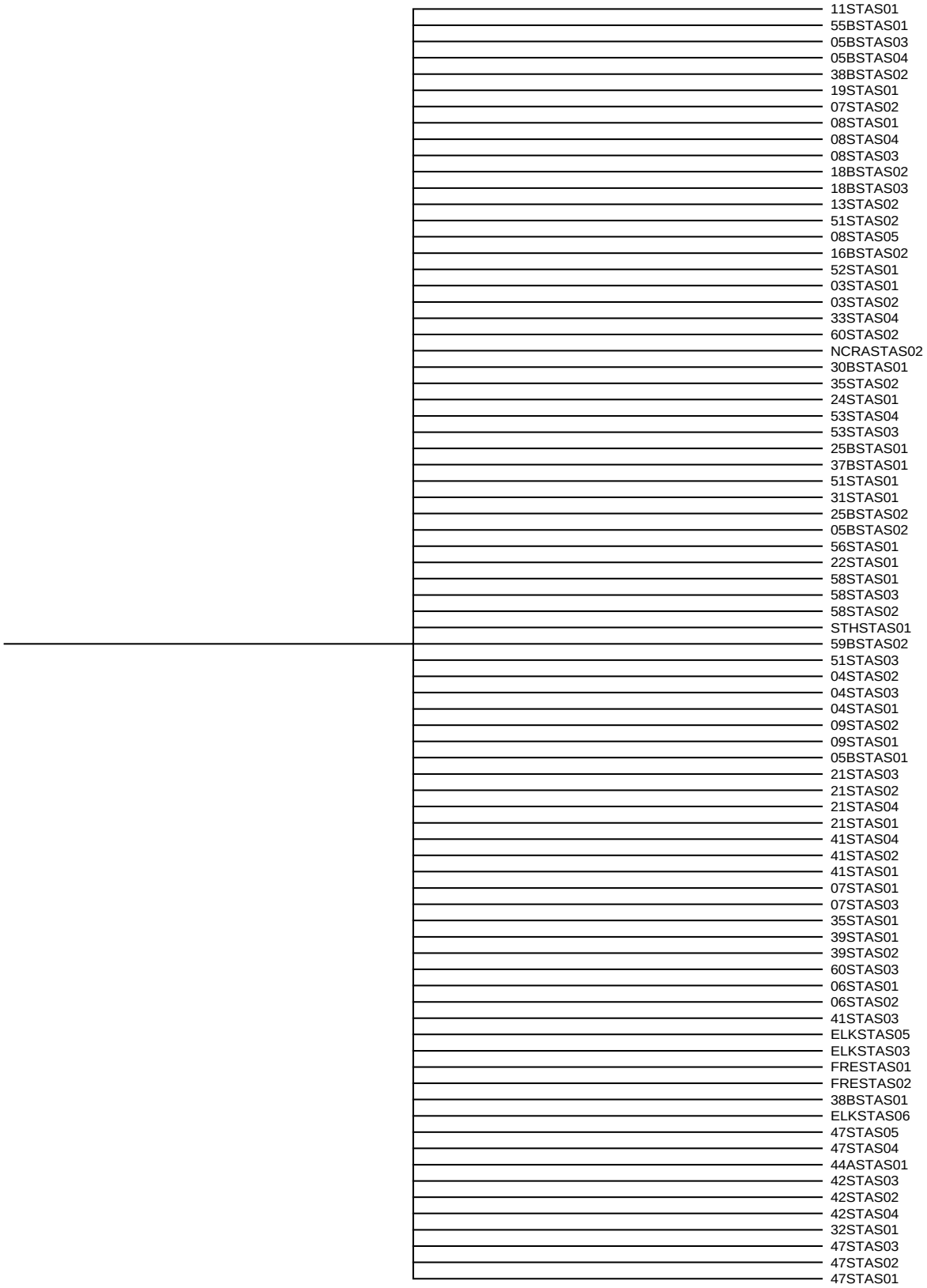


Figure S1. 50% majority-rule consensus tree produced from 633 tree topologies over ten runs. The analysis followed the default settings of a heuristic search in Brownie for species delimitation. The hard polytomy indicates that no putative species could be reliably delimited.

© University of Pretoria

Chapter 3

Geometric morphometric analysis of ocular patterns as a species identifier in the South African endemic trapdoor spider genus *Stasimopus* Simon, 1892 (Araneae, Mygalomorphae, Stasimopidae)

Shannon Brandt[1], Catherine L. Sole[1], Robin Lyle[2] and Christian W. W. Pirk[1]

[1] *Department of Zoology and Entomology, University of Pretoria, Hatfield, Pretoria, South Africa*

[2] *Agricultural Research Council – Plant Health and Protection, Biosystematics, Roodeplaat, Pretoria, South Africa*

This data chapter has been submitted as:

Brandt, S., Sole, C. L., Lyle, R. and Pirk, C. W. W. 2023. Geometric morphometric analysis of ocular patterns as a species identifier in the South African endemic trapdoor spider genus Stasimopus Simon, 1892 (Araneae, Mygalomorphae, Stasimopidae), to Evolutionary Biology.

© University of Pretoria

Abstract

The identification of *Stasimopus* Simon, 1892 species as well as mygalomorph species has been a long-standing challenge. This is due to their conservative morphologies as well as the lack of quantifiable characters. Ocular patterns have historically been used to aid in identification, but have largely been vague and subjective. This study was the first to test for phylogenetic signal in this character to validate its use for species identification and description as well as to test the viability of it in morphospecies and species identification. The results show significant phylogenetic signal for ocular patterns in both sexes, validating its use. The results display the evolutionary change in ocular patterns across various species. Species and morphospecies show distinct clustering in morphospace, but there is overlap due to the continuous shape of the character. The methodology of applying geometric morphometrics to quantify ocular patterns can distinguish between morphospecies and shows great promise for distinguishing species.

Key words

Mygalomorph, Geometric morphometrics, ocular pattern, *Stasimopus*, phylogenetic signal

Statements and Declarations

No conflicting interests to declare.

Acknowledgements

We would like to acknowledge Tshepiso Majelantle and Elmé Brand for their assistance on fieldwork for sample collection. We thank Carmelo Fruciano for his advice with framing the research question for this manuscript. Equipment for field work was supplied by the Agricultural Research Council. We would like to thank the following institutions for loaning the specimens required for specimen identification: Albany Museum, Grahamstown, South Africa; The National Museum, Bloemfontein, South Africa; Ditsong Museum of Natural History, Pretoria, South Africa; Iziko Museum of Cape Town, South Africa; Museum für Naturkunde, Berlin, Germany; National Collection of Arachnida, Pretoria, South Africa.

© University of Pretoria

Funding

The National Research Foundation (NRF) are acknowledged for funding to the second author. The first author would also like to acknowledge the National Research Foundation for funding (Grant no: 120190 and 139125). This work is based on the research supported in part by the Karoo BioGaps Project (NRF Grant Number 98864), which was awarded through the Foundational Biodiversity Information Programme (FBIP), a joint initiative of the Department of Science and Innovation (DSI), the National Research Foundation (NRF) and the South African National Biodiversity Institute (SANBI).

Author contributions

All authors contributed to the study conception and design. Material preparation was performed by Shannon Brandt. Data collection was performed by Shannon Brandt, Catherine Sole and Robin Lyle. Analyses were performed by Shannon Brandt and assisted by Christian Pirk. The manuscript was written by Shannon Brandt and all authors commented on previous versions of the manuscript. All authors read and approved the final manuscript.

© University of Pretoria

Introduction

The taxonomic placement of *Stasimopus*, like other mygalomorph spiders, has historically been based on morphological characters. This can however be confounding as organisms may be cryptic morphologically, display high levels of homoplasy or the characters used to describe them may be vague, indiscriminate and subjective. The characters which are often used to describe mygalomorph species are: the shape of the carapace and fovea; sternum shape and the position of the sigilla; ocular patterns; chelicerae, rastellum and cuspules; the relative leg lengths and spination patterns; the pedipalp shape and relative length to the first legs; the spinnerets; and genitalia (Engelbrecht & Prendini, 2012; Jocque & Dippenaar-Schoeman, 2007). Many of these characters are qualitative in nature, such as relative length and shape, with no quantitative way to distinguish similar species from each other (Bond et al., 2012).

Ocular patterns are commonly used to identify spiders in most families as there is a vast amount of diversity (Crews, 2011; Polotow & Brescovit, 2014). The size and arrangement of the eyes are generally used. For this the standard measurements tend to be eye diameter across the lens, inter-eye distances and the arrangement of the different eye pairs (Crews, 2011). Eye patterns are particularly useful at the family level within the araneomorphs which show a significantly higher degree of morphological variation than the mygalomorphs. (Crews, 2011; Polotow & Brescovit, 2014). Stasimopidae typically have eight eyes, the Anterior Median eyes (AME) are known as the 'principal' eyes, with the other eyes (Anterior Lateral (ALE), Posterior Median (PME) and Posterior Lateral (PLE)) known as 'secondary' eyes (Figure 1). Principal and secondary eyes differ extensively in terms of development, structure and function (Morehouse et al., 2017). Ocular patterns are often included in species descriptions of *Stasimopus* where they are considered diagnostic (Engelbrecht & Prendini, 2011; Hendrixson & Bond, 2004; Hewitt, 1910; Pocock, 1902). It has however never been tested for phylogenetic signal, thus there is no hard evidence that the trait is driven by heritable change and evolution. Phylogenetic signal is based on the observation that closely related species tend to have similar morphological traits and without phylogenetic signal, these traits should not be used to identify nor describe species (Adams, 2014b; Hendrixson & Bond, 2009).

Engelbrecht and Prendini (2012) used ocular patterns and described the distance of the anterior ocelli from the carapace margin, the curvature of the anterior and posterior ocular rows as well as the eye sizes relative to each other. This is a step forward in using ocular patterns as an identifiable character for *Stasimopus*, but is not specific enough for the fine scale variation which exists between the species. The morphological differences between the species of the genus are subtle, making the evolutionary adaptations that would have driven these differences difficult to detect. In having a better understanding of what the differences in the ocular patterns are across the genus, we

Department of Zoology and Entomology
University of Pretoria

© University of Pretoria

may be able to make better predictions about the differing environmental pressures the species historically faced. In order to achieve this, a more quantitative methodology is required.

One solution to this is the implementation of geometric morphometric techniques. Morphometrics is a branch of comparative biology and statistics which finds methods of describing and quantifying variations of shape and relative size between organisms and the analyses make it possible to identify discrete patterns in continuous data (Hendrixson & Bond, 2009; Rohlf & Marcus, 1993; Zelditch et al., 2004c). Geometric morphometrics allows for the capturing of the entire structure being analysed in either two-dimensions or three-dimensions as coordinates of landmark points (Mitteroecker & Gunz, 2009; Rohlf & Marcus, 1993).

Morphometrics has been broadly applied to the Araneae. However, these studies tend to focus on the genitalia, carapace and legs of different spiders to identify species or genera (Bond & Beamer, 2006; Costa-schmidt & de Araujo, 2010; Fernández-Montraveta & Marugán-Lobón, 2017; Hendrixson & Bond, 2009; Prenter et al., 1995; Spasojevic et al., 2016). To the best of our knowledge no study addressed the issue of the use of morphometrics to analyses ocular patterns in the Araneae.

We aim to fill this gap and address the following two related questions: First: can we detect evolutionary signal in the ocular pattern thereby making them useful and robust identifying traits. Second, to test the viability of applying geometric morphometrics to the ocular pattern of *Stasimopus* species to determine their feasibility as quantitative characters to distinguish between morphospecies or possibly species.

Methods and materials

Specimen selection

Specimens were selected to attempt to represent as much of the *Stasimopus* species diversity possible. Material was loaned from various national and international collections: Albany Museum (AMGS), Grahamstown, South Africa; The National Museum (NMBA), Bloemfontein, South Africa; Ditsong Museum of Natural History (TMSA), Pretoria, South Africa; Iziko Museum of Cape Town (SAMC), Cape Town, South Africa; Museum für Naturkunde (ZMB), Berlin, Germany; National Collection of Arachnida (NCA), Pretoria, South Africa. As far as possible only holotypes, allotypes and syntype series were used, as many of the *Stasimopus* identifications after this are incorrect or unvalidated. Specimens collected from the Karoo area of South Africa were included in some analyses in order to test if they could be allocated to the correct species (Specimens information is available in Table S1). GPS coordinates were omitted from Table S1, as the Karoo region is of conservation concern and the IUCN conservation statuses for Stasimopus species are completely known due to the lack of data. In total 35 of the 47 currently recognised *Stasimopus* species were represented between the two sexes (32 species for the females; 20 species for the males) (World Spider Catalog, 2022). As well as nine

© University of Pretoria

previously undescribed species (described in Chapter 4). The categorisation of 'undescribed species' is as described in Chapter 2.

Specimens were also split into 'morphospecies' according to the major biomes in South Africa (A-F in Figure 1). Some species were also grouped due to known phylogenetic relationships.

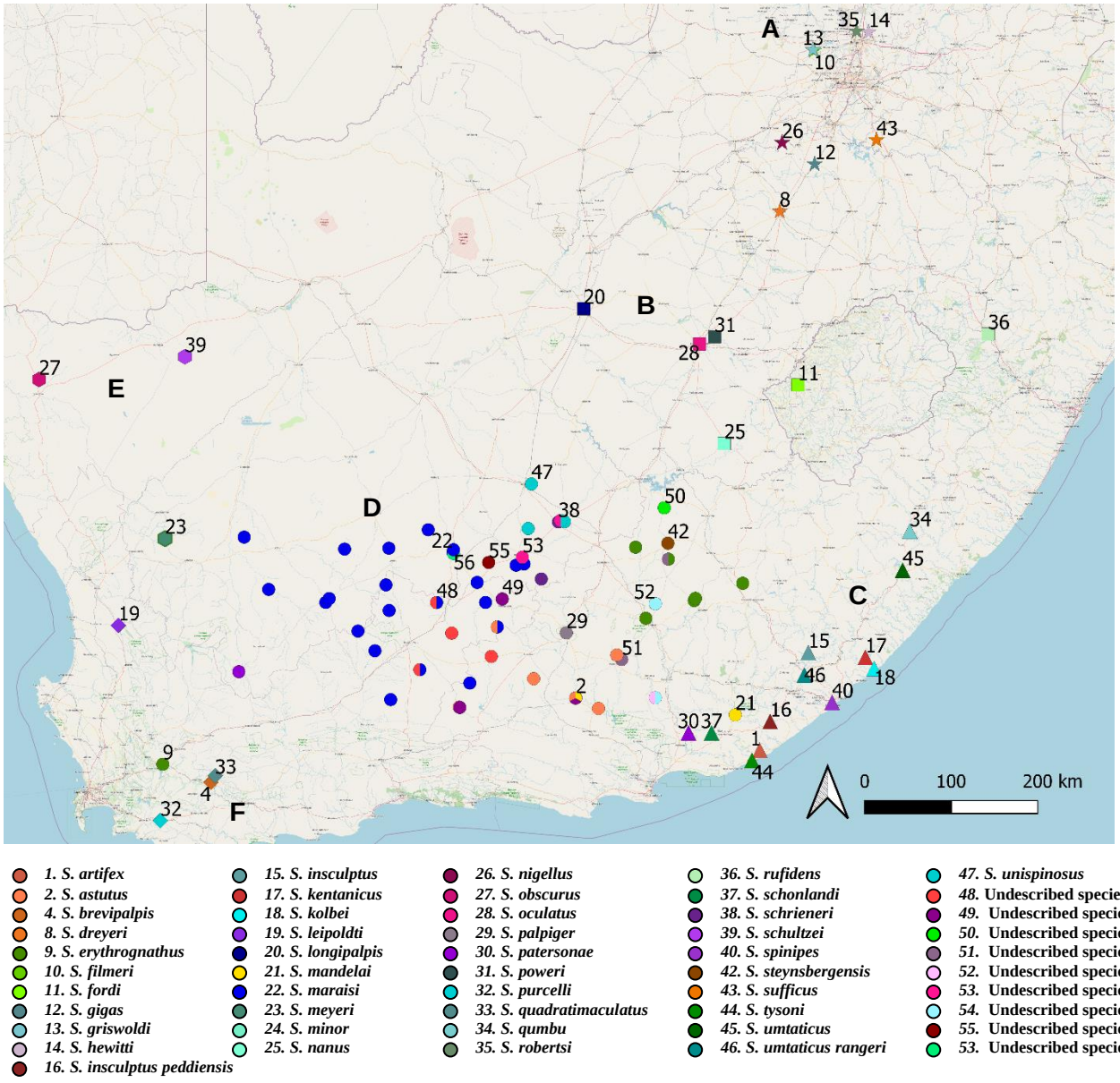


Figure 1. Map of the type localities and general localities of the specimens analysed. The localities are coloured according to the species found there. Numbered markers indicate type localities, unnumbered markers are specimens collected in the Karoo and assigned to species. The various shapes indicated defined locality groupings (A-F) for analyses. A. stars, B. squares, C. triangles, D. circles, E. hexagons, F. diamonds. Map created in QGIS version 3.4.8-Madeira (2019), available at: http://qgis.osgeo.org.

© University of Pretoria

Geometric morphometric data capture

The top angle of the ocular pattern was photographed for 123 females and 66 males belonging to various species of *Stasimopus.* The females were photographed using a Leica M 165C stereomicroscope attached to Leica camera (DMC-2900), whereas males were photographed on a Zeiss Axio Zoom V16 with the Axiocam 512 color and stacked with ZEN 2.3 SPI (Blue Edition). Two different systems were required as the males have a steeper carapace and thus required an imaging system with a greater depth of field. All specimens were photographed on a petri dish of glass beads for ease of adjustment, to ensure similar angles in each photograph. The specimens were selected at random when photographed to ensure that there was no operational bias in the photography process. Operational bias in this context would arise from photographing specimens of the same species directly after one another, this would lead to the operator subconsciously detecting similarities in the positions of the specimens (Bakkes, 2017; Fruciano, 2016).

Once photographed all the images were compiled using tpsUtil v1.79 (Rohlf, 2015) and were imported to tpsDig v.2.31 (Rohlf, 2015) for digitisation. Thirty-two landmarks were selected to capture as much of the shape variation as possible as seen in Figure 2. Landmarks in the context of geometric morphometrics are distinct loci which are homologous in location between different specimens (Rodriguez-Mendoza, 2013; Seetah, 2014; Zelditch et al., 2004a). A list of operational definitions for each landmark are included in Table S2. The specimens were selected at random when digitising to ensure that there was no operational bias.

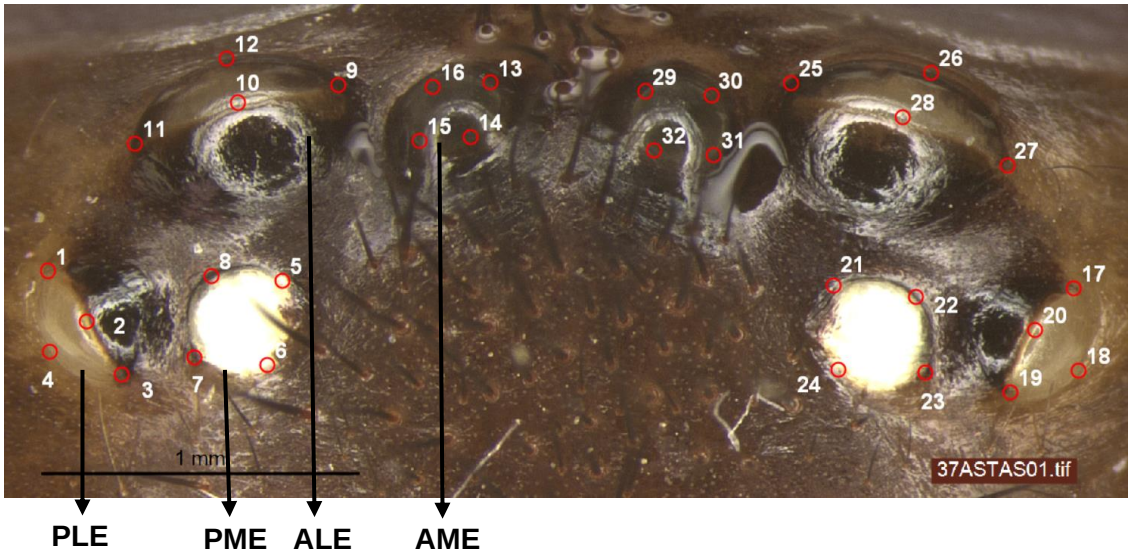


Figure 2. An illustration of the position of the landmarks used in the geometric morphometric analysis of *Stasimopus* ocular patterns. The 32 landmarks correspond with the landmark definitions given in Table S2. In all photographs, the specimen is positioned so that the chelicerae face the top of the image. The following shorthand notations are used; PLE: posterior lateral eye, PME: posterior median eye, ALE: anterior lateral eye and AME: anterior median eye.

Department of Zoology and Entomology
University of Pretoria

© University of Pretoria

Phylogenetic analyses

For sequence generation refer to Chapter 2. Accession numbers for all sequences used are supplied in Table S1. A dated phylogeny was produced using BEAST v1.8.4 (Suchard et al., 2018). The fossil calibration points are as in Chapter 5 and appendix A1. Each family was represented by sequence data from GenBank for 16S rDNA, cytochrome c oxidase subunit 1 (CO1) and elongation factor 1 gamma (EF-1ɣ) if available given in Chapter 5 - Table S1.

The nucleotide substitution rate was determined using jModelTest v2.1.7 (Posada, 2008). This was done for each gene region and the best model was selected based on the Bayesian information criterion (BIC) (Posada, 2008). This was used to set the prior in BEAUTi v1.8.4 (Suchard et al., 2018). Other priors set included, the rate of molecular evolution to a relaxed clock with a lognormal distribution (this allows mutational rates to vary over the tree) (Michonneau, 2017). The tree prior was set to 'Speciation: Birth-Death Incomplete Sampling'. An uncorrelated relaxed clock was used, as this allows for each branch of the phylogeny to have a different evolutionary rate (Drummond et al., 2006). BEAST v1.8.4 (Suchard et al., 2018) was then run for 200,000,000 generations and sampled every 2000 generations. This was repeated twice for each analysis to ensure convergence. BEAST was run in conjunction with BEAGLE (Ayres et al., 2012).

Tracer v1.7.1 was used to confirm convergence (Rambaut et al., 2018). This was tested by checking the log file for each BEAST run and ensuring the ESS values were above 200. The individual runs were then compiled to ensure a normal distribution. Log Combiner v1.8.4 (Suchard et al., 2018) was used to combine the multiple tree files into one file. The subsampling number was set to 50,000 and the burn-in for each tree to 50,000,000. The tree files viewed, annotated and edited in FigTree (Rambaut, 2016).

Statistical analyses

General statistics

All statistical analyses were performed in either MorphoJ v.1.06d (Klingenberg, 2011) or the main packages "geomorph", "Morpho" and "GeometricMorphometricsMix" (Adams et al., 2021; Baken et al., 2021; Collyer & Adams, 2018, 2021; Schlager, 2013) in R (R Core Team, 2017).
A Procrustes fit was created using the landmarks in MorphoJ v.1.06d and R in order to superimpose all the photographs and thus remove the direct effect of size, orientation and position (Zelditch et al., 2004c, 2004b). General procrustes analysis (GPA) was performed on all datasets before any other analyses. This was done by the 'align principal axes' method, which computes the average position in an iterative manner in order to minimise the Procrustes distance (Zelditch et al., 2004b). This analysis produces the distances in three-dimensional space as well as the Procrustes distances which measure

© University of Pretoria

shape dissimilarity. An additional output of this analysis is the centroid size for each specimen photograph.

Determining evolutionary relationships

Phylogenetic signal was tested for the eye patterns of the various species which had available sequence data. Strong phylogenetic signal is present if specimens that are phenotypically more similar are more closely related than specimens that are phenotypically more distinct (Adams, 2014b; Klingenberg & Gidaszewski, 2010). This is expected when organisms have experienced divergent evolution, but can be diluted by homoplasy due to convergence, parallel evolution and reversals (Klingenberg & Gidaszewski, 2010). Phylogenetic signal is tested with morphometric data, by mapping the shape data onto a known phylogeny. Permutations are then performed, simulating the null hypothesis of no phylogenetic structure by randomly assigning the various shapes to the terminal nodes of the phylogeny (Adams, 2014b; Klingenberg & Gidaszewski, 2010; Žikić et al., 2017). This was done for the male and female dataset of sequenced individuals. Phylogenetic signal was tested for average species shape. The phylogenetic signal testing conducted using the package 'geomorph' which is based on a Brownian motion evolutionary model. Brownian motion evolution assumes that the changes in one trait along the phylogeny is expected to have a value of zero and variance among species accumulates proportional to time (Adams, 2014b). The statistic to measure phylogenetic signal by this method is K_{mult}, which is equal to one under Brownian motion. A value above one would imply that more closely related taxa have a morphology in a particular trait which is more similar than expected under Brownian motion (Adams, 2014b). To account for phylogenetic uncertainty, K_{mult} was calculated of every tree of the posterior distribution of the aforementioned BEAST run (Fruciano, 2016). This was done after discarding 25 % of the trees as burn-in.

A Phylogenetic Generalised Least Squares (PGLS) was performed to test for evolutionary allometry in both sexes. Evolutionary allometry describes the covariation between shape and size within a phylogenetic context (Adams, 2014a). This is important in the *Stasimopus* genus as there is a wide variation in average species size, and size is often used to aid in species identification. Two methodologies were tested, both requiring a pruned phylogeny as well as averages for species shape and size (Adams, 2014a). The first method follows Adams (2014b) which implements a distance-based approach to PGLS in the package *geomorph*. The second follows Clavel et al. (2015) and is based on fitting various evolutionary models under a maximum likelihood criterion in the package mvMORPH (Clavel et al., 2015, 2019). The evolutionary models tested included Brownian motion, Ornstein-Uhlenbeck, early burst and Lamba (Clavel et al., 2015).

Partial Least Squares (PLS) is a multivariate statistical technique used to compare multiple response and explanatory variables (Pirouz, 2006; Rohlf & Corti, 2000). The morphometric

© University of Pretoria

implementation is 2B-PLS, this methodology finds pairs of axes in the two blocks of variables which account for the maximal covariation between the blocks (Rohlf & Corti, 2000). PLS is considered more robust than Principal Component Analysis (PCA), Canonical Variates Analysis (CVA) and alternating least squares, as model parameters do not change with new data calibrations (Pirouz, 2006). PLS is also advantageous over regression as it does not assume that the variation in the one variable is caused by the other variable, but rather treats the two variables symmetrically to uncover the relationship between them (Rohlf & Corti, 2000). PLS is better at dealing with small datasets, missing data and data that is multicollinear (Pirouz, 2006). For the analyses, the first variable block was the shape data for all specimens that have genetic sequence data (after GPA), analysed as a pairwise matrix of the Procrustes distances. The second block was the pairwise distances of the various gene regions (CO1, 16S and EF-1ɣ). These distances were obtained by using the sequences generated, and constructing the various matrices in MegaX (Kumar et al., 2018). This block was scaled as it does not share the same units as the shape variable block (Rohlf & Corti, 2000). There is no direct significance test of 2B-PLS available, thus significance was tested by permutations (1000 permutations were used). This tests the null hypothesis that there is no association between the two variable blocks (Rohlf & Corti, 2000). The strength of the covariation is measured by Escoufier RV, which is the multivariate equivalent of the correlation coefficient (Rohlf & Corti, 2000).

Determining if identification is possible

A Principal Component Analysis (PCA) was performed on the whole dataset to test the patterns of covariation of the landmark positions of the eye patterns. The PCA was constructed to provide a graphical representation of the variation in the data.

Regression analyses can be inflated by the multicollinearity of variables within a model (two or more dependent variables being correlated with one another), therefore Variance Inflation Factor (VIF) was used to test if this occurred in the models used in the analysis by testing the correlation and strength between dependent variables (Forthofer et al., 2007). A value of 1 indicates no correlation between variables, 1-5 indicates moderate correlation (not enough to influence results) and >5 indicates a severe correlation which is likely to obscure results such as p-values (Ringle et al., 2018). This was tested in R with the packages “car” (Fox & Weisberg, 2019) and “DAAG” (Maindonald & Braun, 2020). This was tested between centroid size and locality and species separately (as these variables were never run in the same model as they are correlated).

A regression of size and shape was performed in order to quantify the effects of allometry (Klingenberg, 2016). This is important to take into account as real differences in shape between species or populations can be confounded with shape differences due to size (Nakagawa et al., 2017). A regression separates the component of variation of the dependent variable (shape) selected which is

© University of Pretoria

predicted by the independent variable (size) (Rodriguez-Mendoza, 2013). A procrustes regression with residual randomisation was performed in 'geomorph'. A permutation test was included to test the null hypothesis that shape and size are independent for 10,000 runs. It is possible to separate the component of size which is correlated with shape; this was decided against as size is an important predictor of species in *Stasimopus*. Regressions were also performed pooled by species and by locality. As *Stasimopus* species get larger, the eye pattern is more stretched over the carapace, making the ocular pattern sparser by increasing the distance between the various eyes. This means that the size of the specimen directly impacts the shape of the ocular pattern.

Procrustes ANOVA was used to test if there was a significant relationship between procrustes distances (shape) and multiple dependent variables (Goodall, 1991). In this study the null hypothesis was rejected at a significance level of 0.05. Procrustes ANOVA was used to test for a significant relationship between shape and centroid size, species and locality for both sexes separately.

Canonical Variates Analysis (CVA) is an exploratory analysis which generates Mahalanobis distances between groups based on centroids (McKeown & Schmidt, 2013). This produces canonical variates (CVs) from the scaling and rotation of the centroids, thus showing the distances between groups (Manthey & Ousley, 2020; McKeown & Schmidt, 2013). A CVA was conducted for species and locality for both the male and female datasets in R.

Outline files were created to be able to visualise the shape changes between different principal components and discriminant factors. For this tpsDig and MorphoJ were used. The males and females were analysed separately due to a high degree of sexual dimorphism.

Pilot study for error testing

The first pilot study was to test if juveniles could be included in order to increase the sample size. It was found that juveniles experience allometric growth. The ocular pattern tends to be more bulbous in juvenile samples when compared to the adult counterparts. Juvenile specimens of the genus are often left unidentified as the juvenile traits are not well documented. It was therefore decided to exclude juveniles from the study as it would further complicate the results and take away from the straightforward testing if the method can be used to aid in the identification species. A second pilot study was conducted to determine the amount of rotational and digitising error that was incurred and the number of replications that would be required to reduce this. The pilot study found that for the eye patterns there was less than 5 % total error when two replications were used. For this reason, only one replicate was performed in the actual experiment. The documentation of this is available in Appendix A2.

© University of Pretoria

Results

Phylogenetic signal and relationships

The relative position and size of the *Stasimopus* eyes display significant phylogenetic signal for both the female and male dataset (K_{mult}=1.0763; P_{rand}=0.007 and K_{mult}=1.0121; P_{rand}=0.011 respectively). This indicates that closely related species are significantly similar in eye pattern than what would be expected under a Brownian motion evolutionary model. The K_{mult} distribution is shown in Figure S1. This is supported by the positions of the various species in phylomorphospace being reflective of the evolutionary relationships shown in Figure 4 (Figure 3). Here sister species cluster closer together in morphospace than more distantly related species, indicating that they are more morphologically similar. Figure 4 also displays the phylogenetic relationships between the various species, with the average species eye pattern. From this it is clear that more closely related species have more similar eye patterns.

The results of the PGLS analyses yielded significant results for the female datasets following both the method applied in *geomorph* and *mvMORPH* (Lamba model) (p=0.033; p=0.001), indicating that evolutionary allometry is present. For the male dataset evolutionary allometry was not found under *geomorph* but a significant result was found through *mvMORPH* (Early burst model) (p=0.094; p=0.001).

The PLS analyses for the female sequenced dataset produced significant results for all three gene regions, indicating that there is an association between the genetic distances and Procrustes distances. The Escoufier RV is however fairly low, thus the correlation is not strong (CO1: p=0.001, RV=0.43; 16S: p=0.001, RV=0.36; EF-1ɣ: p=0.001, RV=0.37). For the male dataset, only 16S and EF-1ɣ gave significant results, both with average correlation (16S: p=0.008, RV=0.47; EF-1ɣ: p=0.02, RV= 0.55). The figures showing the separation of species in the PLS blocks are available in Figures S2 and S3.

© University of Pretoria

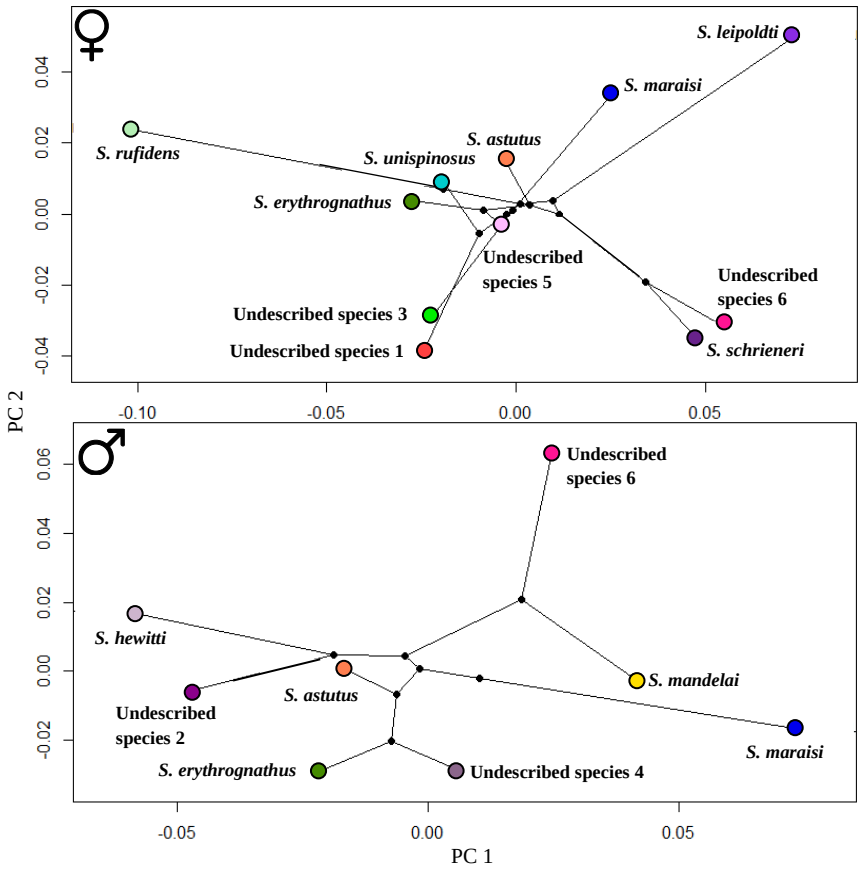


Figure 3. Phylomorphospace plots of the first two principal components for the female and male datasets. Species colours correspond to the map in Figure 1.

© University of Pretoria

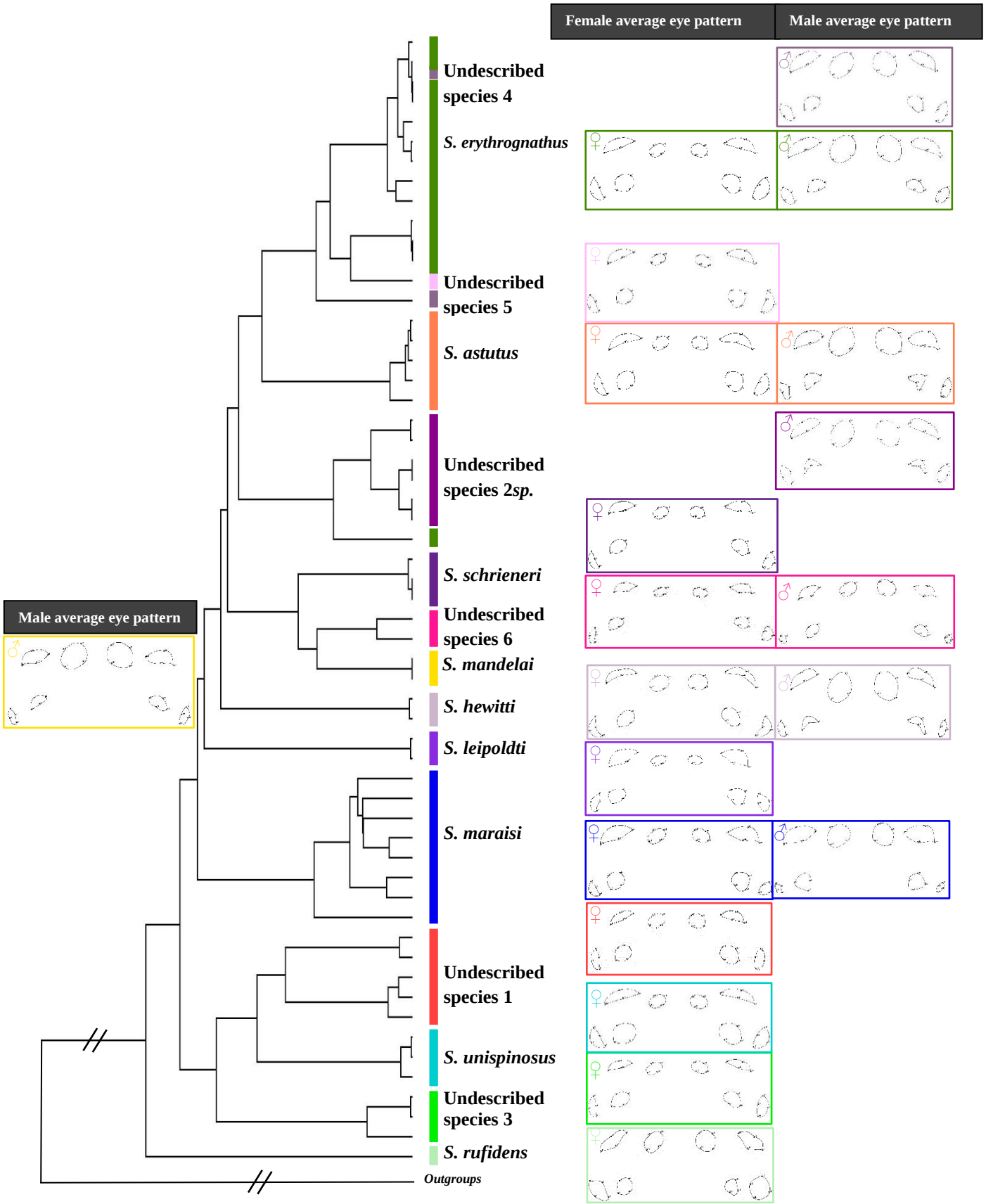


Figure 4. Molecular phylogeny of the sequenced *Stasimopus* specimens. Species colours correspond to the map in Figure 1. The average shape based on thin plate splines averaged by species is given for each sex when available.

© University of Pretoria

Separation of species or morphospecies

Eleven PCs explain 87% of the total variation in the female dataset with PC1 and PC2 explaining 20.79% and 20.15% respectively (Figure S4). For the males nine PCs explain 85% of the total variation and PC1 contributes 26.8% and PC2 23.57% (Figure S5). The PCA for the female dataset shows slight clustering between both species and localities (Figure S4A and S4B). The clusters appear indistinct between species and localities as there are so many species / localities represented. There are distinct changes in relative eye size and position between the PCs in the female dataset (Figure S4C). In the first PC, the anterior eyes are more clustered together than the average shape. The PLEs are also vertically rotated. The second PC saw a reduction in the anterior eye sizes. The PLEs are rotated as in PC1 (Figure S4C). The male dataset PCA shows clustering for the species and locality variable (Figure S5A and S4B). The changes in eye pattern are more extreme for the male dataset than the female. Within the first PC, all eyes are significantly larger. The AMEs shift from being behind the ALEs line, to slightly in front of them (Figure S5C). In the second PC, the opposite pattern is observed, all the eyes are significantly reduced in size (Figure S5C).

The VIF analysis for the female indicated slight correlation between species and centroid size (GVIF: 2.999), and no correlation between locality and centroid size (GVIF: 1.151). There were however, certain species which had VIF values above 5, indicating a severe correlation with centroid size. These species were *S. erythrognathus*, *S. insculptus var peddiensis* and *S. maraisi* (Figure S6A). For the male dataset, severe correlation was found between species and centroid size (GVIF: 19.358), this is seen in the species *S. erythrognathus*, *S. gigas*, *S. griswoldi*, *S. hewitti*, *S. insculptus peddiensis* and Undescribed species 2 (Figure S6C). There was no correlation found between locality and centroid size for the male dataset (GVIF: 1.373).

The regressions between procrustes distances and centroid size (pooled by other variables) are available in Figures S7 and S8. There is a significant relationship between shape (procrustes distances) and centroid size for both sexes (Figure 5, Table S3). The size of an individual accounts for a large percentage of shape variability within both sexes, 7.45% for females and 13.63% for males. This percentage increases when the data are pooled by species for the female dataset (8.61%), but is not significant for males. When pooled by locality, the influence of centroid size on shape decreases, but is still significant (Table S3).

Relative eye position and size is not only significantly influenced by centroid size, but also by the species and locality / morphospecies considered (Table S4). These relationships were observed within both sexes. Pairwise tests to determine the species or locality which influence the relationship were not possible due to sample size constraints.

© University of Pretoria

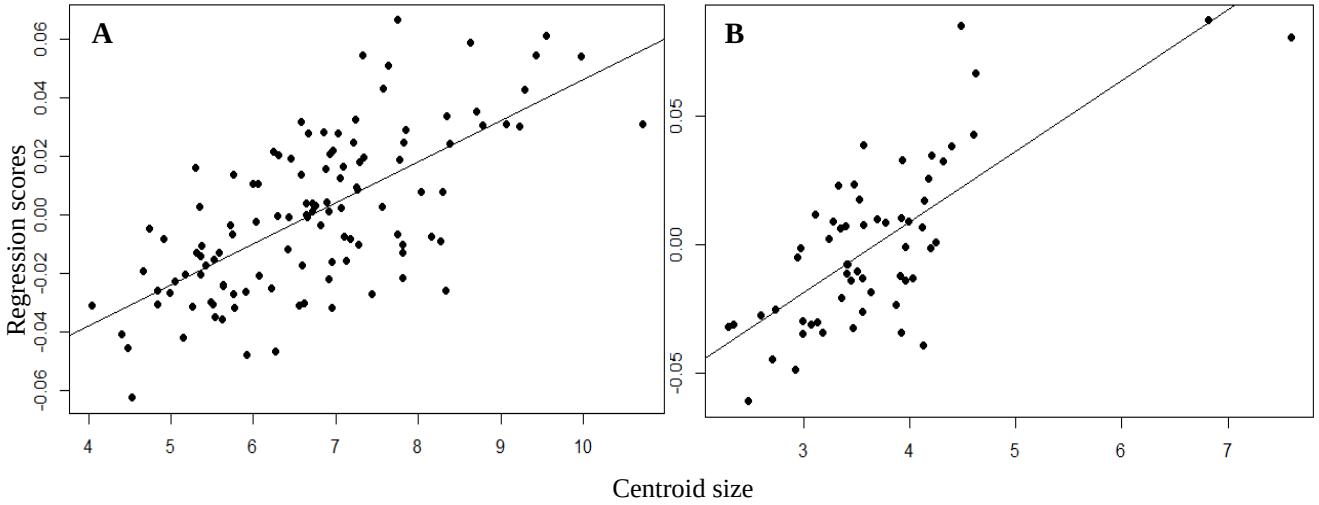


Figure 5. Regression plots. A. Regression of procrustes distances and centroid size for females. B. Regression of procrustes distances and centroid size for males.

Clear clustering is visible in the CVA plots. The clustering is more pronounced when the data are analysed by locality/morphospecies than by species for both sexes. More of the variation in the data is accounted for in a fewer number of CVs for locality than for species. Most species show tight clustering, even though the species overlap. For the female dataset by species, there are subtle changes in ocular pattens along the first and second CV (Figure 5A). In the locality CVA however, the changes are more pronounced, with a reduction in the AMEs and a slight rotation in the PLEs (Figure 5B). For the male dataset, the CVA by species shows a distinct shape change (Figure 6A). There is a reduction in the AMEs size, in the first CV the PLEs and ALEs are also reduced. There is less variation in the CVA by locality for the male dataset (Figure 6B). In CV1 there is a reduction in AMEs, and in CV2 the ALEs are slightly larger. Cross validation could not be performed for the species variable of either dataset as some species only have one representative. For the locality variable for the female dataset the overall classification accuracy was 66.67% and for the male dataset 50.85%.

The between group PCA produced obvious grouping for the various datasets, but these are not as clustered as in the CVA (Figure S9 and S10). Cross validation could again not be performed for the species groupings. The overall classification accuracy for location in the female dataset was 59.64%, and for the male dataset 67.80%.

The separation of the species and morphospecies clusters are validated by the results of the procrustes ANOVA (Table S8). The ANOVA shows that there are significant relationships between shape and species groupings, as well as shape and morphospecies groupings for both sexes.

© University of Pretoria

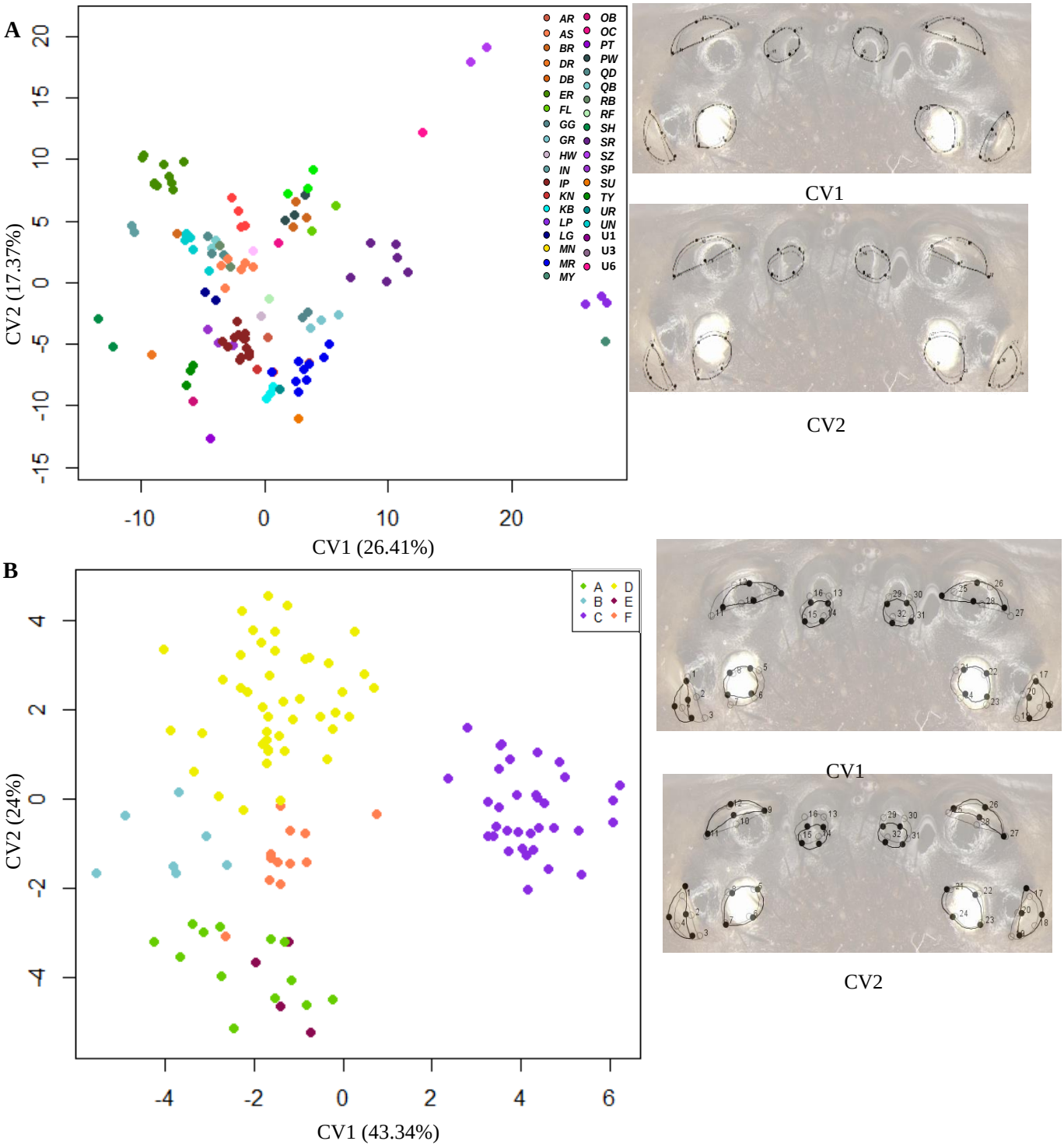


Figure 5. Morphospace plots of the first two CVs for the female dataset. A. CVA by species morphospace plot. The species colours correspond to the map in figure 1. Shape changes in the female ocular pattern for the first and second PC are shown for all the landmarks. The original average shape is indicated in grey and the new target shape in black. B. CVA by locality / morphospecies morphospace plot, also including the shape changes along the CVs.

Department of Zoology and Entomology
University of Pretoria

© University of Pretoria

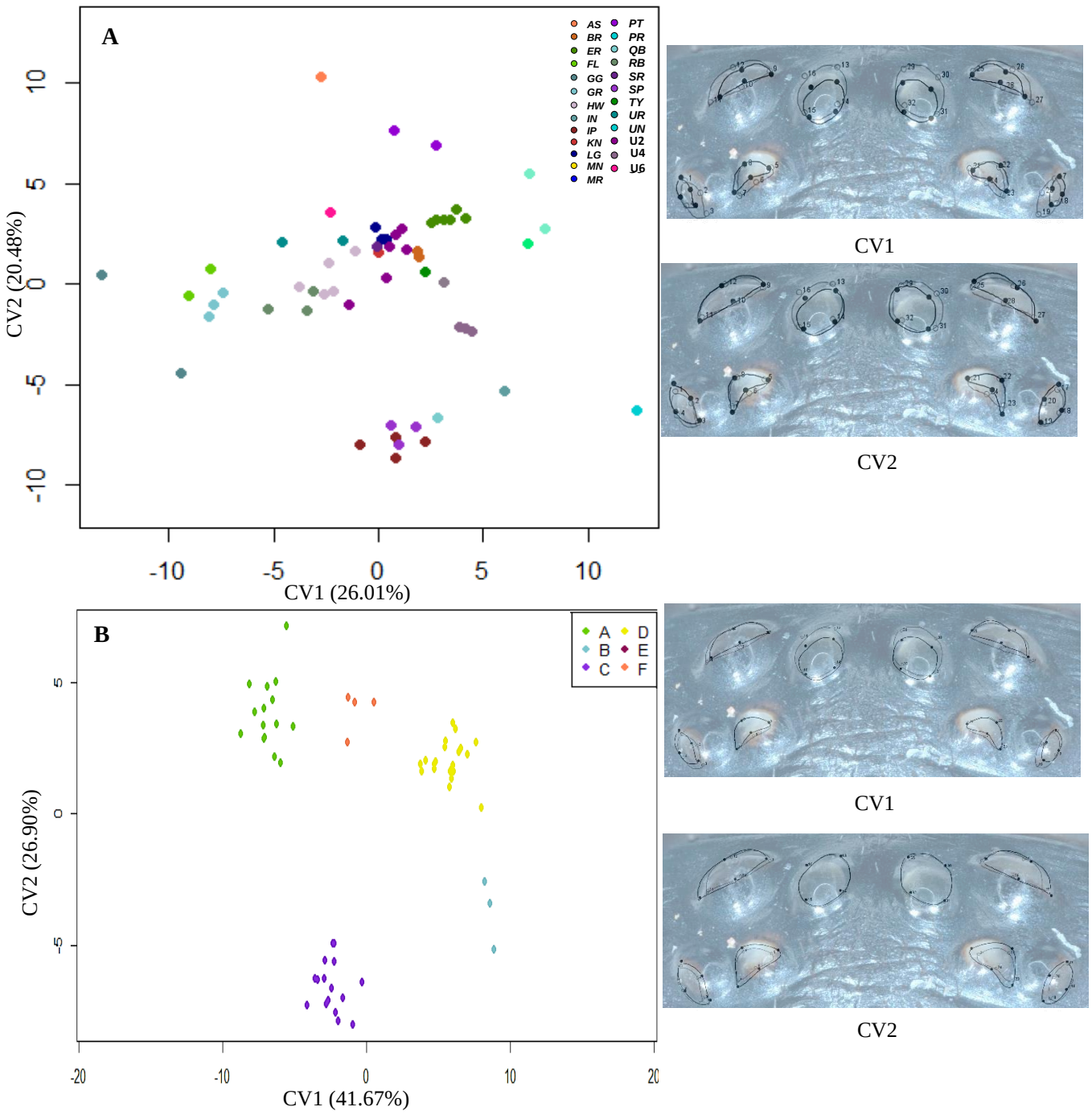


Figure 6. Morphospace plots of the first two CVs for the male dataset. A. CVA by species morphospace plot. The species colours correspond to the map in figure 1. Shape changes in the male ocular pattern for the first and second PC are shown for all the landmarks. The original average shape is indicated in grey and the new target shape in black. B. CVA by locality / morphospecies morphospace plot, also including the shape changes along the CVs.

© University of Pretoria

Discussion

Phylogenetic relationship to eye pattern

This study is the first to test the phylogenetic signal of a trait in *Stasimopus*. The results show that there is significant phylogenetic signal for the relative position and size of eye patterns in the genus. The K_{mult} values for both sexes are above one, this shows that individuals which are more closely related will have morphologically more similar eye patterns than what would be expected under a Brownian evolutionary model (Adams, 2014b). The eye patterns of *Stasimopus* species can thus be used as character for classification of species (Hendrixson & Bond, 2009). The question then becomes, what may drive the observed morphological changes in eye patterns in the various species over evolutionary time? A key pattern which can be observed is that males of a species have larger principal eyes (AMEs) relative to the secondary eyes than females. The primary eyes of arachnids have higher photoreceptor sensitivity and higher spatial accuracy than secondary eyes as well as having the muscularity to allow eye movements (Morehouse et al., 2017). The males may have larger AMEs due to males driving dispersal by actively seeking out females at night and thus having different visual requirements.

Females of *S. rufidens* and Undescribed species 1 also have larger primary eyes relative to secondary when compared to the other species. There is a fundamental gap in the scientific literature concerning the functionality of individual eye pairs within the Araneae and particularly within Mygalomorphae. This oversight is likely due to the assumption that as mygalomorphs occur in low-light environments, they must primarily rely on chemo- and mechanoreception, thus little focus being paid to vision. There is a need for this information as due to the differences in orientation, position and size of each eye pair, it is likely that they all perform different functionalities (Dacke et al., 2001; Kovoor et al., 1993). No eye pairs have ever been tested in isolation for the mygalomorphs, making it difficult to draw concrete reasons as to why there may be differences in the AME of these females. One possibility may be that as the spiderlings have to leave the mothers burrow to construct their own, a larger pair of AMEs may be beneficial in more open habitats as to allow for the detection of predators through the use of active eye movements. If this is the case, then the trait of larger relative AMEs would be shared within a species by both sexes. This could not be confirmed as no male is described for *S. rufidens*.

A high amount of variation was found in the relative position of the PLEs. This may be a new trait to use when identifying species. These eyes would dictate the amount of peripheral vision the spider possess (Morehouse et al., 2017). The females of *S. leipoldti*, Undescribed species 1, Undescribed species 3 and Undescribed species 6 all have PLEs which are angled at 90 degrees, whereas the other species PLEs extend past 90 degrees towards the abdomen. This implies that these species may not require as wide a peripheral vision as the others. Possible reasons for the need of

© University of Pretoria

more peripheral vision may be linked to the density of vegetation around the burrow. If a burrow is not well concealed, the spider may need a wider range of vision in order to detect predators while hunting. Fine scale habitat surveys would be needed to determine if this is the case. Differences in predator and parasitoid fauna may also be a possible reason. Interestingly, these species are not sister taxa, indicating that this has evolved multiple times. The fact that mygalomorph spiders tend to be short-range endemics may explain this (Harvey, 2002; Mason et al., 2018), as genetic drift or isolated and independent selection events over time within these isolated species may have led to the convergent evolution observed.

The PMEs also appear to display variation in relative size between the species in both sexes. In *S. maraisi* and Undescribed species 6, both sexes have PMEs which are significantly larger than the PLEs. The same is seen for females of *S. unispinosus* and Undescribed species 1. Most species appear to have similar sized PMEs and PLEs, except for *S. rufidens*, whose female has larger PLEs than PMEs. The secondary eyes of mygalomorph spiders contain tapetum lining, which is a mechanism for doubling light paths, enabling better detection of dim light (Dahl & Granda, 1989; Morehouse et al., 2017). This has also been linked to the detection of polarized light, for which the secondary eyes are ideally situated on top of the carapace (Dacke et al., 2001). The PMEs of the *Stasimopus* species appear to be the most reflective of the secondary eyes, suggesting that they may be best suited for these functions. The enlargement of these eyes in some species may thus be due to different hunting times. Observational studies would be required to test this postulation. There is again, no clear phylogenetic pattern underlying this trait.

There is a significant relationship between eye pattern and body size when phylogeny is taken into account for both sexes, suggesting evolutionary allometry. This is apparent when looking at the eye pattern of larger species (e.g., *S. gigas*) the eye pattern is sparser and more spread across the carapace than in smaller species.

Eye patterns as an identifier

As clear phylogenetic signal has been confirmed for eye patterns, the next logical step is to determine to what extent it can be applied in a taxonomic context. The morphospace plots (PCA, CVA and between group PCA) show overlap between the sampled species. This is expected due to the continuous nature of the eye patterns as well as the number of species examined (Kallal et al., 2022). Despite this, species still form discrete groupings, implying that the differences between species is greater than within species, this is further supported by the results of the procrustes ANOVA. It is likely that some of the overlap could be reduced by increasing the sample size of each species, as many are only represented by one specimen. The apparent shape differences between the PCs and CVs show that there are distinct shape differences between the various species. This is demonstrated

© University of Pretoria

clearly when looking at the average thin plate splines of the sequenced species. Each species has a distinct eye pattern, but a larger sample size would be necessary to create average shapes for each species.

Another important aspect is that some synoptic species appear to be separate in morphospace (e.g., *S. maraisi* and Undescribed species 6). This could be a useful way of distinguishing species which co-occur in a quantitative manner. There are very few characters which are reliably used to distinguish species not only in *Stasimopus* but the Mygalomorphae generally (Hendrixson & Bond, 2009). Thus, finding a continuous character that can be used to do so would aid in this greatly. This does however, indicate that the morphospecies groupings based on geographic proximity and similarity may be problematic and need to be revised. Cross validation of the locality variable shows fair results. Accuracy is between 50 and 70% for both sexes, which is surprising given the small dataset and geographic groupings.

The results of the regression analyses showed a significant correlation between shape and centroid size for both sexes. These larger specimens are also the data points that affected the VIF results as shape and size are linked. As shown, evolutionary allometry is present in the genus, thus the variation accounted for by this relationship is important when attempting to determine species classifications and should not be removed in subsequent studies. When this relationship is pooled by species, it accounts for below 9% of the variation and is thus, although important, is not a main factor driving shape variation among species. The relationship of size and shape in the eye patterns of *Stasimopus* is important to note as it contributes to shape in larger specimens, but it is not a main contributor to overall eye shape in the genus.

The significant relationship between both species and locality with shape in both sexes reiterates that the relative eye position and size can be used as an identifier. It would be useful to conduct pairwise analyses to determine which species can be differentiated by this technique. This would be a good avenue for future research if a larger sample size can be obtained.

There is clear variation in the relative positions and sizes of the eye patterns in both the males and females of the genus. These differences have qualitatively been used to describe and identify species historically (Engelbrecht & Prendini, 2011; Hendrixson & Bond, 2004; Hewitt, 1910; Pocock, 1902). This study provides the first statistical evidence that this trait carries phylogenetic signal and should and actually can be used for this purpose. We show the power of this method to elucidate the evolutionary history and adaptations of the spider genus. We also show that using geometric morphometrics to quantitatively differentiate morphospecies using this character is possible and there is potential for the methodology to be applied at species level, but this requires validation with more samples or additional species.

© University of Pretoria

References

Adams, D. C. (2014a). A method for assessing phylogenetic least squares models for shape and other high-dimensional multivariate data. *Evolution*, *68*(9), 2675–2688. https://doi.org/10.1111/evo.12463

Adams, D. C. (2014b). A Generalized K Statistic for Estimating Phylogenetic Signal from Shape and Other High-Dimensional Multivariate Data. *Systematic Biology*, *63*(5), 685–697. https://doi.org/10.1093/sysbio/syu030

Adams, D. C., Collyer, M. L., Kaliontzopoulou, A., & Baken, E. K. (2021). *Geomorph: Software for geometric morphometric analyses* (4.0). R package.

Ayoub, N. A., Garb, J. E., Hedin, M., & Hayashi, C. Y. (2007). Utility of the nuclear protein-coding gene, elongation factor-1 gamma (EF-1γ), for spider systematics, emphasizing family level relationships of tarantulas and their kin (Araneae: Mygalomorphae). *Molecular Phylogenetics and Evolution*, *42*, 394–409. https://doi.org/10.1016/j.ympev.2006.07.018

Ayres, D. L., Darling, A., Zwickl, D. J., Beerli, P., Holder, M. T., Lewis, P. O., Huelsenbeck, J. P., Ronquist, F., Swofford, D. L., Cummings, M. P., Rambaut, A., & Suchard, M. A. (2012). BEAGLE: An Application Programming Interface and High-Performance Computing Library for Statistical Phylogenetics. *Systematic Biology*, *61*(1), 170–173. https://doi.org/10.1093/sysbio/syr100

Baken, E. K., Collyer, M. L., Kaliontzopoulou, A., & Adams, D. C. (2021). geomorph v4.0 and gmShiny: Enhanced analytics and a new graphical interface for a comprehensive morphometric experience. *Methods in Ecology and Evolution*, *12*(12), 2355–2363. https://doi.org/10.1111/2041-210X.13723

Bakkes, D. K. (2017). Evaluation of measurement error in rotational mounting of larval *Rhipicephalus* (Acari: Ixodida: Ixodidae) species in geometric morphometrics. *Zoomorphology*, *136*(3), 403–410. https://doi.org/10.1007/s00435-017-0357-8

Bond, J. E., & Beamer, D. A. (2006). A morphometric analysis of mygalomorph spider carapace shape and its efficacy as a phylogenetic character (Araneae). *Invertebrate Systematics*, *20*(1), 1–7. https://doi.org/10.1071/IS05041

Bond, J. E., Hendrixson, B. E., Hamilton, C. A., & Hedin, M. (2012). A reconsideration of the classification of the spider infraorder Mygalomorphae (Arachnida: Araneae) based on three nuclear genes and morphology. *PLoS ONE*, *7*(6), e38753. https://doi.org/https://doi.org/10.1371/journal.pone.0038753

Clavel, J., Aristide, L., & Morlon, H. (2019). A Penalized Likelihood Framework for High-Dimensional Phylogenetic Comparative Methods and an Application to New-World Monkeys Brain Evolution. *Systematic Biology*, *68*(1), 93–116. https://doi.org/10.1093/sysbio/syy045

© University of Pretoria

Clavel, J., Escarguel, G., & Merceron, G. (2015). mvMORPH: an R package for fitting multivariate evolutionary models to morphometric data. *Methods in Ecology and Evolution*, *6*(11), 1311–1319. https://doi.org/10.1111/2041-210X.12420

Collyer, M. L., & Adams, D. C. (2018). RRPP: An R package for fitting linear models to high-dimensional data using residual randomization. *Methods in Ecology and Evolution*, *9*(7), 1772–1779. https://doi.org/10.1111/2041-210X.13029

Collyer, M. L., & Adams, D. C. (2021). *RRPP: Linear Model Evaluation with Randomized Residuals in a Permutation Procedure* (4.0). R package.

Costa-schmidt, L. E., & de Araujo, A. M. (2010). Genitalic variation and taxonomic discrimination in the semi-aquatic spider genus *Paratrechalea* (Araneae: Trechaleidae). *The Journal of Arachnology*, *38*, 242–249. https://doi.org/10.1636/JOA_A09-75.1

Crews, S. C. (2011). A revision of the spider genus *Selenops* Latreille, 1819 (Arachnida, Araneae, Selenopidae) in North America, Central America and the Caribbean. *Zookeys*, *105*, 1–182. https://doi.org/10.3897/zookeys.105.724

Dacke, M., Doan, T. A., & O'Carroll, D. C. (2001). Polarized light detection in spiders. *Journal of Experimental Biology*, *204*(14), 2481–2490. https://doi.org/10.1242/jeb.204.14.2481

Dahl, R. D., & Granda, A. M. (1989). Spectral sensitivities of photoreceptor in the ocelli of the tarantula, *Aphonopelma chalcodes* (Araneae, Theraphosidae). *Journal of Arachnology*, *17*, 195–205.

Doyle, J.J. (1992). Gene trees and species trees: Molecular systematic one-character taxonomy. *Systematic Botany*, *17*, 144–163. https://doi.org/10.2307/2419070

Drummond, A. J., Ho, S. Y. W., Phillips, M. J., & Rambaut, A. (2006). Relaxed phylogenetics and dating with confidence. *PLoS Biology*, *4*(5), 0699–0710. https://doi.org/10.1371/journal.pbio.0040088

Dunlop, J. A., Penney, D., & Jekel, D. (2020). A summary list of fossil spiders and their relatives. World Spider Catalog; Natural History Museum Bern. http://wsc.nmbe.ch

Engelbrecht, I., & Prendini, L. (2011). Assessing the taxonomic resolution of southern African trapdoor spiders (Araneae: Ctenizidae; Cyrtaucheniidae; Idiopidae) and implications for their conservation. *Biodiversity and Conservation*, *20*(13), 3101–3116. https://doi.org/10.1007/s10531-011-0115-z

Engelbrecht, I., & Prendini, L. (2012). Cryptic diversity of South African trapdoor spiders: Three new species of *Stasimopus* Simon, 1892 (Mygalomorphae, Ctenizidae), and redescription of *Stasimopus robertsi* Hewitt, 1910. *American Museum Novitates*, *3732*, 1–42. https://doi.org/https://doi.org/10.1206/3732.2

© University of Pretoria

Fernández-Montraveta, C., & Marugán-Lobón, J. (2017). Geometric morphometrics reveals sex-differential shape allometry in a spider. *PeerJ*, *5*, e3617. https://doi.org/10.7717/peerj.3617

Forthofer, R. N., Lee, E. S., & Hernandez, M. (2007). Linear Regression. *Biostatistics*, 349–386. https://doi.org/10.1016/B978-0-12-369492-8.50018-2

Fox, J., & Weisberg, S. (2019). *An R Companion to Applied Regression* (Third). Sage.

Fruciano, C. (2016). Measurement error in geometric morphometrics. *Development Genes and Evolution*, *226*(3), 139–158. https://doi.org/10.1007/s00427-016-0537-4

Goodall, C. (1991). Procrustes Methods in the Statistical Analysis of Shape. *Journal of the Royal Statistical Society: Series B (Methodological)*, *53*(2), 285–321. https://doi.org/10.1111/j.2517-6161.1991.tb01825.x

Harvey, M. S. (2002). Short-range endemism among the Australian fauna: some examples from non-marine environments. *Invertebrate Systematics*, *16*, 555–570. https://doi.org/10.1071/IS02009

Hendrixson, B. E., & Bond, J. E. (2004). A new species of *Stasimopus* from the Eastern Cape Province of South Africa (Araneae, Mygalomorphae, Ctenizidae), with notes on its natural history. *Zootaxa*, *619*, 1–14. http://dx.doi.org/10.5281/zenodo.10101

Hendrixson, B. E., & Bond, J. E. (2009). Evaluating the efficacy of continuous quantitative characters for reconstructing the phylogeny of a morphologically homogeneous spider taxon (Araneae, Mygalomorphae, Antrodiaetidae, *Antrodiaetus*). *Molecular Phylogenetics and Evolution*, *53*(1), 300–313. https://doi.org/10.1016/j.ympev.2009.06.001

Hewitt, J. (1910). Description of two trapdoor spiders from Pretoria (female of *Acanthodon pretoriae* Poc. and *Stasimopus robertsi*, n. sp.). *Annals of the Transvaal Museum*, *2*, 74–76.

Jocque, R., & Dippenaar-Schoeman, A. S. (2007). *Spider families of the world* (Second ed.). Royal Museum for Central Africa.

Kallal, R. J., de Miranda, G. S., Garcia, E. L., & Wood, H. M. (2022). Patterns in schizomid flagellum shape from elliptical Fourier analysis. *Scientific Reports*, *12*(1), 3896. https://doi.org/10.1038/s41598-022-07823-y

Katoh, K. (2005). MAFFT version 5: improvement in accuracy of multiple sequence alignment. *Nucleic Acids Research*, *33*, 511–518. https://doi.org/10.1093/nar/gki198

Katoh, K., Toh, H. (2008). Recent developments in the MAFFT multiple sequence alignment program. *Briefings in Bioinformatics*, *9*, 286–298. https://doi.org/10.1093/bib/bbn013

© University of Pretoria

Klingenberg, C. P. (2011). MorphoJ: an integrated software package for geometric morphometrics. *Molecular Ecology Resources*, *11*, 353–357. https://doi.org/10.1111/j.1755-0998.2010.02924.x

Klingenberg, C. P. (2016). Size, shape, and form: concepts of allometry in geometric morphometrics. *Development Genes and Evolution*, *226*(3), 113–137. https://doi.org/https://doi.org/10.1007/s00427-016-0539-2

Klingenberg, C. P., & Gidaszewski, N. A. (2010). Testing and Quantifying Phylogenetic Signals and Homoplasy in Morphometric Data. *Systematic Biology*, *59*(3), 245–261. https://doi.org/10.1093/sysbio/syp106

Kornilios, P., Thanou, E., Kapli, P., Parmakelis, A., & Chatzaki, M. (2016). Peeking through the trapdoor: Historical biogeography of the Aegean endemic spider *Cyrtocarenum Ausserer*, 1871 with an estimation of mtDNA substitution rates for Mygalomorphae. *Molecular Phylogenetics and Evolution*, *98*, 300–313. https://doi.org/10.1016/j.ympev.2016.01.021

Kovoor, J., Cuevas, A. M., & Escobar, J. O. (1993). Microanatomy of the anterior median eyes and its possible relation to polarized-light reception in *Lycosa tarentula* (Araneae, Lycosidae). *Bolletino Di Zoologia*, *60*(4), 367–375. https://doi.org/10.1080/11250009309355841

Leavitt, D. H., Starrett, J., Westphal, M. F., & Hedin, M. (2015). Multilocus sequence data reveal dozens of putative cryptic species in a radiation of endemic Californian mygalomorph spiders (Araneae, Mygalomorphae, Nemesiidae). *Molecular Phylogenetics and Evolution*, *91*, 56–67. https://doi.org/10.1016/j.ympev.2015.05.016

Kück, P., & Meusemann, K. (2010). FASconCAT: Convenient handling of data matrices. *Molecular Phylogenetics and Evolution*, *56*, 1115–1118. https://doi.org/10.1016/j.ympev.2010.04.024

Kumar, S., Stecher, G., Li, M., Knyaz, C., & Tamura, K. (2018). MEGA X: Molecular Evolutionary Genetics Analysis across Computing Platforms. *Molecular Biology and Evolution*, *35*(6), 1547–1549. https://doi.org/10.1093/molbev/msy096

Maddison, W.P. (1997). Gene trees in species trees. *Systematic Bibliology*, *46*, 523–536. https://doi.org/10.1093/sysbio/46.3.523

Maindonald, J. H., & Braun, W. J. (2020). *DAAG: Data Analysis and Graphics Data and Functions* (1.24). R package.

Manthey, L., & Ousley, S. D. (2020). Geometric morphometrics. *Statistics and Probability in Forensic Anthropology*, 289–298. https://doi.org/10.1016/B978-0-12-815764-0.00023-X

Mason, L. D., Wardell-Johnson, G., & Main, B. Y. (2018). The longest-lived spider: mygalomorphs dig deep, and persevere. *Pacific Conservation Biology*, *24*(2), 203. https://doi.org/10.1071/PC18015

© University of Pretoria

McKeown, A. H., & Schmidt, R. W. (2013). Geometric Morphometrics. In DiGangi, E.A & Moore, M. K. (Eds.), *Research Methods in Human Skeletal Biology* (pp. 325–359). Elsevier. https://doi.org/10.1016/B978-0-12-385189-5.00012-1

Michonneau, F. (2017). Using GMYC for species delimitation. *Zenodo*. https://doi.org/10.5281/zenodo.838259

Mitteroecker, P., & Gunz, P. (2009). Advances in Geometric Morphometrics. *Evolutionary Biology*, *36*, 235–247. https://doi.org/10.1007/s11692-009-9055-x

Mora, E., Paspati, A., Decae, A. E., & Arnedo, M. A. (2017). Rafting spiders or drifting islands? Origins and diversification of the endemic trap-door spiders from the Balearic Islands, Western Mediterranean. *Journal of Biogeography*, *44*, 924–936. https://doi.org/10.1111/jbi.12885

Morehouse, N. I., Buschbeck, E. K., Zurek, D. B., Steck, M., & Porter, M. L. (2017). Molecular evolution of spider vision: New opportunities, familiar players. *Biological Bulletin*, *233*(1), 21–38. https://doi.org/10.1086/693977

Nakagawa, S., Kar, F., O'Dea, R. E., Pick, J. L., & Lagisz, M. (2017). Divide and conquer? Size adjustment with allometry and intermediate outcomes. *BMC Biology*, *15*(1), 107. https://doi.org/10.1186/s12915-017-0448-5

Opatova, V., Bond, J. E., & Arnedo, M. A. (2013). Ancient origins of the Mediterranean trap-door spiders of the family Ctenizidae (Araneae, Mygalomorphae). *Molecular Phylogenetics and Evolution*, *69*, 1135–1145. https://doi.org/10.1016/j.ympev.2013.08.002

Opatova, V., Hamilton, C. A., Hedin, M., de Oca, L. M., Král, J., & Bond, J. E. (2020). Phylogenetic Systematics and Evolution of the Spider Infraorder Mygalomorphae Using Genomic Scale Data. *Systematic Biology*, *69*(4), 671–707. https://doi.org/10.1093/sysbio/syz064

Pirouz, D. M. (2006). An Overview of Partial Least Squares. *SSRN Electronic Journal*. https://doi.org/10.2139/ssrn.1631359

Pocock, R. I. (1902). Descriptions of some new species of African Solifugae and Araneae. *Annals and Magazine of Natural History*, *7*(10), 6–27.

Polotow, D., & Brescovit, A. D. (2014). Phylogenetic analysis of the tropical wolf spider subfamily Cteninae (Arachnida, Araneae, Ctenidae). *Journal of the Linnean Society*, *170*, 333–361. https://doi.org/10.1111/zoj.12101

Posada, D. (2008). jModelTest: Phylogenetic model averaging. *Molecular Biology and Evolution*, *25*(7), 1253–1256. https://doi.org/10.1093/molbev/msn083

© University of Pretoria

Prenter, J., Montgomery, I. W., & Elwood, R. W. (1995). Multivariate morphometrics and sexual dimorphism in the orb-web spider *Metellina segmentata* (Clerck, 1757) (Araneae, Metidae). *Biological Journal of the Linnean Society*, *55*, 345–354.

R Core Team. (2017). *R: A language and environment for statistical computing* (3.3.3). R Foundation for Statistical Computing. www.R-project.org

Rambaut, A. (2016). *FigTree* (1.4.3). Institute of Evolutionary Biology, University of Edinburgh, Edinburgh.
http://tree.bio.ed.ac.uk/software/figtree/

Rambaut, A., Drummond, A. J., Xie, D., Baele, G., & Suchard, M. A. (2018). Posterior Summarization in Bayesian Phylogenetics Using Tracer 1.7. *Systematic Biology*, *67*(5), 901–904.
https://doi.org/10.1093/sysbio/syy032

Ringle, C. M., Sarstedt, M., Mitchell, R., & Gudergan, S. P. (2018). Partial least squares structural equation modelling in HRM research. *The International Journal of Human Resource Management*, *31*(12), 1617–1643.
https://doi.org/10.1080/09585192.2017.1416655

Rodriguez-Mendoza, R. (2013). *Population structure of the bluemouth, Helicolenus dactylopterus (Teleostei: Sebastidae), in the Northeast Atlantic and Mediterranean using geometric morphometric techniques* [Thesis]. University of Vigo.

Rohlf, F. J. (2015). The tps series of software. *Hystrix, the Italian Journal of Mammalogy*, *26*, 1–4.
https://doi.org/10.4404/hystrix-26.1-11264

Rohlf, F. J., & Corti, M. (2000). Use of Two-Block Partial Least-Squares to Study Covariation in Shape. *Systematic Biology*, *49*(4), 740–753.
https://doi.org/10.1080/106351500750049806

Rohlf, F. J., & Marcus, L. F. (1993). A Revolution in Morphometrics. *TREE*, *8*(4), 129–132.
https://doi.org/10.1016/0169-5347(93)90024-J

Schlager, S. (2013). *Soft-tissue reconstruction of the human nose: population differences and sexual dimorphism* [Thesis]. Freiburg University.

Seetah, T. K. (2014). Geometric Morphometrics and Environmental Archaeology. In C. Smith (Ed.), *Encyclopaedia of Global Archaeology*. Springer.
https://doi.org/10.1007/978/1-4419-0465-2

Selden, P. A. (2002). First British Mesozoic spider, from Cretaceous amber of the Isle of Wight, southern England. *Palaeontology, 45*, 973–983.
https://doi.org/10.1111/1475-4983.00271

Selden, P. A., & Gall, J. C. (1992). A Triassic mygalomorph spider from the northern Vosges, France. *Palaeontology*, *35*(1), 211–235.

Simon, E. (1892). Histoire naturelle des araignées. *Deuxième Édition, Tome Premier*, 1–256.

© University of Pretoria

Spasojevic, T., Kropf, C., Nentwig, W., & Lasut, L. (2016). Combining morphology, DNA sequences and morphometrics: revising closely related species in the orb-weaving spider genus *Araniella* (Araneae, Araneidae). *Zootaxa*, *4111*(4), 488–470. https://doi.org/10.11646/zootaxa.4111.4.6

Suchard, M. A., Lemey, P., Baele, G., Ayres, D. L., Drummond, A. J., & Rambaut, A. (2018). Bayesian phylogenetic and phylodynamic data integration using BEAST 1.10. *Virus Evolution*, *4*(1), vey016. https://doi.org/10.1093/ve/vey016

Wheeler, W. C., Coddington, J. A., Crowley, L. M., Dimitrov, D., Goloboff, P. A., Griswold, C. E., Hormiga, G., Prendini, L., Ramirez, M. J., Sierwald, P., Almeida-Silva, L., Alvarez-Padilla, F., Arnedo, M. A., Benavides Silva, L. R., Benjamin, S. P., Bond, J. E., Grismado, C. J., Hasan, E., Hedin, M., …, & Zhang, J. (2016). The spider tree of life: phylogeny of Araneae based on target-gene analyses from an extensive taxon sampling. *Cladistics*, 33. https://doi.org/10.1111/cla.12182

World Spider Catalog. (2022). *World Spider Catalog Version 23.5*. Natural History Museum Bern. Retrieved June 5, 2022 from https://doi.org/10.24436/2

Wunderlich, J. (1998). Beschreibung der ersten fossilen Spinnen der Unterfamilien Mysmeninae (Anapidae) und Erigoninae (Linyphiidae) im Dominikanischen Bernstein (Arachnida: Araneae). *Entomologische Zeitschrift, 108*, 363–367.

Wunderlich, J. (2000). Zwei neue Arten der Familie Falltürspinnen (Araneae: Ctenizidae) aus dem Baltischen Bernstein. *Entomologische Zeitschrift, 110*, 345–348.

Zelditch, M. L., Swiderski, D. L., Sheets, H. D., & Fink, W. L. (2004a). Landmarks. In M. L. Zelditch, D. L. Swiderski, & H. D. Sheets (Eds.), *Geometric Morphometrics For Biologists: A Primer* (2nd ed., pp. 23–50). Elsevier Academic Press.

Zelditch, M. L., Swiderski, D. L., Sheets, H. D., & Fink, W. L. (2004b). Superimposition methods. In M. L. Zelditch, D. L. Swiderski, & H. D. Sheets (Eds.), *Geometric Morphometrics For Biologists: A Primer* (2nd ed., pp. 105–128). Elsevier Academic Press.

Zelditch, M. L., Swiderski, D. L., Sheets, H. D., & Fink, W. L. (2004c). Theory of Shape. In M. L. Zelditch, D. L. Swiderski, & H. D. Sheets (Eds.), *Geometric Morphometrics For Biologists: A Primer* (2nd ed., pp. 73–104). Elsevier Academic Press.

Žikić, V., Stanković, S. S., Petrović, A., Ilić Milošević, M., Tomanović, Ž., Klingenberg, C. P., & Ivanović, A. (2017). Evolutionary relationships of wing venation and wing size and shape in Aphidiinae (Hymenoptera: Braconidae). *Organisms Diversity & Evolution, 17*(3), 607–617. https://doi.org/10.1007/s13127-017-0338-2

© University of Pretoria

Supplementary material

Table S1. Specimen information for samples used in Geometric morphometric analyses. GenBank ascension numbers are given for each gene region for sequenced specimen.

No.	CODE	Sex	Species	Museum	Museum Voucher	CO1	Efɣ-1
1	SAR01FLC	F	*S. artifex*	BMNH	BMNH-1899.7.24.47	---	---
2	SAR02FLC	F	*S. artifex*	AMGS	AMGS-1562	---	---
3	SAS01FLD	F	*S. astutus*	BMNH	BMNH-1902-3-8-2-3	---	---
4	SAS02FLD	F	*S. astutus*	BMNH	BMNH-1902-3-8-2-3	---	---
5	SAS03FLD	F	*S. astutus*	BMNH	BMNH-1902-3-8-2-3	---	---
6	SAS01KLD	F	*S. astutus*	NCA	NCA 2017/1906	MK923804	MK923916
7	SAS02KLD	F	*S. astutus*	NCA	NCA 2019/638	MK923819	---
8	SAS03KLD	F	*S. astutus*	NCA	NCA 2019/635	MK923820	MK923927
9	SAS04KLD	F	*S. astutus*	NCA	NCA 2019/647	MK923844	---
10	SBR01FLF	F	*S. brevipalpis*	SAMC	SAMC-12394	---	---
11	SBR02FLF	F	*S. brevipalpis*	SAMC	SAMC-12758	---	---
12	SBR03FLF	F	*S. brevipalpis*	SAMC	SAMC-12758	---	---
13	SDR01FLA	F	*S. dreyeri*	AMGS	AMGS-2180	---	---
14	SDB01FLA	F	*S. dubious*	TMSA	TMSA-2745	---	---
15	SER01FLF	F	*S. erythrognathus*	AMGS	AMGS-84633	---	---
16	SER02FLF	F	*S. erythrognathus*	AMGS	AMGS-84636	---	---
17	SER03FLF	F	*S. erythrognathus*	AMGS	AMGS-84646	---	---
18	SER01KLD	F	*S. erythrognathus*	NCA	NCA 2019/625	MK923811	---
19	SER02KLD	F	*S. erythrognathus*	NCA	NCA 2019/626	---	---
20	SER03KLD	F	*S. erythrognathus*	NCA	NCA 2019/627	MK923812	---
21	SER04KLD	F	*S. erythrognathus*	NCA	NCA 2019/645	---	MK923965
22	SER05KLD	F	*S. erythrognathus*	NCA	NCA 2019/665	MK923853	MK923966
23	SER06KLD	F	*S. erythrognathus*	NCA	NCA 2019/666	MK923854	MK923967
24	SER07KLD	F	*S. erythrognathus*	NCA	NCA 2017/1916	MK923862	MK923975
25	SFL01FLA	F	*S. filmeri*	TMSA	TMSA-23996	---	---
26	SFL03FLA	F	*S. filmeri*	TMSA	TMSA-23998	---	---
27	SGG01FLA	F	*S. gigas*	BMNH	Unavailable	---	---
28	SGG03FLA	F	*S. gigas*	SAMC	SAMC-10068	---	---
29	SGR01FLA	F	*S. griswoldi*	TMSA	TMSA-24001	---	---
30	SGR02FLA	F	*S. griswoldi*	TMSA	TMSA-24001	---	---
31	SGR03FLA	F	*S. griswoldi*	TMSA	TMSA-24001	---	---
32	SHW01FLA	F	*S. hewitti*	TMSA	TMSA-23989	---	---
33	SIN01FLC	F	*S. insculptus*	AMGS	AMGS-Oct_1912	---	---
34	SIN02FLC	F	*S. insculptus*	AMGS	AMGS-84603	---	---
35	SIP01FLC	F	*S. insculptus peddiensis*	AMGS	NM15345	---	---
36	SIP02FLC	F	*S. insculptus peddiensis*	AMGS	NM15337	---	---
37	SIP03FLC	F	*S. insculptus peddiensis*	AMGS	NM15327	---	---
38	STS01FLC	F	*S. insculptus peddiensis*	AMGS	AMGS-84578	---	---
39	STS02FLC	F	*S. insculptus peddiensis*	AMGS	AMGS-84590	---	---
40	STS03FLC	F	*S. insculptus peddiensis*	AMGS	AMGS-84594	---	---
41	STS04FLC	F	*S. insculptus peddiensis*	AMGS	AMGS-84583	---	---
42	STS05FLC	F	*S. insculptus peddiensis*	AMGS	AMGS-84577	---	---
43	STS06FLC	F	*S. insculptus peddiensis*	AMGS	AMGS-84589	---	---
44	STS07FLC	F	*S. insculptus peddiensis*	AMGS	AMGS-84584	---	---

© University of Pretoria

Table S1 (cont.). Specimen information for samples used in Geometric morphometric analyses. GenBank ascension numbers are given for each gene region for sequenced specimen.

No.	16S	Locality
1	---	SOUTH AFRICA, Eastern Cape, Cuylerville
2	---	SOUTH AFRICA, Eastern Cape, Rokeby Park
3	---	SOUTH AFRICA, Eastern Cape, Pearston
4	---	SOUTH AFRICA, Eastern Cape, Pearston
5	---	SOUTH AFRICA, Eastern Cape, Pearston
6	MK935609	SOUTH AFRICA, Eastern Cape, Somerset East; BioGaps site 3230_2510
7	MK935625	SOUTH AFRICA, Eastern Cape, Aberdeen; near Biogaps site 3245_2405
8	MK935626	SOUTH AFRICA, Eastern Cape, Aberdeen; near Biogaps site 3245_2405
9	MK935651	SOUTH AFRICA, Western Cape, Waterkloof; near Biogaps site 3210_2345
10	---	SOUTH AFRICA, Western Cape, Robertson, Ashton
11	---	SOUTH AFRICA, Western Cape, Robertson, Ashton
12	---	SOUTH AFRICA, Western Cape, Robertson, Ashton
13	---	SOUTH AFRICA, Free State, Kroonstad
14	---	SOUTH AFRICA, North West, Potchefstroom
15	---	SOUTH AFRICA, Western Cape, Worster
16	---	SOUTH AFRICA, Western Cape, Worster
17	---	SOUTH AFRICA, Western Cape, Worster
18	MK935616	SOUTH AFRICA, Eastern Cape, Queenstown; Biogaps site 3140_2640
19	MK935617	SOUTH AFRICA, Eastern Cape, Queenstown; Biogaps site 3140_2640
20	MK935618	SOUTH AFRICA, Eastern Cape, Queenstown; Biogaps site 3140_2640
21	MK935666	SOUTH AFRICA, Eastern Cape, Kambrokop.
22	MK935667	SOUTH AFRICA, Eastern Cape, Kambrokop.
23	MK935668	SOUTH AFRICA, Eastern Cape, Kambrokop.
24	MK935675	SOUTH AFRICA, Eastern Cape, Cradock
25	---	SOUTH AFRICA, Gauteng, Krugersdorp, Hartebeestfontien farm
26	---	SOUTH AFRICA, Gauteng, Krugersdorp, Hartebeestfontien farm
27	---	SOUTH AFRICA, Free State, Vredefort
28	---	SOUTH AFRICA, Free State, Vredefort
29	---	SOUTH AFRICA, North-West, Brits, Hartebeestfontien farm
30	---	SOUTH AFRICA, North-West, Brits, Hartebeestfontien farm
31	---	SOUTH AFRICA, North-West, Brits, Hartebeestfontien farm
32	---	SOUTH AFRICA, Gauteng, Pretoria, Roodeplaat dam nature reserve
33	---	SOUTH AFRICA, Eastern Cape, King William's Town
34	---	SOUTH AFRICA, Eastern Cape, nr. King William's town, Debe Nek
35	---	SOUTH AFRICA, Eastern Cape, Peddie
36	---	SOUTH AFRICA, Eastern Cape, Peddie
37	---	SOUTH AFRICA, Eastern Cape, Peddie
38	---	SOUTH AFRICA, Eastern Cape, Peddie
39	---	SOUTH AFRICA, Eastern Cape, Peddie
40	---	SOUTH AFRICA, Eastern Cape, Peddie
41	---	SOUTH AFRICA, Eastern Cape, Peddie
42	---	SOUTH AFRICA, Eastern Cape, Peddie
43	---	SOUTH AFRICA, Eastern Cape, Peddie
44	---	SOUTH AFRICA, Eastern Cape, Peddie

© University of Pretoria

Table S1 (cont.). Specimen information for samples used in Geometric morphometric analyses. GenBank ascension numbers are given for each gene region for sequenced specimen.

No.	CODE	Sex	Species	Museum	Museum Voucher	CO1	Efy-1
45	STS08FLC	F	*S. insculptus peddiensis*	AMGS	AMGS-84581	---	---
46	STS09FLC	F	*S. insculptus peddiensis*	AMGS	AMGS-84587	---	---
47	STS010FLC	F	*S. insculptus peddiensis*	AMGS	AMGS-84575	---	---
48	SKN01FLC	F	*S. kentanicus*	SAMC	SAMC-12411	---	---
49	SKN03FLC	F	*S. kentanicus*	AMGS	AMGS-84621	---	---
50	SKB01FLC	F	*S. kolbei*	SAMC	SAMC-5317	---	---
51	SKB02FLC	F	*S. kolbei*	SAMC	SAMC-13690	---	---
52	SKB03FLC	F	*S. kolbei*	SAMC	SAMC-14296	---	---
53	SLP01FLF	F	*S. leipoldti*	SAMC	SAMC-2909	---	---
54	SLP01KLF	F	*S. leipoldti*	NCA	NCA 2017/1870	MK923786	MK923898
55	SLP02KLF	F	*S. leipoldti*	NCA	NCA 2017/1871	MK923787	MK923899
56	SLG01FLB	F	*S. longipalpis*	AMGS	NM14949	---	---
57	SLG02FLB	F	*S. longipalpis*	AMGS	NM14948	---	---
58	SMR01FLD	F	*S. maraisi*	AMGS	NM14631	---	---
59	SMR03FLD	F	*S. maraisi*	AMGS	NM14632	---	---
60	SMR01KLD	F	*S. maraisi*	NCA	NCA 2017/1845	MK923772	MK923883
61	SMR02KLD	F	*S. maraisi*	NCA	NCA 2017/1853	MK923777	MK923888
62	SMR03KLD	F	*S. maraisi*	NCA	NCA 2017/1862	MK923784	MK923895
63	SMR04KLD	F	*S. maraisi*	NCA	NCA 2017/1882	MK923791	MK923902
64	SMR05KLD	F	*S. maraisi*	NCA	NCA 2017/1885	MK923794	MK923905
65	SMR07KLD	F	*S. maraisi*	NCA	NCA 2019/636	MK923825	MK923932
66	SMR08KLD	F	*S. maraisi*	NCA	NCA 2019/689	MK923839	---
67	SMY02FLE	F	*S. meyeri*	ZMBH	ZMBH-2903	---	---
68	SOB01FLE	F	*S. obscurus*	ZMBH	ZMBH-9412	---	---
69	SOC01FLB	F	*S. oculatus*	BMNH	BMNH-1883-70	---	---
70	SPT01FLC	F	*S. patersonae*	AMGS	AMGS-1634	---	---
71	SPW01FLB	F	*S. poweri*	AMGS	NM15358	---	---
72	SPW02FLB	F	*S. poweri*	AMGS	NM15357	---	---
73	SPW03FLB	F	*S. poweri*	AMGS	NM15354	---	---
74	SQD01FLF	F	*S. quadratimaculatus*	SAMC	SAMC-12398	---	---
75	SQD02FLF	F	*S. quadratimaculatus*	SAMC	SAMC-12399	---	---
76	SQD03FLF	F	*S. quadratimaculatus*	SAMC	SAMC-12400	---	---
77	SQB01FLC	F	*S. qumbu*	AMGS	AMGS-84734	---	---
78	SQB02FLC	F	*S. qumbu*	AMGS	AMGS-84734	---	---
79	SRB01FLA	F	*S. robertsi*	TMSA	TMSA-3109-3112	---	---
80	SRB02FLA	F	*S. robertsi*	TMSA	TMSA-3109-3112	---	---
81	SRF01FLB	F	*S. rufidens*	NCA	NCA 2019/704	---	---
82	SSH01FLC	F	*S. schonlandi*	BMNH	STAS_425	---	---
83	SSH02FLC	F	*S. schonlandi*	AMGS	AMGS-84755	---	---
84	SSR01FLD	F	*S. schrieneri*	SAMC	SAMC-9513	---	---
85	SSR02FLD	F	*S. schrieneri*	SAMC	SAMC-9516	---	---
86	SSR03FLD	F	*S. schrieneri*	SAMC	SAMC-9558	---	---
87	SSR01KLD	F	*S. schrieneri*	NCA	NCA 2019/671	MK923849	MK923958
88	SSR02KLD	F	*S. schrieneri*	NCA	NCA 2019/672	MK923850	MK923959

© University of Pretoria

Table S1 (cont.). Specimen information for samples used in Geometric morphometric analyses. GenBank ascension numbers are given for each gene region for sequenced specimen.

No.	16S	Locality
45	---	SOUTH AFRICA, Eastern Cape, Peddie
46	---	SOUTH AFRICA, Eastern Cape, Peddie
47	---	SOUTH AFRICA, Eastern Cape, Peddie
48	---	SOUTH AFRICA, Eastern Cape, Transkei, Kentani
49	---	SOUTH AFRICA, Eastern Cape, Transkei, Kentani
50	---	SOUTH AFRICA, Eastern Cape, Transkei, Kentani
51	---	SOUTH AFRICA, Eastern Cape, Transkei, Kentani
52	---	SOUTH AFRICA, Eastern Cape, Transkei, Kentani
53	---	SOUTH AFRICA, Western Cape, Clanwilliam
54	---	SOUTH AFRICA, Northern Cape, Laingsburg; near BioGaps site 3240_2020
55	MK935596	SOUTH AFRICA, Northern Cape, Laingsburg; near BioGaps site 3240_2020
56	---	SOUTH AFRICA, Northern Cape, Kimberly
57	---	SOUTH AFRICA, Northern Cape, Kimberly
58	---	SOUTH AFRICA, Northern Cape, Victoria West, Driefontien
59	---	SOUTH AFRICA, Northern Cape, Victoria West, Driefontien
60	MK935581	SOUTH AFRICA, Western Cape, Victoria West; BioGaps site 3155_2330
61	MK935586	SOUTH AFRICA, Western Cape, Beaufort West; BioGaps site 3155_2250
62	MK935593	SOUTH AFRICA, Northern Cape, Victoria West; BioGaps site 3105_2245
63	---	SOUTH AFRICA, Western Cape, Beaufort West; BioGaps site 3225_2205
64	MK935601	SOUTH AFRICA, Western Cape, Prince Albert; BioGaps site 3255_2220
65	MK935631	SOUTH AFRICA, Northern Cape, Farm Draai Drift, Biogaps site 3210_2150
66	MK935646	SOUTH AFRICA, Northern Cape, Bakenskop; Biogaps site 3120_2140
67	---	SOUTH AFRICA, Northern Cape, Hantam
68	---	SOUTH AFRICA, Northern Cape, Little Namaqualand
69	---	SOUTH AFRICA, Free State, Bloemfontien
70	---	SOUTH AFRICA, Eastern Cape, Perserverence
71	---	SOUTH AFRICA, Free State, Bloemfontien, Modder rivier
72	---	SOUTH AFRICA, Free State, Bloemfontien, Modder rivier
73	---	SOUTH AFRICA, Free State, Bloemfontien, Modder rivier
74	---	SOUTH AFRICA, Western Cape, Montague Baths
75	---	SOUTH AFRICA, Western Cape, Montague Baths
76	---	SOUTH AFRICA, Western Cape, Montague Baths
77	---	SOUTH AFRICA, Eastern Cape, Transkei, Qumbu
78	---	SOUTH AFRICA, Eastern Cape, Transkei, Qumbu
79	---	SOUTH AFRICA, Gauteng, Pretoria, Lyttelton junction
80	---	SOUTH AFRICA, Gauteng, Pretoria, Lyttelton junction
81	MK935681	SOUTH AFRICA, KwaZulu-Natal, Ukuwela, Hhluhluwe
82	---	SOUTH AFRICA, Eastern Cape, Grahamstown
83	---	SOUTH AFRICA, Eastern Cape, King William's Town
84	---	SOUTH AFRICA, Eastern Cape, Hanover
85	---	SOUTH AFRICA, Eastern Cape, Hanover
86	---	SOUTH AFRICA, Eastern Cape, Hanover
87	MK935659	SOUTH AFRICA, Northern Cape, Richmond; near Biogaps site 3135_2410
88	MK935660	SOUTH AFRICA, Northern Cape, Richmond; near Biogaps site 3135_2410

© University of Pretoria

Table S1 (cont.). Specimen information for samples used in Geometric morphometric analyses. GenBank ascension numbers are given for each gene region for sequenced specimen.

No.	CODE	Sex	Species	Museum	Museum Voucher	CO1	Efy-1
89	SSR03KLD	F	*S. schrieneri*	NCA	NCA 2019/673	MK923851	MK923960
90	SSZ01FLE	F	*S. shultzei*	SAMC	SAMC-150,154	---	---
91	SSZ02FLE	F	*S. shultzei*	SAMC	SAMC-B8497	---	---
92	SSZ03FLE	F	*S. shultzei*	SAMC	SAMC-B8497	---	---
93	SSP01FLC	F	*S. spinipes*	AMGS	NM16728	---	---
94	SSP02FLC	F	*S. spinipes*	AMGS	NM16728	---	---
95	SSP03FLC	F	*S. spinipes*	AMGS	NM14825	---	---
96	SSU01FLA	F	*S. sufficus*	TMSA	TMSA-2742	---	---
97	STY01FLC	F	*S. tysoni*	AMGS	NM14965	---	---
98	STY02FLC	F	*S. tysoni*	AMGS	NM14963	---	---
99	STY03FLC	F	*S. tysoni*	AMGS	NM14964	---	---
100	SUR01FLC	F	*S. umtaticus rangeri*	AMGS	NM14772	---	---
101	SUN01FLD	F	*S. unispinosus*	SAMC	SAMC-9523	---	---
102	SUN02FLD	F	*S. unispinosus*	SAMC	SAMC-9579	---	---
103	SUN03FLD	F	*S. unispinosus*	SAMC	SAMC-9426	---	---
104	SUN01KLD	F	*S. unispinosus*	NCA	NCA 2017/1835	MK923764	MK923875
105	SUN03KLD	F	*S. unispinosus*	NCA	NCA 2019/654	---	MK923961
106	SUN04KLD	F	*S. unispinosus*	NCA	NCA 2019/655	---	MK923962
107	S1N01KLD	F	Undescribed 1 / *S. hamartia* n. sp.	NCA	NCA 2017/1849	MK923774	MK923885
108	S1N02KLD	F	Undescribed 1 / *S. hamartia* n. sp.	NCA	NCA 2017/1852	MK923776	MK923887
109	S1N03KLD	F	Undescribed 1 / *S. hamartia* n. sp.	NCA	NCA 2017/1888	MK923797	MK923908
110	S1N04KLD	F	Undescribed 1 / *S. hamartia* n. sp.	NCA	NCA 2017/1889	MK923798	MK923909
111	S1N05KLD	F	Undescribed 1 / *S. hamartia* n. sp.	NCA	NCA 2019/660	MK923823	MK923930
112	S3N01KLD	F	Undescribed 3 / *S. venterstadensis* n. sp.	NCA	NCA 2019/608	MK923808	MK923920
113	S3N02KLD	F	Undescribed 3 / *S. venterstadensis* n. sp.	NCA	NCA 2019/609	---	---
114	S3N03KLD	F	Undescribed 3 / *S. venterstadensis* n. sp.	NCA	NCA 2019/610	MK923809	---
115	S5N01KLD	F	Undescribed 5 / *S. theaei* n. sp.	NCA	NCA 2019/606	MK923818	---
116	S6N01KLD	F	Undescribed 6 / *S. ignis* n. sp.	NCA	NCA 2019/653	MK923852	MK923964
117	SAS01KLD	M	*S. astutus*	NCA	NCA 2019/703	MK923873	---
118	SBR01MLF	M	*S. brevipalpis*	SAMC	SAMC-B778	---	---
119	SER01MLF	M	*S. erythrognathus*	AMGS	AMGS-84628	---	---
120	SER01KLD	M	*S. erythrognathus*	NCA	NCA 2017/1913	MK923806	MK923918
121	SER02KLD	M	*S. erythrognathus*	NCA	NCA 2019/611	---	MK923968
122	SER03KLD	M	*S. erythrognathus*	NCA	NCA 2019/613	MK923855	MK923969
123	SER04KLD	M	*S. erythrognathus*	NCA	NCA 2019/614	MK923856	MK923970
124	SER05KLD	M	*S. erythrognathus*	NCA	NCA 2019/615	MK923857	MK923971
125	SFL01MLA	M	*S. filmeri*	TMSA	TMSA-23992	---	---
126	SFL02MLA	M	*S. filmeri*	TMSA	TMSA-23994	---	---
127	SGG01MLA	M	*S. gigas*	SAMC	SAMC-9943	---	---
128	SGG02MLA	M	*S. gigas*	SAMC	SAMC-9943	---	---
129	SGR01MLA	M	*S. griswoldi*	TMSA	TMSA-23999	---	---

© University of Pretoria

Table S1 (cont.). Specimen information for samples used in Geometric morphometric analyses. GenBank ascension numbers are given for each gene region for sequenced specimen.

No.	16S	Locality
89	MK935661	SOUTH AFRICA, Northern Cape, Farm Auguskraal, ca. 40km SE Richmond, near Biogaps site 3135_2410
90	---	SOUTH AFRICA, Northern Cape, Steinkopf
91	---	SOUTH AFRICA, Northern Cape, Steinkopf
92	---	SOUTH AFRICA, Northern Cape, Steinkopf
93	---	SOUTH AFRICA, Eastern Cape, East London
94	---	SOUTH AFRICA, Eastern Cape, East London
95	---	SOUTH AFRICA, Eastern Cape, East London
96	---	SOUTH AFRICA, Gauteng, Heidelberg, Beerlaagte farm
97	---	SOUTH AFRICA, Eastern Cape, Port Alfred
98	---	SOUTH AFRICA, Eastern Cape, Port Alfred
99	---	SOUTH AFRICA, Eastern Cape, Port Alfred
100	---	SOUTH AFRICA, Free State, Gleniffer
101	---	SOUTH AFRICA, Eastern Cape, Hanover
102	---	SOUTH AFRICA, Eastern Cape, Hanover
103	---	SOUTH AFRICA, Eastern Cape, Poortjiesfontein
104	MK935574	SOUTH AFRICA, Northern Cape, Richmond; BioGaps site 3105_2400
105	MK935662	SOUTH AFRICA, Northern Cape, Hanover
106	MK935663	SOUTH AFRICA, Northern Cape, Hanover
107	MK935583	SOUTH AFRICA, Western Cape, Beaufort West; BioGaps site 3215_2305
108	MK935585	SOUTH AFRICA, Western Cape, Beaufort West; BioGaps site 3155_2250
109	MK935602	SOUTH AFRICA, Eastern Cape, Willowmore; BioGaps site 3225_2335
110	MK935603	SOUTH AFRICA, Eastern Cape, Willowmore; BioGaps site 3225_2335
111	MK935629	SOUTH AFRICA, Western Cape, Beaufort West; Biogaps site 3235_2240
112	MK935612	SOUTH AFRICA, Eastern Cape, Kleinvie; near Biogaps site 3055_2540
113	MK935613	SOUTH AFRICA, Eastern Cape, Kleinvie; near Biogaps site 3055_2540
114	MK935614	SOUTH AFRICA, Eastern Cape, Kleinvie; near Biogaps site 3055_2540
115	MK935624	SOUTH AFRICA, Eastern Cape, 2.2km SW Farm Bloemhof, 25km SSE Somerset East, Biogaps site 3255_2535
116	MK935665	SOUTH AFRICA, Northern Cape, Hanover
117	MK935687	SOUTH AFRICA, Eastern Cape, Farm Osplaat, 18km WNW Jansenville.
118	---	SOUTH AFRICA, Western Cape, Robertson, Ashton
119	---	SOUTH AFRICA, Western Cape, Worster
120	---	SOUTH AFRICA, Eastern Cape, Tarkastad; BioGaps site 3150_2605
121	MK935669	SOUTH AFRICA, Eastern Cape, Farm Elandskuil, road to farmhouse
122	MK935670	SOUTH AFRICA, Eastern Cape, Farm Elandskuil, road to farmhouse
123	---	SOUTH AFRICA, Eastern Cape, Farm Elandskuil, road to farmhouse
124	MK935671	SOUTH AFRICA, Eastern Cape, Farm Elandskuil, road to farmhouse
125	---	SOUTH AFRICA, Gauteng, Krugersdorp, Hartebeestfontien farm
126	---	SOUTH AFRICA, Gauteng, Krugersdorp, Hartebeestfontien farm
127	---	SOUTH AFRICA, Free State, Vredefort
128	---	SOUTH AFRICA, Free State, Vredefort
129	---	SOUTH AFRICA, North-West, Brits, Hartebeestfontien farm

© University of Pretoria

Table S1 (cont.). Specimen information for samples used in Geometric morphometric analyses. GenBank ascension numbers are given for each gene region for sequenced specimen.

No.	CODE	Sex	Species	Museum	Museum Voucher	CO1	Efy-1
130	SGR02MLA	M	*S. griswoldi*	TMSA	TMSA-24001	---	---
131	SGR03MLA	M	*S. griswoldi*	TMSA	TMSA-24001	---	---
132	SHW01MLA	M	*S. hewitti*	TMSA	TMSA-23988	---	---
133	SHW02MLA	M	*S. hewitti*	TMSA	TMSA-23989	---	---
134	SHW03MLA	M	*S. hewitti*	TMSA	TMSA-23989	---	---
135	SHW01KLA	M	*S. hewitti*	NCA	NCA 2019/695	---	---
136	SHW02KLA	M	*S. hewitti*	NCA	NCA 2019/696	MK923865	---
137	SIN01MLC	M	*S. insculptus*	BMNH	BMNH-78.3	---	---
138	SIP04MLC	M	*S. insculptus peddiensis*	AMGS	NM15347	---	---
139	SIP01MLC	M	*S. insculptus peddiensis*	AMGS	NM15347	---	---
140	SIP02MLC	M	*S. insculptus peddiensis*	AMGS	NM15349	---	---
141	SIP03MLC	M	*S. insculptus peddiensis*	AMGS	NM15350	---	---
142	SKN01MLC	M	*S. kentanicus*	SAMC	SAMC-14685	---	---
143	SKN02MLC	M	*S. kentanicus*	SAMC	SAMC-B782	---	---
144	SLG01MLB	M	*S. longipalpis*	AMGS	NM14946	---	---
145	SLG02MLB	M	*S. longipalpis*	AMGS	NM14945	---	---
146	SLG03MLB	M	*S. longipalpis*	AMGS	NM14947	---	---
147	S9N01MLD	M	Undescribed 9 / *S. malesociatus* n. sp.	AMGS	AMGS-5367	---	---
148	SMN01KLD	M	*S. mandelai*	NCA	NCA 2019/700	MK923870	---
149	SMN02KLD	M	*S. mandelai*	NCA	NCA 2019/701	MK923871	---
150	SPL01MLD	M	*S. palpiger*	BMNH	STAS_429	---	---
151	SPT01MLC	M	*S. patersonae*	SAMC	SAMC-B4655	---	---
152	SPT02MLC	M	*S. patersonae*	SAMC	SAMC-B4655	---	---
153	SPR01MLF	M	*S. purcelli*	SAMC	SAMC-150432	---	---
154	SQB01MLC	M	*S. qumbu*	AMGS	NM14594	---	---
155	SRB01MLA	M	*S. robertsi*	TMSA	TMSA-2746	---	---
156	SRB02MLA	M	*S. robertsi*	TMSA	TMSA-3188-3189	---	---
157	SRB03MLA	M	*S. robertsi*	TMSA	TMSA-3188-3189	---	---
158	SSR01MLD	M	*S. schrieneri*	SAMC	SAMC-9159	---	---
159	SSP01MLC	M	*S. spinipes*	AMGS	NM14861	---	---
160	SSP02MLC	M	*S. spinipes*	AMGS	NM14834	---	---
161	SSP03MLC	M	*S. spinipes*	AMGS	NM14851	---	---
162	STY01MLC	M	*S. tysoni*	AMGS	NM14956	---	---
163	SUR01MLC	M	*S. umtaticus rangeri*	AMGS	NM14770	---	---
164	SUR02MLC	M	*S. umtaticus rangeri*	AMGS	NM14771	---	---
165	S2N01KLD	M	Undescribed 2/*S. dylani* n. sp.	NCA	NCA 2019/663	MK923859	MK923973
166	S2N02KLD	M	Undescribed 2/*S. dylani* n. sp.	NCA	NCA 2019/664	MK923860	MK923974
167	S2N03KLD	M	Undescribed 2/*S. dylani* n. sp.	NCA	NCA 2019/697	MK923867	---
168	S2N04KLD	M	Undescribed 2/*S. dylani* n. sp.	NCA	NCA 2019/698	MK923868	---
169	S2N05KLD	M	Undescribed 2/*S. dylani* n. sp.	NCA	NCA 2019/699	MK923869	---
170	S2N06KLD	M	Undescribed 2/*S. dylani* n. sp.	NCA	NCA 2019/702	MK923872	---
171	S4N01KLD	M	Undescribed 4 / *S. karooensis* n. sp.	NCA	NCA 2019/616	MK923858	MK923972
172	S4N02KLD	M	Undescribed 4 / *S. karooensis* n. sp.	SAMC	SAM-ENW-C007293	MK923864	---
173	S4N03KLD	M	Undescribed 4 / *S. karooensis* n. sp.	SAMC	SAM-ENW-C007746	---	---
174	S6N01KLD	M	Undescribed 6 / *S. ignis* n. sp.	NCA	NCA 2019/642	MK923866	MK923976

© University of Pretoria

Table S1 (cont.). Specimen information for samples used in Geometric morphometric analyses. GenBank ascension numbers are given for each gene region for sequenced specimen.

No.	16S	Locality
130	---	SOUTH AFRICA, North-West, Brits, Hartebeestfontien farm
131	---	SOUTH AFRICA, North-West, Brits, Hartebeestfontien farm
132	---	SOUTH AFRICA, Gauteng, Pretoria, Roodeplaat dam nature reserve
133	---	SOUTH AFRICA, Gauteng, Pretoria, Roodeplaat dam nature reserve
134	---	SOUTH AFRICA, Gauteng, Pretoria, Roodeplaat dam nature reserve
135	MK935678	SOUTH AFRICA, Gauteng, Wonderboom Distr.
136	MK935679	SOUTH AFRICA, Gauteng, Wonderboom Distr.
137	---	SOUTH AFRICA, Eastern Cape, King William's Town
138	---	SOUTH AFRICA, Eastern Cape, Peddie
139	---	SOUTH AFRICA, Eastern Cape, Peddie
140	---	SOUTH AFRICA, Eastern Cape, Peddie
141	---	SOUTH AFRICA, Eastern Cape, Peddie
142	---	SOUTH AFRICA, Eastern Cape, Transkei, Kentani
143	---	SOUTH AFRICA, Eastern Cape, Transkei, Kentani
144	---	SOUTH AFRICA, Northern Cape, Kimberly
145	---	SOUTH AFRICA, Northern Cape, Kimberly
146	---	SOUTH AFRICA, Northern Cape, Kimberly
147	---	SOUTH AFRICA, Northern Cape, Victoria West
148	MK935684	SOUTH AFRICA, Eastern Cape, Farm Osplaat, 18km WNW Jansenville.
149	MK935685	SOUTH AFRICA, Eastern Cape, Farm Osplaat, 18km WNW Jansenville.
150	---	SOUTH AFRICA, Eastern Cape, Graaff Reinet
151	---	SOUTH AFRICA, Eastern Cape, Alicedale
152	---	SOUTH AFRICA, Eastern Cape, Alicedale
153	---	SOUTH AFRICA, Western Cape, Caledon
154	---	SOUTH AFRICA, Eastern Cape, Transkei, Qumbu
155	---	SOUTH AFRICA, Gauteng, Pretoria, Mayville
156	---	SOUTH AFRICA, Free State, near Bothaville
157	---	SOUTH AFRICA, Free State, near Bothaville
158	---	SOUTH AFRICA, Eastern Cape, Hanover
159	---	SOUTH AFRICA, Eastern Cape, East London
160	---	SOUTH AFRICA, Eastern Cape, East London
161	---	SOUTH AFRICA, Eastern Cape, East London
162	---	SOUTH AFRICA, Eastern Cape, Port Alfred
163	---	SOUTH AFRICA, Free State, Gleniffer
164	---	SOUTH AFRICA, Free State, Gleniffer
165	MK935673	SOUTH AFRICA, Western Cape, Murraysburg
166	MK935674	SOUTH AFRICA, Western Cape, Murraysburg
167	MK935682	SOUTH AFRICA, Eastern Cape, Farm Osplaat, 18km WNW Jansenville.
168	---	SOUTH AFRICA, Eastern Cape, Farm Osplaat, 18km WNW Jansenville.
169	MK935683	SOUTH AFRICA, Eastern Cape, Farm Osplaat, 18km WNW Jansenville.
170	MK935686	SOUTH AFRICA, Eastern Cape, Farm Osplaat, 18km WNW Jansenville.
171	MK935672	SOUTH AFRICA, Eastern Cape, Farm Elandskuil, road to farmhouse
172	MK935677	SOUTH AFRICA, Eastern Cape, Pearston, Plains of Camdeboo Game Reserve
173	---	SOUTH AFRICA, Eastern Cape, Pearston, Plains of Camdeboo Game Reserve
174	MK935680	SOUTH AFRICA, Northern Cape, Richmond

© University of Pretoria

Table S2. The definitions for each landmark used in the geometric morphometric analysis of *Stasimopus* ocular patterns. The landmarks correspond with those illustrated in figure 1. The following shorthand notations are used; PLE: posterior lateral eye, PME: posterior median eye, ALE: anterior lateral eye and AME: anterior median eye.

Landmark	Definition
1	Left PLE, the middle of the lens facing outwards.
2	Left PLE, the meeting of the lens with the eye socket, most facing the chelicerae.
3	Left PLE, middle of the lens embedded in the eye socket.
4	Left PLE, the meeting of the lens with the eye socket, furthest from the chelicerae.
5	Left PME, the meeting of the lens with the eye socket, furthest from the chelicerae.
6	Left PME, the middle of the lens facing outwards.
7	Left PME, the meeting of the lens with the eye socket, closest to the chelicerae.
8	Left PME, middle of the lens embedded in the eye socket.
9	Left ALE, the meeting of the lens with the eye socket, furthest from the chelicerae.
10	Left ALE, the middle of the lens facing outwards.
11	Left ALE, the meeting of the lens with the eye socket, closest to the chelicerae.
12	Left ALE, middle of the lens embedded in the eye socket.
13	Left AME, the furthest left point of the lens from the chelicerae.
14	Left AME, the closest edge of the lens to the chelicerae.
15	Left AME, the closest right point of the lens from the chelicerae.
16	Left AME, the furthest edge of the lens to the chelicerae.
17	Right PLE, middle of the lens embedded in the eye socket.
18	Right PLE, the meeting of the lens with the eye socket, most facing the chelicerae.
19	Right PLE, the middle of the lens facing outwards.
20	Right PLE, the meeting of the lens with the eye socket, furthest from the chelicerae.
21	Right PME, the meeting of the lens with the eye socket, furthest from the chelicerae.
22	Right PME, middle of the lens embedded in the eye socket.
23	Right PME, the meeting of the lens with the eye socket, closest to the chelicerae.
24	Right PME, the middle of the lens facing outwards.
25	Right ALE, the meeting of the lens with the eye socket, furthest from the chelicerae.
26	Right ALE, middle of the lens embedded in the eye socket.
27	Right ALE, the meeting of the lens with the eye socket, closest to the chelicerae.
28	Right ALE, the middle of the lens facing outwards.
29	Right AME, the furthest left point of the lens from the chelicerae.
30	Right AME, the closest edge of the lens to the chelicerae.
31	Right AME, the closest right point of the lens from the chelicerae.
32	Right AME, the furthest edge of the lens to the chelicerae.

© University of Pretoria

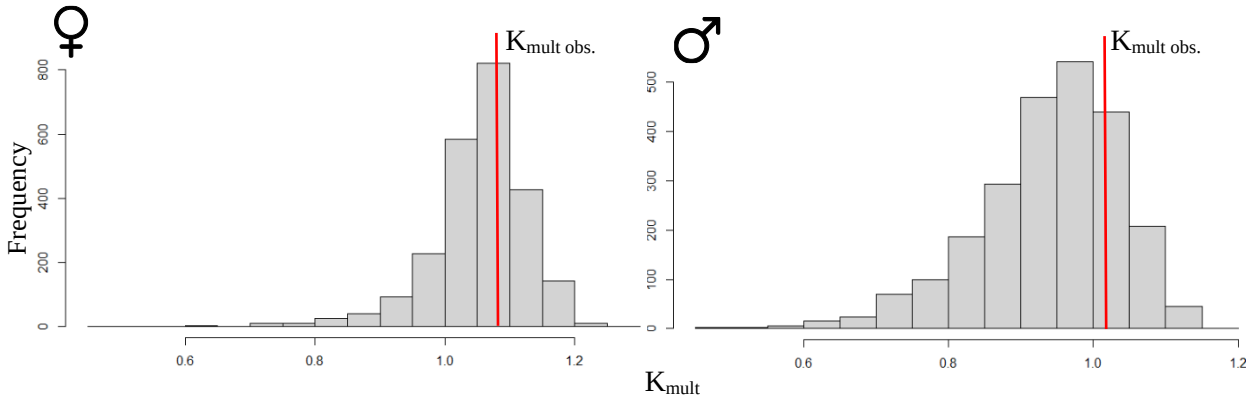


Figure S1. Histograms of K_{mult} values for the female and male datasets. Values were obtained through permutating the eye pattern shape data on the tips of the phylogeny for 999 permutations. The observed K_{mult} is indicated on each histogram.

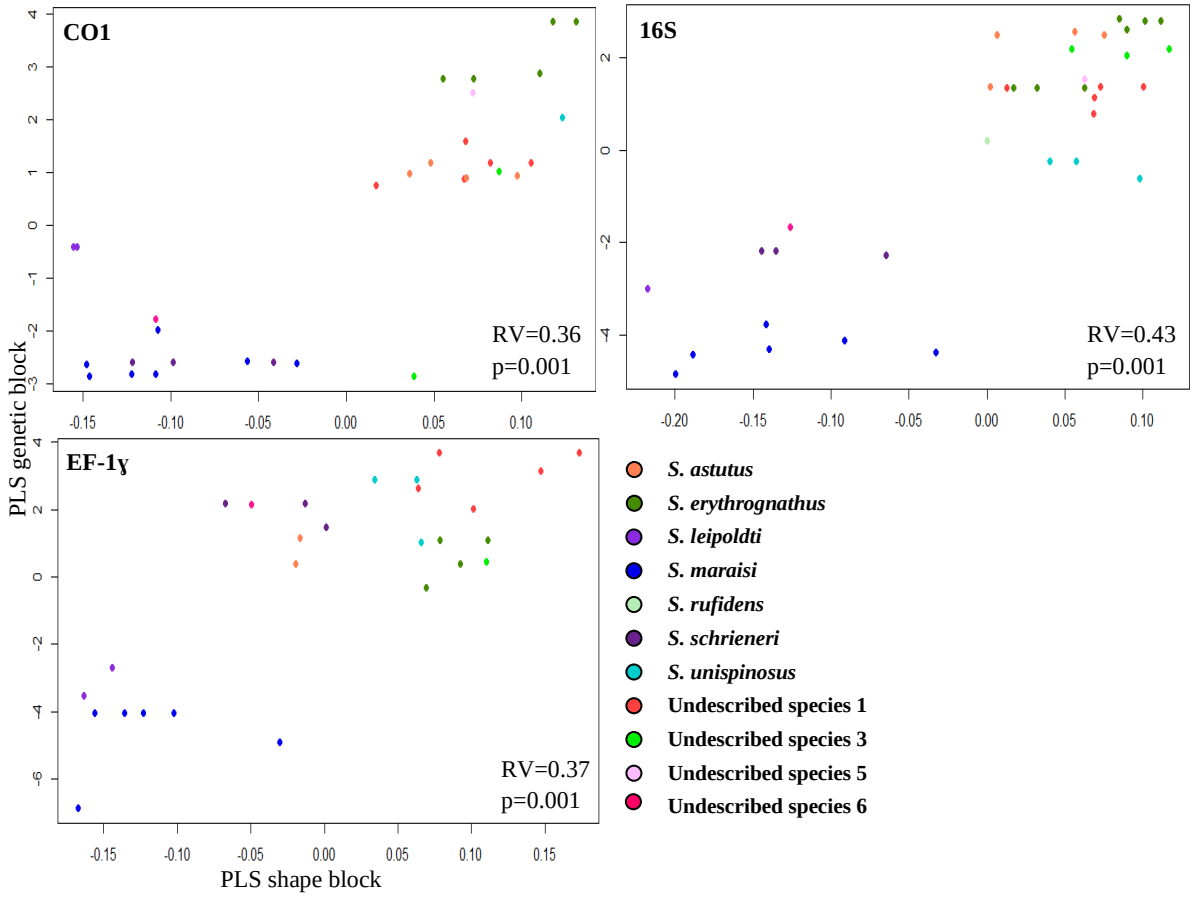


Figure S2. Ordinations based on the PLS of the genetic distances and procrustes distances of various *Stasimopus* species for the female dataset. The species colours correspond to the map in figure 1. The Escoufier RV correlation coefficient and the p-value based on permutation testing is given for each test.

© University of Pretoria

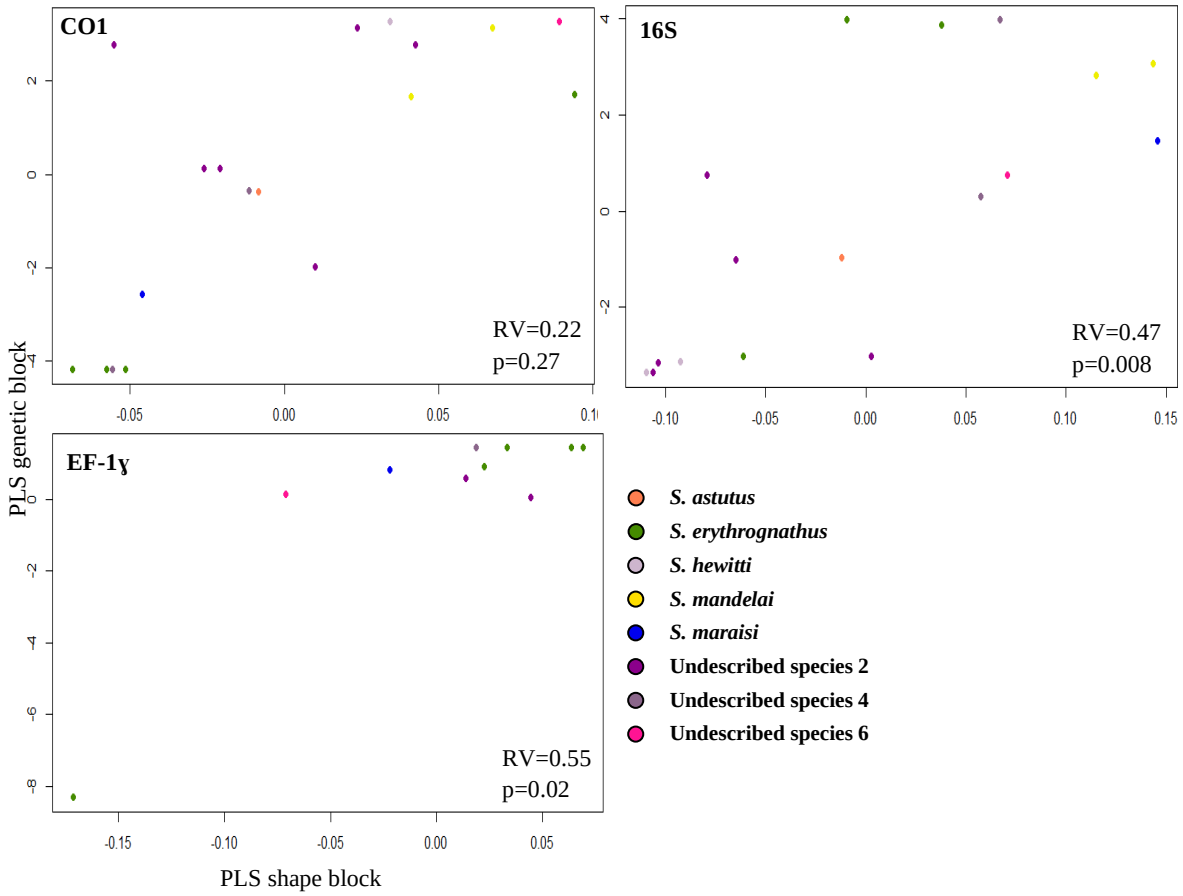


Figure S3. Ordinations based on the PLS of the genetic distances and procrustes distances of various *Stasimopus* species for the male dataset. The species colours correspond to the map in figure 1. The Escoufier RV correlation coefficient and the p-value based on permutation testing is given for each test.

Department of Zoology and Entomology
University of Pretoria

© University of Pretoria

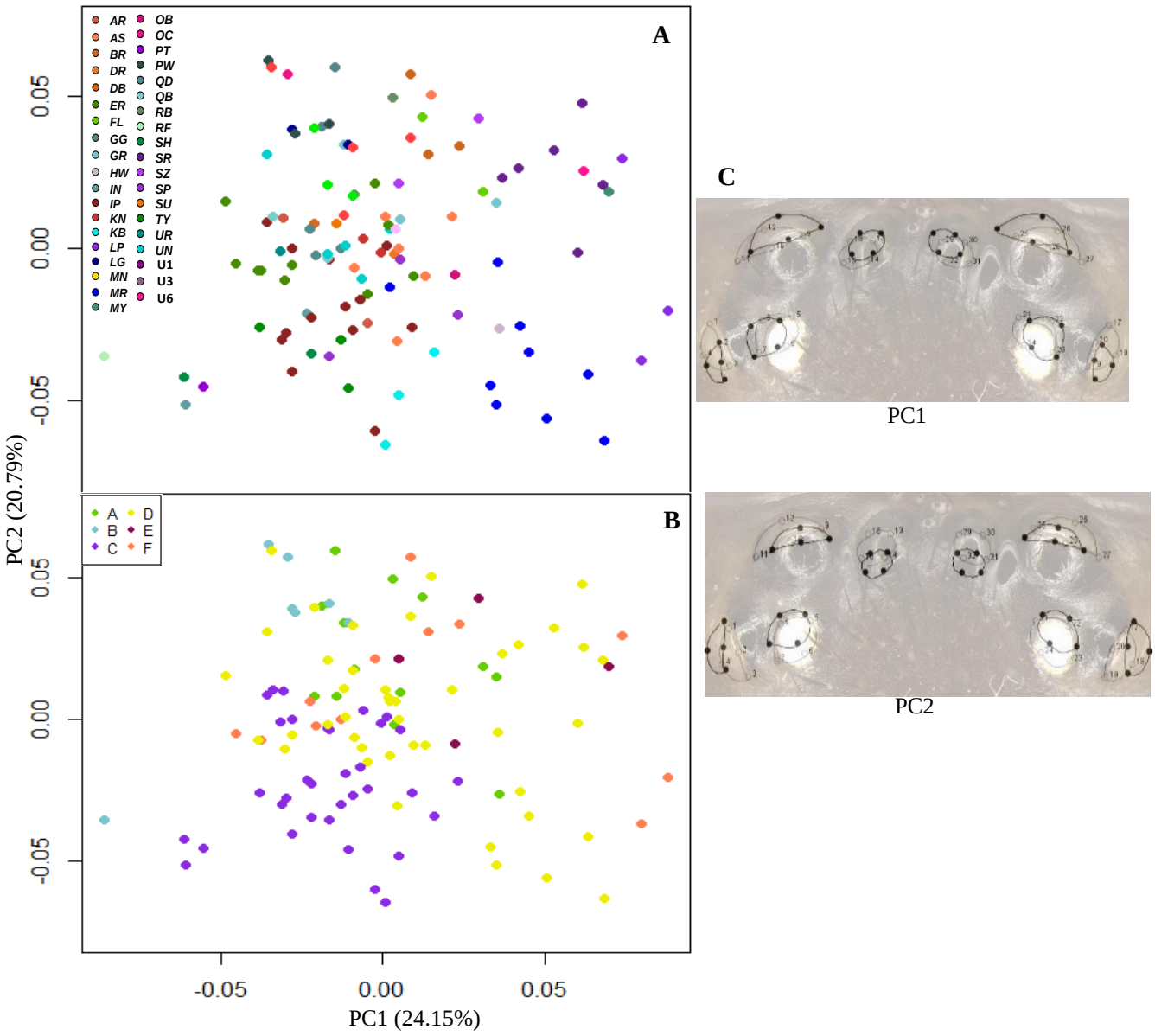


Figure S4. Morphospace plots of the first two PCs for the female dataset. The colours match that of Figure 1. A. The morphospace plot coloured by species. B. The morphospace plot coloured by locality / morphospecies. C. Shape changes in the female ocular pattern for the first and second PC are shown for all the landmarks. The original average shape is indicated in grey and the new target shape in black.

© University of Pretoria

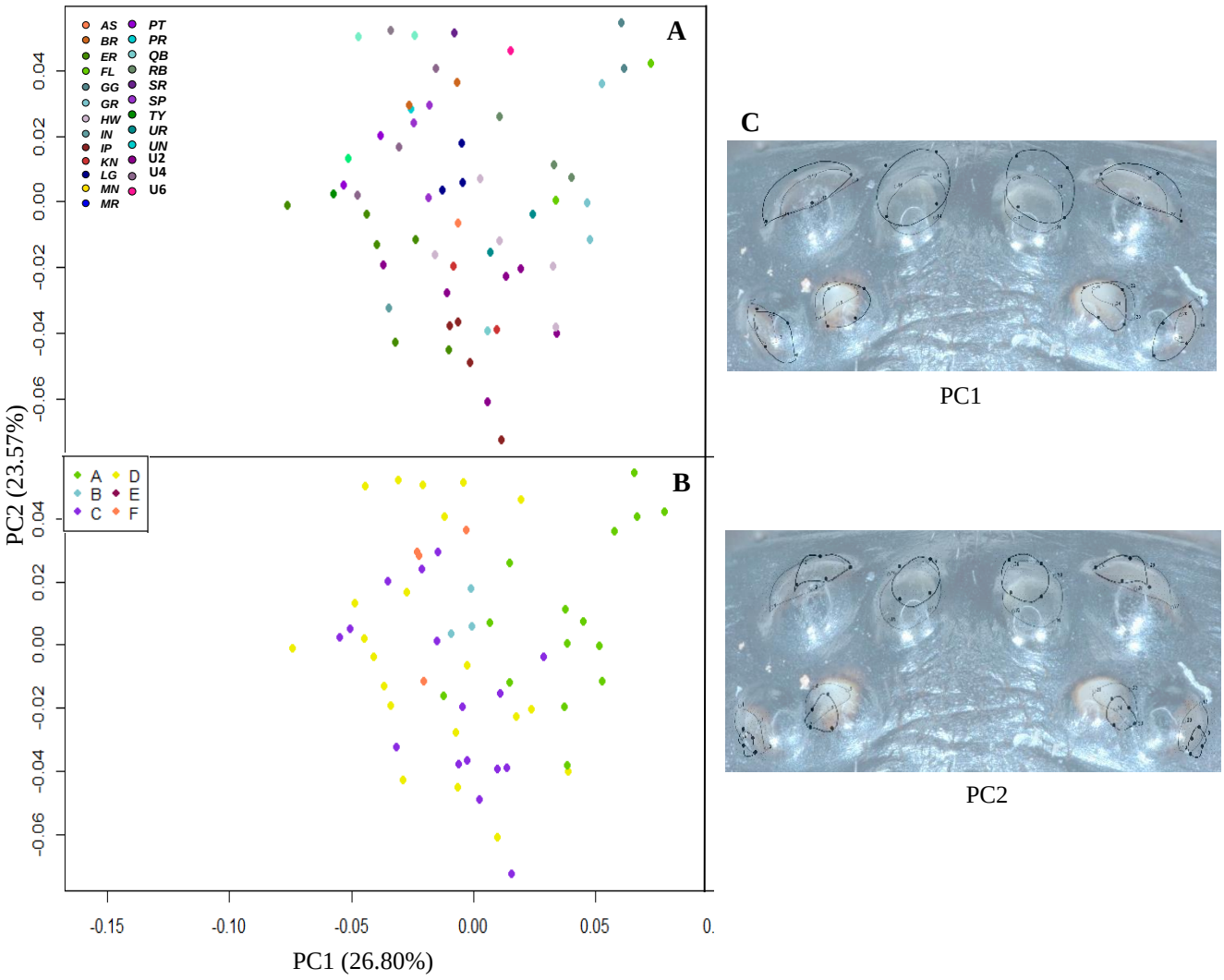


Figure S5. Morphospace plots of the first two PCs for the male dataset. A. The morphospace plot coloured by species. The species colours correspond to the map in figure 1. B. The morphospace plot coloured by locality / morphospecies. C. Shape changes in the male ocular pattern for the first and second PC are shown for all the landmarks. The original average shape is indicated in grey and the new target shape in black.

© University of Pretoria

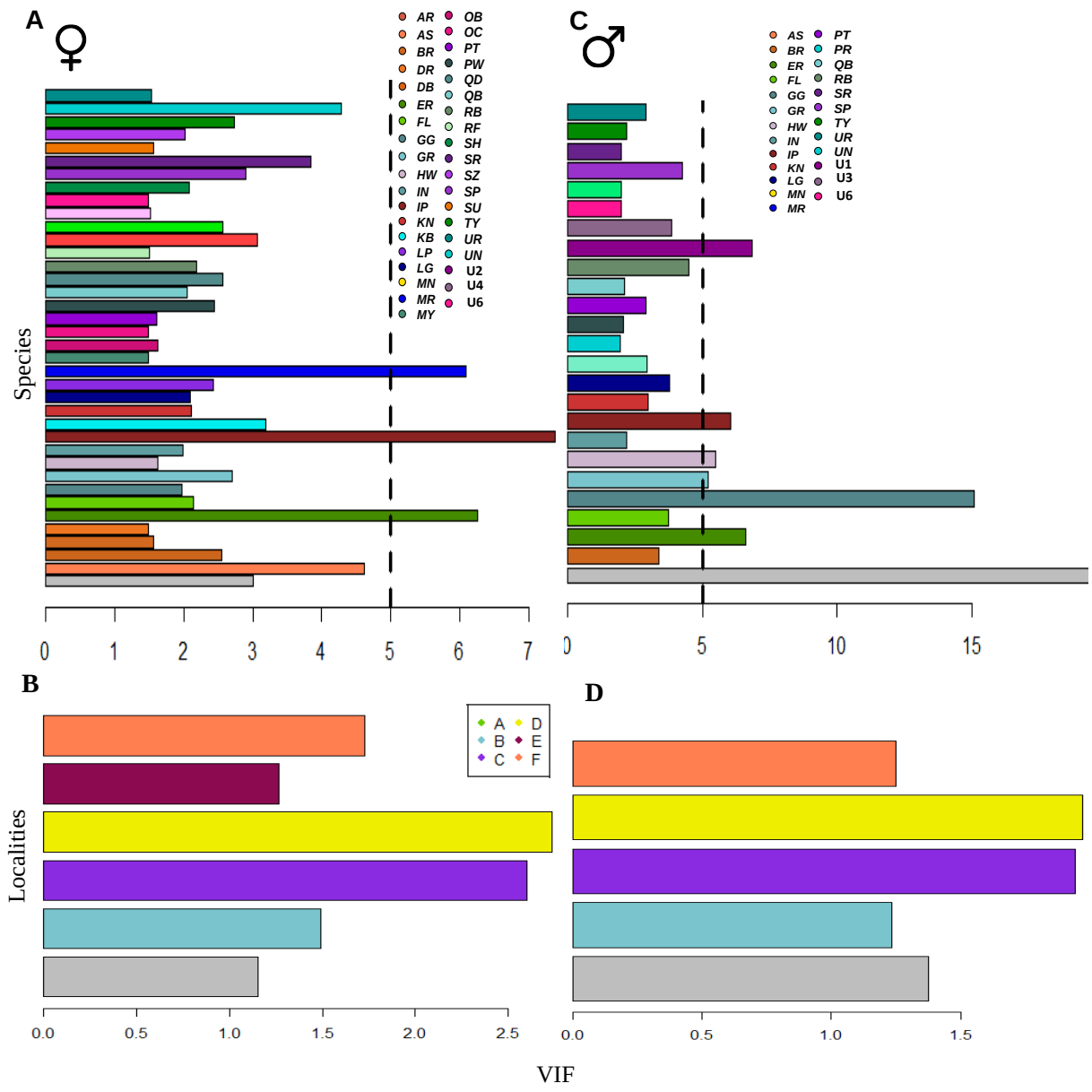


Figure S6. The VIF results for the correlation tests between species and centroid size, and locality and centroid size for each sex. VIF values above 5 are considered severe and may influence the p-values of subsequent analyses. The grey bars indicate centroid size.

Table S3. Results of the regressions of centroid size and procrustes distances pooled by other variables. The percentage predicted is the amount of variation in the dataset accounted for by the variable.

Sex	Trait	Effect	% Predicted	p value
Female	Centroid size	Procrustes scores	7.468%	<0.0001
		Pooled by species	8.608%	<0.0001
		Pooled by locality	6.578%	<0.0001
Male	Centroid size	Procrustes scores	13.625%	<0.0001
		Pooled by species	4.392%	0.0066
		Pooled by locality	8.068%	0.0001

Department of Zoology and Entomology
University of Pretoria

© University of Pretoria

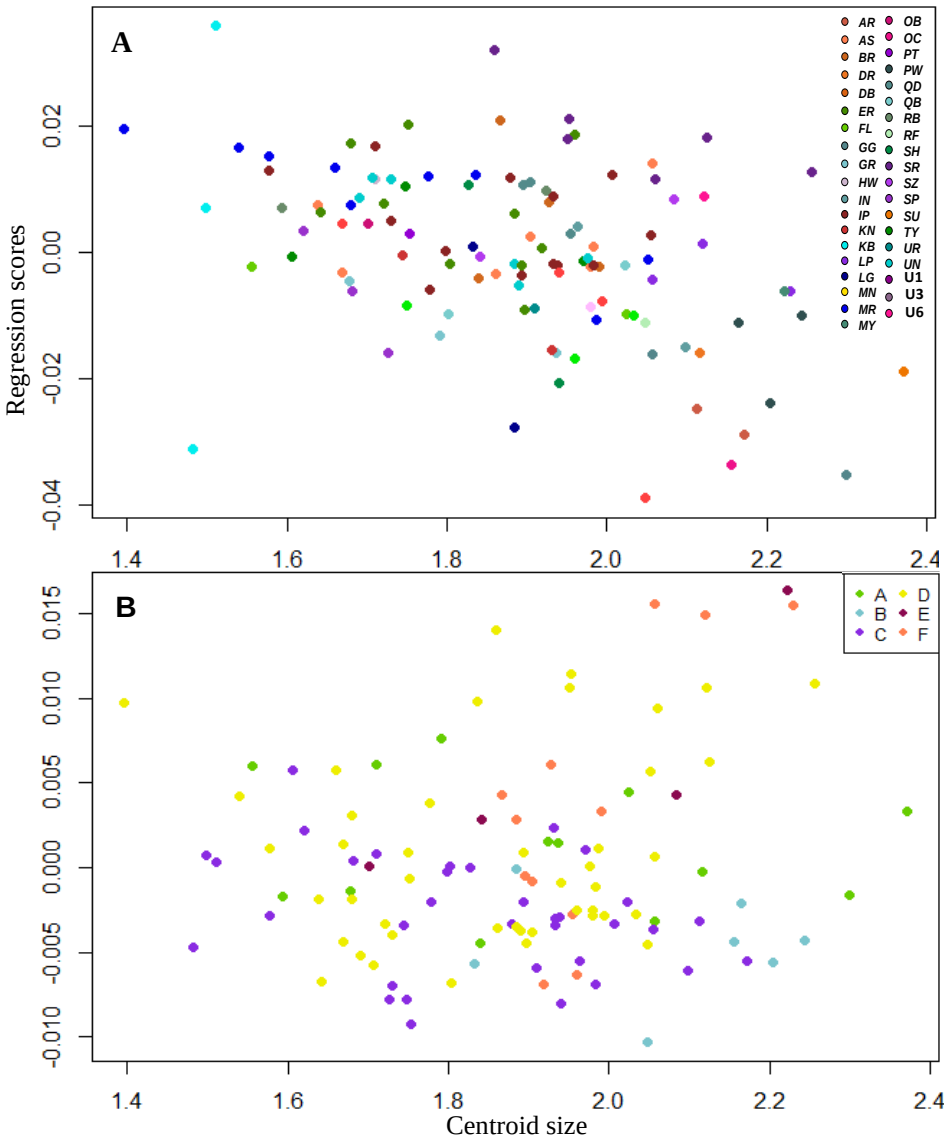


Figure S7. Female regression plots. A. Regression of procrustes distances and centroid size pooled by species. B. Regression of procrustes distances and centroid size pooled by locality.

Department of Zoology and Entomology
University of Pretoria

© University of Pretoria

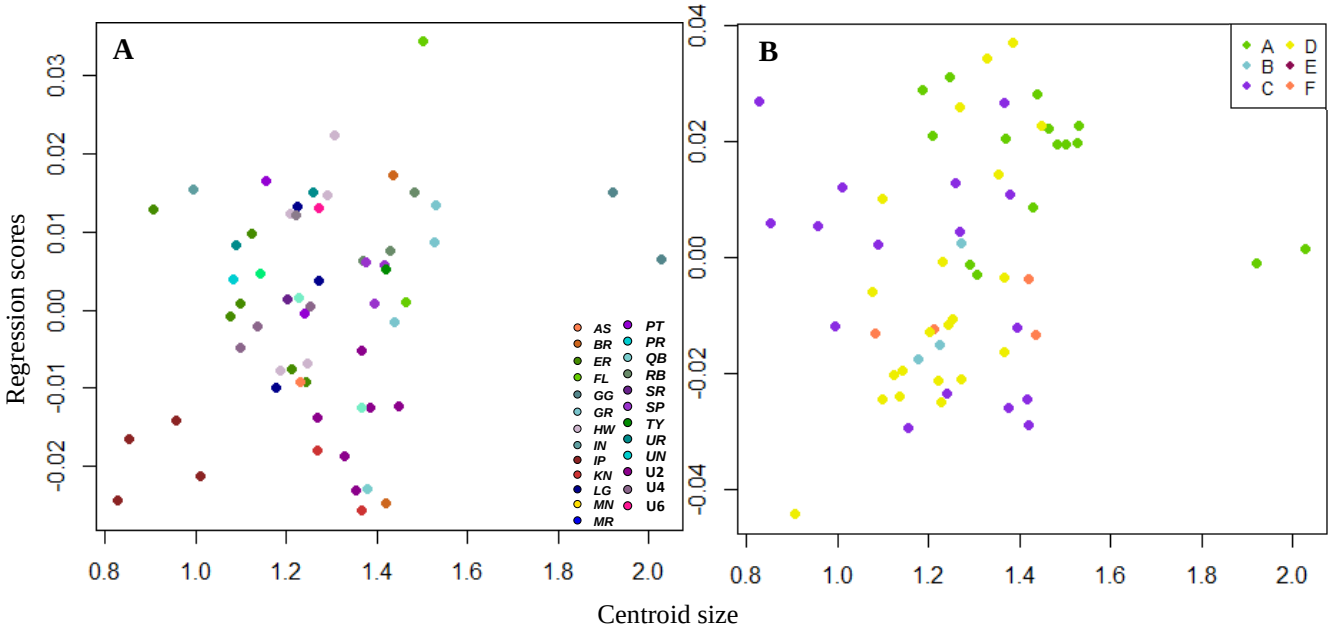


Figure S8. Male regression plots. A. Regression of procrustes distances and centroid size pooled by species. B. Regression of procrustes distances and centroid size pooled by locality.

Table S4. Results of procrustes ANOVAs. Significant values indicted in red.

Sex	Trait	Effect	df	F	Z	p value
Female	Shape	Centroid size	1	9.0969	4.5777	0.001
		Species	37	3.9931	11.8994	0.001
		Locality	5	4.7443	6.9358	0.001
Male	Shape	Centroid size	1	8.9913	4.5395	0.001
		Species	24	2.3984	6.0755	0.001
		Locality	4	3.1142	4.2255	0.001

© University of Pretoria

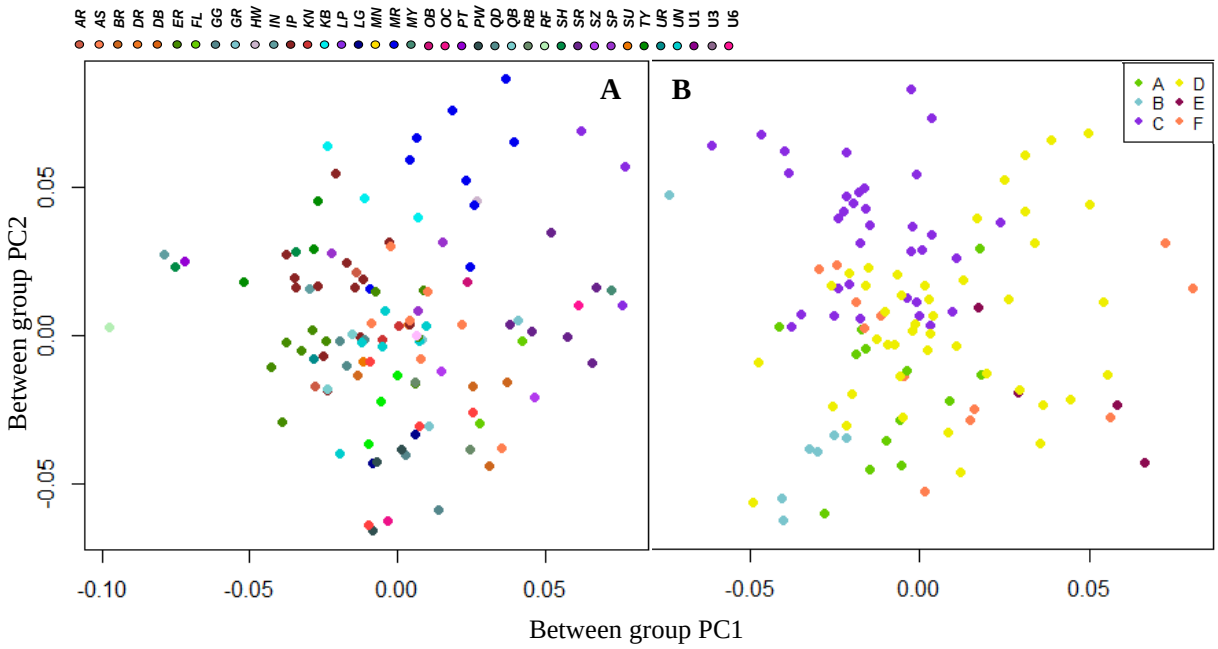


Figure S9. Morphospace plots of the first two PCs for between group PCAs for the female dataset. A. Between group PCA by species. B. Between group PCA by locality / morphospecies. The species colours correspond to the map in figure 1.

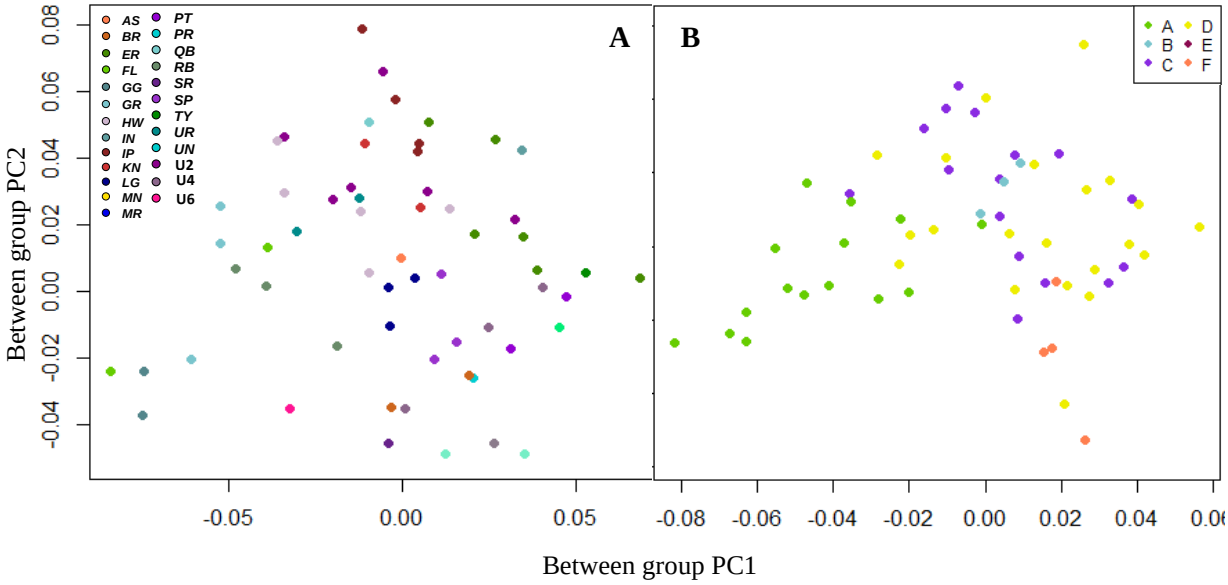


Figure S10. Morphospace plots of the first two PCs for between group PCAs for the male dataset. A. Between group PCA by species. B. Between group PCA by locality / morphospecies. The species colours correspond to the map in figure 1.

© University of Pretoria

Chapter 4

An integrative taxonomy of the genus *Stasimopus* Simon 1892 (Araneae: Mygalomorphae) of the Karoo with the description of nine new species and a *Stasimopus maraisi* Hewitt 1914 male

Shannon Brandt[1], Catherine L. Sole[1] and Robin Lyle[2]

[1] *Department of Zoology and Entomology, University of Pretoria, Hatfield, Pretoria, South Africa*

[2] *Agricultural Research Council – Plant Health and Protection, Biosystematics, Roodeplaat, Pretoria, South Africa*

This data chapter has been submitted as:

Brandt, S., Sole, C. L. and Lyle, R. 2023. An integrative taxonomy of the genus *Stasimopus* Simon 1892 (Araneae: Mygalomorphae) of the Karoo with the description of nine new species and a *Stasimopus maraisi* Hewitt 1914 male, to Zootaxa.

© University of Pretoria

Abstract

The genus *Stasimopus* Simon 1892 is endemic to Southern Africa, but is historically largely understudied. This paper provides a taxonomic revision for the *Stasimopus* species of the Karoo region of South Africa and includes the description of nine new species (*S. dylani* **sp. nov.**, *S. finni* **sp. nov.**, *S. hamartia* **sp. nov.**, *S. ignis* **sp. nov.**, *S. karooensis* **sp. nov**., S. *malesociatus* **sp. nov.,** *S. tera* **sp. nov.**, *S. theaei* **sp. nov.** and *S. venterstadensis* **sp. nov.**). A description of the genetically matched *S. maraisi* Hewitt 1914 male is provided. The original *S. maraisi* male is designated to its own new species (S. *malesociatus* **sp. nov.**). An identification key is provided for species occurring in the Karoo region. This is the first integrative taxonomy for the genus that includes morphological, geometric morphometric as well as genetic data.

Keywords

Integrative taxonomy, *Stasimopus*, Karoo, new species, trapdoor spider

© University of Pretoria

UNIVERSITEIT VAN PRETORIA
UNIVERSITY OF PRETORIA
YUNIBESITHI YA PRETORIA

1. Introduction

The genus *Stasimopus* is a group of trapdoor spiders endemic to Southern Africa, recorded in the Western Cape, Eastern Cape, Northern Cape, Free State, Kwazulu-Natal, North-West and Gauteng provinces of South Africa and in Lesotho. The genus currently comprises 47 species (World Spider Catalog 2022), but the actual species diversity is likely much higher.

The first member of the genus was originally described by Koch (1842) under the name *Actinopus caffrus*. Two more species were later described under two separate genera; *Cyrtocarenum rufidens* Ausserer, 1871 and *Pachlyomerus natalensis* Cambridge, 1889. These species were later synonomised and placed in the genus *Stasimopus*, as *S. rufidens* (Ausserer, 1871) by Simon (1892). The genus *Stasimopus* was established by Simon (1892) to accommodate the species, *S. caffrus* (Koch, 1842). This is the type species for the genus.

An abundance of species was described following this by the following researchers; Karsch (1879), Pocock (1897, 1900, 1901, 1902a, 1902b), Purcell (1902, 1903a, 1903b, 1908), Hewitt (1910, 1913, 1914, 1915a, 1915b, 1916, 1917, 1919, 1927), Tucker (1917), Hendrixson & Bond (2004) and Engelbrecht & Prendini (2012). No subsequent taxonomic treatments of the genus have since occurred.

There has historically been extensive debate around the phylogenetic placement of the genus *Stasimopus*. The genus was originally placed within the family Ctenizidae Thorell 1887 by Raven (1885). This was based on a range of plesiomorphic characteristics: three claws on the tarsi; in females, claws are paired with few teeth; on the first and second legs are patches of dense short spines on the lateral surfaces on the distal segments in females; males have a simple, pyriform pedipalpal bulb; the chelicerae have two rows of teeth; fang's outer surface is smooth and a strongly procurved fovea on the carapace (Engelbrecht & Prendini 2012). The genus was often found to be paraphyletic in phylogenetic studies regardless of morphological conservancy (Ayoub *et al.* 2007; Hedin & Bond 2006; Opatova *et al.* 2013). In 2020 the genus was elevated to its own family Stasimopidae Bond, Opatova and Hedin 2020 based on extensive genetic data (Opatova *et al.* 2020). No studies have looked at the phylogenetic relationships within the genus or the phylogeography.

Due to the confounding morphological characters of the genus and reoccurring incorrect placement, there is a need for a more integrative taxonomic approach (Bond *et al.* 2012; Bond *et al.* 2021; Newton *et al.* 2020). The integrative taxonomic approach we employ will make use of the generalised species concept to separate and diagnose species by identifying a species as separately evolving metapopulation lineages using multiple lines of evidence (De Queiroz 2007; Rix et al. 2018). Thus, the first criterion for identifying a species is that it must be a lineage, which is evolving separately from other such lineages (monophyletic) (Bond *et al.* 2021). The species delimitation is then proven or falsified by secondary properties, viewed as lines of evidence for the species delimitation (Yeates *et al*. 2011). Secondary properties are of vital importance as they may be what is

© University of Pretoria

used to actually identify the species (such as morphological characters), because of this, numerous sources state the importance of using more than one line of evidence when looking at a species' taxonomy (Dayrat 2005; De Queiroz 2007; Fujita *et al.* 2012; Yeates *et al.* 2011). For this reason, standard morphological characters and the geometric morphometric determined ocular patterns will be used to aid in species designation (Chapter 3).

The Karoo region of South Africa is an arid/semi-arid area that spans one third of the land surface of South Africa over four provinces (Northern Cape, Western Cape, Eastern Cape and Free State) (Henschel *et al.* 2018). The Karoo contains unique and sensitive ecosystems which respond poorly to disturbance and have slow recovery rates (Holness *et al.* 2016). This region has long been neglected in studies due to the assumption of low biodiversity in semi-arid regions (Roth-Monzón *et al.* 2018). The area has recently undergone a Strategic Environmental Assessment (SEA) under the BioGaps project due to the threat of impending land-use change (Holness *et al.* 2016). All the *Stasimopus* material collected during this assessment is used to form this integrative taxonomy for the Karoo region of South Africa.

The aim of this article is to produce an integrative taxonomy for the *Stasimopus* of the Karoo region using genetics, geometric morphometrics and morphology. Nine new species found in the Karoo are described, as well as a description of the *S. maraisi* male.

2. Methods and Materials

2.1. Sample collection

Stasimopus specimens were collected from part of the Great Karoo, South Africa. The area is within the demarcated area for potential shale gas fracking (Figure 1). The sites were selected by the Karoo BioGaps team to cover the range of environmental conditions present in the region. Within each site drainage line habitats were targeted for sampling as they are favoured by trapdoor spiders. A total of 79 sites were sampled, on average 50 km apart (Figure 1). At each site four people spent one-hour, thereby four man-hours soil scraping. Soil scraping involves removing the top layer of soil to expose burrow entrances. Once entrances were exposed, the burrows were excavated using a hand shovel and taking care to not injure the specimens. This methodology was effective for collecting female and juvenile specimens. In order to collect male specimens, road cruising was done after rain in the evenings. This involves slowly driving on isolated roads with torches to find males which are crossing in search of potential mates. All specimens were preserved in a solution of cold alcohol and kept in an ice box.

© University of Pretoria

Specimens were later preserved in 80% ethanol in glass polytop vials for long-term storage. All locality information is available in Chapter 2 - Table S1. All newly collected material was deposited in the National Collection of Arachnida (NCA) of the Agricultural Research Council (ARC), Pretoria, South Africa.

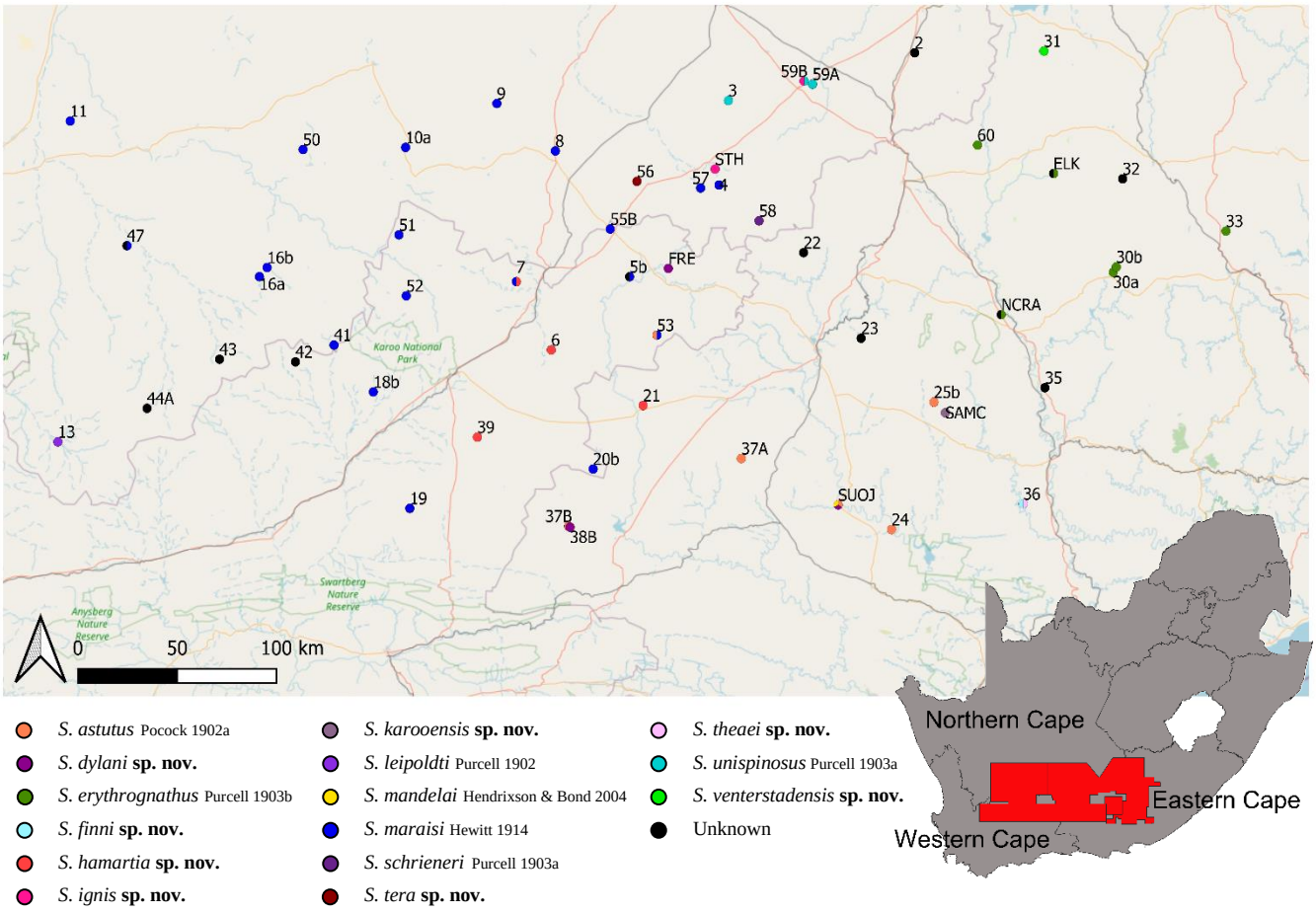


Figure 1. Map of the study area in the greater Karoo region, in the south-western part of South Africa. Markers indicate the 55 sites where *Stasimopus* specimens were found. If sites were near one another, they are denoted as 'a' and 'b'. The localities are coloured according to the species found there. Red polygons indicate areas identified for shale gas exploration. Map created in QGIS version 3.4.8-Madeira (2019), available at: http://qgis.osgeo.org.

2.2. Taxonomic methods

The taxonomic methods largely follow that of Ríos Tamayo & Lyle (2020). Photographs were taken with either a Zeiss Axio Zoom V16 with the Axiocam 512 color and stacked with ZEN 2.3 SPI (Blue Edition) for smaller characters or Canon EOS 5D camera equipped with a 100 mm macro lens for habitus photographs and larger characters. Rendering of the image slices was done with Helicon Focus software.

© University of Pretoria

All measurements are given in millimeters (mm). If multiple specimens were used to describe the species, a range of lengths are provided, with the holotype / allotype value given in parentheses. Ocular measurements, leg lengths and spination is only given for the largest specimen. Lengths of leg segments are always given in the order: femur, patella, tibia, metatarsus, tarsus. Legs are described from I to IV and from the proximal to distal end (femur to tarsus). Each segment surface will be described in the order of prolateral, dorsal, retrolateral, ventral. Genitalia are dissected and were examined in alcohol. Epygines cleared and photographed in clove oil.

All specimen were examined and identified against existing species descriptions and type specimens. The following collections were accessed; Albany Museum (AMGS) – T. Bellingan, Grahamstown, South Africa; The National Museum (NMBA) – J. A. Neethling, Bloemfontein, South Africa; Ditsong Museum of Natural History (TMSA) – T. Bird, Pretoria, South Africa; Iziko Museum of Cape Town (SAMC) – S. van Nooit, Cape Town, South Africa; Museum für Naturkunde (ZMB) – B. Huber, Berlin, Germany; National Collection of Arachnida (NCA) – P. Marais, Pretoria, South Africa. Species that occur in the Karoo region were reexamined for the species diagnoses, this includes *S. artifex* Pocock 1902a, *S. astutus* Pocock 1902a, *S. erythrognathus* Purcell 1903b, *S. leipoldti* Purcell 1902, *S. maraisi* Hewitt 1914, *S. mandelai* Hendrixson & Bond 2004, *S. palpiger* Pocock 1902a, *S, patersonae* Hewitt 1913, *S. schonlandi* Pocock 1900, *S. schrieneri* Purcell 1903a, *S. spinosus* Hewitt 1914, *S. steynsbergensis* Hewitt 1915b and *S. unispinosus* Purcell 1903a. *Stasimopus bimaculatus* Purcell 1903b could not be examined as it is missing from the museum collections.

All the examined morphological characters are in a character matrix and is available in Table 1 and 2. The matrices includes all species for which types could be located excluding species from Gauteng province and the Free State province localities which border Gauteng. This information was used to form species diagnoses.

Where geographical locality co-ordinates were not provided on specimen labels or were unavailable on institutional databases, they were searched for using the Global Gazetteer Version 2.2 (www.fallingrain.com/world/) and are indicated in square brackets.

2.3. Phylogenetic analyses

DNA extraction, sequencing and alignment are as stated in Chapter 2.

All analyses were applied to a concatenated-molecular dataset. The Akaike information criterion (AIC) and the Bayesian information criterion (BIC) were both implemented within jModelTest v2.1.7 (Posada 2008). This allows for the selection of the best model to account for varying base pair substitution rates (Posada 2008).

Maximum likelihood (RAxML v8.1.20; (Stamatakis 2014)) analyses were performed in RAxML implementing a General Time Reversible (GTR) model. A maximum likelihood search was

© University of Pretoria

done followed by bootstrapping for support of 1000 pseudoreplicates (Felsenstein 1985). To ensure the effective sampling of the tree space, the analyses were repeated, using a different starting seed. For the analysis the rapid hill-climbing algorithm was implemented (Stamatakis *et al.* 2008).

For Bayesian inference (MrBayes v3.2.5 (Ronquist & Huelsenbeck 2003)) analyses, the parameters for each partition were unlinked in order to obtain separate estimates for each gene region, the rate-prior was set to variable and flat Dirichlet-priors used. The analysis was run by two simultaneous Monte-Carlo-Markov-Chains (Drummond & Rambaut 2007). These were run for 10 million iterations, sampling every 500th iteration. The first 25 % was discarded as burn-in. The analysis was repeated and all four runs combined to create a majority-rule consensus tree (Drummond *et al.* 2006). Outgroup selection also follows Chapter 2.

2.4. Geometric morphometric analysis of ocular patterns

Ocular patterns have long been used in the identification of the Araneae, but not in a quantitative manner. A study by Brandt *et al.* (IN REVIEW - b) (Chapter 3) showed that ocular patterns can be used to distinguish between morphospecies of the genus *Stasimopus*. For this reason, the average ocular pattern (relative eye size and position) for each species is included, so that it can be used to distinguish between the species of the Karoo. The methodology of how this was obtained is as stated in Chapter 3.

2.5. List of abbreviations

Morphology: anterior eye row (AER); anterior lateral eyes (ALE); anterior median eyes (AME); bootstrap value (BS); dorsal (*do*); median ocular quadrangle (MOQ); posterior eye row (PER); prolateral (*pl*); posterior lateral eyes (PLE); posterior median eyes (PME); posterior probability (PP); retrolateral (*rl*); ventral (*v*).

© University of Pretoria

3. Results

3.1. Morphological character matrices

List of characters and character states (codification) for table 1 & 2 (Both sex characters):

1 Eye pattern clustering: (0) highly clustered (Fig 17); (1) fairly clustered (Fig 17D); (2) not clustered (Fig 17A); (3) sparse (*S. patersonae*). **2** Largest eye: (0) AME; (1) ALE; (2) PME; (3) PLE. **3** Smallest eye: (0) AME; (1) ALE; (2) PME; (3) PLE. **4** Eyes of similar sizes: (0) yes; (1) no.

List of characters and character states (codification) for table 1 (male characters):

5 PLE in separate line: (0) yes (Fig 11C); (1) no (Fig 11A). **6** Carapace texture: (0) smooth (Fig 7D); (1) rugose (Fig 6C); (2) highly rugose (Fig 5B). **7** Shape of sternal sigilla: (0) narrow (Fig 21C); (1) broad; (2) fused (Fig 8A). **8** Sternum shape/ coxa imprints: (0) absent (Fig 25E); (1) shallow (Fig 21C); (2) distinct (Fig 8A). **9** Number of cheliceral teeth in proventral row: (0) 3; (1) 4; (2) 5. **10** Number of cheliceral teeth in retroventral row: (0) 3; (1) 4; (2) 5. **11** Number of cheliceral denticles: (0) 0-5; (1) 6-10; (2) 11-15; (3) 16-20. **12** Length of pedipalp relative to leg I segments: (0) tibia; (1) metatarsus; (2) tibia; (3) exceeds leg I. **13** Distance pedipalp reaches of segment in 12: (0) $\frac{1}{10}$; (1) $\frac{1}{8}$; (2) $\frac{1}{6}$; (3) $\frac{1}{5}$; (4) $\frac{1}{3}$; (5) $\frac{1}{2}$; (6) $\frac{3}{4}$; (7) full length; (8) exceeds. **14** Bulb shape: (0) compact (Fig 10B); (1) oval (Fig 14B); (2) elliptical (Fig 25B). **15** Embolus direction in relation to tibia (when palpal bulb is perpendicular to tibia): (0) parallel (Fig 10B); (1) perpendicular (Fig 21B); (2) distal (Fig 25B); (3) posterior (Fig 40B). **16** Leg I & II tarsus spines present: (0) 0-5; (1) 6-10; (2) 11-15; (3) 16-20; (4) 21-25. **17** Leg I & II metatarsus spines present: (0) 0-5; (1) 6-10; (2) 11-15; (3) 16-20; (4) 21-25; (5) 26-30; (6) >30. **18** Leg I & II tibia spines present: (0) 0-5; (1) 6-10; (2) 11-15; (3) 16-20; (4) 21-25; (5) 26-30; (6) >30. **19** Scopula extends onto metatarsus I & II: (0) no; (1) yes. **20** Leg III tarsus spines present: (0) 0-5; (1) 6-10; (2) 11-15; (3) 16-20; (4) 21-25; (5) 26-30; (6) >30. **21** Leg III metatarsus spines present: (0) 0-5; (1) 6-10; (2) 11-15; (3) 16-20; (4) 21-25; (5) 26-30; (6) >30. **22** Leg III tibia dorsal spines present: (0) 0-5; (1) 6-10; (2) 11-15; (3) 16-20; (4) 21-25; (5) 26-30; (6) >30. **23** Leg IV tarsus spines present: (0) 0-5; (1) 6-10; (2) 11-15; (3) 16-20; (4) 21-25; (5) 26-30; (6) >30. **24** Leg IV metatarsus spines present: (0) 0-5; (1) 6-10; (2) 11-15; (3) 16-20; (4) 21-25; (5) 26-30; (6) >30. **25** Leg IV tibia spines present: (0) 0-5; (1) 6-10; (2) 11-15.

List of characters and character states (codification) for table 2 (female characters):

5 Number of labial cuspules present: (0) None; (1) 0-5; (2) 6-10; (3) 11-15. **6** Sternal sigilla (0) distinct; (1) indistinct. **7** Sternal sigilla shape: (0) narrow (Fig 34A); (1) broad (Fig 19A); (2) fused (Fig 8A). **8** number of maxillary cuspules (0) none; (1) 0-5; (2) 6-10; (3) 11-15; (4) 16-20; (5) 21-25; (6) >26. **9** Number of cheliceral teeth in proventral row: (0) 4; (1) 5; (2) 6; (3) 7. **10** Number of cheliceral teeth in retroventral row: (0) 4; (1) 5; (2) 6; (3) 7. **11** Number of cheliceral denticles: (0) 0-10; (1) 11-15; (2) 16-20; (3) 21-30; (4) 31-40; (5) 41-50; (6) >51. **12** Pedipalp tarsus retrolateral spines present: (0) 0-5; (1) 6-10; (2) 11-15; (3) 16-20; (4) 21-25; (5) >26. **13** Pedipalp tarsus prolateral

© University of Pretoria

spines present: (0) 0-5; (1) 6-10; (2) 11-15; (3) 16-20; (4) 21-25; (5) >26. **14** Pedipalp tarsus prolateral spines length: (0) short; (1) long. **15** Pedipalp tibia retrolateral spines present: (0) 0-5; (1) 6-10; (2) 11-15; (3) 16-20; (4) 21-25. **16** Pedipalp tibia retrolateral spines present: (0) 0; (1) 1; (2) 2; (3) 3; (4) 4; (5) 5; (6) >6. **17** Extent of spine patch on metatarsus I: (0) $< \frac{1}{10}$; (1) $< \frac{1}{8}$; (2) $< \frac{1}{6}$; (3) $< \frac{1}{4}$; (4) $\frac{1}{3}$; (5) $\frac{1}{2}$; (6) $> \frac{3}{4}$. **18** Extent of spine patch on metatarsus II: (0) $< \frac{1}{10}$; (1) $< \frac{1}{8}$; (2) $< \frac{1}{6}$; (3) $< \frac{1}{4}$; (4) $\frac{1}{3}$; (5) $\frac{1}{2}$; (6) $> \frac{3}{4}$. **19** Spine patch extends onto tibia I & II: (0) yes; (1) no. **20** Metatarsus III covered in small red spinules: (0) yes; (1) no. **21** Metatarsus III with two rows of red spines: (0) yes; (1) no. **22** Number of spines in each row stated in 21: (0) 10-15; (1) 16-20; (2) 21-25; (3) 26-30; (4) >30. **23** Apical tuft present on metatarsus III: (0) yes (Fig 20E); (1) no. **24** Number of spines present in metatarsus III apical tuft: (0) 0; (1) 1-3; (2) 4-5; (3) 6-8; (4) 9-10; (5) 11-13; (6) >14. **25** Number of spines present in metatarsus IV apical preening comb: (0) comb absent; (1) 1; (2) 2; (3) 3; (4) 4-5; (5) 6-7; (6) 8-10; (7) 11-15. **26** Spermathecae terminus shape: (0) inflated (Fig 22A); (1) same width as spermathecae base (Fig 22B). **27** Spermathecae tubes shape: (0) straight (Fig 22A); (1) slightly curved inwards (Fig 22B); (2) extremely curved inwards (Fig 22D).

It is noted that some of the characters described are not discrete but are rather continuous. These characters have been placed into categories to attempt to capture the variation across the various species. These characters were used to inform the species diagnoses and can be used to do so in future.

3.2. Phylogenetic results

The results of the JModel test, infer a best model for the analysis of the data was GTR+G+I. The results for only identified specimens are given in Figure 4, but the phylogenies for all specimens collected (including unidentified juveniles) is given in figure S1-S2. These phylogenies demonstrate that the species diversity is significantly higher than suggested in Figure 4, as the unidentified specimens form multiple distinct genetic clades (S1, S2). The Bayesian inference phylogeny and the maximum likelihood phylogeny are fairly congruent, with only a few topological differences (Figure S2 – Maximum likelihood phylogeny). The largest difference is the placement of clade B. In the Bayesian inference tree, clade B is sister to clade A, where as in the maximum likelihood tree it is sister to clade H. The only other differences are small changes in the placement of individuals within species.

© University of Pretoria

Table 1. Morphological matrix of characters and character states used to identify males of the various *Stasimopus* species. Unknown character, due to damage or missing (-); Unknown, due to not being dissected (?).

Species	Specimen	1	2	3	4	5	6	7	8	9	10	11	12	13	14	15	16	17	18	19	20	21	22	23	24	25
S. astutus	AMGS-1829	1	1	2	1	1	1	-	2	-	-	-	0	3	-	-	0	3	4	1	0	3	1	1	2	0
S. brevipalpis	SAMC-B778	1	1	2	1	1	1	0	1	1	1	2	-	-	-	-	-	3	3	0	1	1	0	2	1	0
***S. dylani* sp. nov.**	NCA 2019/663	1	0	2	1	1	1	2	2	1	2	2	2	4	0	0	1	4	2	0	0	2	1	1	2	0
S. erythrognathus	AMGS-84628	1	1	2	1	1	2	-	2	2	2	2	0	5	0	1	0	4	3	1	0	0	1	0	1	0
***S. finni* sp. nov.**	NCA 2019/605	1	1	0	1	1	1	2	2	1	1	2	2	3	1	0	0	4	3	0	1	2	0	2	3	0
***S. hamartia* sp. nov.**	NCA 2017/1891	-	-	-	-	1	1	0	1	-	-	-	-	-	0	1	0	4	1	0	-	-	-	2	2	0
***S. ignis* sp. nov.**	NCA 2019/642	1	0	3	1	0	1	-	0	0	0	0	2	7	1	2	0	3	2	0	1	1	1	1	1	0
S. insculptus	BMNH-78.3	2	1	3	1	1	1	2	1	1	1	2	0	7	1	1	2	4	3	0	2	2	2	5	3	0
S. insculptus peddiensis	AMGS-2717 (NM15348)	2	1	3	1	1	2	-	2	1	1	1	0	6	0	1	0	1	0	0	2	2	1	2	3	1
***S. karooensis* sp. nov.**	SAM-ENW-C007293	1	0	2	1	1	1	2	2	1	1	1	1	3	0	1	0	2	4	0	0	3	1	1	2	0
S. kentanicus	SAMC-14685	1	4	3	0	1	1	0	1	1	2	2	0	6	0	2	2	6	6	0	5	6	2	6	6	2
S. longipalpis	AMGS-4222	1	0	2	1	1	1	-	0	-	-	-	3	8			0	5	2	0	1	1	3	1	1	0
***S. malesociatus* sp. nov.**	AMGS-8367	2	0	2	1	1	1	2	2	0	1	0	0	4	2	2	0	2	2	0	0	2	1	2	2	0
S. maraisi	NCA 2019/630	1	1	3	1	1	0	0	1	1	1	1	2	0	1	3	0	3	3	0	0	1	0	1	1	0
S. palpiger	BMNH-1901.3.13.112	1	0	2	1	0	2	0	2	1	1	2	3	8	0	1	0	3	3	0	0	2	6	3	1	0
S. patersonae	SAMC-B4655	1	0	2	1	1	1	0	2	1	1	0	0	6	2	3	1	4	3	0	1	2	0	1	1	0
S. purcelli	SAMC-150432	1	0	2	1	1	1	0	2	-	-	-	0	5	0	2	0	3	3	1	0	1	0	1	0	0
S. qumbu	AMGS-2052	1	0	2	1	1	2	-	2	-	-	-	-	-	0	0	2	6	4	0	-	-	-	1	2	0
S. schrieneri	SAMC-9159	2	1	3	1	0	1	0	1	1	1	0	2	4	1	2	0	4	2	0	0	2	4	1	0	0
S. spinipes	AMGS-16728 (2785)	1	1	3	1	1	1	0	1	1	1	2	0	3	0	2	4	6	6	0	3	6	6	6	4	0
S. steynsbergensis	BMNH – 1905.3.30.32	1	0	2	1	1	2	1	1	-	-	-	1	6	0	2	2	4	3	0	1	4	4	0	2	0
S. tysoni	AMGS-3068 (NM14956)	1	0	2	1	1	2	-	2	-	-	-	-	-	0	1	2	6	6	0	6	5	4	4	4	0
S. umtaticus rangeri	AMGS (NM14770)	1	1	3	1	1	1	0	1	-	-	-	1	7	1	3	4	6	2	0	5	6	1	4	4	1

© University of Pretoria

Table 2. Morphological matrix of characters and character states used to identify females of the various *Stasimopus* species. Unknown character, due to damage or missing (-); Unknown, due to not being dissected (?).

Species	Specimen	1	2	3	4	5	6	7	8	9	10	11	12	13	14	15	16	17	18	19	20	21	22	23	24	25	26	27
S. artifex	BMNH1899-7-24-47	1	1	2	1	2	-	-	4	-	-	-	5	3	0	2	6	0	0	0	0	0	3	0	3	6	?	?
S. astutus	BMNH-01-3-13-110-111	0	1	4	0	3	1	0	4	1	1	2	3	2	1	2	3	3	3	0	0	0	3	1	0	6	?	?
S. brevipalpis	SAMC 12394	2	1	0	1	2	0	2	6	-	-	-	3	1	1	1	2	4	3	0	0	0	1	1	0	5	?	?
S. erythrognathus	AMGS-84633	1	1	0	1	2	0	1	4	0	1	1	5	2	1	2	2	6	4	0	0	0	1	0	3	5	?	?
***S. hamartia* sp. nov.**	NCA 2017/1852	1	4	4	0	2	1	1	3	0	0	3	4	1	1	1	4	5	5	0	0	0	2	0	5	5	0	0
***S. ignis* sp. nov.**	NCA 2019/653	2	1	2	1	1	0	1	4	0	0	1	4	2	1	2	3	2	2	0	0	0	3	1	0	6	1	1
S. insculptus	AMGS- OCT-1912	1	1	2	1	2	0	1	6	0	1	5	5	3	0	2	4	0	0	0	0	0	4	0	2	4	?	?
S. insculptus peddiensis	AMGS2717 (NM15345)	1	1	3	1	1	1	0	4	0	1	4	5	4	0	2	5	1	2	0	0	0	4	1	0	4	?	?
S. kentanicus	SAMC-12411	1	1	3	1	-	-	-	3	0	0	3	-	-	-	-	-	-	-	-	-	-	-	-	-	-	?	?
S. kolbei	SAMC-5317	0	4	3	0	1	0	0	3	-	-	-	3	2	1	3	6	2	2	0	0	0	1	1	0	5	?	?
S. leipoldti	SAMC-2909	2	1	0	1	1	0	0	3	1	1	2	4	0	1	2	1	1	2	0	0	0	4	1	0	4	?	?
S. maraisi	AMGS1806 (NM14631)	1	1	3	1	1	0	0	3	0	2	3	3	2	1	1	2	2	3	0	0	0	1	1	0	3	?	?
S. meyeri	ZMBH-2903	2	1	0	1	2	1	0	4	1	1	0	3	1	1	1	2	1	2	0	0	0	1	1	0	6	?	?
S. obscurus	ZMBH-9412	1	1	0	1	2	0	0	4	-	-	-	4	3	0	1	2	6	6	0	0	0	2	1	0	4	?	?
S. patersonae	AMGS1634 (NM14650)	3	1	0	1	1	0	1	5	1	1	3	4	3	0	1	6	1	2	0	0	0	2	1	0	4	?	?
S. poweri	NM15358 (AMGS)	2	1	2	1	2	-	-	4	0	1	6	3	1	1	1	1	6	4	0	0	0	1	0	6	7	?	?
S. quadratimaculatus	SAMC-12398	3	1	2	1	1	0	0	3	0	0	1	4	2	0	1	4	5	5	0	0	0	1	-	-	6	?	?
S. qumbu	AMGS-84734	2	1	2	1	1	1	0	4	0	1	4	5	2	1	4	3	5	4	0	0	0	3	0	3	4	?	?
S. schoenlandi	BMNH1899-7-24-45-46	3	2	4	0	2	1	0	5	0	0	3	5	5	0	2	3	2	1	0	0	0	3	0	3	5	?	?
S. schrieneri	SAMC-9513	3	1	0	1	1	1	0	3	0	0	1	5	3	0	1	4	1	0	0	0	0	3	1	0	4	?	?
S. schultzei	SAMC-150514	1	1	0	1	1	1	0	3	0	1	0	5	1	0	1	2	5	4	0	0	0	1	1	0	5	?	?
S. spinipes	AMGS/ NM14861	1	1	0	1	3	1	0	5	0	1	1	5	3	1	2	5	3	2	0	0	0	2	1	0	6	?	?
S. shonlandi var. spinosus	AMGS (NM15172)	3	1	0	1	2	0	1	3	3	3	6	5	5	0	3	5	4	2	0	0	0	3	0	6	5	?	?
***S. teras* sp. nov.**	NCA 2019/643	-	-	-	-	1	1	-	3	0	1	1	3	2	1	1	3	2	2	0	0	0	2	1	0	6	1	1
***S. theaei* sp. nov.**	NCA 2019/606	1	1	0	1	3	0	0	4	0	1	6	4	2	1	1	2	5	4	0	0	0	2	1	0	6	0	0
S. tysoni	AMGS (NM14965)	3	2	3	1	2	0	1	5	1	1	4	5	4	0	2	5	2	1	0	0	0	2	0	1	4	?	?
S. umtaticus	SAMC 8848	1	0	2	1	1	-	-	5	-	-	-	-	-	-	-	-	2	2	0	0	0	3	0	5	6	?	?
S. umtaticus rangeri	AMGS (NM14772)	1	1	0	1	1	0	1	6	0	0	3	5	4	0	4	6	1	0	0	0	0	4	1	0	6	?	?
S. unispinosus	SAMC 5923	1	1	4	0	2	0	0	4	0	1	1	4	1	1	3	2	5	4	0	0	0	1	0	3	1	?	?
***S. venterstadensis* sp. nov.**	NCA 2019/610	0	1	2	1	2	0	1	3	0	1	3	4	1	1	2	2	3	3	0	0	0	2	0	3	4	0	2

© University of Pretoria

3.3. Geometric morphometric ocular patterns

There are clear differences between the ocular patterns of each species (Figure 2-3). The patterns scaled by centroid size make it easier to detect the differences visually, and when analysed statistically, the species are distinct (Chapter 3).

The eye pattern photographs and landmark data is available so that it can be used by future researchers to distinguish species in this manner (Brandt et al. IN REVIEW – Figshare database).

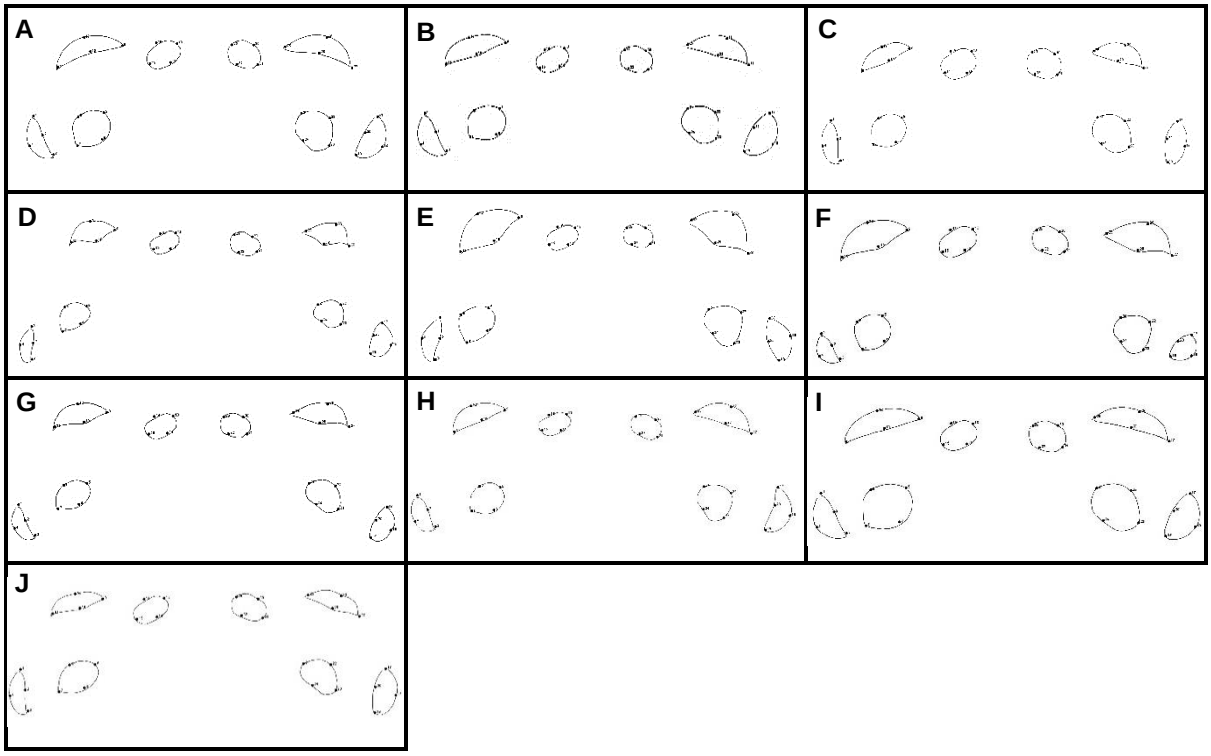


Figure 2. Average ocular pattern for the female *Stasimopus* species occurring in the Karoo region. A. *S. astutus*. B. *S. erythrognathus*. C. *S. hamartia* **sp. nov.** D. *S. ignis* **sp. nov.** E. *S. leipoldti*. F. *S. maraisi*. G. *S. schrieneri*. H. *S. theaei* **sp. nov.** I. *S. unispinosus*. J. *S. venterstadensis* **sp. nov.**

© University of Pretoria

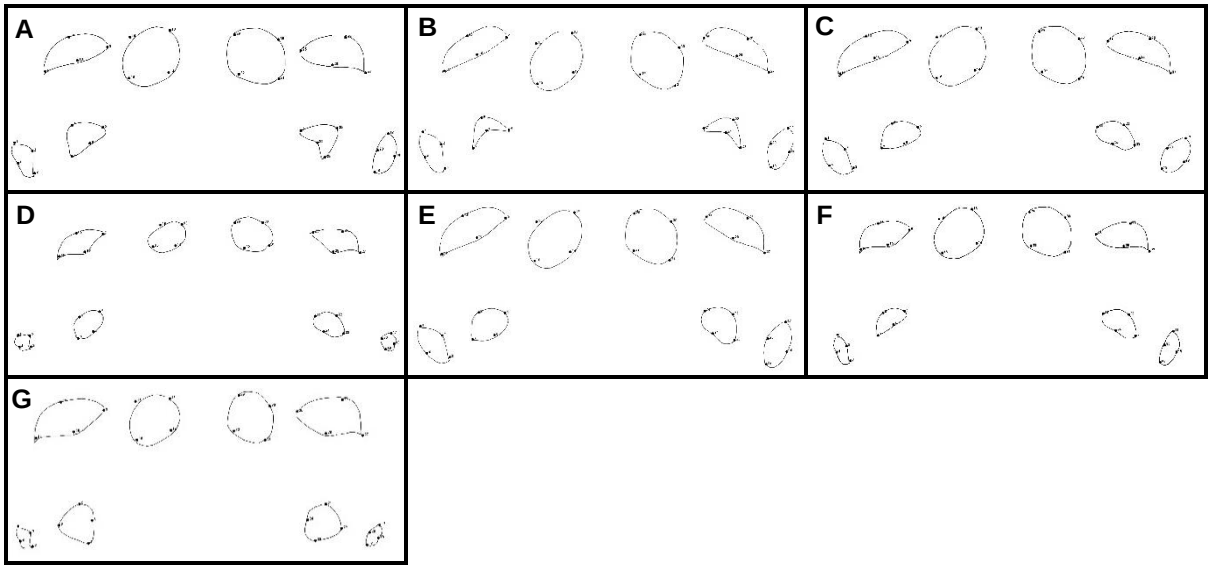


Figure 3. Average ocular pattern for the male *Stasimopus* species occurring in the Karoo. A. *S. astutus*. B. *S. dylani* **sp. nov.** C. *S. erythrognathus*. D. *S. ignis* **sp. nov.** E. *S. karooensis* ***sp. nov.*** F. *S. mandelai*. G. *S. maraisi*.

3.4. Integrative taxonomy

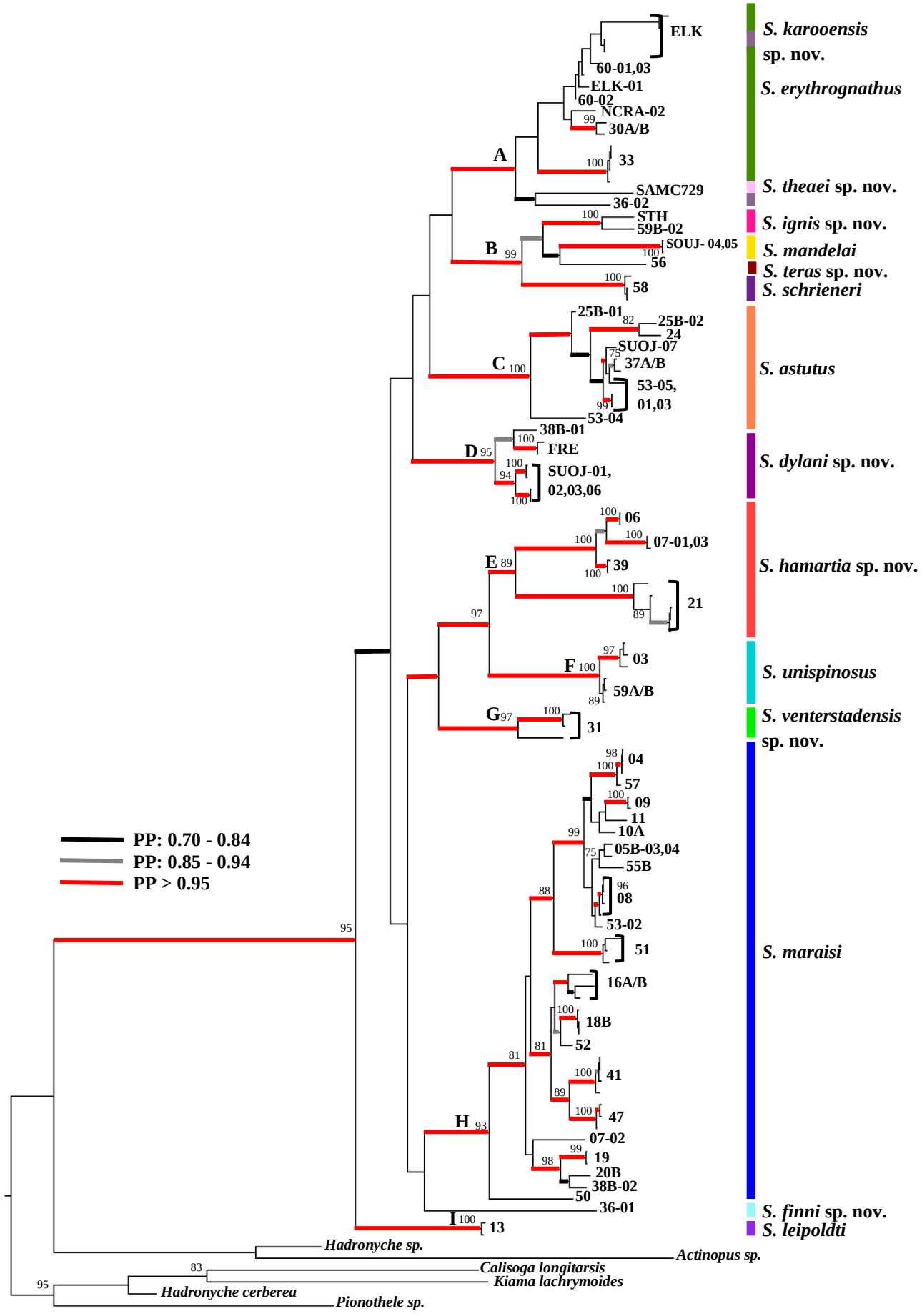
Stasimopus is a well-supported monophyletic clade from the data (BS: 95; PP:1.00) (Figure 4). Fifteen distinct species were recovered. The phylogeny is divided into nine clades (A-I) for ease of discussion.

The first clade (Figure 4, A) comprises an apparent species complex. The clade has high PP support (1.00), the species identified in the genetic complex are *S. erythrognathus*, *S. karooensis* **sp. nov.** and *S. theaei* **sp. nov.** These species are however, morphologically distinct. The males of *S. erythrognathus* and *S. karooensis* **sp. nov.** are distinguishable based on the length of the pedipalp in relation to leg I, ocular pattern, the pedipalpal bulb shape as well as the spination pattern on the metatarsus of all legs (Figures 3E, 11D, 27A, B, D-F, Table 1). The females of *S. erythrognathus* and *S. theaei* **sp. nov.** are differentiated based on the density of cheliceral denticles (Figure 34C, Table 2). Clade B consists of many species, each with very few representatives (Figure 4). These species are *S. mandelai*, *S. schrieneri*, *S. ignis* **sp. nov.** and *S. teras* **sp. nov.** The two individuals from *S. ignis* **sp. nov.** are grouped with high support (BS: 100; PP:1.00), the same is true for *S. mandelai* (BS: 100; PP:1.00) and *S. schrieneri* (BS: 100; PP:1.00). *Stasimopus schrieneri* females can be differentiated from *S. ignis* **sp. nov.** and *S. teras* **sp. nov.** based on the preening comb on metatarsus IV as well as the extent of spination on leg I (Figures 24A & E, 31D, 32B, Table 1). Clade C (Figure 4) is a well-supported monophyletic group (BS: 100; PP:1.00) and was morphologically identified as *S. astutus*, based on the following characteristics, the females having distinctly high number of labial cuspules, the length of spine extent on leg I and II and the preening comb on leg IV (Table 1). The male was identified based on the length of the pedipalp and the pedipalp bulb (Table 2). Clade D is identified

© University of Pretoria

as *S. dylani* **sp. nov.** (Figure 4), this is a strongly supported monophyletic group (BS: 100; PP:1.00). The was identified by the male ocular pattern (Figures 3B, 11A, Table 2) and relative length of the pedipalp. Clade E is a monophyletic group with high support and identified as *S. hamartia* **sp. nov.** (BS: 89; PP:1.00). This clade has good representation, but the male cannot be used for identification as it was found in poor condition. The females are identified based on the tuft present on metatarsus III, spination on leg I and cheliceral denticles (Figures 19C, 20A, E, Table 2). Clade F has been identified as *S. unispinosus* and is also a well-supported monophyletic linage (BS: 100; PP:1.00). The clade consists of only female specimens and were primarily identified based on the preening comb on metatarsus IV and the extent of spination on legs I and II (Table 2). Clade G is comprised of three females from one locality and described as *S. venterstadensis* **sp. nov.** This clade has high support (BS: 97; PP:1.00) and is morphologically distinct based on the tuft present on metatarsus III and the preening comb on metatarsus IV (Figures 38E, F, Table 2). Clade H is the clade with the most representation. It is a well-supported monophyly (Figure 4; BS: 93; PP:1.00) and was identified based on the females as *S. maraisi*. The key identifying characters were the preening comb on metatarsus IV, the labial and maxillary cuspules as well as Leg I spination (Table 2). The male (NCA 2019/630) which was genetically identified as *S. maraisi* did however, not match the type nor description of *S. maraisi* (Hewitt 1927). For this reason, the male (NCA 2019/630), has been described as the true male for the species *S. maraisi*, and the originally described male (AMGS-5367), has been redescribed as a new species, *S. malesociatus* **sp. nov.** *Stasimopus finni* **sp. nov.** is sister to clade H, but is represented by only one male specimen (thus not forming a clade) (Figure 4). This species is however morphologically distinct due to the relative length of the pedipalp, the pedipalp bulb and cheliceral denticles (Figures 13A, 14A, B, Table 1). The last clade (Figure 4; clade I), is identified as *S. leipoldti* and is a well-supported lineage (BS: 100; PP:1.00). The species was identified by the spination on leg I metatarsus, cuspules on the maxilla and labium and the spination on metatarsus III (Table 2).

© University of Pretoria



© University of Pretoria

Figure 4. Bayesian inference consensus tree for the concatenated dataset of CO1, 16S and EF-1ɣ for the *Stasimopus* dataset from the Karoo region. Posterior probabilities are shown by the use of coloured bars. Bootstrap support values above 70 are given on the corresponding node. The phylogeny is divided into nine clades for ease of discussion (A-I). The numbers for each specimen correspond to localities in figure 1.

3.5. Taxonomic results

The species diversity of *Stasimopus* for the Karoo region has been increased by 11 species; two of which have range expansions and nine are newly described species. The male which genetically matched the female specimens identified as *S. maraisi*, is described below. The original *S. maraisi* male is described further under the new name *S. malesociatus* **sp. nov.** The new species are described below as well as the description for *S. maraisi* male.

Systematics

Stasimopidae Bond, Opatova and Hedin 2020

Genus *Stasimopus* Simon 1892

Simon 1892: 82; Pocock 1897: 726-728; Hewitt 1915b: 75-85; Roewer 1942: 159; Raven 1985: 143-144; Dippenaar-Schoeman 2002: 31-38; Engelbrecht and Prendini 2012: 8.

Type species: *Stasimopus caffrus* (Koch 1842).

Diagnosis: The family Stasimopidae is monogeneric (Opatova *et al.* 2020. The characters for distinguishing this genus thus applies to the family. The family differs from other Ctenizid-like taxa based on the following suite of characteristics based on Raven (1985): The tibia of leg III lacking a saddle-like excavation, the ocelli is twice as wide as it is long and the anterior lobe of the maxillae is anteriorly produced (Engelbrecht & Prendini 2012; Opatova *et al.* 2020).

Description:

General: Medium to large bodied spiders (22-42 mm) (Dippenaar-Schoeman 2002).

Carapace: Cephalic region dome shaped with procurved fovea (Dippenaar-Schoeman 2002). In *S. filmeri*, the fovea forms into horn-like protrusion (Engelbrecht & Prendini 2012).

Ocelli: The eyes occur in single cluster on forefront of cephalic region and eyes arranged in two transverse rows (Dippenaar-Schoeman 2002; Pocock 1897). Posterior row wider than anterior row (Dippenaar-Schoeman 2002; Raven 1985).

Chelicerae: Distinct rastellum with thick spines, as well as cheliceral furrow with two rows of teeth (Dippenaar-Schoeman 2002).

© University of Pretoria

Sternum, labium and maxillae: The sternum has single pair of sigilla present. Sigilla are situated opposite III coxa (Dippenaar-Schoeman 2002; Pocock 1897). In some male species sigilla are fused at anterior end, forming an arrow-like shape. Labium cuspules present in females and bare in males (Dippenaar-Schoeman 2002). Maxilla has longer process only at distal end forming a long cone (Pocock 1897; Raven 1985). Maxilla has few basal teeth present (Pocock 1897).
Abdomen: Varies in colour. Four spinnerets. Posterior spinnerets have domed apical segments (Dippenaar-Schoeman 2002).
Pedipalps: Male bulb is simple pyriform (Dippenaar-Schoeman 2002).
Legs: Female legs are short and stocky. Three tarsal claws present, the paired claw with one large tooth and two smaller teeth below, third claw is untoothed (Dippenaar-Schoeman 2002). Distal segments of leg I and II densely spined (Dippenaar-Schoeman 2002). Males have long slender legs.
Spermathecae: Multilobular (Dippenaar-Schoeman 2002).

Distribution: The genus is currently recorded from Lesotho and South Africa, in all provinces except Limpopo. It is an endemic to the Afrotropical region.

Included taxa: In this paper, nine new species are described and a description of a *S. maraisi* male. This increases the number of species in the genus to 56, with 23 of them found in the Karoo region.

© University of Pretoria

Key to adult females of five *Stasimopus* species in the Karoo region

1. Tuft of spines present ventrally on metatarsus III (Fig 20E) ……2
- Tuft of spines not present ventrally on metatarsus III……3
2. Patch of spinules on metatarsus I extends ½ the segment length (Fig 20A) ……... ……. *S. hamartia* **sp. nov.**
- Patch of spinules on metatarsus I extends ¼ the segment length (Fig 3A) ……... ……..…… *S. venterstadensis* **sp. nov.**
3. Chelicera with extremely dense denticles (>45) (Fig 34C) ……..... *S. theaei* **sp. nov.**
- Chelicera with few denticles (<15) (Fig 23C) ……...4
4. Metatarsus III with >26 spines in each row dorsally (Fig 24C) ……..…. *S. ignis* **sp. nov.**
- Metatarsus III with <21 spines in each row dorsally (Fig 31E) ……..…. *S. teras* **sp. nov.**

Key to adult males of six *Stasimopus* species in the Karoo region*

* *S. hamartia* not included due to damaged state.

1. The largest eye is the AME (Fig 11D) ……...……2
- The largest eye is the ALE (Fig 11B) …...…….……3
2. Embolus extends posteriorly in relation to pedipalp tibia (Fig 29B) ... *S. malesociatus* **sp. nov.**
- Embolus extends perpendicularly in relation to pedipalp tibia (Fig 27A) ……... ……. *S. karooensis* **sp. nov.**
3. Pedipalp reaches <1/5 of tibia I length…….…….....4
- Pedipalp reaches >1/3 of tibia I length……...5
4. The carapace is smooth in texture (Fig 7D) ……..…. *S. maraisi* **sp. nov.**
- The carapace is rugose in texture (Fig 5B) …… *S. finni* **sp. nov.**
5. Embolus extends almost parallel in relation to pedipalp tibia (Fig 10B) ….. *S. dylani* **sp. nov.**
- Embolus extends distally in relation to pedipalp tibia (Fig 25B).…… *S. ignis* **sp. nov.**

© University of Pretoria

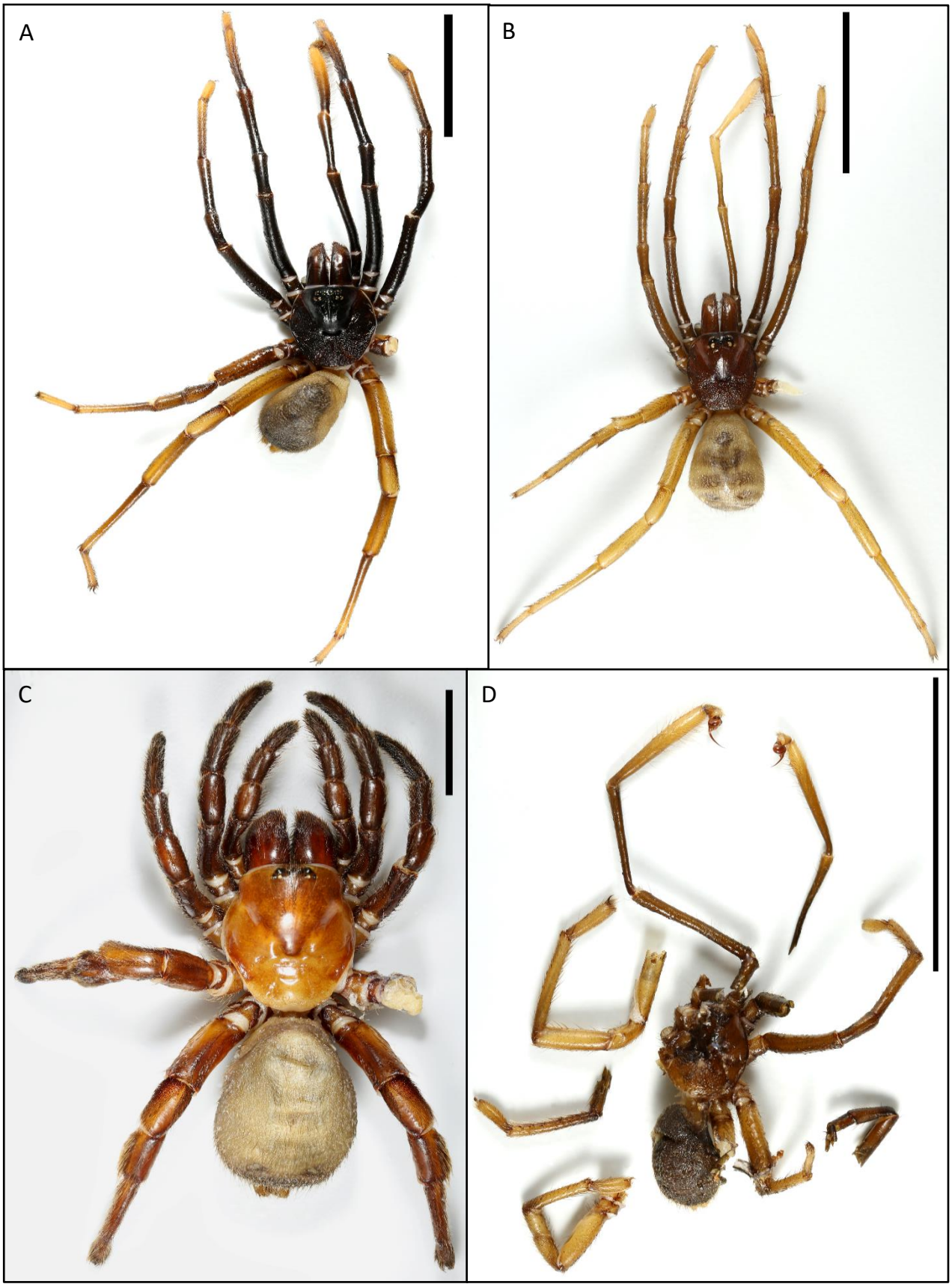


Figure 5. Three *Stasimopus* species in habitus view. (A) Male of *Stasimopus dylani* **sp. nov.** (NCA 2019/663). (B) Male of *Stasimopus finni* **sp. nov.** (NCA 2019/605). (C) Female of *Stasimopus hamartia* **sp. nov.** (NCA 2017/1852). (D) Male of *Stasimopus hamartia* **sp. nov.** (NCA 2017/1891). Scale: 1cm.

© University of Pretoria

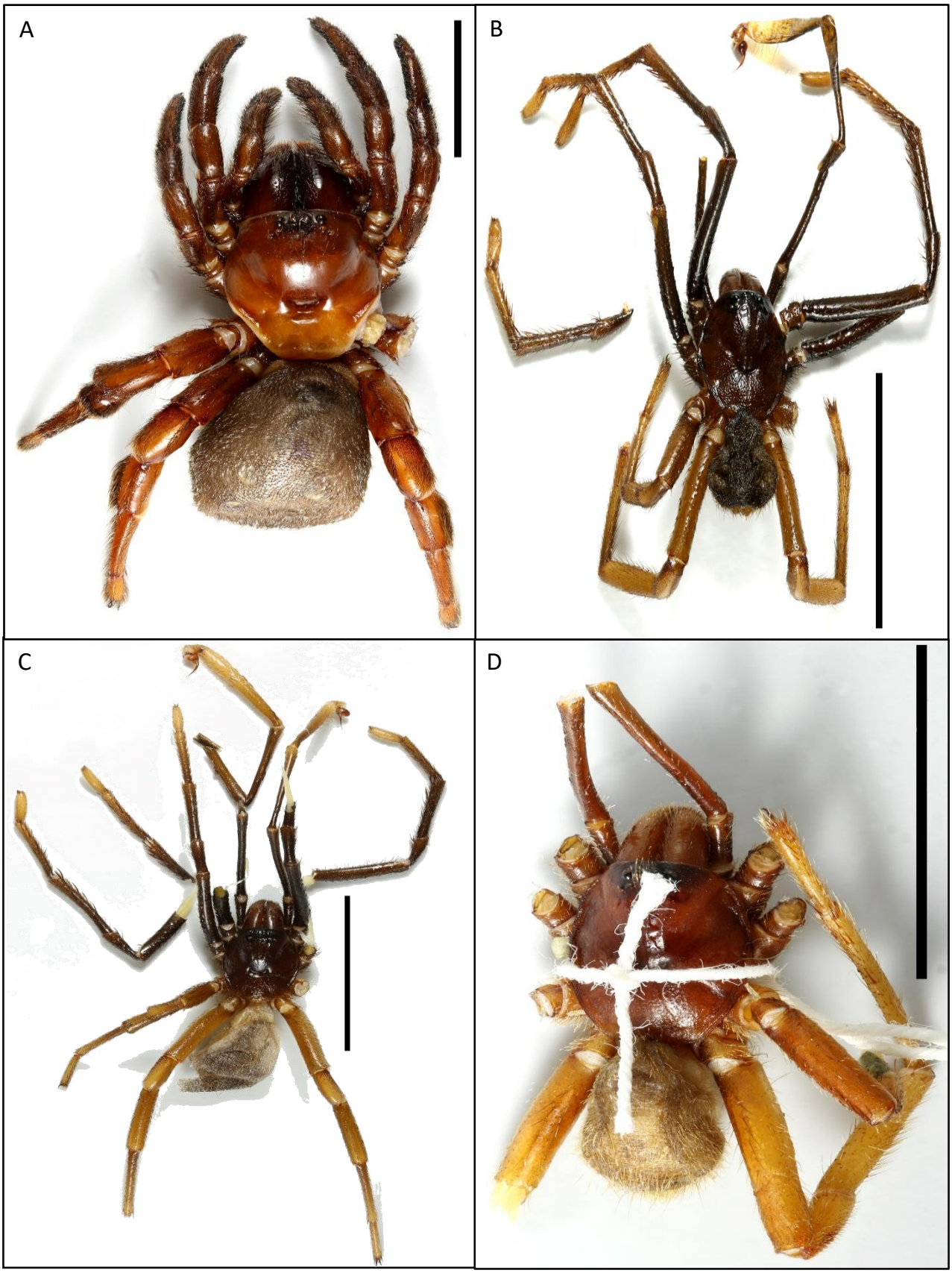


Figure 6. Three *Stasimopus* species in habitus view. (A) Female of *Stasimopus ignis* **sp. nov.** (NCA 2019/653). (B) Male of *Stasimopus ignis* **sp. nov.** (NCA 2019/642). (C) Male of *Stasimopus karooensis* **sp. nov.** (SAM- ENW-C007293). (D) Male of *Stasimopus malesociatus* **sp. nov**. (AMGS-5367). Scale: 1cm.

© University of Pretoria

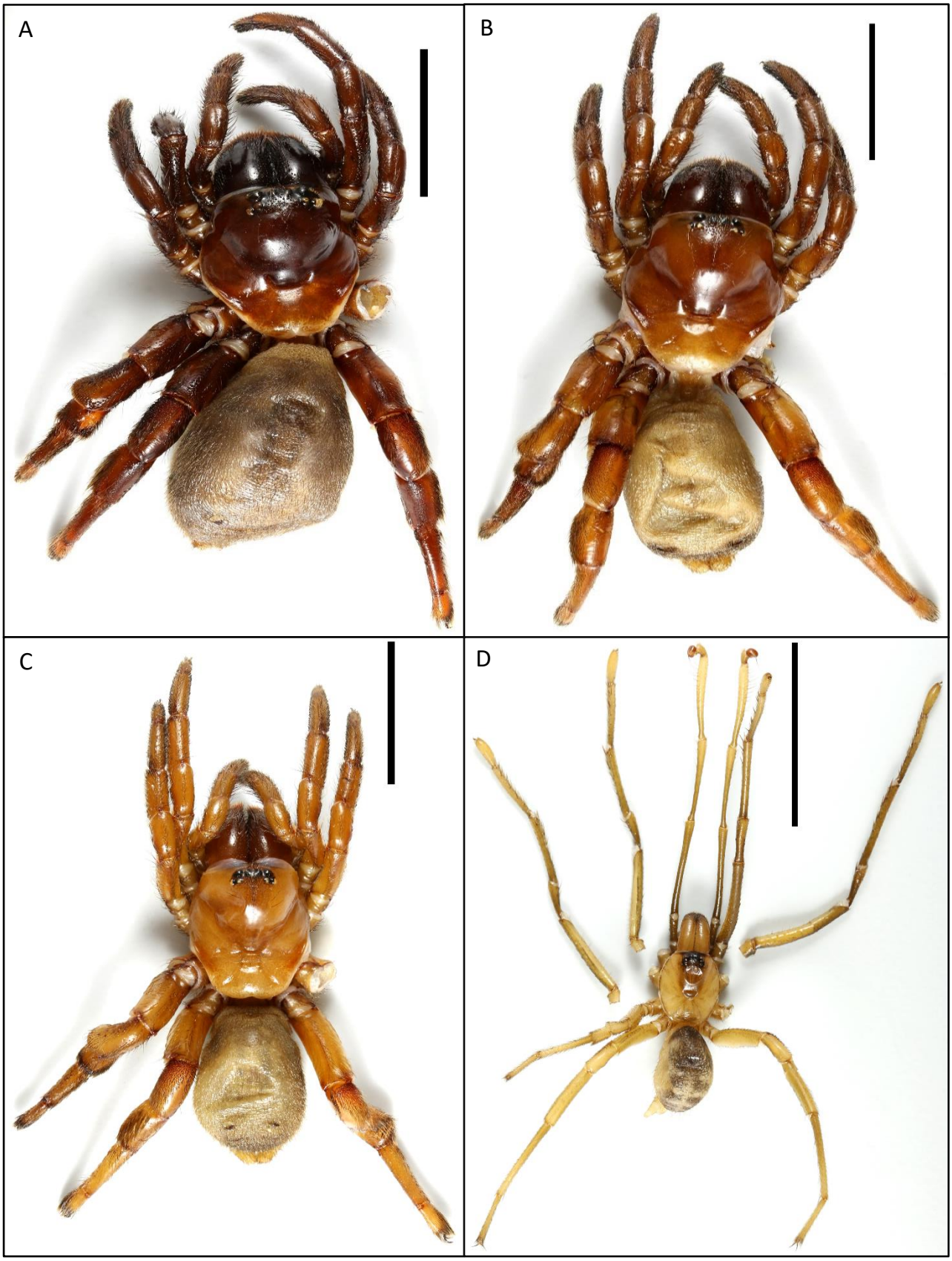


Figure 7. Four *Stasimopus* species in habitus view. (A) Female of *Stasimopus teras* **sp. nov.** (NCA 2019/643). (B) Female of *Stasimopus theaei* **sp. nov.** (NCA 2019/606). (C) Female of *Stasimopus venterstadensis* **sp. nov.** (NCA 2019/610). (D). Male of *Stasimopus maraisi* (NCA 2019/630). Scale: 1cm.

© University of Pretoria

***Stasimopus dylani* sp. nov.**

(Figures 3B, 5A; 8, 9, 10, 11A)

Type material: Holotype ♂ SOUTH AFRICA: Western Cape Province: Murraysburg (-31.8884, 23.7310), 21.v.2018, S. Brandt, C. Sole, E. Engelbrecht and E. Brand, (NCA 2019/663). Paratypes. Same data, 21.v.2018, 1♂ (NCA 2019/664); Eastern cape Province: Jansenville (-32.8772, 24.4952), 17.vii.2015, I. Engelbrecht and D. Kambas, 4♂♂ (NCA 2019/697, NCA 2019/698, NCA 2019/699, NCA 2019/702), Willowmore (-33.0423, 23.1958), 15.v.2018, S. Brandt, C. Sole, E. Engelbrecht and E. Brand, 1♀ *juv.* (NCA 2019/676).

Etymology: This species is a patronym in recognition of Dylan Cecil Brandt, for his unending support and encouragement of the first author during her postgraduate studies.

Diagnosis: The males of *S. dylani* **sp. nov.** are distinguishable from other members of the genus occurring in the Karoo based on the following combination of characters. Differentiated from *S. astutus*, *S. erythrognathus*, *S. malesociatus* **sp. nov.**, *S. patersonae*, *S. steynsbergensis*, *S. karooensis* **sp. nov.** and *S. mandelai* based on the pedipalp not extending beyond the tarsus of leg I. It is distinguished from *S. palpiger* by the pedipalp that is longer than leg I, which is not the case with *S. dylani* **sp. nov.** The species can be distinguished from *S. schrieneri*, *S. ignis* **sp. nov.**, *S. finni* **sp. nov.** and *S. maraisi* based on the largest eye, which in these species is the ALE, whereas in *S. dylani* **sp. nov.** it is the AME.

Description: Based on the holotype ♂ (NCA 2019/663) and paratypes 5♂ (NCA 2019/664, NCA 2019/697, NCA 2019/698, NCA 2019/699, NCA 2019/702).
Remarks: ♀: Known only from males.
General: ♂: (Fig 5A) Medium bodied spiders, ranging between 10.68 – 13.03 (13.03) total length.
Carapace: ♂: Carapace length 4.78 – 6.28 (6.28); width 4.42 – 5.74 (5.74). Black colouration, thoracic region with rugose texture. The fovea strongly procurved, between 1.00 – 1.38 (1.11) in length.
Ocelli: ♂: (Fig 11A, Fig 3B) AME diameter 0.26 – 0.28 (0.28), PME diameter 0.16 – 0.20 (0.19), MOQ anterior width 1.30 – 1.67 (1.67), MOQ posterior width 1.72 – 2.09 (2.05); AME-AME 0.25, AME-ALE 0.15, ALE-ALE 1.08, PME-PME 1.02, PME-PLE 0.16, PLE-PLE 1.62. AER arrangement slightly recurved, PER recurved.
Chelicerae: ♂: (Fig 8B) Two teeth rows present, 4 teeth in proventral row, 5 teeth in retroventral row; 12 cuspules in between.
Sternum, labium and maxillae: ♂: (Fig 8A) Sternum length 2.27 – 3.48 (3.48); sternum width 2.47 – 3.05 (3.05). Sternum shape has distinct impressions of where the coxa are situated. Sigilla in the shape

© University of Pretoria

of a fused arrow, distal end fused, proximal end 1.06 – 1.45 (1.12) apart; cuspules absent on labium and maxilla.

Abdomen: ♂: (Fig 5A) Abdomen length 5.56 – 6.75 (6.75); width 3.45 – 4.63 (4.63). Colour, *do*- dark grey, *v*- and laterally beige.

Pedipalps: ♂: (Fig 10A, B) Total length 19.01; Segment lengths 1.77, 6.41, 4.82, - ,6.02. Spination: spines absent. Bulb compact, embolus elongated, tapering into sharp point, extending downwards, almost parallel to tibia.

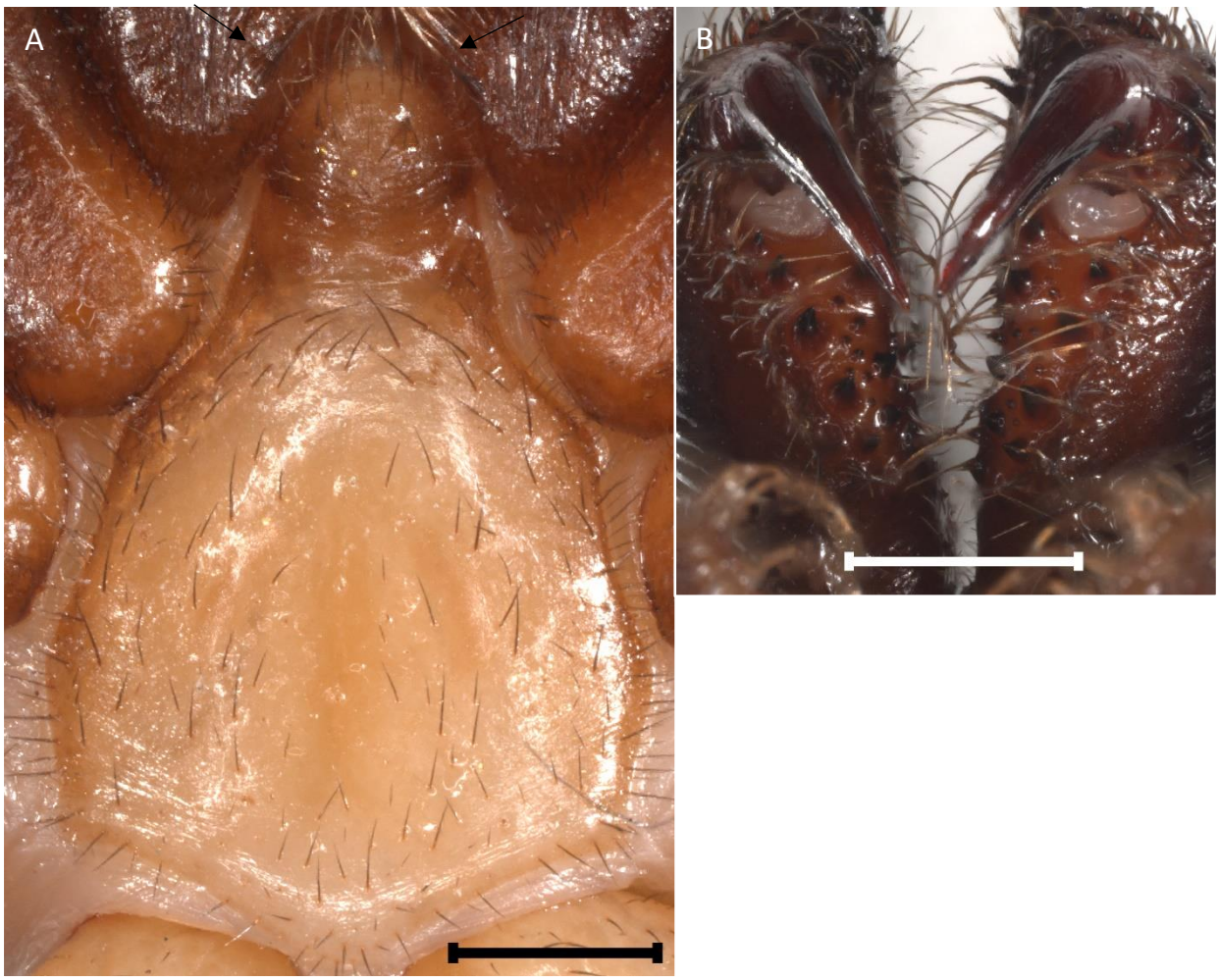


Figure 8. Male of *Stasimopus dylani* **sp. nov.** (NCA 2019/663). (A) Sternum with fused labium and visible sigilla (as shown by the arrows). (B) Fangs with cheliceral teeth. Scale: 1mm.

Legs: ♂: Length order: I, IV, II, III. I Total length 22.94; Segment lengths 7.07, 3.23, 4.86, 5.62, 2.16; Spination: spines absent on femur and patella, with sparse setae. Tibia *v*- 19 large spines (extending *pl*&*rl*), covering only distal half. Metatarsus (Fig 10C) *pl*- 19 large spines extending *v*, 21 large spines *rl* (slightly *v*). Tarsus (Fig 10C) *pl*- 4 spines, *rl*- 4 spines, *v*- scopulate. II Total length 20.88; Segment lengths 6.42, 2.86, 4.32, 5.21, 2.07; Spination: spines absent on femur and patella, with sparse setae.

© University of Pretoria

Tibia *v*- 5-7 spines distally. Metatarsus *pl*- 12-13 large spines extending *v*, *rl*- 10-11 large spines extending *v*. Tarsus *pl*- 4 spines, rl- 3-4 spines, *v*- scopulate. III Total length 16.45; Segment lengths 4.64, 2.26, 2.55, 4.35, 2.66; Spination: spines absent on femur, with sparse setae. Patella, *do* (slightly *pl*)- 7 small spines. Tibia (Fig 10F), *do*- Distally dense patch of spines (Approx. 25), extend to metatarsus. Metatarsus (Fig 10D), *pl*- 11 spines, *do*- small patch of spines proximally (Approx. 15) connecting to tibia, *rl*- 3 spines, *v*- 5 spines. Tarsus (Fig 10D) *pl*- 8 spines, *rl*- 7 spines. IV Total length 22.85; Segment lengths 5.32, 2.65, 4.50, 7.42, 2.96; Spination: spines absent on femur, with sparse setae. Patella (Fig 10G), *do*- short red spines proximally, less dense distally, interspersed with black setae. Tibia short black setae. Metatarsus (Fig 10E) *pl*- 5 spines, *rl*- 6 spines. Tarsus (Fig 10E) *pl*- 10 spines, *rl*- 9 spines.

Distribution and environment notes:

The species is found in the localities indicated in Figure 9. The species appears to have a broader distribution in the Western and Eastern Cape provinces of South Africa. The areas typically had sandy soils. The juvenile female was collected from a flat pan. All the males were collected while they were crossing quite roads. The SUOJ locality had no rain on the day collected, but a slight drizzle did occur after collection, whereas the males from FRE were collected after very heavy rain.

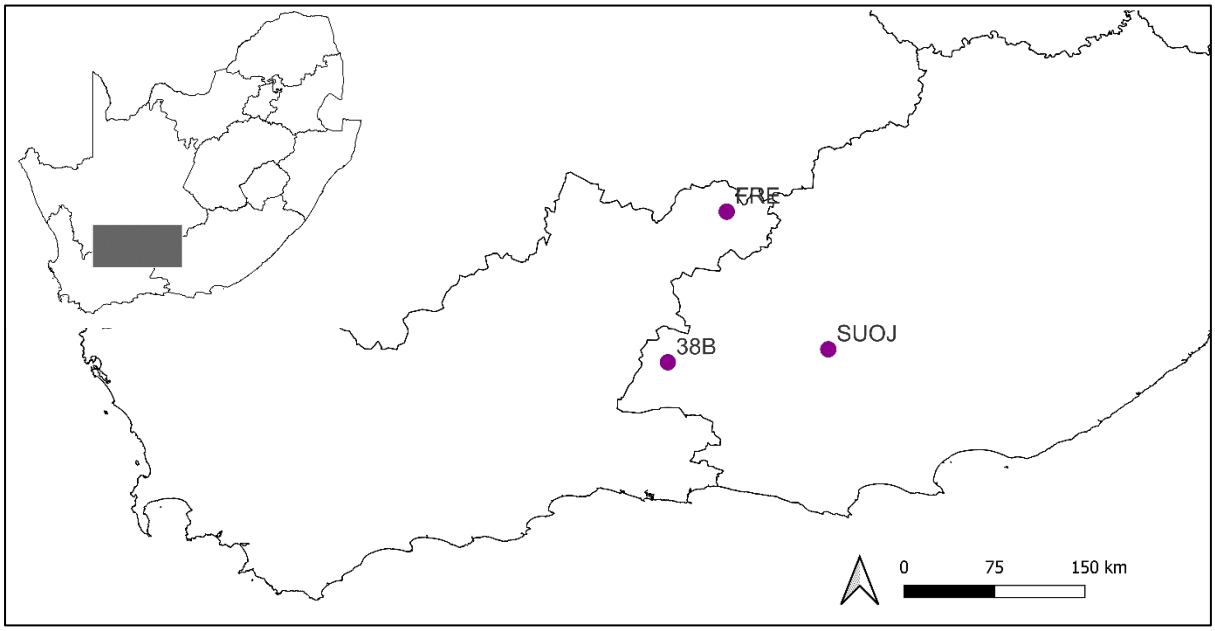


Figure 9. Map of the localities where *Stasimopus dylani* **sp. nov.** specimens were collected. Numbers match the site numbers in Figure 1. Map created in QGIS version 3.4.8-Madeira (2019), available at: http://qgis.osgeo.org.

© University of Pretoria

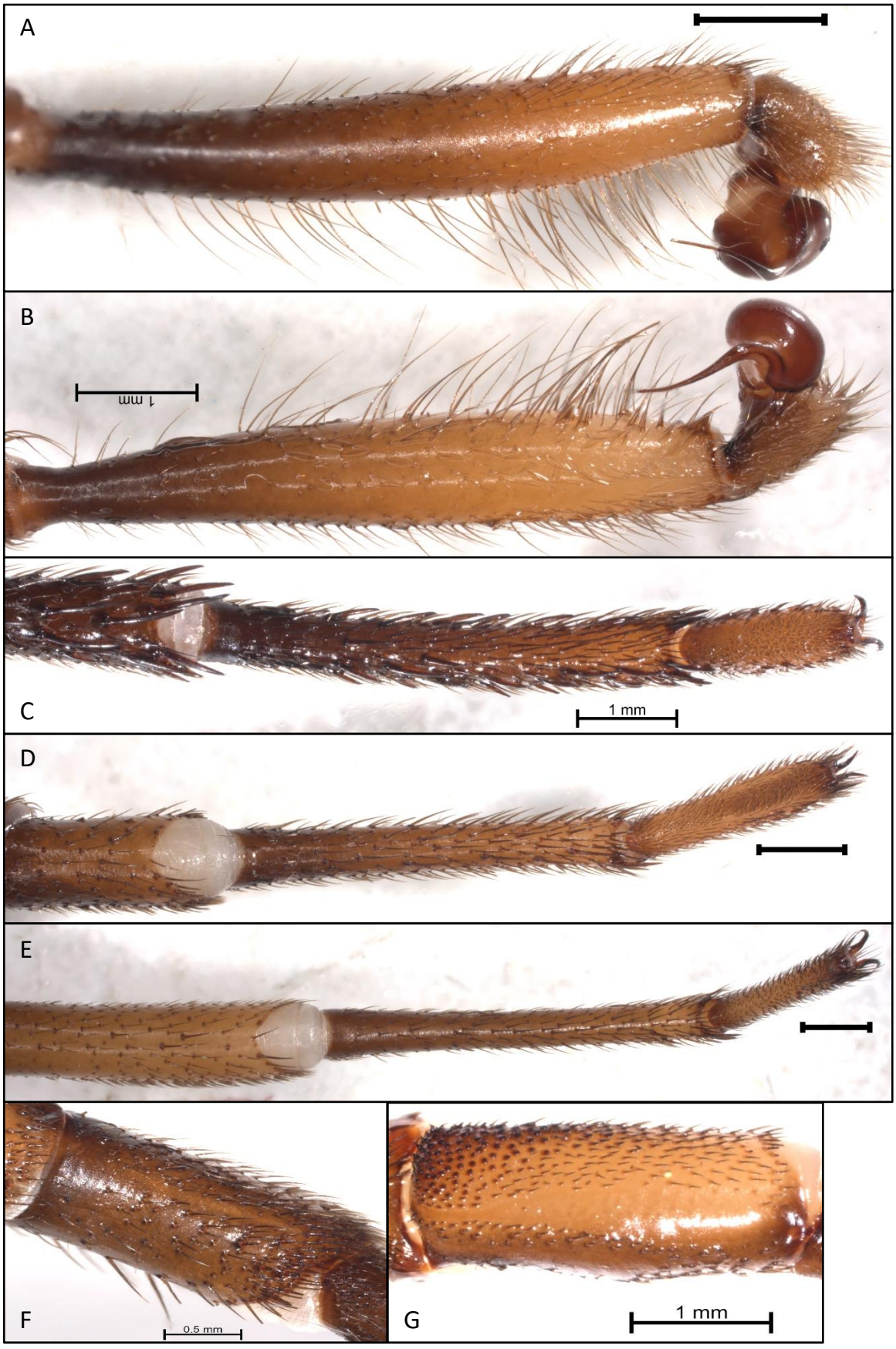


Figure 10. Male of *Stasimopus dylani* **sp. nov.** (NCA 2019/663). (A) Pedipalp tibia, bulb, retrolateral aspect. (B) Pedipalp tibia, bulb, prolateral aspect. (C) Leg I metatarsus, tarsus. Ventral aspect. (D) Leg III metatarsus, tarsus. Ventral aspect. (E) Leg IV metatarsus, tarsus. Ventral aspect. (F) Leg III tibia, dorsal aspect. Scale: 0.5mm. (G) Leg IV patella, dorsal aspect. Scale: 1mm.

© University of Pretoria

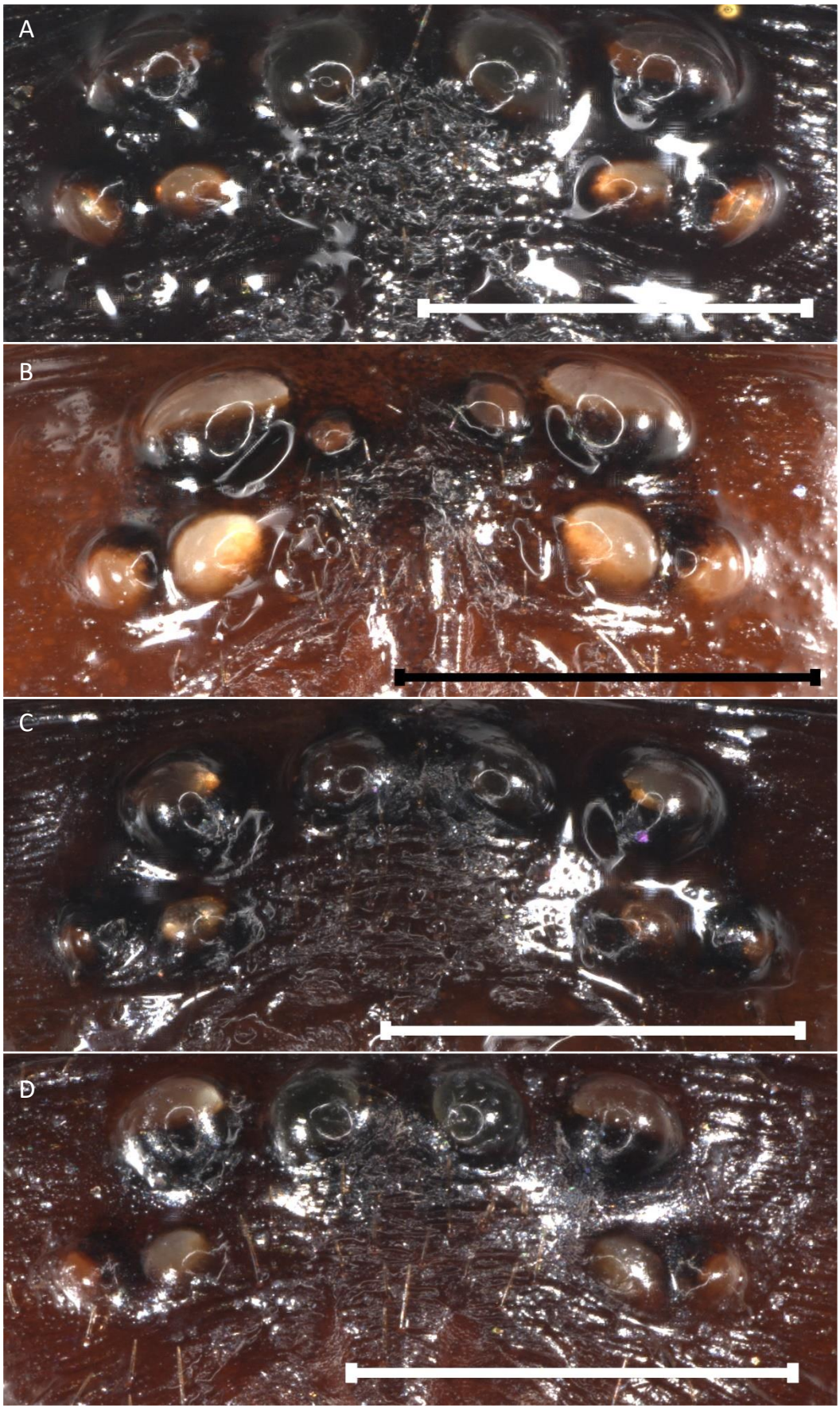


Figure 11. Ocular patterns for the male *Stasimopus* Simon, 1892 species. (A) *S. dylani* **sp. nov.** (NCA 2019/663). (B) *Stasimopus finni* **sp. nov.** (NCA 2019/605). (C) *Stasimopus ignis* **sp. nov.** (NCA 2019/642). (D) *Stasimopus karooensis* **sp. nov.** (SAM-ENW-C007293). Scale: 1mm.

© University of Pretoria

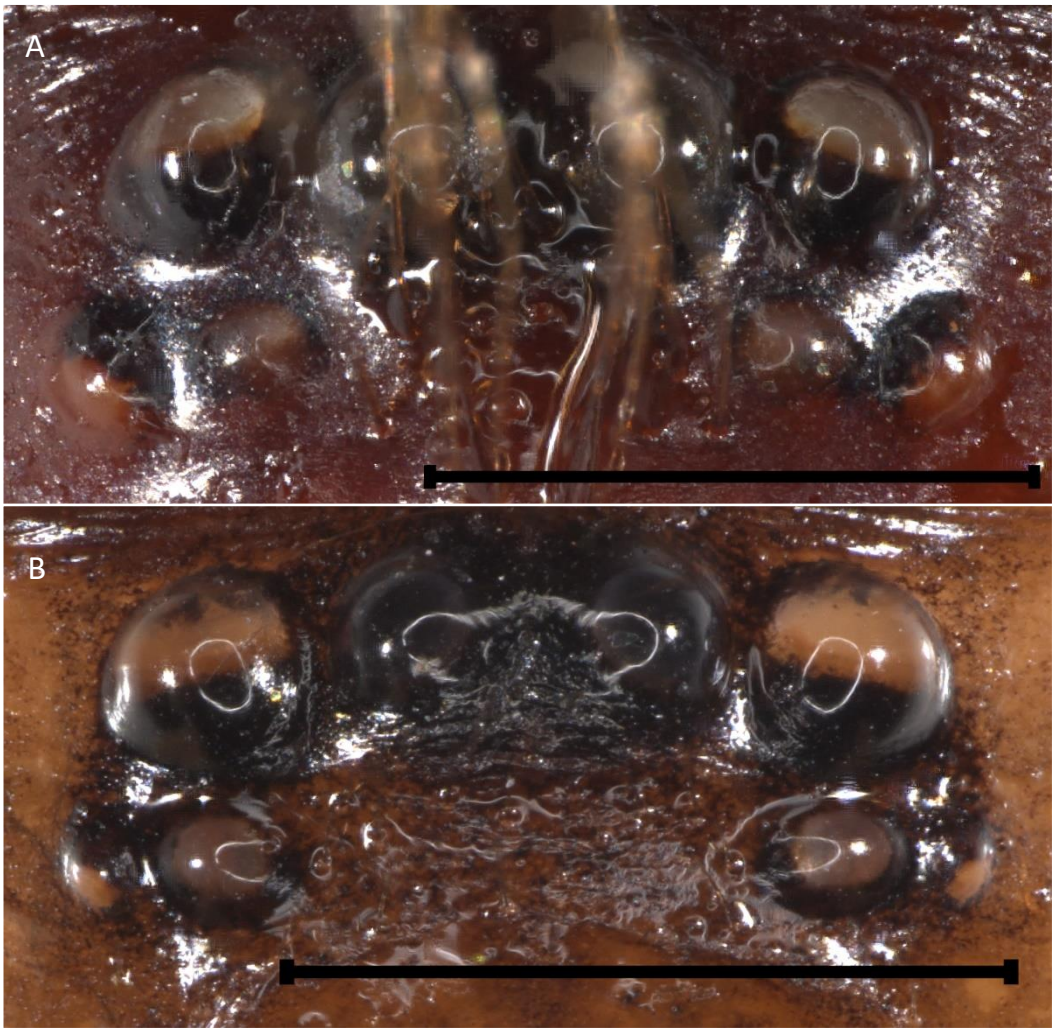


Figure 12. Ocular patterns for the male *Stasimopus* Simon, 1892 species. (A) *Stasimopus malesociatus* **sp. nov.** (AMGS-5367). (B) *Stasimopus maraisi* (NCA 2019/630). Scale: 1mm.

***Stasimopus finni* sp. nov.**

(Figures 5B, 11B, 13A, 14, 15)

Type material: Holotype ♂ SOUTH AFRICA: Eastern Cape Province, Somerset East (-32.9386, 25.6612), 14.v.2018, S. Brandt, C. Sole, E. Engelbrecht and E. Brand, (NCA 2019/605).

Etymology: The specific epithet is patronym in honour of Finn Robert Pirk the son of the third author, who loves all creepy crawlies.

Diagnosis: The males of *S. finni* **sp. nov.** are distinguishable from other members of the genus occurring in the Karoo based on the following combination of characters. It is differentiated from *S. astutus*, *S. erythrognathus*, *S. malesociatus* **sp. nov.**, *S. patersonae*, *S. steynsbergensis*, *S. karooensis* **sp. nov.** and *S. mandelai* based on the pedipalp not reaching the tarsus of leg I.

© University of Pretoria

Distinguished from *S. palpiger* as the pedipalp is longer than leg I, which *S. finni* **sp. nov.** is not. The species has denser cheliceral denticles (>11) than *S. schrieneri* (<5), *S. ignis* **sp. nov.** (<5) and *S. maraisi* (<10). *Stasimopus finni* **sp. nov.** is in general more spinose on the legs than *S. dylani* **sp. nov.** (Tibia of leg I and IV).

Description: Based on the holotype ♂ (NCA 2019/605).
Remarks: ♂: The left AME is reduced in size, making some eye measurements unreliable. ♀: Known only from the type male.
General: ♂: (Fig 5B) Medium bodied spider, 10.84 total length.
Carapace: ♂: Carapace length 4.76; width 4.05. Deep red-brown colouration, thoracic region with rugose texture. Fovea procurved, 0.81 in length.
Ocelli: ♂: (Fig 11B) AME diameter 0.14, PME diameter 0.19, MOQ anterior width 1.22 (may not be accurate due to deformity), MOQ posterior width 1.71; AME-AME 0.31 (may not be accurate due to deformity)., AME-ALE 0.10, ALE-ALE 0.65, PME-PME 0.79, PME-PLE 0.16, PLE-PLE 1.14. AER procurved, PER recurved.
Chelicerae: ♂: (Fig 13A) Two teeth rows present, 4 teeth proventral row, 4 in retroventral row; 11-13 cuspules between rows.
Sternum, labium and maxillae: ♂: (Fig 14C) Sternum length 2.66; sternum width 2.19. Sternum shape has distinct impressions of where the coxa are situated. Sigilla in the shape of a fused arrow, distal end fused, proximal end 0.69 apart; cuspules on labium absent; maxilla absent.
Abdomen: ♂: (Fig 5B) Abdomen length 6.08; width 4.30. Pale beige colouration with dark grey banding, smaller band near carapace, followed by broader and wider band, then a narrower band, lastly two shorter bands next to one another.
Pedipalps: ♂: (Fig 14A, B) Total length 16.03; Segment lengths 1.57, 5.42, 4.15, -, 4.88. Spines absent. Bulb oval, embolus elongated, tapering retrolaterally into sharp point.
Legs: ♂: Length order: I, IV, II, III. I Total length 17.40; Segment lengths 5.54, 2.36, 4.22, 3.93, 1.35; Spination: spines absent on femur, with sparse setae. Patella *v*- 2-3 spines distally. Tibia (Fig 14D) *v*- 16-18 large spines extend *pl*&*rl*, denser distally. Metatarsus (Fig 14D) *v*- 15-16 large spines extend *pl*&*rl*. Tarsus (Fig 14D) *pl*&*rl*- 1-2 small spines, *v*- scopulate. II Total length 15.53; Segment lengths 4.77, 2.23, 3.63, 3.57, 1.33; Spination: spines absent on femur, with sparse setae. Patella *v*- 2-3 spines distally. Tibia *v*- 16 large spines extend *pl*&*rl*, denser distally. Metatarsus *v*- 14-16 large spines, 1 distinctly large spine distally on *pl* and *rl* aspects. Tarsus *pl*&*rl*- 2-3 small spines, *v*- scopulate. III Total length 11.75; Segment lengths 3.01, 1.54, 1.38, 3.68, 2.14; Spination: spines absent on femur, with sparse setae. Patella *do*- 11 small spines. Tibia *pl*- 1 spine, almost *v*, *do*- 2 unorganised rows of red spinules (11 *pl*/*do*; 8-9 *rl*/*do*). Metatarsus *do*- 8 spines in two 2, *v* (Fig 14E) – 18 spines, 3 are large and distal. Tarsus *v* (Fig 14E) – 7 small spines, extend *pl*&*rl*, dense setae covering spines. IV

© University of Pretoria

Total length 17.38; Segment lengths 4.27, 2.31, 3.66, 4.85, 2.29; Spination: spines absent on femur, with sparse setae. Patella *do*- short dense red spines proximally, less dense distally; interspersed with fine black setae. Tibia *pl*/*v*- 2-3 small spines. Metatarsus *pl*- 8 spines, *v* (Fig 14F) – I5 spines (4 large spines distally), spines extend *pl*. Tarsus (Fig 14F) *pl*- 11-14 spines, extend *v*, *v*- 7 small spines.

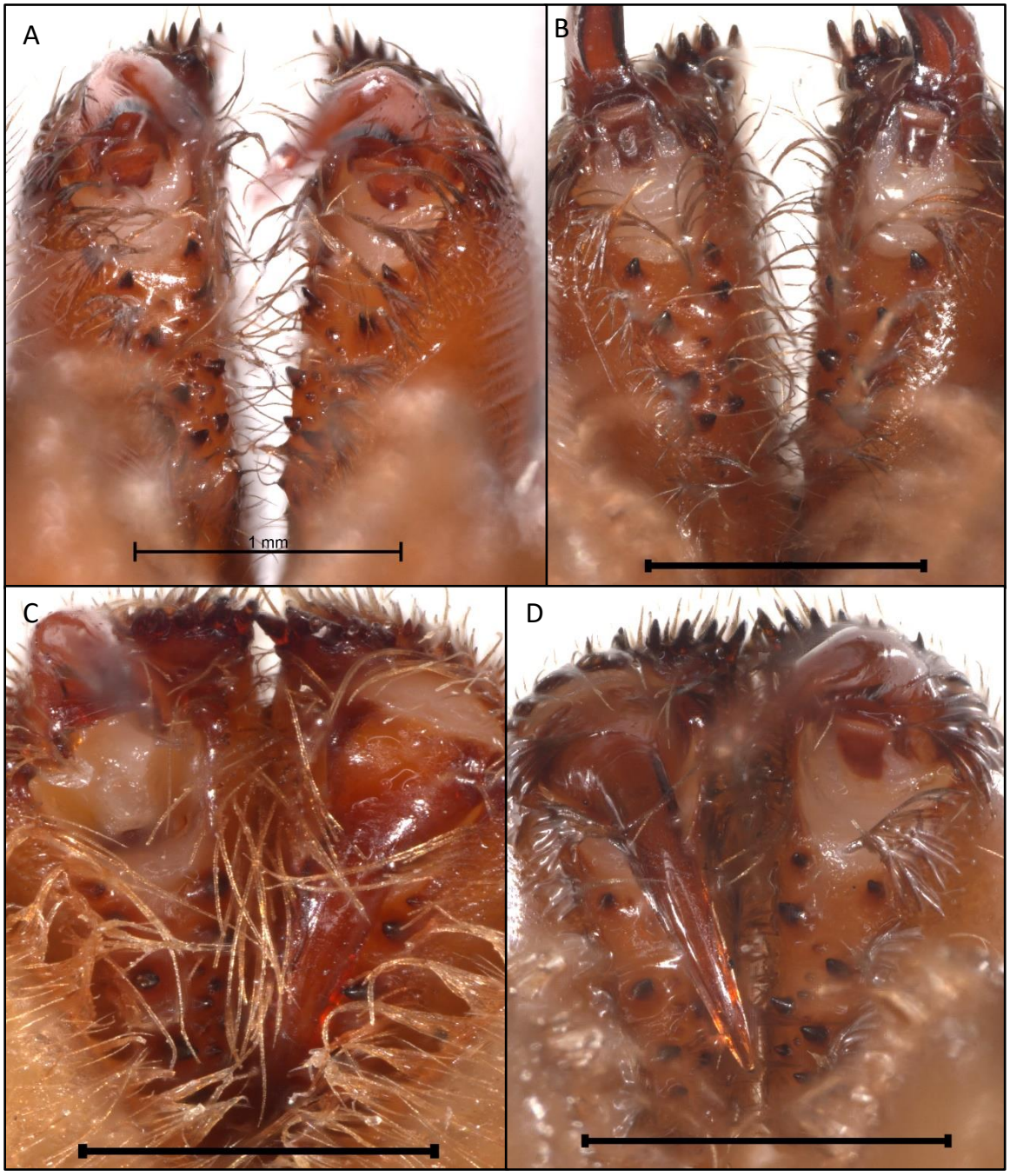


Figure 13. Cheliceral teeth of various male *Stasimopus* species. (A) *Stasimopus finni* **sp. nov.** (NCA 2019/605). (B) *Stasimopus karooensis* **sp. nov.** (SAM-ENW-C007293). (C) *Stasimopus malesociatus* **sp. nov.** (AMGS-5367). (D) *Stasimopus maraisi* (NCA 2019/630). Scale: 1mm.

© University of Pretoria

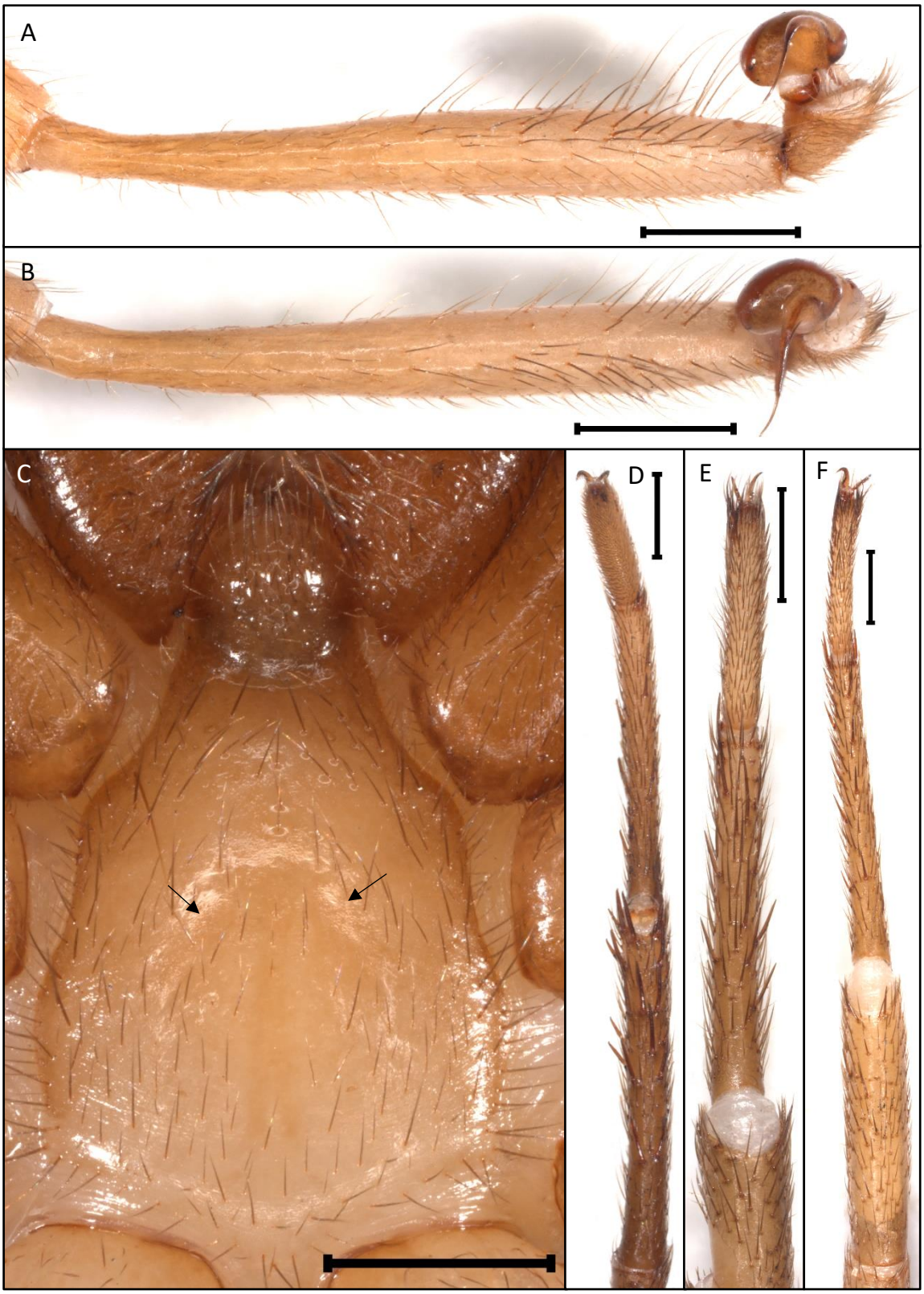


Figure 14. Male of *Stasimopus finni* **sp. nov.** (NCA 2019/605). (A) Pedipalp tibia, bulb, retrolateral aspect. (B) Pedipalp tibia, bulb, prolateral aspect. (C) Sternum with fused labium and visible sigilla (as shown by the arrows). (D) Leg I tibia, metatarsus, tarsus. Ventral aspect. (E) Leg III partial tibia, metatarsus, tarsus. Ventral aspect. (F) Leg IV tibia, metatarsus, tarsus. Ventral aspect. Scale: 1mm.

© University of Pretoria

Distribution and environment notes:

The species is found in the localities indicated in Figure 15. The species is only known from the type locality near Somerset East in the Eastern Cape province. The location was a flat between small hills. The vegetation was dominated by low shrubs and aloe plants. The soil was very hard, chalky and pale. The specimen was found in a short burrow (Approx. 10cm deep).

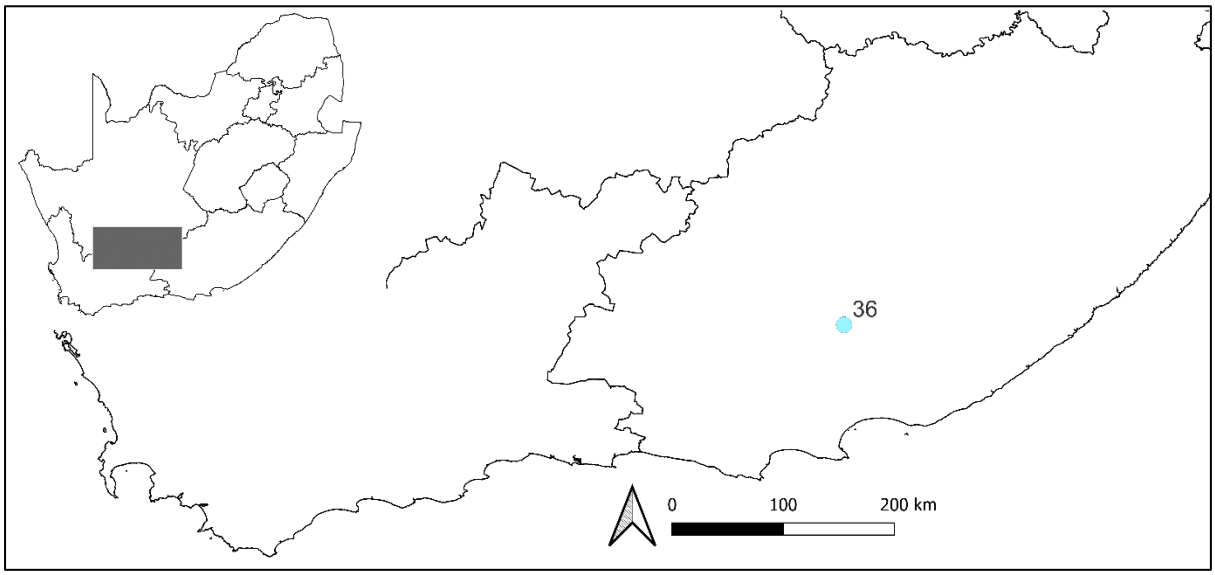


Figure 15. Map of the locality where the *Stasimopus finni* **sp. nov.** specimen was collected. Numbers match the site numbers in Figure 1. Map created in QGIS version 3.4.8-Madeira (2019), available at: http://qgis.osgeo.org.

***Stasimopus hamartia* sp. nov.**

(Figures 2C, 5C&D, 16, 17A, 19, 20, 21, 22A)

Type material: Holotype ♀ SOUTH AFRICA: Western Cape Province, Beaufort West (-31.9265, 22.9042), 20.iv.2017, S. Brandt, C. Sole, E. Engelbrecht and T. Majelantle, (NCA 2017/1852). Allotype ♂ Eastern Cape Province, Willowmore (-32.5015, 23.5935), 14.iv.2017, S. Brandt, C. Sole, E. Engelbrecht and T. Majelantle, (NCA 2017/1891). Paratypes. Western Cape Province, Beaufort West (-32.2535,23.0939), 20.iv.2017, S. Brandt, C. Sole, E. Engelbrecht and T. Majelantle, (1♀ NCA 2017/1849, 1♀ *juv.* NCA 2017/1850); same data, 20.iv.2017, 1♀ *juv.* (NCA 2017/1854); same data, 14.iv.2017, 2♀♀ (NCA 2017/1888, NCA 2017/1889), 2♀♀ *juv.* (NCA 2017/1890, NCA 2017/1892); Western Cape Province, Farm Tulpleegte (-32.6422, 22.6914), 15.v.2018, S. Brandt, C. Sole, E. Engelbrecht and E. Brand, 1♀ (NCA 2019/660), 1♀ *juv.* (NCA 2019/661).

Etymology: The specific epithet is a Greek noun ‘hamartia’ meaning fatal error or flaw. It is so because the allotype specimen when collected was being eaten by an Idiopidae species found in her burrow.

© University of Pretoria

Diagnosis: The females of *S. hamartia* **sp. nov.** are distinguishable from other members of the genus occurring in the Karoo based on the following combination of characters. It is differentiated from *S. astutus*, *S. leipoldti*, *S. maraisi*, *S. patersonae*, *S. schrieneri*, *S. theaei* **sp. nov.**, *S. ignis* **sp. nov.** and *S. teras* **sp. nov.** by the presence of an apical tuft being present on metatarsus III. Further differentiation can be made based on the extent of the spination present on the dorsal surface of metatarsus I. Only *S. hamartia* **sp. nov.**, *S. erythrognathus* and *S. unispinosus* have spines extending half or more of the segment. This species can then be differentiated from *S. erythrognathus* and *S. unispinosus* as these species have less than 15 cheliceral denticles, whereas *S. hamartia* **sp. nov.** has over 20 denticles present. The male of this species is difficult to diagnose due to the state of the allotype, which was found half-eaten by a female idiopid.

Description: Based on the holotype ♀ (NCA 2017/1852) and paratypes 4♀ (NCA 2017/1849, NCA 2017/1888, NCA 2017/1889, NCA 2019/660) and the allotype ♂ (NCA 2017/1891).
Remarks: ♂: The allotype is in poor condition as it was found half-eaten in a female idiopid burrow (Fig 5D). For this reason, many measurements and characters could not be determined.
General: ♀: (Fig 5C) Large bodied spiders, ranging between 20.10 – 31.30 (27.30) total length. ♂: (Fig 5D) Length could not be determined.
Carapace: ♀: Carapace length 8.62 – 14.01 (12.07); width 7.45 – 12.06 (10.88). Reddish orange colouration. Smooth texture, with some pleats in thoracic region. Fovea strongly procurved, between 1.36 – 2.82 (2.09) in length. ♂: Length and width undetermined. Reddish orange colouration, thoracic region with rugose texture. Fovea length undetermined.
Ocelli: ♀: (Fig 2C, 17A) AME diameter 0.25 – 0.36 (0.30), PME diameter 0.27 – 0.30 (0.28), MOQ anterior width 1.81 – 2.92 (2.62), MOQ posterior width 3.05 – 4.80 (4.16); AME-AME 0.72, AME-ALE 0.51, ALE-ALE 2.39, PME-PME 2.51, PME-PLE 0.39, PLE-PLE 3.83. AER slightly procurved, PER almost straight. ♂: Eye measurements could not be taken.
Chelicerae: ♀: (Fig 19C) Two teeth rows present, 3-4 teeth in proventral row, 4 teeth in retroventral row; 16 cuspules in between.
Sternum, labium and maxillae: ♀: (Fig 19A) Sternum length 5.20 – 7.74 (6.78); sternum width 4.25 – 6.99 (6.20). Longitudinally elongated sigilla, distal end 0.47 – 0.95 (0.70) apart, proximal end 1.75 – 3.14 (2.27) apart; labium with 6-11 cuspules present (Fig 19B); maxillae with 8-14 cuspules present. ♂: (Fig 21C) Sternum length 2.73; sternum width undetermined. Sternum shape has shallow impressions of where the coxa are situated. Longitudinally elongated sigilla, distal end 0.43 apart, proximal end 0.93 apart; cuspules on labium absent; maxilla absent.
Abdomen: ♀: Abdomen length 11.48 – 17.29 (15.13); width 7.62 – 12.18 (11.56). Grey colour, two black spots posteriorly situated, closer towards spinnerets, some specimens with larger darker patch

© University of Pretoria

connecting the two dots and extending further towards the spinnerets. ♂: Length and width are undetermined. Dark brown in colour.

Pedipalps: ♀: Total length 16.79; Segment lengths 5.78, 3.75, 3.49, - ,3.79. Spination: spines absent in femur and patella, with sparse setae. Tibia *pl*- 2 tibial spurs, 1 proximal, 1 distal, *do* – small patch of spinules distally extend onto the tarsus. *Rl*- 20-21 spinules along the segment. Tarsus *pl*- 5 large spines on the distal end, *do*- patch of 15-17 spinules, less dense distally, extend $\frac{1}{4}$ - $\frac{1}{5}$ of segment, *rl*- covered in dense spines (20-24). ♂: (Fig 21A, B) Total length not determined; Segment lengths damaged, 6.38, 4.83, - ,5.89. Spines absent. Bulb compact, embolus elongated tapering into sharp point, perpendicular to tibia.

Legs: ♀: Length order: IV, I, III, II. I Total length 24.43; Segment lengths 7.58, 4.75, 4.68, 5.56, 1.86; Spination: spines absent on femur and patella, with sparse setae. Tibia *pl*&*rl* – dense spines extend entire segment, less dense proximally, *do* (Fig 20A)- patch of dense spines distally, extend onto metatarsus, reaches $\frac{1}{8}$ of segment. Metatarsus *pl*&*rl*- dense spines extend entire segment, *do* (Fig 20A) – patch of dense spines extending $\frac{1}{2}$ segment from proximal end, *v*- highly scopulate. Tarsus *pl*&*rl*- dense spines extend entire segment, *v*- highly scopulate. II Total length 21.30; Segment lengths 6.58, 4.49, 3.77, 4.89, 1.58; Spination: spines absent on femur and patella, with sparse setae. Tibia *pl*- dense spines extend $\frac{1}{6}$ of segment from distal end, 2-3 spines proximally, *do* (Fig 20B)- patch of dense spines distally reaching $\frac{1}{8}$ of segment length. *Rl*- dense spines extend entire segment, less dense proximally. Metatarsus and tarsus same as in I (Fig 20B). III Total length 22.63; Segment lengths 6.36, 6.02, 2.09, 5.17, 3.03; Spination: spines absent on femur with sparse setae. Patella *do*/*rl* with 2-3 short spines. Tibia *do* (Fig 20C) – stout red spines dense patch distally, hidden by long setae. Metatarsus *do* (Fig 20C)- 2 rows of stout red spines (14-18 in each), between smaller red spinules, *v*- Terminally 8-9 long spines present (Fig 20E). Tarsus *pl*- dense patch of red spines on the distal $\frac{1}{3}$ of the segment. IV Total length 28.04; Segment lengths 7.14, 5.73, 5.42, 6.87, 2.88; Spination: spines absent on femur with sparse setae. Patella *do*- short dense red spines proximally, less dense distally, interspersed with short black setae. Tibia (Fig 20D) *pl*- 12-13 spines along segment, *do*- dense setae. Metatarsus (Fig 20D) *pl*- 9-10 spines along segment, denser distally, *v*- 5-6 randomly scattered spinules, six spines in a transverse row in the preening comb (Fig 20F). Tarsus *pl*- dense patch of red spines extending distally. ♂: Length order undetermined. I Total length undetermined; Segment lengths -, -, -, 4.63, 1.96; Spination: Metatarsus *v* (Fig 21D) – 25 spines segment. Tarsus *v*- scopulate. II Total length 14.41; Segment lengths 4.35, 2.18, 3.54, 2.9, 1.45; Spination: spines absent on femur. Patella *v*- 4 small thickened setae distally. Tibia *v*- 11 long spines along segment, 2 most distal are thicker. Metatarsus *v*- 23 spines along segment. Tarsus *do*- dense patch of spinules (7-8) distally, *v*- scopulate. III Total length 12.21; Segment lengths 3.41, 2.05, 1.37, 3.36, 2.02; Spination: spines

© University of Pretoria

absent on femur. Patella *pl*- 2-3 spines distally. Tibia *do*- dense patch of spinules (9-10 each) on distal end more *pl&rl*. Metatarsus *pl*- 1 spine, *do*- 9-10 spines along segment, *v*- 4 spines scattered. Tarsus *pl*- 1 spine distally, *v*- scopulate. IV Length order undetermined. I Total length undetermined; Segment lengths -, 2.14, 3.46, 5.01, 2.6; Spination: Patella *do*- dense red spines proximally (extends *rl*). Tibia *pl*- 1 small spine. Metatarsus *v* (Fig 21E)- 5 spines, distal 3 are larger. Tarsus *pl&rl*- 12 small spines along surface, denser distally, *v*- scopulate.

Spermathecae: (Fig 22A) Entire, with inflated terminus, similar to a giraffe's ossicones.

Distribution and environment notes:

The species is found in the localities indicated in Figure 16. The species occurs on the border of the Western and Eastern Cape provinces of South Africa. All the sample locations were flat pans near drainage lines, with typical low to medium height Karoo shrubs. All the soil was hard and compact, except for at site 21 where the soil was softer (this was the most specimen rich site). The burrow trapdoor lids were visible on the surface only at sites 6 and 7. At site 39 several empty *Stasimopus* burrows were excavated, and a pompilid wasp was found in one. One burrow which had a live female specimen in was deep (Approx. 30cm).

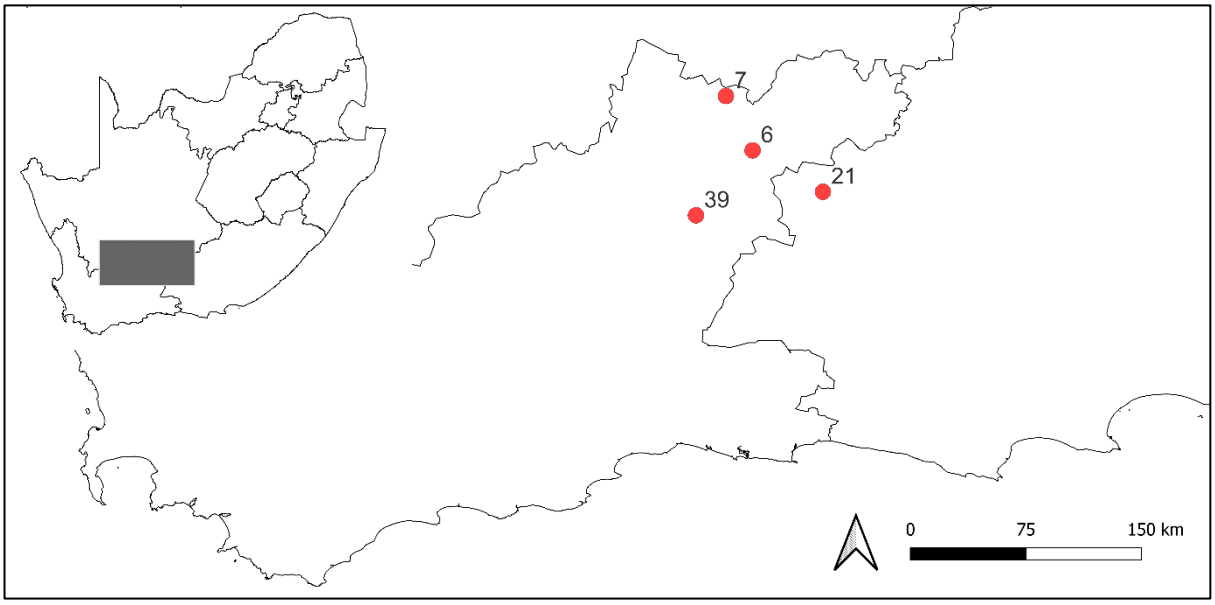


Figure 16. Map of the localities where *Stasimopus hamartia* **sp. nov.** specimens were collected. Numbers match the site numbers in Figure 1. Map created in QGIS version 3.4.8-Madeira (2019), available at: http://qgis.osgeo.org.

© University of Pretoria

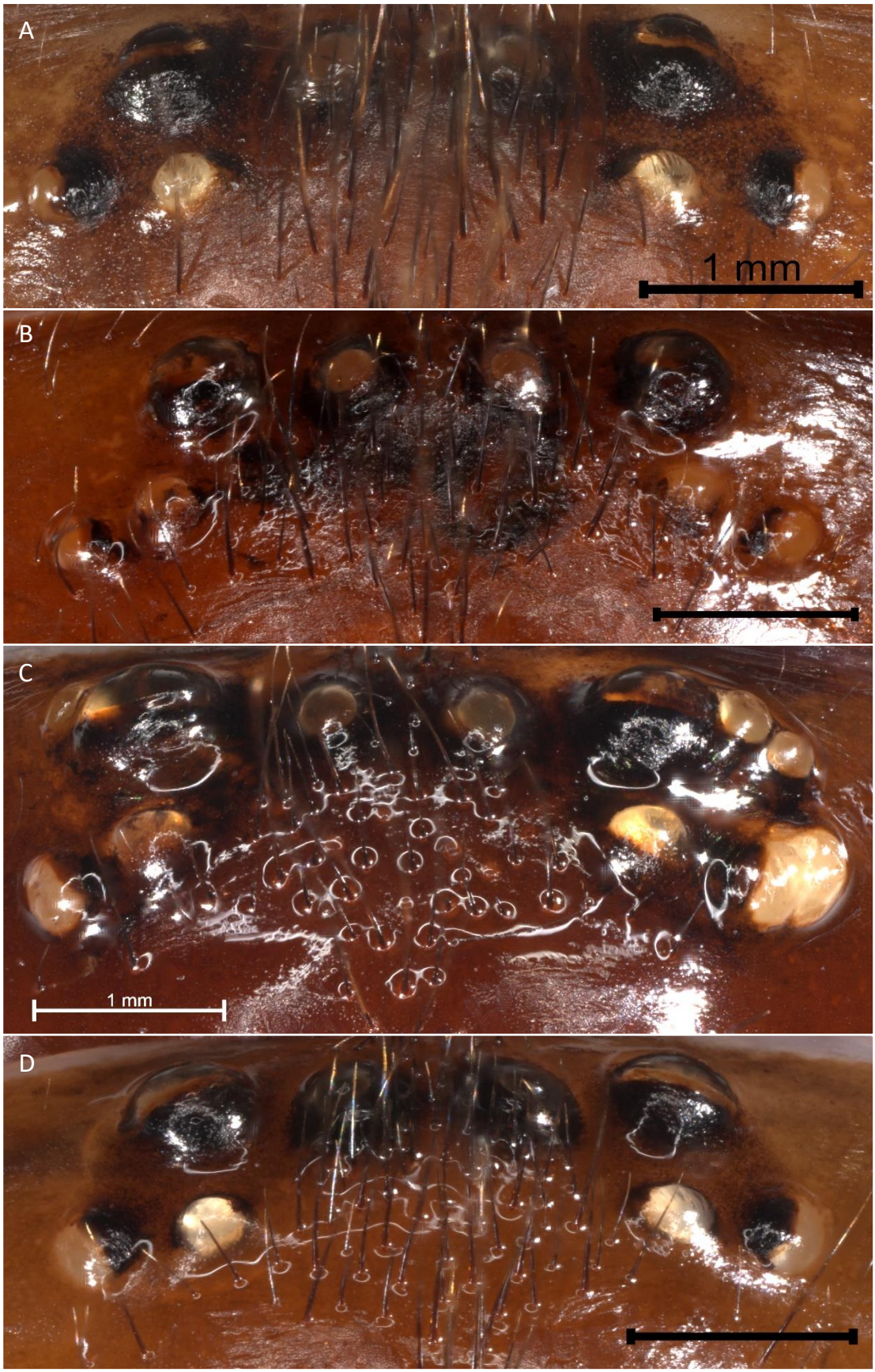


Figure 17. Ocular patterns for the newly described female *Stasimopus* Simon, 1892 species. (A) *S. hamartia* **sp. nov.** (NCA 2017/1852). (B) *S. ignis* **sp. nov.** (NCA 2019/653). (C) *S. teras* **sp. nov.** (NCA 2019/643). (D) *S. theaei* **sp. nov.** (NCA 2019/606). Scale: 1mm.

© University of Pretoria

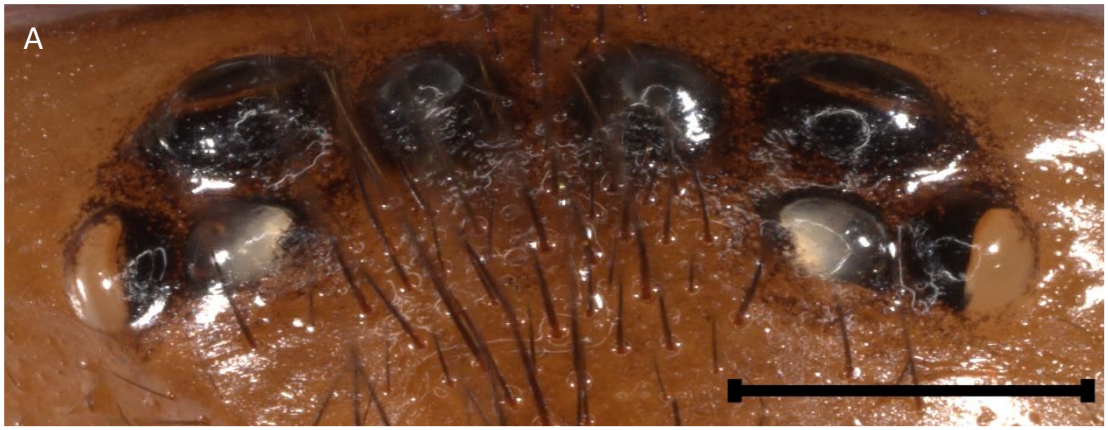


Figure 18. Ocular patterns for the *Stasimopus* Simon, 1892 species. (A) Female of *Stasimopus venterstadensis* **sp. nov.** (NCA 2019/610). Scale: 1mm.

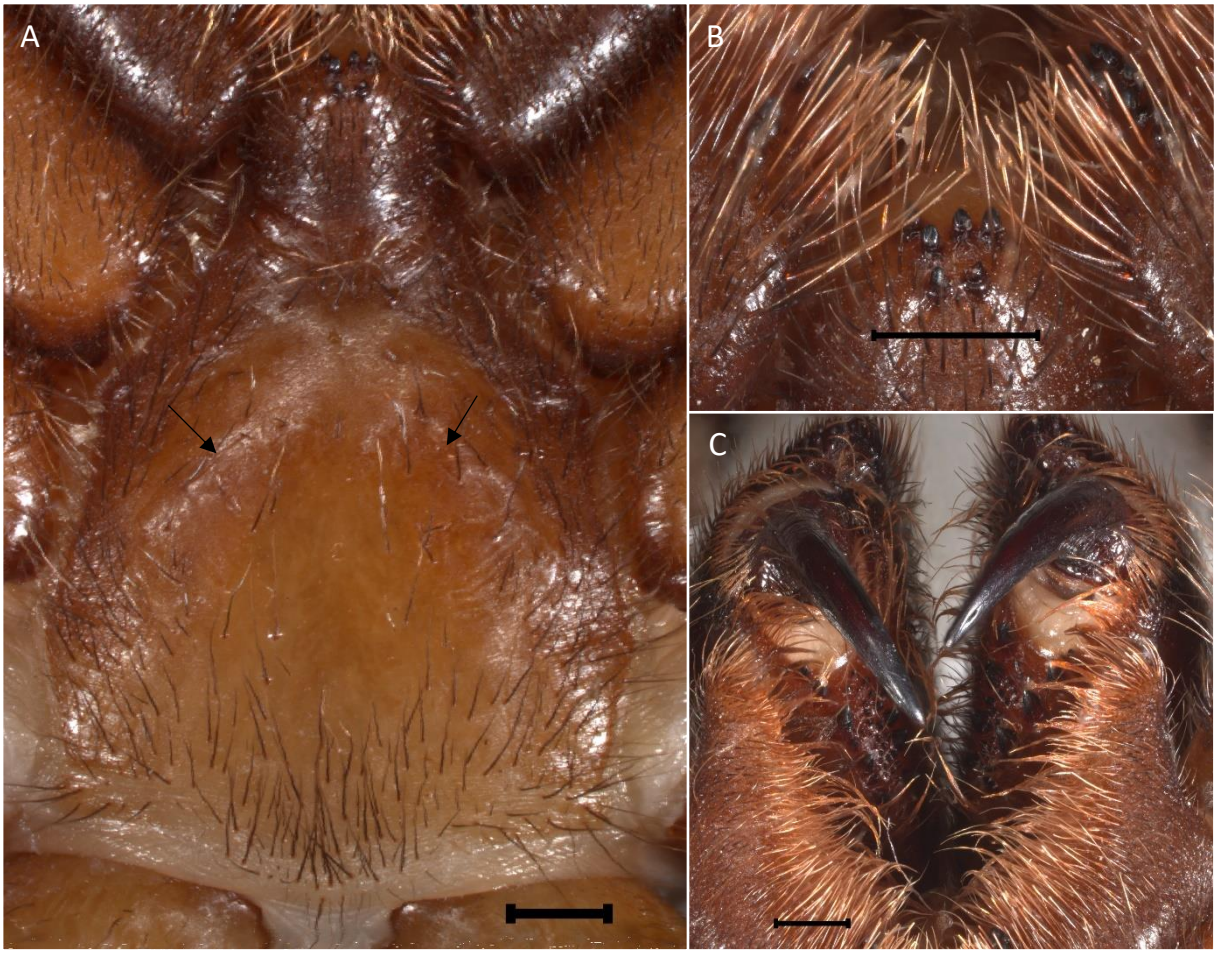


Figure 19. Female of *Stasimopus hamartia* **sp. nov.** (NCA 2017/1852). (A) Sternum with fused labium and visible sigilla (as shown by the arrows). (B) Labium teeth. (C) Fangs with cheliceral teeth. Scale: 1mm.

© University of Pretoria



Figure 20. Female of *Stasimopus hamartia* **sp. nov.** (NCA 2017/1852). (A) Leg I tibia, metatarsus, tarsus. Dorsal aspect. (B) Leg II tibia, metatarsus, tarsus. Dorsal aspect. (C) Leg III tibia, metatarsus, tarsus. Dorsal aspect. (D). Leg IV partial tibia, metatarsus, tarsus. Prolateral aspect. (E) Leg III metatarsal tuft. Ventral aspect. (F) Leg IV metatarsus preening comb. Scale: 1mm.

© University of Pretoria

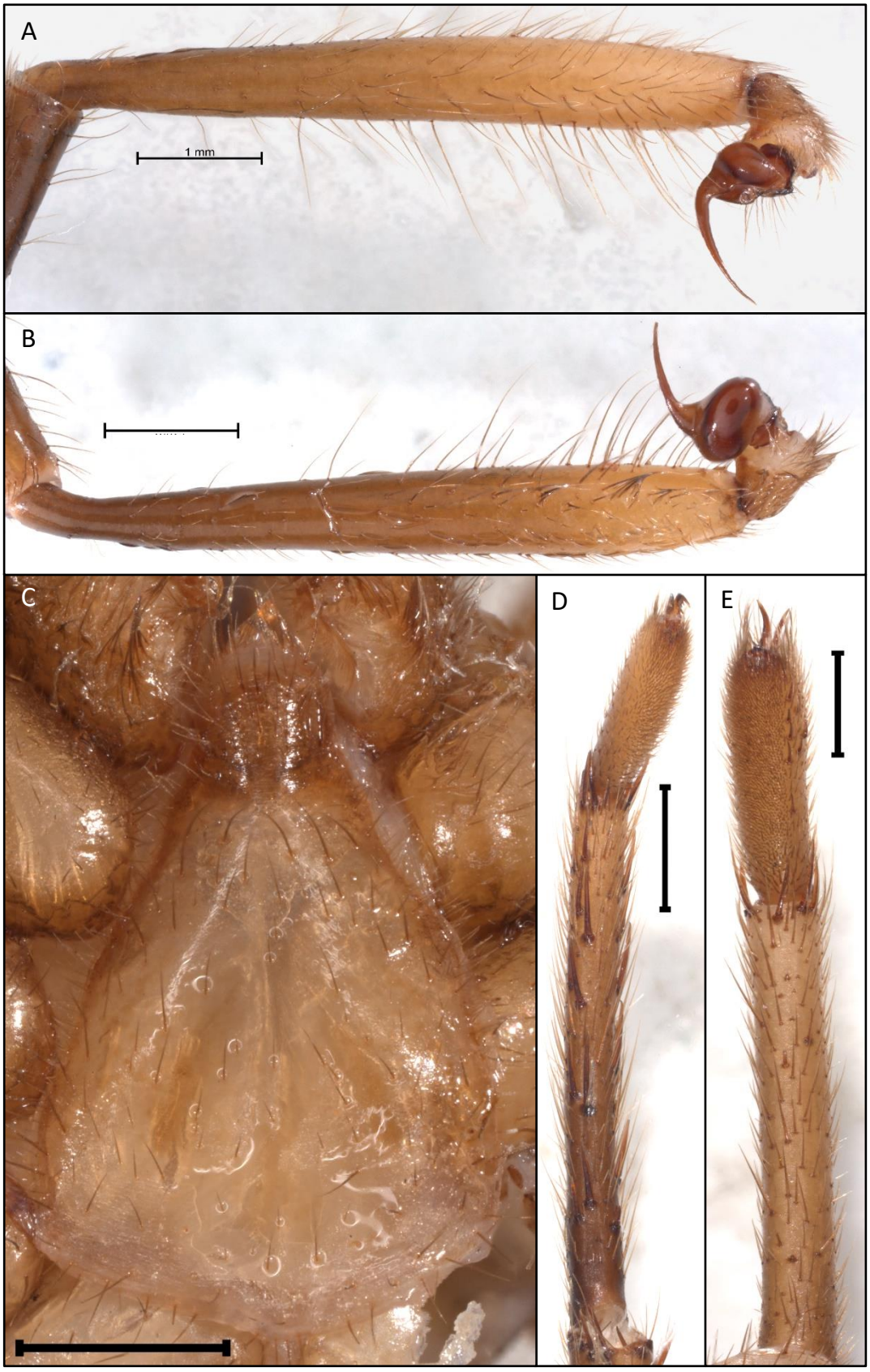


Figure 21. Male of *Stasimopus hamartia* **sp. nov.** (NCA 2017/1891). (A) Pedipalp tibia, bulb, retrolateral aspect. (B) Pedipalp tibia, bulb, prolateral aspect. (C) Sternum with fused labium and visible sigilla (as shown by the arrows). (D). Leg I metatarsus, tarsus. Ventral aspect. (E) Leg IV metatarsus, tarsus. Ventral aspect. Scale: 1mm.

© University of Pretoria

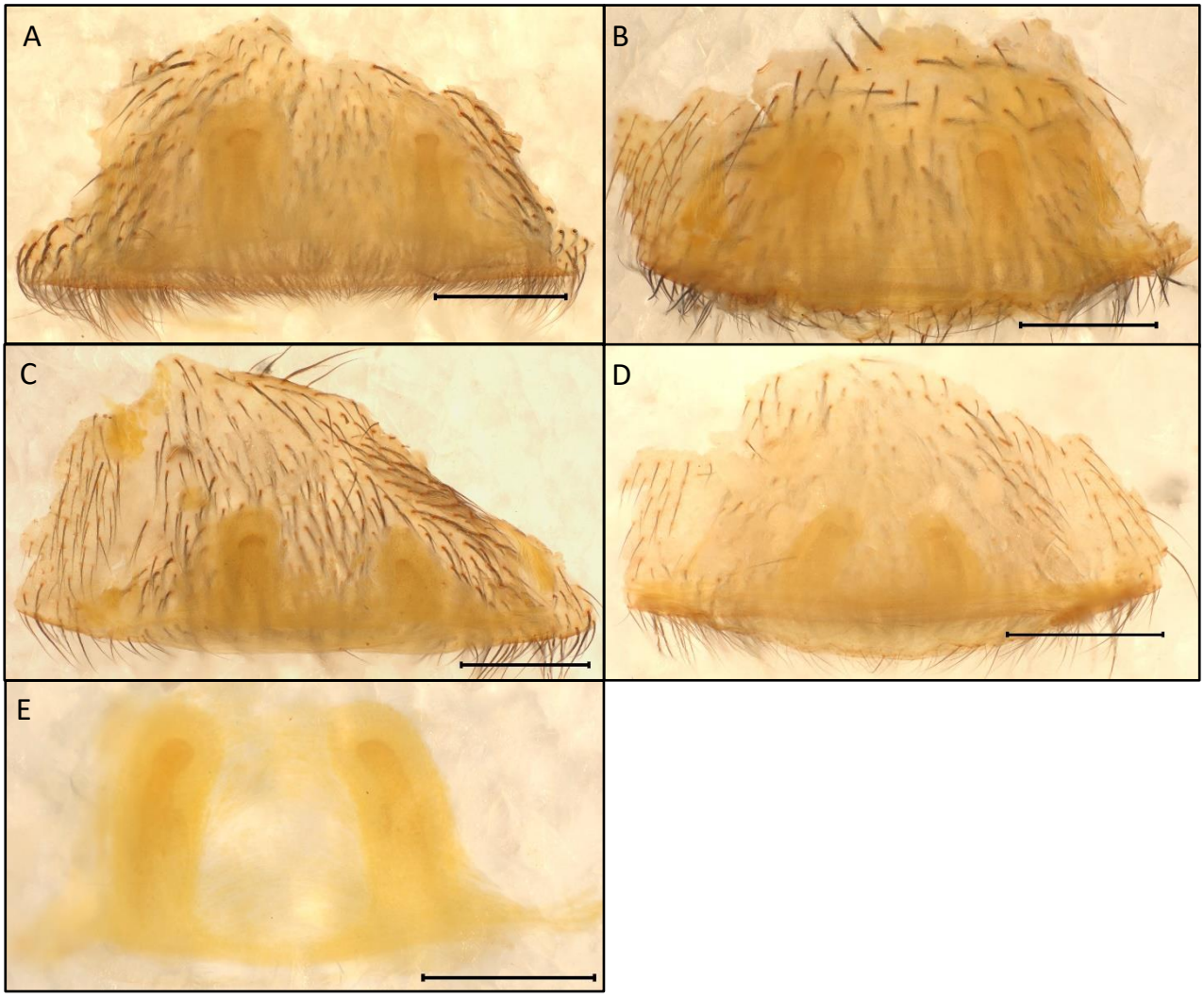


Figure 22. Spermathecae for the newly described female *Stasimopus* Simon, 1892 species. (A) *S. hamartia* **sp. nov.** (NCA 2017/1852). (B) *S. ignis* **sp. nov.** (NCA 2019/653). (C) *S. theaei* **sp. nov.** (NCA 2019/606). (D) *S. venterstadensis* **sp. nov.** (NCA 2019/610). (E) Spermathecae of *S. tera* **sp. nov.** (NCA 2019/643). The spermathecae detached from the vulva, and the vulva is thus not apparent. Scale: 1mm.

***Stasimopus ignis* sp. nov.**

(Figures 2D, 3D, 6A&B, 11C, 17B, 22B, 23, 24, 25, 26)

Type material: Holotype ♂ SOUTH AFRICA: Northern Cape Province, Richmond (-31.4412, 23.9851), 22.v.2018, S. Brandt, C. Sole, E. Engelbrecht and E. Brand, (NCA 2019/642). Allotype ♀. Hanover (-31.0439, 24.4689), 24.v.2018, S. Brandt, C. Sole, E. Engelbrecht and E. Brand, (NCA 2019/653).

Etymology: The specific epithet is a Latin noun ‘ignis’ taken in apposition meaning fire/flame. This is in reference to both the colouration of the female of the species, as well as an allusion to the increasing fire frequency (historically rare) in the Nama Karoo which is likely due to climate change.

© University of Pretoria

Diagnosis: The males of *S. ignis* **sp. nov.** are distinguishable from other members of the genus occurring in the Karoo based on the following combination of characters. It is differentiated from *S. astutus*, *S. erythrognathus*, *S. malesociatus* **sp. nov.**, *S. patersonae*, *S. steynsbergensis*, *S. karooensis* **sp. nov.** and *S. mandelai* based on the pedipalp not reaching the tarsus of leg I. It is further distinguished from *S. palpiger* by the pedipalp which is longer than leg I, that is not the case with *S. ignis* **sp. nov.** The species can be differentiated from the rest of the species (*S. schrieneri*, *S. dylani* **sp. nov.**, *S. finni* **sp. nov.** and *S. maraisi*) as *S. ignis* **sp. nov.** only has 3 cheliceral teeth in the inner cheliceral row whereas the other species have 4 or more.

The females of *S. ignis* **sp. nov.** are distinguishable from other members of the genus occurring in the Karoo based on the following combination of characters. The preening comb on metatarsus IV has 8 or more spines in a transverse row, only shared or exceeded by *S. artifex*, *S. theaei* **sp. nov.** and *S. teras* **sp. nov.** The species can be differentiated from *S. artifex* ($< \frac{1}{10}$ segment) and *S. theaei* **sp. nov.** ($> \frac{1}{2}$ segment) by the extent of spination on metatarsus I, extending less than $\frac{1}{6}$ the segment. Can be separated from *S. teras* **sp. nov.** by the extent of spination on the tarsus of the pedipalp (*S. teras* **sp. nov.** is less spinose).

Description: Based on the holotype ♀ (NCA 2019/642) and the allotype ♂ (NCA 2019/653).
Remarks: ♂: male specimen abdomen is severely dehydrated, making abdomen and total length measurements challenging.
General: ♂: (Fig 6B) Medium bodied spiders, 8.29 total length. ♀: (Fig 6A) total length 22.54.
Carapace: ♂: Carapace length 4.73; width 4.30. Reddish brown colouration, thoracic region with rugose texture. Fovea strongly procurved, 0.88 in length. ♀: Carapace length 9.98; width 9.55. Reddish orange colouration, smooth texture, with some pleats in thoracic region. Fovea procurved, 1.99 in length.
Ocelli: ♂: (Fig 3D, 11C) AME diameter 0.20, PME diameter 0.13, MOQ anterior width 1.21, MOQ posterior width 1.80; AME-AME 0.20, AME-ALE 0.19, ALE-ALE 0.98, PME-PME 1.02, PME-PLE 0.19, PLE-PLE 1.62. AER and PER slightly recurved. ♀: (Fig 2D, 17B). AME diameter 0.31, PME diameter 0.26, MOQ anterior width 2.79, MOQ posterior width 4.27; AME-AME 0.62, AME-ALE 0.61, ALE-ALE 2.29, PME-PME 2.55, PME-PLE 0.42, PLE-PLE 3.66. AER slightly procurved, PER strongly recurved.
Chelicerae: ♂: (Fig 25D) Two teeth rows present, 3-4 teeth in proventral row, 3 in retroventral row; no cuspules in between. ♀: (Fig 23C) Two teeth rows present, 4 teeth in proventral row and 4 in retroventral row; 10-11 cuspules in between.

© University of Pretoria

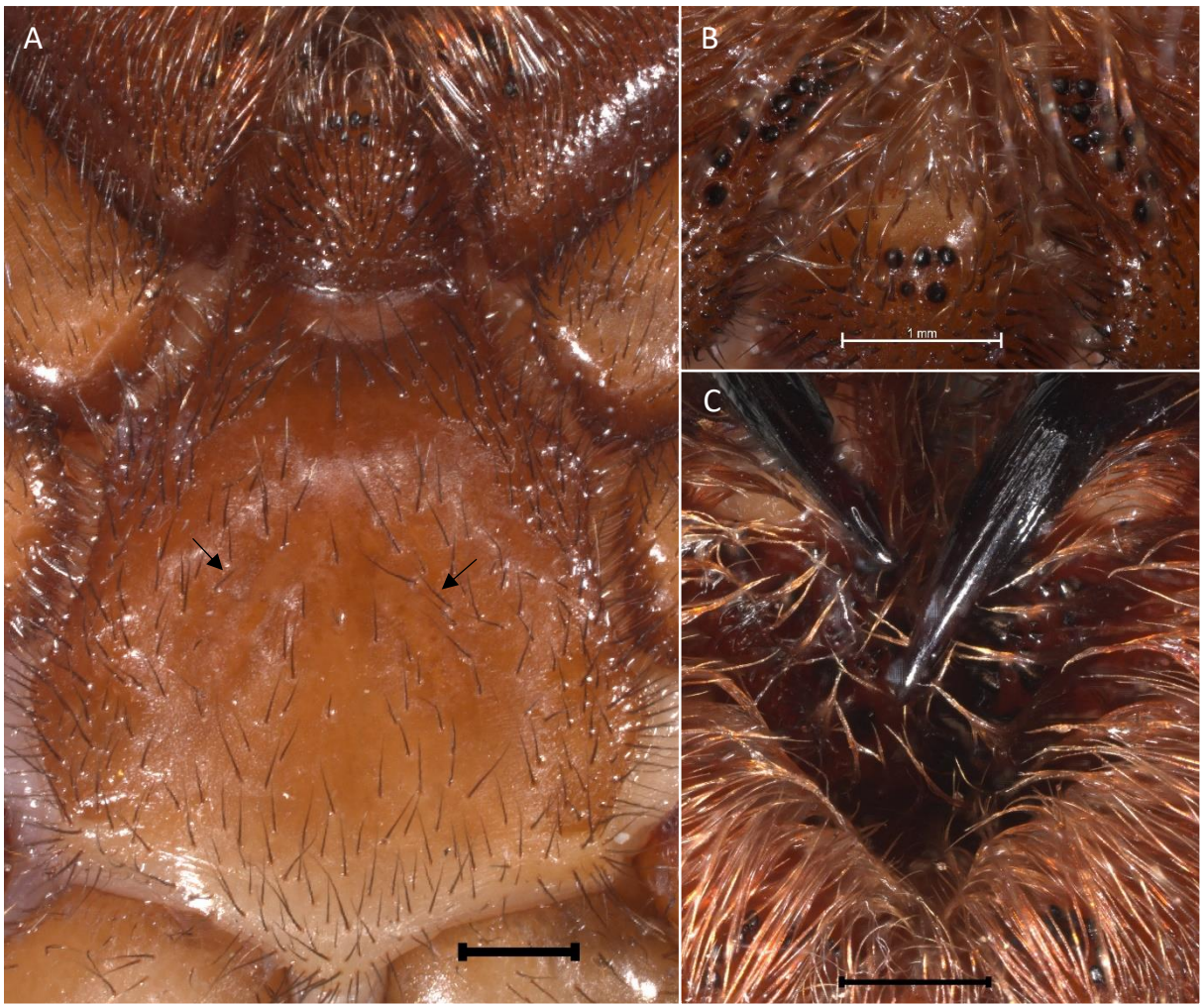


Figure 23. Female of *Stasimopus ignis* **sp. nov.** (NCA 2019/653). (A) Sternum with fused labium and visible sigilla (as shown by the arrows). (B) Labium teeth. (C) Fangs with cheliceral teeth. Scale: 1mm.

Sternum, labium and maxillae: ♂: (Fig 25E) Sternum length 2.22; sternum width 2.17. Sternum shape has no impressions of where the coxa are situated. Sigilla in the shape of a fused arrow, distal end fused, proximal end 0.89 apart. Cuspules on labium absent; cuspules on maxilla absent. ♀: (Fig 23A) Sternum length 6.02; sternum width 5.68. Longitudinally elongated sigilla, distal end 0.71 apart, proximal end 1.82 apart. Labium with 5 cuspules present (Fig 25B), maxillae with 13-16 cuspules present.

Abdomen: ♂: Abdomen length 3.56; width 3.18. Mottled grey colouration. ♀: Abdomen length 12.56; width 11.28. Grey/brown colouration, with one large dark spot near the carapace followed by a smaller one, two small black markings terminally.

Pedipalps: ♂: (Fig 25A-C) Total length 16.22; Segment lengths, 4.55, 1.48, 5.16, - ,5.05. Spines absent. Bulb small, embolus with broad base, tapering distally away from tibia. ♀: Total length 12.65; Segment lengths 4.25, 2.44, 2.76, - ,3.20. Spination: spines absent on femur, with sparse setae. Patella *pl*- 3-4 long thin spines. Tibia *pl*- 2-3 tibial spurs, 1 proximal and 1 distal, *do*- small patch of spinules

© University of Pretoria

distally extends onto tarsus (7-9 spinules), *rl*- 23 spinules along segment. Tarsus *pl*- 12-13 large spines distally, *do*- patch of 15-17 spinules, less dense distally, extend $\frac{1}{4}-\frac{1}{5}$ segment, *rl*- covered in dense spines (>30).

Legs: ♂: Length order: I, IV, II, III. I Total length 17.18; Segment lengths 4.88, 2.40, 3.98, 3.82, 2.10; Spination: spines absent on femur, with sparse setae. Patella *v*- 2 long spines distally. Tibia (Fig 25F) *v*- 8-10 large spines. Metatarsus (Fig 25F) *v*- 18-19 large spines, extending *pl*&*rl*. Tarsus (Fig 25F) *v*- highly scopulate. II Total length 14.57; Segment lengths 3.92, 2.12, 3.42, 3.32, 1.79; Spination: spines absent on femur, with sparse setae. Patella *v*- 2 small thickened setae distally. Tibia *v*- 12 long spines along segment. Metatarsus *v* – 18 spines along segment, extend *pl*&*rl*. Tarsus *pl*- 1 small spine, *rl*- 3 small red spines, *v*- scopulate. III Total length 11.82; Segment lengths 3.10, 1.99, 1.41, 3.30, 2.03; Spination: spines absent on femur, with sparse setae. Patella *pl*- 17 spines, 9 distally situated, *do*- 8 spines, extend *rl*. Tibia *do*- dense patch of spinules (12) distally. Metatarsus *do*- 8 spines along segment (4 distal), *rl*- 2 spines, *v* (Fig 25G)- 4 spines scattered. Tarsus *rl*- 4-5 small spines, *v* (Fig 25G) – scopulate, 7 spines more distally situated. IV Total length 16.87; Segment lengths 4.70, 2.20, 3.19, 4.61, 2.18; Spination: spines absent on femur, with sparse setae. Patella *do*- dense red spines proximally, interspersed with black setae. Tibia *pl*- 2 small spines. Metatarsus *pl*- 3 spines (one large distally), *rl*- 1 large spine distally, *v* (Fig 25H)- 7 spines. Tarsus *v*- 12 spines scattered, almost *pl*, *v*- Scopulate. ♀: Length order: IV, III, I, II. I Total length 18.05; Segment lengths 5.93, 2.88, 3.61, 3.91, 1.72; Spination: spines absent on femur and patella, with sparse setae. Tibia *pl*- small spines extend $\frac{1}{2}$ distally along segment, *do* (Fig 24A)- patch of dense spines distally, extend approx. $\frac{1}{6}$ segment, *rl*- small spines extend entire segment, less dense proximally. Metatarsus *pl*&*rl*- dense spines extend entire segment, *do* (Fig 24A)- patch of dense spines extend $\frac{1}{4}$ segment length from the proximal end, *v*- highly scopulate. Tarsus *pl*&*rl*- dense spines extend entire segment, *v*- highly scopulate. II Total length 17.58; Segment lengths 5.33, 3.12, 3.66, 3.69, 1.79; Spination, follows that of leg I (Fig 24B). III Total length 19.00; Segment lengths 5.10, 4.18, 2.87, 4.16, 2.71; Spination: spines absent on femur, with sparse setae. Patella *pl*- 8-9 red spinules with rows of black setae. Tibia *do* (Fig 24C)- dense patch of stout red spines distally situated, hidden by long setae. Metatarsus *do* (Fig 24C)- 2 rows of stout red spines (26-30 in each), between smaller red spinules. Tarsus *pl*- >15 spines along surface, dense distally
covered in setae). IV Total length 21.20; Segment lengths 5.12, 3.76, 4.40, 5.25, 2.39; Spination: spines absent on femur, with sparse setae. Patella *pl*- 3-4 long spines. Tibia *pl* (Fig 24D)- 4-8 spines along segment, *do*- dense setae. Metatarsus *pl* (Fig 24D)- 22 spines along segment, *v*- 5-6 (spines in transverse row in the preening comb (Fig 24E). Tarsus *pl* (Fig 24D)- dense patch of red spines extending distally (>25 spines), covered in setae.

© University of Pretoria



Figure 24. Female of *Stasimopus ignis* **sp. nov.** (NCA 2019/653). (A) Leg I tibia, metatarsus, tarsus. Dorsal aspect. (B) Leg II tibia, metatarsus, tarsus. Dorsal aspect. (C) Leg III tibia, metatarsus, tarsus. Dorsal aspect. (D). Leg IV partial tibia, metatarsus, tarsus. Prolateral aspect. (E) Leg IV metatarsus preening comb. Scale: 1mm.

© University of Pretoria

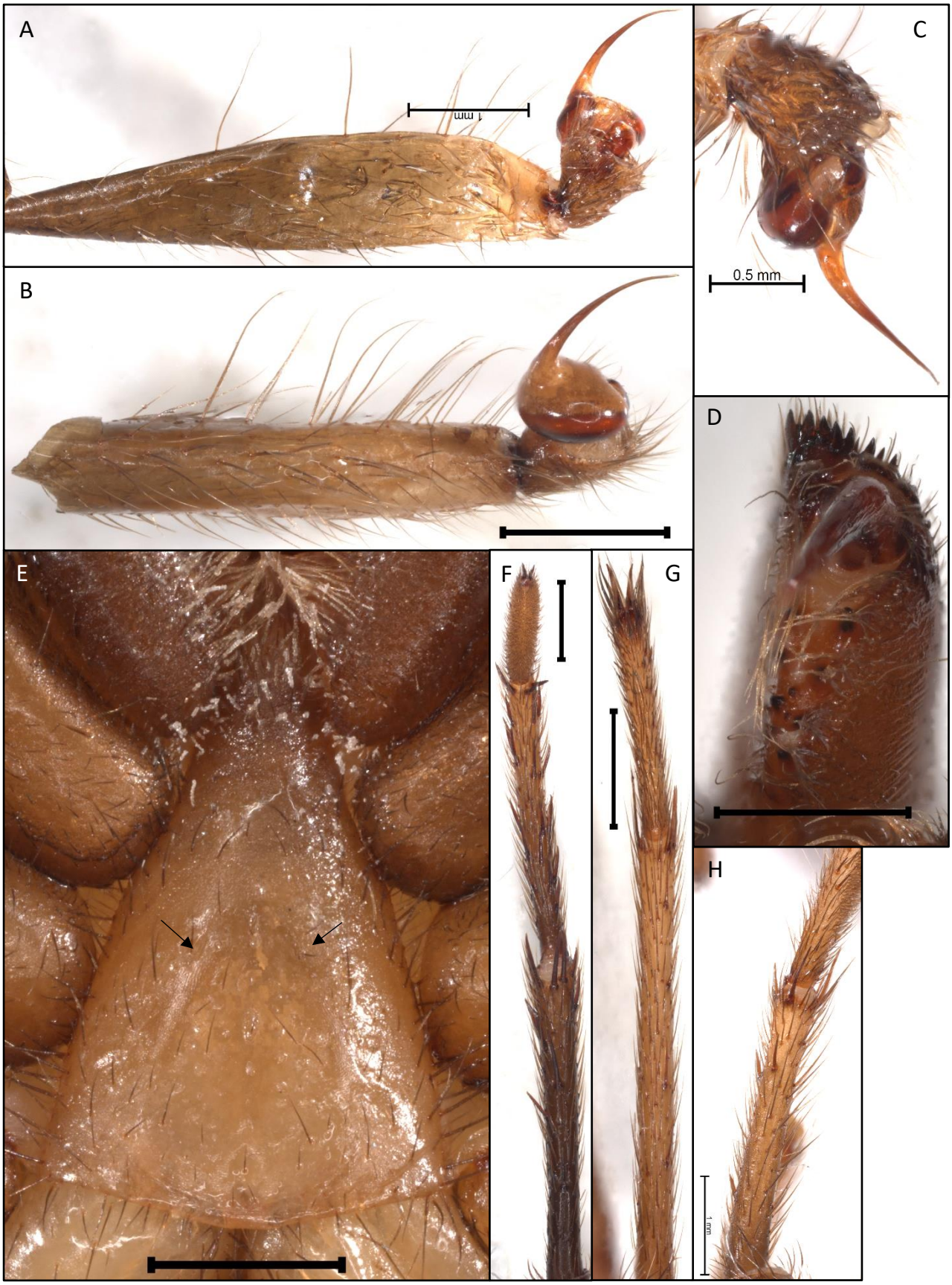


Figure 25. Male of *Stasimopus ignis* **sp. nov.** (NCA 2019/642). (A) Pedipalp tibia, bulb, retrolateral aspect. (B) Pedipalp tibia, bulb, prolateral aspect. (C) Pedipalpal bulb, ventral aspect. (D) Cheliceral teeth. (E) Sternum with fused labium and visible sigilla (as shown by the arrows). (F) Leg I tibia, metatarsus, tarsus. Ventral aspect. (G) Leg III metatarsus, tarsus. Ventral aspect. (H) Leg IV metatarsus. Ventral aspect. Scale: 1mm.

© University of Pretoria

Spermathecae: (Fig 22B) Entire, with terminus as broad as base.

Distribution and environment notes:

The species is found in the localities indicated in Figure 26. The species is only known from two localities in the Northern Cape province. Female found on a gentle slope in loamy soil which had a hard subsoil layer. The vegetation was dominated by typical Karoo low shrubs and grasses. The male was found under a door mat at the Toonbothasfontein farm.

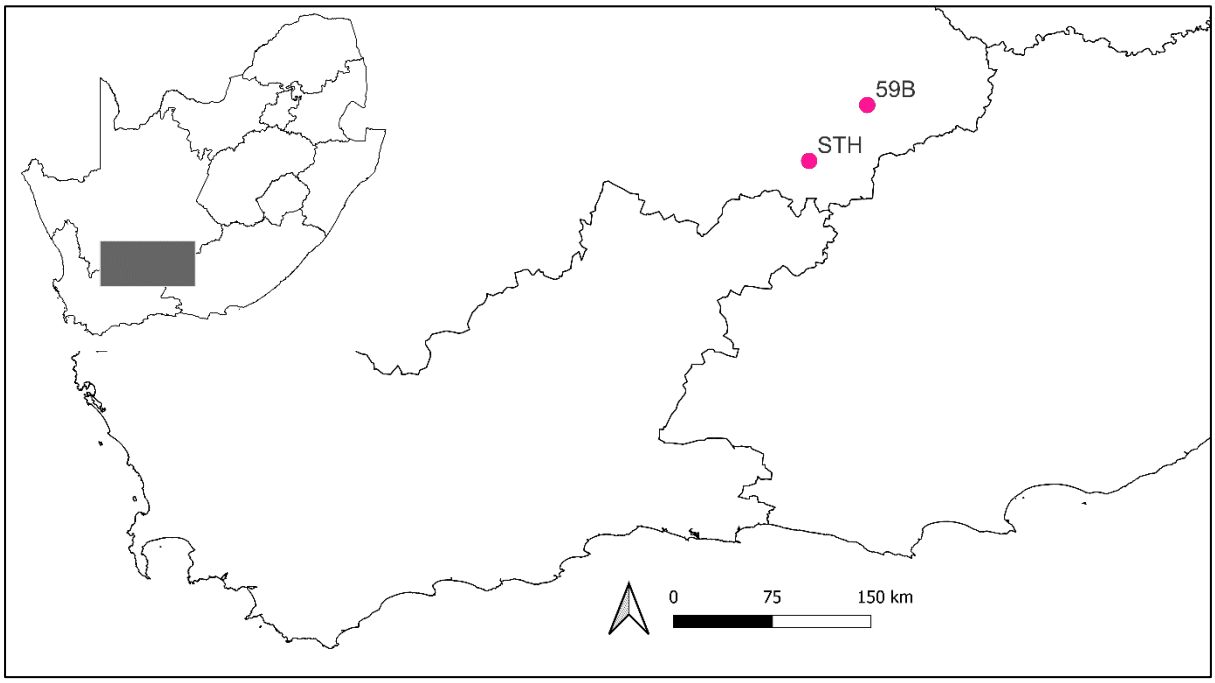


Figure 26. Map of the localities where *Stasimopus ignis* **sp. nov.** specimens were collected. Numbers match the site numbers in Figure 1. Map created in QGIS version 3.4.8-Madeira (2019), available at: http://qgis.osgeo.org.

***Stasimopus karooensis* sp. nov.**

(Figs 3E, 6C, 11D, 13B, 27, 28)

Type material: Holotype ♂ SOUTH AFRICA: Eastern Cape Province, Pearston, Camdeboo Game Reserve (-32.5339, 25.2378), 09.iv.2010-26.vi.2010, S. van Noort, (SAM-ENW-C007293). Paratypes. Same data, 1♂ (SAM-ENW-C007746). Jansenville (-32.8772, 24.4952), 17.vii.2015, I. Engelbrecht and D. Kambas, 1♂ (NCA 2019/616).

Etymology: The specific species name refers to the large distribution of the species within the Karoo. It is an acknowledgement to the Karoo BioGaps project, which provided some funding and the sampling organisation for this project.

© University of Pretoria

Diagnosis: The males of *S. karooensis* **sp. nov.** are distinguishable from other members of the genus occurring in the Karoo based on the following combination of characters. It is differentiated from *S. schrieneri*, *S. dylani* **sp. nov.**, *S. ignis* **sp. nov.**, *S. finni* **sp. nov.**, *S. maraisi* and *S. palpiger* by the pedipalp being shorter in relation to leg I (only reaching metatarsus I). It is distinguished from *S. astutus*, *S. erythrognathus*, *S. malesociatus* **sp. nov.** and *S. patersonae* as the pedipalp is longer in relation to leg I (extending past the tibia). Lastly, it is differentiated from *S. mandelai* and *S. steynsbergensis* by being more spinose on tarsus IV.

Description: Based on the holotype ♂ (SAM-ENW-C007293) and paratypes 2♂ (SAM-ENW-C007746, NCA 2019/616).
Remarks: ♀: Known only from males.
General: ♂: (Fig 6C) Medium bodied spiders, ranging between 8.34 – 9.29 (8.34) total length.
Carapace: ♂: Carapace length 3.99 – 4.98 (3.99); width 3.62 – 4.35 (3.62). Dark red colouration, thoracic region with rugose texture. Fovea procurved, between 0.78 – 0.94 (0.78) in length.
Ocelli: ♂: (Fig 3E, 11D) AME diameter 0.20 – 0.22 (0.20), PME diameter 0.12 – 0.15 (0.15), MOQ anterior width 1.08 – 1.23 (1.08), MOQ posterior width 1.29 -1.69 (1.29); AME-AME 0.18, AME-ALE 0.10, ALE-ALE 0.84, PME-PME 0.15, PME-PLE 0.78, PLE-PLE 1.20; AER almost straight, PER slightly recurved.
Chelicerae: ♂: (Fig 13B) Two teeth rows present, 4 teeth in proventral row, 4 in retroventral row. Number of cuspules could not be determined as the fangs could not be opened without damaging an old specimen.
Sternum, labium and maxillae: ♂: (Fig 27C) Sternum length 2.56 – 2.76 (2.73); sternum width 2.12 – 2.54 (2.12). Sternum shape has distinct impressions of where the coxa are situated. Sigilla in the shape of a fused arrow, distal end fused, proximal ends 0.68 – 1.14 (0.68) apart; cuspules on labium absent; maxilla absent.
Abdomen: ♂: Abdomen length 4.31 – 4.36 (4.36); width 2.78 – 3.07 (2.78). Mottled grey colouration.
Pedipalps: ♂: (Fig 27A, B) Total length 16.60; Segment lengths 4.64, 4.68, 3.14, -, 4.14. Spination: spines absent. Bulb compact and flattened. Embolus elongated tapering to sharp point, extending perpendicular from tibia.
Legs: ♂: Length order: I, IV, II, III. I Total length 19.32; Segment lengths 5.83, 2.66, 4.21, 4.61, 2.02; Spination: spines absent on femur and patella, with sparse setae. Tibia *v*- 13 large spines extending *pl&rl*. Metatarsus *v* (Fig 27D)- 10-12 large spines. Tarsus *v*- scopulate. II Total length 16.82; Segment lengths 5.16, 2.30, 3.70, 3.87, 1.81; Spination: spines absent on femur, with sparse setae. Patella *pl*- 1 large spine. Tibia *v*- 13-14 large spines extend *pl&rl*. Metatarsus *v*- 14-15 large spines. Tarsus *v*- scopulate. III Total length 12.12; Segment lengths 3.25, 1.75, 1.45, 3.52, 2.16;

© University of Pretoria

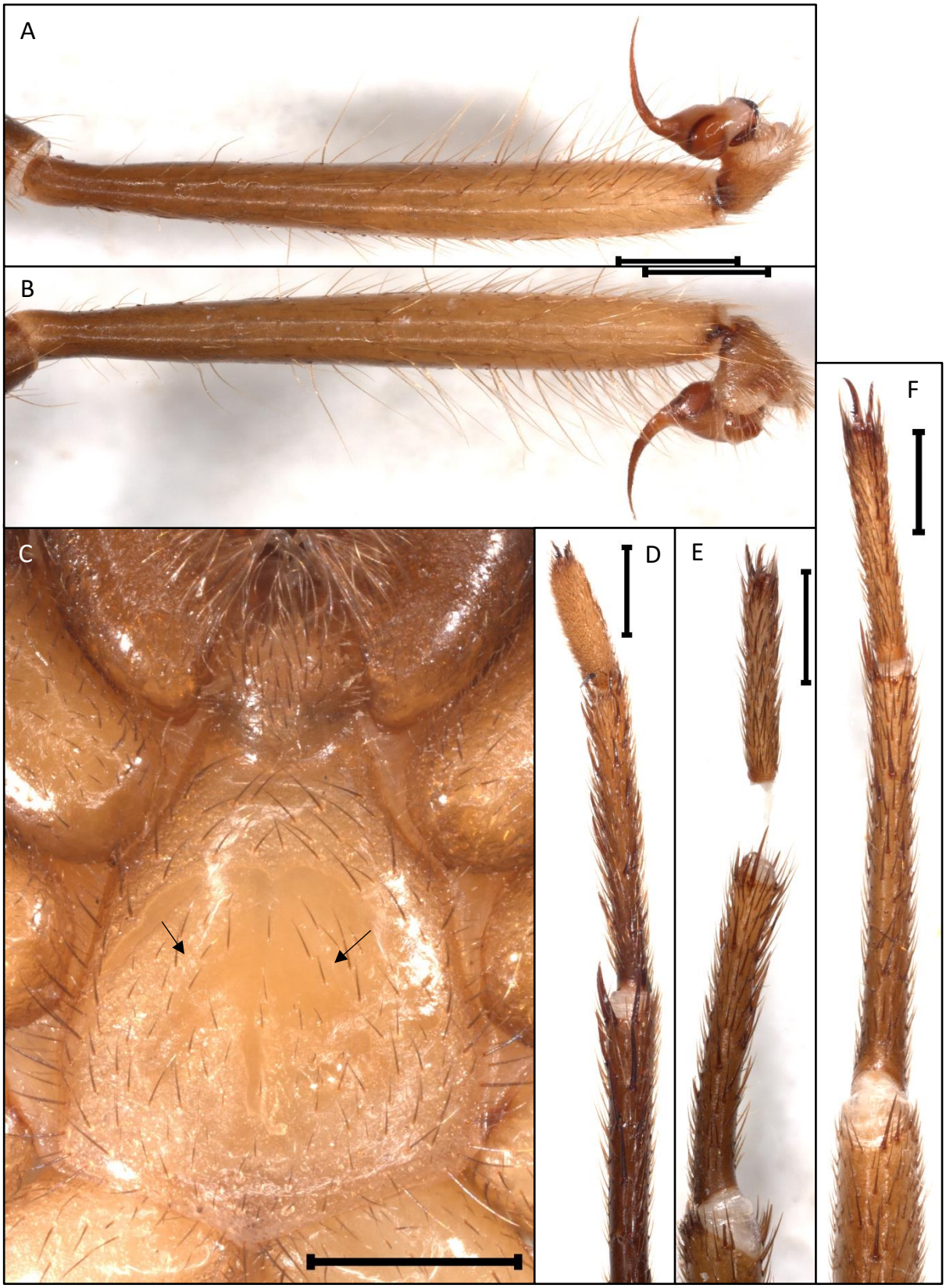


Figure 27. Male of *Stasimopus karooensis* **sp. nov.** (SAM-ENW-C007293). (A) Pedipalp tibia, bulb, retrolateral aspect. (B) Pedipalp tibia, bulb, prolateral aspect. (C) Sternum with fused labium and visible sigilla (as shown by the arrows). (D) Leg I partial tibia, metatarsus, tarsus. Ventral aspect. (E) Leg III metatarsus, tarsus. Ventral aspect. (F) Leg IV metatarsus, tarsus. Ventral aspect. Scale: 1mm.

© University of Pretoria

Spination: spines absent on femur, with sparse setae. Patella *do*- 4 red spines. Tibia *pl&rl*- dense patches of short spines distally (9-10 in each patch). Metatarsus (Fig 27E) *pl&rl*- dense spines along each surface (15-17 in each patch), extend *do&v*. Tarsus *pl&rl*- small spines along each surface (10-11 in each patch), denser distally, *v*- scopulate. IV Total length 18.85; Segment lengths 4.50, 2.39, 3.67, 5.34, 2.96; Spination: spines absent on femur, with sparse setae. Patella *do*- short dense red spines proximally, less dense distally, interspersed with fine black setae. Tibia *pl*- 5 spines. Metatarsus *pl*- 10 spines, *v* (Fig 27F)- 1 spine. Tarsus *pl&rl*- 15-16 spines along each surface, denser distally, *v* (Fig 27F)- scopulate.

Distribution and environment notes:

The species is found in the localities indicated in Figure 28. The species is only known from two localities in the Eastern Cape province. These two localities are a great distance apart. The SAMC specimens were collected in Camdeboo Escarpment Thicket vegetation in yellow pan traps. The ELK specimens were all collected while crossing a quite road after heavy rains.

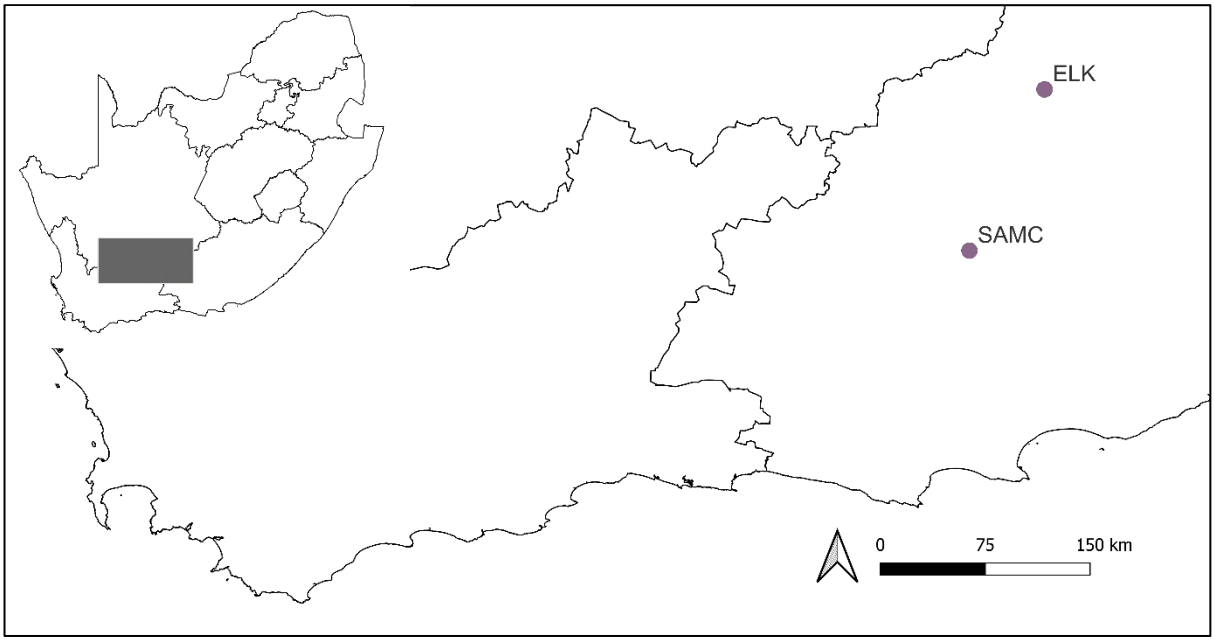


Figure 28. Map of the localities where *Stasimopus karooensis* **sp. nov.** specimens were collected. Numbers match the site numbers in Figure 1. Map created in QGIS version 3.4.8-Madeira (2019), available at: http://qgis.osgeo.org.

© University of Pretoria

***Stasimopus malesociatus* sp. nov.**

(Figures 6D, 12A, 13C, 29, 30)

Type material: Holotype ♂ SOUTH AFRICA: Northern Cape Province, Victoria West, no collection date, H. James, (AMGS-5367).

Etymology: The specific epithet is a Latin adjective 'malè sociatus' taken in apposition meaning mismatched. This is in reference to this specimen being incorrectly assigned as the allotype to the previously described species *Stasimopus maraisi*.

Diagnosis: The males of *S. malesociatus* **sp. nov.** are distinguishable from other members of the genus occurring in the Karoo based on the following combination of characters. It is differentiated from *S. astutus, S. erythrognathus, S. schrieneri, S. finni* **sp. nov.** and *S. maraisi* by the AME being the largest eye. It is distinguished from *S. ignis* as PLE is the smallest eye. The species is distinguished from *S. patersonae, S. karooensis* **sp. nov.**, *S. dylani* **sp. nov.** and *S. palpiger* as *S. malesociatus* **sp. nov.** only has 3 cheliceral teeth in the inner row, whereas the others have 4. The metatarsus of legs I and II are less spinous than *S. steynsbergensis.*

Description: ♂: Originally described in Hewitt 1927 pg. 425-426. Additional description is given below.
Remarks: The specimen is in poor condition with various limbs severed or damaged. The spination patterns may be inaccurate due to the removal of a hard clay-like substance.
General: ♂: (Fig 6D) Medium bodied spider, 9.09 total length.
Carapace: ♂: Carapace length 4.93; width 4.61. Reddish orange colouration, thoracic region with rugose texture. Fovea procurved, 0.77 in length.
Ocelli: ♂: (Fig 12A) AME diameter 0.23, PME diameter 0.13, MOQ anterior width 1.21, MOQ posterior width 1.68; AME-AME 0.20, AME-ALE 0.12, ALE-ALE 0.87, PME-PME 0.77, PME-PLE 0.16, PLE-PLE 1.29; AER slightly recurved, PER recurved.
Chelicerae: ♂: (Fig 13C) Two teeth rows present, 3 teeth in proventral row, 4 in retroventral row; 4-5 cuspules in between.
Sternum, labium and maxillae: ♂: (Fig 29D) Sternum length 2.77; sternum width 2.65. Sternum shape has distinct impressions of where the coxa are situated. Sigilla in the shape of a fused arrow, distal end fused, proximal ends 1.0 apart; cuspules on labium absent; maxilla absent.
Abdomen: ♂: Abdomen length 4.16; width 3.48. Mottled brownish red colouration.
Pedipalps: ♂: (Figs 29A-C) Total length 13.48; Segment lengths 1.39, 4.37, 3.18, -, 4.54. Spination: spines absent. Bulb elliptical, embolus with broad base, tapering into sharp point, curving distally.

© University of Pretoria

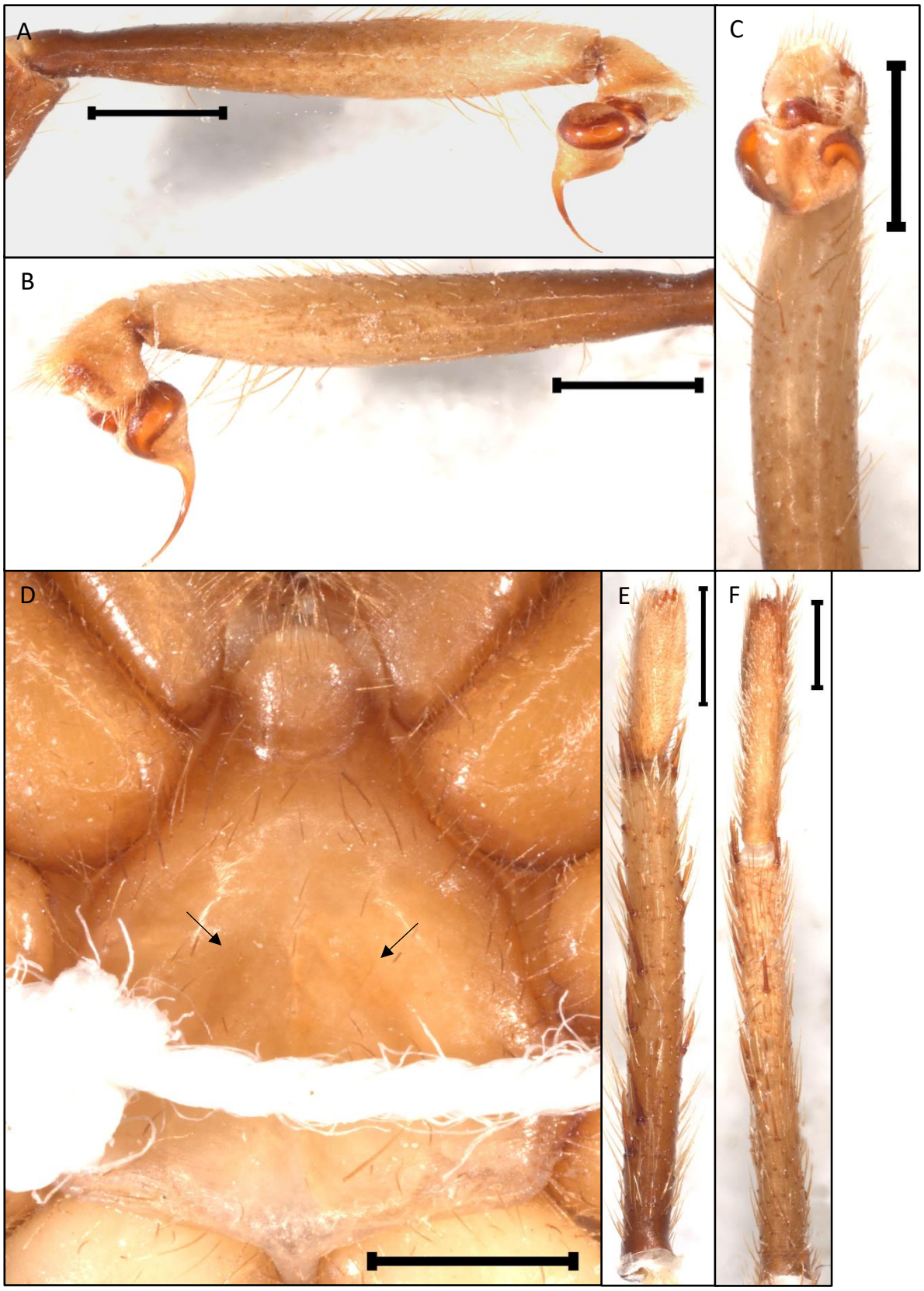


Figure 29. Male of *Stasimopus malesociatus* **sp. nov.** (AMGS-5367). (A) Pedipalp tibia, bulb, retrolateral aspect. (B) Pedipalp tibia, bulb, prolateral aspect. (C) Pedipalpal bulb, ventral aspect. (D) Sternum with fused labium and visible sigilla (as shown by the arrows). (E) Leg I tibia, metatarsus, tarsus. Ventral aspect. (F) Leg IV metatarsus. Ventral aspect. Scale: 1mm.

© University of Pretoria

Legs: ♂: Length order: undetermined. I Total length undetermined; Segment lengths -, -, -, 4.78, 1.98; Spination: spines absent on femur, with sparse setae. Metatarsus *v* (Fig 29E)- 13 large spines. Tarsus *v*- scopulate. II Total length 18.31; Segment lengths 5.63, 2.55, 3.96, 4.15, 2.02; Spination: spines absent on femur, with sparse setae. Patella *v*- 1 large spine. Tibia *v*- 12-14 large spines. Metatarsus *v*- 8 spines. Tarsus *v*- scopulate. III Total length undetermined; Segment lengths 3.81, 2.00, 1.78, -, -; Spination: spines absent on femur, with sparse setae. Patella *do*- damaged, 8 red spines, extend *pl*, *v*- 1 spine. Tibia *pl&rl*- dense patches of short red spines distally (7-9 in each patch), *v*- 3 thin spines. IV Total length 20.68; Segment lengths 5.06, 2.69, 4.26, 5.81, 2.87; Spination: spines absent on femur, with sparse setae. Patella *do*- short dense red spines proximally (Approx. 50-60), less dense distally, interspersed with fine black setae. Tibia *pl*/*v* (Fig 29F)- 5 spines. Metatarsus *v* (Fig 29F)- 9 spines. Tarsus *pl* (Fig 29F)- 11 spines along surface.

Distribution and environment notes:

The species is found in the locality indicated in Figure 30. The species is only known from the type locality near Victoria West in the Northern Cape province. The original description does not describe the area where the specimen was collected.

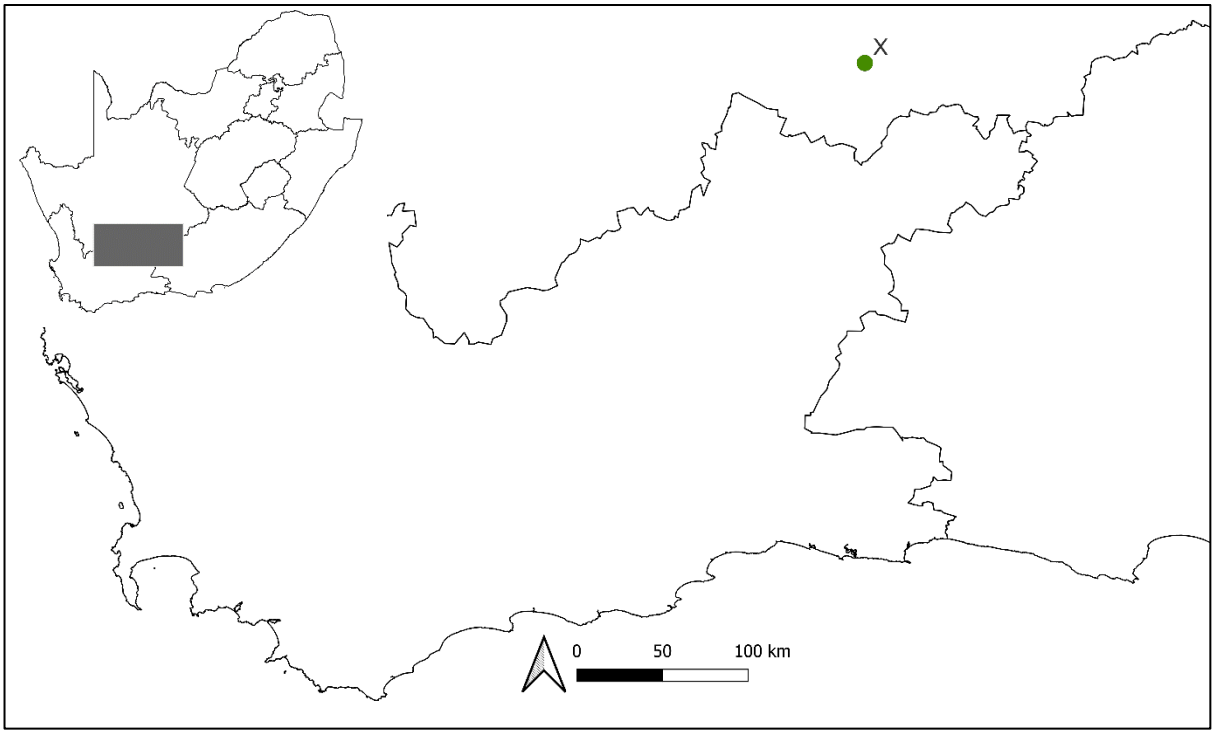


Figure 30. Map of the locality where the *Stasimopus malesociatus* **sp. nov.** specimen was collected. Map created in QGIS version 3.4.8-Madeira (2019), available at: http://qgis.osgeo.org.

© University of Pretoria

***Stasimopus teras* sp. nov.**
(Figs 7A, 17C, 22E, 31, 32, 33)

Type material: Holotype ♀ SOUTH AFRICA: Northern Cape Province, Victoria West (-31.4965, 23.5597), 22.v.2018, S. Brandt, C. Sole, E. Engelbrecht and E. Brand, (NCA 2019/643).

Etymology: The specific epithet is a Greek noun 'teras' taken in apposition meaning monster or marvel. This is in reference to the extreme eye deformity of the type specimen. It is also a homage to the field of teratology which is the "study of marvels and monstrosities".

Diagnosis: The authors acknowledge that the type specimen being used to describe the species is deformed, but despite this we believe this to be a valid species. The other characters and the genetic evidence (clear genetic distance from all other species) are overwhelming to support this deduction. The females of *S. teras* **sp. nov.** are distinguishable from other members of the genus occurring in the Karoo based on the following combination of characters. The preening comb on metatarsus IV has 8 or more spines in a transverse row, only shared or exceeded by *S. artifex, S. theaei* **sp. nov.** and *S. ignis* **sp. nov.** The species can be differentiated from *S. artifex* (< 1/10 segment) and *S. theaei* **sp. nov.** (>1/2 segment) by the extent of spination on metatarsus I, extending less than 1/6 the segment. Can be separated from S. *ignis* **sp. nov.** by the extent of spination on the tarsus of the pedipalp (*S. teras* **sp. nov.** is less spinose).

Description: Based on the holotype ♀ (NCA 2019/643).
Remarks: ♀: Severe eye deformity present, thus many eye measurements were not taken. For more information, please see Mitchell *et al.* (2020). ♂: Known only from the type female.
General: ♀: (Fig 7A) Medium bodied spider, 23.20 total length.
Carapace: ♀: Carapace length 9.16; width 9.27. Reddish orange colouration, smooth texture, with pleats in thoracic region. Fovea strongly procurved, 2.29 in length.
Ocelli: ♀: (Fig 17C) AME diameter 0.29, PME diameter 0.42; AME-AME 0.55, AME-ALE 0.52, ALE-ALE 2.11, PME-PME 2.19, PME-PLE 0.40, PLE-PLE 3.59. AER procurved, PER strongly recurved.
Chelicerae: ♀: (Fig 31C) Two teeth rows present, 4 teeth in proventral row, 5 teeth in retroventral row; 11-12 cuspules in between which vary in sizes.
Sternum, labium and maxillae: ♀: (Fig 31A) Sternum length 5.70; sternum width 5.44. Sigilla indistinct. Labium (Fig 31B) with 5 cuspules present, maxillae with 12-15 cuspules present.
Abdomen: ♀: Abdomen length 14.04; width 9.57. Greyish brown colouration, with long vertical band marking along the ventral surface, less apparent towards the spinnerets.
Pedipalps: ♀: Total length 12.38; Segment lengths 4.10, 2.67, 2.68, -, 2.94. Spination: spines absent on femur, with sparse setae. Patella *pl-* 2-3 long thin spines. Tibia *pl-* 3 tibial spurs, *do-* small patch of

© University of Pretoria

spinules distally extend onto tarsus with 3-4 spines, *rl*- 8-10 spinules along segment. Tarsus *pl*- 10-11 long spines, *do*- patch of 12-13 spinules, less dense distally, extend $\frac{1}{4}$ - $\frac{1}{5}$ of segment, *rl*- covered in dense spines (22-25), difficult to see distally due to dense setae.

Legs: ♀: Length order: IV, I, II, III. I Total length 16.67; Segment lengths 4.74, 3.39, 3.39, 3.62, 1.52; Spination: spines absent on femur and patella, with sparse setae. Tibia *pl*&*rl*- spinules extend entire segment, less dense proximally, *do* (Fig 31D)- distal dense patch of spines, reach $\frac{1}{5}$ of segment length, continued on metatarsus. Metatarsus *pl*&*rl*- dense spinules along entire segment, *do* (Fig 31D)- patch of dense spines proximally, covering approx. $\frac{1}{6}$ of segment, *v*- scopulate. Tarsus *pl*&*rl*- dense spinules along entire segment, *v*- scopulate. II Total length 16.07; Segment lengths 4.98, 3.24, 2.96, 3.45, 1.44; Spination: spines absent on femur and patella, with sparse setae. Tibia *pl*&*rl*- spinules extend entire segment, less dense proximally, *do*- distally dense patch of spines, reach $\frac{1}{4}$ of segment, continues on metatarsus. Metatarsus and tarsus have same spination as leg I. III Total length 15.99; Segment lengths 4.52, 3.89, 1.39, 4.07, 2.12; Spination: spines absent on femur, with sparse setae. Patella *pl*- 8 spinules interspersed with thick setae, *do*- 5 spinules. Tibia *do* (Fig 31E)- stout red spines dense distally, covered in long setae (extending *pl*&*rl*), *rl*- 3 spinules proximally. Metatarsus *do* (Fig 31E)- 2 rows of stout red spines, 17-21 in each, with small red spinules between. Tarsus *pl*- 11-12 large red spines extend from distal tip to half segment. IV Total length 19.54; Segment lengths 5.05, 3.79, 3.82, 4.88, 1.99; Spination: spines absent on femur, with sparse setae. Patella *do*- short dense red spines proximally, less dense distally, interspersed with stout black setae. Tibia *pl*- many spines extending under the dorsal setae, *do*- very dense setae cover randomly scattered spinules. Metatarsus *pl* (Fig 32A)- 9-13 spines denser distally, *v*- 9-10 spines in a transverse row (preening comb) (Fig 32B). Tarsus *pl* (Fig 32A)- 15 short spines, denser distally, *rl*- 4-5 spines distally.

Spermathecae: (Fig 22E) Entire, with terminus gradually curving inwards, spermathecae equal width entire length.

© University of Pretoria



Figure 31. Female of *Stasimopus teras* **sp. nov.** (NCA 2019/643). (A) Sternum with fused labium and visible sigilla (as shown by the arrows). (B) Labium teeth. (C) Fangs with cheliceral teeth. (D) Leg I tibia, metatarsus, tarsus. Dorsal aspect. (E) Leg III tibia, metatarsus, tarsus. Dorsal aspect. Scale: 1mm.

© University of Pretoria

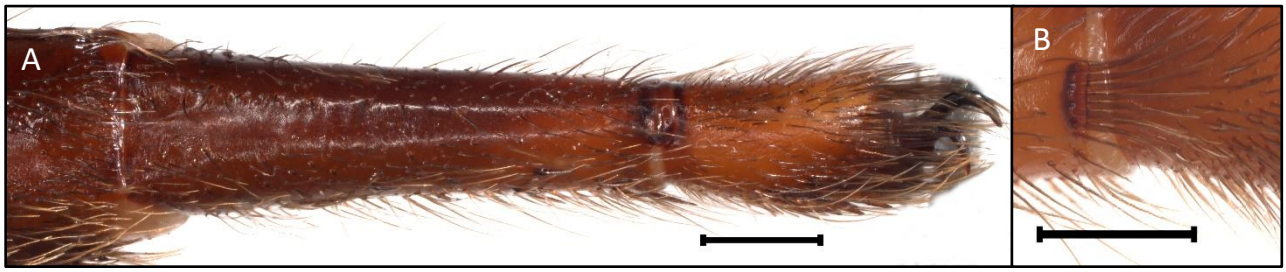


Figure 32. Female of *Stasimopus teras* **sp. nov.** (NCA 2019/643) (A). Leg IV partial tibia, metatarsus, tarsus. Prolateral aspect. (B) Leg IV metatarsus preening comb. Scale: 1mm.

Distribution and environment notes:

The species is found in the localities indicated in Figure 33. The species is only known from the type locality near Victoria West in the Northern Cape province. The site where the specimen was found was under powerlines on a flat plain. The vegetation was dominated by typical Karoo low to medium shrubs with some grass patches. The soil was grey with a russet-coloured surface layer which was slightly cracked. The burrow lid was clearly visible.

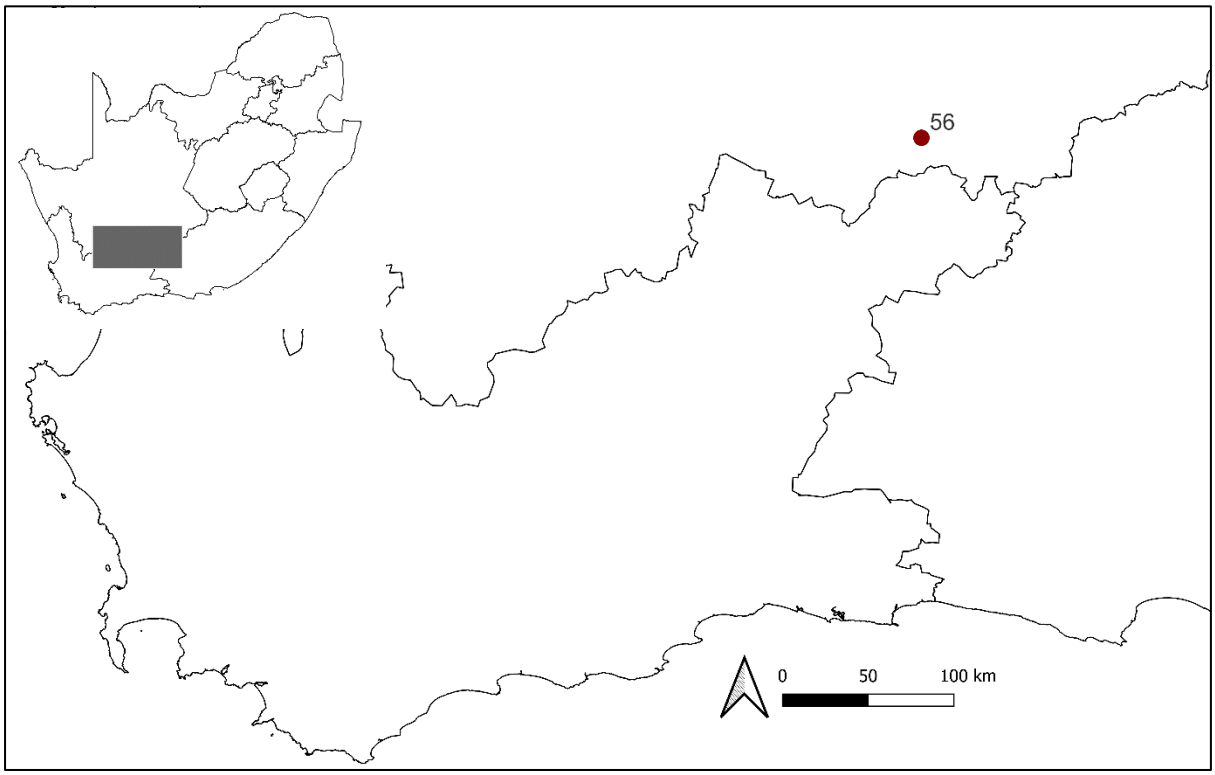


Figure 33. Map of the locality where the *Stasimopus teras* **sp. nov.** specimen was collected. Numbers match the site numbers in Figure 1. Map created in QGIS version 3.4.8-Madeira (2019), available at: http://qgis.osgeo.org.

© University of Pretoria

***Stasimopus theaei* sp. nov.**

(Figures 2H, 7B, 17D, 22C, 34, 35, 36)

Type material: Holotype ♀ SOUTH AFRICA: Eastern Cape Province, Somerset East (-32.9386, 25.6612), 14.v.2018, S. Brandt, C. Sole, E. Engelbrecht and E. Brand, (NCA 2019/606).

Etymology: The specific epithet is a patronym in homage to Thea Lyle Subramoney the daughter of the second author.

Diagnosis: The females of *S. theaei* **sp. nov.** are distinguishable from other members of the genus occurring in the Karoo based on the following combination of characters. Easily distinguished by the highly dense denticles on the chelicera (>50), all other species but *S. spinosus* have less than 30. Distinguishable from *S. spinosus* by the extent of spines on metatarsus 1 extending more than half the segment (only matched or exceeded by *S. unispinosus*, *S. hamartia* **sp. nov.** and *S. erythrognathus*).

Description: Based on the holotype ♀ (NCA 2019/606).
Remarks: ♂: Known only from the type female.
General: ♀: (Fig 7B) Medium bodied spider, 21.66 total length.
Carapace: ♀: Carapace length 10.29; width 9.61. Reddish colour, smooth texture, with some pleats in the thoracic region. The fovea strongly procurved, 2.20 in length.
Ocelli: ♀: (Fig 2H, 17D) AME diameter 0.25, PME diameter 0.26, MOQ anterior width 2.57, MOQ posterior width 3.89; AME-AME 0.58, AME-ALE 0.34, ALE-ALE 1.83, PME-PME 1.86, PME-PLE 0.48, PLE-PLE 3.10. AER fairly straight, PER slightly recurved.
Chelicerae: ♀: (Fig 34C) Two teeth rows present, 4 teeth in proventral row, 5 in retroventral row; 48 - 50 cuspules in between which vary in sizes.
Sternum, labium and maxillae: ♀: (Fig 34A) Sternum length 5.51; sternum width 5.75. Longitudinally elongated sigilla, distal end 0.72 apart, proximal end 1.66 apart. Labium (Fig 34B) 14 cuspules present, maxillae 13 -14 cuspules present.
Abdomen: ♀: Abdomen length 11.37; width 8.41. Greyish yellow colouration, end of abdomen towards the spinnerets darker grey than the rest of abdomen.
Pedipalps: ♀: Total length 11.49; Segment lengths 3.58, 2.41, 2.62, -, 2.89. Spination: spines absent on femur, with sparse setae. Patella *pl*- 2-3 long thin spines. Tibia *pl*- 2 tibial spurs, 1 proximal and 1 distal, *do*- small patch of spinules distally extend onto tarsus. *rl*- 22 spinules along segment. Tarsus *pl*- 12-14 large spines, *do*- patch of 17-19 spinules, less dense distally, extend $\frac{1}{3}$ - $\frac{1}{4}$ of segment, *rl*- covered in dense spines (25-30).
Legs: ♀: Length order: IV, III, I, II. I Total length 17.76; Segment lengths 5.97, 3.56, 3.81, 3.98, 1.40; Spination: spines absent on femur and patella, with sparse setae. Tibia *pl*- small spines extending $\frac{1}{2}$ -

© University of Pretoria

$\frac{1}{3}$ from the distal end, *do* (Fig 35A)- distally dense patch of spines, extend to $\frac{1}{7}$ of segment, continues on metatarsus, *rl*- spinules extend entire segment less dense proximally. Metatarsus *pl*&*rl*- very dense spinules along the entire segment, *do* (Fig 35A)- patch of dense spines proximally, cover approx. $\frac{2}{3}$ of segment, *v*- scopulate. Tarsus *pl*&*rl*- dense spinules along entire segment, *v*- scopulate. II Total length 15.38; Segment lengths 4.59, 3.05, 2.95, 3.53, 1.26; Spination: spines absent on femur and patella, with sparse setae. Tibia *pl*- small spines extending $\frac{1}{2}$ of section from distal end, *do* (Fig 35B)- distally dense patch of spines, extend $\frac{1}{5}$ of segment, continues on metatarsus, *rl*- spinules extend entire segment, less dense proximally. Metatarsus *pl*&*rl*- dense spinules along the entire segment, *do* (Fig 35B)- patch of dense spines proximally, covering approx. $\frac{1}{3}$ of segment, *v*- scopulate. Tarsus *pl*&*rl*- dense spinules along the entire segment, *v*- scopulate. III Total length 17.85; Segment lengths 4.80, 4.21, 2.10, 4.12, 2.62; Spination: spines absent on femur, with sparse setae. Patella *pl*- 12 red spinules, has rows of black setae. Tibia *do* (Fig 35C)- stout red spines very dense distally, covered in long setae. Metatarsus *do* (Fig 35C)- 2

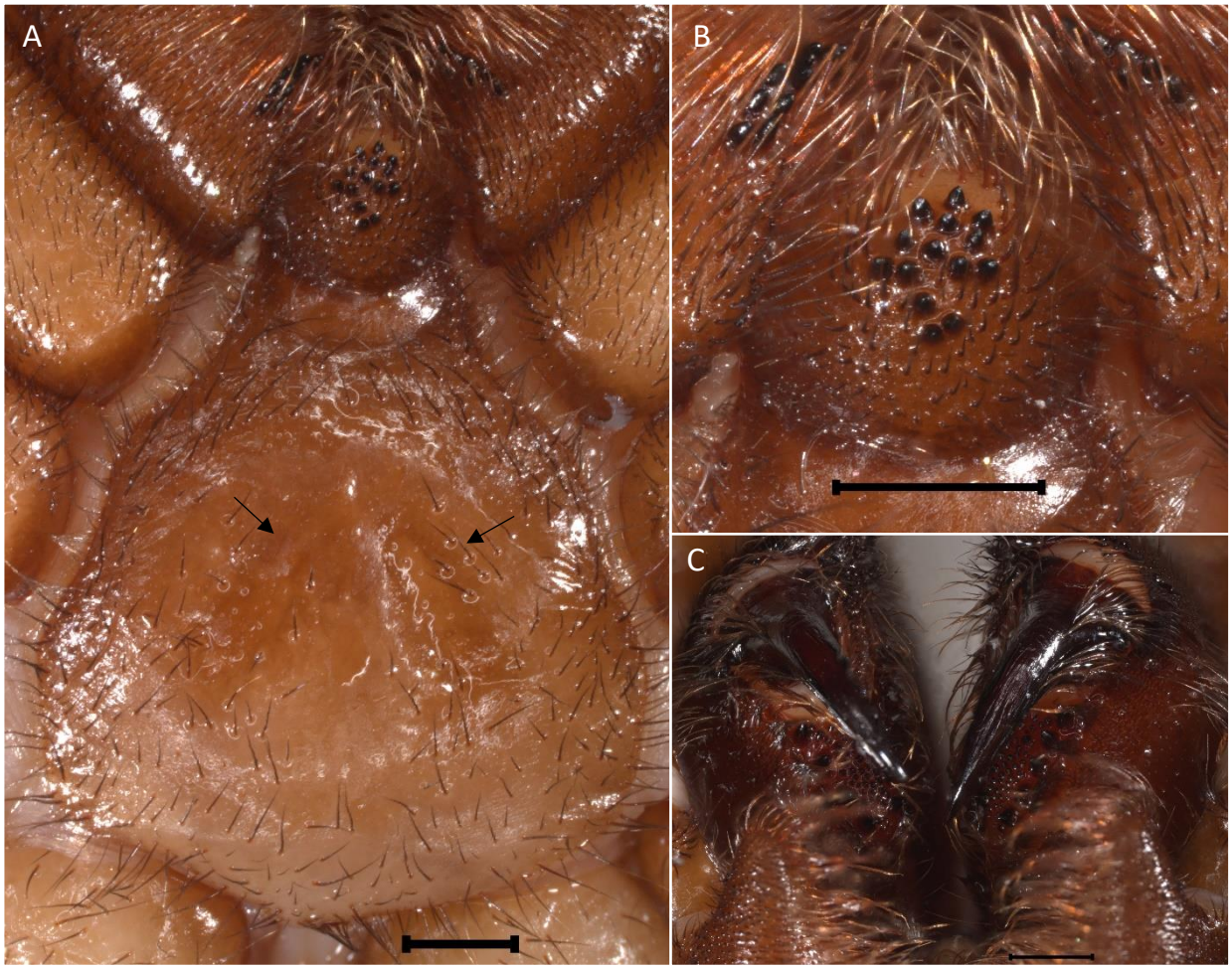


Figure 34. Female of *Stasimopus theaei* **sp. nov.** (NCA 2019/606). (A) Sternum with fused labium and visible sigilla (as shown by the arrows). (B) Labium teeth. (C) Fangs with cheliceral teeth. Scale: 1mm.

© University of Pretoria



Figure 35. Female of *Stasimopus theaei* **sp. nov.** (NCA 2019/606). (A) Leg I tibia, metatarsus, tarsus. Dorsal aspect. (B) Leg II tibia, metatarsus, tarsus. Dorsal aspect. (C) Leg III tibia, metatarsus, tarsus. Dorsal aspect. (D). Leg IV tibia, metatarsus, tarsus. Prolateral aspect. (E) Leg IV metatarsus preening comb. Scale: 1mm.

© University of Pretoria

rows of stout red spines (18-22 in each), between small red spinules. Tarsus *pl*- dense patch of red spines extend distally and covered in dense setae, *pl*&*rl*- 3-5 stout black spines along both surfaces, denser distally, *v*- scopulate. IV Total length 20.93; Segment lengths 5.05, 4.52, 4.17, 5.03, 2.17; Spination: spines absent on femur, with sparse setae. Patella *do*- short dense red spines proximally, less dense distally, interspersed with stout black setae. Tibia *pl* (Fig 35D)- many spines extending under the dorsal setae, *do*- dense setae covering randomly scattered spinules. Metatarsus *pl* (Fig 35D)- 17-20 spines extending ventrally, *v*- 7-8 spines in a transverse row (preening comb) (Fig 35E). Tarsus *pl* (Fig 35D)- very dense setae covering randomly scattered spinules.

Spermathecae: (Fig 22C) Entire, with short inflated terminus, one appears 2/3 length of other spermathecae.

Distribution and environment notes:

The species known from the type locality indicated in Figure 36. It has been collected near Somerset East in the Eastern Cape province. The location was a flat between small hills. The vegetation was dominated by low shrubs and aloe plants. The soil was very hard, chalky and pale. The specimen was found in a deep vertical burrow (approx. 30 cm deep), which angled slightly near the bottom.

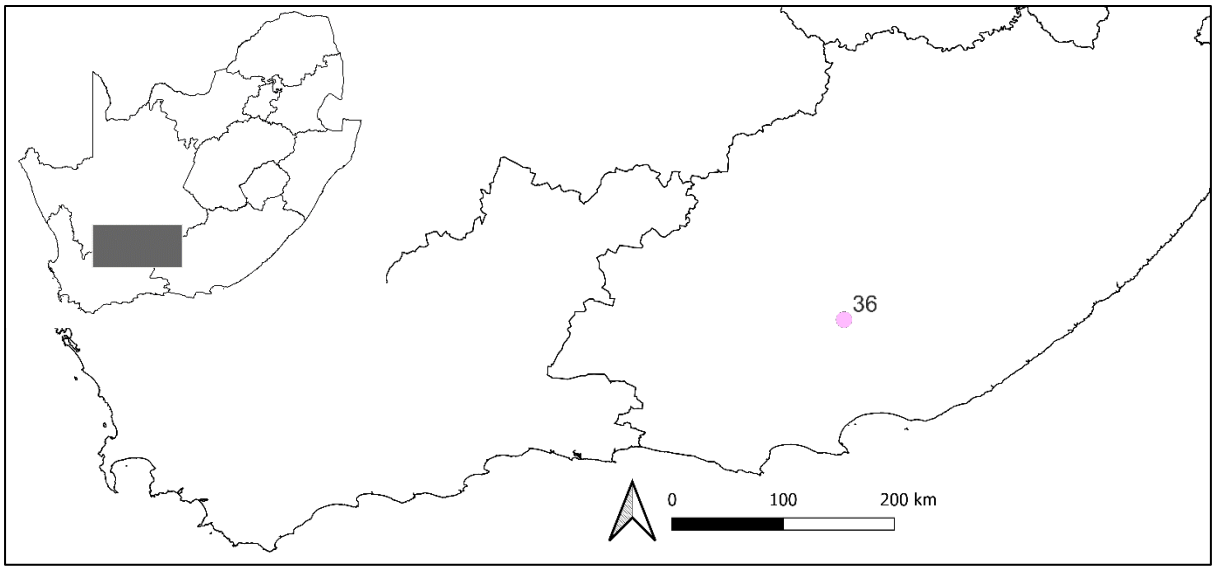


Figure 36. Map of the locality where the *Stasimopus theaei* **sp. nov.** specimen was collected. Numbers match the site numbers in Figure 1. Map created in QGIS version 3.4.8-Madeira (2019), available at: http://qgis.osgeo.org.

© University of Pretoria

***Stasimopus venterstadensis* sp. nov.**
(Figures 2J, 7C, 18, 22D, 37, 38, 39)

Type material: Holotype ♀ SOUTH AFRICA: Eastern Cape Province, Venterstad (-30.9077, 25.7738), 12.v.2018, S. Brandt, C. Sole, E. Engelbrecht and E. Brand, (NCA 2019/610). Paratypes: Same data, 12.v.2018, 2♀♀ (NCA 2019/608, NCA 2019/609).

Etymology: The species is named after the type locality, Venterstad, on the Eastern Cape province in South Africa.

Diagnosis: The females of *S. venterstadensis* **sp. nov.** are distinguishable from other members of the genus occurring in the Karoo based on the following combination of characters. It is differentiated from *S. astutus*, *S. leipoldti*, *S. maraisi*, *S. patersonae*, *S. schrieneri*, *S. theaei* **sp. nov.**, *S. ignis* **sp. nov.** and *S. teras* **sp. nov.** by the presence of an apical tuft being present on metatarsus III. This species is distinguishable from the other species based on the number of spines in the preening comb on metatarsus IV, *S. unispinosus* having less than 3, whereas, *S. schonlandi*, *S. artifex* and *S. spinosus* all have more than 6.

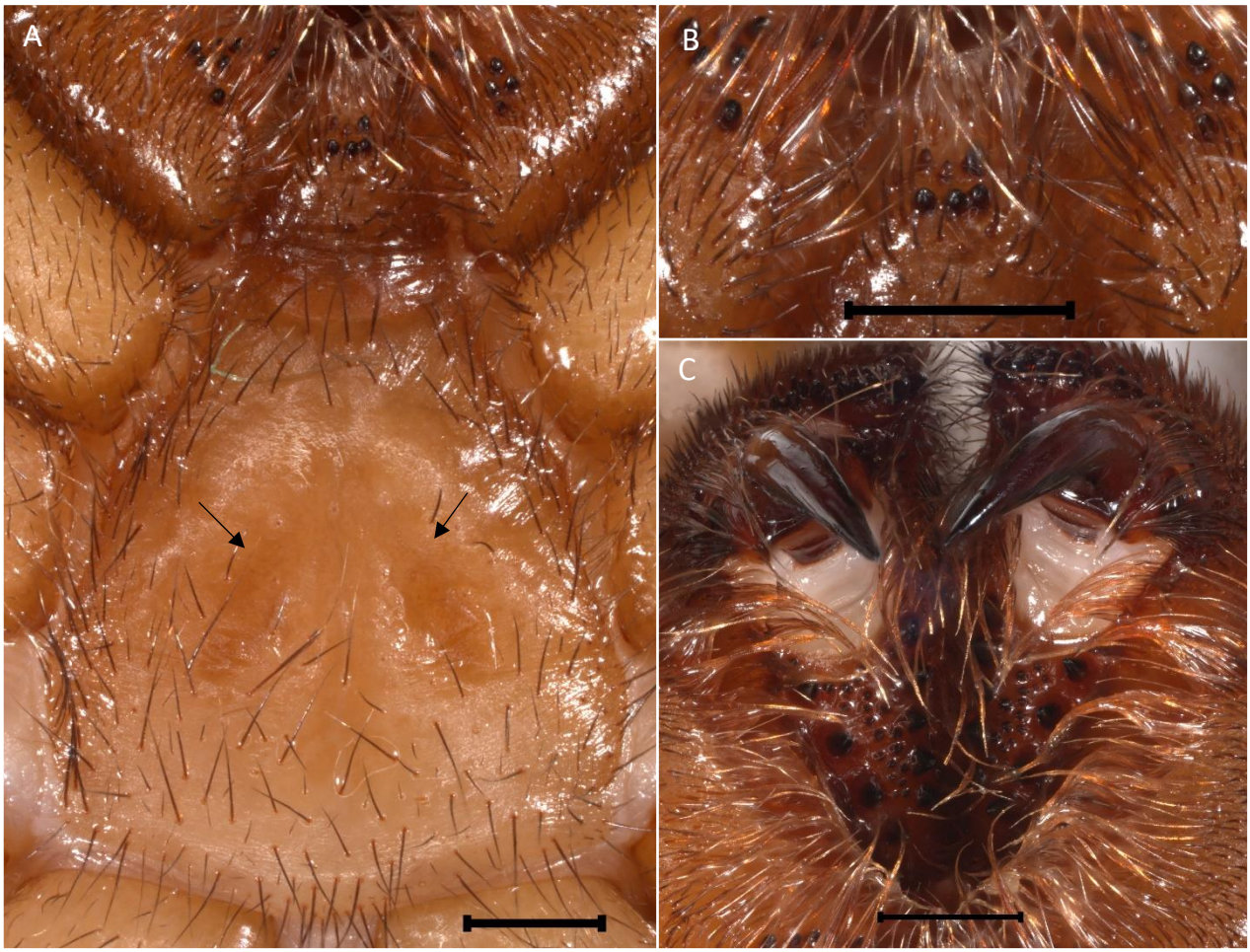


Figure 37. Female of *Stasimopus venterstadensis* **sp. nov.** (NCA 2019/610). (A) Sternum with fused labium and visible sigilla (as shown by the arrows). (B) Labium teeth. (C) Fangs with cheliceral teeth. Scale: 1mm.

© University of Pretoria

Description: Based on the holotype ♀ (NCA 2019/610) and the paratypes 2♀ (NCA 2019/608, NCA 2019/609).

Remarks: ♂: Known only from females. *General:* ♀: (Fig 7C) Large bodied spiders, ranging between 18.48 - 25.32 (18.48) total length.

Carapace: ♀: Carapace length 8.98 - 11.12 (8.98); width 7.52 - 10.40 (7.52). Dark reddish orange colouration. Smooth texture, with pleats in thoracic region. Fovea strongly procurved, between 1.63 - 1.94 (1.63) in length.

Ocelli: ♀: (Fig 2J, 18) AME diameter 0.28 - 0.34 (0.28), PME diameter 0.30 - 0.38 (0.30), MOQ anterior width 2.04 - 2.64 (2.04), MOQ posterior width 3.26 - 4.17 (3.26); AME-AME 0.56, AME-ALE 0.30, ALE-ALE 1.81, PME-PME 1.83, PME-PLE 0.38, PLE-PLE 3.19. AER and PER almost straight.

Chelicerae: ♀: (Fig 37C) Two teeth rows present, 6 teeth in proventral row, 6 teeth in retroventral row; 29 - 31 cuspules in between.

Sternum, labium and maxillae: ♀: (Fig 37A) Sternum length 5.00 - 5.88 (5.00); sternum width 4.47 - 6.14 (4.47). Longitudinally elongated sigilla, distal end 0.64 - 0.72 (0.67) apart, proximal end 1.61 - 1.87 (1.80) apart; labium (Fig 37B) 12 - 16 cuspules present; maxillae 5 - 7 cuspules present.

Abdomen: ♀: Abdomen length 9.50 - 14.20 (9.50); width 7.02 - 10.12 (7.02). Grey colour, with one large dark spot near the carapace followed by a smaller one towards the spinnerets.

Pedipalps: ♀: Total length 13.08; Segment lengths 4.45, 2.90, 2.69, - ,3.05. Spination: spines absent on femur, with sparse setae. Patella *pl*- 2-3 long thin spines. Tibia *pl*- 2 tibial spurs, 1 proximal and 1 distal, *do*- small patch spinules distally extending onto the tarsus, *rl*- 15-16 spinules along segment. Tarsus *pl*- 8-10 large spines, *do*- a patch of 16-18 spinules, less dense distally, extend $\frac{1}{3}$ - $\frac{1}{4}$ of segment, *rl*- covered in dense spines (24-27).

Legs: ♀: Length order: IV, III, I, II. I Total length 18.72; Segment lengths 5.97, 3.56, 3.81, 3.98, 1.40; Spination: spines absent on femur and patella, with sparse setae. Tibia *pl*- small spines extending $\frac{1}{2}$ - $\frac{1}{3}$ segment from distal end, *do* (Fig 38A)- distally dense patch of spines, extending $\frac{1}{6}$ segment, and continued on metatarsus, *rl*- spinules extending entire segment, less dense proximally. Metatarsus *pl*&*rl*- very dense spinules along entire segment, *do* (Fig 38A)- patch of dense spines proximally, extending approx. $\frac{1}{3}$ segment, *v*- scopulate. Tarsus *pl*&*rl*- very dense spinules along entire segment, *v*- scopulate. II Total length 16.52; Segment lengths 5.20, 3.22, 2.98, 3.61, 1.51; Spination follows that of leg I (Fig 38B). III Total length 19.35; Segment lengths 4.89, 4.52, 3.12, 4.12, 2.71; Spination: spines absent on femur and patella, with sparse setae. Tibia *do* (Fig 38C)- stout red spines dense distally, hidden by long setae. Metatarsus *do* (Fig 38C)- 2 rows of stout red

© University of Pretoria



Figure 38. Female of *Stasimopus venterstadensis* **sp. nov.** (NCA 2019/610). (A) Leg I tibia, metatarsus, tarsus. Dorsal aspect. (B) Leg II tibia, metatarsus, tarsus. Dorsal aspect. (C) Leg III tibia, metatarsus, tarsus. Dorsal aspect. (D). Leg IV metatarsus, tarsus. Prolateral aspect. (E) Leg III metatarsal tuft. Ventral aspect. (F) Leg IV metatarsus preening comb. Scale: 1mm.

© University of Pretoria

spines (22-27 in each), between smaller red spinules, *V*- 8 spines distally (Fig 38E). Tarsus *pl&rl*- 10-15 stout black spines along both surfaces, denser distally, *v*- scopulate. IV Total length 23.03; Segment lengths 6.00, 4.66, 4.31, 5.41, 2.66; Spination: spines absent on femur, with sparse setae. Patella *do*- covered in red dense spinules. Tibia *do*- dense setae covering randomly scattered spinules. Metatarsus *pl* (Fig 38D)- 22 spines, *v*- 8 spines in a transverse row (preening comb) (Fig 38F). Tarsus *pl* (Fig 38D)- dense setae covering randomly scattered spinules.

Spermathecae: (Fig 22D) Entire, with inflated terminus directed inwards.

Distribution and environment notes:

The species is found in the localities indicated in Figure 39. The species is only known from one locality near Venterstad in the Eastern Cape province. Specimen collected from a flat plain with sandy soil. The vegetation was dominated by typical Karoo shrubs and buffalo grass.

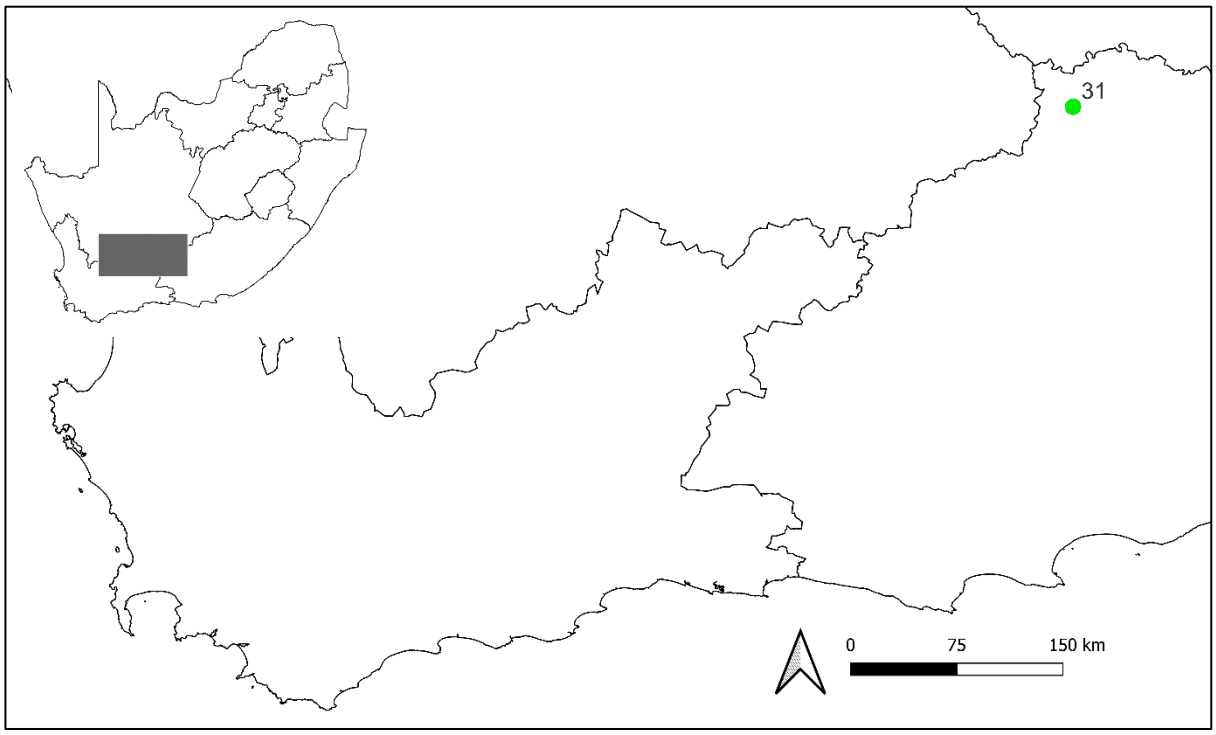


Figure 39. Map of the locality where *Stasimopus venterstadensis* **sp. nov.** specimens were collected. Numbers match the site numbers in Figure 1. Map created in QGIS version 3.4.8-Madeira (2019), available at: http://qgis.osgeo.org.

© University of Pretoria

***Stasimopus maraisi* male description**

(Figs 3G, 7D, 12B, 13D, 40, 41)

Type material: Allotype ♂ SOUTH AFRICA: Northern Cape Province, Williston (-31.7863, 20.7857), 19.v.2018, S. Brandt, C. Sole, E. Engelbrecht and E. Brand, (NCA 2019/630).

Diagnosis: The males of *S. maraisi* are distinguishable from other members of the genus occurring in the Karoo based on the following combination of characters. The main distinguishing feature is that *S. maraisi* has a carapace which is smooth in texture, whereas other species are more rugose. Further differentiation can be made from *S. astutus*, *S. erythrognathus*, S. *malesociatus* **sp. nov.**, *S. patersonae*, *S. steynsbergensis*, *S. karooensis* **sp. nov.** and *S. mandelai* based on the pedipalp not reaching the tarsus of leg I. Distinguished from *S. palpiger* as the pedipalp is longer than leg I, which *S. maraisi* is not.

Description: ♀: The female description is available in Hewitt 1914. Based on the new ♂ (NCA 2019/630).
Remarks: ♂: The original male described in Hewitt 1927 pg. 425-426 was found to not be a genetic match for the characters describing the female holotype for the species. For this reason, the male that does match genetically is described here.
General: ♂: (Fig 7D) Medium bodied spider, 8.46 total length.
Carapace: ♂: Carapace length 3.86; width 3.46. Orange yellow colouration, smooth in texture. Fovea procurved, 0.85 in length.
Ocelli: ♂: (Fig 3G, 12B) AME diameter 0.18, PME diameter 0.13, MOQ anterior width 1.11, MOQ posterior width 1.34; AME-AME 0.16, AME-ALE 0.10, ALE-ALE 0.69, PME-PME 0.73, PME-PLE 0.11, PLE-PLE 1.15 AER strongly recurved, PER also recurved.
Chelicerae: ♂: (Fig 13D) Two teeth rows present, 3 teeth in proventral row, 4 in retroventral row. 5-6 cuspules between rows.
Sternum, labium and maxillae: ♂: (Fig 40C) Sternum length 2.21; sternum width 1.93. Sternum shape has shallow impressions of where the coxa are situated. Sigilla in the shape of fused arrow, distal end fused, proximal end 0.93 apart. Cuspules on labium absent; maxilla cuspules absent.
Abdomen: ♂: Abdomen length 4.61; width 3.10. Light grey colouration with dark bands. Large dark patch proximally covering 1/3 total abdomen dorsally, followed by 4 smaller dark bands which are lighter in the middle.
Pedipalps: ♂: (Fig 40A, B) Total length 15.32; Segment lengths 1.34, 5.15, 4.22, -, 4.61. Spination: spines absent. Bulb oval, embolus elongated tapering into sharp point, curving posteriorly.
Legs: ♂: Length order: I, IV, II, III. I Total length 17.76; Segment lengths 5.31, 2.29, 4.40, 3.97, 1.79; Spination: spines absent on femur, with sparse setae. Patella *do*- 1 small spine, *v*- 4 spines

© University of Pretoria

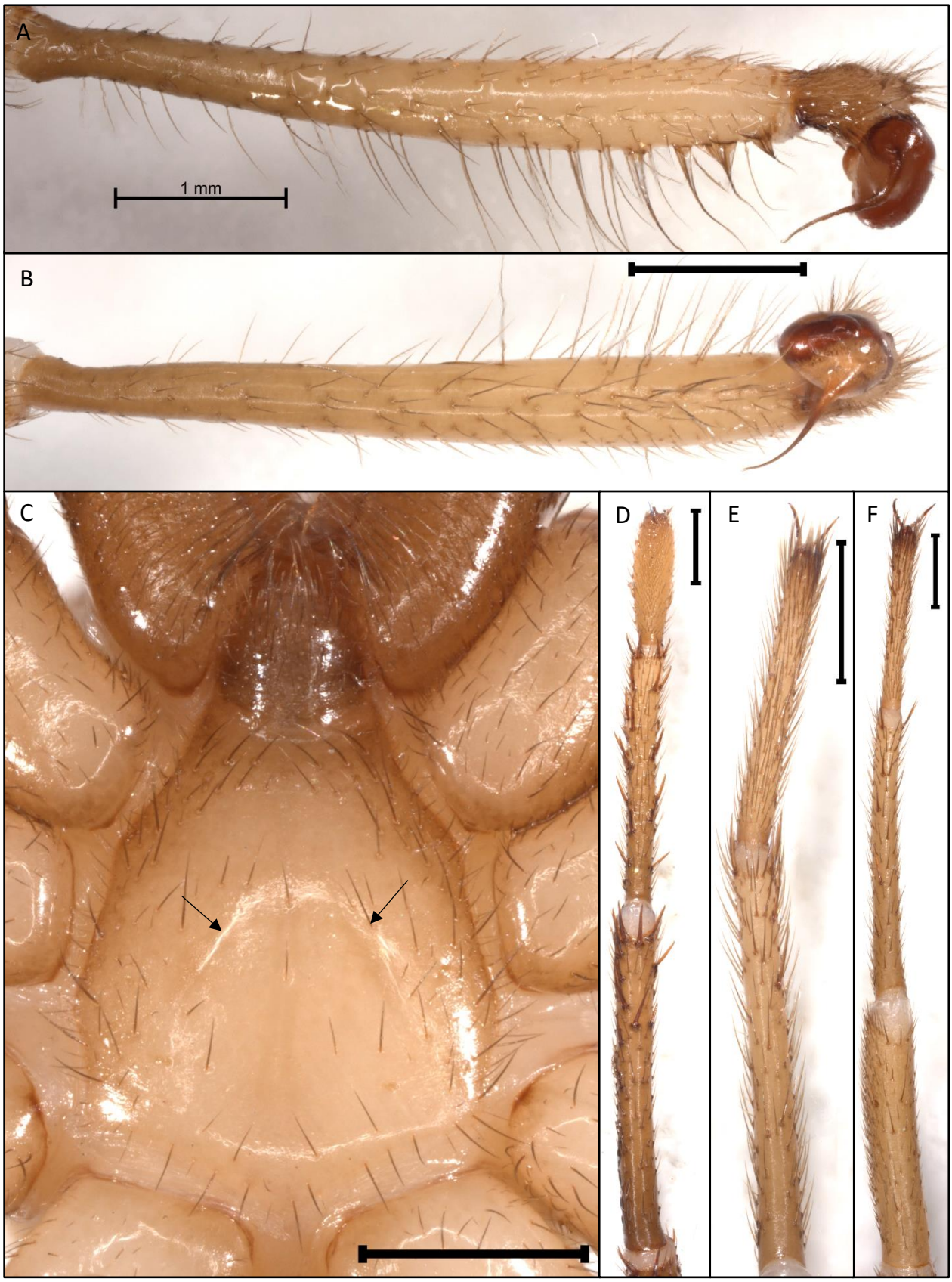


Figure 40. Male of *Stasimopus maraisi* (NCA 2019/630). (A) Pedipalp tibia, bulb, retrolateral aspect. (B) Pedipalp tibia, bulb, prolateral aspect. (C) Sternum with fused labium and visible sigilla (as shown by the arrows). (D) Leg I tibia, metatarsus, tarsus. Ventral aspect. (E) Leg III metatarsus, tarsus. Ventral aspect. (F) Leg IV tibia, metatarsus, tarsus. Ventral aspect. Scale: 1mm.

© University of Pretoria

distally (slightly *rl*). Tibia *v* (Fig 40D)- 12 large spines extending *rl*, only on distal half. Metatarsus *v* (Fig 40D)- 17 large spines extending *pl*&*rl*. Tarsus *v* (Fig 40D)- scopulate. II Total length 15.10; Segment lengths 4.52, 2.02, 3.59, 3.24, 1.73; Spination: Femur 4 randomly scattered spines. Spines absent on patella. Tibia *v*- 11 large spines extending *rl*. Metatarsus *v*- 18 large spines, extending *pl*&*rl*. Tarsus *v*- scopulate. III Total length 11.56; Segment lengths 3.10, 1.63, 1.37, 3.31, 2.16; Spination: spines absent on femur, with sparse setae. Patella *do*- 8 small spines along surface, *rl*- 6 spines. Tibia *pl*- 1 spine, *do*- 6-8 spines distally, *v*- 2 spines. Metatarsus *pl*- 3 red spines, *v* (Fig 40E)- 4 spines, *rl*- 2 spines. Tarsus *pl*&*rl*- 2-3 spines on either edge, *v* (Fig 40E)- 7 small spines, dense setae covering spines. IV Total length 16.63; Segment lengths 4.39, 1.87, 3.43, 4.40, 2.55; Spination: spines absent on femur, with sparse setae. Patella *do*- short dense red spines proximally (approx. 30), less dense distally, interspersed with fine black setae. Tibia *v* (Fig 40F)- 1 small spine. Metatarsus *pl*- 5-6 spines, *v* (Fig 40F)- 8 spines, *rl*- 1 spine distally. Tarsus *pl*- 4-5 spines, *v* (Fig 40F)- 9 spines (extend *pl*), *rl*- 1 spine distally.

Distribution and environment notes:

This species is widely distributed across the Karoo region, mostly in the Western and Northern Cape provinces of South Africa as seen in Figure 41. The species occurs in a range of soil and vegetation types. The soil types include clay, loam, sand and occasionally silt, but the specimens were most often found in clay or loam soils. All the specimens were collected on open plains near to drainage lines. In these areas the vegetation was mostly low shrubs, with grasses present at few sites.

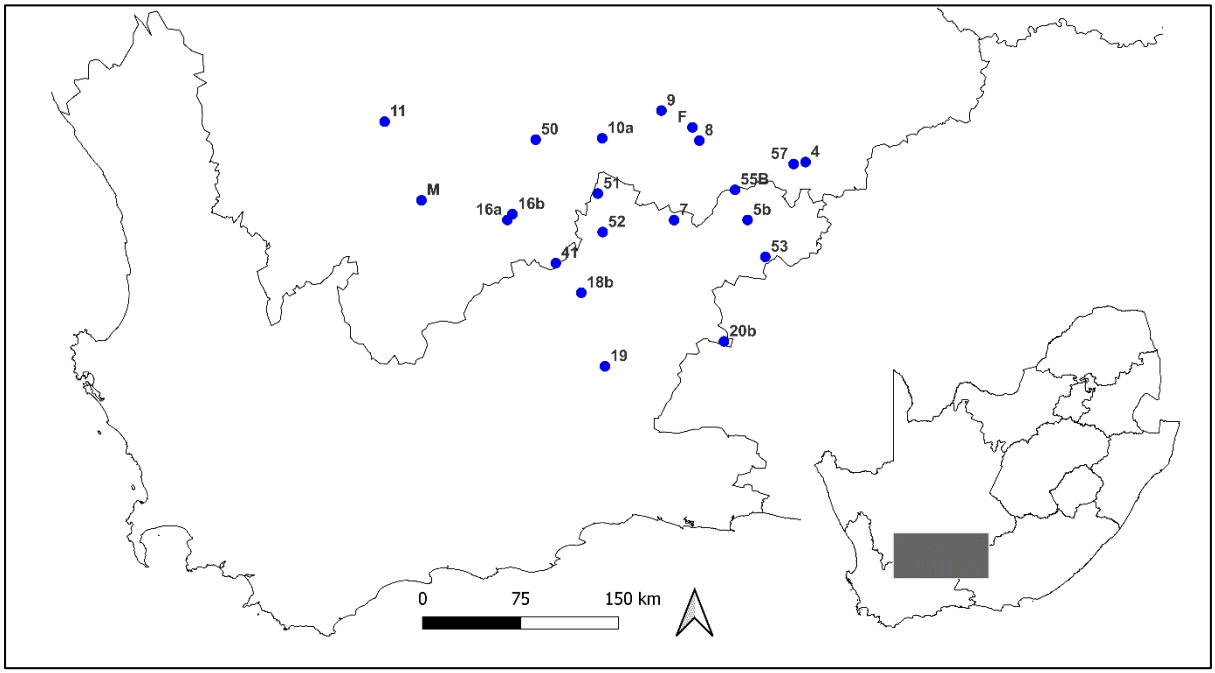


Figure 41. Map of the localities where *S. maraisi* Hewitt 1914 specimens were collected. Numbers match the site numbers in Figure 1. The points denoted as F and M represent the female and male type localities for this species. Map created in QGIS version 3.4.8-Madeira (2019), available at: http://qgis.osgeo.org.

© University of Pretoria

4. Discussion

4.1. Karoo species diversity

Based on the taxonomic literature, 12 species of *Stasimopus* are known from within or nearby this part of the Karoo (Dippenaar-Schoeman *et al.* 2010). Our study has increased the number of species from the Karoo region to 23 species. Two of these additional species were already described, but they had never been recorded in the Karoo region. *Stasimopus erythrognathus* was initially believed to only occur in the Western cape (Worster), but its range has been expanded to the Easten Cape (700km in distance). *Stasimopus leipoldti* is reported from Clanwilliam in the Western Cape and has now also been recorded in the Tankwa Karoo.

4.2. Integrative taxonomy

Integrative taxonomy stresses the importance of using multiple lines of evidence when testing taxonomic hypotheses (Bond 2012; Ferretti *et al.* 2019; Hedin & Bond 2006). Under this framework we have examined distinct evolutionary lineages (genetic monophyletic groups) as well as morphological characters to find a higher than expected species diversity present in the Karoo region of South Africa.

Each species identified and described in this manuscripts is supported following the integrated taxonomic framework. Within this context, a species complex was found. There is a genetic species complex between *S. erythrognathus*, *S. karooensis* **sp. nov.** and *S. theaei* **sp. nov.** Each of these species is however, morphologically distinct based on a range of charateristics. In order to resolve this genetic complex, more samples of *S. karooensis* **sp. nov.** and *S. theaei* **sp. nov.** are required, as this is currently based on small sample sizes (two and one specimen respectively) as well as possibly including additional gene regions. The integrative framework allows us to be confident in the description of *S. teras* despite the physical deformity in the ocular pattern. The other characters used to identify and describe the species are distinct enough without the use of the ocular pattern to separate the species from others. This is further supported by the molecular phylogeny which clearly separates the species. It would be useful for the type locality to be sampled to find an undeformed member of the species (so that the true ocular pattern can be described) and a male representative.

Mygalomorph spiders are notorious for their homoplasious morphology, making identification and taxonomy challenging (Bond *et al.* 2021; Ferretti *et al.* 2019; Hamilton *et al.* 2011; Montes de Oca *et. al.* 2022; Wilson *et al.* 2023). This is apparent from the mismatch of the original *S. maraisi* holotype and allotype. Further inflating the morphological identification problem is that the majority of *Stasimopus* species (and mygalomorphs generally) are described on the basis of only one sex (53%) of which most are described only based on females (40%) (Bond *et al.* 2021; Engelbrecht & Prendini 2012). This is especially problematic as males of the genus are known to be more

© University of Pretoria

diagnostic than females (Engelbrecht & Prendini 2012; Hendrixson & Bond 2004). In this manuscript however, females did display a few distinct diagnostic charaters, most prominently the presence or absence of an apical tuft on metatrasus III, the spination of the preening comb, extent of spination on legs I and II as well as the density of cuspules on the labium, maxilla and chelicera.

The species described here, add to the issue of species described by only one sex. This is a challenging issue to resolve due to the difficulty of sampling of spiders with the life histories observed here. To compensate for this the DNA evidence is important. In this study both mitochondrial and nuclear DNA was used. Mitcohondrial DNA is faster evolving than nuclear, leading to an increased amount of informative sites, often recoving deeper population divergences (Ferretti *et al.* 2019; Hendrixson & Bond 2005). Mitochondrial DNA does tend to conflate population structure to species diverity due to the sedentary habits of females of the species (Ferretti *et al.* 2019; Harvey *et al.* 2015). This emphasises the need to include both mitochondrial and nuclear DNA when constructing phylogenies for taxonomies (Ferretti *et al.* 2019; Hedin *et al.* 2013; Satler *et al.* 2013). The DNA data generated for this study as well as the morphological matrices are invaluable resources. It is suggested that if a wider range of *Stasimopus* species can be genetically sequenced, these data should feed into a combined molecular and morphology analyses. This would create a fully integrated taxonomy for the entire genus if the funding for sequencing can be obtained.

The field of taxonomy is of vital importance as it is foundational to all other biological sciences. This study is a first step to understanding the diversity of *Stasimopus* which will enable us to better understand their conservation status and our understanding of the Karoo ecosystem.

5. Conclusion

This study is the first integrative taxonomy for the genus *Stasimopus*. It is however, limited to the species occuring in the Karoo, and future studies should extend this to the entire genus. The information gathered greatly increases the species diverity as well as expanding the distribution range for various species. It is apparent that there is a great amount of undiscovered diversity present within the mygalomorphs in southern Africa and more comprehensive sampling is needed. It is also important that going forward in the field of mygalomorph systematics that DNA evidence is considered when identifying and describing species due to the conservative nature of the morphology.

© University of Pretoria

Acknowledgements

We would like to acknowledge Carmen Jacobs and Ishtiag Abdalla Mohammed for assistance with molecular work and phylogenetic analyses. Tshepiso Majelantle and Elmé Brand for their assistance on fieldwork. Elsa van Niekerk for assistance with photo editing and graphic design. Equipment for fieldwork was supplied by the Agricultural Research Council. We would like to thank the following institutions for loaning the specimens required for specimen identification: Albany Museum, Grahamstown, South Africa; The National Museum, Bloemfontein, South Africa; Ditsong Museum of Natural History, Pretoria, South Africa; Iziko Museum of Cape Town, South Africa; Museum für Naturkunde, Berlin, Germany; National Collection of Arachnida, Pretoria, South Africa.

Funding

The National Research Foundation (NRF) are acknowledged for funding to the second author. The first author would also like to acknowledge the National Research Foundation for funding (Grant no: 120190 and 139125). This work is based on the research supported in part by the Karoo BioGaps Project (NRF Grant Number 98864), which was awarded through the Foundational Biodiversity Information Programme (FBIP), a joint initiative of the Department of Science and Innovation (DSI), the National Research Foundation (NRF) and the South African National Biodiversity Institute (SANBI).

© University of Pretoria

References

Ausserer, A. (1871) Beiträge zur Kenntniss der Arachniden-Familie der Territelariae Thorell (Mygalidae Autor). *Verhandlungen der Kaiserlich-Königlichen Zoologisch-Botanischen Gesellschaft in Wien*, 21, 117–224.

Ayoub, N.A., Garb, J.E., Hedin, M. & Hayashi, C.Y. (2007) Utility of the nuclear protein-coding gene, elongation factor-1 gamma (EF-1γ), for spider systematics, emphasizing family level relationships of tarantulas and their kin (Araneae: Mygalomorphae). *Molecular Phylogenetics and Evolution*, 42, 394–409. https://doi.org/10.1016/j.ympev.2006.07.018

Bond, J.E. (2012) Phylogenetic treatment and taxonomic revision of the trapdoor spider genus *Aptostichus* Simon (Araneae, Mygalomorphae, Euctenizidae). *Zookeys*, 252, 1–209. https://doi.org/10.3897/zookeys.252.3588

Bond, J.E., Hendrixson, B.E., Hamilton, C.A. & Hedin, M. (2012) A reconsideration of the classification of the spider infraorder Mygalomorphae (Arachnida: Araneae) based on three nuclear genes and morphology. *PLoS ONE*, 7, e38753. https://doi.org/https://doi.org/10.1371/journal.pone.0038753

Bond, J.E., Godwin, R.L., Colby, J.D., Newton, L.G., Zahnle, X.J., Agnarsson, I., Hamilton, C.A. & Kuntner, M. (2021) Improving Taxonomic Practices and Enhancing Its Extensibility—An Example from Araneology. *Diversity*, 14, 5. https://doi.org/10.3390/d14010005

Brandt, S., Sole, C.L., Lyle, R. & Pirk, C.W.W. IN REVIEW. Geometric morphometric analysis of ocular patterns as a species identifier in the South African endemic trapdoor spider genus *Stasimopus* Simon, 1892 (Araneae, Mygalomorphae, Stasimopidae). Submitted to *Evolutionary Biology*. (Chapter 3)

Dayrat, B. (2005) Towards integrative taxonomy. *Biological Journal of the Linnean Society* 85, 407–415. https://doi.org/10.1111/j.1095-8312.2005.00503.x

Dippenaar-Schoeman, A.S. (2002) *Baboon and Trapdoor Spiders of Southern Africa: An Identification Manual*. Plant Production Research Institute, Agricultural Research Council, Pretoria, 29–38 pp.

Dippenaar-Schoeman, A.S., Haddad, C.R., Foord, S.H., Lyle, R., Lotz, L., Helberg, L., Mathebula, S., van der Berg, A., van Niekerk, E. & Jocque, R. (2010) *First atlas of the spiders of South Africa (Arachnida: Araneae)*. Plant Production Research Institute, Agricultural Research Council, Pretoria, 1160 pp.

Drummond, A.J., Ho, S.Y.W., Phillips, M.J. & Rambaut, A. (2006) Relaxed phylogenetics and dating with confidence. *PLoS Biology*, 4, 0699–0710. https://doi.org/10.1371/journal.pbio.0040088

Drummond, A.J. & Rambaut, A. (2007) BEAST: Bayesian evolutionary analysis by sampling trees. *BMC Evolutionary Biology*, 7, 1–8. https://doi.org/10.1186/1471-2148-7-214

© University of Pretoria

Engelbrecht, I. & Prendini, L. (2012) Cryptic diversity of South African trapdoor spiders: Three new species of *Stasimopus* Simon, 1892 (Mygalomorphae, Ctenizidae), and redescription of *Stasimopus robertsi* Hewitt, 1910. *American Museum Novitates*, 1–42. https://doi.org/https://doi.org/10.1206/3732.2

Felsenstein, J. (1985) Confidence limits on phylogenetics: an approach using the bootstrap. *Evolution*, 783–791. https://doi.org/10.2307/2408678

Ferretti, N.E., Soresi, D.S., González, A. & Arnedo, M. (2019) An integrative approach unveils speciation within the threatened spider *Calathotarsus simoni* (Araneae: Mygalomorphae: Migidae). *Systematics and Biodiversity*, 17, 439–457. https://doi.org/10.1080/14772000.2019.1643423

Fujita, M.K., Leaché, A.D., Burbrink, F.T., McGuire, J.A. & Moritz, C. (2012) Coalescent-based species delimitation in an integrative taxonomy. *Trends in Ecology & Evolution*, 27, 480–488. https://doi.org/10.1016/j.tree.2012.04.012

Hamilton, C.A., Formanowicz, D.R. & Bond, J.E. (2011) Species delimitation and phylogeography of *Aphonopelma hentzi* (Araneae, Mygalomorphae, Theraphosidae): Cryptic diversity in North American tarantulas. *PLoS ONE*, 6, e26207. https://doi.org/10.1371/journal.pone.0026207

Harvey, M.S., Main, B.Y., Rix, M.G. & Cooper, S.J.B. (2015) Refugia within refugia: in situ speciation and conservation of threatened *Bertmainius* (Araneae: Migidae), a new genus of relictual trapdoor spiders endemic to the mesic zone of south-western Australia. *Invertebrate Systematics*, 29 (6), 511–553. https://doi.org/10.1071/IS15024

Hedin, M. & Bond, J.E. (2006) Molecular phylogenetics of the spider infraorder Mygalomorphae using nuclear rRNA genes (18S and 28S): Conflict and agreement with the current system of classification. *Molecular Phylogenetics and Evolution*, 41, 454–471. https://doi.org/10.1016/j.ympev.2006.05.017

Hedin, M., Starrett, J. & Hayashi, C. (2013) Crossing the uncrossable: Novel trans-valley biogeographic patterns revealed in the genetic history of low-dispersal mygalomorph spiders (Antrodiaetidae, *Antrodiaetus*) from California. *Molecular Ecology*, 22, 508–526. https://doi.org/10.1111/mec.12130

Hendrixson, B.E. & Bond, J.E. (2004) A new species of *Stasimopus* from the Eastern Cape Province of South Africa (Araneae, Mygalomorphae, Ctenizidae), with notes on its natural history. *Zootaxa*, 619, 1–14. https://doi.org/10.11646/zootaxa.619.1.1

Hendrixson, B.E. & Bond, J.E. (2005) Testing species boundaries in the *Antrodiaetus unicolor* complex (Araneae: Mygalomorphae: Antrodiaetidae): "Paraphyly" and cryptic. *Molecular Phylogenetics and Evolution*, 36 (2), 405–416. https://doi.org/10.1016/j.ympev.2005.01.021

Henschel, J.R., Hoffman, M.T. & Walker, C. (2018) Introduction to the Karoo Special Issue: Trajectories of Change in the Anthropocene. *African Journal of Range & Forage Science*, 35, 151–156. https://doi.org/10.2989/10220119.2018.1535214

© University of Pretoria

Hewitt, J. (1910) Description of two trapdoor spiders from Pretoria (female of *Acanthodon pretoriae* Poc. and *Stasimopus robertsi*, n. sp.). *Annals of the Transvaal Museum*, 2, 74–76.

Hewitt, J. (1913) Descriptions of new and little-known species of trapdoor spiders (Ctenizidae and Migidae) from South Africa. *Records of the Albany Museum Grahamstown*, 2, 404–434.

Hewitt, J. (1914) Descriptions of new Arachnida from South Africa. *Records of the Albany Museum Grahamstown*, 3, 1–37.

Hewitt, J. (1915a) Descriptions of new South African Arachnida. *Records of the Albany Museum Grahamstown*, 3, 70–106. https://doi.org/10.5962/bhl.part.7433

Hewitt, J. (1915b) New South African Arachnida. *Annals of the Natal Museum*, 3, 289–327. https://doi.org/10.5962/bhl.part.7433

Hewitt, J. (1916) Descriptions of new South African spiders. *Annals of the Transvaal Museum*, 5, 180–213.

Hewitt, J. (1917) Descriptions of new South African Arachnida. *Annals of the Natal Museum*, 3, 687–711.

Hewitt, J. (1919) Descriptions of new South African Araneae and Solifugae. *Annals of the Transvaal Museum*, 6, 63–111.

Hewitt, J. (1927) On some new arachnids from South Africa. *Records of the Albany Museum Grahamstown*, 3, 416–429.

Holness, S., Driver, A., Todd, S., Snaddon, K., Hamer, M., Raimondo, D., Daniels, F., Alexander, G., Bazelet, C., Bills, R., Bragg, C., Branch, B., Bruyns, P., Chakona, A., Child, M., Clarke, R.V., Coetzer, A., Coetzer, W., Colville, J., Conradie, W., Dean, R., Eardley, C., Ebrahim, I., Edge, D., Gaynor, D., Gear, S., Herbert, D., Kgatla, M., Lamula, K., Leballo, G., Lyle, R., Malatji, N., Mansell, M., Mecenero, S., Midgley, J., Mlambo, M., Mtshali, H., Simaika, J., Skowno, A., Staude, H., Tolley, K.A., Underhill, L., van der Colff, D., van Noort, S. & von Staden, L. (2016) Biodiversity and Ecological Impacts: Landscape Processes, Ecosystems and Species. *In:* Scholes, R., Lochner, P., Schreiner, G., Snyman-Van der Walt, L. & de Jager, M (Eds.), *Shale Gas Development in the Central Karoo: A Scientific Assessment of the Opportunities and Risks*. CSIR, Pretoria, pp. 7-1–7-72.

Karsch, F. (1879) Zur Theraphosiden-Gattung Moggridgea. *Zeitschrift für die Gesammten Naturwissenschaften*, 52, 383–385.

Koch, C.L. (1842) Zeh'sche Buchhandlung, Nürnberg, Neunter Band. *Die Arachniden*, 98.

Mitchell, S., Sole, C. & Lyle, R. (2020) Teratological cases of the ocular patterns in the South African endemic trapdoor spider genus *Stasimopus* Simon (1892) (Araneae, Mygalomorphae, Stasimopidae). *African Zoology*, 55, 363–367. https://doi.org/10.1080/15627020.2020.1842241

Montes de Oca, L., Indicatti, R.P., Opatova, V., Almeida, M., Pérez-Miles, F. & Bond, J.E. (2022) Phylogenomic analysis, reclassification, and evolution of South American nemesioid burrowing mygalomorph spiders. *Molecular Phylogenetics and Evolution*, 168, 107377. https://doi.org/10.1016/j.ympev.2021.107377

© University of Pretoria

Newton, L.G., Starrett, J., Hendrixson, B.E., Derkarabetian, S. & Bond, J.E. (2020) Integrative species delimitation reveals cryptic diversity in the southern Appalachian *Antrodiaetus unicolor* (Araneae: Antrodiaetidae) species complex. *Molecular Ecology*, 29, 2269–2287. https://doi.org/10.1111/mec.15483

Opatova, V., Bond, J.E. & Arnedo, M.A. (2013) Ancient origins of the Mediterranean trap-door spiders of the family Ctenizidae (Araneae, Mygalomorphae). *Molecular Phylogenetics and Evolution*, 69, 1135–1145. https://doi.org/10.1016/j.ympev.2013.08.002

Opatova, V., Hamilton, C.A., Hedin, M., de Oca, L.M., Král, J. & Bond, J.E. (2019) Phylogenetic Systematics and Evolution of the Spider Infraorder Mygalomorphae Using Genomic Scale Data. *Systematic Biology*, 69 (4), 671–707. https://doi.org/10.1093/sysbio/syz064

Pickard-Cambridge, O. (1889) On some new species and a new genus of Araneida. *Proceedings of the Zoological Society of London*, 57, 34–46. https://doi.org/10.1111/j.1469-7998.1889.tb06745.x

Pocock, R.I. (1897) On the Spiders of the Suborder Mygalomorphae from the Ethiopian Region contained in the Collection of the British Museum. *Proceedings of the Zoological Society of London*, 65, 724–774. https://doi.org/10.1111/j.1096-3642.1897.tb03116.x

Pocock, R.I. (1900) Some new Arachnida from Cape Colony. *Annals and Magazine of Natural History*, 7, 316–333. https://doi.org/10.1080/00222930008678382

Pocock, R.I. (1901) Descriptions of some new African Arachnida. *Annals and Magazine of Natural History*, 7, 284–288. https://doi.org/10.1080/00222930108678472

Pocock, R.I. (1902a) Descriptions of some new species of African Solifugae and Araneae. *Annals and Magazine of Natural History*, 10, 6–27. https://doi.org/10.1080/00222930208678627

Pocock, R.I. (1902b) Some new African spiders. *Annals and Magazine of Natural History*, 7, 315–330. https://doi.org/10.1080/00222930208678678

Posada, D. (2008) jModelTest: Phylogenetic model averaging. *Molecular Biology and Evolution*, 25, 1253–1256. https://doi.org/10.1093/molbev/msn083

Purcell, W.F. (1902) New South African trap-door spiders of the family Ctenizidae in the collection of the South African Museum. *Transactions of the South African Philosophical Society*, 11, 348–382. https://doi.org/10.1080/21560382.1900.9525972

Purcell, W.F. (1903a) New Arachnida collected by Mr. S. C. Cronwright Schreiner at Hanover, Cape Colony. *Annals of the South African Museum*, 3, 13–40.

Purcell, W.F. (1903b) New South African spiders of the families Migidae, Ctenizidae, Barychelidae Dipluridae, and Lycosidae. *Annals of the South African Museum*, 3, 69–142.

© University of Pretoria

Purcell, W.F. (1908) Araneae (I). *In:* Schultze, L. (Ed.), *Zoologische und anthropologische Ergebnisse einer Forschungsreise im westlichen und zentralen Südafrika*. Denkschriften der Medizinisch-Naturwissenschaftlichen Gesellschaft zu Jen, pp. 203–246.

De Queiroz, K. (2007) Species Concepts and Species Delimitation. *Systematic Biology*, 56, 879–886. https://doi.org/10.1080/10635150701701083

Raven, R.J. (1985) The spider infraorder Mygalomorphae (Araneae): cladistics and systematics. *Bulletin of the American Museum of Natural History*, 182, 1–180.

Ríos Tamayo, D. & Lyle, R. (2020) The South African genus *Lepthercus* Purcell, 1902 (Araneae: Mygalomorphae): phylogeny and taxonomy. *Zootaxa*, 4766, 261–305. https://doi.org/10.11646/zootaxa.4766.2.2

Rix, M.G., Huey, J.A., Cooper, S.J.B., Austin, A.D. & Harvey, M.S. (2018) Conservation systematics of the shield-backed trapdoor spiders of the nigrum-group (Mygalomorphae, Idiopidae, *Idiosoma*): integrative taxonomy reveals a diverse and threatened fauna from south-western Australia. *ZooKeys*, 756, 1–121. https://doi.org/10.3897/zookeys.756.24397

Roewer, C.F. (1942) Katalog der Araneae von 1758 bis 1940. *Bremen*, 1, 1–1040.

Ronquist, F. & Huelsenbeck, J.P. (2003) MrBayes 3: Bayesian phylogenetic inference under mixed models. *Bioinformatics*, 19, 1572–1574. https://doi.org/10.1093/bioinformatics/btg180

Roth-Monzón, A.J., Mendoza-Hernández, A.A. & Flores-Villela, O. (2018) Amphibian and reptile biodiversity in the semi-arid region of the municipality of Nopala de Villagrán, Hidalgo, Mexico. *PeerJ*, 6, e4202. https://doi.org/10.7717/peerj.4202

Satler, J.D., Carstens, B.C. & Hedin, M. (2013) Multilocus Species Delimitation in a Complex of Morphologically Conserved Trapdoor Spiders (Mygalomorphae, Antrodiaetidae, *Aliatypus*). *Systematic Biology*, 62, 805–823. https://doi.org/10.1093/sysbio/syt041

Simon, E. (1892) Histoire naturelle des araignées. *Deuxième édition, tome premier*, 1–256. https://doi.org/10.5962/bhl.title.51973

Stamatakis, A. (2014) RAxML version 8: a tool for phylogenetic analysis and post-analysis of large phylogenies. *Bioinformatics*, 30, 1312–1313. https://doi.org/10.1093/bioinformatics/btu033

Stamatakis, A., Hoover, P., Rougennant, J. & Renner, S. (2008) A rapid bootstrap algorithm for the RAxML web servers. *Systematic Biology*, 57, 758–771. https://doi.org/10.1080/10635150802429642

Thorell, T. (1887) Viaggio di L. Fea in Birmania e regioni vicine. II. Primo saggio sui ragni birmani. *Annali del Museo Civico di Storia Naturale di Genova*, 25, 5-417

Tucker, R.W.E. (1917) On some South African Avicolariidae (Arachnida). Families Migidae, Ctenizidae, Diplotheleae and Dipluridae. *Annals of the South African Museum*, 17, 79–138.

© University of Pretoria

Wilson, J.D., Bond, J.E., Harvey, M.S., Ramírez, M.J. & Rix, M.G. (2023) Correlation with a limited set of behavioural niches explains the convergence of somatic morphology in mygalomorph spiders. *Ecology and Evolution*, 13. https://doi.org/10.1002/ece3.9706

World Spider Catalog (2022) World Spider Catalog Version 23.5. Natural History Museum Bern. Available from: http://wsc.nmbe.ch (accessed 19 July 2022)

Yeates, D.K., Seago, A., Nelson, L., Cameron, S.L., Joseph, L. & Trueman, J.W.H. (2011) Integrative taxonomy, or iterative taxonomy? *Systematic Entomology*, 36, 209–217. https://doi.org/10.1111/j.1365-3113.2010.00558.x

© University of Pretoria

Supplementary material

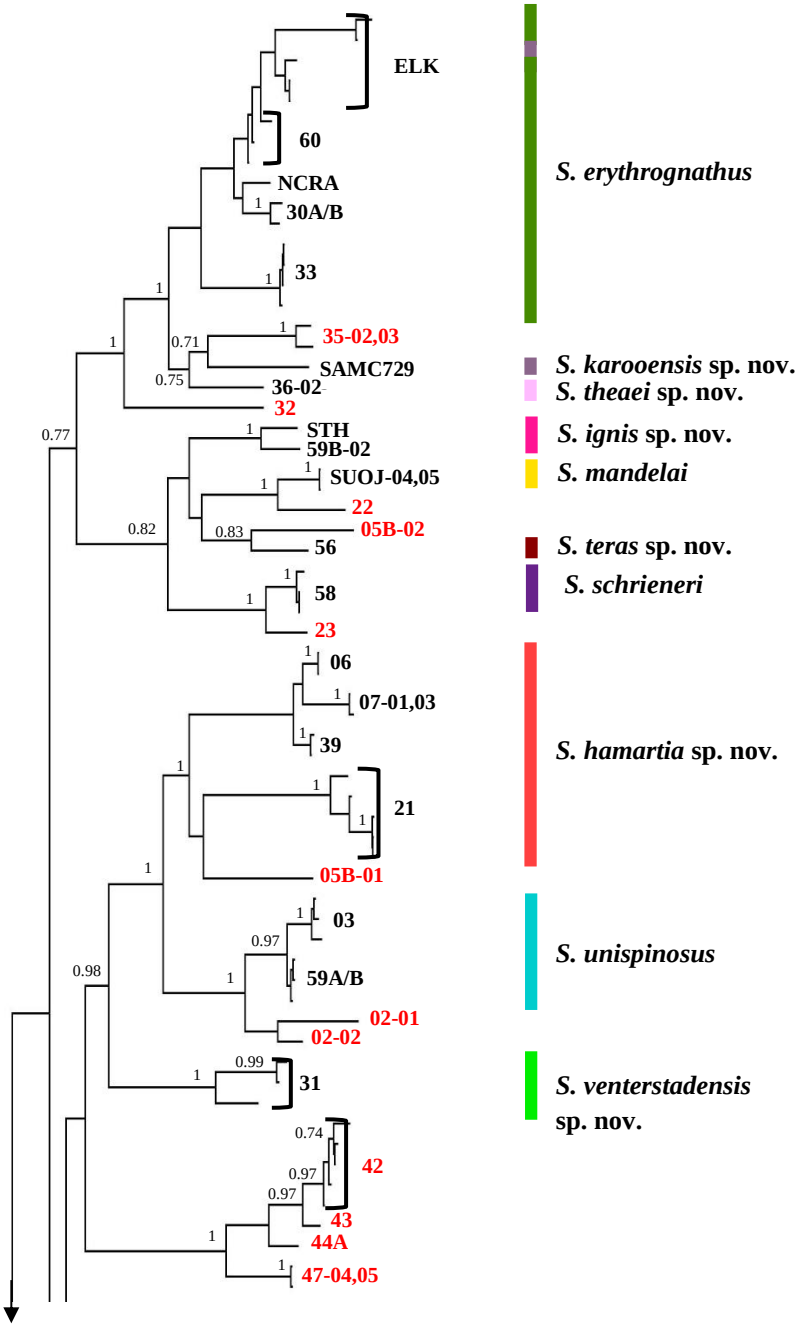


Figure S1 (part A). Bayesian Inference consensus tree for the concatenated dataset of CO1, 16S and EF-1ɣ for the Stasimopus dataset from the Karoo. All Stasimopus specimens are included. Juveniles that could not be morphologically or genetically identified are indicated in red. Posterior probabilities above 0.7 are given on the corresponding node. The numbers for each specimen correspond to localities in figure 1.

© University of Pretoria

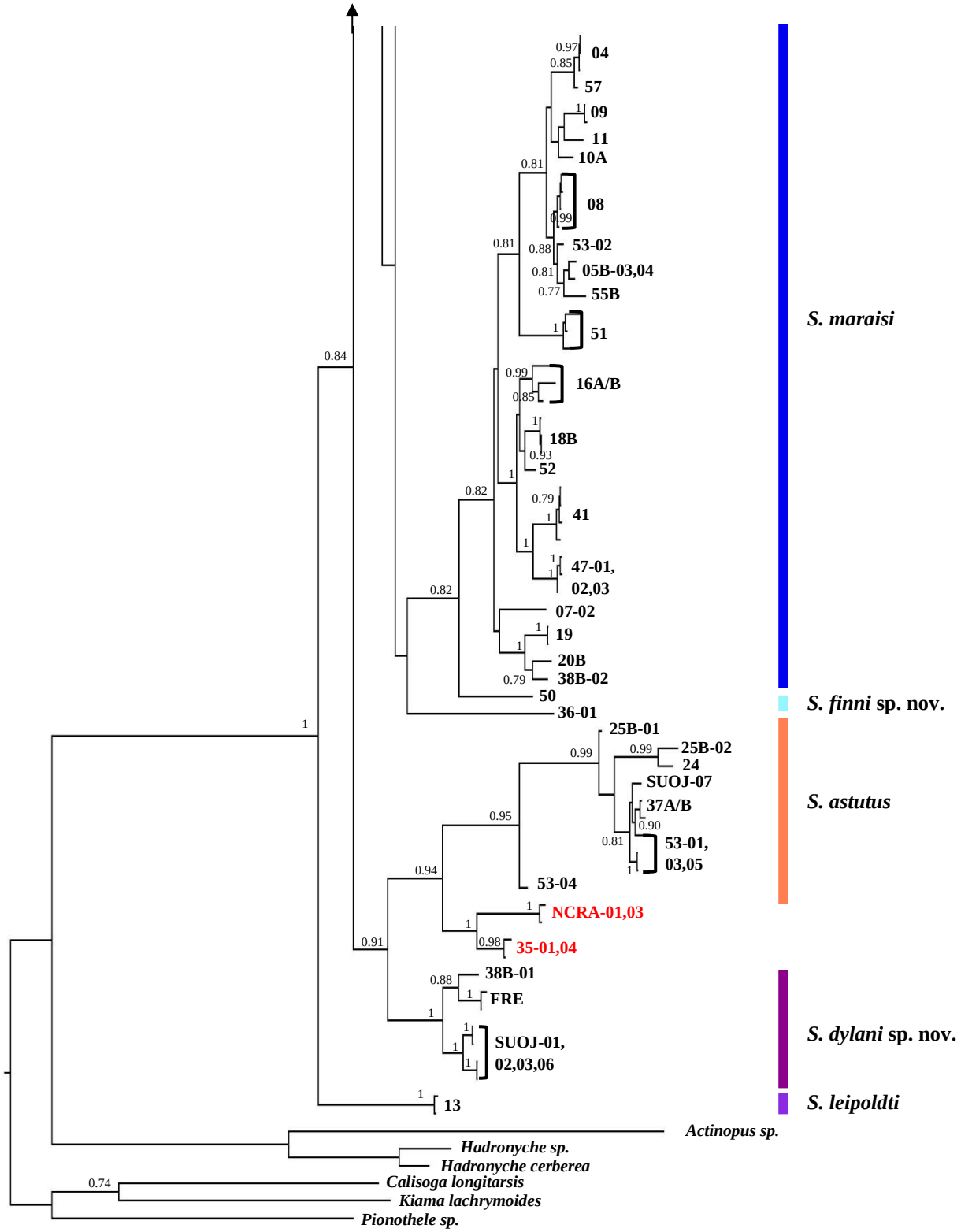


Figure S1 (part B). Bayesian Inference consensus tree for the concatenated dataset of CO1, 16S and EF-1ɣ for the *Stasimopus* dataset from the Karoo. All *Stasimopus* specimens are included. Juveniles that could not be morphologically or genetically identified are indicated in red. Posterior probabilities above 0.7 are given on the corresponding node. The numbers for each specimen correspond to localities in figure 1.

© University of Pretoria

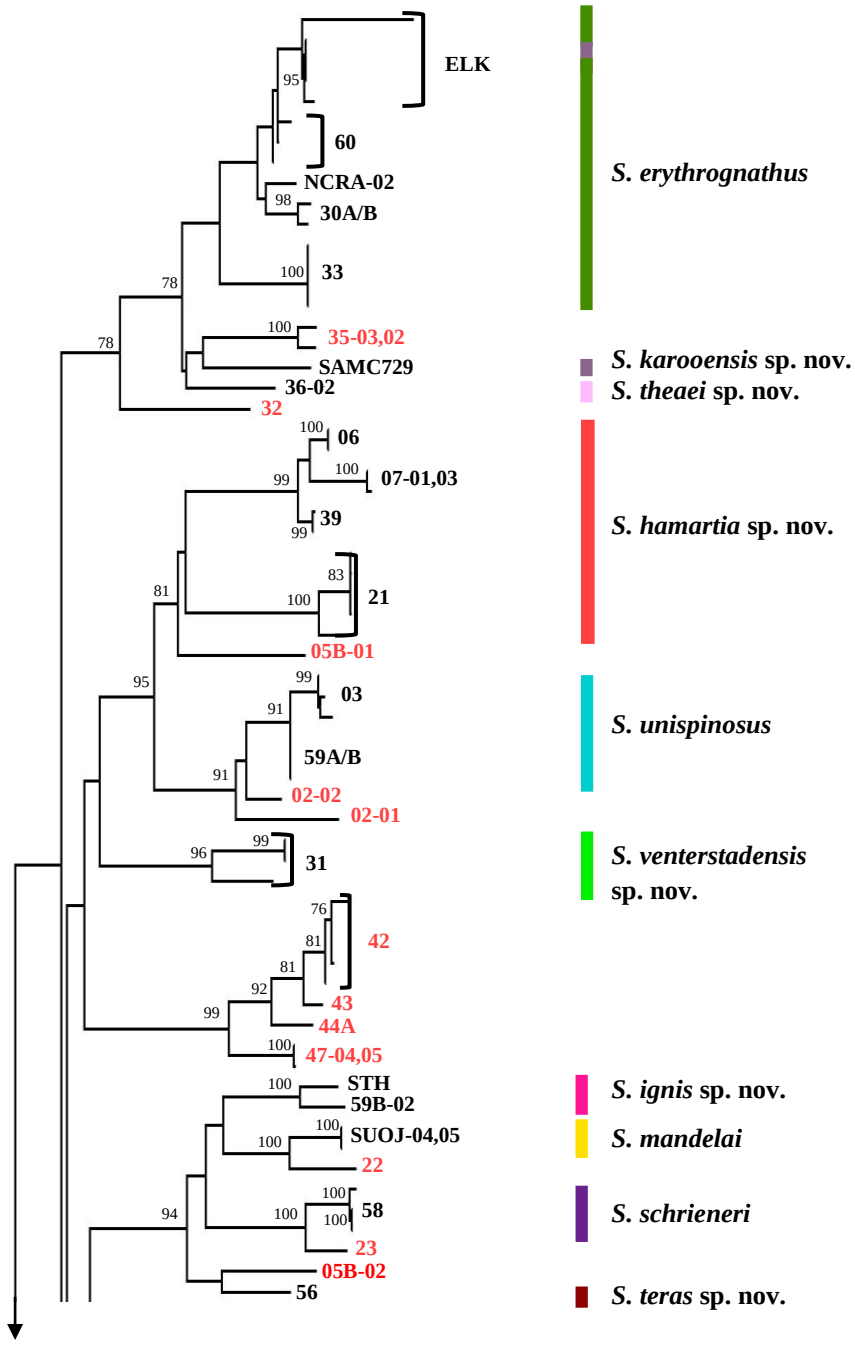


Figure S2 (part A). Maximum likelihood consensus tree for the concatenated dataset of CO1, 16S and EF-1ɣ for the *Stasimopus* dataset from the Karoo. All *Stasimopus* specimens are included. Juveniles that could not be morphologically or genetically identified are indicated in red. Bootstrap support values above 70 are given on the corresponding node. The numbers for each specimen correspond to localities in figure 1.

© University of Pretoria

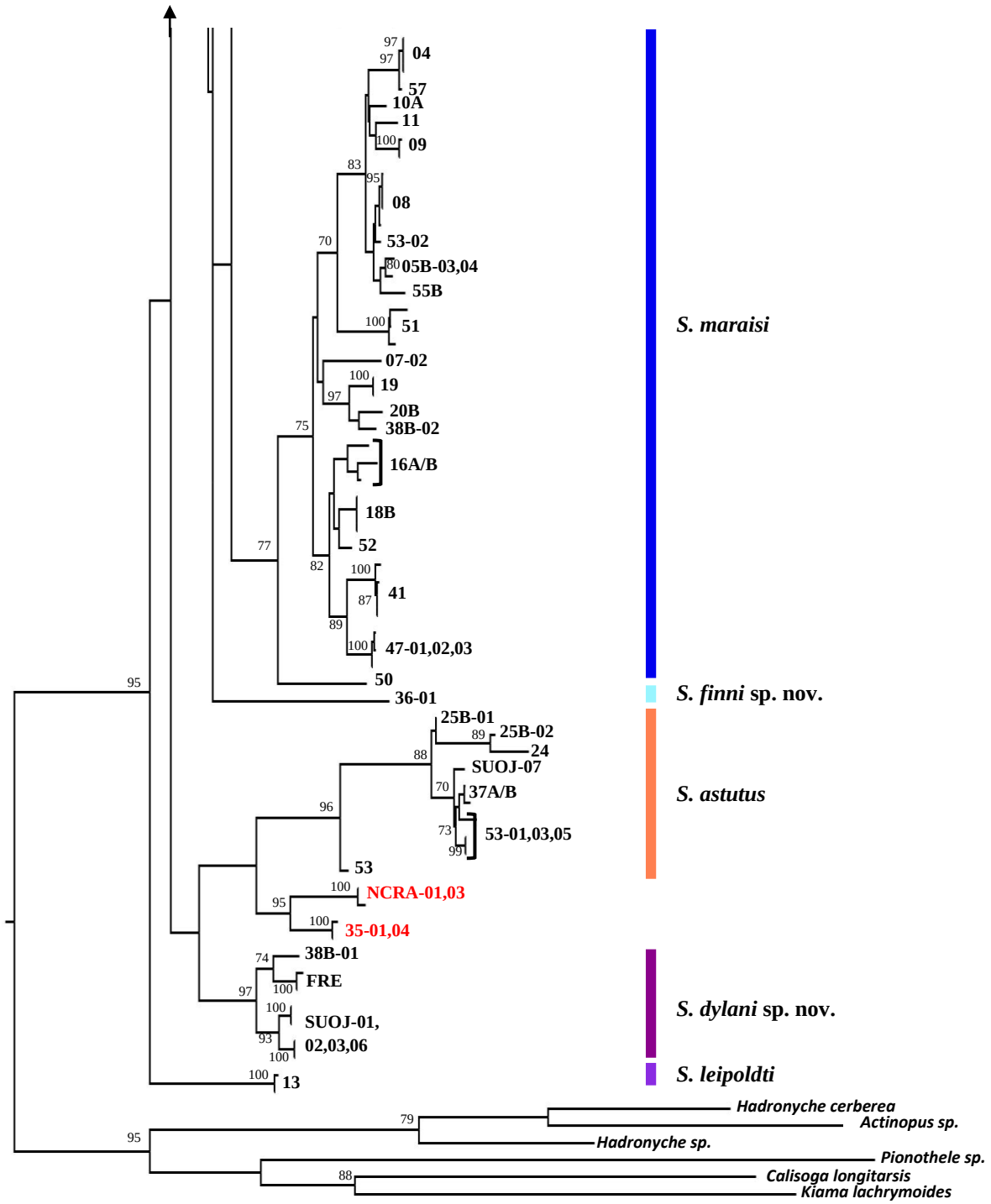


Figure S2 (part B). Maximum likelihood consensus tree for the concatenated dataset of CO1, 16S and EF-1ɣ for the *Stasimopus* dataset from the Karoo. All *Stasimopus* specimens are included. Juveniles that could not be morphologically or genetically identified are indicated in red. Bootstrap support values above 70 are given on the corresponding node. The numbers for each specimen correspond to localities in figure 1.

© University of Pretoria

Chapter 5

Phylogeography and diversification of an endemic trapdoor spider genus, *Stasimopus* Simon 1892 in the Karoo

Shannon Brandt[1], Robin Lyle[2] and Catherine L. Sole[1]

[1] *Department of Zoology and Entomology, University of Pretoria, Hatfield, Pretoria, South Africa*

[2] *Agricultural Research Council – Plant Health and Protection, Biosystematics, Roodeplaat, Pretoria, South Africa*

This data chapter will be submitted as:

Brandt, S., Lyle, R. L., and Sole, C. L. 2023. Phylogeography and diversification of an endemic trapdoor spider genus, *Stasimopus* Simon 1892 in the Karoo, to Ecology and Evolution.

© University of Pretoria

Abstract

The Karoo region of South Africa has long been neglected, with few studies investigating the fauna and their phylogeographic history in the area. Mygalomorph spiders are prime candidates for these types of studies due to their life history traits. The genus *Stasimopus* is endemic to South Africa but has also never undergone a phylogeographic review. This study aims to unravel the phylogeographic patterns and history of the many *Stasimopus* species which occur in the greater Karoo region. It was found that 15 species occur in the Karoo and that the genus radiation in the area is in the early Paleocene. Most species radiated between the late Eocene and the Miocene. The Tankwa Karoo has been identified as a possible Pleistocene glacial cycle refugia for the species *S. leipoldti*, but this is tentative as it is based on a very small sample size. The species *S. maraisi* was found to have undergone extensive population expansion in the mid-Miocene leading to its extensive modern range. This study highlights the similar phylogeographic histories of Mygalomorph spiders in the arid region of western Australia and that of the Karoo.

Keywords

Araneae, divergence dating, endemic, Karoo, Mygalomorphae, phylogeography, South Africa, *Stasimopus*

© University of Pretoria

Introduction

The Karoo region of South Africa has long been neglected in studies due to the assumption of low biodiversity in semi-arid regions (Roth-Monzón et al., 2018). This began to change in 2015 when a Strategic Environmental Assessment (SEA) was undertaken to produce a report on the state of biodiversity in the region to assist governmental policy-makers in making informed decisions about land use change in the area through the Karoo BioGaps project (Scholes et al., 2016). This became imperative as in previous years pressure for land use change increased due to economic incentives such as mining, farming, renewable energy, intensive shale gas exploration and the Square Kilometre Array (SKA) (Sethusa, 2016). However, to date there are still, few studies on the faunal diversity in the area (Main et al., 2019).

The Karoo region of South Africa has a geologically rich history. The Karoo basin of South Africa in combination with four other basins globally form the Gondwanan foreland basins which were formed by collisions and terrain accretion tectonics along Gondwana's southern edge (Götz & Ruckwied, 2014). The Karoo basin sedimentation dates from the late Carboniferous to the middle Jurassic (323 – 174 MYA) (Johnson et al., 2006). During this time the sedimentation recorded a gradual change from a glacial environment to an arid desert, as South Africa changed in latitude from the polar region to the tropics (Johnson et al., 2006; Meadows & Watkeys, 1999; Tankard et al., 1982b). The Karoo basin is the only basin globally to record this 200 MY change in its sedimentation (Johnson et al., 2006). It spans 700,000 km^2, covering 60 % of South Africa's land surface (Johnson et al., 2006). Only the south-western portion of this is the modern-day Karoo region. Due to the geological history of the basin, it is now of large economic value due to expansive coal deposits (Holness et al., 2016; Johnson et al., 2006).

The modern-day Karoo region of South Africa is an arid/semi-arid area (Henschel et al., 2018). The Karoo comprises two separate biomes, namely Nama Karoo and Succulent Karoo, which are distinguished by climate and vegetation (Henschel et al., 2018). The Nama Karoo is on the central plateau in the western portion of the country (Mucina, Rutherford, et al., 2006). It experiences unreliable summer rainfall with periods of prolonged drought (Desmet & Cowling, 1999; Henschel et al., 2018). The vegetation is dominated by dwarf shrub vegetation which are xeromorphic as well as succulents in the west and grasses in the east (Desmet & Cowling, 1999; Werger, 1978). This is the second largest biome in South Africa covering 260,295 km^2 (Henschel et al., 2018; Mucina, Rutherford, et al., 2006). Due to past land use practices approximately 60 % of the biome has moderate to severe degredation of soils and vegetation (Mucina, Rutherford, et al., 2006). Only 2 % of the entire Nama Karoo biome is under conservation (Henschel et al., 2018). The Succulent Karoo covers a belt from Lüderitz (Namibia) through Namaqualand and includes smaller areas of Hantam, Tanqua (or Tankwa), Roggeveld and the little Karoo (Mucina, Jürrgens, et al., 2006). The biome

© University of Pretoria

experiences reliable winter rainfall (100-200 mm anually) which aids in the sustainability of vegetation (Desmet & Cowling, 1999; Henschel et al., 2018). The vegetation is dominated by succulent plants and following good rains by annuals (Asteraceae and Brassicaceae) (Desmet & Cowling, 1999; Werger, 1978). This biome is the forth largest in South Africa and covers 87,001 km^2 (Henschel et al., 2018; Mucina, Jürrgens, et al., 2006). The succulent Karoo is bordered by the Cape Fold mountains, which caused isolation leading to high levels of endemisim and species richness of many taxa including hopliniid beetles, aculeate Hymenoptera, reptiles and arachnids (Milton & Dean, 1999). The succulent Karoo is also the world's only entirely arid region diversity hotspot (Henschel et al., 2018; Mucina, Jürrgens, et al., 2006). Despite high levels of endemisim and being a biodiversity hotspot, only 8% of the biome is conserved (Henschel et al., 2018).

Stasimopidae is a family of trapdoor spiders endemic to Southern Africa (Opatova et al., 2020). The family consists of one genus, *Stasimopus* and 47 described species (World Spider Catalog, 2022). These spiders have life history traits which make it easy to detect population structuring and dispersal events increasing the likelihood of inferring phylogeographic events. Mygalomorphs are exceptionally long lived for spiders, reportedly living to 43 years old (Mason et al., 2018). Most mygalomorph spiders live in retreats comprising vertical burrows or chambers under rocks or on trees which are lined with silk (Dippenaar-Schoeman, 2002; Mason et al., 2018; Wilson et al., 2023). The females show great fidelity to their burrows, hunting from burrow entrances (Buchli, 2015; Engelbrecht & Prendini, 2011; Satler et al., 2013). The males are nomadic, wandering to locate females to mate with and are thus responsible for nuclear gene flow between populations. The offspring, once mature enough, will leave the mothers burrow but only move a few meters before making a new burrow to live in (Satler et al., 2013). This combination of behaviours leads to extensive population structuring and isolated geographic locations for the populations (Rix et al., 2017). These characteristics are often associated with species which are classified as 'short range endemics', which if found to be true for the species of the genus, may make them of conservation concern. *Stasimopus* and other mygalomorph spiders are model species for phylogeographic studies due to these factors (Ferretti et al., 2014; Hedin et al., 2013, 2015; Kremen et al., 1993; Leavitt et al., 2015; Newton et al., 2020; Rix et al., 2017; Satler et al., 2013; Wilson et al., 2018). Performing this study on the *Stasimopus* genus, could possibly serve as a proxy for other mygalomorph spiders living under similar environmental conditions.

Several phylogeographic studies have been performed on Mygalomorphae species, but none have to date been performed in South Africa, nor on the *Stasimopus* genus (Beavis et al., 2011; Beavis & Rowell, 2006; Cooper et al., 2011; Ferretti et al., 2014; Graham et al., 2015, 2020; Hamilton et al., 2011; Harrison et al., 2017; Hedin et al., 2013, 2015; Hendrixson & Bond, 2007; Kornilios et al., 2016; Opatova et al., 2013, 2016, 2020; Rix et al., 2017; Starrett et al., 2018; Starrett & Hedin, 2007; Wilson et al., 2018). Phylogeographic inference is of immense importance to conservation as there is

© University of Pretoria

the possibility of defining areas for conservation based on the evolutionary potential of various taxa (Rolland et al., 2011). This is vital in light of the sensitivity of the Karoo ecosystem, the life history of *Stasimopus* and the drastic land-use and climate change predicted for the area.

The aims of this study are threefold; first, to create a dated phylogeny for the *Stasimopus* species occurring in the Karoo region using CO1, 16S and EF-1ɣ genes. This will be used to understand the diversification of the genus over geological time. Second, using haplotype networks to understand the distribution of genetic diversity in the landscape. Lastly, evaluating the phylogeographic pattern underlying the phylogeny and assessing the potential drivers thereof.

Materials and Methods

Taxon sampling

Stasimopus specimens were collected from part of the Great Karoo, South Africa. The area is within the demarcated area for potential shale gas fracking. The boundary of the area is set approximately by the following coordinates: -30.88688, 26.29295 and -33.03079, 20.01661 (Figure 1). Sites were selected by the Karoo BioGaps team to cover the range of environmental conditions present in the region and within each site drainage line habitats were targeted for sampling as they are favoured by trapdoor spiders. *Stasimopus* specimens were collected at 55 sites. At each site four people spent one-hour, thereby four man-hours soil scraping. Soil scraping involves removing the top layer of soil to expose burrow entrances. Once entrances were exposed, the burrows were excavated using a hand shovel, taking care to not injure the specimens. This methodology was effective for collecting female and juvenile specimens. In order to collect male specimens, road cruising was done after rain in the evenings. This involves slowly driving on isolated roads with torches to find males which are crossing in search of potential mates. All specimens were preserved in a solution of cold alcohol and kept in an ice box. Specimens were later preserved in 80% ethanol in glass polytop vials for long term storage. All locality information is available in Chapter 2 - Table S1. All newly collected material was deposited in the National Collection of Arachnida (NCA) of the Agricultural Research Council (ARC), Roodeplaat, South Africa.

Sequence data generation

The genetic sequences used in this study were generated in Chapter 2. For the methodology, please consult that chapter, accession numbers for all sequences used are supplied in Chapter 2 - Table S1.

© University of Pretoria

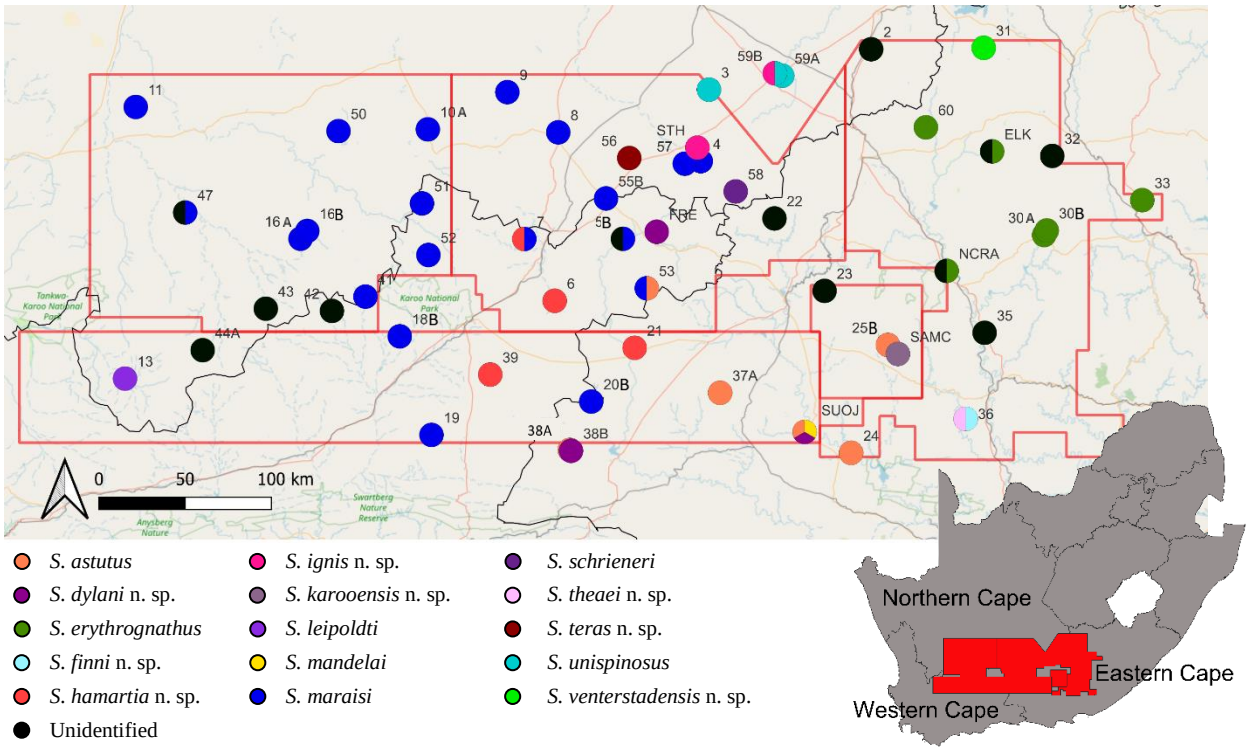


Figure 1. Map of the study area in the greater Karoo, in the south-western part of South Africa. Markers indicate the 55 sites where *Stasimopus* specimens were found. If sites were near one another, they are denoted as 'a' and 'b'. The localities are coloured according to the species found there. Red polygons indicate areas identified for shale gas exploration. Map created in QGIS version 3.4.8-Madeira (2019), available at: http://qgis.osgeo.org.

Divergence dating

Dating the phylogeny was done using BEAST v1.8.4 (Suchard et al., 2018). All identical sequences were removed from the analysis. In order to determine the most appropriate fossil calibration points, numerous combinations were tested varying the fossil calibrations used, as explained in Appendix A.

The final fossil calibration points used were as follows: the Hexathelidae fossil, *Rosamygale grauvogely* (Gresa-Voltzia formation, France, Triassic) (Dunlop et al., 2020; Opatova et al., 2020; Selden & Gall, 1992). *Rosamygale grauvogely* is thus, the first mygalomorph appearance in the fossil record, dating to 250 – 240 MYA (Opatova et al., 2020). The Nemesiidae fossil, *Cretamygale chasei* (Isle of Wight, Cretaceous) (Selden, 2002), two Ctenizidae/Halonoproctidae fossils, *Ummidia damzeni* and *U. malonowskii* (both from Baltic amber, Palaeogene) (Wunderlich, 2000). Lastly, a fossil from the family Cyrtaucheniidae, *Bolostromus destructus* (Dominican amber, Neogene) (Dunlop et al., 2020; Wunderlich, 1998). Each family was represented by available sequence data from GenBank for 16S rDNA, cytochrome oxidase 1 (CO1) and elongation factor 1 gamma (EF-1ɣ) (Table S1). Each calibration point was set by setting a hard minimum bound (the youngest possible age of the fossil based on the deposit in which it was found) and a soft upper bound (the oldest

© University of Pretoria

possible age). The nucleotide substitution rate was determined using jModelTest v2.1.7 (Posada, 2008). This was done for each gene region and the best model to account for varying base pair substitution rates was selected based on the Bayesian information criterion (BIC) (Posada, 2008). This was used to set the prior in BEAUTi v1.8.4 (Suchard et al., 2018). Other priors set included, the rate of molecular evolution to a relaxed clock with a lognormal distribution (this allows mutational rates to vary over the tree) (Michonneau, 2017). As the dataset includes intraspecific and interspecific sampling the study follows the protocol of (Hedin et al., 2013) by testing four different tree priors. All analyses were thus repeated using 'Speciation: Birth-Death Incomplete Sampling', 'Speciation: Birth-Death', 'Speciation: Yule Process' and 'Coalescent: Constant Size' at tree priors. This allowed testing at both the population level of diversity and species level diversity. An uncorrelated relaxed clock was used, as this allows for each branch of the phylogeny to have a different evolutionary rate (Drummond et al., 2006). BEAST was then run for 200,000,000 (250,000,000 for the yule model) generations and sampled every 5000 generations. This was repeated twice for each analysis to ensure convergence. BEAST was run in conjunction with BEAGLE (Ayres et al., 2012).

Tracer v1.7.1 was used to confirm convergence (Rambaut et al., 2018). This was tested by checking the log file for each BEAST run and ensuring the ESS values were above 200. The individual runs were then compiled to ensure a normal distribution. Log Combiner v1.8.4 (Suchard et al., 2018) was used to combine the multiple tree files into one file. The subsampling number was set to 50,000 and the burn-in for each tree to 50,000,000.

The tree files viewed, annotated and edited in FigTree (Rambaut, 2016).

Demography analyses

DNA sequence polymorphism (DnaSP) v6.12.03 (Rozas et al., 2017) was used to gather baseline statistics of gene region for each species with more than four representatives. Ambiguous nucleotides were removed, and all other settings left on default. The basic statistics recorded were as follows: nucleotide diversity (π), gene diversity (H_d), number of haplotypes (H), mean number of pairwise differences (k) and number of segregating sites (S). Tajima's test and Fu and Li's tests were also run (Graham et al., 2020). Tajima's D compares the number of segregating sites (S) and the mean pairwise differences between different sequences (Ramírez-Soriano et al., 2008; Tajima, 1989). Fu and Li's D* is similar but compares the total amount of nucleotide variations to the number of singleton mutations, this was done without an outgroup (Fu & Li, 1993; Ramírez-Soriano et al., 2008). Both tests are statistical tests of neutrality and are used to determine historic population demographic changes (Graham et al., 2020; Ramírez-Soriano et al., 2008).

© University of Pretoria

Haplotype networks

DnaSP was also used to prepare the sequence data for input into Network v5.0.0.0 (Fluxus-engineering.com, 2019) in order to construct haplotype networks. The 16S data was exported in Rdf format with gaps/missing data not considered, whereas the coding regions (CO1 and EF-1ɣ) were exported with gaps considered. In order to accurately estimate the relationship between closely related *Stasimopus* individuals of the same species (which have not yet undergone speciation), a haplotype network was constructed in Network. The Network software uses the method of Maximum Parsimony to select the shortest and least complex tree. The haplotype network was constructed using the median-joining (MJ) network algorithm. This allows for multistate data (A, T, G, C or N at any nucleotide position) (Bandelt et al., 1999). All settings for network calculation were left on default. The post-processing option of Maximum parsimony was used in order to remove all unnecessary median vectors.

Pie charts of haplotypes were plotted onto a map of the Karoo region using the coordinates of each locality. This allowed for the visualisation of the different haplotypes in geographic space.

Mantel test and isolation by distance

A mantel test was performed to determine if geographic distance and genetic distance are correlated. This determines if there is isolation by distance. A distance matrix for the sampling localities was constructed by determining the distance between each set of coordinates using the online tool, Movable Type Scripts: Calculate distance, bearing and more between Latitude/Longitude points (Available at: https://www.movable-type.co.uk/scripts/latlong.html) (Veness, 2019). This tool uses the haversine formula to calculate the distance between coordinate pairs (Veness, 2019). A distance matrix was constructed from the pairwise genetic distance for the CO1 dataset (as this is the most complete dataset) using Mega 7 (Kumar et al., 2016).

The Mantel test was conducted for two different datasets in R (R Core Team, 2017), using the packages ‘Ade4’ (Dray et al., 2018) and ‘vegan’ (Oksanen et al., 2019) and were both run for 10,000 permutations. First was to determine if there is genetic isolation for each locality, this thus included the 48 localities for which CO1 data is available and one representative sequence per locality, in their respective distance matrix. The second test was to test if there is isolation by distance across the various species, for this, localities which were at the edges of the species distribution were chosen across the various species. The specimens used are available in Table S2.

© University of Pretoria

Results

Divergence dating

The dated phylogeny for the *Stasimopus* genus in the Karoo can be seen in Figure 2. Samples indicated in red text could not be identified to species level as they are juveniles. Divergence estimates indicate that the genus *Stasimopus* in the Karoo dates to between 48.30 - 84.15 MYA, towards the beginning of the Paleocene under the birth-death speciation model (Figure 2, node i). This range is shared by the birth-death incomplete and coalescent models (Figures S1 and S2). The yule speciation model gives older node ages across the entire phylogeny (Figure S3, Table 1). Due to the consistent dating of the birth-death, birth-death incomplete and coalescent models, the discussion will revolve around these dates.

The phylogeny is divided into 11 clades for the ease of discussion (labelled A - K). Clade A is the oldest clade across all models. This clade is well supported and consists of a species complex of *S. erythrognathus* and *S. karooensis* n. sp. as well as a single individual representing *S. theaei* n. sp. This clade is dated to 24.13 – 50.25 MYA (Figure 2, node ii). The age of the species complex is younger 9.36 - 22.35 MYA (Figure 2, node iii), the inclusion of *S. theaei* n. sp. and the unidentified samples make the clade significantly older. Clade B is a well-supported monophyletic clade, consisting of *S. astutus* and *S. finni* n. sp. The species *S. astutus* is young from the Miocene (6.89- 16.46 MYA) (Figure 2, node iv), but Clade B is dated between 22.69 - 50.78 MYA due to the inclusion of *S. finni* n. sp. (Figure 2, node v). Clade C is dated within the Oligocene, the individual species cannot be accurately dated due to small sample sizes. *Stasimopus dylani* n. sp. (Clade D) (Figure 2, node vi), *S. venterstadensis* n. sp. (Clade I) (Figure 2, node iiv) and *S. unispinosus* (Clade H) (Figure 2, node iiiv) are all dated to the Miocene. Clade F (*S. maraisi*) is one of the older species dated between 16.2 – 39.32 MYA (Figure 2, node ix), followed by clade G (*S. hamartia* n. sp.) between 22.53 – 43.56 MYA (Figure 2, node x). *Stasimopus leipoldti* (Clade K) is very recently diverged in the Pleistocene (Figure 2, node xi). This may however, be inaccurate due to the small sample size and that the samples are from the same locality. Clades E and J are comprised of only unidentifiable juveniles. It is however apparent that these specimens likely comprise separate species.

© University of Pretoria

Table 1. Comparison of the divergence dates for the various clades (indicated on figure 2), and species under different speciation models (tree priors) in BEAST. The mean date estimates are given in millions of years (Ma) and the confidence intervals (based on the 95% highest posterior density – HPD) are given in parentheses. The species complex referred to is that between *S. erythrognathus* and *S. karooensis* n. sp.

Clade / lineage	**Birth-death (Ma)**	**Birth-death incomplete (Ma)**	**Coalescent (Ma)**	**Yule (Ma)**
Karoo Genus	64.30 (48.30-84.15)	64.31 (48.12-83.36)	59.53 (44.62-76.51)	94.89 (66.70-130.74)
A	37.38 (26.37-50.25)	37.54 (26.47-50.24)	34.11 (24.13-45.35)	54.24 (36.75-77.67)
B	36.86 (24.92-50.78)	36.99 (24.75-50.59)	31.22 (22.69-40.72)	50.97 (32.03-73.54)
C	34.31 (24.64-45.27)	34.39 (24.89-45.12)	33.65 (22.34-45.93)	50.17 (34.61-71.17)
D	20.66 (13.20-29.55)	20.69 (13.25-29.37)	18.71 (12.07-26.65)	29.59 (17.18-46.46)
E	18.31 (12.03-25.99)	18.30 (11.78-25.83)	16.57 (10.77-23.29)	26.77 (15.40-41.66)
F (*S. maraisi*)	27.30 (17.83-39.26)	27.37 (18.11-39.32)	24.78 (16.20-35.19)	40.34 (23.11-63.37)
G (*S. hamartia* n. sp.)	32.36 (22.61-43.01)	32.55 (22.97-43.56)	29.55 (20.53-39.41)	43.85 (30.09-63.41)
H (*S. unispinosus*)	16.90 (10.63-24.53)	16.94 (10.40-24.56)	15.36 (9.40-21.96)	24.38 (13.78-39.45)
I (*S. venterstadensis* n. sp.)	11.25 (6.01-17.75)	11.28 (6.20-17.82)	10.21 (5.51-15.92)	16.70 (7.66-31.49)
J	18.99 (12.44-27.42)	19.01 (12.41-27.23)	17.31 (11.37-24.44)	29.19 (16.84-48.28)
K (*S. leipoldti*)	0.57 (0.01-1.75)	0.57 (0.01-1.73)	0.51 (0.01-1.57)	0.94 (0.24-3.21)
**Species complex*	15.76 (10.19-22.35)	15.79 (10.18-22.34)	14.22 (9.36-20.12)	23.34 (14.28-50.88)
S. astutus	11.57 (7.47-16.46)	11.58 (7.58-16.38)	10.49 (6.89-14.74)	17.37 (9.92-28.48)
S. dylani n. sp.	10.29 (6.36-15.29)	10.31 (6.37-15.29)	9.34 (5.77-13.66)	16.07 (8.68-26.80)

© University of Pretoria

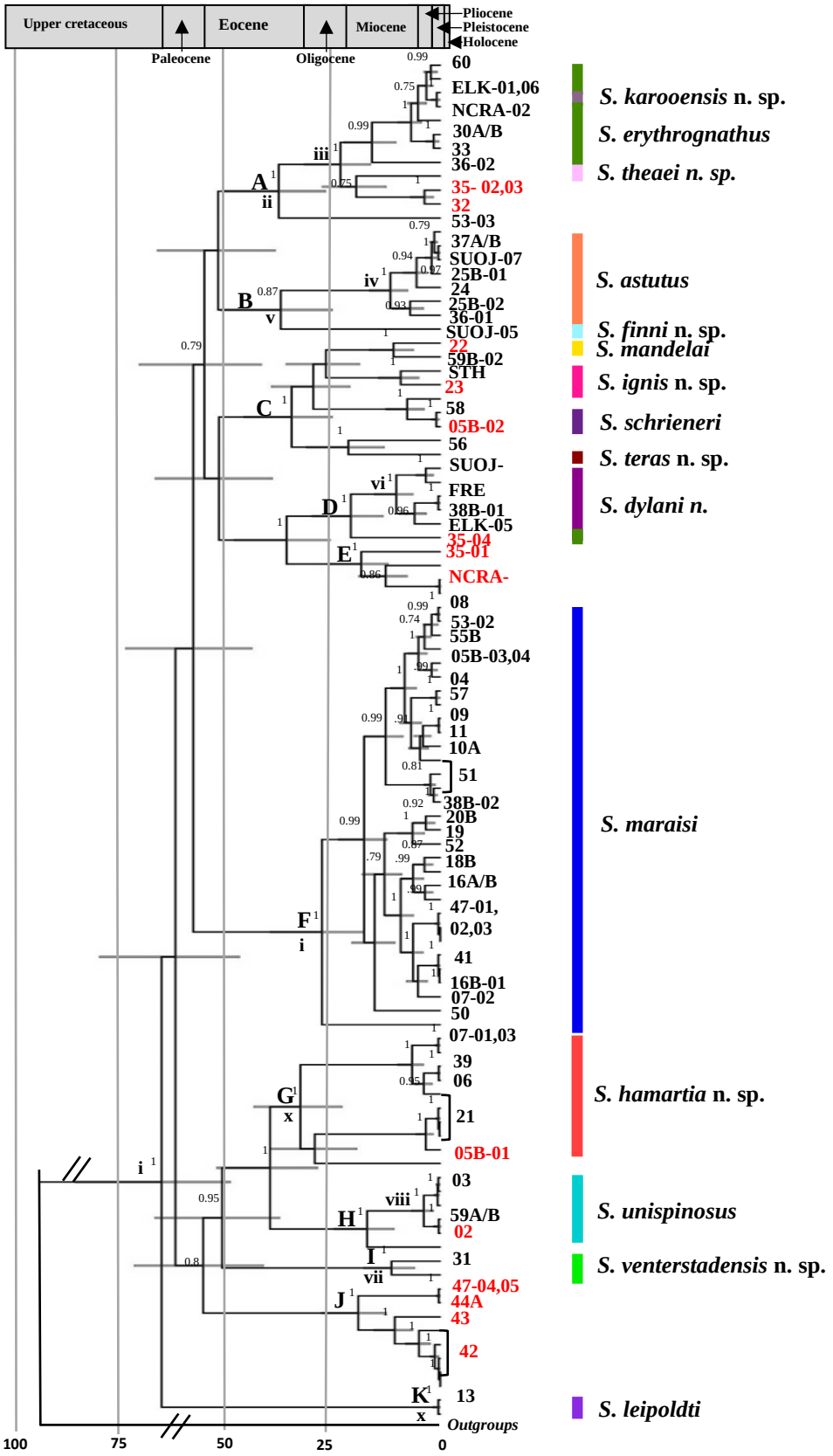


Figure 2. Maximum clade credibility tree from the BEAST analysis of CO1, 16S and EF-1γ for the *Stasimopus* specimens occurring in the Karoo under the birth-death speciation model. The grey bars indicate the confidence intervals for the dating. Outgroups available in table S1. Posterior probabilities above 0.70 are given on the corresponding nodes. Specimen numbers correspond to localities in Figure 1, and red specimens indicate juveniles which could not be identified. Identified species are indicated by the coloured bars. Clades are numbered for the ease of discussion. Discussed nodes are indicated by roman numerals.

© University of Pretoria

Demographic history

The haplotypes and demographic results for CO1 are presented in Figure 3 and Table 2 and the data for 16S and EF-1ɣ in Figures S4, S5 and Tables S3, S4, respectively. The haplotype networks are largely in agreement with the phylogeny, except for the placement of the *S. venterstadensis* n. sp. (Clade I, light green) individuals in the CO1 network (Figure 3) which are split and group with *S. maraisi* (Clade F, dark blue) and *S. astutus* (Clade B, coral) separately. The species complex of clade A (Figure 2) appears to be present across all three haplotype networks. The networks reveal that there is a higher degree of genetic differentiation in the CO1 gene within species than the other two gene regions, this is apparent from the higher number of mutational steps between haplotypes. EF-1ɣ consistently has the least number of mutational steps between haplotypes within species. This is further substantiated by the differences in *k*, *S* and π values across the three gene regions for each species (Table 2, Tables S3 and S4). This should however be interpreted with caution as all sample sizes (except for *S. maraisi*) are quite low.

The haplotype diversity is high across all species considered for the CO1 gene region (Table 2). *Stasimopus unispinosus* has a lower haplotype diversity for the 16S and EF-1ɣ regions, both of 0.6 (Tables S3 and S4). Nucleotide diversity is relatively low across species and gene regions (>0.1) (Table 2, S3 and S4).

In the EF-1ɣ network (Figure S5) the *S. maraisi* network shows a clear expansion pattern, but this is not shown in the other two gene regions. This expansion of *S. maraisi* for the EF-1ɣ gene region is further proven by the significant negative result of the Tajima's D (-1.825*) and Fu & Li's D* (-3.140*) statistics. The only other significant result is for *S. hamartia* n. sp. for 16S, where Fu & Li's D* is significant (1.418).

There is clear phylogeographic structuring across all three gene regions. Most species appear to be isolated to one or a few locations, except for *S. maraisi* which is widespread across the region. *Stasimopus leipoldti* was only found in one location in the Tankwa Karoo, but the type locality for the species is Clanwilliam (Western Cape), over 150 km away. A similar trend is seen for *S. erythrognathus* which was in found in the eastern Karoo, but the type locality is Worcester (Western cape), 700 km away.

There are many species occurring sympatrically at multiple locations. These include *S. maraisi* and *S. hamartia* n. sp.; *S. maraisi* and *S. dylani* n. sp.; *S. theaei* n. sp. and *S. finni* n. sp.; *S. erythrognathus* and *S. karooensis* n. sp.; *S. astutus*, *S. mandelai* and *S. dylani* n. sp.; *S. maraisi* and Clade J. Clade J likely comprises a new species based on the degree of genetic variation, but no adults were found to confirm their identity.

© University of Pretoria

Table 2. Demographic parameters for the CO1 gene region for the *Stasimopus* of the Karoo region. The number of sequences (n), nucleotide diversity (π), haplotypes (H), gene diversity (H_d), mean number of pairwise differences (k) and segregating sites (S) (out of 401) are given. The results of Tajima's D and Fu & Li's D* are also given. Significant results ($p<0.05$) are indicated by an asterisk. The species complex referred to is that between *S. erythrognathus* and *S. karooensis* n. sp. Species with less than four representatives were omitted.

Species	**n**	**π**	**H**	**H_d**	**k**	**S**	**Tajima's D**	**Fu & Li's D***
S. astutus	9	0.043	7	0.917	17.222	45	0.089	1.030
S. dylani n. sp.	7	0.048	4	0.857	19.429	41	0.472	0.794
S. maraisi	36	0.078	25	0.973	23.651	101	-0.682	0.419
S. erythrognathus	11	0.068	6	0.873	27.382	55	0.694	0.896
Species complex*	12	0.079	7	0.894	22.924	73	-0.090	0.111
S. hamartia n. sp.	10	0.098	6	0.889	37.622	80	0.776	0.921

Mantel test

The Mantel tests yielded significant results for all tests conducted ($p<0.05$). The results by locality indicate the same weak positive correlation for both software packages (Ade: r =0.1413, p =0.0022; Vegan: r =0.1413, p =0.0032). The results for the mantel test across the various species are not significant (Ade: r =0.0157, p =0.4333; Vegan: r =0.0157, p =0.437).

© University of Pretoria

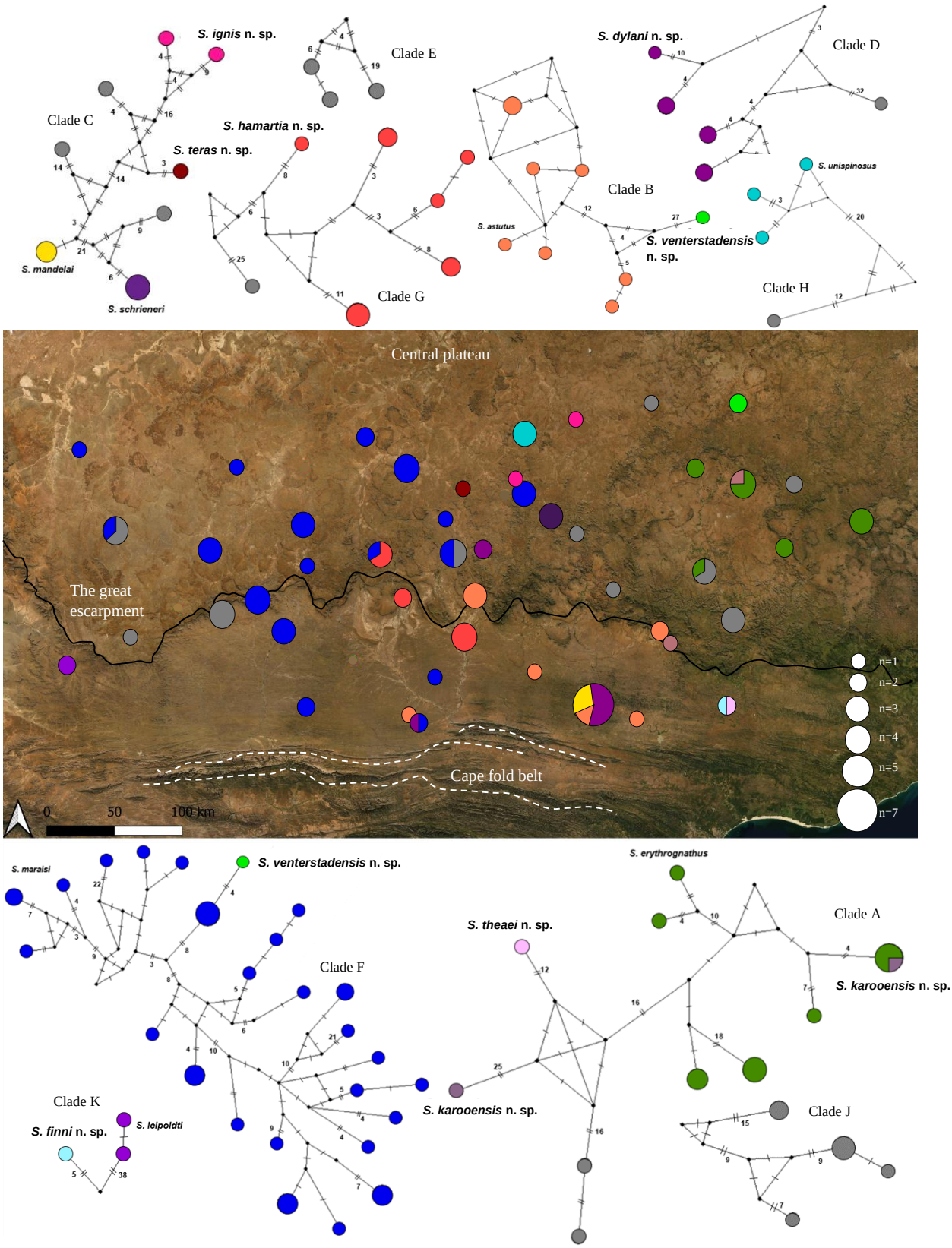


Figure 3. Map of the Karoo area sampled with haplotype networks for the CO1 gene region. Each circle in the networks represents a unique *Stasimopus* haplotype. The black dots on each network represents a hypothetical intermediate haplotype. Mutational steps are indicated by lines, and more than two steps by the corresponding number. The haplotype networks and map circles are proportional to the given sample size.

© University of Pretoria

Discussion

Divergence dating

From the divergence dated phylogenies, it appears that the genus *Stasimopus* radiated in the Karoo region approximately 64.30 MYA (CI: 48.30 - 84.15), towards the beginning of the Paleocene. The beginning of the Paleocene is marked by the Cretaceous - Paleogene extinction event approximately 66MYA (Meadows & Watkeys, 1999). The new niche gaps, along with high temperatures contributed to many radiation events, which would have aided the origin of the *Stasimopus* genus (Meadows & Watkeys, 1999).

Diversification of the genus ramps up towards the end of the Eocene and beginning of the Oligocene (seen by the rise of clades A, B, C, G and F). This Eocene - Oligocene boundary has been noted as 'the great divide' due to large shifts in climate (increasing temperatures in southern Africa), leading to changes in fauna globally (Meadows & Watkeys, 1999). This trend of mygalomorph diversification and geological desertification was mirrored in Australia, which saw the radiation of the Idiopidae and Halonoproctidae families at this time (Harvey et al., 2020).

The genus continued to radiate in the Miocene, with the rise of the rest of the clades, except K. The late Miocene coincides with an increase in temperature and onset of aridification once again (Meadows & Watkeys, 1999; Tankard et al., 1982a). This is also mirrored in south-western Australia which experienced similar environmental conditions and the speciation of many plants and animals (Cooper et al., 2011; Harvey et al., 2020). The late Miocene and early Pliocene are noted as vitally important in the establishment of arid zone diversity in Australia in mygalomorph taxa such as Idiopidae (Rix et al., 2017). This same time period appears to be important for the diversification of the arid adapted *Stasimopus* species.

Stasimopus leipoldti (Clade K) may have arisen in the Pleistocene, this is however a tentative conclusion due to the small sample size of the species in this study. The Pleistocene saw southern Africa becoming more arid. It is also marked by alternating glacial and interglacial cycles (Barlow et al., 2013; Tankard et al., 1982a). These cycles are known to have had impacts on various species ranges (Gruber et al., 2017). There is however, evidence to suggest that Fynbos and Succulent Karoo biomes were decoupled from these effects and experienced climate stability (Potts et al., 2013). This may have led to the high levels of diversity and endemism present in these biomes today (Potts et al., 2013). *Stasimopus leipoldti* is originally described from Clanwilliam (Western Cape), over 150 km away, falling into the Succulent Karoo biome, the samples collected for this study were from the Tankwa Karoo, which is a small, isolated enclave of this biome nestled in the harsher Nama Karoo biome (Henschel et al., 2018). This Tankwa Karoo area may thus be a Pleistocene glacial cycle refugia for the species. A larger sample size as well as genetic sampling of the type locality is needed to show this more definitively. The same pattern of a Pleistocene glacial refugia was reported for the

© University of Pretoria

Aname genus in Pilbara, Western Australia, which experienced a similar geological history to the Karoo region (Gruber et al., 2017).

A similar relationship is seen between the type of *S. erythrognathus* (Worster, Eastern Cape) and the specimens occurring over 700 km away. This species could not be accurately dated in isolation due to forming part of a genetic species complex. The distance between the type locality and the specimens assessed here may indicate another species complex, but sampling the type locality would be required to test this.

Aridification has played a large role in shaping the evolutionary history of *Stasimopus* in the Karoo. The region is however, experiencing rapid desertification due to climate change and habitat degradation (Hoffmann, 1995; Hoffmann et al., 1999). This change may thus continue to drive the diversification of the genus, or the conditions could become too harsh over too short a time span leading to the extinction of these arid adapted species.

Demography

The lower degree of genetic variation in the EF-1ɣ region is expected due to this being a nuclear gene and having a lower mutational rate than the two mitochondrial genes (Allio et al., 2017). The high haplotype diversity across the various species and gene regions indicates that enough time has elapsed for diversification to occur. Majority of the species display high haplotype diversity and low nucleotide diversity across the gene regions (except for *S. unispinosus* which does not have a high haplotype diversity). This trend is indicative of a rapid expansion from a relatively small population (Beavis et al., 2011; Hewitt, 2000). In order to gain further insight into the demographic history of these species for which only a few specimens were available, more samples are required. The incongruence of the placement of *S. venterstadensis* in the haplotype network of CO1 is potentially due to mitochondrial introgression from an ancient admixture between the two species (Croucher et al., 2004; Horoiwa et al., 2021; Kornilios et al., 2016). This could explain why the same pattern is not observed in the other gene regions, but a larger sample size of *S. venterstadensis* is required to fully explore this possibility.

The EF-1ɣ results for *S. maraisi* indicate that the population has undergone a recent expansion event based on the negative Tajima's D and Fu and Li's D as well as the shape of the haplotype network (Avise, 2000; Graham et al., 2020, 2015). This expansion based on the dated phylogeny likely occurred in the mid-Miocene, coinciding with the formation of the Benguela current, leading to the Karoo experiencing a more tropical climate (Meadows & Watkeys, 1999). This may have given males, which are vulnerable to desiccation, more favourable conditions to disperse further than is usually possible under arid conditions. This could have contributed to the wide species range of *S. maraisi* seen today. The influence of the Benguela current formation on accelerated speciation

© University of Pretoria

has previously been recorded in southern Africa. In Namibia and the Northern Cape, the formation of the Benguela current led to xeric conditions which caused local speciation events such as the formation of the aeolian sand dune system in Namibia, which in turn influenced the speciation of the *Pachysoma* dung beetles as well as *Senecio* genus of daisies (Milton et al., 2020; Sole et al., 2005). The influence of this current on the succulent Karoo and Fynbos biomes are also well linked to speciation, such as on the tent tortoise, *Psammobates tentorius* as well as numerous plant species (Klak et al., 2004; Verboom et al., 2009; Zhao et al., 2020). The effect of the Benguela on the Nama Karoo fauna, where *S. maraisi* is found is however largely unexplored, and requires further research.

Mantel test and geographic influence

Individuals from localities which are in close geographic proximity tend to be more related to each other than individuals which are located further away from each other, this is supported by the results of the Mantel test. The Mantel tests showed that there is a relationship between geographic distance and genetic distance in our samples. There is a weak positive correlation in both cases, meaning that with greater geographic distance the samples are slightly less related (Diniz-Filho et al., 2013). This is termed isolation by distance and is a common artefact in mygalomorph spiders due to their poor dispersal abilities and sedentary lifestyles (Satler et al., 2013; Thanou et al., 2017). This is important information to note given the possible fragmentation of the habitat due to land use changes.

This also leads to many species being considered short range endemics and occuring at only one or a few localities (Harvey, 2002; Mason et al., 2018). This is true for many of the species considered here, except for *S. astutus*, *S. maraisi*, *S. leipoldti* and *S. erythrognathus*. Most of these species have ranges of less than 10,000 km^2 (Harvey, 2002). This is vital as this makes these species a conservation concern as they are more at risk of extinction due to climate change, habitat loss as well as habitat degredation (Gruber et al., 2017; Harvey et al., 2011).

The species sampled appear to experience sympatry at multiple locations. This indicates that the species may have an unknown ecological niche separation or are syntopic in nature (Ríos Tamayo & Lyle, 2020). Sympatry and syntopy are common in distantly related mygalomorph spiders and has been reported several times (Leavitt et al., 2015; Satler et al., 2011; Wilson et al., 2018). But in this case, the lineages are not as distantly related, posing the question of whether there is a possible niche divergence (occupying a new ecological or behavioural role than what was occupied before) and what this may be. In the genera *Aliatypus* (North America) and *Euoplos* (Australia) the niche divergence was observed in the structure of the trapdoor lid and the habitat around the burrow (slopes and leaf litter) (Satler et al., 2011; Wilson et al., 2017). The further study of the species co-occuring at these localities and habitats may shed light on the speciation mechanisims within the genus.

© University of Pretoria

Conclusions

Stasimopus is an ancient group of spiders in the Karoo region. The genus has radiated from the late Eocene and through the Miocene resulting in 15 extant species in the region. The similarities in biogeographic histories between the Karoo and arid region of western Australia have seemingly affected the mygalomorph fauna in similar ways. More mygalomorph genera are needed to see if this holds true. The Tankwa Karoo is possibly of importance as a Pleistocene glacial cycle refugia for the species *S. leipoldti*. The area should receive additional sampling to determine if it is a refugia for other taxa. Many of the species are short range endemics, making them of higher conservation concern. This is important to note as the Karoo is undergoing further desertification due to factors such as climate change. The genus has thrived under arid conditions, but this rapid desertification may push the various species to their adaptational limits.

Acknowledgements

We would like to acknowledge Carmen Jacobs and Ishtiag Abdalla Mohammed for assistance with molecular work and phylogenetic analyses. Tshepiso Majelantle and Elmé Brand for their assistance on fieldwork. Equipment for field work was supplied by the Agricultural Research Council. The National Research Foundation (NRF) are acknowledged for funding to the last author. The first author would also like to acknowledge the National Research Foundation for funding (Grant no: 120190). This work is based on the research supported in part by the Karoo BioGaps Project (NRF Grant Number 98864), which was awarded through the Foundational Biodiversity Information Programme (FBIP), a joint initiative of the Department of Science and Innovation (DSI), the National Research Foundation (NRF) and the South African National Biodiversity Institute (SANBI).

© University of Pretoria

References

Allio, R., Donega, S., Galtier, N., & Nabholz, B. (2017). Large variation in the ratio of mitochondrial to nuclear mutation rate across animals: Implications for genetic diversity and the use of mitochondrial DNA as a molecular marker. *Molecular Biology and Evolution, 34*(11), 2762–2772. https://doi.org/10.1093/molbev/msx197

Avise, J. C. (2000). *Phylogeography: the history and formation of species*. Harvard University Press. https://doi.org/10.2307/j.ctv1nzfgj7

Ayres, D. L., Darling, A., Zwickl, D. J., Beerli, P., Holder, M. T., Lewis, P. O., Huelsenbeck, J. P., Ronquist, F., Swofford, D. L., Cummings, M. P., Rambaut, A., & Suchard, M. A. (2012). BEAGLE: An Application Programming Interface and High-Performance Computing Library for Statistical Phylogenetics. *Systematic Biology, 61*(1), 170–173. https://doi.org/10.1093/sysbio/syr100

Bandelt, H. J., Forster, P., & Rohl, A. (1999). Median-joining networks for inferring intraspecific phylogenies. *Molecular Biology and Evolution, 16*(1), 37–48. https://doi.org/10.1093/oxfordjournals.molbev.a026036

Barlow, A., Baker, K., Hendry, C. R., Peppin, L., Phelps, T., Tolley, K. A., Wüster, C. E., & Wüster, W. (2013). Phylogeography of the widespread African puff adder (*Bitis arietans*) reveals multiple Pleistocene refugia in southern Africa. *Molecular Ecology, 22*(4), 1134–1157. https://doi.org/10.1111/mec.12157

Beavis, A. S., & Rowell, D. M. (2006). Phylogeography of two Australian species of funnel web spider (Araneae: Mygalomorphae: Hexathelidae) in Tallaganda State Forest, New South Wales. Insect Biodiversity and Dead Wood: Proceedings of a Symposium for the 22nd International Congress of Entomology, 23–29.

Beavis, A. S., Sunnucks, P., & Rowell, D. M. (2011). Microhabitat preferences drive phylogeographic disparities in two Australian funnel web spiders. *Biological Journal of the Linnean Society, 104*(4), 805–819. https://doi.org/10.1111/j.1095-8312.2011.01753.x

Buchli, H. H. R. (2015). Hunting behaviours in the Ctenizidae. *Integrative and Comparative Biology, 9*, 175–193. https://doi.org/10.1093/icb/9.1.175

Cooper, S. J., Harvey, M. S., Saint, K. M., & Main, B. Y. (2011). Deep phylogeographic structuring of populations of trapdoor spider *Moggridgea tingle* (Migidae) from southwestern Australia: evidence for long-term refugia within refugia. *Molecular Ecology, 20*(15), 3219–3236. https://doi.org/10.1111/j.1365-294X.2011.05160.x

Croucher, P. J. P., Oxford, G. S., & Searle, J. B. (2004). Mitochondrial differentiation, introgression and phylogeny of species in the *Tegenaria atrica* group (Araneae: Agelenidae). *Biological Journal of the Linnean Society, 81*(1), 79–89. https://doi.org/10.1111/j.1095-8312.2004.00280.x

Desmet, P. G., & Cowling, R. M. (1999). The climate of the Karoo - a functional approach. In W. R. J. Dean & S. J. Milton (Eds.), *The Karoo: Ecological Patterns and Processes* (pp. 3–16). Cambridge, UK: Cambridge University Press.

© University of Pretoria

Diniz-Filho, J. A. F., Soares, T. N., Lima, J. S., Dobrovolski, R., Landerio, V. L., de Campos Telles, M. P., … Bini, L. M. (2013). Mantel test in population genetics. *Genetics and Molecular Biology*, *36*(4), 475–485. https://doi.org/10.1590/S1415-47572013000400002

Dippenaar-Schoeman, A. S. (2002). *Baboon and Trapdoor Spiders of Southern Africa: An Identification Manual* (Handbook, Issue 13). Plant production research institute. Agricultural Research Council, Pretoria.

Doyle, J.J. (1992). Gene trees and species trees: Molecular systematic one-character taxonomy. *Systematic Botany*, *17*, 144–163. https://doi.org/10.2307/2419070

Dray, S., Dufour, A.-B., & Thioulouse, J. (2018). Analysis of ecological data: Exploratory and euclidean methods in environmental sciences.

Drummond, A. J., Ho, S. Y. W., Phillips, M. J., & Rambaut, A. (2006). Relaxed phylogenetics and dating with confidence. *PLoS Biology*, *4*(5), 0699–0710. https://doi.org/10.1371/journal.pbio.0040088

Dunlop, J. A., Penney, D., & Jekel, D. (2020). A summary list of fossil spiders and their relatives. World Spider Catalog; Natural History Museum Bern. http://wsc.nmbe.ch [Accessed 14th November 2020].

Engelbrecht, I., & Prendini, L. (2011). Assessing the taxonomic resolution of southern African trapdoor spiders (Araneae: Ctenizidae; Cyrtaucheniidae; Idiopidae) and implications for their conservation. *Biodiversity and Conservation*, *20*(13), 3101–3116. https://doi.org/10.1007/s10531-011-0115-z

Ferretti, N., González, A., & Pérez–Miles, F. (2014). Identification of priority areas for conservation in Argentina: quantitative biogeography insights from mygalomorph spiders (Araneae: Mygalomorphae). *Journal of Insect Conservation*, *18*(6), 1087–1096. https://doi.org/10.1007/s10841-014-9718-5

Fluxus-engineering.com. (2019). *Network* (5.0.1.1).

Fu, Y. X., & Li, W. H. (1993). Statistical tests of neutrality of mutations. *Genetics*, *133*(3), 693–709. https://doi.org/10.1093/genetics/133.3.693

Götz, A. E., & Ruckwied, K. (2014). Palynological records of the Early Permian postglacial climate amelioration (Karoo Basin, South Africa). *Palaeobiodiversity and Palaeoenvironments*, *94*(2), 229–235. https://doi.org/10.1007/s12549-013-0134-8

Graham, M. R., Hendrixson, B. E., Hamilton, C. A., & Bond, J. E. (2015). Miocene extensional tectonics explain ancient patterns of diversification among turret-building tarantulas (*Aphonopelma mojave* group) in the Mojave and Sonoran deserts. *Journal of Biogeography*, *42*(6), 1052–1065. https://doi.org/10.1111/jbi.12494

© University of Pretoria

Graham, M. R., Santibáñez-López, C. E., Derkarabetian, S., & Hendrixson, B. E. (2020). Pleistocene persistence and expansion in tarantulas on the Colorado Plateau and the effects of missing data on phylogeographical inferences from RADseq. *Molecular Ecology*, *29*(19), 3684–3701. https://doi.org/10.1111/mec.15588

Gruber, K., Harvey, M., Didham, R., & Huey, J. (2017). *Phylogeography of trapdoor spiders of the genus Aname: using genes and genomes to reveal biogeographic and evolutionary history* [Master in Science]. University of Western Australia. Retrieved from https://research-repository.uwa.edu.au/en/publications/phylogeography-of-trapdoor-spiders-of-the-genus-aname-using-genes

Hamilton, C. A., Formanowicz, D. R., & Bond, J. E. (2011). Species delimitation and phylogeography of *Aphonopelma hentzi* (Araneae, Mygalomorphae, Theraphosidae): Cryptic diversity in North American tarantulas. *PLoS ONE*, *6*(10), e26207. https://doi.org/10.1371/journal.pone.0026207

Harrison, S. E., Harvey, M. S., Cooper, S. J. B., Austin, A. D., & Rix, M. G. (2017). Across the Indian Ocean: A remarkable example of trans-oceanic dispersal in an austral mygalomorph spider. *PLoS ONE*, *12*(8), E0180139. https://doi.org/10.1371/journal.pone.0180139

Harvey, M. S. (2002). Short-range endemism among the Australian fauna: some examples from non-marine environments. *Invertebrate Systematics*, *16*, 555–570. https://doi.org/10.1071/IS02009

Harvey, M. S., Johnson, M. S., & Humphreys, W. F. (2011). Protecting the innocent: Studying short-range endemic taxa enhances conservation outcomes. *Invertebrate Systematics*, *25*, 1–10. https://doi.org/10.1071/IS11011

Harvey, M. S., Rix, M. G., Hillyer, M. J., & Huey, J. A. (2020). The systematics and phylogenetic position of the troglobitic Australian spider genus *Troglodiplura* (Araneae: Mygalomorphae), with a new classification for Anamidae. *Invertebrate Systematics*, *34*, 799–822. https://doi.org/10.1071/is20034

Hedin, M., Carlson, D., & Coyle, F. (2015). Sky island diversification meets the multispecies coalescent – divergence in the spruce-fir moss spider (*Microhexura montivaga*, Araneae, Mygalomorphae) on the highest peaks of southern Appalachia. *Molecular Ecology*, *24*, 3467–3484. https://doi.org/10.1111/mec.13248

Hedin, M., Starrett, J., & Hayashi, C. (2013). Crossing the uncrossable: Novel trans-valley biogeographic patterns revealed in the genetic history of low-dispersal mygalomorph spiders (Antrodiaetidae, *Antrodiaetus*) from California. *Molecular Ecology*, *22*(2), 508–526. https://doi.org/10.1111/mec.12130

Hendrixson, B. E., & Bond, J. E. (2007). Molecular phylogeny and biogeography of an ancient Holarctic lineage of mygalomorph spiders (Araneae: Antrodiaetidae: *Antrodiaetus*). *Molecular Phylogenetics and Evolution*, *42*(3), 738–755. https://doi.org/10.1016/j.ympev.2006.09.010

© University of Pretoria

Henschel, J. R., Hoffman, M. T., & Walker, C. (2018). Introduction to the Karoo Special Issue: Trajectories of Change in the Anthropocene. *African Journal of Range & Forage Science*, *35*(3–4), 151–156. https://doi.org/10.2989/10220119.2018.1535214

Hewitt, G. (2000). The genetic legacy of the Quaternary ice ages. *Nature*, *405*(6789), 907–913. https://doi.org/10.1038/35016000

Hoffmann, M. T., Cousins, B., Meyer, T., Petersen, A., & Hendricks, H. (1999). Historical and contemporary land use and the desertification of the Karoo. In W. R. J. Dean & S. J. Milton (Eds.), *The Karoo: Ecological Patterns and Processes* (pp. 257–273). Cambridge University Press.

Hoffmann, T. M. (1995). Environmental history and the desertification of the Karoo, South Africa. *Plant Biosystematics*, *129*(1), 261–273. https://doi.org/10.1080/11263509509436134

Holness, S., Driver, A., Todd, S., Snaddon, K., Hamer, M., Raimondo, D., Daniels, F., Alexander, G., Bazelet, C., Bills, R., Bragg, C., Branch, B., Bruyns, P., Chakona, A., Child, M., Clarke, R. V., Coetzer, A., Coetzer, W., Colville, J., … von Staden, L. (2016). Biodiversity and Ecological Impacts: Landscape Processes, Ecosystems and Species. In R. Scholes, P. Lochner, G. Schreiner, L. Snyman-Van der Walt, & M. de Jager (Eds.), *Shale Gas Development in the Central Karoo: A Scientific Assessment of the Opportunities and Risks* (pp. 7–1 to 7–72). CSIR. http://seasgd.csir.co.za/scientific-assessment-chapters/

Horoiwa, M., Mandagi, I. F., Sutra, N., Montenegro, J., Tantu, F. Y., Masengi, K. W. A., Nagano, A. J., Kusumi, J., Yasuda, N., & Yamahira, K. (2021). Mitochondrial introgression by ancient admixture between two distant lacustrine fishes in Sulawesi Island. *PLOS ONE*, *16*(6), e0245316. https://doi.org/10.1371/journal.pone.0245316

Johnson, M. R., van Vuuren, C. J., Visser, J. N. J., Cole, D. I., Wickens, H., Robers, D. L., & Brandl, G. (2006). Sedimentary rocks of the Karoo supergroup. In M. R. Johnson, C. R. Anhaeusser, & R. J. Thomas (Eds.), *The geology of South Africa*. Council for Geoscience.

Katoh, K. (2005). MAFFT version 5: improvement in accuracy of multiple sequence alignment. *Nucleic Acids Research*, *33*(2), 511–518. https://doi.org/10.1093/nar/gki198

Katoh, K., & Toh, H. (2008). Recent developments in the MAFFT multiple sequence alignment program. *Briefings in Bioinformatics*, *9*(4), 286–298. https://doi.org/10.1093/bib/bbn013

Klak, C., Reeves, G., & Hedderson, T. (2004). Unmatched tempo of evolution in Southern African semi-desert ice plants. *Nature*, *427*(6969), 63–65. https://doi.org/10.1038/nature02243

© University of Pretoria

Kornilios, P., Thanou, E., Kapli, P., Parmakelis, A., & Chatzaki, M. (2016). Peeking through the trapdoor: Historical biogeography of the Aegean endemic spider *Cyrtocarenum* Ausserer, 1871 with an estimation of mtDNA substitution rates for Mygalomorphae. *Molecular Phylogenetics and Evolution*, *98*, 300–313. https://doi.org/10.1016/j.ympev.2016.01.021

Kremen, C., Cowell, R. K., Erwin, T. L., Murphy, D. D., Noss, R. F., & Sanjayan, M. A. (1993). Terrestrial arthropod assemblages their use in conservation planning. *Conservation Biology*, *7*(4), 796–808. https://doi.org/10.1046/j.1523-1739.1993.740796.x

Kück, P., & Meusemann, K. (2010). FASconCAT: Convenient handling of data matrices. *Molecular Phylogenetics and Evolution*, *56*(3), 1115–1118. https://doi.org/10.1016/j.ympev.2010.04.024

Kumar, S., Stecher, G., & Tamura, K. (2016). MEGA7: Molecular Evolutionary Genetics Analysis Version 7.0 for bigger datasets. *Molecular Biology and Evolution*, *33*(7), 1870–1874. https://doi.org/10.1093/molbev/msw054

Leavitt, D. H., Starrett, J., Westphal, M. F., & Hedin, M. (2015). Multilocus sequence data reveal dozens of putative cryptic species in a radiation of endemic Californian mygalomorph spiders (Araneae, Mygalomorphae, Nemesiidae). *Molecular Phylogenetics and Evolution*, *91*, 56–67. https://doi.org/10.1016/j.ympev.2015.05.016

Maddison, W. P. (1997). Gene trees in species trees. *Systematic Biology*, *46*(3), 523–536. https://doi.org/10.1093/sysbio/46.3.523

Main, D., Tensen, L., Gihring, K., Bronner, G., Aboul-Hassan, N., Blanckenberg, M., & van Vuuren, B. J. (2019). Unravelling the taxonomy and distribution of two problematic small mammal genera in the Karoo biome. *African Zoology*, *54*(3), 125–135. https://doi.org/10.1080/15627020.2019.1628661

Mason, L. D., Wardell-Johnson, G., & Main, B. Y. (2018). The longest-lived spider: mygalomorphs dig deep, and persevere. *Pacific Conservation Biology*, *24*(2), 203. https://doi.org/10.1071/PC18015

Meadows, M. E., & Watkeys, M. K. (1999). Paleoenvironments. In W. R. J. Dean & S. J. Milton (Eds.), *The Karoo: Ecological Patterns and Processes* (pp. 27–41). Cambridge University Press.

Michonneau, F. (2017). Using GMYC for species delimitation. *Zenodo*. https://doi.org/10.5281/zenodo.838259

Milton, J. J., Affenzeller, M., Abbott, R. J., & Comes, H. P. (2020). Plant speciation in the Namib Desert: origin of a widespread derivative species from a narrow endemic. In *BioRxiv* [Preprint]. https://doi.org/10.1101/2022.01.04.474907

Milton, S. J., & Dean, W. R. J. (1999). The Karoo: past and future. In W. R. J. Dean & S. J. Milton (Eds.), *The Karoo: Ecological Patterns and Processes* (pp. 314–318). Cambridge University Press.

© University of Pretoria

Mucina, L., Jürrgens, N., le Roux, A., Rutherford, M. C., Schmiedel, U., Elser, K. J., Powrie, L. W., Desmet, P. G., Milton, S. J., Boucher, C., Ellis, F., Lambrechts, J. J. N., Ward, R. A., Manning, J. C., & Midgley, G. F. (2006). Succulent Karoo Biome. In L. Mucina & M. C. Rutherford (Eds.), *The Vegetation of South Africa, Lesotho and Swaziland* (Vol. 19, pp. 220–299). South African National Biodiversity Institute.

Mucina, L., Rutherford, M. C., Plamer, A. R., Milton, S. J., Scott, L., Lloyd, J. W., van der Merwe, B., Horae, D. B., Bezuidenhout, H., Vlok, J. H. J., Euston-Brown, D. I. W., Powrie, L. W., & Dold, A. P. (2006). Nama-Karoo Biome. In L. Mucina & M. C. Rutherford (Eds.), *The Vegetation of South Africa, Lesotho and Swaziland* (pp. 324–347). South African National Biodiversity Institute.

Newton, L. G., Starrett, J., Hendrixson, B. E., Derkarabetian, S., & Bond, J. E. (2020). Integrative species delimitation reveals cryptic diversity in the southern Appalachian *Antrodiaetus unicolor* (Araneae: Antrodiaetidae) species complex. *Molecular Ecology*, *29*(12), 2269–2287. https://doi.org/10.1111/mec.15483

Opatova, V., Bond, J. E., & Arnedo, M. A. (2013). Ancient origins of the Mediterranean trap-door spiders of the family Ctenizidae (Araneae, Mygalomorphae). *Molecular Phylogenetics and Evolution*, *69*(3), 1135–1145. https://doi.org/10.1016/j.ympev.2013.08.002

Opatova, V., Bond, J. E., & Arnedo, M. A. (2016). Uncovering the role of the Western Mediterranean tectonics in shaping the diversity and distribution of the trap-door spider genus *Ummidia* (Araneae, Ctenizidae). *Journal of Biogeography*, *43*(10), 1955–1966. https://doi.org/10.1111/jbi.12838

Opatova, V., Hamilton, C. A., Hedin, M., de Oca, L. M., Král, J., & Bond, J. E. (2020). Phylogenetic Systematics and Evolution of the Spider Infraorder Mygalomorphae Using Genomic Scale Data. *Systematic Biology*, *syz064*. https://doi.org/10.1093/sysbio/syz064

Posada, D. (2008). jModelTest: Phylogenetic model averaging. *Molecular Biology and Evolution*, *25*(7), 1253–1256. https://doi.org/10.1093/molbev/msn083

Potts, A. J., Hedderson, T. A., Vlok, J. H. J., & Cowling, R. M. (2013). Pleistocene range dynamics in the eastern Greater Cape Floristic Region: A case study of the Little Karoo endemic *Berkheya cuneata* (Asteraceae). *South African Journal of Botany*, *88*, 401–413. https://doi.org/10.1016/j.sajb.2013.08.009

Rambaut, A. (2016). *FigTree* (1.4.3). Institute of Evolutionary Biology, University of Edinburgh, Edinburgh. http://tree.bio.ed.ac.uk/software/figtree/

Rambaut, A., Drummond, A. J., Xie, D., Baele, G., & Suchard, M. A. (2018). Posterior Summarization in Bayesian Phylogenetics Using Tracer 1.7. *Systematic Biology*, *67*(5), 901–904. https://doi.org/10.1093/sysbio/syy032

© University of Pretoria

Ramírez-Soriano, A., Ramos-Onsins, S. E., Rozas, J., Calafell, F., & Navarro, A. (2008). Statistical power analysis of neutrality tests under demographic expansions, contractions and bottlenecks with recombination. *Genetics*, *179*(1), 555–567. https://doi.org/10.1534/genetics.107.083006

Ríos Tamayo, D., & Lyle, R. (2020). The South African genus *Lepthercus* Purcell, 1902 (Araneae: Mygalomorphae): phylogeny and taxonomy. *Zootaxa*, *4766*(2), 261–305. https://doi.org/10.11646/zootaxa.4766.2.2

Rix, M. G., Cooper, S. J., Meusemann, K., Klopfstein, S., Harrison, S. E., Harvey, M. S., & Austin, A. D. (2017). Post-Eocene climate change across continental Australia and the diversification of the Australasian spiny trapdoor spiders (Idiopidae: Arbantinae). *Molecular Phylogenetics and Evolution*, *109*, 302-320. https://doi.org/10.1016/j.ympev.2017.01.008

Rolland, J., Cadotte, M. W., Davies, J., Devictor, V., Lavergne, S., Mouquet, N., Pavoine, S., Rodrigues, A., Thuiller, W., Turcati, L., Winter, M., Zupan, L., Jabot, F., & Morlon, H. (2011). Using phylogenies in conservation: new perspectives. *Biology Letters*, 10–12. https://doi.org/10.1098/rsbl.2011.1024

Roth-Monzón, A. J., Mendoza-Hernández, A. A., & Flores-Villela, O. (2018). Amphibian and reptile biodiversity in the semi-arid region of the municipality of Nopala de Villagrán, Hidalgo, Mexico. *PeerJ*, *6*, e4202. https://doi.org/10.7717/peerj.4202

Rozas, J., Ferrer-Mata, A., Sánchez-DelBarrio, J. C., Guirao-Rico, S., Librado, P., Ramos-Onsins, S. E., & Sánchez-Gracia, A. (2017). DnaSP 6: DNA Sequence Polymorphism Analysis of Large Data Sets. *Molecular Biology and Evolution*, *34*(12), 3299–3302. https://doi.org/10.1093/molbev/msx248

Satler, J. D., Carstens, B. C., & Hedin, M. (2013). Multilocus Species Delimitation in a Complex of Morphologically Conserved Trapdoor Spiders (Mygalomorphae, Antrodiaetidae, *Aliatypus*). *Systematic Biology*, *62*(6), 805–823. https://doi.org/10.1093/sysbio/syt041

Satler, J. D., Starrett, J., Hayashi, C. Y., & Hedin, M. (2011). Inferring species trees from gene trees in a radiation of Californian trapdoor spiders (Araneae, Antrodiaetidae, *Aliatypus*). *PLoS ONE*, *9*, E25355. https://doi.org/10.1371/journal.pone.0025355

Selden, P. A. (2002). First British Mesozoic spider, from Cretaceous amber of the Isle of Wight, southern England. *Palaeontology*, *45*, 973–983. https://doi.org/10.1111/1475-4983.00271

Selden, P. A., & Gall, J. C. (1992). A Triassic mygalomorph spider from the northern Vosges, France. *Palaeontology*, *35*(1), 211–235.

Sethusa, T. (2016). *Karoo BioGaps Project*. SANBI [ONLINE]. https://www.sanbi.org/karoo-biogaps-project/

© University of Pretoria

Sole, C. L., Scholtz, C. H., & Bastos, A. D. S. (2005). Phylogeography of the Namib Desert dung beetles Scarabaeus (*Pachysoma*) MacLeay (Coleoptera: Scarabaeidae). *Journal of Biogeography*, *32*(1), 75–84. https://doi.org/10.1111/j.1365-2699.2004.01124.x

Starrett, J., Hayashi, C. Y., Derkarabetian, S., & Hedin, M. C. (2018). Cryptic elevational zonation in trapdoor spiders (Araneae, Antrodiaetidae, *Aliatypus janus* complex) from the Californian southern Sierra Nevada. *Molecular Phylogenetics and Evolution*, *118*, 403–413. https://doi.org/10.10016/j.ympev.2017.09.003

Starrett, J., & Hedin, M. L. (2007). Multilocus genealogies reveal multiple cryptic species and biogeographical complexity in the California turret spider *Antrodiaetus riversi* (Mygalomorphae, Antrodiaetidae). *Molecular Ecology*, *16*, 583–604. https://doi.org/10.1111/j.1365-294X.2006.03164.x

Suchard, M. A., Lemey, P., Baele, G., Ayres, D. L., Drummond, A. J., & Rambaut, A. (2018). Bayesian phylogenetic and phylodynamic data integration using BEAST 1.10. *Virus Evolution*, *4*(1). https://doi.org/10.1093/ve/vey016

Tajima, F. (1989). Statistical method for testing the neutral mutation hypothesis by DNA polymorphism. *Genetics*, *123*(3), 585–595. https://doi.org/10.1093/genetics/123.3.585

Tankard, A. J., Jackson, M. P. A., Eriksson, K. A., Hobday, D. K., Hunter, D. R., & Minter, W. E. L. (1982a). Changing climates and sea levels: The Cenozoic record. In A. J. Tankard, M. P. A. Jackson, K. A. Eriksson, D. K. Hobday, D. R. Hunter, & W. E. L. Minter (Eds.), *Crustal evolution of Southern Africa: 3.8 billion years of Earth history* (pp. 433–454). Springer-Verlag.

Tankard, A. J., Jackson, M. P. A., Eriksson, K. A., Hobday, D. K., Hunter, D. R., & Minter, W. E. L. (1982b). The intercratonic Karoo basin. In A. J. Tankard, M. P. A. Jackson, K. A. Eriksson, D. K. Hobday, D. R. Hunter, & W. E. L. Minter (Eds.), *Crustal evolution of Southern Africa: 3.8 billion years of Earth history* (pp. 346–402). Springer-Verlag.

Thanou, E., Kornilios, P., Poursanidis, D., Parmakelis, A., Arnedo, M. A., & Chatzaki, M. (2017). Exploring the role of within-island ecogeographical factors: insights from the genetic diversity of Cretan trap-door spiders (*Cyrtocarenum cunicularium*, Ctenizidae: Araneae). *Invertebrate Systematics*, *31*(4), 506. https://doi.org/10.1071/IS16082

Veness, C. (2019). *Movable Type Scripts: Calculate distance, bearing and more between Latitude/Longitude points*.

Verboom, G. A., Archibald, J. K., Bakker, F. T., Bellstedt, D. U., Conrad, F., Dreyer, L. L., Forest, F., Galley, C., Goldblatt, P., Henning, J. F., Mummenhoff, K., Linder, H. P., Muasya, A. M., Oberlander, K. C., Savolainen, V., Snijman, D. A., Niet, T. van der, & Nowell, T. L. (2009). Origin and diversification of the Greater Cape flora: ancient species repository, hot-bed of recent radiation, or both? *Molecular Phylogenetics and Evolution*, *51*(1), 44–53. https://doi.org/10.1016/j.ympev.2008.01.037

© University of Pretoria

Werger, M. J. A. (1978). The Karoo-Namib region. In M. J. A. Werger (Ed.), *Biogeography and ecology of southern Africa* (pp. 231–300). Springer.

Wilson, J. D., Bond, J. E., Harvey, M. S., Ramírez, M. J., & Rix, M. G. (2023). Correlation with a limited set of behavioural niches explains the convergence of somatic morphology in mygalomorph spiders. *Ecology and Evolution*, *13*(1). https://doi.org/10.1002/ece3.9706

Wilson, J. D., Hughes, J. M., Raven, R. J., Rix, M. G., & Schmidt, D. J. (2018). Spiny trapdoor spiders (*Euoplos*) of eastern Australia: Broadly sympatric clades are differentiated by burrow architecture and male morphology. *Molecular Phylogenetics and Evolution*, *122*, 157–165. https://doi.org/10.1016/j.ympev.2018.01.022

World Spider Catalog. (2022). *World Spider Catalog Version 23.5*. Natural History Museum Bern. https://doi.org/10.24436/2 [Accessed 8th August 2022].

Wunderlich, J. (1998). Beschreibung der ersten fossilen Spinnen der Unterfamilien Mysmeninae (Anapidae) und Erigoninae (Linyphiidae) im Dominikanischen Bernstein (Arachnida: Araneae). *Entomologische Zeitschrift*, *108*, 363–367.

Wunderlich, J. (2000). Zwei neue Arten der Familie Falltürspinnen (Araneae: Ctenizidae) aus dem Baltischen Bernstein. *Entomologische Zeitschrift*, *110*, 345–348.

Zhao, Z., Heideman, N., Bester, P., Jordaan, A., & Hofmeyr, M. D. (2020). Climatic and topographic changes since the Miocene influenced the diversification and biogeography of the tent tortoise (*Psammobates tentorius*) species complex in Southern Africa. *BMC Evolutionary Biology*, *20*(1), 153. https://doi.org/10.1186/s12862-020-01717-1

© University of Pretoria

Data Accessibility Statement

All genetic sequence data is available on NCBI Nucleotide Database (MK923763-MK935687).
All specimens collected for this research have been deposited in the National Collection of Arachnida (NCA) of the Agricultural Research Council (ARC), Roodeplaat, South Africa.

Benefit-Sharing Statement

Benefits Generated: Benefits from this research accrue from the sharing of our data and results on public databases as described above

Author Contributions

All authors contributed to the study conception and design. Material preparation was performed by Shannon Brandt. Data collection was performed by Shannon Brandt, Catherine Sole and Robin Lyle. Specimen identification was performed by Shannon Brandt and overseen by Robin Lyle. DNA sequencing was performed by Shannon Brandt and overseen by Catherine Sole. Analyses were performed by Shannon Brandt. The first draft of the manuscript was written by Shannon Brandt and all authors commented on previous versions of the manuscript. All authors read and approved the final manuscript.

© University of Pretoria

Supplementary material

Table S1. Specimen information for samples used in divergence dating. GenBank ascension numbers are given for each gene region as well as original publication reference.

No.	Family	Species	CO1	Efɣ-1	16S	Voucher codes
1	**Ctenizidae**	*Cyrtocarenum grajum*	KU854158	KU854191	KU854101	---
2	**Ctenizidae**	*Cteniza moggridgei*	---	KF471462	---	CRBAMM000793
3	**Cyrtaucheniidae**	*Ancylotrypa* sp.	---	JQ358724	---	---
4	**Cyrtaucheniidae**	*Homostola pardalina*	---	JQ358746	KY15815	16S: ARAMY000530; EF-1ɣ: MY 0530
5	**Hexathelidae**	*Bymainiella terraereginae*	KY017749	---	KY015907	ARAMY002045
6	**Hexathelidae**	*Mediothele australis*	KY017751	---	KY015909	ARAMR000287
7	**Hexathelidae**	*Paraembolides cannoni*	KY017752	---	KY015910	ARAMY002083
8	**Nemesiidae**	*Calisoga longitarsis*	---	DQ680314	KY015979	16S: ARAMY000281; EF-1ɣ: MY77
9	**Nemesiidae**	*Iberesia brauni*	---	KX418046	KX418441	CRBAAP000087
10	**Nemesiidae**	*Iberesia machadoi*	KR182534	KR182476	---	MY1008
11	**Nemesiidae**	*Nemesia bristowei*	---	KX418049	KX418375	CRBAAP000053
12	**Nemesiidae**	*Nemesia carminans*	---	KX418072	KX418413	CRBAMM000844

Table S1 (cont.). Specimen information for samples used in divergence dating. GenBank ascension numbers are given for each gene region as well as original publication reference.

No.	Museum Voucher	Locality	Coordinates	Reference
1	---	GREECE, Taygetos Mt., Peloponnese	---	(Kornilios et al., 2016)
2	Z627	FRANCE: Monti, Sospel	N43.82472 E7.48162	(Opatova et al., 2013)
3	EF-1ɣ: MY 0500	---	---	(Bond et al., 2012)
4	AUM MY530	SOUTH AFRICA, Mpumalanaga Province	16S: 26º10'38.64"S, 31º13'00.84"E; S26.1774 E31.2169	(Wheeler et al., 2016); EF-1ɣ :(Bond et al., 2012)
5	AUM MY2045	AUSTRALIA, Queensland, Lamington National Park.	---	(Wheeler et al., 2016)
6	MACN	CHILE, Araucania (Reg. IX), Malleco Prov., Mt. Nat. Contulmo.	---	(Wheeler et al., 2016)
7	AUM MY2083	AUSTRALIA, Queensland, Binna Burra, Lamington Nat. Park	---	(Wheeler et al., 2016)
8	16S: AUM MY281	USA, California, vic Mariposa	16S: 37º30'14.04"N, 119º59'38.76"W	(Wheeler et al., 2016); EF-1ɣ: (Ayoub et al., 2007)
9	H10	SPAIN, Balearic Islands, Majorca rd. Orient to Banyola; red. Slopes	39.7271N, 2.7342E	(Mora et al., 2017)
10	---	---	---	(Leavitt et al., 2015)
11	H128	SPAIN, Balearic Islands, Majorca, Can Planiol, MA-10 Deia-Andratx, after Valldemossa crossrd, rd. slope	39.6889 N, 2.5775 E	(Mora et al., 2017)
12	RA191	FRANCE: Provence-Alpes-Cote d'AzurFontvielle, PN des Alpilles	43.7592N, 4.6951E	(Mora et al., 2017)

© University of Pretoria

Table S2. The locality coordinates and samples used to conduct the mantle test. The "By locality" section indicates the test that was run on 48 samples each with a unique locality to test for isolation by distance between the CO1 dataset and the geographic distances. The "By species" section indicates the subset of samples and localities tested to determine if there is a correlation between geographic distance and genetic differences across the various species.

By locality		
Site number	**Specimen code**	**Species**
02	NCA 2017/1834	Unidentified
03	NCA 2017/1835	*S. unispinosus*
04	NCA 2017/1839	*S. maraisi*
05B	NCA 2017/1843	Unidentified
06	NCA 2017/1849	*S. hamartia* n. sp.
07	NCA 2017/1852	*S. hamartia* n. sp.
08	NCA 2017/1855	*S. maraisi*
09	NCA 2017/1861	*S. maraisi*
11	NCA 2017/1866	*S. maraisi*
13	NCA 2017/1870	*S. leipoldti*
16A	NCA 2017/1874	*S. maraisi*
16B	NCA 2017/1875	*S. maraisi*
18B	NCA 2017/1882	*S. maraisi*
19	NCA 2017/1885	*S. maraisi*
20B	NCA 2017/1887	*S. maraisi*
21	NCA 2017/1888	*S. hamartia* n. sp.
22	NCA 2017/1897	Unidentified
23	NCA 2017/1899	Unidentified
24	NCA 2017/1903	*S. astutus*
25B	NCA 2017/1906	*S. astutus*
30A	NCA 2017/1913	*S. erythrognathus*
30B	NCA 2017/1914	*S. erythrognathus*
31	NCA 2019/610	*S. venterstadensis* n. sp.
32	NCA 2019/603	Unidentified
33	NCA 2019/625	*S. erythrognathus*
35	NCA 2019/620	Unidentified
36	NCA 2019/605	*S. finni* n. sp.
37A	NCA 2019/638	*S. astutus*
37B	NCA 2019/635	*S. astutus*
38B	NCA 2019/676	*S. dylani* n. sp.
39	NCA 2019/660	*S. hamartia* n. sp.
41	NCA 2019/636	*S. maraisi*
42	NCA 2019/691	Unidentified
44A	NCA 2019/662	Unidentified
47	NCA 2019/630	*S. maraisi*
50	NCA 2019/689	*S. maraisi*

© University of Pretoria

Table S2 (cont.). The locality coordinates and samples used to conduct the mantle test. The "By locality" section indicates the test that was run on 48 samples each with a unique locality to test for isolation by distance between the CO1 dataset and the geographic distances. The "By species" section indicates the subset of samples and localities tested to determine if there is a correlation between geographic distance and genetic differences across the various species.

By locality (cont.)		
Site number	**Specimen code**	**Species**
51	NCA 2019/640	*S. maraisi*
52	NCA 2019/688	*S. maraisi*
53	NCA 2019/647	*S. astutus*
55B	NCA 2019/680	*S. maraisi*
56	NCA 2019/643	*S. teras* n. sp.
58	NCA 2019/671	*S. schrieneri*
59B	NCA 2019/655	*S. unispinosus*
60	NCA 2019/665	*S. erythrognathus*
ELK	NCA 2019/613	*S. erythrognathus*
FRE	NCA 2019/663	*S. dylani* n. sp.
NCRA	NCA 2017/1915	Unidentified
STH	NCA 2019/642	*S. ignis* n. sp.
By Species		
Site number	**Specimen code**	**Species**
21	NCA 2017/1888	*S. hamartia* n. sp.
24	NCA 2017/1903	*S. astutus*
60	NCA 2019/665	*S. erythrognathus*
13	NCA 2017/1870	*S. leipoldti*
08	NCA 2017/1855	*S. maraisi*
19	NCA 2017/1885	*S. maraisi*
52	NCA 2019/688	*S. maraisi*
58	NCA 2019/671	*S. schrieneri*
03	NCA 2017/1835	*S. unispinosus*
06	NCA 2017/1849	*S. hamartia* n. sp.
FRE	NCA 2019/663	*S. dylani* n. sp.
31	NCA 2019/610	*S. venterstadensis* n. sp.
36	NCA 2019/605	*S. finni* n. sp.
STH	NCA 2019/642	*S. ignis* n. sp.
56	NCA 2019/643	*S. teras* n. sp.

© University of Pretoria

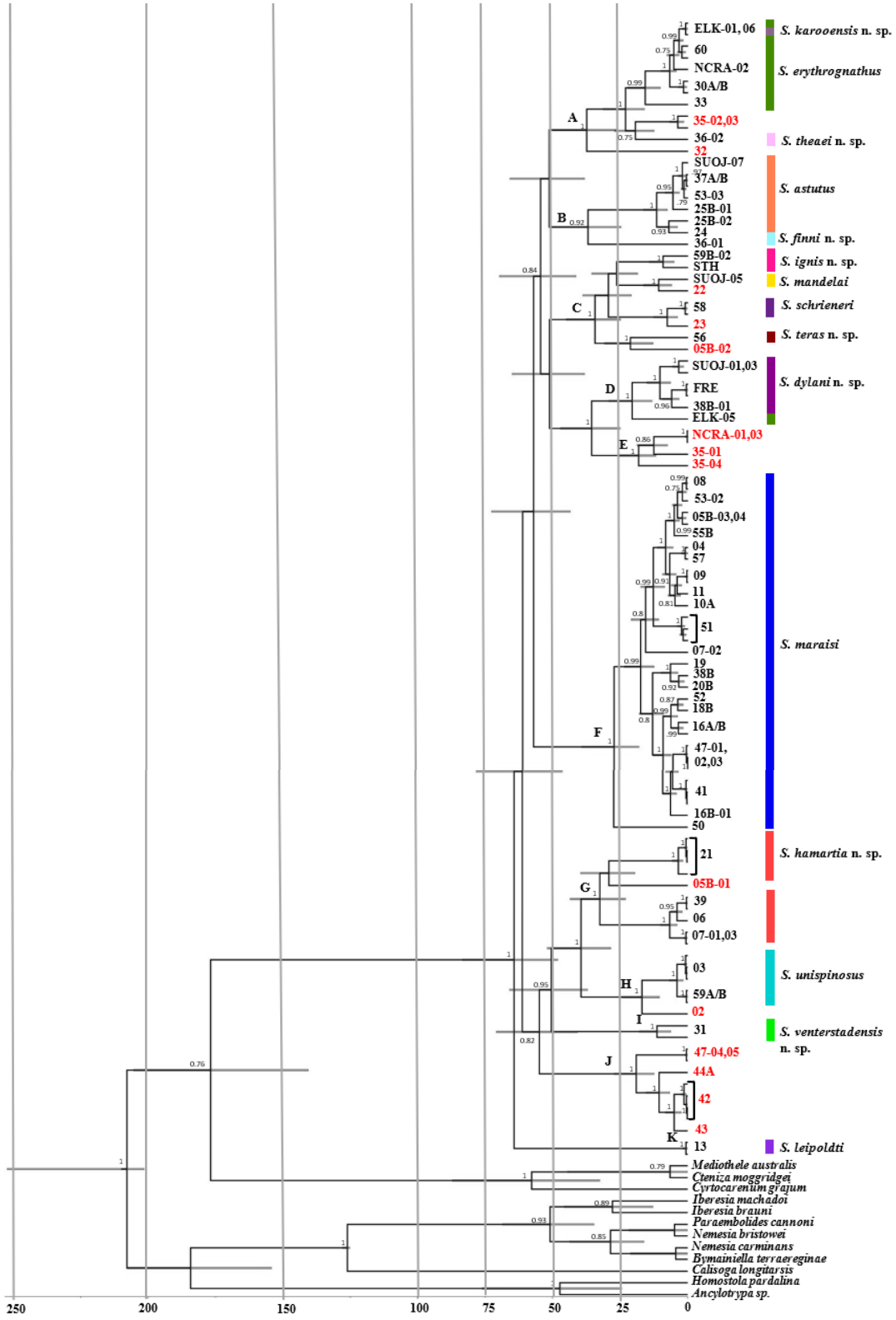


Figure S1. Maximum clade credibility tree from the BEAST analysis of CO1, 16S and EF-1ɣ for the *Stasimopus* specimens occurring in the Karoo under the Birth-death incomplete speciation model. The grey bars indicate the confidence intervals for the dating. Posterior probabilities > 0.70 are given on the corresponding nodes. Specimen numbers correspond to localities in figure 1, and red specimens indicate juveniles which could not be identified. Identified species are indicated by the coloured bars. Clades are numbered for the ease of discussion.

© University of Pretoria

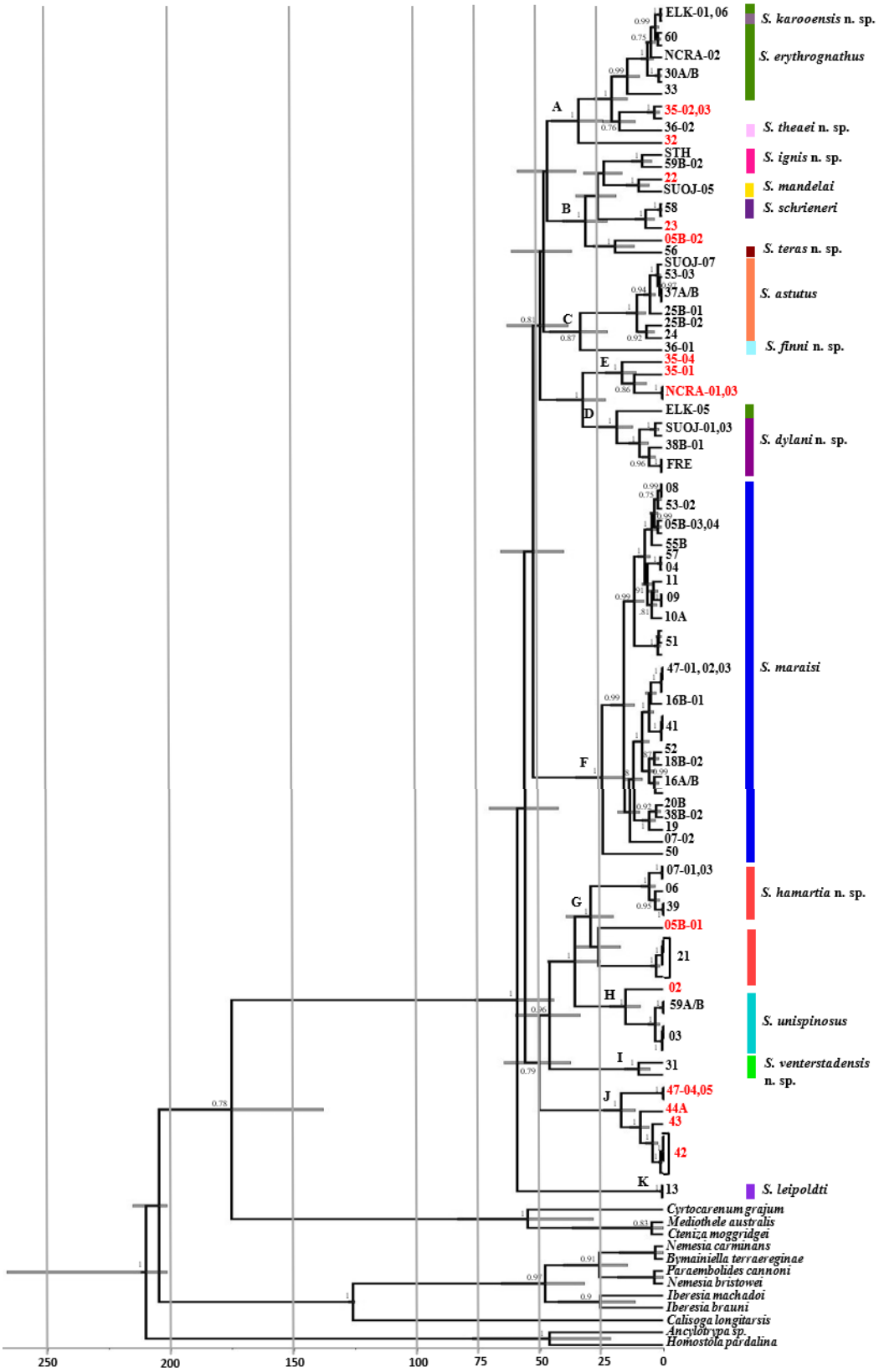


Figure S2. Maximum clade credibility tree from the BEAST analysis of CO1, 16S and EF-1ɣ for the *Stasimopus* specimens occurring in the Karoo under the coalescent speciation model. The grey bars indicate the confidence intervals for the dating. Posterior probabilities > 0.70 are given on the corresponding nodes. Specimen numbers correspond to localities in figure 1, and red specimens indicate juveniles which could not be identified. Identified species are indicated by the coloured bars. Clades are numbered for the ease of discussion.

© University of Pretoria

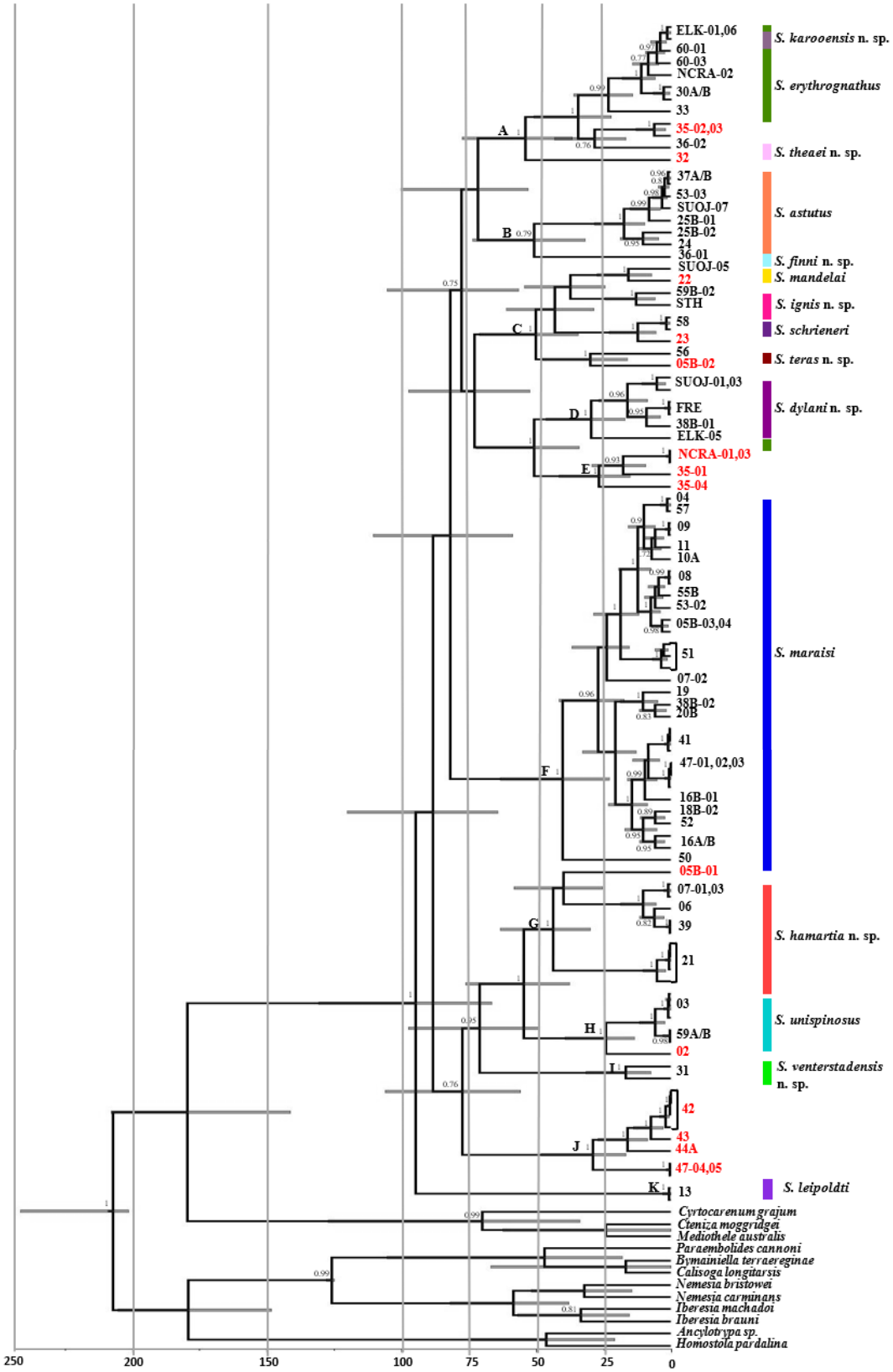


Figure S3. Maximum clade credibility tree from the BEAST analysis of CO1, 16S and EF-1ɣ for the *Stasimopus* specimens occurring in the Karoo under the Yule speciation model. The grey bars indicate the confidence intervals for the dating. Posterior probabilities > 0.70 are given on the corresponding nodes. Specimen numbers correspond to localities in figure 1, and red specimens indicate juveniles which could not be identified. Identified species are indicated by the coloured bars. Clades are numbered for the ease of discussion.

© University of Pretoria

Table S3. Demographic parameters for the 16S gene region for the *Stasimopus* of the Karoo region. The number of sequences (n), nucleotide diversity (π), haplotypes (H), gene diversity (H_d), mean number of pairwise differences (k) and segregating sites (S) (out of 317) are given. The results of Tajima's D and Fu & Li's D* are also given. Significant results ($p<0.05$) are indicated by an asterisk. The species complex referred to is that between *S. erythrognathus* and *S. karooensis* n. sp. Species with less than four representatives were omitted.

Clade / Lineage	n	π	H	H_d	k	S	Tajima's D	Fu & Li's D*
S. astutus	11	0.080	7	0.818	23.182	79	-1.402	-1.286
S. dylani n. sp.	6	0.042	5	0.933	12.867	25	0.556	0.627
S. maraisi	35	0.068	23	0.973	20.225	70	0.310	-0.108
S. erythrognathus	12	0.065	8	0.897	19.256	56	-0.092	0.444
Species complex*	13	0.078	8	0.894	23.242	67	-0.569	-0.926
S. hamartia n. sp.	11	0.095	6	0.800	28.000	56	1.850	1.418**
S. unispinosus	5	0.006	2	0.600	1.800	3	1.573	1.572

Table S4. Demographic parameters for the EF-1ɣ gene region for the *Stasimopus* of the Karoo region. The number of sequences (n), nucleotide diversity (π), haplotypes (H), gene diversity (H_d), mean number of pairwise differences (k) and segregating sites (S) (out of 539) are given. The results of Tajima's D and Fu & Li's D* are also given. Significant results ($p<0.05$) are indicated by an asterisk. The species complex referred to is that between *S. erythrognathus* and *S. karooensis* n. sp. Species with less than four representatives were omitted.

Clade / Lineage	n	π	H	H_d	k	S	Tajima's D	Fu & Li's D*
S. astutus	7	0.014	7	1.000	7.330	21	-0.813	-0.651
S. maraisi	37	0.005	11	0.698	2.928	26	-1.825**	-3.140**
S. erythrognathus	11	0.006	7	0.873	3.309	10	-0.131	-0.478
Species complex*	12	0.083	7	0.833	3.167	10	-0.180	-0.550
S. hamartia n. sp.	11	0.005	6	0.836	2.509	7	0.202	-0.193
S. unispinosus	6	0.003	2	0.600	1.800	3	1.910	1.400

© University of Pretoria

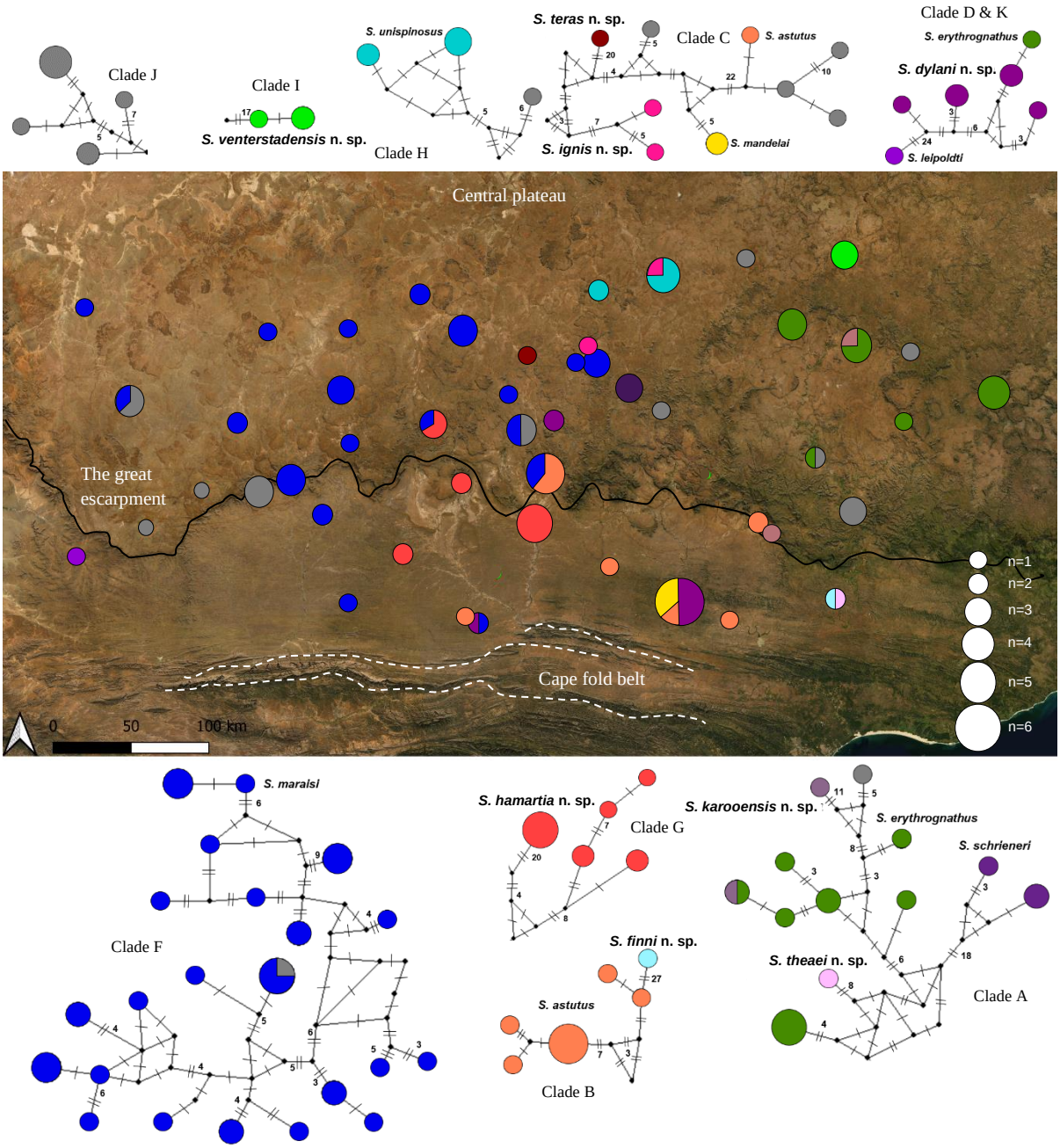


Figure S4. Map of the Karoo area sampled with haplotype networks for the 16S gene region. Each circle in the networks represents a unique haplotype. The black dots on each network represents a hypothetical intermediate haplotype. Mutational steps are indicated by lines, and more than two steps by the corresponding number. The haplotype networks and map circles are proportional to the given sample size.

© University of Pretoria

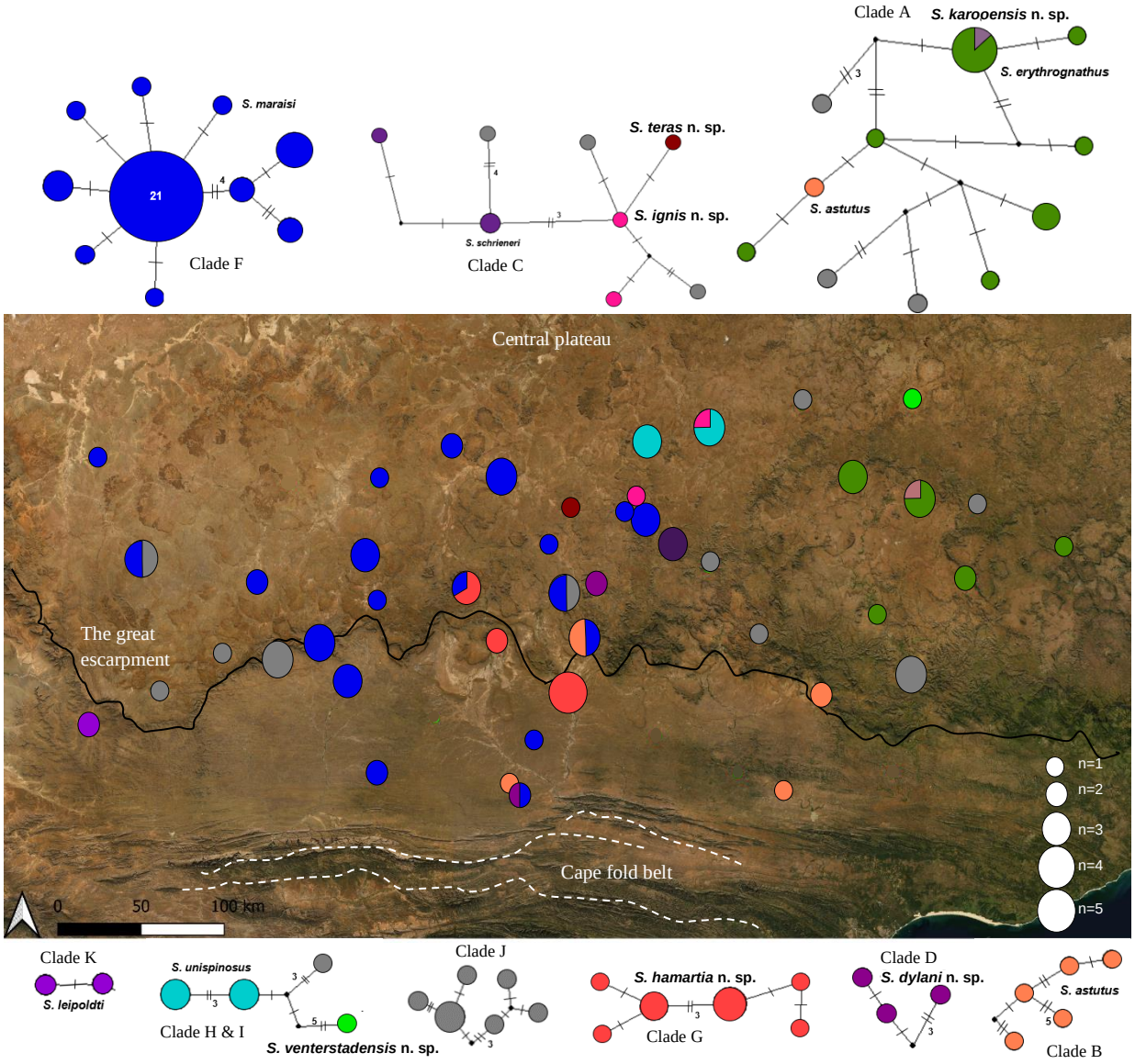


Figure S5. Map of the Karoo area sampled with haplotype networks for the EF-1ɣ gene region. Each circle in the networks represents a unique haplotype. The black dots on each network represents a hypothetical intermediate haplotype. Mutational steps are indicated by lines, and more than two steps by the corresponding number. The haplotype networks and map circles are proportional to the given sample size.

© University of Pretoria

Chapter 6

General discussion

Stasimopus Simon 1892 and mygalomorphs in general all struggle with the issue of identification. There are very few characters used in identification and conservative morphologies compound this issue (Hamilton et al., 2014; Hendrixson and Bond, 2009; Newton et al., 2020; Opatova et al., 2020; Rix et al., 2018). The challenge of identification confounds taxonomy, as many species are misidentified, or shelved in museums, unidentified, due to a lack of expertise (Gruber et al., 2017). This was the first main aim of this research, find different methodologies to aid in specimen identification at the species level.

The first avenue to aid in species identification was the use of various species delimitation methodologies (Chapter 2). This chapter included the first phylogenetic study of the genus *Stasimopus*, which produced valuable sequence data for the various species. Seventeen *Stasimopus* species were found to occur in the Karoo region, including nine previously unidentified species. These species are all morphologically and genetically distinct, except for *S. erythrognathus* (Purcell, 1903b) and *S. karooensis* n. sp. (Undescribed species 4). which form a genetic species complex. The species delimitation results themselves revealed the ineffectiveness of this methodology for the genus. All methodologies failed to delimit the actual species. The Automatic barcode Gap discovery method, which works only on cytochrome c oxidase 1 (CO1) data, gave the closest results, delimiting 21 species due to oversplitting *S. hamartia* n. sp. (Undescribed species 1), *S. ignis* n. sp. (Undescribed species 6) and the *S. erythrognathus / S. karooensis* n. sp. (Undescribed species 4) complex. Cytochrome oxidase 1 data may however, need to be interpreted with caution when used in isolation, as it may not capture all the variation present and may be lacking some resolving power (Galtier et al., 2009). The other two single locus methods, Bayesian Poisson Tree Process (bPTP) and General Mixed Yule Coalescent (GMYC) were completely inaccurate, severly oversplitting the species, to the extent that each locality was mistaken for a separate species or lumping everything into one or two species. This oversplitting seems to be a common issue amoung the Mygalomorphae, due to the strong population structuring observed in spiders with sedentary lifestyles (Hamilton et al., 2014; Hedin, 2015; Leavitt et al., 2015; Newton et al., 2020; Opatova and Arnedo, 2014; Satler et al., 2013). The multilocus approach, Brownie was also ineffective, as the results were inconclusive, due to no congruence being found between the trees produced by the analysis. Species delimitation methods appear to be more effective to answer questions of possible species complexes for taxa which do not

© University of Pretoria

have intense population structuring. These methods have been effective at this for a multitude of different taxa, such as frogs, certain fish families, lizards and fungi to mention a few (Domingos et al., 2017; García-Melo et al., 2019; O'Connell et al., 2018; Singh et al., 2015). These methods have also been shown to work in resolving cases of crypsis in some mygalomorph taxa such as for the genus *Aliatypus* in work done by Satler et al. (2013), but this was not the case for the genus *Stasimopus*. This chapter shows conclusively that species delimitation tools cannot be used to aid in the identification of *Stasimopus* species, as in most other mygalomorph species it delimits genetic structure, not species (Sukumaran and Knowles, 2017).

The second methodology investigated for aiding species identification was the use of geometric morphometrics. The first determining factor was to confirm the link between differences in eye pattern and a phylogenetic pattern which would be driven by evolution. Chapter 3 showed that there is significant phylogenetic signal present for the relative size and position of the eyes for the *Stasimopus* species. This shows that individuals which are more closely related have morphologically more similar eye patterns than what would be expected under a Brownian evolutionary model (Adams, 2014). The eye patterns of *Stasimopus* species can thus be used as a character for classification of species as it is informative of evolutionary decent (Hendrixson and Bond, 2009). The various average eye patterns for the species raised some questions about the evolution of this trait. The first being the distinct difference in relative size of the primary eyes, Anterior Median Eyes (AME) between males and females between species. The primary eyes of arachnids have higher photoreceptor sensitivity and higher spatial accuracy than secondary eyes as well as having the muscularity to allow eye movements (Morehouse et al., 2017). It was hypothesised that the males with larger primary eyes may be due to the higher level of activity of males outside the burrows, as males actively seek out mates at night. Some female species also have larger relative primary eyes compared to other species. It is challenging to draw conclusive answers as to why this may be the case as there is a large gap in the literature concerning the functionality of the different eye pairs in the mygalomorphs. One possibility may be that as the spiderlings have to leave the mothers burrow to construct their own, a larger pair of AMEs may be beneficial in more open habitats as to allow for the detection of predators through the use of active eye movements. The other interesting morphological difference between female species was the relative position of the posterior lateral eyes (PLE). Posterior lateral eyes play a role in the wideness of the spider's peripheral vision (Morehouse et al., 2017). The females of *S. leipoldti* (Purcell, 1902), *S. hamartia* n. sp. (Undescribed species 1), *S. venterstadensis* n. sp. (Undescribed species 3) and *S. ignis* n. sp. (Undescribed species 6) all have PLE which are angled at 90 degrees, whereas the other species PLE are angled further back past 90 degrees, more towards the abdomen. A possible reason for this may be due to differing densities of vegetation surrounding the burrow. If a spider's burrow is poorly concealed by vegetation, a wider

© University of Pretoria

peripheral vision would be beneficial to allow for the detection of predators. This also raised an interesting evolutionary question, as these species are not sister taxa, implying that a wider peripheral vision evolved multiple times. The analysis of evolutionary affect also showed that evolutionary allometry is present for both sexes. This validates the observation that when looking at a larger bodied species, the eye pattern is more spread over the carapace and appears sparser.

The evidence of evolutionary influence on the trait clearly demonstrates that it is a good character which can be used to distinguish between species as it demonstrates evolutionary decent, the question remained, to what extent? The morphospace plots show clustering, demonstrating that the between species variation is greater than within species. The clusters do however overlap, this is an expected result due to the continuous nature of the eye patterns. Although clear clusters were not found, all significance testing showed that there are differences in eye pattern among species and morphospecies. The exact species that displayed these differences could not be analysed due to the small sample size of each species. An interesting result to come of this methodology is that some synoptic species were separate in morphospace. This is an interesting result, as the niche separation between *Stasimopus* species is unknown, and this character should be further investigated to understand what prevents interbreeding or fatal mating mistakes between the syntopic species. This method can also now be used to distinguish between co-occurring species of a homoplasious genus. Chapter 3 showed that eye patterns can be used to identify species to some extent, which is a step forward in finding a quantitative methodology. A larger sample size would be needed to test this more definitively and determine which species can be clearly separated by this character. This methodology was included when constructing an integrative taxonomy for the genus.

Integrative taxonomy stresses the importance of using multiple lines of evidence when testing taxonomic hypotheses (Bond, 2012; Bond et al., 2021; Ferretti et al., 2019; Hedin and Bond, 2006). This is vitally improtant in the Mygalomorphae which has historically been classified solely based on morphology. This study demonstrated why species identification based only on morphology is problematic. Through the use of a genetic phylogeny it was found that the original male allotype described as *S. maraisi* (Hewitt, 1914) was incorrectly matched to the female of the species. The correct male for the species was detected based on genetic information and described morphologically. The original *S. maraisi* allotype was redescribed as *S. malesociatus* n. sp. (Undescribed species 9). Further inflating the morphological identification problem is that the majority of *Stasimopus* species (and mygalomorphs generally) are described on the basis of only one sex (53%) of which most are described only based on females (40%) (Engelbrecht and Prendini, 2012; Bond et al., 2021). Genetic data also alleviates the problem of mismatching a sex to the incorrect species as illustrated above. If a database of *Stasimopus* sequence data can be compiled, then idividuals can be assigned to already existing species. The sequence data obtained in Chapter 2 is an

© University of Pretoria

invaluable resource towards this. These data were added to GenBank where it can be used as reference sequences for other researchers.

The integrative taxonomy also took into account morphology. Typically males of the genus are considered more diagnostic than females (Engelbrecht and Prendini, 2012; Hendrixson and Bond, 2004). In this manuscript however, females did display a few distinct diagnostic characters, most prominently the presence or absence of an apical tuft on metatarsus III, the spination of the preening comb, extent of spination on legs I and II as well as the density of cuspules on the labium, maxilla and chelicera. All of the morphological data was compiled into a matrix for future researchers to access when trying to identify *Stasimopus* species. Along with this a new character was added, the geometeric morphometric eye pattern. This character was used to differentiate between species and the outline drawings are an easy to use morphological character.

Chapter 4 describes nine new *Stasimopus* species using the array of different data types. This increases the known genus diversity from 47 species to 56. As well as greatly increasing the diversity of the Karoo region, which until recently was serverely under studied, it is likely that the mygalomorph fauna is too underrepresented and needs to be reassessed. This chapter demonstrates the importance of having a solid taxonomic understanding of taxa so that more focused reseach can ensue. The field of taxonomy is of vital importance as it is foundational to all other biological sciences (Bond et al., 2021). This study a first step to understanding the diversity of *Stasimopus* which will enable us to better understand their conservation status and our understanding of the Karoo ecosystem. The results of chapters 2-4 allowed for the resolution of the taxonomy of the *Stasimopus* in the Karoo, enabling a phylogeographic investigation.

The fifth chapter of this thesis provided interesting insights into the phylogeography of the genus in the Karoo. It was estimated that the genus radiated in the Karoo region 64.30 MYA in the early Paleocene. This is shortly after the Cretatceous – Paleogene extinction event (66 MYA), which has been shown to have sparked many radition events due to the new niche gaps alongside higher temperatures (Meadows and Watkeys, 1999). The radiation of the genus shares striking similarities with the evolution of the mygalomorph fauna of Australia. Many clades arose towards the end of the Eocene and beginning of the Oligocene (clades A, B, C, G and F). This Eocene – Oligocene boundary has been noted as ‘the great divide’ due to large shifts in climate leading to changes in fauna globally (Meadows and Watkeys, 1999). This trend of mygalomorph diversification and geological desertification was again mirrored in Australia, which saw the radiation of the Idiopidae and Halonoproctidae families (Harvey et al., 2020). Radiation continued into the Miocene with an increase in temperature and aridification (Meadows and Watkeys, 1999; Tankard et al., 1982). This is again seen in South Western Australia with similar conditions and the speciation of many plants and

© University of Pretoria

animals including the mygalomorph family Idiopidae (Cooper et al., 2011; Harvey et al., 2020; Rix et al., 2017b). The last radiation of note is clade K (*S. leipoldti*), which arose in the Pleistocene. This dating is contentious and should be interpreted with caution due to the lack of divergent samples. This period is marked by increased aridity and alternating glacial and interglacial cycles (Barlow et al., 2013; Tankard et al., 1982). This is known to have affected faunal ranges greatly, however, the succulent Karoo biome (in which the clade K samples were found) is believed to have been decoupled from these effects and experienced climate stability at this time (Potts et al., 2013). *Stasimopus leipoldti* is originally described from Clanwilliam (Western Cape), over 150 km away, the samples collected for this study were from the Tankwa Karoo, which is a small, isolated enclave of the Succulent Karoo nestled in the harsher Nama Karoo Biome (Henschel et al., 2018). This Tankwa Karoo area may thus be a Pleistocene glacial cycle refugia for the species. The same pattern was reported for the *Aname* genus in Pilbara, Western Australia, which experienced a similar geological history to the Karoo region (Gruber et al., 2017).

The demography analyses in chapter 5 showed that many of the species occurring in the Karoo have undergone a rapid expansion from a relatively small population (Beavis et al., 2011; Hewitt, 2000). This was especially pronounced in *S. maraisi* (the only species of which a substantial sample size was obtained). This likely occurred in the mid-Miocene, coinciding with the formation of the Benguela current, leading to the Karoo experiencing a more tropical climate (Meadows and Watkeys, 1999). This may have given males, which are vulnerable to desiccation, more favourable conditions to disperse further than is usually possible under arid conditions. This could have contributed to the wide species range of *S. maraisi* seen today. The effect of the Benguela current formation on speciation is well recorded in the Namib desert, Succulent Karoo and Fynbos biomes (Klak et al., 2004; Milton et al., 2022; Sole et al., 2005; Verboom et al., 2009; Zhao et al., 2020). It is however largely unexplored in the Nama Karoo where *S. maraisi* is found.

Chapter 5 provided evidence that *Stasimopus* species experience isolation by distance, meaning that with greater geographic distance the samples are slightly less related (Diniz-Filho et al., 2013). This is common in mygalomorph spiders due to their poor dispersal abilities and sedentary lifestyles (Satler et al., 2013; Thanou et al., 2017). This finding has important conservation implications as many of the species are considered short range endemics and occur at only one or a few localities (Gruber at al., 2017; Harvey, 2002; Mason et al., 2018). Most of these species have ranges of less than 10,000 km^2 (Harvey, 2002). These species are more at risk of extinction due to climate change, habitat loss as well as habitat degredation (Gruber et al., 2017; Harvey et al., 2011). A recent taxonomic revision of the genus *Euoplos* from the semi-arid Avon Wheatbelt and Geraldton Sandplains bioregions of south-western Western Australia by Rix et al. (2019), demonstrated that many species should be listed as threatened or critically endangered based on the small ranges and population declines. Many species of the *Stasimopus* genus may need the same IUCN listing as many

© University of Pretoria

are short range endemics known from a sole locality. Long term pit fall trapping like those referenced in Rix et al. (2019) is required to confirm the population of these spiders and urgently address their IUCN listing, which is currently data deficient.

This chapter provided invaluable insight into the evolutionary history of the genus and the role of aridification in driving diversification. The region is however, experiencing rapid desertification due to climate change and habitat degradation (Hoffmann et al., 1999; Hoffmann, 1995). This change may thus continue to drive the diversification of the genus, or the conditions could become too harsh over too short a time span leading to the extinction of these arid adapted species. The larger species distribution of some species is an unexpected insight and may provide hope for the survival of some species due to refugia within these ranges.

The finding that many of the *Stasimopus* species found in the Karoo region are short range endemics raises conservation concerns. Short-range endemics often have life history traits such as poor dispersal ability, reliance on rare or fragmented habitats and low fecundity (Harvey et al., 2011). *Stasimopus*, like most of the Mygalomorphae, are known to exhibit sedentarily habits and have short dispersal distances (Leavitt et al., 2015; Wilson et al., 2023). These factors would make a species which is a short-range endemic especially sensitive to climate change, degradation of the habitat or habitat loss (Harvey et al., 2011). This is vital information in light of the land use change proposed for the Karoo region due to its richness of natural resources. Further study is needed of these spiders (including long term monitoring) to understand their conservation status. It is a critical that these *Stasimopus* species are considered in conservation planning initatives in order to conserve the biodiversity of the region.

It is also important to highlight certain areas for conservation priority. The results of chapter 5 show the possible importance of the Tankwa Karoo as a Pleistiocene refugia for *S. leipolti* due to historic climate stability. This area is likely a refugia for many more species and should be highlighted for conservation. The slew of new species described in chapter 4 indicates that the biodivesity of the Karoo region has been serverly underestimated, and this will likely be true not only for other mygalomorph species, but numerous different taxa. This again emphasises the importantance of conducting further research in this region, but also considering the conservational value the Karoo region may have.

© University of Pretoria

Future directions

There are numerous ways in which this research can be carried forward. Firstly, addressing the issue of species identification. A possible way forward would to sequence additional species to have a database of all known *Stasimopus* species. This would simplify the identification process as well as allow for a full genus phylogeny. The amounts of unidentified *Stasimopus* material within the various museum collections in South Africa is phenomenal, a great step forward would be to identify this material, as it would likely greatly increase the known distributions for many species which would assist in conservation initiatives and providing species with an IUCN status other than data deficient. This would also likely lead to the discovery of many new species which would add to the overall diversity of the genus. Alongside this more comprehensive sampling for specimens is required in areas where there has historically been little sampling performed (e.g., North-West province), in order to truly understand the current standing of the genus as well as to use them in future studies. For species which are only known from one or two localities, long term monitoring or pitfall trapping should be implemented. This is also a vital step in understanding the range and rarity of these spiders to be able to gauge what conservation status they should have. Mygalomorph spiders have life history traits which make it easy to detect population structuring and dispersal events increasing the likelihood of inferring phylogeographic events (Ferretti et al., 2014; Hedin et al., 2013, 2015; Kremen et al., 1993; Leavitt et al., 2015; Newton et al., 2020; Rix et al., 2017; Satler et al., 2013; Wilson et al., 2018). Thus, if the entire country could be sampled it may provide great insight into the phylogeographic history of mygalomorph spiders generally. This may also shed light on critical areas for conservation as demonstrated by the identification of the Tankwa Karoo in chapter 5. If a more comprehensive phylogeographic study can be conducted, an interesting line of study may be to perform computer modelling on the historic data as well as make predictions on the future species ranges based on a range on environmental variables such as rainfall, aridity and temperature. This would allow for predictions of range shifts under different climate change scenarios and would thus be a valuable tool for outlining conservation areas for the future. The next line of investigation suggested would be to use the additional samples to validate the geometric morphometric technique of eye patterns of species identification as well as trying to identify additional characters to aid in the challenging identification process.

© University of Pretoria

Conclusion

This thesis is the most comprehensive research done to date on a mygalomorph genus in southern Africa. The first data chapters demonstrate the difficulty of species identification. It was shown that species delimitation is ineffective at delimiting species for the *Stasimopus* genus due to the extensive population substructure at fine geographical scales, leading to 'microallopatric populations'. Chapter 3 showed that eye patterns do carry phylogenetic signal and are driven by evolutionary decent, strengthening the case of their validity for species description and identification. The results show promise for the use of geometric morphometrics as separating species based on this character, but a larger sample size is required to test this more conclusively. This research is a step forward in finding methods to aid in species identification, but more work is needed in this area.

Chapter 4 is the first integrative taxonomy to be constructed for the genus. This showed the vast diversity of the genus in the Karoo, which was previously underestimated. This taxonomy used multiple lines of evidence (genetic, morphology and morphometric) to identify species. This framework should be taken forward when assessing future specimens. This also led to the discovery and subsequent description of nine new *Stasimopus* species, greatly increasing diversity.

The final data chapter provided novel phylogeographic insight. It unravelled the complex history of the genus in the Karoo which has an ancient beginning in the Paleocene, with extensive radiation from the late Eocene and through the Miocene resulting in 15 extant species in the region. This showed the extensive influence aridification has had on the genus as well as highlighting the similarities of this on the mygalomorph fauna of the Karoo and arid region of western Australia. The chapter also showed the importance of the Tankwa Karoo as a possible Pleistocene glacial cycle refugia for the species *S. leipoldti*. Many of the species are short range endemics, making them of higher conservation concern. This demonstrates the importance of long-term studies to understand the distribution of the species so that we may better gauge their conservation status. This is important to note as the Karoo is undergoing further desertification due to factors such as climate change and habitat degradation. The genus has thrived under arid conditions, but this rapid desertification may push the various species to their adaptational limits.

© University of Pretoria

References

Adams, D.C., 2014. A Generalized K Statistic for Estimating Phylogenetic Signal from Shape and Other High-Dimensional Multivariate Data. Systematic Biology 63, 685–697. https://doi.org/10.1093/sysbio/syu030

Barlow, A., Baker, K., Hendry, C.R., Peppin, L., Phelps, T., Tolley, K.A., Wüster, C.E., Wüster, W., 2013. Phylogeography of the widespread African puff adder (*Bitis arietans*) reveals multiple Pleistocene refugia in southern Africa. Molecular Ecology 22, 1134–1157. https://doi.org/10.1111/mec.12157

Beavis, A.S., Sunnucks, P., Rowell, D.M., 2011. Microhabitat preferences drive phylogeographic disparities in two Australian funnel web spiders. Biological Journal of the Linnean Society 104, 805–819. https://doi.org/10.1111/j.1095-8312.2011.01753.x

Bond, J.E., 2012. Phylogenetic treatment and taxonomic revision of the trapdoor spider genus *Aptostichus* Simon (Araneae, Mygalomorphae, Euctenizidae). Zookeys 252, 1–209. https://doi.org/10.3897/zookeys.252.3588

Bond, J.E., Godwin, R.L., Colby, J.D., Newton, L.G., Zahnle, X.J., Agnarsson, I., Hamilton, C.A., Kuntner, M., 2021. Improving Taxonomic Practices and Enhancing Its Extensibility—An Example from Araneology. Diversity 14(1), 5. https://doi.org/10.3390/d14010005

Cooper, S.J., Harvey, M.S., Saint, K.M., Main, B.Y., 2011. Deep phylogeographic structuring of populations of trapdoor spider *Moggridgea tingle* (Migidae) from southwestern Australia: evidence for long-term refugia within refugia. Molecular Ecology 20, 3219–3236. https://doi.org/10.1111/j.1365-294X.2011.05160.x

Diniz-Filho, J.A.F., Soares, T.N., Lima, J.S., Dobrovolski, R., Landerio, V.L., de Campos Telles, M.P., Rangel, T.F., Bini, L.M., 2013. Mantel test in population genetics. Genetics and Molecular Biology 36, 475–485. https://doi.org/10.1590/S1415-47572013000400002

Domingos, F.M.C.B., Colli, G.R., Lemmon, A., Lemmon, E.M., Beheregaray, L.B., 2017. In the shadows: Phylogenomics and coalescent species delimitation unveil cryptic diversity in a Cerrado endemic lizard (Squamata: *Tropidurus*). Molecular Phylogenetics and Evolution 107, 455–465. https://doi.org/10.1016/j.ympev.2016.12.009

Engelbrecht, I., Prendini, L., 2012. Cryptic diversity of South African trapdoor spiders: Three new species of *Stasimopus* Simon, 1892 (Mygalomorphae, Ctenizidae), and redescription of *Stasimopus robertsi* Hewitt, 1910. American Museum Novitates 1–42. https://doi.org/https://doi.org/10.1206/3732.2

Ferretti, N., González, A., Pérez–Miles, F., 2014. Identification of priority areas for conservation in Argentina: quantitative biogeography insights from mygalomorph spiders (Araneae: Mygalomorphae). Journal of Insect Conservation 18(6), 1087–1096. https://doi.org/10.1007/s10841-014-9718-5

© University of Pretoria

Ferretti, N.E., Soresi, D.S., González, A., Arnedo, M., 2019. An integrative approach unveils speciation within the threatened spider *Calathotarsus simoni* (Araneae: Mygalomorphae: Migidae). Systematics and Biodiversity 17, 439–457. https://doi.org/10.1080/14772000.2019.1643423

Galtier, N., Nabholz, B., Glemin, S., Hurst, G.D.D., 2009. Mitochondrial DNA as a marker of molecular diversity: a reappraisal. Molecular Ecology 18, 4541–4550. https://doi.org/https://doi.org/10.1111/j.1365-294X.2009.04380.x

García-Melo, J.E., Oliveira, C., da Costa Silva, G.J., Ochoa-Orrego, L.E., Garcia Pereira, L.H., Maldonado-Ocampo, J.A., 2019. Species delimitation of neotropical Characins (Stevardiinae): Implications for taxonomy of complex groups. PLOS ONE 14, e0216786. https://doi.org/10.1371/journal.pone.0216786

Gruber, K., Harvey, M., Didham, R., Huey, J., 2017. Phylogeography of trapdoor spiders of the genus *Aname*: using genes and genomes to reveal biogeographic and evolutionary history (Master in Science). University of Western Australia.

Hamilton, C.A., Hendrixson, B.E., Brewer, M.S., Bond, J.E., 2014. An evaluation of sampling effects on multiple DNA barcoding methods leads to an integrative approach for delimiting species: A case study of the North American tarantula genus *Aphonopelma* (Araneae, Mygalomorphae, Theraphosidae). Molecular Phylogenetics and Evolution 71, 79–93. https://doi.org/10.1016/j.ympev.2013.11.007

Harvey, M.S., 2002. Short-range endemism among the Australian fauna: some examples from non-marine environments. Invertebrate Systematics 16, 555–570. https://doi.org/10.1071/IS02009

Harvey, M.S., Johnson, M.S., Humphreys, W.F., 2011. Protecting the innocent: Studying short-range endemic taxa enhances conservation outcomes. Invertebrate Systematics 25, 1–10. https://doi.org/10.1071/IS11011

Harvey, M.S., Rix, M.G., Hillyer, M.J., Huey, J.A., 2020. The systematics and phylogenetic position of the troglobitic Australian spider genus *Troglodiplura* (Araneae: Mygalomorphae), with a new classification for Anamidae. Invertebrate Systematics 34, 799–822. https://doi.org/10.1071/is20034

Hedin, M., 2015. High-stakes species delimitation in eyeless cave spiders (*Cicurina*, Dictynidae, Araneae) from central Texas. Molecular Ecology 24, 346–361. https://doi.org/10.1111/mec.13036

Hedin, M., Bond, J.E., 2006. Molecular phylogenetics of the spider infraorder Mygalomorphae using nuclear rRNA genes (18S and 28S): Conflict and agreement with the current system of classification. Molecular Phylogenetics and Evolution 41, 454–471. https://doi.org/10.1016/j.ympev.2006.05.017

Hedin, M., Starrett, J., Hayashi, C., 2013. Crossing the uncrossable: Novel trans-valley biogeographic patterns revealed in the genetic history of low-dispersal mygalomorph spiders (Antrodiaetidae, *Antrodiaetus*) from California. Molecular Ecology 22(2), 508–526. https://doi.org/10.1111/mec.12130

© University of Pretoria

Hendrixson, B.E., Bond, J.E., 2004. A new species of *Stasimopus* from the Eastern Cape Province of South Africa (Araneae, Mygalomorphae, Ctenizidae), with notes on its natural history. Zootaxa 619, 1–14. https://doi.org/10.11646/zootaxa.619.1.1

Hendrixson, B.E., Bond, J.E., 2009. Evaluating the efficacy of continuous quantitative characters for reconstructing the phylogeny of a morphologically homogeneous spider taxon (Araneae, Mygalomorphae, Antrodiaetidae, *Antrodiaetus*). Molecular Phylogenetics and Evolution 53, 300–313. https://doi.org/10.1016/j.ympev.2009.06.001

Henschel, J.R., Hoffman, M.T., Walker, C., 2018. Introduction to the Karoo Special Issue: Trajectories of Change in the Anthropocene. African Journal of Range & Forage Science 35, 151–156. https://doi.org/10.2989/10220119.2018.1535214

Hewitt, G., 2000. The genetic legacy of the Quaternary ice ages. Nature 405, 907–913. https://doi.org/10.1038/35016000

Hoffmann, M.T., 1995. Environmental history and the desertification of the Karoo, South Africa. Plant Biosystematics 129, 261–273.

Hoffmann, M.T., Cousins, B., Meyer, T., Petersen, A., Hendricks, H., 1999. Historical and contemporary land use and the desertification of the Karoo, in: Dean, W.R.J., Milton, S.J. (Eds.), The Karoo: Ecological Patterns and Processes. Cambridge University Press, Cambridge, pp. 257–273.

Klak, C., Reeves, G., Hedderson, T., 2004. Unmatched tempo of evolution in Southern African semi-desert ice plants. Nature 427, 63–65. https://doi.org/10.1038/nature02243

Kremen, C., Cowell, R.K., Erwin, T.L., Murphy, D.D., Noss, R.F., Sanjayan, M.A., 1993. Terrestrial arthropod assemblages their use in conservation planning. Conservation Biology 7(4), 796–808. https://doi.org/10.1046/J.1523-1739.1993.740796.X

Leavitt, D.H., Starrett, J., Westphal, M.F., Hedin, M., 2015. Multilocus sequence data reveal dozens of putative cryptic species in a radiation of endemic Californian mygalomorph spiders (Araneae, Mygalomorphae, Nemesiidae). Molecular Phylogenetics and Evolution 91, 56–67. https://doi.org/10.1016/j.ympev.2015.05.016

Mason, L.D., Wardell-Johnson, G., Main, B.Y., 2018. The longest-lived spider: mygalomorphs dig deep, and persevere. Pacific Conservation Biology 24, 203. https://doi.org/10.1071/PC18015

Meadows, M.E., Watkeys, M.K., 1999. Paleoenvironments, in: Dean, W.R.J., Milton, S.J. (Eds.), The Karoo: Ecological Patterns and Processes. Cambridge University Press, Cambridge, pp. 27–41.

Milton, J.J., Affenzeller, M., Abbott, R.J., Comes, H.P., 2022. Plant speciation in the Namib Desert: origin of a widespread derivative species from a narrow endemic. BioRxiv. [Preprint].

Morehouse, N.I., Buschbeck, E.K., Zurek, D.B., Steck, M., Porter, M.L., 2017. Molecular evolution of spider vision: new opportunities, familiar players. Biological Bulletin 233, 21–38. https://doi.org/10.1086/693977

© University of Pretoria

Newton, L.G., Starrett, J., Hendrixson, B.E., Derkarabetian, S., Bond, J.E., 2020. Integrative species delimitation reveals cryptic diversity in the southern Appalachian *Antrodiaetus unicolor* (Araneae: Antrodiaetidae) species complex. Molecular Ecology 29(12), 2269–2287. https://doi.org/10.1111/mec.15483

O'Connell, K.A., Smith, E.N., Shaney, K.J., Arifin, U., Kurniawan, N., Sidik, I., Fujita, M.K., 2018. Coalescent species delimitation of a Sumatran parachuting frog. Zoologica Scripta 47, 33–43. https://doi.org/10.1111/zsc.12248

Opatova, V., Arnedo, M.A., 2014. Spiders on a hot volcanic roof: Colonisation pathways and phylogeography of the Canary Islands endemic trap-door spider *Titanidiops canariensis* (Araneae, Idiopidae). PLoS ONE 9, e115078. https://doi.org/10.1371/journal.pone.0115078

Opatova, V., Hamilton, C.A., Hedin, M., de Oca, L.M., Král, J., & Bond, J.E., 2020. Phylogenetic Systematics and Evolution of the Spider Infraorder Mygalomorphae Using Genomic Scale Data. Systematic Biology, syz064. https://doi.org/10.1093/sysbio/syz064

Potts, A.J., Hedderson, T.A., Vlok, J.H.J., Cowling, R.M., 2013. Pleistocene range dynamics in the eastern Greater Cape Floristic Region: A case study of the Little Karoo endemic *Berkheya cuneata* (Asteraceae). South African Journal of Botany 88, 401–413. https://doi.org/10.1016/j.sajb.2013.08.009

Rix, M.G., Cooper, S.J., Meusemann, K., Klopfstein, S., Harrison, S.E., Harvey, M.S., Austin, A.D., 2017. Post-Eocene climate change across continental Australia and the diversification of the Australasian spiny trapdoor spiders (Idiopidae: Arbantinae). Molecular Phylogenetics and Evolution 109, 302-320. https://doi.org/10.1016/j.ympev.2017.01.008

Rix, M.G., Huey, J.A., Cooper, S.J.B., Austin, A.D., Harvey, M.S., 2018. Conservation systematics of the shield-backed trapdoor spiders of the nigrum-group (Mygalomorphae, Idiopidae, *Idiosoma*): integrative taxonomy reveals a diverse and threatened fauna from south-western Australia. ZooKeys 756, 1–121. https://doi.org/10.3897/zookeys.756.24397

Rix, M.G., Wilson, J.D., & Harvey, M.S., 2019. A revision of the white-headed spiny trapdoor spiders of the genus *Euoplos* (Mygalomorphae: Idiopidae: Arbanitinae): a remarkable lineage of rare mygalomorph spiders from the south-western Australian biodiversity hotspot. The Journal of Arachnology 47(1), 63. https://doi.org/10.1636/0161-8202-47.1.63

Satler, J.D., Carstens, B.C., Hedin, M., 2013. Multilocus Species Delimitation in a Complex of Morphologically Conserved Trapdoor Spiders (Mygalomorphae, Antrodiaetidae, *Aliatypus*). Systematic Biology 62, 805–823. https://doi.org/10.1093/sysbio/syt041

Singh, G., Dal Grande, F., Divakar, P.K., Otte, J., Leavitt, S.D., Szczepanska, K., Crespo, A., Rico, V.J., Aptroot, A., Cáceres, M.E. da S., Lumbsch, H.T., Schmitt, I., 2015. Coalescent-Based Species Delimitation Approach Uncovers High Cryptic Diversity in the Cosmopolitan Lichen-Forming Fungal Genus *Protoparmelia* (Lecanorales, Ascomycota). PLOS ONE 10, e0124625. https://doi.org/10.1371/journal.pone.0124625

Sole, C.L., Scholtz, C.H., Bastos, A.D.S., 2005. Phylogeography of the Namib Desert dung beetles Scarabaeus (*Pachysoma*) MacLeay (Coleoptera: Scarabaeidae). Journal of Biogeography 32, 75–84. https://doi.org/10.1111/j.1365-2699.2004.01124.x

© University of Pretoria

Sukumaran, J., Knowles, L.L., 2017. Multispecies coalescent delimits structure, not species. Proceedings of the National Academy of Sciences 114, 1607–1612. https://doi.org/10.1073/pnas.1607921114

Tankard, A.J., Jackson, M.P.A., Eriksson, K.A., Hobday, D.K., Hunter, D.R., Minter, W.E.L., 1982. Changing climates and sea levels: The Cenozoic record, in: Tankard, A.J., Jackson, M.P.A., Eriksson, K.A., Hobday, D.K., Hunter, D.R., Minter, W.E.L. (Eds.), Crustal Evolution of Southern Africa: 3.8 billion Years of Earth History. Springer-Verlag, New York, pp. 433–454.

Thanou, E., Kornilios, P., Poursanidis, D., Parmakelis, A., Arnedo, M.A., Chatzaki, M., 2017. Exploring the role of within-island ecogeographical factors: insights from the genetic diversity of Cretan trap-door spiders (*Cyrtocarenum cunicularium*, Ctenizidae: Araneae). Invertebrate Systematics 31, 506. https://doi.org/10.1071/IS16082

Verboom, G.A., Archibald, J.K., Bakker, F.T., Bellstedt, D.U., Conrad, F., Dreyer, L.L., Forest, F., Galley, C., Goldblatt, P., Henning, J.F., Mummenhoff, K., Linder, H.P., Muasya, A.M., Oberlander, K.C., Savolainen, V., Snijman, D.A., Niet, T. van der, Nowell, T.L., 2009. Origin and diversification of the Greater Cape flora: ancient species repository, hot-bed of recent radiation, or both? Molecular Phylogenetics and Evolution 51, 44–53. https://doi.org/10.1016/j.ympev.2008.01.037

Wilson, J.D., Bond, J.E., Harvey, M.S., Ramírez, M.J., Rix, M.G., 2023. Correlation with a limited set of behavioural niches explains the convergence of somatic morphology in mygalomorph spiders. Ecology and Evolution 13(1). https://doi.org/10.1002/ece3.9706

Wilson, J.D., Hughes, J.M., Raven, R.J., Rix, M.G., Schmidt, D.J., 2018. Spiny trapdoor spiders (*Euoplos*) of eastern Australia: Broadly sympatric clades are differentiated by burrow architecture and male morphology. Molecular Phylogenetics and Evolution 122, 157–165. https://doi.org/10.1016/j.ympev.2018.01.022

Zhao, Z., Heideman, N., Bester, P., Jordaan, A., Hofmeyr, M.D., 2020. Climatic and topographic changes since the Miocene influenced the diversification and biogeography of the tent tortoise (*Psammobates tentorius*) species complex in Southern Africa. BMC Evolutionary Biology 20, 153. https://doi.org/10.1186/s12862-020-01717-1

© University of Pretoria

Appendix A1

Detailed methodology for divergence dating

(supporting the methods stated in Chapter 5)

Divergence dating

Dating the phylogeny was done using BEAST v1.8.4 (Suchard et al., 2018). All identical sequences were removed from the analysis. In order to determine the most appropriate fossil calibration points, numerous combinations were tested varying the fossil calibrations used. The families were selected based on the most recent Mygalomorphae revision by Opatova et al. (2020). The sister clade to Stasimopidae in this study is the 'Venom clade', composed of Atracidae and Actinopodidae, but these families lack appropriate fossil representatives. The sister clades to Stasimopidae which have fossil representatives were Halonoproctidae, Ctenizidae, Barychelidae and Theraphosidae. On the more derived end of the phylogeny is Nemesiidae and Cyrtaucheniidae. And the most basal group in the mygalomorphs which was selected was Hexathelidae as it has the oldest fossil representative.

Based on this, the following combinations were tested: 1. Nemesiidae and Cyrtaucheniidae (outgroup: Anamidae); 2. Nemesiidae, Cyrtaucheniidae and Halonoproctidae (outgroup: Anamidae); 3. Nemesiidae, Cyrtaucheniidae and Ctenizidae (outgroup: Anamidae); 4. Nemesiidae, Cyrtaucheniidae, Ctenizidae and Halonoproctidae (outgroup: Anamidae); 5. Cyrtaucheniidae, Ctenizidae and Halonoproctidae (outgroup: Anamidae); 6. Cyrtaucheniidae, Barychelidae, Theraphosidae (outgroup: Idiopidae). All of these groupings were retested with Hexathelidae as an alternative outgroup.

The fossils used for this testing were as in Table A1-1. Each combination's results were compared and the result with the highest support values and the most realistic divergence dates (based on that of Opatova et. al., 2020) were selected to be used.

The final fossil calibration points used were as follows: the Hexathelidae fossil, *Rosamygale grauvogely* (Gresa-Voltzia formation, France, Triassic) (Dunlop et al., 2020; Opatova et al., 2020; Selden and Gall, 1992). *Rosamygale grauvogely* is thus, the first mygalomorph appearance in the fossil record, dating to 250 – 240 MYA (Opatova et al., 2020). The Nemesiidae fossil, *Cretamygale chasei* (Isle of Wight, Cretaceous) (Selden, 2002), two Ctenizidae/Halonoproctidae fossils, *Ummidia damzeni* and *U. malonowskii* (both from Baltic amber, Palaeogene) (Wunderlich, 2000). Lastly a fossil from the family Cyrtaucheniidae, *Bolostromus destructus* (Dominican amber, Neogene)

© University of Pretoria

(Dunlop et al., 2020; Wunderlich, 1998). Each family was represented by sequence data from GenBank for 16S rDNA, cytochrome c oxidase subunit 1 (CO1) and elongation factor 1 gamma (EF-1ɣ) if available as given in Chapter 4, Table S1. Each calibration point was set by setting a hard minimum bound (the youngest possible age of the fossil based on the deposit in which it was found) and a soft upper bound (the oldest possible age).

Table A11-. The various fossils used for the divergence dating combinations.

Family	**Fossil**	**Period**	**Reference**
Cyrtaucheniidae	*Bolostromus destructus*	Neogene	Wunderlich, 1998
Nemesiidae	*Cretamygale chasei*	Cretaceous	Selden, 2002
Barychelidae	*Psalistops hispaniolensis*	Neogene	Wunderlich, 1998
Theraphosidae	*Hemirraghus sp.*	Neogene	García-Villafuerte, 2008
	Ischnocolinopsis acutus	Neogene	Wunderlich 1998
Ctenizidae / Halonoproctidae	*Baltocteniza kulickae*	Palaeogene	Eskov and Zonstein, 2000
	Electrocteniza sadilenkoi	Palaeogene	Eskov and Zonstein, 2000
	Ummidia damzeni, U. makinowskii	Palaeogene	Wunderlich, 2000
Hexathelidae	*Rosamygale grauvogeli*	Triassic	Selden and Gall, 1992

© University of Pretoria

References

Ayoub, N.A., Garb, J.E., Hedin, M., Hayashi, C.Y., 2007. Utility of the nuclear protein-coding gene, elongation factor-1 gamma (EF-1γ), for spider systematics, emphasizing family level relationships of tarantulas and their kin (Araneae: Mygalomorphae). Molecular Phylogenetics and Evolution 42, 394–409. https://doi.org/10.1016/j.ympev.2006.07.018

Bond, J.E., Hendrixson, B.E., Hamilton, C.A., Hedin, M., 2012. A reconsideration of the classification of the spider infraorder Mygalomorphae (Arachnida: Araneae) based on three nuclear genes and morphology. PLoS ONE 7, e38753. https://doi.org/https://doi.org/10.1371/journal.pone.0038753

Dunlop, J.A., Penney, D., Jekel, D., 2020. A summary list of fossil spiders and their relatives. World Spider Catalog; Natural History Museum Bern. http://wsc.nmbe.ch

Eskov, K.Y., Zonstein, S.L., 2000. The first ctenizoid mygalomorph spiders from Eocene Baltic amber (Araneida: Mygalomorphae: Ctenizidae). Paleontological Journal 34, S268–S274.

García-Villafuerte, M.Á., 2008. Primer registro fósil del género Hemirraghus (Araneae, Theraphosidae) en ámbar del Terciario, Chiapas, México. Revista Ibérica de Aracnología 16, 43–47.

Kornilios, P., Thanou, E., Kapli, P., Parmakelis, A., Chatzaki, M., 2016. Peeking through the trapdoor: Historical biogeography of the Aegean endemic spider *Cyrtocarenum Ausserer*, 1871 with an estimation of mtDNA substitution rates for Mygalomorphae. Molecular Phylogenetics and Evolution 98, 300–313. https://doi.org/10.1016/j.ympev.2016.01.021

Leavitt, D.H., Starrett, J., Westphal, M.F., Hedin, M., 2015. Multilocus sequence data reveal dozens of putative cryptic species in a radiation of endemic Californian mygalomorph spiders (Araneae, Mygalomorphae, Nemesiidae). Molecular Phylogenetics and Evolution 91, 56–67. https://doi.org/10.1016/j.ympev.2015.05.016

Mora, E., Paspati, A., Decae, A.E., Arnedo, M.A., 2017. Rafting spiders or drifting islands? Origins and diversification of the endemic trap-door spiders from the Balearic Islands, Western Mediterranean. Journal of Biogeography 44, 924–936. https://doi.org/10.1111/jbi.12885

Opatova, V., Bond, J.E., Arnedo, M.A., 2013. Ancient origins of the Mediterranean trap-door spiders of the family Ctenizidae (Araneae, Mygalomorphae). Molecular Phylogenetics and Evolution 69, 1135–1145. https://doi.org/10.1016/j.ympev.2013.08.002

Opatova, V., Hamilton, C.A., Hedin, M., de Oca, L.M., Král, J., Bond, J.E., 2020. Phylogenetic Systematics and Evolution of the Spider Infraorder Mygalomorphae Using Genomic Scale Data. Systematic Biology, syz064. https://doi.org/10.1101/531756

Selden, P.A., Gall, J.C., 1992. A Triassic mygalomorph spider from the northern Vosges, France. Palaeontology 35, 211–235.

Selden, P.A., 2002. First British Mesozoic spider, from Cretaceous amber of the Isle of Wight, southern England. Palaeontology 45, 973–983. https://doi.org/10.1111/1475-4983.00271

© University of Pretoria

Suchard, M.A., Lemey, P., Baele, G., Ayres, D.L., Drummond, A.J., Rambaut, A., 2018. Bayesian phylogenetic and phylodynamic data integration using BEAST 1.10. Virus Evolution 4, vey016.

Wheeler, W.C., Coddington, J.A., Crowley, L.M., Dimitrov, D., Goloboff, P.A., Griswold, C.E., Hormiga, G., Prendini, L., Ramirez, M.J., Sierwald, P., Almeida-Silva, L., Alvarez-Padilla, F., Arnedo, M.A., Benavides Silva, L.R., Benjamin, S.P., Bond, J.E., Grismado, C.J., Hasan, E., Hedin, M., Izquierdo, M.A., Labarque, F.M., Ledford, J., Lopardo, L., Maddison, W.P., Miller, J.A., Piacentini, L.N., Platnick, N.I., Polotow, D., Silva-Davila, D., Scharff, N., Szuts, T., Ubick, D., Vink, C.J., Wood, H.M., Zhang, J., 2016. The spider tree of life: phylogeny of Araneae based on target-gene analyses from an extensive taxon sampling. Cladistics 33. https://doi.org/10.1111/cla.12182

Wunderlich, J., 1998. Beschreibung der ersten fossilen Spinnen der Unterfamilien Mysmeninae (Anapidae) und Erigoninae (Linyphiidae) im Dominikanischen Bernstein (Arachnida: Araneae). Entomologische Zeitschrift 108, 363–367.

Wunderlich, J., 2000. Zwei neue Arten der Familie Falltürspinnen (Araneae: Ctenizidae) aus dem Baltischen Bernstein. Entomologische Zeitschrift 110, 345–348.

© University of Pretoria

Appendix A2

Pilot study supporting documentation to Chapter 3

(Submitted alongside chapter 3 to Evolutionary Biology)

Methods

A pilot study to test two variables was conducted. The first variable tested the number of replicates necessary to reduce operational error to a tolerable amount. For this, three adult females are used from three species: *S. brevipalpis*, *S. rufidens* and Undescribed species 3. The second variable is allometry within species to determine if juveniles can be included in the study. For this, three adult female and three juveniles of *S. maraisi* were also included. Each specimen was reset and photographed in a random order five times to ensure that there was no operational bias in the photography process (Bakkes, 2017). A Leica M 165C stereomicroscope attached to Leica camera (DMC-2900) was used for the photography and the specimens were set in a petri dish of glass beads for ease of adjustment, to ensure similar angles in each photograph.

Once photographed all the images were compiled using tpsUtil v1.79 (Rohlf, 2015) and were imported to tpsDig v.2.31 (Rohlf, 2015) for digitisation. The photographs were selected at random when digitising to ensure that there was no operational bias. The photography and landmarking were performed by the same operator for the entire process to ensure that no additional error was introduced (Bakkes, 2017).

The statics used to complete the pilot study were performed in MorphoJ v.1.06d (Klingenberg, 2011). A general procrustes analyses (GPA) was performed to standardise the data. Thereafter, a principal component analyses (PCA) was done to determine if the between species differences are greater than the within species. A regression was performed to test for allometry for the different female life stages. Lastly, a procrustes ANOVA was performed to test if there is a significant influence of maturity, species and replication. Procrustes ANOVA was also used to determine the percentage error due to orientation (error introduced during photography) and digitisation for the different numbers of replications. This was calculated using the mean sum of squares (Bakkes 2017, Fruciano 2016). For further information on each statistical analysis, please see the methods stated in the manuscript.

© University of Pretoria

Results & Discussion

The results of the PCA shows clear separation between species. The clustering is tighter between species than within species (Figure P1). This indicates that this character may be useful for separating species, but is not too fine-scale to detect within species differences. The tightness of each individual cluster also indicates that the replications were very similar and not mistaken for within species variation. The distinct separating between the juveniles and adults of *S. maraisi* shows that the differences in the relative positions and sizes of the eyes are highly variable between the two life stages. The two life stages can thus not be compared with in a species and juveniles should not be included in downstream analyses.

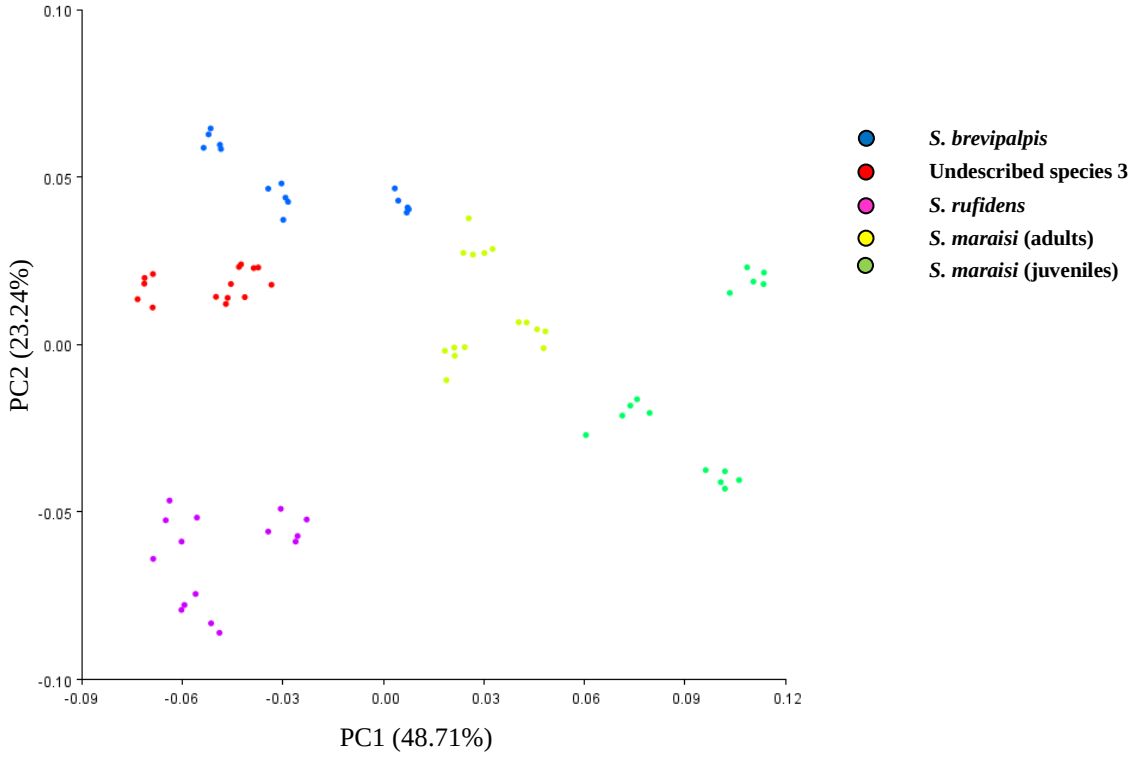


Figure P1. Morphospace plots of the first two PCs for the female pilot dataset. A. The morphospace plot coloured by species. *S. maraisi* is shown for juveniles (green) and adults (yellow) of the species.

© University of Pretoria

The regressions of shape and centroid size show that there is a significant relationship between the two variables. When juveniles are included with the other species, the amount of variation explained by size is 40.32%, this is reduced to 12.11% when the juveniles are removed and species are accounted for (Figure P2). When only the *S. maraisi* specimens are tested, 46.58% of the variation is due to size. This shows that the variation in allometry within a species between two life stages is too great to be included with the species variation, as these relationships would be obscured. The species pooled regression displays evolutionary allometry, this is expected as size is used as an identifying feature between *Stasimopus* species (Figure P2C).

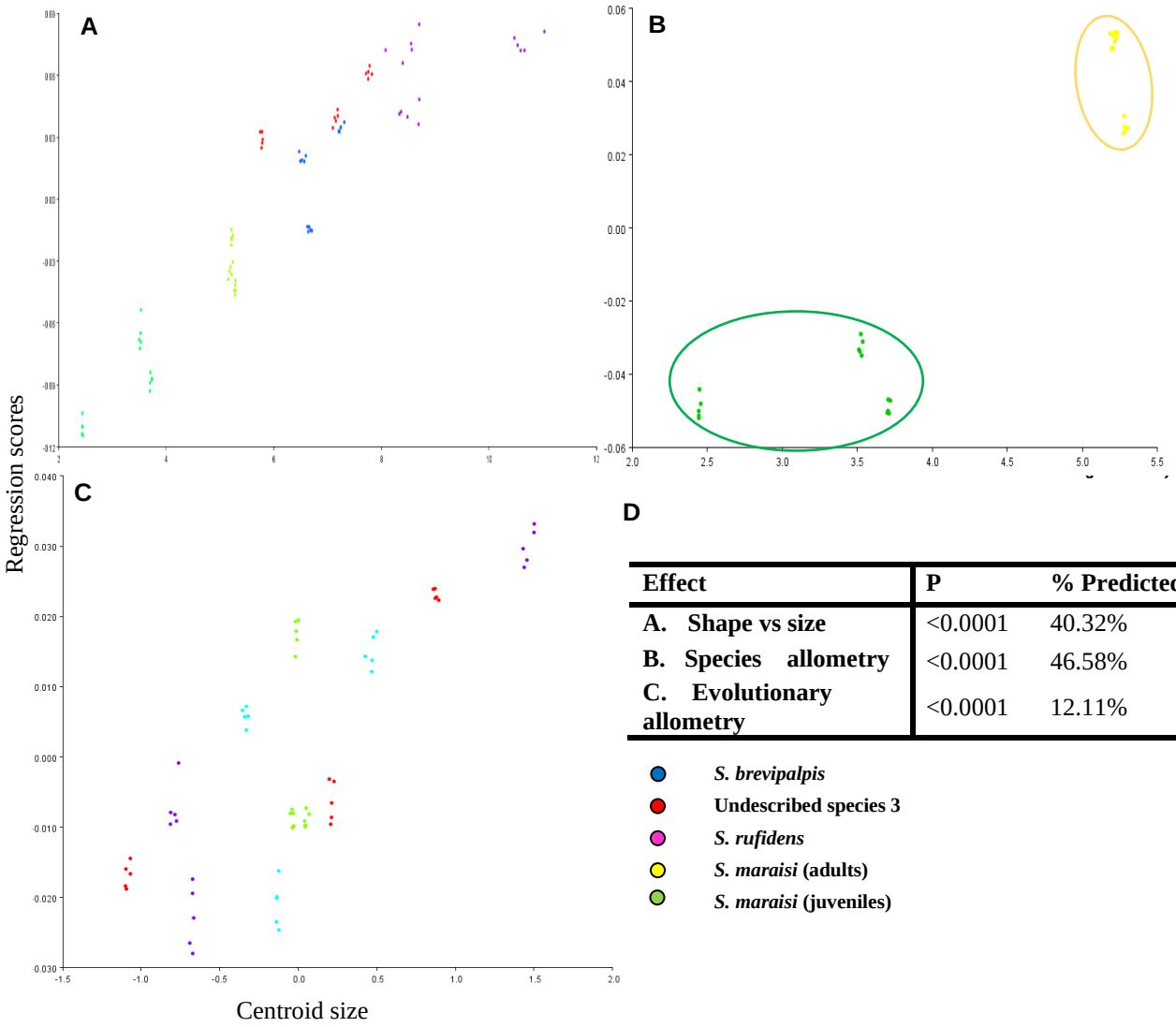


Figure P2. Various regressions of procrustes distances against centroid size. A. Regression of all four species (including the *S. maraisi* juveniles – yellow). B. Regression of the *S. maraisi* specimens to test allometry within the species. C. Regression pooled by species (not including juveniles) to test evolutionary allometry. D. Table showing the significance of the regressions and the percentage variation in the dataset which is predicted by centroid size.

© University of Pretoria

The Procrustes ANOVA of various variables and shape shows that there is a significant relationship between species as well as maturity and shape (Table P1). There are differences between the various species relative eye positions and sizes, indicating that this character could be used to separate species. The same pattern is true for the juveniles and adults of *S. maraisi*, indicating again that the juveniles cannot be included in the analyses. There is no significance between shape and replications, indicating that each replication was similar enough and that multiple replications may not be necessary.

Table P1. Procrustes ANOVA of the various variable relationship with shape of *Stasimopus* ocular patterns.

Effect	SS	MS	Df	F	P
Species	0.20681	0.001149	180	180	<0.0001
Maturity	0.18172	0.003029	60	40.53	<0.0001
Replications	0.00257	0.000011	240	0.12	1.000

The testing for error between replications is shown in Table P2. The error which contributed the most to total error in each replication was orientation error. This is the placement and photography of the specimens. This is likely due to the specimen not facing the camera lens at exactly the same angle in every photograph. This however, still contributes to a small amount of the total variation in the dataset (3.287% at most). The total variation is also at a manageably low level (<5%) even with only two replications.

Table P2. Procrustes ANOVA of the digitisation and orientation error associated with different numbers of replication. The percentage error is calculated based on the mean sum of squares (MS).

Reps	Effect	SS	MS	Df	F	P	% Error	Total error
5	**Individual**	0.95867	0.001141	840	95.06	<.0001		
	Orientation	0.05403	0.000012	4500	1.98	<.0001	1.052%	
	Digitisation	0.02180	0.000006	3600			0.531%	1.583%
4	**Individual**	0.76671	0.000913	840	72.08	<.0001		
	Orientation	0.04559	0.000013	3600	2.10	<.0001	1.387%	
	Digitisation	0.01630	0.000006	2700			0.662%	2.049%
3	**Individual**	0.57726	0.000687	840	51.20	<.0001		
	Orientation	0.03624	0.000013	2700	2.09	<.0001	1.953%	
	Digitisation	0.01153	0.000006	1800			0.932%	2.885%
2	**Individual**	0.38862	0.000463	840	30.42	<.0001		
	Orientation	0.02738	0.000015	1800	2.24	<.0001	3.287%	
	Digitisation	0.00650	0.000007	960			1.464%	4.751%

© University of Pretoria

Conclusion

The results of the pilot study that there are significant and quantifiable differences in the relative position and size of eyes between *Stasimopus* species. The differences between eye patterns of juveniles and adults within the same species is too great and will likely confound the between species results. For this reason, juveniles will not be included in the study. The error testing showed that there is more error introduced from the photography process than digitisation. The total error with only two replicates is still below 5%. The decision was made to only use on replication for the study.

References

Bakkes, D. K. (2017). Evaluation of measurement error in rotational mounting of larval *Rhipicephalus* (Acari: Ixodida: Ixodidae) species in geometric morphometrics. *Zoomorphology*, *136*(3), 403–410. https://doi.org/10.1007/s00435-017-0357-8

Fruciano, C. (2016). Measurement error in geometric morphometrics. *Development Genes and Evolution*, *226*(3), 139–158. https://doi.org/10.1007/s00427-016-0537-4

Klingenberg, C. P. (2011). MorphoJ: an integrated software package for geometric morphometrics. *Molecular Ecology Resources*, *11*, 353–357. https://doi.org/10.1111/j.1755-0998.2010.02924.x

Rohlf, F. J. (2015). The tps series of software. *Hystrix, the Italian Journal of Mammalogy*, *26*, 1–4. https://doi.org/10.4404/hystrix-26.1-11264

© University of Pretoria

Appendix B1

Teratological cases of the ocular patterns in the South African endemic trapdoor spider genus *Stasimpus* Simon (1892) (Araneae, Mygalomorphae, Stasimopidae)

Shannon Brandt[1], Robin Lyle[2] and Catherine L. Sole[1]

[1] *Department of Zoology and Entomology, University of Pretoria, Hatfield, Pretoria, South Africa*

[2] *Agricultural Research Council – Plant Health and Protection, Biosystematics, Roodeplaat, Pretoria, South Africa*

This appendix has been published as:

Mitchell, S. (Brandt, S.), Lyle, R. and Sole, C. L. (2020). Teratological cases of the ocular patterns in the South African endemic trapdoor spider genus *Stasimopus* Simon (1892) (Araneae, Mygalomorphae, Stasimopidae). African Zoology, 55 (4): 363-367.

© University of Pretoria

Abstract

Teratology is the science that deals with the causes and patterns of deformities, abnormalities and defects in the physical development of animals. Teratological occurrences can be due to genetic or environmental conditions. Ocular teratologies are common in hypogean spiders. This communication reports on the occurrence of ocular teratologies of the South African endemic spider family, Stasimopidae. Various museum collections resulting in 181 spiders were examined for cases of ocular teratologies. Six females and one male were found to display some form of teratology. The species found to exhibit these were, *Stasimopus patersonae*, *S. robertsi*, *S. insculptus peddiensis*, *S. griswoldi*, and three unidentified specimens. The teratologies range from reduced eye size to numerous additional eyes. The exact cause of the teratologies is unknown. They could, however, be linked to embryonic trauma or developmental issues, juvenile injury, or unusual environmental conditions during embryonal development. The spiders all survived to adulthood as in hypogeal spiders, eye sight is not the most relied on sense. Understanding the causes of teratologies is important as it may enable researchers to predict the effect of increasing chemical use and global climate change on the embryology of spiders.

Keywords

arachnid, deformity, environmental impacts, hypogean, South Africa, teratology

© University of Pretoria

Introduction

Teratology has long been documented and studied in the field of arachnology (Kaston 1982, Jimenez and Llinas 2002). It is the science that deals with the causes and patterns of deformities, abnormalities and defects in the physical development of animals (Balazuc 1948, Ujhazy *et al.* 2012, Burke *et al.* 2018). Reporting teratological cases is important because they may indicate the effect a particular environmental condition may play during development and may be of general interest (Burke *et al.* 2018).

Ocular teratologies are the most frequently reported deformity of the external features of spiders (Jimenez and Llinas 2002). The documentation of teratological cases of the ocular patterns in the Araneae started with Kaston in 1937 in which he described a spider from the family Amaurobiidae and another from the family Corinnidae, both with missing eyes (Kaston 1937). Many other cases have been reported since Kaston (Kaston 1962, 1982, Marer 1972, Savory 1977, Ono and Kudo 1996, Noordijk and Heijerman 2016). It has been noted that the teratology of the eyes of spiders tends to be more common in hypogean spiders, due to a stronger reliance on senses other than vision (Jimenez and Llinas 2002). These types of studies have advanced to experimental phases in which researchers are testing different environmental conditions (e.g., temperature changes, high humidity and different chemicals) and how this influences the development of structural abnormalities. These studies were not only carried out on spiders, for example the giant house spider, *Eratigena atrica* (Temperature), but also on other organisms, such as Japanese horseshoe crabs, *Tachypleus tridentatus* (Chemicals) and the tick, *Hyalomma marginatum Hyalomin* (Humidity) (Itow 1980, Itow and Sekiguchi 1980, Buczek 2000, Napiórkowska *et al.* 2007, Napiórkowska and Templin 2017, 2018). In multiple studies carried out on the giant house spider, it was found that alternating between high and low temperatures during embryogenesis, causes deformities in the pedipalp, legs and prosoma of spiders, which often leads to fatality.

Spiders typically have eight eyes, the Anterior Median eyes (AME) are known as the ‘principal’ eyes, with the other eyes (Anterior Lateral (ALE), Posterior Median (PME) and Posterior Lateral (PLE)) known as ‘secondary’ eyes (Figure 1). Principal and secondary eyes differ extensively in terms of development, structure and function (Morehouse *et al.* 2017).

This communication serves to report the extent of some ocular teratological occurrences found in the South African spider genus *Stasimopus* Simon (1892), which is endemic to Southern Africa. The genus has recently been placed into its own family, Stasimopidae (Opatova *et al.* 2019). It is a large genus comprising of 47 species (World Spider Catalog 2020). These spiders live in retreats comprising vertical burrows or chambers under rocks or on trees which are lined with silk (Dippenaar-Schoeman 2002). The females lead sedentary lifestyles, only exiting the burrow to capture

© University of Pretoria

prey within reach of the burrow entrance (Engelbrecht and Prendini 2011, Satler *et al.* 2013). However, the males are nomadic in nature, spending time wandering to locate females and are the drivers of dispersal.

Methods and Materials

Multiple national and international museum collections (Albany Museum, Grahamstown, South Africa; The National Museum, Bloemfontein, South Africa; Ditsong Museum of Natural History, Pretoria, South Africa; Iziko Museum of Cape Town, South Africa; Museum für Naturkunde, Berlin, Germany; National Collection of Arachnida, Pretoria, South Africa) were examined. A total of 142 females and 70 males examined from 39 different species between the sexes. The examined material yielded six females and one male that display some form of teratology (Table 1).

All the specimens were photographed using Zeiss Axio Zoom V16 with the Axiocam 512 colour and stacked with ZEN 2.3 SP1 (Blue Edition) or a Leica M 165C stereomicroscope attached to Leica camera (DMC-2900). Two different systems were required because the males and some females have a steeper carapace and thus required an imaging system with a greater depth of field. All specimens were photographed on a petri dish of glass beads for ease of adjustment.

An ocular teratology is considered to be a deviation from the normal ocular pattern for the genus. This standard pattern is shown in Figure 1.

© University of Pretoria

Table 1. Specimen information for the *Stasimopus* individuals showing some form of teratology.

Species	**Sex**	**Locality**	**Accession**
Stasimopus patersonae (Hewitt, 1913)	Female	SOUTH AFRICA, Eastern Cape province, Perseverance	Albany Museum (Collector number: 1955)
Stasimopus griswoldi (Engelbrecht and Prendini, 2012)	Female	SOUTH AFRICA, North-West province, Brits, Hartebeespoort dam	Ditsong Museum of Natural History (TMSA-24001)
Stasimopus robertsi (Hewitt, 1910)	Female	SOUTH AFRICA, Gauteng province, Pretoria, Lyttelton junction	Ditsong Museum of Natural History (TMSA -3109-3112)
Stasimopus insculptus peddiensis (Hewitt, 1917)	Female	SOUTH AFRICA, Eastern Cape province, Peddie	Albany Museum (AMGS-84594)
Stasimopus sp.	Female	SOUTH AFRICA, Western Cape province, Kleinwaterval	National Collection of Arachnida (NCA) (NCA 2017/1885)
Stasimopus sp.	Female	SOUTH AFRICA, Northern Cape province, Sandkop	National Collection of Arachnida (NCA) (NCA 2019/643)
Stasimopus sp.	Male	SOUTH AFRICA, Eastern Cape province, Bloemhof farm	National Collection of Arachnida (NCA) (NCA 2019/605)

© University of Pretoria

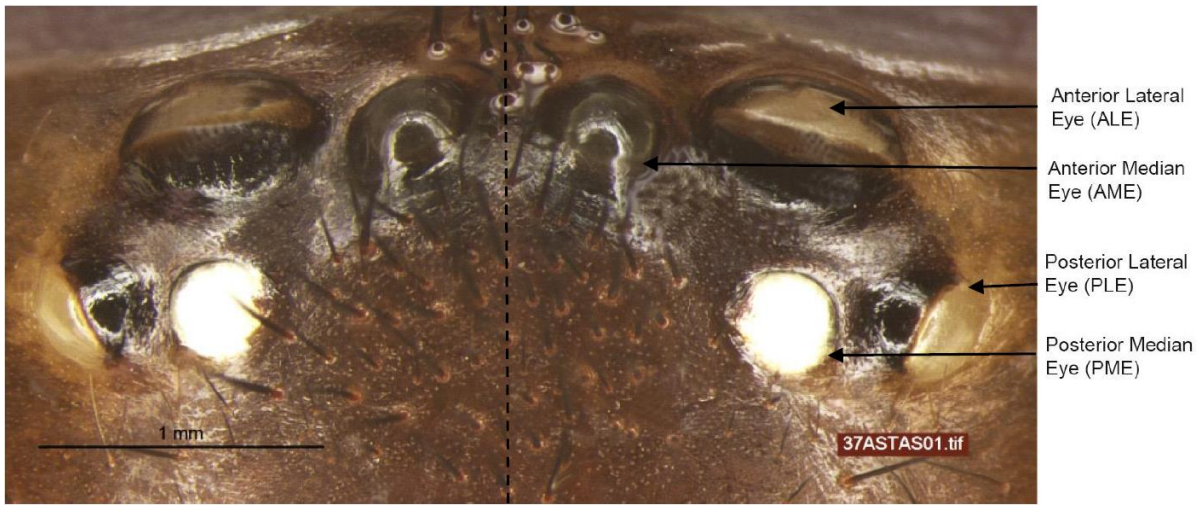


Figure 1: The ocular pattern of a *Stasimopus* female trapdoor spider. This represents the standard number and arrangement of eyes for this genus of spider. Any additional or reduced number indicates a teratology. Any change in the position of the eye in relation to the other eyes is also regarded as an abnormality

Results

The *S. patersonae* female has a growth protruding from the left PME (Figure 2A). The specimen of *S. robertsi* has a teratology of the right PME, which appears to be bifurcating (Figure 2B). *Stasimopus insculptus peddiensis* specimen has a number of deformities (Figure 2C). The right AME is absent entirely. There are six eye-like protrusions to the left of and beneath the right ALE. The right PME is split into two. Both PMEs are bifurcating and the left is partially split. The female of *S. griswoldi* has two smaller, presumably non-functional eyes on either side of the right ALE and one small growth on the outside of the left ALE (Figure 2D). The unidentified female from Kleinwaterval farm (NCA 2017/1885) has what appears to be cuticles for multiple (at least seven) additional eyes, but none of them are completed with lenses (Figure 2E). The additional cuticles to support a lens span from the ALE to the PLE on both sides of the ocular pattern. The other unidentified *Stasimopus* female from Sandkop (NCA 2019/643), has multiple deformities (Figure 2F). The right ALE has two additional eyes to the right. The left ALE has a small additional eye to the left. The right PLE appears to be split into three separate compartments. The unidentified male from Bloemhof farm (NCA 2019/605) has a smaller than usual left AME (Figure 2G).

© University of Pretoria



Figure 2: Ocular teratologies of various specimens of the genus *Stasimopus*. All teratologies are indicated by white arrows. (a). *Stasimopus patersonae* with an additional growth on the left posterior median eye. (b). *Stasimopus robertsi* with an additional growth on the right posterior median eye. (c). *Stasimopus insculptus peddiensis* with a number of deformities. (d). *Stasimopus griswoldi* with three small growths around the anterior lateral eyes. (e). *Stasimopus* species (female, NCA 2017/1885) with many additional growths/eyes surrounding the entire ocular pattern. (f). *Stasimopus* species (female, NCA 2019/643) with multiple additional eyes and bifurcating eyes. (g). *Stasimopus* species (male, NCA 2019/605) with a smaller right anterior median eye.

© University of Pretoria

Discussion

The exact causes of these deformities are unknown.

The secondary eyes of spiders and scorpions initially develop from a common eye field during embryonic development, this eye field is then split into the separate units (ommatidia) and each unit develops into an eye (Loria and Prendini 2014, Morehouse *et al.* 2017). It is thus plausible that any form of trauma during the splitting of the eye field could cause the deformities seen in Figure 2A, B, C (excluding the AMEs), D, E and F. The development of the separate ommatidia has also been linked to gene expression and an error in this process could lead to the aforementioned deformations.

Jimenez and Llinas (2002) stated that deformities could be linked to illness or injury during the juvenile stages of a spider's life. This is also recognised in Balazuc (1955) as heteromorphosis which was reported in the ocellus of the spur-throated grasshopper, *Melanoplus* (Orthoptera: Acrididae). It is possible that in the case of additional eyes (Figure 2E and F), a duplication of part of the cephalic region may have occurred during embryonic development (Jimenez and Llinas 2002). The formation of photoreceptors without lenses is believed to be caused by the failure of photoreceptors at recruiting the cuticular lens secreting cells, thus inhibiting the formation of the lens (Morehouse *et al.* 2017). This could be the cause of the deformities seen in Figure 2E. The reasons for the photoreceptor failure are not yet known.

Multiple genes which play a role in general arthropod eye development have been identified in spiders, which implies that the developmental process likely follows a similar pattern (Morehouse *et al.* 2017). From this it can be deduced that loss of the *dac* -gene would lead to the loss of a secondary eye, but not the primary eye. The genetic pathway responsible for primary eye development must still be investigated further to understand what may lead to the loss of AMEs such as in Figure 2C.

It is most likely that these teratologies are the result of environmental conditions during embryonal development. Multiple studies have shown the effects of different temperatures causing various teratologies under laboratory conditions (Napiórkowska *et al.* 2007, Napiórkowska and Templin 2017, 2018). Another possible cause for the deformities reported in this paper is exposure to pesticides during embryonal or post-embryonal development (Holmberg and Kokko 1983, Noordijk and Heijerman 2016). The Karoo region in which the non-identified individuals were collected has been documented to have undergone extensive spraying with the pesticide Deltamethrin for the control of brown locusts (Brown *et al.* 1993, Brown and Kriel 1994, Stewart *et al.* 1994, Price *et al.* 2000). In addition, to Deltamethrin being used in the area, the Northern Cape part of the Karoo underwent many different chemical trials for locust control using Fipronil, Fenvalerate, Tralomethrin, Pyridaphenthion and Alpha-cypermethrin (Price *et al.* 1994, 1996, 2000, Stewart and Napier Bax

© University of Pretoria

1995, Stewart *et al.* 1995, Chambers and de Klerk 1997, Price 2001). These studies stated that the chemicals cause a 'knock-down state', in which the locusts become paralysed for varying amounts of time (Brown *et al.* 1993, Brown and Kriel 1994, Price *et al.* 1996). The locusts either die during the knock-down due to environmental conditions, die after the knock-down due to the pesticide action, or make a full recovery (Brown *et al.* 1993, Brown and Kriel 1994, Price *et al.* 1996). Only two of these studies considered the impact of these trials on non-target organisms, thus the impact this may have had on the spider fauna is unknown (Brown *et al.* 1994, Stewart *et al.* 1994).

For most species of spider, sight is not the main avenue for prey capture. Spiders such as those in this study, live in burrows and are nocturnal. These spiders are more reliant on mechanical and chemical stimuli (Foelix 1996, Jimenez and Llinas 2002). Thus, the impairment of vision would likely not lead to mortality, which may explain how these specimens survived to maturity (Jimenez and Llinas 2002).

More studies are needed to investigate why and how ocular teratologies occur in the Araneae as to better understand the environmental and/or genetic conditions, which underlie this. Long term studies are also suggested which will investigate the impact ocular teratologies have on spider behaviour and survival. It is vital to understand the underlying causes of teratological cases to be able to predict the effects of increasing use of chemicals (pesticides and herbicides) and changing global climate, which may affect the embryology of spiders.

© University of Pretoria

References

Balazuc J. 1948. La Tératologie dês Coléoptères et expériences de transplantation chez *Tenebrio molitor* L. *Mémoires Du Muséum National d'Histoire Naturelle, (Nouvelle série), Paris*, 25: 1–293.

Balazuc J. 1955. La Tératologie des Orthoptéroïdes. A propos de quelques nouveaux faits observationnels et expérimentaux. *Bollettino del Laboratorio di Entomologia Agraria "Filippo Silvestre" di Portici*, 14: 48–64.

Brown HD, Kriel CF. 1994. *Evaluating Deltamethrin UL under operational conditions for the control of the brown locust in South Africa*. Pretoria.

Brown HD, Kriel CF, Butler ET. 1993. *Operational use of Deltamethrin 0.7 ULV formulation by the SADA's locust control organisation and efficacy of RU's is 081-A against African migatory locust, Locusta migratoria migratorioides, in South Africa*. Pretoria.

Brown HD, Price RE, Seesink LD. 1994. *Impact of Deltamethrin on a Dipteran parasite of locusts in South Africa*. Pretoria.

Buczek A. 2000. Experimental teratogeny in the tick *Hyalomma marginatum marginatum* (Acari: Ixodida: Ixodidae): effect of high humidity on embryonic development. *Journal of Medical Entomology* 37 (6): 807–814.

Burke AF, Sole CL, Scholtz CH. 2018. A remarkable teratological case for *Eucymatodera parva* Schenkling, 1908 (Cleridae: Tillinae) from Namibia. *African Entomology* 26 (1): 250–253.

Chambers BQ, de Klerk JC. 1997. *Evaluation of Alpha-Cypermethrin for the control of the brown locust in the karoo, South Africa*. Pretoria.

Dippenaar-Schoeman AS. 2002. *Baboon and Trapdoor Spiders of Southern Africa : An Identification Manual*. Handbook. Pretoria: Plant production research institute. Agricultural Research Council, Pretoria.

Engelbrecht I, Prendini L. 2011. Assessing the taxonomic resolution of southern African trapdoor spiders (Araneae: Ctenizidae; Cyrtaucheniidae; Idiopidae) and implications for their conservation. *Biodiversity and Conservation* 20 (13): 3101–3116.

Foelix RF. 1996. The Biology of Spiders. *In*: *The Biology of Spiders*. Oxford University Press. pp 330.

© University of Pretoria

Holmberg RG, Kokko EG. 1983. A blind *Homolophus biceps* (Arachnida: Opiliones). *Entomological News* 94: 49–52.

Itow T. 1980. Teratogenesis of the horseshoe crab by alpha-lipoic amide (6,8-thioctic amide) in marketed vitamin tablets. *Journal of Nutritional Science and Vitaminology* 26: 237–245.

Itow T, Sekiguchi K. 1980. Morphogenic movement and experimentally induced decrease in number of embryonic segments in the Japanese horseshoe crab, *Tachypleus tridentatus*. *Biological Bulliten* 158: 324–338.

Jimenez ML, Llinas J. 2002. Revision of ocular anomalies in epigean spiders (Arachnida:Araneae) with notes on four new records. *Anales del Instituto de Biología, Universidad Nacional Autónoma de México, Serie Zoología* 73 (2): 241–250.

Kaston BJ. 1937. Structural anomalies in spiders. *Bulletin of the Brooklyn Entomological Society* 32: 104.

Kaston BJ. 1962. Ocular anomalies in spiders. *Bulletin of the Brooklyn Entomological Society* 57: 17–21.

Kaston BJ. 1982. Additional ocular anomalies in spiders. *Journal of Arachnology* 10 (281).

Loria SF, Prendini L. 2014. Homology of the lateral eyes of Scorpiones: A six-ocellus model. *PLoS ONE* 9 (12): 1–30.

Marer PJ. 1972. An eye deformity in a tarantula spider, *Aphonopelma reversum*. *Pan-Pacific Entomology* 48: 221–225.

Morehouse NI, Buschbeck EK, Zurek DB, Steck M, Porter ML. 2017. Molecular evolution of spider vision: New opportunities, familiar players. *Biological Bulletin* 233 (1): 21–38.

Napiórkowska T, Jacuński L, Templin J. 2007. Epimorphosis and repair processes of schistomelic pedipalps and walking appendages in *Tegenaria atrica* (Araneae, Agelenidae). *Biologia, Bratislava* 62 (6): 756–762.

Napiórkowska T, Templin J. 2017. Teratological changes on the prosoma of *Eratigena atrica* spiders caused by alternating temperatures. *Invertebrate Survival Journal* 14: 480–487.

Napiórkowska T, Templin J. 2018. Heterosymely and accompanying anomalies in the spider *Eratigena atrica* (C .L. Kock, 1843) (Araneae: Agelenidae). *Annales Zoologici* 68 (4): 909–914.

Noordijk J, Heijerman T. 2016. A rare teratology in the harvestman *Lophopilio palpinalis* (Opiliones:

© University of Pretoria

Phalangiidae). *Arachnology* 17 (2): 100–102.

Ono H, Kudo Y. 1996. The Ocular Anomaly in a Ground Spider (Araneae: Gnaphosidae) from Japan. *Acta Arachnologica* 45 (1): 73–75.

Opatova V, Hamilton CA, Hedin M, De Oca LM, Král J, Bond JE. 2019. Phylogenetic Systematics and Evolution of the Spider Infraorder Mygalomorphae Using Genomic Scale Data. *Systematic Biology* syz064.

Price RE. 2001. *Efficacy of Alpha-cypermethrin (Fastac) against brown locust nymphal bands under cool climatic conditions in the Karoo, South Africa*. Pretoria.

Price RE, Brown HD, Mitchell JD, Coetzee KE. 2000. *Efficacy of Fipronil in barrier treatments for the control of nymphal bands of the brown locust*. Pretoria.

Price RE, Butler ET, Brown HD. 1994. *Efficacy of Fipronil against nymphal bands of the brown locust in the karoo, South Africa*. Pretoria.

Price RE, Butler ET, du Preez I. 1996. *Field trials of Filpronil UL against brown locust nymphal bands in the karoo, South Africa*. Pretoria.

Satler JD, Carstens BC, Hedin M. 2013. Multilocus Species Delimitation in a Complex of Morphologically Conserved Trapdoor Spiders (Mygalomorphae, Antrodiaetidae, *Aliatypus*). *Systematic Biology* 62 (6): 805–823.

Savory T. 1977. Ontogeny. *In*: *Arachnida*. London: Academic Press Inc. pp 49–59.

Sonnini CS, Latreille PA. 1802. Histoire Naturelle des Reptiles. *Librairie Encycopédique de Roret*, 4 volumes: xxii, 280, 332, 335; 4.

Stewart DAB, Butler ET, du Preez I. 1995. *Efficacy of ISOO3N and IS044B against the brown locust in the karoo, South Africa*. Pretoria.

Stewart DAB, Napier Bax P. 1995. *Efficacy of Fenvalerate against the brown locust Locustana pardalina in the karoo, South Africa*. Pretoria.

Stewart DAB, Price RE, Butler ET. 1994. *Environmental impact of Deltamethrin on non-target organisms in the Karoo*. Pretoria.

Ujhazy E, Mach M, Navarova J, Brucknerova I, Bubovicky M. 2012. Teratology- past, present and future. *Interdisciplinary Toxicology* 5: 163–168.

© University of Pretoria

World Spider Catalog, 2020. World Spider Catalog Version 21.0. *Natural History Museum Bern*. Available at http://wsc.nmbe.ch [accessed 1 October 2020].

Acknowledgements

We would like to thank the following institutions for loaning the specimens reported on in the communication: Albany Museum, Grahamstown, South Africa; The National Museum, Bloemfontein, South Africa; Ditsong Museum of Natural History, Pretoria, South Africa; Iziko Museum of Cape Town, South Africa; Museum für Naturkunde, Berlin, Germany; National Collection of Arachnida, Pretoria, South Africa. The first author would also like to acknowledge the National Research Foundation for funding (Grant no: 120190). This work is based on the research supported in part by the Karoo BioGaps Project (NRF Grant Number 98864), which was awarded through the Foundational Biodiversity Information Programme (FBIP), a joint initiative of the Department of Science of Technology (DST), the National Research Foundation (NRF) and the South African National Biodiversity Institute (SANBI).

© University of Pretoria